Université Pierre et Marie Curie

École doctorale CERVEAU, COGNITION et COMPORTEMENT

Laboratoire Développement oligodendrocytaire et interactions neurovasculaires

Institut du Cerveau et de la Moelle épinière Hôpital de la Pitié Salpêtrière

UMRS 975. CRICM UMRS 975, U975, UMR 7225.

Ascl1 and Olig2 transcriptional regulations of oligodendrogenesis

Par Adrien Clavairoly

Thèse soutenue le 19 septembre 2014 pour obtenir le titre de Docteur en neuroscience de l'Université Pierre et Marie Curie

devant un jury composé de :

Pr Ann Lohof : Président du jury

Dr Alexandra Pieranni : Rapporteur

Dr Diogo Sampaio et Castro : Rapporteur

Dr Matthias Grozcer : Examinateur

Dr Antoine de Chevigny : Examinateur

Dr Carlos Parras : Directeur de Thèse

Except where otherwise noted, this work is licensed under
http://creativecommons.org/licenses/by-nc-nd/3.0/

Dédicace

A mes parents Laure et François, mon frère Fabian et ma sœur Olivia, à Gabriel et Morwena et à tous ceux qui par amitié et par amour m‘ont construit.

Remerciements

Je tiens à remercier chaleureusement l'ensemble des membres du jury pour avoir accepté d'évaluer ce travail de doctorat. Je remercie en particulier le Pr Anne Lohof d'avoir accepté de présider ce jury, ainsi que le Dr Alessandra Pierrani et le Dr Diogo Sampaio e Castro d'y participer en qualité de rapporteur. Enfin, je remercie le Dr Matthias Groszer et Dr Antoine de Chevigny en leur qualité d'examinateur. J'exprime ma sincère gratitude au Dr Carlos Parras de m'avoir accepté au sein de son équipe lors de mon Master 2 ainsi que pour son soutien compréhensif et patient tout au long de ces 4 années ainsi que pour l'aide inestimable apporté lors de la rédaction de ce travail. Je remercie également chaleureusement tous les membres de l'équipe « origine des oligodendrocytes » qui ont partagé ces 4 années avec moi et ont fortement contribué à l'aboutissement de ce travail. Je remercie en particulier le Dr Boris Zalc de m'avoir accueilli au sein du Centre de Recherche de l'Institut du Cerveau et de la Moelle épiniere et pour tous les échanges que nous avons pu avoir lors de nos réunions d'équipe hebdomadaires. Je remercie chaleureusement le Dr Karim Mannioui, le Dr Romain Fontaine, le Dr Charles-Felix Calvo, le Dr Hessameh Hassani et le Dr Hiroko Nakatani, Marie-Stephane Aigrot , Hatem Hmidan, Corentine Marie et Magalie Frah pour leur présence, leur humour et l'aide qu'ils ont pu m'apporter tout au long de ces années. Enfin je remercie tous ceux que j'aime, ma famille et mes amis, en particulier François et Laure, mes parents, Fabian et Olivia, mon frère et ma sœur, et Morwena Latouche mon Amour.

Table of Contents

Remerciements 3

PREFACE 9

INTRODUCTION....16

PART I: THEORETICAL BACKGROUND....16

CHAPTER I: GENOME REGULATION AND NUCLEAR ORGANIZATION....17

General consideration on genome structure and conservation 17

Basal transcription machinery and core promoter elements....18

Transcription initiation, elongation and termination and nuclear export 20

The looping model of promoter-enhancer gene activation....21

Chromatin structure and gene regulation 25

Transcription factors diversity and phylogenetic origin....28

Transcription factor functions in gene regulation....29

Transcription factors combinatorial regulation of transcription....30

Epigenetic regulation of the chromatin: The histone code hyposthesis 31

Network regulation, information flow and central dogma of the molecular biology....37

Transcriptomic technologies 39

Chromatin immuno-precipitation techniques....42

Chromosome conformation capture assays 44

CHAPTER II: Nervous system development and cell type specification....46

Neurulation: the prosomeric model....46

Neural stem cell diversity and cell fate competency 58

Mechanisms of Intrinsic and extrinsic regulations of neural stem cells....65

Stem cell niche, stemness maintance and growth factors....65

CHAPTER III: Oligodendrogenesis and myelination....84

Myelination of the central nervous system 84

Functional organization of myelinated axons....87

Lipid composition of myelinating oligodendrocytes....87

Protein composition of myelin 88

Glial network in brain energy metabolism and axonal support....91

Oligodendrogenesis throughout development....94

Transcriptional control of oligodendrocyte progenitor cells specification.....94
Oligodendrogenesis during postnatal development and adulthood.....97
Molecular mechanisms involved in myelination and remyelination.....102
Therapeutic Aspect of oligodendroglial pathologies.....109
Conclusions and Future Directions.....111
PART II: EXPERIMENTAL WORK.....111
Chapter I: Material and methods.....111
Animals and genotyping.....111
Immunofluorescence.....112
Demyelinating.....113
Microarray experiments.....113
Technical aspects of microarray processing.....115
Cell culture.....119
Cell transfection.....121
Drug screening.....121
Chapter II: Data analysis and interpretation.....122
ChIP-Sequencing Peak-Calling and Data Analysis.....122
RT-PCR Analysis of ver-expression of Ascl1 and Olig2 in neurosphere.....122
Transcription factor binding site enrichement analysis.....123
OBJECTIVES & HYPOTHESES.....123
RESULTS.....125
Role of Ascl1 and Olig2 in neural stem cell and oligodendrocyte differentiation.....125
Identification of Cdh7 as putative regulator of oligodendrogenesis and myelination. ...146
Identification of TNS3 expression in premyelinating oligodendrocyte.....154
Myelinating oligodendrocyte control the creatine metabolism in the brain.....160
ARTICLE I: Ascl1/Mash1 Promotes Brain Oligodendrogenesis during Myelination and Remyelination.....165
ARTICLE II: Development of the prethalamus is crucial for thalamocortical projection formation and is regulated by Olig2.....186
PART III: DISCUSSION.....204
Creatine.....209
Chd7.....210
Chd8.....211

Tns3 211
CONCLUSION AND PERSPECTIVES 212
ANNEX 213
REFERENCES 228
ABSTRACT 258
RESUME EN FRANÇAIS 259

PREFACE

The question of the embryonic development has always questioned the curious minds. Aristotle in his book –On the Generation of Animals" was already developing a theory of –epigenesis" based on the observation of developing chick eggs. As opposed to preformationist views that lived long until the 18th century, Aristotle defined epigenesis as the progressive formation of the organism as being not fully formed at the beginning of embryonic development. In 1768 Caspar Friedrich Wolff was the first to observe that the embryo was constructed in –leaf-like layers" and it is Christian Heinrich Pander in 1817 that described for the first time the fate of the 3 germ layers of the embryo, the endorderm, the mesoderm and endoderm. Pionneer of the germ layer theory, he wrote in 1817 –A unique metamorphosis begins in each of these three layers, and each hurries toward its goal; although each is not yet independent enough to indicate what it truly is; it still needs its sister travellers, and therefore, although already designated for different ends, all three influence each other collectively" (Pander, C. 1817). A few year later, Rudolf Virchow developed the –cellular theory" affirming that –Omnis cellula e cellula" (Virchow 1858), a statement still standing

despite numerous efforts (Miller, 1953, Gibson DG 2014; Keber F C 2014) indeed, today cells are still generated exclusively from cells by successive division. One year later, in 1859, Charles Darwin writes in "The Origin of Species by Means of Natural Selection (…)": ―I should infer from analogy that probably all the organic beings which have ever lived on this earth have descended from some one primordial form, into which life was first breathed (Darwin C., "The Origin of Species by Means of Natural Selection, or the Preservation of Favoured Races in the Struggle For Life", (1859) p. 490). Darwin's theory lead today to the ―modern evolutionary synthesis" (Huxley J 1942) and allowed the rise of modern genetics and evolutionary developmental biology (The Structure of Evolutionary Theory Harvard University Press, Cambridge, Gould MA 2002).

In 1908, Alexander Maksimov is the first to propose the term "stem cell" as cells able to maintain an undifferentiated state (self renewal) as well as to differentiate. The term ―embryonic stem cell" giving rise to the three germ layers (potency) was later coined by Gail R. Martin who developped the technics to extract stem cell from the mouse blastocyst (Gail R. Martin 1981). During the process of differentiation, cells become restricted progressively from totipotency (3 germ layers ability), to pluripotency (3 germ layers but primed), multipotency (a subset of the 3 germ layers) or unipotency (only one germ layer). Carcinogenic and stem cells, able to self-renew but unable to differentiate, were later called nullipotent. In 1957, Conrad Hal Waddington published, the ―epigenetic landscape" model depicting how a cell cell progresses during development to generate all the alternative cell fates necessary to the formation of the whole organism. Waddington depicted cell fate choices as a ball rolling down to different valleys in a three dimensional landscape defined by the X-axis as the concentration of each molecules in the cell, the Y-axis as time and the Z-axis representing the system being monostable, bistable and then multistable (Figure 1).

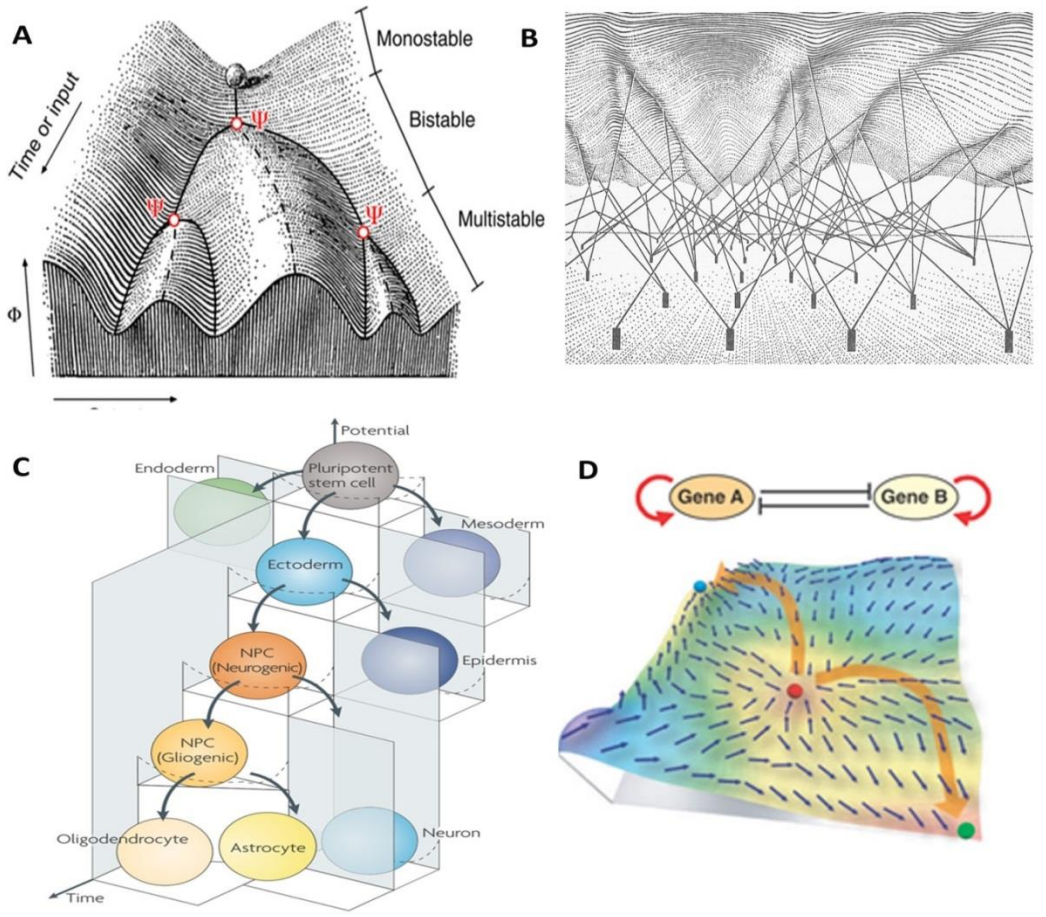

Figure 1. Evolution of Epigenetic landscape. A. Original drawing of Waddington (Waddington, C.H. 1957) where cells are depicted as a ball rolling down to a valley. New valleys represent different cell fates, and ridges maintain cells in particular epigenetic state. Landscape can be monostable, bi-stable or multistable. The solid black lines represent stable steady states, the dashed lines represent unstable steady states, and in red the bifurcations. B. Original drawing from Waddington showin correlation between the height of the ridges and combinatorial gene expression. C. Schématic representic the progressive cell fate restriction occurring during neural development. D. Mordern mathematical representation of the epigenetic landscape. Oscillatory gene expressions are generated by positive or negative feedback in the regulation network (red and black arrows) which lead to cell differentiation, a process driven by positive feedbacks stabilizing ~~ir~~reversible" stochastic events (adapted from S Newman 2012).

After a succession of identity crises, cells can –abruptly" shift from one fate to another and become –canalized" in a particular fate –buffering" subsequent genetic and environmental variations to maintain their identity. Waddington also emphasizes in his drawing the direct relationship existing between the ridges of the valley and specific gene expression of individual genes that cooperate to form what he called –Creodes", the different pathways followed by the cell during the process of differentiation (Waddington 1957). Aware of the complexity of the regulations in living systems, making the cell behaviour and evolution –quasi finalistic" (Waddington 1962a, 88), Waddington introduced the term epigenetics as –the branch of biology which studies the causal interactions between genes and their products which bring the phenotype into being." (Waddington CH. Towards a Theoretical Biology. Edinburgh, Scotland: Edinburgh University Press; 1968. The Basic Ideas of Biology).The concept of Epigenetics evolved with the emergence of modern biology and is defined today as –the study of changes in gene function that are mitotically and/or meiotically heritable and that do not entail a change in DNA sequence (Wu Ct, Morris JR Science. 2001). Waddington also defined –Attractors" describing the mechanism that restrict the cellular states to certain region of the three dimensional space and which allow perturbations to be bufferd. Waddington was really a pioneer in defining his model using references to thermodynamics. In 1877, Boltzman defined Entropy as a measure of –molecular disorder", Entropy of closed system being by definition always increasing toward a point of maximum entropy that defines the state of equilibrium of the system. However, cells and organisms are open systems exchanging matter, energy and information with their environnement. In 1977, Ilya Prigogine characterized the belousov-zhabotinsky reaction as a –dissipative Systems" which is an ensemble of non-linear chemical reactions passing by phase of increasing and decreasing entropy and able to form oscillating pattern. Such life mimicking reactions are maintained out-of-equilibrium and can generate self-organization, complex pattern formation and increase the level of order of the system upon time thanks to continuous metabolic transformation of energy and information (Prigogine, 1977). Dissipative reaction does not last infinitly. As only the intial and final equilibrium states are important to measure entropy, the second law of thermodynamics is preserved. Production of entropy (from catabolic processes) is balanced by the Production of structure (from

anabolic processes) or a change of the system as a whole called phase transitions, lowering the entropy of the system. In cells, while steady-state is achieved when the net change in entropy is close to zero, growth implies a net decrease in entropy for the system. In both cases, a production of entropy towards the environnement occurs to preserve the second law. Prigogine writes in ―Order out of chaos" ―We grow in direct proportion to the amount of chaos we can sustain and dissipate" (Ilya Prigogine, Order Out of Chaos: Man's New Dialogue with Nature).

Francisco Varela then developed the central concept of ―autopoiesis" (self-action) to describe caracteristics of living systems. He states that ―An autopoietic machine is a network of processes that produces and degrades their own components which through their interactions continuously maintain the network of processes that produced them as a concrete unit in space. (Maturana and Varela On Machines and Living Beings, 1972). This model of self-organization highlight the fundamental role of frontiers in biology (Mulkidjanian 2009) , the notion of homeostasis (dynamic maintenance of internal environment), metabolism (reactions that create and break down molecules), but also emphasized the fact that a system is made of a network of non-linear (positive and negative feedback) processes from which ―emerge" the necessary functions used for its self-maintenance and organization. It is important to note that all living organism are autopoietic but not all autopoietic system are alive (for example economic systems or chemical dissipative reactions). To propose a possible definition of living systems, we could describe it as a non-linear autopoietic and dissipative system that (once) emerged from physical properties of matter and evolved since by means of natural selection.

Many studies showed evidence in support of the epigenetic landcape model. It is now recognized that most of the genes exhibit a low expression level in stem cells but are maintained in a chromatin state ready for subsequent activation upon activation (T.I. Lee, R.G. Jenner2006). Moreover, genes whose changes in expressions levels are correlated have greater probability to physically interact and increase the level of order of the cell (Jansen 2002). However, it is only recently that the epigenetic landscape model validity was formally demonstrated in a study covering 800 different cell types

of all differentiation stages where gene expression profiles and inferred global protein network interactions were under analysis. In the "epigenetic landscape" paradigm, pluripotent stem cells have high entropy and low level ordering while cell differentiation lead to a decrease of entropy through progressive ordering. This study shows using a quantitative measure of "signaling entropy" that this parameter is sufficient to discriminate embryonic stem cell from cancer cell and differentiated cell. However, this study failed to discriminate between more differentiated cell types (R. Banerji, D. Miranda-Saavedra 2013).

Since Waddington proposed his model, many studies have used is to describe developmental processes. However, the number of cell type and cell type transitions that exist is impossible to describe using only 3 dimensions. Moreover, a paradigm shift came with the demonstration that transdifferentiation, the conversion of cell types in different lineages, was possible. Indeed, exogenous expression of the transcription factor MyoD was shown to induce muscle-specific (mesodermal) properties in fibroblasts (ectodermal) (Davis Weintraub 1987). After the pioneer work from John Gurdon who showed that cloning of a somatic nucleus into an enucleated egg was able to generate a complete organism (Gurdon 1967), cell fusion induced cell-fate reprogramming to pluripotent stem cells became possible (Gurdon, 2006). More recently, the revolutionary work of Yamanaka's group demonstrated that overexpression of only four transcription factors, Oct4, Sox2, Klf4, and c-Myc in adult fibroblasts, was sufficient to reprogram differentiated cells into induced pluripotent cells (iPSCs) (Takahashi and Yamanaka, 2006). "Direct" reprogramming of adult somatic cells into alternative cell types then became possible after the discovery that three neuronal transcription factors, Ascl1, Brn2, and Myt1l (BAM factors) were able to convert cells originating from the same (ectodermic fibroblast) or different (endodermic hepatocytes) germ layer, into functional neurons called induced neuronal (iN) cells (Vierbuchen et al., 2010; Maro s 2011). This ground breaking discovery showed that a small number of "master regulators" are able to shift the expression of hundreds of genes and convert directly a cell type into another without passing by a pluripotent stage or a cell division. It is now of primary interest to understand how those cell fate change are driven at an epigenetic level and to describe precisely the

gene regulatory network underlying this puzzling phenomenon. Indeed, transdifferentiation requires jumping over two or more epigenetic ridges and dedifferentiation requires uphill movement in the Waddington landscape. Moreover, actual direct conversion yiel are really small and models fail to provide any quantification of the probability of any transition states.Waddington himself cautioned that the epigenetic landscape was an abstraction that could not be rigorously interpreted (Waddington 1957). Understanding how deterministic cell behaviour emerges from complex stochastic pattern of dynamic molecular interactions between so many intra and extracellular components is highly challenging. Efforts in ―system biology"are made to develop new mathematical tools that describe the complex dynamical nature of living systems (M. Hecker, 2009). Bayesian inference are particulary fitted to explain biological system as this mathematical tool can use prior knowledge such as transcriptomic, proteomic, metabolic, epigenetic or phenomic data to assess simultaneous bottom-up and top-down causality. A number of studies already showed the great utility of such network-based analysis (M.J. Lee, A.S. Ye,2012, J.T. Erler, R. Linding 2012). However, ―the gene regulatory network inference problem" is particularly hard (de Jong H, Page M. 2008) as interactions between components of the system have to be reconstructed from small data sets, generally containing a few replicates. The increasing availability of high-dimensional and temporal data and structured information stored in online database is now paving the way for a data-driven biology (Altaf-Ul-Amin M 2014) where a multi-level data integration together with further understanding of the relation between biological structure, entropy and information will surely lead to the emergence of new models explain the ability for the cell to manage the strict constraints of thermodynamics as well as their changing environnement. (Smith JM 2000; Longo 2012;)

INTRODUCTION

PART I: THEORETICAL BACKGROUND

Conrad Waddington had a really rich scientific carreer. He published in paleonthology, genetics, biochemistry, population genetics and embryology. In 1934, he demonstrated that the grafting of a duck "organizer" (the hensen's node) into a chick or a rabbit embryo at the blastoderm stage was able to induce a full sond second body axis formation (Waddington 1934; Jonathan M. W. Slack 2002). As the secondary axis was containing many tissue types, Waddington understood that this "organizer effect" was not arising from a single molecule and more interestingly that the signals were conserved between species. He employed the word "evocation" as the priming of the future fate choice and the word "individuation" as the production of different cell responses induced by an "evocator". During years, Waddington tried to find the neural-inducing activity of the node and thought to find it when he purified steroids from the embryo (Waddington 1935). However in the 1930s, biochemists had no chance at all of purifying "this evocator"and we had to wait the 1990s to finally identify the fibroblast growth factor (FGF) and transforming growth factor-β (TGFβ) families only present at picomolar concentratrion in early embryos (Slack, J. M. W.1994; Baedke 2013). Two different mechanisms were identified for creating spatially restricted patterns in living systems. The first one, proposed by Alan Turing in 1952 in "The chemical basis of morphogenesis" defines "morphogenes" as diffusing molecules able to drive morphogenetic changes (Turing A 1952). He developed a model now called "diffusion-driven instability" where a competition betwen a slow diffusing activator and a faster diffusing inhibitor generate periodic patterns. Even if this phenomenon was biologicaly demonstrated only recently (Maini 2012, Marcon 2012), Turing's work introduced algorithmic and booelan logic in biology (Davidson 2010) and thus paved the way for modern computational model of gene regulatory network occurring during development (Corominas-Murtra, 201; Alexander Spirov2013). The second model under analysis was "the french flag gradient model", a system of diffusible molecule which, produced asymmetrically, creates a spatial concentration gradient. Each position along this gradient receives different

concentrations of signal and gives cells access to positional information allowing them to trigger discrete response depending on their location (Wolpert L, 1969). This model was later on demonstrated and refined for sonic hedgehog signaling thanks to a quantitative correlation between Shh morphogen concentration and intracellular gradual Gli signaling responses (E Dessaud 2007).

Life seems to be more than complex chemistry. Indeed, its unique informational management properties and modular functionality seem to be its specificity. Embryonic development is accomplished by a dynamic regulation of gene expression that lead to growth and differentiation (Bruneau, 2008; Kang et al., 2011; SiTayeb et al., 2010). Striking differences in epigenetic landscape exist between normal and pathological embryonic, adult and cultured cells (Gifford et al., 2013; Heintzman et al., 2009; Shen et al., 2012; Stergachis et al., 2013; Zhu et al., 2013; Ziller et al., 2013). Identifying the temporal dynamics of the genetic regulatory landscapes driving normal and pathological biological processes is thus of primary interest.

CHAPTER I: GENOME REGULATION AND NUCLEAR ORGANIZATION

General consideration on genome structure and conservation

In human, only 1.5% of the $3{,}38.10^9$ bp of the genome serves as a template for the 20389 genes identified so far (Lander, E. S. 2001; Ensembl GRCh38). The remaining proportion of the genome, mainly composed of repetitive sequences of viral origins (45%), intronic sequences (25%), intergenic sequences (~25%) and centromeric/telomeric sequences (~5%) were long thought to be ~~"j~~unk DNA" (Ehret and de Haller 1963; Ohno S 1972; Venter, J.C 2001; Mandal PK, 2008). Mouse models have been used extensively to improve our understanding of mammalian development. With their $2.7.10^9$ bp and 99% of genes having human orthologs, mice played a great role in both the annotation and the study of gene function and regulation (Buecker and Wysocka, 2012). It is now well recognized that an important part of the non protein coding part of the eukaryotic genome is actually essential for the control of gene expression (Nord AS 2013). Indeed, the genome is now known to undergo ~~"p~~ervasive transcription" (P Kapranov2007, MB Clark 2011) and despite a very low abundance for the majority of the RNA molecules present in a cell, around 75% of the genome is

found to be transcribed in human cells in average (Cheng et al. 2005; Manak et al. 2006; The ENCODE Project Consortium 2007; Kapranov et al. 2007; Efroni et al. 2008; Clark MB et al. 2011). Nontheless, low expression of many non-protein coding RNA have tremendous effects in many developmental process and are frequently disregulated in diseases (M Esteller 2011). While recent comparative analysis showed that only 8.2% of the human genome is under purifying selection and thus phylogenetically conserved in mammals (Rands CM 2014), 80 % of the human genome is said to be functional, as defined by the ENCODE project by the participation of the genomic sequence under investigation in at least one biochemical RNA and/or DNA event in at least one cell type (ENCODE project consortium 2011; Dunham I 2012). However this definition of functionality is pretty loose as transcription or replication of a genomic element does not imply its functionality (D Graur 2013). A high level of sequence conservation is frequently used as evidence of functionality (Pennacchio and Rubin, 2001). However, transcription regulatory regions evolve faster than protein-coding regions and play a key role in evolution of species and specialization of organs, such as the brain (Clarke SL, 2012). Indeed, 11% and 40% of the human regulatory regions emerged since the rhesus or mouse divergence, respectively (J Cotney 2013). Moreover, conservation of regulatory regions is tissue and developmental stage dependent (Nord AS 2013). Interestingly, while a rapid turnover of regulatory DNA sequences occurs during evolution (Schmidt, D. 2010; Villar D Flicek P 2014), many studies showed a high functional conservation of these regulatory regions (Arnold CD 2014; J Cotney 2013). Thus, sequence conservation and functional conservation are not strictly correlated. Nonetheless, strong regulatory functions are most of the time associated with strong purifying selection (Q. He, A.F. Bardet, B., 2011).Thus, despite usefull correlation between biological functionality and phylogenetic conservation substantial work remains to be done to understand the regulatory logic of transcription operating during development and evolution.

Basal transcription machinery and core promoter elements

Transcription is the mechanism by which genes are converted into mRNA before translation into proteins. This process needs to be tightly controlled to achieve a

proper development and maintenance of the organism. Transcription of protein-coding genes and most non-coding RNA genes is driven by RNA polymerase II (pol II). Transcription involves three steps: Initiation, the recruitment of the polymerase to the gene promoter; Elongation, the synthesis of the RNA, and Termination, the dissociation of the RNA from DNA and the transcription machinery (Shandilya J 2012). Pol II is part of molecular complex known as the pre-initiation complex (PIC) composed of the general initiation factors, pol II and the mediator complex (Hahn, 2004; Kornberg, 2005). The general initiation transcription factors TFIID, TFIIA, TFIIB, TFIIF, TFIIE, and TFIIH are the minimum factors required to drive pol II binding to the ~~"c~~ore promoter", the proximal cis-regulatory element (CRE) to initiate transcription (Thomas chiang, 2006). The mediator is a ubiquitous complex composed of 33 subunits required to link the core promoter with their proximal and distant cis-regulatory element known as enhancers or silencers (Takagi & Kornberg, 2006; Poss 2013, Malik & Roeder, 2010; Borggrefe & Yue, 2011). Core promoters are positioned between −50 and +50 relative to the +1 transcription start site (TSS) of genes and arecomposed of 4 obligatory consensus motifs: An upstream TFIIB responsive element (BREu; SSRCGCC), the TATA box consensus (TATAWAWR), the downstream BRE (BREd; RTDKKKK) and the initiator Inr (YYA+1NWYY). Additional sites were identified more recently known as the DPE (downstream promoter element), the MTE (motif ten element), the Motif 1/6 elements, the DRE (DNA replication-related-element), the DCE (downstream core element), the XCPE (X core promoter element), the TCE (translational control element), and the PB (the pause button) (Ohler, U.2010). As about 160,000 PICs are detected genome-wide, the complexity of core promoter elements makes bioinformatics inference usefull but inadequate for in-vivo inference (Müller F 2014). Accurate genome wide in-vivo identification of TSS in different cell types are now possible based on analysis of high-throughput sequencing (U. Ohler, D.A. Wassarman, 2010; B. Lenhard, A. Sandelin, 2010; P. Batut, A. Dobin, 2013). Core promoters are divided in two categories: ~~"n~~arrow promoters", where Pol II transcription initiates at at a unique TSS, and ~~"b~~road promoters" where Pol II can initiate transcription at multiple TSS (A. Sandelin 2007). Genes with ~~"n~~arrow promoters" have low GC-content and mainly correspond to tissue-specific genes, while genes with ~~"b~~road promoters" have high GC content and are associated with

developmentally regulated or housekeeping genes (B. Lenhard, A. Sandelin, P 2010). A former classification discriminating TATA-containing and TATA-less promoters (S.T. Smale,1997) should be abandoned. Indeed, precise analysis of TATA-less promoters demonstrated the existence of a TATA-like motif in all promoters (HS Rhee, 2012).

Transcription initiation, elongation and termination and nuclear export

After formation of the PIC, the polymerase initiate RNA synthesis in a process called elongation. Briefly, the phosphorylation of serine residues in the carboxy-terminal repeat domain (CTD) of Pol II by TFIIH or P-TEFb triggers elongation (Zhou, Li, 2012). However, Pol II elongates inefficiently and often pauses within the first 100 nucleotides. Pol II pausing is caused by the association of DSIF (Wada, T. et al. 1998), NELF (Yamaguchi, Y. et al. 1999) and GRINL1A (Cheng, B. et al. 2012). Pausing of Pol II is a way to generate an accessible promoter region that can be quickly bound by activators and co-activators (TFIIH or P-TEFb) to trigger elongation. The open promoter associated with the GTFs remains after Pol II escapes and allows rapid entry of new PIC (Yudkovsky, N., Ranish, J. A. & Hahn, S. 2000). Paused Pol II has been observed at genes that are rapidly induced or genes involved in early embryonic development (Aida, M. et al 2006 Adelman, K. et al.2009). However, pausing seems to be a general mechanism as it was also observed in constitutively expressed genes (Gilchrist, D. A. et al 2012). Transcription occurs in bursts, where a gene is transcribed for a short period followed by a period of inactivity (JM, O'Shea EK. 2005). Different groups of genes can be divided depending on their bursting activity (Raj A, van Oudenaarden A. 2008). Transcription termination, the process by which mRNA is released after synthesis, is coupled with RNA poly(A) and capping maturation (Kuehner J 2011). Most of the mRNAs have a highly conserved poly (A) signal (5′-AAUAAA-3′ followed by a G/U-rich sequence). Once the poly (A) signal is transcribed, Pol II stops. The endoribonucleolytic cleavage of the nascent transcript occurs and is followed by polyadenylation of the mRNA thanks to the recruitment of the polyadenylation specificity factor (CPSF), the cleavage stimulatory factor (CstF)

and the Poly (A) polymerase on the carboxy-terminal domain (CTD) of the Pol II subunit Rpb1. (J.N. Kuehner 2011). Maturation of the pre-mature mRNA is a cotranscriptional process that occurs concomitantly with alternative splicing before export in the cytoplasm for translation into protein. Maturation stabilizes RNA molecules against exosomal or alternative RNA degradation pathways (Chlebowski A 2013). Disruption of the RNA degradation pathways reveals the phenomenon of pervasive transcription and highlights the importance of the degradation machinery in the control of gene expression (A. Jacquier 2009). Recent studies estimate that in human, up to 94% of multi-exon genes undergo alternative splicing (Pan Q, Shai O et al. 2008; Wang ET, Sandberg R et al. 2008) a phenomenon shown to underly the developmental complexity of the organism (L Chen SJ. Bush 2014). Finally, mature RNAs are exported via the nuclear pore complex thanks to receptors that directly recognize the RNA or interact with the mRNA ribonucleoprotein (mRNP) complex (Adams RL 2013). This level of RNA regulation, together with cytoplasmic P-bodies (involved in RNA degradation and strorage) as well as mechanism of riboswitch (temporary inactivation for local translation) explain the discrepancy between transcriptome and proteome. Indeed, in mice, mRNA levels explain only 40% of the variability in protein levels (Schwanhäusser 2011; Ghazalpour et al., 2011).

The looping model of promoter-enhancer gene activation

Enhancers are proximal or distal cis-regulatory DNA sequences, commonly 20–500 bp in length, containing clustered transcription factor binding sites (TFBS) and representing 11% of the genome (Spitz and Furlong, 2012; Shen 2012).More likely associated with developmentally regulated genes (Levine, 2010), enhancers are responsible for the tissue specificity of gene expression (Bernstein et al., 2012; Ernst et al., 2011; Shen et al., 2012; Visel et al., 2009). Strikingly, enhancers are modular and work in an additive way to drive specific spatially restricted expression patterns in vivo (Visel et al., 2009, 2013) independently on their location (up or downstream of the promoter) or their orientation compared to their related promoter (Banerji, J., Rusconi, S. 1981). Intensive work allowed significant progress to identify these elements in

mammalian genomes (Bernstein et al., 2012; Ernst et al., 2011; Shen et al., 2012). The major model of promoter-enhancer interaction driving gene activation is the looping model‘‘where multiple enhancers (4-5 enhancer per promoter in average) activate transcription by delivering activating factors to the promoter to increase the probability of activation of the preinitiation complex as well as the probability of transition from initiation to elongation during transcription (Bulger and Groudine, 2011; Ghavi-Helm, Y. & Furlong, 2012; Shen 2010). This model was higly validated by recent studies (Ong and Corces, 2011, 2012) and the emergence of technologies such as chromosome conformation capture and their derivatives (Wit and de Laat, 2012; Gibcus and Dekker, 2013), allowed the identification of the chromatin features associated with enhancers. Interestingly, gene expression from a particular promoter is positively correlated with the number of enhancers contacting it. Promoters can be enhancers for different genes and enhancer can regulate different genes. Promoter-enhancer long range interactions display striking asymmetry with a bias for interactions with elements located ~120 Kb upstream of the TSS. Moreover, 57% of the interactions span >100 kb with a median distance of 124 kb and only ~7% occur with the nearest gene, suggesting that genomic proximity is not a good predictor for long-range interactions inference (Sanyal A, Lajoie BR 2012; Fulai Jin, et al., & Bing Ren. Nature 13 Nov 2013). The ENCODE project which is in charge of only 1% of the genome already revealed 400,000 distinct enhancers mapped in a set of human cell lines (Buecker and Wysocka, 2012; Maston1 et al., 2012). Current estimate compiling bioinformatics predictions and experimental inferences of enhancers in the human genome reach many millions (Dunham et al., 2012). High throughput in-vivo transgenic validations were recently done in mouse embryos and comprehensive enhancer databases are currently under construction (Vista Enhancer Browser http://enhancer.lbl.gov).

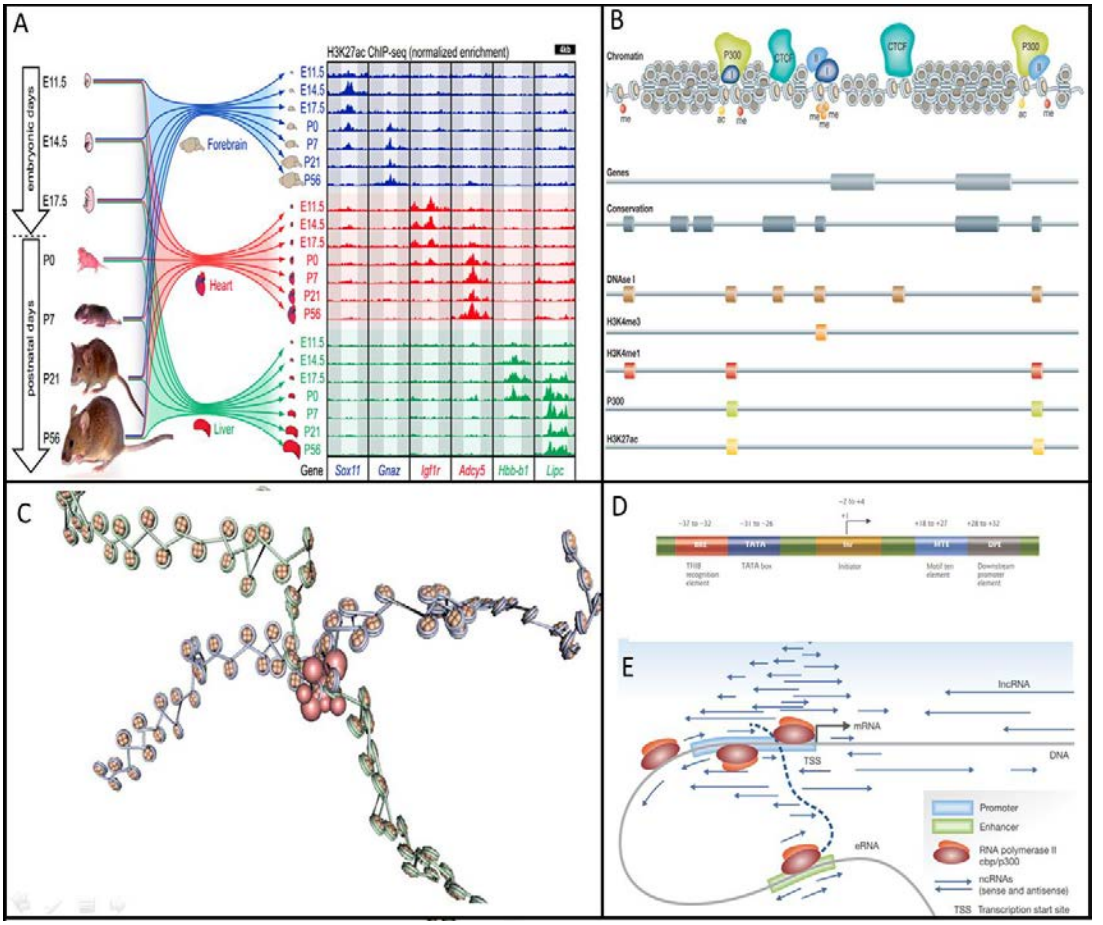

Figure (A) Figure 1. Epigenetic change during development. Schematic showing the mouse developmental change in epigenetic profile between E11.5 and P56. The Chip-seq profiles of the active enhancer mark H3K27Ac are shown for 3 different tissues, the brain, the heart and the liver. (B) Parrallel analysis of Chip-seq peaks. The absence of overlap between peaks of each tissue indicated cell type specificity of the identified enhancers. (adapted from B van Steensel 2011.(B) Stuctural organization of the chromatin and gene regulation. Schematin showinh the DNA packed around histone and forming globules of nucleosomes. DNA accessibility is driver by Histone turn over and competition with TFs and chromatin remodelers. P300 is shown to bind on active enhancer and acetylate H3k27. Pararallele view of different epigenetic marks or DNAse accessibility regions.(C) Model of chromatin organization in an interphase mammalian nuclei.(D) RNA PolII core promoter element motifs. Sequence elements that can contribute to basal transcription from the core promoter are indicated.The location given for the different motis are indicated relative to the start site
(adapted from AS Nord 2013; B van Steensel 2011; Mirny et al 2011)

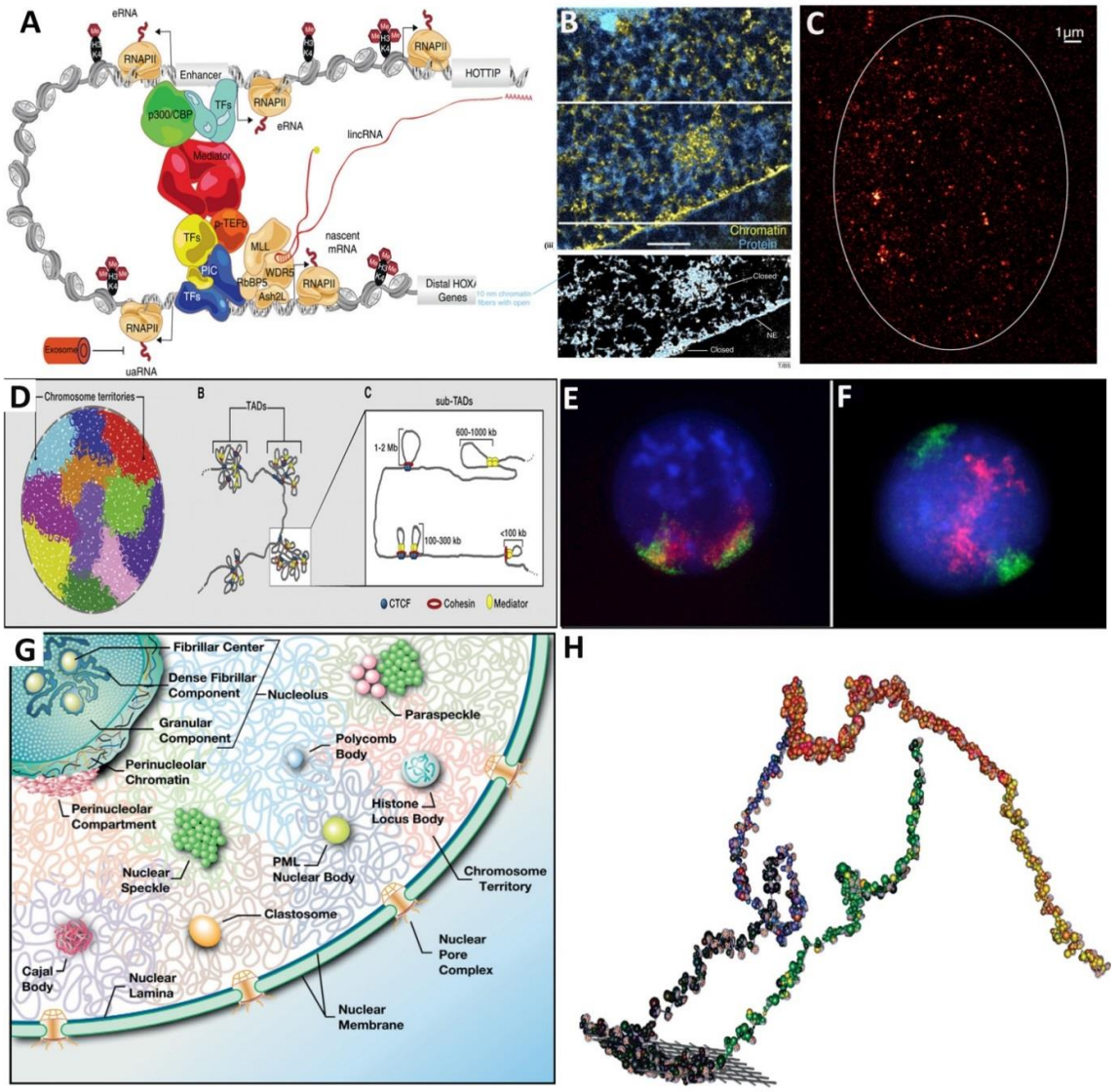

Figure 2. Principles of 3D organization of the chromatin. A: Promoter-enhancer loop model. Schematic showing chromatin looping stabilizing the pre-initiation complex (RNApolII, GTFs) thanks to the mediator complex together with Long non coding RNA, cohesins and CTCF. Production of RNA is pervasive and directed down and upstream of the gene with the production of non-coding RNA such as eRNA transcribed at distant enhancer sites. The action of the exosome, in charge of RNA degradation, is central for the control of gene expression. B: Chromatin organization. Compacted chromatin is inactive and maintained in periphery of the nucleus (D. Fussner 2011). C. Transcription factory in a mammalian cell. Super-resolution microscopy showing spatial clustering of RNA polII (see also W hao 2014). D. Nuclear organization and chromosome territories. Schematic showing chromosomes occupying defined nuclear territory with little overlap with others. Despite some trans-regulation (inter-chromosomic), the majority of long range interaction are cis-

regulatory events (intra-chromosomic). Chromatin folding generates globules of nucleosomal DNA that are organized in topologically associating domains (TADs) and SubTADs with different size and shapes. E-F. High resolution visualization of chromatin in an interphase mammalian nuclei. Chromosomes are compartmentalized and are formed of fractal successive ordering of 10 nm chromatin fibers (Mirny et al 2011). G. Subnuclear organization. Schematic representation of the nuclear bodies (adapted from YS Mao 2011). H. Chromatin regulation. Chromatin types were recently divided in five colors: Yellow (active and ubiquitously expressed genes; ~15% of the genome), Red (active and tissue specific genes; ~10%), Blue (developmentally regulated gene; ~20%), Green (heterochromatic but active genes; ~5%) and Black (heterochromatic silent genes; ~50% of the genome). Silent chromatin is characterized by lamina associated domains (LADs) which are large (0.1–10 Mb) silent domains located in periphery of the nucleus. (adapted from B van Steensel 2011).

Chromatin structure and gene regulation

Chromatin is formed of nucleosomes wrapping 147 bp of DNA around an octamer of histone (two molecules each of histone H2A, H2B, H3 and H4) in a highly stable unit that is maintained by over 120 protein-DNA interactions (Luger K, Mäder AW 1997). Chromatin is a ―bead-on-a-string" structure with 20-60 bp long DNA linkers connecting the nucleosomes together (Grosberg and Khokhlov 1994. Routh et al. 2008) .While the volume of DNA of a human diploid genome is around 6.4 mm^3 and would occupy 5.7% of the nuclear volume, the DNA wrapped around nucleosomes occupy 20.6 mm^3 which represent 18.2% of the nuclear volume. Thus, chromatin does not compact DNA (Fussner 2011). Rather, chromatin is a highly dynamic packaging of chromosomes which allow a tight control of gene expression, DNA replication and DNA repair (Bickmore 2013). Early electron microscopy studies showed that nucleosomes formed repetitive coiled structures of ~30nm diameter called solenoids (JD McGhee, JM Nickol, 1983; Horowitz, R.A. et al. 1994). However, recent studies in unfixed interphase nuclei or mitotic chromosomes failed to detect solenoids in-vivo (Maeshima et al, 2010; Fussner et al, 2011). Rather, most nuclei show irregular patches of local compaction consisting of globules of nucleosomes which aggregations are facilitated for example by the linker histone H1 or the Polycomb Group (PcG) protein complexes (Francis NJ, Kingston RE et al, 2004; Hizume et al, 2005). Moreover, the early distinction between ―compacted and inactive heterochromatin" and ―open and

active euchromatin" is now recognized as an oversimplification. Indeed, accessibility of chromatin was measured in-vitro by exposing detergent-permeabilized nuclei to endonucleases DNase I and quantitative mapping of the cutting sites; the cutting frequency being thought to be proportional to the accessibility of the DNA (Weintraub and Groudine, 1976). However, more recent measures of DNA accessibility by an in-vivo mapping of DNA methylation by Dam methyltransferase that marks any accessible GATC sequences with an adenine tag that does not occur endogenously, established that most of the genome is actually accessible (Sha K, Gu SG, 2010). Indeed, other studies showed no differences in DNA accessibility for molecules below a 10 nm (1MDa) size (Verschure et al, 2003; Gorisch et al, 2005; Pack et al, 2006). Thus, changes in chromatin organization do not control the binding of proteins to DNA through changes in DNA accessibility. Rather, different chromatin types may act as guides to favor targeting of specific DNA regions (van Steensel B 2011). Indeed, the mapping of more than 100 chromatin associated proteins divided the drosophila chromatin into five main types, each chromatin type being specifically bound by specific proteins (Filion GJ, van Bemmel JG 2010; van Bemmel JG 2013). Chromatin types were divided as follow: Yellow (active and ubiquitously expressed genes; ~15% of the genome), Red (active and tissue specific genes; ~10%), Blue (developmentally regulated gene; ~20%), Green (heterochromatic but active genes; ~5%) and Black (heterochromatic silent genes; ~50% of the genome). In human or mouse, similar chromatin types (4-5 types and 51 subtypes) were also described based on the study of post translational epigenetic marks of histone proteins (Ernst and Kellis, 2010; Oren Ram goren A 2011). The BLACK chromatin drives gene silencing thanks to histone H1 which stabilize nucleosome positions and decrease histone turnover (Laybourn and Kadonaga, 1991, Woodcock et al., 2006) as well as by lamina anchoring of the chromatin to the internal nuclear membrane (Pickersgill et al., 2006, Towbin et al., 2009). Silent chromatin is characterized by lamina associated domains (LADs) which are large (0.1–10 Mb) silent domains located in periphery of the nucleus (L. Guelen, L. Pagie, 2008). The recent development of chromosome conformation capture techniques (3C, 4C, 5C and Hi-C) unraveled the 3D organization of chromatin at high resolution and enabled the modelization of genome-wide interactions map independently of any DNA binding factor (E. de Wit, W. de Laat 2012). Briefly, all these techniques uses

formaldehyde fixation to cross-link genomic regions that interact in vivo, the sequencing of the ligation products of interacting DNA regions and reconstruction of an interaction map (E. Lieberman-Aiden 2009). ChIA-PET, a variant technique, includes an additional immuno-precipitation step that allows modelization of the interaction map for a specific TF (Jingyao Zhang, Huay Mei Poh 2012). These techniques identified in chromosomes, large discrete interacting domains called topologically associating domains (TADs) which have an average size of ~900kb in mammals (Dixon 2012). Mammalian genomes are composed of ~2,000 TADs, covering 90% of the genome. Regions located within TADs are shown to be much more likely to interact with each other than regions being in different TADs (E. Lieberman-Aiden 2009). Long range interaction between promoter and cis-regulatory elements such as enhancers are particularly frequent within TADs (Shen Y 2012). Moreover, analysis of boundary regions between TADs showed enrichment for CTCF protein, although CTCF also frequently binds sites within TADs and does not block physical long-range interactions (Sanyal A, Lajoie BR 2012). Modelization of the mammalian chromatin demonstrated a ―fractal globule" organization where nucleosomes are organized in knot-free globules that crumple together successively (as in fractal motifs) to form higher order globules (A. Y. Grosberg, S. K. Nechaev, E. I. 1998; Lieberman-Aiden et al. 2009). Hi-C analyses of mammalian genomes (Lieberman-Aiden et al., 2009; Kalhor et al., 2012; Zhang R.P. McCord et al., 2012), showed that chromosomes largely occupy individual territories where the captured long-range DNA interactions are mainly in cis (intra-chromosomic) within TADs (Simonis et al., 2006; Lieberman-Aiden et al., 2009; Hou et al., 2012; Kalhor et al., 2012; Sexton et al., 2012). Despite this territorial organization, interactions in trans (inter-chromosomic) occur at the boundaries between chromosomes and through infiltration of looped-out genomic region into the territories of another chromosome (Branco and Pombo, 2006). This spatial organization allow the formation of ―transcription factories" (concept first proposed to describe the clustering of transcription factors as discrete foci in the nucleus) comprising interacting chromatin regions, clustered transcription machinery and high concentration of TFs, RNA maturation and splicing machineries (Jackson et al. 1993; Melnik et al. 2011; Edelman and Fraser 2012). A well known example of transcription factory is the nucleolus

which produces rRNA from 2000 clustered rRNA copies dispersed in five different chromosomes that are recruited to the nucleolus to be cotranscribed (Hernandez-Verdun et al. 2010; Nemeth and Langst 2011). Many other membrane-less subnuclear nuclear structures such as Histone bodies, Cajal bodies, speckles, paraspeckles, and Polycomb bodies (Yuntao S. Mao 2011) are ordered in the nucleus by the nucleoskeleton composed of lamins, titin, actin, myosins, and kinesin–s associated with chromatin (Simon and Wilson 2011; de Lanerolle and Serebryannyy 2011).

Transcription factors diversity and phylogenetic origin

Transcription factors (TFs) are a class of DNA-binding proteins that typically recognize small 6–12 bp-long DNA sequences (Spitz,François 2012). TFs regulate transcription through binding to defined ~~–e~~is-regulatory elements" that are present in promoters, enhancers and silencers DNA sequences (Wingender et al 2012). In human, TFs represent 1558 genes encoding 2904 proteins grouped in 9 superclasses, 40 classes and 111 different families. Repository of every known transcription factors associated with a known transcription factor binding site (TFBS) are available on TRANSFAC (Kel-Margoulis,O.V. 2006), JASPAR (Mathelier, A. et al 2013) or Matinspector (K. Cartharius et al 2005) databases. Among the nine TFs superclasses, Zinc-finger domain represent 53% of all TFs, Helix-turn-helix domain represents 26% and Basic domain factors 11%. These three superclasses have in common an alpha-helix able to bind the major groove of the DNA (Wingender et al 2012).

Recent phylogenetic analysis showed that helix-turn-helix eukaryotic superclasse of transcription factors has a prokaryotic origin (D. Wilson, Charoensawan 2007). However, most of the mammalian TFs classes are metazoan specific and originate from a diversification through duplication and divergence from their common ancestor (Larroux et al. 2008; Degnan 2009; Sebé-Pedrós et al. 2011, Ereskovsky 2013). This diversification of TFs classes was a key step in the evolution from the early metazoan to a progressive complexification of organism development (Andrew H. Knoll 2011).

Transcription factor functions in gene regulation

Direct target genes are genes bound by a TF in promoter or cis-regulatory element whose transcription is regulated as a consequence of that binding. Typically, direct target genes are identified combining chromatin immuno-precipitation to identify TFBS (Gerstein et al., 2010) and observation of gene regulation after an over-expression or down-regulation (Pavlopoulos and Akam, 2011; Ririe et al., 2008). In bacteria, early studies showed a clear correlation between binding events and transcription regulation (Lin, S. and Riggs, A.D. 1975. Elf, J. et al. 2007). However, in eukaryotes, TFBS occupancy and gene expression are not strictly correlated (F. Gao, et al.2004, Z. Hu, et al. 2007). In prokariotes, transcription factors are expressed at low levels (typically 1 to 10^2 molecules/cell) and occupy TFBS only with the help of other transcription factors in allosteric cooperative DNA binding. The co-occurrence of appropriately spaced recognition sites in the genome (TFBS modules) is necessary to allow highly selective binding of transcription factors in vivo (Biggin 2011; Bolouri and Davidson, 2003; Johnson, 1995; Mann et al., 2009; Thanos and Maniatis, 1995). Even if clustering of TFBS and TFBS modules increase specificity in eukaryotic gene regulation (Wunderlich et al 2009), the prokaryotic ―deterministic allosteric model" does not explain the majority of transcription events in eukaryotes. Indeed, eukaryotic TFs are expressed at really high concentration (10^3 to 10^5 molecules/nucleus) and are able to bind DNA without the help of allosteric interactions (Biggin M, 2011). Moreover, TFBS are frequently degenerate sequences that evolve rapidly without strong evolutionary constraint (Gwenael Badis 2009; Villar D Flicek P 2014). TFs binding specificities are described with a position weight matrices (PWM) which are consensus binding sequences associated with probabilistic frequencies of nucleotide distribution for each single position. Indeed, in-vitro and in-vivo experimental methods (Geertz M 2010) showed that each eukaryotic TF is able to bind TFBS with different or equal affinities to primary, secondary (50% of TFs) and sometimes tertiary TFBS but also for some of them in the absence of any detectable sequence motif (Gwenael Badis 2009; Wingender et al 2012, J.A., Snyder 2012). In eukaryotes, most of the TFs are bound to thousands of genomic regions (Myers et al., 2011; Gerstein et al., 2010; Ne` gre et al., 2011; Rey et al., 2011), and around 10,000-60,000 regions (Chen et al., 2008;

Bieda et al., 2006; Cao et al., 2010). Importantly, the genomic regions identified in those studies typically use a 1% false discovery rate (FDR) cut-off. However, genomic regions identified at less stringent FDR cannot be explained by experimental noise. Rather, many DNA binding are not involved in the transcriptional regulation (Boj et al., 2009; Cao et al., 2010; Hoffman et al., 2010; John et al., 2011). Eukaryotic and more specifically mammalian transcription is most likely a continuous phenomenon where TFs bind essentially to a continuum of occupancy levels. In this "Continuous model" (Carr 1999; Biggin, 2001), genes the most highly bound by a transcription factor are the most likely to be regulated in overexpression or downregulation experiment while genes moderately bound show moderate regulation and genes bound at lower levels shows no significant regulation (Fullwood et al., 2009; MacArthur et al., 2009; Rey et al., 2011). In support of this model, data indicate that functionally and structurally different TFs bind identical genomic regions (Elf et al., 2007; Kao-Huang et al., 1977; Phair et al., 2004; Yang and Nash, 1995 / Roy et al., 2010; Chen et al., 2008; Jenner et al., 2009). Moreover, combining the fact that heterozygotic null mutation rarely leads to a phenotype (Ashburner, 1989) and the fact that if such mutation is associated with a mutation in a second gene of the same pathway, a strong phenotype occurs (Simon et al., 1991), this "ontinuous model" seems to be more appropriate to explain the pervasive redundant cross-regulations observed between transcription factors (Davidson, 2010; Young, 2011). However, for the ease of representation, the majority of the proposed gene regulation networks involves a short list of direct target where each transcription factor directly regulates only a defined number of genes (Georgescu et al., 2008; Oliveri et al., 2008; Ririe et al., 2008; Stathopoulos and Levine, 2005). A great effort is now made to propose networks that are far more highly connected and are more representative of the reality of eukaryotic transcription regulation (Chen et al., 2008; Gerstein et al., 2010; Negre et al., 2011; Sandmann et al., 2007).

Transcription factors combinatorial regulation of transcription

Different modes of TFs binding lead to different types of transcriptional outputs (Spitz F. Furlong 2012). The fact that enhancer activation is proportional to the

concentration of the individual TFs, as recently demonstrated (Giorgetti, L. et al 2010) allowed the identification of super-enhancers defined by high-density TFBS clustering and strong gene activation capacities (Hnisz D, Abraham BJ 2013; Whyte WA, Orlando DA 2013). Contrary to these graded enhancer outputs, cooperative homotypic or heterotypic bindings allow the same or different set of TFs, respectively, to demonstrate nonlinear relationship between TFs concentration, occupancy and gene regulation. In this context, cooperative binding between two TFs results in a net increase in the affinity of the two factors for their motifs, while their inherent sequence specificity remains the same (Spitz F. Furlong 2012). Cooperative binding can be driven by direct TFs interaction bound to adjacent sites as described above; however, an indirect cooperation mechanism termed ‚assisted loading' or ‚hit and run model' can occur when two TFs that compete for the same TFBS does not inhibit the activity of each other but rather increases the occupancy of each TFs via increased nucleosome depletion rate (Voss, T. C. 2011). TFs binding or chromatin associated protein can also trigger a change in the bending of DNA which assist the binding of neighbouring TFs keeping their DNA affinity unchanged (Falvo, J. V., 1995 ; Siggers, T., 2011). Finally, TFs interactions or cofactors can increase, decrease or change the DNA sequence specificity (Siggers, T, Duyzend, M. 2011). Together these results show how modular and context-dependent is the combinatorial action of TFs on cis-regulatory elements.

Epigenetic regulation of the chromatin: The histone code hyposthesis

In 2000, the ‚histone code hyposthesis" postulated that multiple histone post-translational modifications acting in a combinatorial and sequential way to control chromatin remodeling (B.D. Strahl, C.D. Allis 200). Indeed, the four core histones are subject to covalent modifications, including methylation, acetylation, phosphorylation, and ubiquitination (among many others), on the N-terminal histone tails that protrude from the nucleosomal surface or present in the histone globular domains (Vaquero et al. 2003; Campos and Reinberg 2009). These ‚epigenetic marks" modulate chromatin structure through effector proteins that can write, read or erase the histone code (Taverna et al. 2007; Voigt and Reinberg 2011; de CA Musselman 2012). Thus, ‚histone marks" have been shown to carry epigenetic information that can be

transmitted through cell division and instruct specific gene expression in daughter cells (Probst et al. 2009; Margueron and Reinberg 2010). Proteins such as chromatin remodelers, histone modification enzymes and histone chaperones are involved in chromatin regulation (Khorasanizadeh S. 2004). Chromatin remodelers act with other chromatin component to control the activity of cis-regulatory elements which can be defined by specific histone epigenetic marks (Scott B 2014). Chromatin remodelers are key proteins that use the energy of ATP hydrolysis to move, eject, or restructure the composition of nucleosomes (Becker PB, Horz W. 2002., Saha A, Wittmeyer J, Cairns BR. 2006). There are four different families of chromatin remodelers conserved from yeast to humans, the SWI/SNF, ISWI, CHD and INO80 families (for review C. Clapier2009; Narlikar G 2013). All share six basic properties: They have an affinity for the nucleosome; they recognize covalent histone marks; they have a DNA-dependent ATPase domain; they have domains that regulate the ATPase domain; they interact with other chromatin and transcription factors and they have the ability to translocate on DNA (Weake and Workman, 2010). Remodelers share the ability to translocate along DNA in an ATP dependant manner at an average speed of 25 bp/s and to bind DNA at an internal nucleosomal location to release DNA out of the nucleosome (singleton 2007 sirinakis 2011). Nucleosome repositioning is triggered without histone disassembly by the conformational change of a DNA-binding domain located on the linker DNA (between two nucleosomes) that propagates to a DNA translocation domain which generates a small DNA loop that is resolved by nucleosome sliding (C. Clapier2009). Movement of the histone is energy demanding as the hydrolysis of 2 to 4 ATP molecules is needed to move a nucleosome of one base pair (Fyodorov DV 2002). The action of the remodelers is facilitated by the histone chaperones, which collect the histones after the histone–DNA interactions have been broken. The dynamic turnover of histones from DNA is termed histone exchange. During nucleosome formation, histones H3/H4 are deposited first onto the DNA before H2A/H2B. Conversely nucleosome disassembly involves that peripherally located histone H2A/H2B dimers are first removed, followed by removal of H3/H4 (Das, C. 2012). RNA polymerase processing facilitates histone exchange thanks to the histone chaperone FACT (Belotserkovskaya R2009). Other histone chaperone such as Sp6, Asf1, HIR, and Rtt106 promote chromatin reassembly following Pol II passage (Das C, Tyler JK.

2013). Like promoters, enhancers show a high sensitivity to the DNase I (Gross and Garrard, 1988). However, rather than being nucleosome free, these regions are associated with nucleosomes constituted by histone variants H3.3 and H2A.Z (Goldberg et al., 2010; Jin et al., 2009). H3.3/H2A.Z-containing nucleosomes have a hyperdynamic turnover which explains the DNase I profiles (Jin et al., 2009). However, nucleosomes flanking enhancers are far less dynamic and expose specific histone marks such as H3K4me1/2/3 (Histone 3 lysine 4 mono/di/tri methylation) and H3K27Ac (Histone 3 lysine 27 acetylation) that are now frequently used to map enhancers (Creyghton et al., 2010; Heintzman et al., 2009; Rada-Iglesias et al., 2011; Zentner et al., 2011). Enhancers commonly span 200–500 bp in length and containing hundreds of clustered transcription factor binding sites (TFBS) (Spitz and Furlong, 2012). Enhancer activation involves „pioneer" TFs (aret and Carroll, 2011) which can directly associate with DNA in packed nucleosomes (J Xu, SD Pope 2007; AA Sérandour, S Avner, 2011).

Table 2 | Summary of ENCODE histone modifications and variants

Histone modification or variant	Signal characteristics	Putative functions
H2A.Z	Peak	Histone protein variant (H2A.Z) associated with regulatory elements with dynamic chromatin
H3K4me1	Peak/region	Mark of regulatory elements associated with enhancers and other distal elements, but also enriched downstream of transcription starts
H3K4me2	Peak	Mark of regulatory elements associated with promoters and enhancers
H3K4me3	Peak	Mark of regulatory elements primarily associated with promoters/transcription starts
H3K9ac	Peak	Mark of active regulatory elements with preference for promoters
H3K9me1	Region	Preference for the 5′ end of genes
H3K9me3	Peak/region	Repressive mark associated with constitutive heterochromatin and repetitive elements
H3K27ac	Peak	Mark of active regulatory elements; may distinguish active enhancers and promoters from their inactive counterparts
H3K27me3	Region	Repressive mark established by polycomb complex activity associated with repressive domains and silent developmental genes
H3K36me3	Region	Elongation mark associated with transcribed portions of genes, with preference for 3′ regions after intron 1
H3K79me2	Region	Transcription-associated mark, with preference for 5′ end of genes
H4K20me1	Region	Preference for 5′ end of genes

Figure 3. Histone code of functional elements in mammalian genomes. Table 2. Numerous other epigenetic marks define the epigenetic code (adapted from ENCODE project consortium).

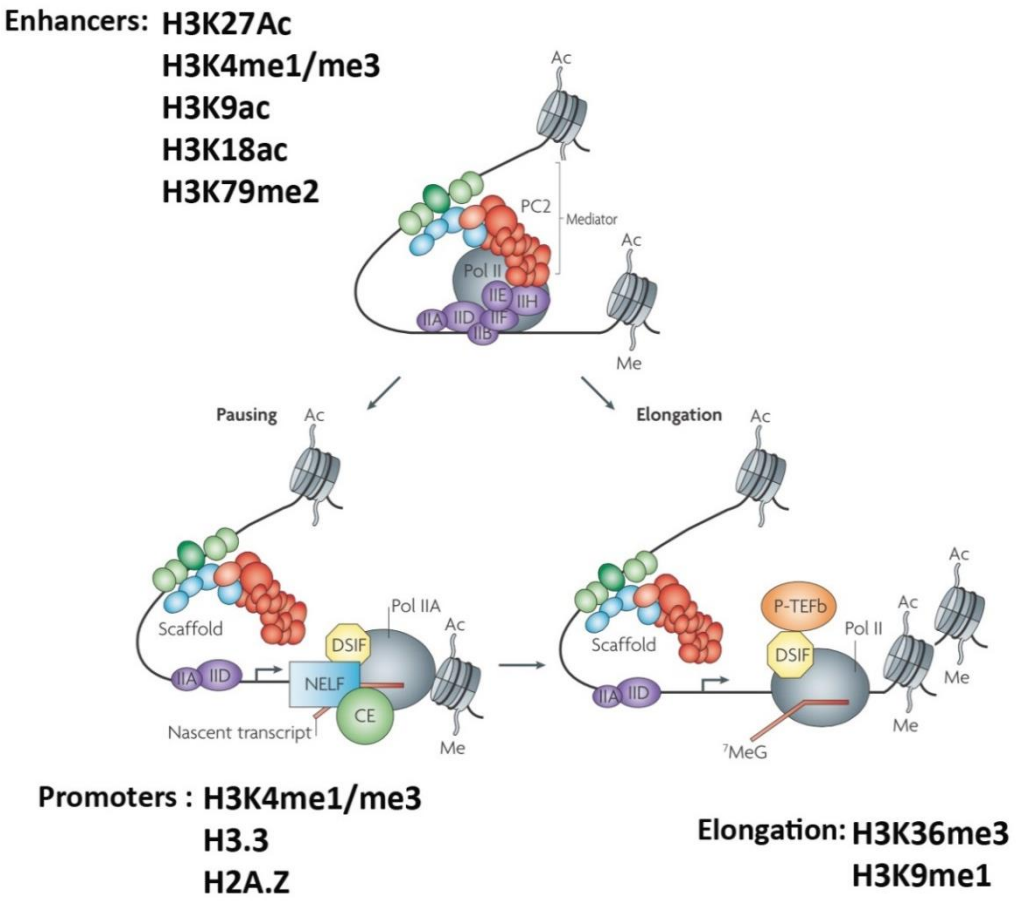

Figure 3. Histone code of functional elements in mammalian genomes. Schematic showing the epigenetic marks associated with promoters, enhancer and transcription elongation. Active promoters are marked by histone H3 lysine 4 dimethylation (H3K4me2), H3K4me3, acetylation (ac), and H2A.Z. Transcribed regions are enriched for H3K36me3 and H3K79me2. Repressed genes may be located in large domains of H3K9me2 and/or H3K9me3 or H3K27me3. Enhancers are relatively enriched for H3K4me1, H3K4me2, H3K27ac and the histone acetyltransferase p300.

Preceding occupancy of other TFs, pioneer factors help to the recruit chromatin ~~–r~~eaders", writers", and ~~–r~~emodeler" (Kouzarides, 2007 and Ruthenburg et al., 2007) and participate to the initial decompaction of the chromatin as well as the protection against inhibiting DNA methylation (ghisletti et al., 2010; serandour et al., 2011; zaret and carroll, 2011). Enhancers are associated with developmentally regulated genes

(Levine, 2010) and drive tissue specificity of gene expression (Bernstein et al., 2012; Ernst et al., 2011; Shen et al., 2012; Visel et al., 2009). Mutations occurring in enhancers underlie evolutionary differences between species (Jones et al., 2012) and contribute to many diseases (Dickel et al., 2013; Bernstein et al., 2012; Ernst et al., 2011). When enhancers are active, they bind general RNA polymerase II and mediator complex and trigger mRNA and enhancer RNAs (eRNAs) transcription (Natoli and Andrau, 2012) thanks to CTCF and cohesion long range interaction DNA stabilization (Phillips and Corces 2009; Nasmyth and Haering 2009). eRNAs are short bidirectional and nonpolyadenylated or long unidirectional and polyadenylated which function is still under investigation (Natoli and Andrau, 2012). Intensive work allowed significant progress to identify enhancers in mammalian genomes (Bernstein et al., 2012; Ernst et al., 2011; Shen et al., 2012). H3K4me1 and H3K27Ac were the first histone modifications associated to enhancer function (Heintzman et al., 2007; MP Creyghton 2010). H3K4me1 is enriched at distal enhancer sites, in contrast to H3K4me3, which is present at active promoters (Heintzman et al., 2007). However, H3K4me1 is also present at promoter regions. While a high ratio of H3K4me1 to H3K4me3 better distinguishes enhancers from promoters, an opposite ratio better define promoters (Djebali et al., 2012; Heintzman et al., 2007; Koch and Andrau, 2011). Interestingly, early priming of enhancers by H3K4me1 in the absence of H3K27Ac is observed before cell differentiation (Creyghton et al., 2010; Bogdanovic et al., 2012; Bonn et al., 2012; Mercer et al., 2011; Rada-Iglesias et al., 2012; Wamstad et al., 2012, Zaret and Carroll, 2011). Thus, H3K4me1 priming defines an enhancer state of potental activation and H3K27ac distinguishes active enhancers from inactive or poised enhancer containing H3K4me1 alone (MP Creyghton 2010). Moreover, an ‗‗enhancer decommissing‘‘ mechanism involving Pol II and TFs clearance, is mediated by demethylation of H3K4me1 by LSD1 (Whyte et al., 2012). H3K4me2 is present at both enhancers and promoters and seems to be an intermediate state of activation (Koch and Andrau, 2011; Pekowska et al., 2011). H3K27Ac is associated with active enhancers and is acquired exclusively in the context of the pre-existing H3K4me1 (Bonn et al., 2012). Many distinct Histone acetyl transferase (HATs) are involved in transcriptional activation (Brown et al., 2000; Lee and Workman, 2007). Recently, binding of p300/CBP HATs complex, was shown to map enhancers in different cell

types (Ghisletti et al., 2010; Heintzman et al., 2009; Kim et al., 2010; Rada-Iglesias et al., 2011; Visel et al., 2009). p300/CBP are ubiquitously expressed

Numerous H3K4 methylation readers have been discovered in mammalian cells (Ruthenburg et al., 2007). Unmodified H3K4 is read by BHC80 (CoREST complex), Dnmt3L (cofactor of DNA methyltransferases Dnmt3a/b), and Uhrf1 (cofactor of methyltransferase Dnmt1). Interestingly, all those proteins lead to transcription inhibition (Lan et al., 2007; Nady et al., 2011; Ooi et al., 2007). Most of the H3K4 readers prefer trimethylated over the monomethylated form. However, chromodomains of the ATP-dependent remodelers CHD1 and CHD7 recognize all forms of methylated H3K4. Interestingly, CHD7 appears to be preferentially associated with enhancer regions (Schnetz et al., 2009). So far, the only reader reported to prefer H3K4me1 binding is the chromodomain of the acetyltransferase TIP60 involved in the deposition and acetylation of H2A.Z (Jeong et al., 201). One of the functions of H3K4me1 could be to promote incorporation of the H2A.Z-in nucleosomes to initiate TFs accessibility (Altaf et al., 2010).

Numerous histone methylation writers have also been reported. For example, genes of the Trithorax family Set1a/1b, MLL1/2/3/4 methylate histone H3K4 (Ruthenburg et al., 2007). Studies shows that Set1a/1b/Wdr82 methylate H3K4me3 (Ardehali et al., 2011; Hallson et al., 2012; Wu et al., 2008, Lee and Skalnik, 2008; Wu et al., 2008). In human and mouse ESCs, a large subclass of enhancers enriched for H3K4me1, but lacking H3K27Ac, is also marked by H3K27me3 and bound by the Polycomb complex (Rada-Iglesias et al., 2011; Zentner et al., 2011). These elements, termed ‗‗poised enhancers,'' are located near key early developmental genes and share most of the properties of active enhancers, including similar levels of nucleosomal depletion, p300, and BRG1 binding. The loss of H3K27me3 and the gain of H3K27Ac then trigger a switch from poised enhancers to active enhancers (Rada-Iglesias et al., 2011). Poised enhancers are already looped to their target promoters via cohensin and CTCF looping, ready for gene activation upon proper receiving of developmental signals (Sanyal et al., 2012). Genes interacting with H3K27me3 enhancers commonly have bivalently marked promoters that are characterized by the simultaneous presence of the H3K4me3 and H3K27me3 and association with PRC2 (Bernstein et al. 2006; Buecker, C. 2012 ; Voigt T 2013).

Recently, other enhancer histone modifications have been identified such as H3K9ac and H3K18ac (Ernst et al., 2011; Zentner et al., 2011), or histone crotonylation (Tan et al., 2011), H3K79me2/3 (Bonn et al., 2012; Djebali et al., 2012).

As many new histone and DNA epigenetic modifications are yet to be charachterized (Rothbart SB 2014) and many others will be identified in more diverse functions and cellular states, the ~~–h~~istone code" seems to be extraordinary versatile and cell type specific. Thus, the epigenetic code seems to be far from being hacked. Despite the discovery of several important epigenetic constants in differentiating cells by different leading teams (Visel et al 2013) as well as the ENCODE project (which only investigated 1% (30 Mb) of the human genome in carcinogenous cell line and cost more than 300 million dollars), unraveling the in-vivo epigenetic network in most cell types at different developmental time points remains to be done (D Graur 2013).

Network regulation, information flow and central dogma of the molecular biology

The transcriptional program that controls gene expression is highly flexible and able to adapt to a great range of perturbations. TFs are the genes that demonstrate the most cross-regulation capacities and underwent the most genomic duplications during evolution and are thus often called the master genes of the genome (Levine and Tjian, 2003). In yeast, only ~20% of the 6000 yeast genes confer lethality when deleted (Dixon et al. 2009). In this context biological systems are defined as robust and redundant systems. In order to understand how genes regulate each other to orchestrate cell differentiation, the reconstruction of gene regulatory networks (GNR) is often done by perturbation of each component of the network via single or multiple gene knock-in and knock-out (Kholodenko et al., 2002). As these perturbations propagate rapidly and cause global changes in gene expression that are stabilized to a new attractor state (if not lethal), differentiating between direct interactions and indirect interaction is one of the main challenges in genomic studies. The spatial and temporal dynamic of GNR have been extensively described with Boolean logic (Mangan and Alon 2003). GRNs are composed of ~~–n~~odes," representing the network components, joined by ~~–e~~dges,"

which represent physical and/or regulatory interactions. While most of the nodes have a relatively low (in or out)-degrees, some (for example TFs) are highly connected and are called ―hubs" (Yu and Gerstein 2006).This work allowed the description of network motifs frequently occurring in GNR such as positive or negative auto-regulatory loops, activation or inhibition cascade, positive and negative feed-back loops and coherent and incoherent feedforward loops (Shoval Alon 2013). Working together as a complex logical clockwork, these motifs lead to different pattern of gene expression such as indefinite or finite oscillatons, single pulse responses or cellular state transition that are maintained and integrated by the cells (Yosef Regev 2011). In order to generate bistable or multistable cell systems able to differentiate, GNR must include positive or double-negative feedback loops (E.H. Snoussi 1998) or paradoxical motifs (such as the incoherent feedforward loop type 1) which are defined as motifs that simultaneously drive two opposite effects on the same target or biological process (Hart et al., 2011a, 2012). All these motifs are pervasive in GNR (Shoval and Alon, 2010) and cells have to process and integrate in time and space this information to allow the emergence of bistable or multistable cellular states as well as the maintenance of the final monostable state (James E. Ferrell 2012). However, biological interactions are not strictly specific and despite strict constraints, biological systems are stochastic by nature (non-linear) and degenerate (composed of elements that are structurally different but share the same function). In this context, GNR specificity is mainly driven by the subcellular and cellular spatiotemporal constraints that confer the specificity to the molecular interactions, such as cell compartmentalization and temporal separation of gene expression (Schwartz and Madhani, 2004; Komarova et al., 2005). In the nucleus, while TFs and co-factors are rapidly produced and degraded upon developmental signals and mechanisms of negative titration, nuclear export or post translational regulations, chromatin epigenetic structural constraints drive the specificity of their action on specific cis-regulatory region as a continuous dialogue. Regulation of gene expression was originally conceived as a one directional flow of information, going from one gene coded on DNA in the nucleus, to transcription of the corresponding mRNA then translated into one protein to perform its particular function. This view has been abandoned after accumulating evidence of pervasive transcription of non-coding RNA discovered between the 1950‘s and today (tRNA,

rRNA, miRNA, LncRNA, piRNA, eRNA, PALR, PROMPT, SUTs CUTs, lincRNA) together with the discovery of alternative promoter usage, alternative splicing (>90% genes), alternative polyadenylation, RNA editing and posttranscriptional, posttranslational or epigenetic regulations. It is now well recognized that information flow goes downward, from DNA to RNA and protein as well as backward from protein to RNA and from RNA to DNA. Thus, despite local hierarchies in GNRs, a global hierarchical causality is impossible to define as both top-down and bottom-up causation are at work in cells. The gene-centric view, illustrated by Richard Dawkins in his book "The selfish gene" postulating that any DNA sequence aims at replicating itself even sometimes at the disadvantage of the organism (Dawkin 1976), restrained for decades our conception about evolution, putting the focus on genetic selection. Besides DNA replication and genetic information transmission, the information flow generated by the interactions of actors operating in the cell as a whole (genome, epigenome, transcriptome, lipidome, metabolome) is subject to maintenance, transmission, variation and natural selection (H Nam, NE Lewis 2012). In this context, DNA sequence conservation seems to be among others a convenient hallmark (easy to conceptualize, to read, and interpret) for a more abstract multi-level –functional" selection (Hogeweg P. 2012).

Methodological considerations

Transcriptomic technologies

Isolation and differential measure of RNA sequences are generally performed with different purification techniques to isolate different fractions of RNA followed by high-throughput sequencing or microarray analysis. These technics have the capacity to simultaneously measure tens of thousands of transcripts and allowed important progress in a wide range of biological questions. Despite recent progress single cell RNA experiments, generally averaged RNA content of a cell population are measured. Microarrays remain the most used and the cheapest approach for transcriptomic analysis. However, several drawbacks, such as platform specificities (Affymetrix, Illumina, Agilent), noisy background hybridization, measurement problems with low

abundance transcripts or fixed chip design. We used in this study the Affymetrix microarray (Mouse Genome 430 2.0 Array) which involves hybridization of biotinylated cDNA (obtained from reverse transcription of mRNA) against synthetic oligonucleotides (probes of 25 bases long, directed in the 3‘ region of each gene) directly synthesized and spotted in defined order onto a glass array. Each array contains 900,000 different oligos and each oligo is present in millions of copies. After hybridization between oligos and cDNA, the chip is stained with a fluorescent molecule (streptavidin-phycoerythrin) that binds to biotin. A series of stains AND washes with reagents binds the biotin which provides light emission that is detected by microarray scanning with a confocal laser. The distribution pattern of signal in the array is recorded and signal intensities for each gene are interpreted in relation with their locations on the array. Subsequently, replicates experiments are normalized and summarized to perform differential measure between different biological conditions. RNA-Seq, which allows sequencing of all transcripts present in biological samples is more appropriate to study refined biological differences such as novel transcripts splicing events, allele-specific expression or any non-coding RNA processes. Both techniques need powerful technical and algorithmic challenges for experimental design, sample preparation, data analysis, storage and exchange. Despite the fact that RNA-Seq better estimates absolute transcript levels, both techniques show great overlap of genes differential expression results. Details on each microarray platform and RNA-Seq technology and the challenges and benefits associated with its technology and application are reviewed (S Zhao W P F-Leung, 2014). Raw (CEL files) and processed data (tab files) are submitted to GEO Gene Expression Omnibus database (Edgar R, Domrachev M, 2013)which store all the Chip-seq dataset published so far.

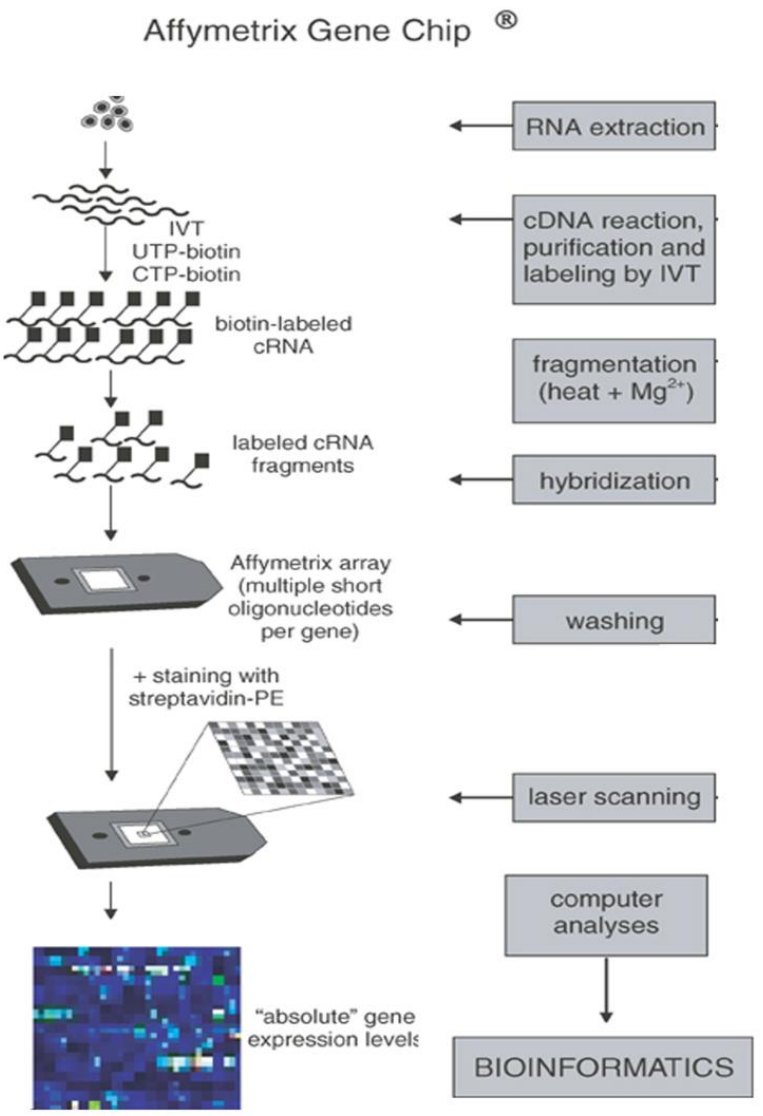

Figure 4. Affymetrix arrays, one population is used as starting material. Total RNA is extracted and cDNA is prepared. The cDNA is used in an IVT reaction to generate biotinylated cRNA. After fragmentation, this cRNA is hybridized to microarrays, washed and stained with PE-conjugated streptavidin, and subsequently scanned on a laser scanner (adapted from F J T Staal, 2003).

Chromatin immuno-precipitation techniques

ChIP-seq is a technique of chromatin immuno-precipitation followed by DNA sequencing (Iyer et al., 2001) which identifies specific DNA sequences bound by a specific chromatin associated protein (generally TFs or histone epigenetic marks). Briefly, Protein-DNA interactions are fixed by formaldehyde cross-linking, chromatin is sheared in 400bp fragments by sonication, and DNA sequences binding to a specific protein are selectively enriched by immuno-precipitation with a specific antibody targeting a protein of interest. After PCR amplification and sequencing, DNA reads of the enriched fraction are aligned against the reference genome using Bowtie (Langmead B 2009) and reads distributions are plotted to define peaks region and peaks summit that are then analysed to locate the protein bound regions. However, non-specific immuno-precipitation generate noisy signal that need to be handle by statistical methods in order to locate individual high-confidence binding sites against background sequence enrichment. MACS, a Model-based Analysis of ChIP-seq (Feng, Liu, Liu 2012) is the most commonly used algorithm that identifies binding peaks (Peak calling) in ChIP-seq data. MACS consists of four steps: removing duplicate reads generated by PCR, adjusting read position by alignments to form peaks, calculating peak enrichment against background, and estimating the false discovery rate. Because TFs DNA binding is a continuous phenomenon, many weak sites are identified. Thus, the final peak list depends on the algorithm parameter settings, the FDR cut-off as well as the quality of the biological signal. An appropriate control sample is critical to estimate the background level. Two methods are used to produce control DNA samples. Either ‟Input‟ DNA is isolated from cells that have been cross-linked and fragmented under the same conditions but not immunoprecipitated or a ‟mock‟ ChIP reaction is performed using a control antibody that reacts with an irrelevant, non-nuclear antigen such as IgG. Many drawbacks are associated with this step as mock antibody rarely yield enough non-specific DNA during precipitation and the optimal input DNA level to use is hard to define a-priori. Other statistical methods have been developed to measure the intrinsic background level directly from the experimental sample and seem more appropriate to measure the background level (BA de Boer, 2014).

Similarly to microarray experiments, biological samples used in Chip-seq are cell populations rather than single cells. Thus, peaks enrichment reflects the average probability for a protein to be bound on DNA at specific regions where the most frequent binding event are the highest peaks identified. The ENCODE project defined a set of standards and guidelines to follow to increase the quality of ChIP experiments (Landt S 2014) and raw sequencing results (SRA, BAM files) and processed data (Bed files) are submitted to GEO database which store all the Chip-seq dataset published so

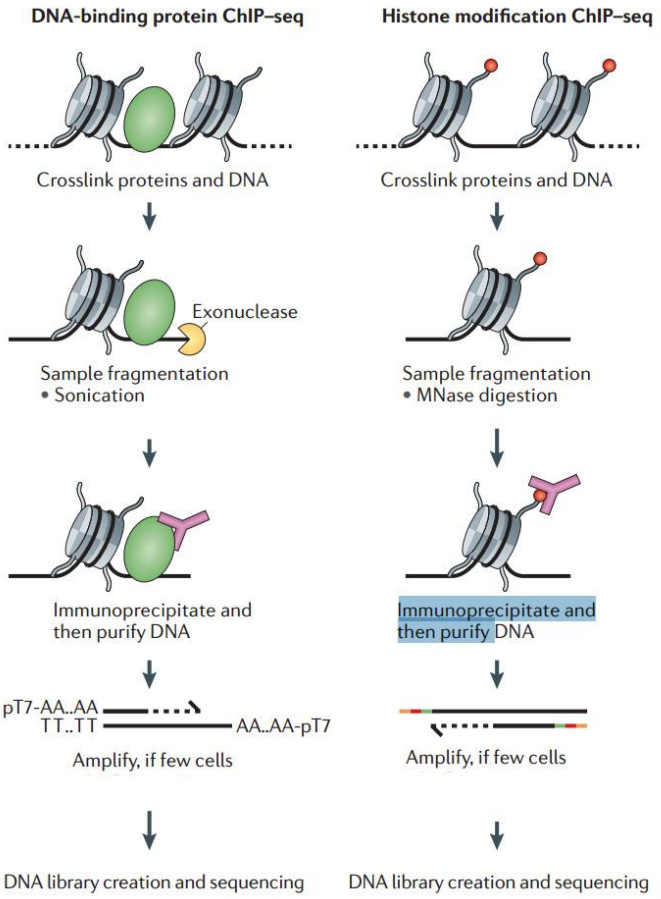

far.

Figure 5 Chromatin immunoprecipitation techniques. Simplified schematics of the main steps are shown. Left: Chromatin immunoprecipitation followed by sequencing (ChIP–seq) for DNA-binding proteins such as transcription factors. Right: ChIP–seq for histone modifications (adapated from S. Furey 2012).

Chromosome conformation capture assays

Following the pioneering work of Job Dekker in 2002, nuclear architecture and 3D chromosome folding have been extensively studied using chromosome conformation capture techniques and derivatives (J Dekker 2002; J Dekker 2013). These methods rely on cross-linking of spatially interacting chromatin, fragmentation and re-ligation of cross-linked chromatin and identification by sequencing of cis-regulatory sequences (promoter, enhancers, silencers) that interact with each other via long range interactions. Hundred of thousands of significant long-range interactions between gene promoters and distal cis-regulatory are identified genome-wide thanks to complex algorithmic reconstruction of interaction probability map. As almost all of the genes engage in long range interactions, chromosome capture analysis allowed the identification of important new general concepts of gene regulation as well as a new understanding of the nuclear organization. Generalization of these techniques to the study of cell-type specific differentiation processes leads to a global overview of the chromatin remodeling mechanism at work during development. Computational inference based on correlations between gene activity and activity of distal elements across panels of cell lines are now the next frontier in our understanding of genetic and epigenetic gene regulation (Visel et al., 2009, 2013).

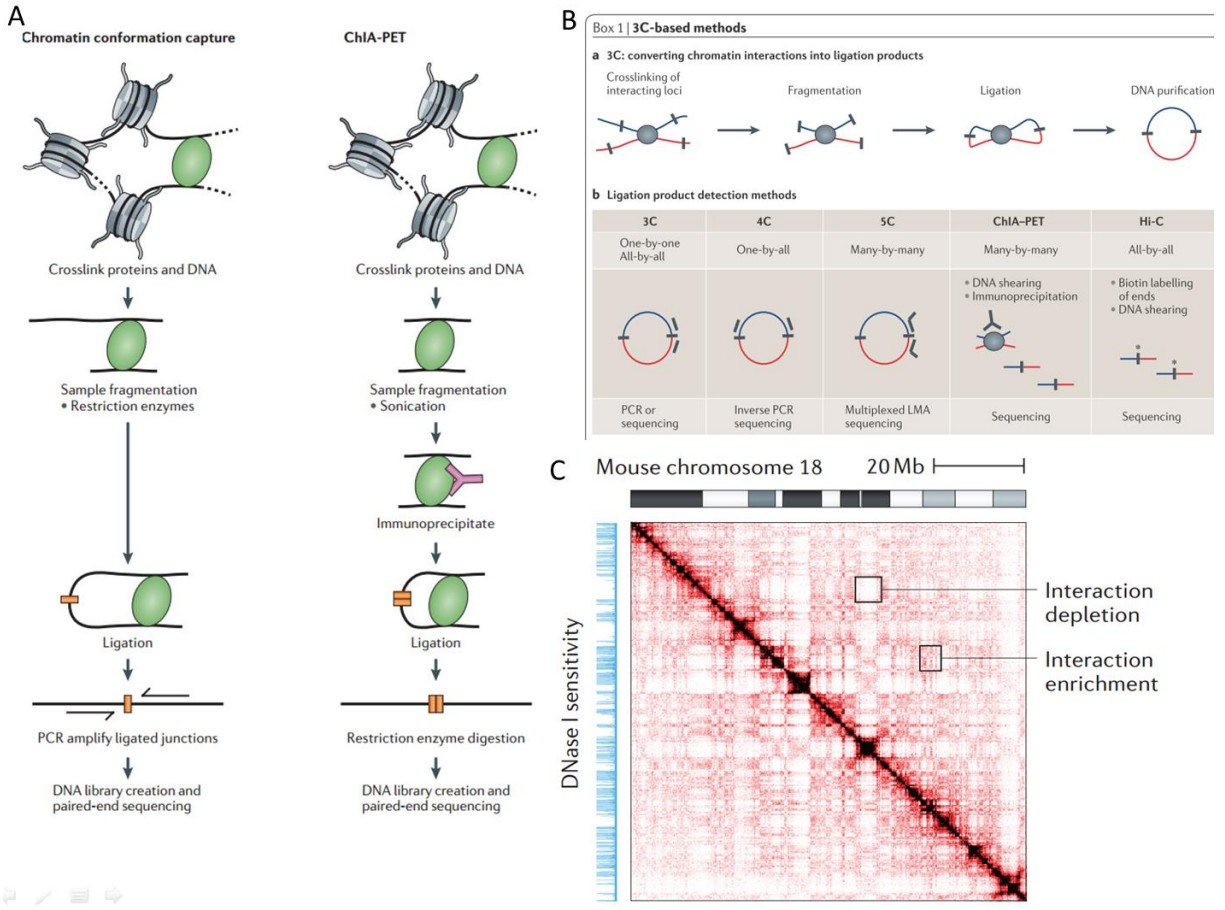

Figure 6. Detecting chromatin interactions with chromosome capture. A. Distant genomic regions interaction are mediated by DNA-binding proteins. Chromatin conformation capture technics (3C and derivatives) use a cromatin cross-linking folled by a fragmentation and a ligation step to join distant fragments that are interacting in 3D space, thus providing information on possible promoter-enhancer interactions. Chromatin interaction analysis with paired-end tag sequencing (ChIA-PET) detects chromatin interactions. However, ChIA-PET uses a chromatin immunoprecipitation (ChIP) step to more specifically identify interactions with a particular bounchrod protein, such as RNA polymerase II. (adapated from S. Furey 2012 and J Dekker 2013). B. Schematic of the chromatin capture technic. C. Schematic of Hi-C data from mouse chromosome 18. Hi-C method is a genome-wide 3C. Hi-C provides a true all-by-all genome-wide interaction map, but the resolution of this map depends on the depth of sequencing. Hi-C data are represented as two-dimensional heat maps. While the probability of long range interaction is invertionaly proportional to the distance, shift from this linear model define interaction enrichement or interaction depletetion. Interacting regions detection depends on sequencing depth. Bioinformatic reconstruction allow the inference of long range regulation of gene expression (adapted from Dekker J 2013).

CHAPTER II: Nervous system development and cell type specification

The early organization of the CNS is made by the action of morphogenetic signals starting during the gastrula stage and evolving throughout the embryonic and postnatal development (echevarria D 2003). Neural development starts when ectodermal cells are specified into neurectodermal cells at the origin of the entire nervous system. Primary neural induction and antero-posterior or dorso-ventral regionalization of the early neural tube is due to the activity of the ~~"p~~rimary organizer". Indeed, after the discovery by Hans Spemann and Hilde Mangold in 1924 that grafting a salamander embryo with the dorsal blastopore lip ~~"o~~rganizer" of another embryo was sufficient to induce a secondary full body axis comprising a full neural axis (Spemann & Mangold 1924; De Robertis & Kuroda 2004), similar ~~"o~~rganizers" were identified in all vertebrates and in some nonvertebrates (Cobos et al., 2001; Darras et al. 2011, Meinhardt 2006, Nakamoto et al. 2011). A large number of factors expressed by ~~"th~~e node", the mammalian organizer, have now been identified. Later on, local signaling known as ~~"se~~condary organizers", drive the antero-posterior specification of the three main domains of the brain: the forebrain, the midbrain and the hindbrain. Patterning of the central nervous system into different areas by the action of different gradients of morphogens such as Fgfs, Wnts, Shh, and BMPs lead to regional expression of homeodomain and bHLH transcription factors that specify neural precursors cells (NPC) into all specific cell types neural cell type of the central nervous system.

Neurulation: the prosomeric model

Neurulation starts at the end of gastrulation from an inductive interaction between the ~~"n~~ode" and the neighboring ectoderm and endoderm. The presomptive neural plate formation is first triggered by Fgf8 signaling coming from the primary endoderm (Viera C 2010). The ectoderm surrounding the neural plate expresses BMPs while the node and the extending axial mesendoderm express Wnts and the BMP inhibitors Noggin and Chordin(De Robertis & Kuroda 2004, Munoz-Sanjuan & Brivanlou 2002; Stern 2006). Two orthogonal gradients are established: a Wnt gradient along the Antero-posterior axis and a BMP gradient along the mediolateral axis and the

axial mesendoderm (Meinhardt 2006, Niehrs 2010). Interestingly, ectodermal cells undergo neural differentiation as their default state. Indeed, neural differentiation must be suppressed in the lateral ectoderm by TGFβ signaling in order to develop as epidermis (Wittler and Kessel, 2004). Subsequent suppression of BMP signaling maintains neural differentiation (Linker et al. 2009; Stern, 2005). Neural plate formation involves pseudostratification of the neurectoderm, lengthening of the neural plate along the anteroposterior axis and bending of the neural plate triggering the formation the neural folds (Colas and Schoenwolf, 2001). Elevation of the neural folds creates the neural groove becoming, after closure at the dorsal midline, the lumen of the neural tube. At this stage, the initial medio-lateral patterning is transposed into dorso-ventral polarity.

The early neural tube is formed by three primary vesicles: the forebrain (prosencephalon), the midbrain (mesencephalon) and hindbrain (rhombencephalon). Cephalic and cervical flexures of the neural tube then start and the subdividion of the prosencephalon into telencephalon and diencephalon occurs (Pombero and Martinez, 2009). Early patterning events driven by the ―primary organizer" are then refined through the establishment of ―secondary organizers". Secondary organizers are domains of the neural plate where localized expression of transcription factors and morphogenes gradient control morphogenesis (Martinez, 2001; Echevarria et al., 2003; Aroca and Puelles 2005). The ―prosomeric segmental model" is used to describe the dorso-ventral and antero-posterior neural regionalization thanks to a grid-like representation of the histogenic domains by longitudinal (columnar) and transverse (segmental) boundaries based on regionalized gene expression pattern (Puelles et al., 1987; Viera C 2010). Three regions in the neural tube have been identified as secondary organizers: the anterior neural ridge (ANR) at the rostral part of the neural tube, the zona limitans intrathalamica (ZLI) in the diencephalon and the isthmic organizer (IsO) at the midbrain-hindbrain boundary.

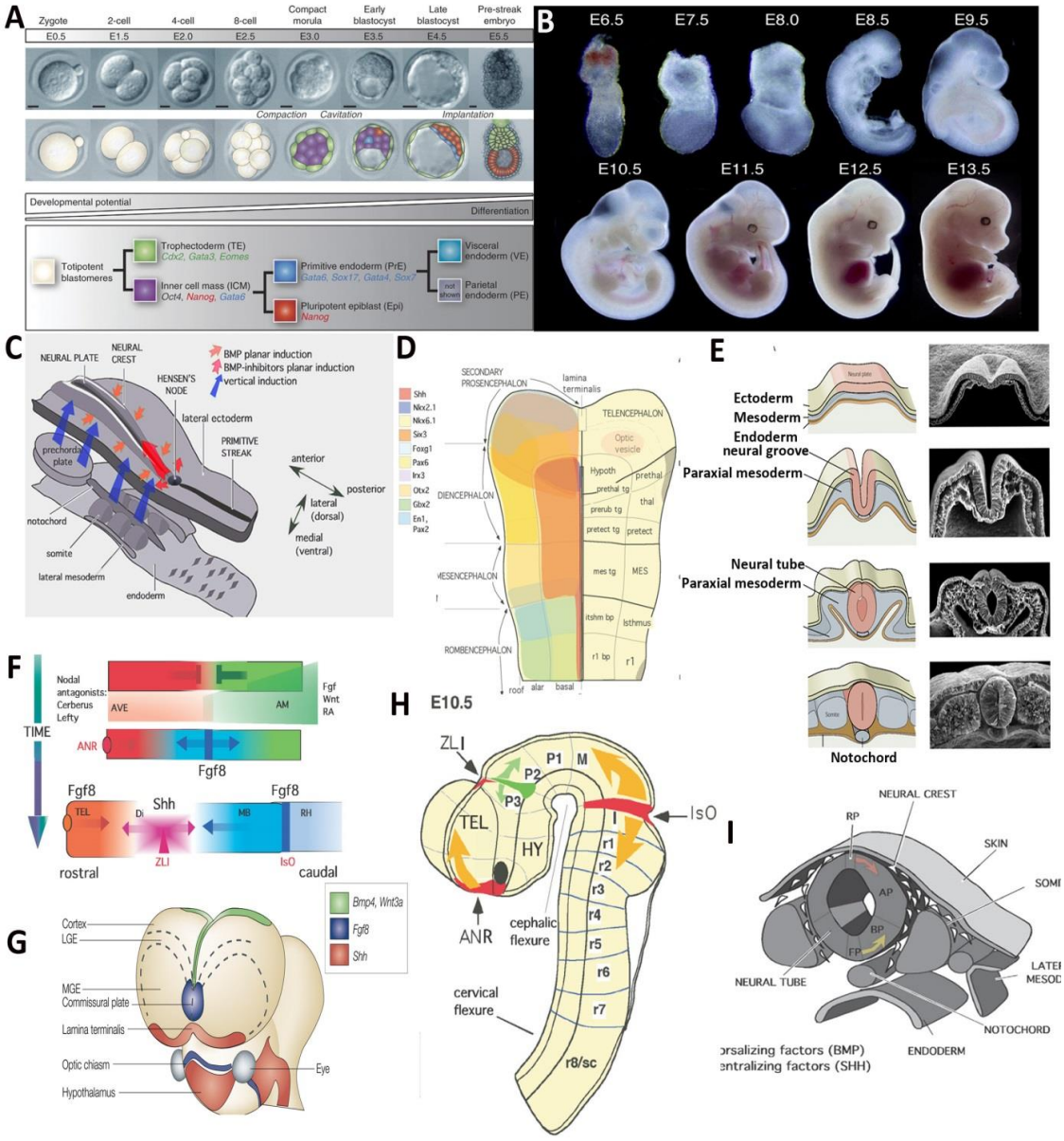

Figure 7. Neural and brain development. (A).Schematic representing the mouse embryonic development from E0.5 to E5.5. Embryonic Pluripotency factors, Nanog, Gata6, Oct4 are indicated. Epiblast cells are the embryonic stem cells. (**B**) From E6.5, neurulation begins and lead to the formation of the neural system. (**C**) Neurulation. At the neural plate stage, vertical induction from the mesendoderm (notochord and prechordal plate), and planar induction from Hensen‘s node and ectoderm drive dorsoventral and antero-posterior patterning of the nervous system. (**D**) Schematic representations of TFs expression domains at the neural plate stage. Gene symbol and color codes are identified. Medio-lateral (dorso-ventral) and antero- posterior (rostro-

caudal) regionalization are identifiable by the limits between expression domains. (**E**) During neurulation, neural folds close at the dorsal midline. the initial medio-lateral orientation of the neural plate becomes the dorso-ventral organization of the neural tube. (**F**) Schematic representation of secondary organizer. Morphogenetic signals from the anterior ventral endoderm (AVE) and axial mesendoderm (AM) drive the anterero posterior posterior organization of the neuroepithelium and induce patterning of cellular domain. TFs genetic interactions at the boundary between domains specify the development of secondary organizers that produce a second wave of inductive signals (arrows) (**H**) Representation of an E10.5 mouse neural tube showing the anterior neural ridge. (ANR); the anterior ventral endoderm. (AVE); the axial mesoderm.(AM); the diencephalon. (DI) the midbrain.(MB); the hypothalamus (HY); the isthmus (I); the isthmic organizer (IsO); the rhombencephalon (RH); the telencephalon (TEL); ZLIthe zona limitans intrathalamica (ZLI); the prosomeres (p1-p3); the r1-r8 rhombomeres (r1-r8); the spinal cord (sc) **(G)** Morphogenetic signals. schematic view of the mouse brain at E13.5. Patterning molecules include bone morphogenetic proteins, members of the wingless-type MMTV integration site family (green), fibroblast growth factors (blue) and sonic hedgehog (red) (**H**) brain organisers (**I**) spinal cord organisers (adapted from Martinez 2001, 2010; G. Schoenwolf 2009; Marín O 2001).

Dorso-ventral patterning

Dorso-Ventral (DV) patterning generate four longitudinal territories which are from ventral to dorsal, the floor plate, the basal plate, the alar plate and the roof plate (Kiecker, Clemens 2012). Sonic Hedgehog (Shh) signaling is necessary and sufficient to specify the ventral identity of the nervous system (Placzek et al. 1990, van Straaten et al. 1985). Shh starts to be produced by the notochord, a structure underlying the midline of the neural plate. Later on, Shh is produced by the floor plate overlying the notochord (Echelard et al., 1993; Roelink et al., 1994, 1995; Placzek & Briscoe 2005). Shh is secreted and exchanged from cell to cell to form a molecular gradient that specifies different cell fates in a dose-dependent manner (Echelard et al. 1993, Krauss et al. 1993, Roelink et al. 1994 ; Chiang et al. 1996; Dessaud et al. 2008, Lupo et al. 2006). This ventral-to-dorsal gradient of shh is visible in the ventral neural tube as well

as the ventral telencephalon (Chamberlain et al. 2008). Shh downstream effectors are the activating transcription factors Gli1 and Gli2 and the inhibitor Gli3. In this context, the Shh gradient is converted into two gradients of opposite transcriptional response involving Gli1/2 and Gli3 activity along the DV axis (Fuccillo et al. 2006, Lei et al. 2004, Stamataki et al. 2005). While genes such as Foxa2, Nkx2.2, Olig2, Nkx6.1, Dbx1, and Dbx2, are induced upon Gli activation, genes such as Pax6, Pax7, and Irx3 are repressed. Interestingly, repressed and activated genes cross-repress each other to define the boundaries between their expression domains (Briscoe et al. 2000). Differential exposure duration of Shh signal and subsequent combinatorial expression of Gli participate to the cell fate diversity of diverse neural cell types in the telencephalon, the hindbrain or the spinal cord (Dessaud et al. 2008, Pattyn et al. 2003). In the early forebrain, the prechordal plate expresses Shh. However, Shh is not sufficient for ventralization (Pera & Kessel 1997). BMP7, which is expressed in the prechordal mesoderm synergizes with Shh to induce ventral forebrain identity (Dale et al. 1997). Moreover, Wnt inhibitors expressed in the prechordal plate contribute to ventralization (Kiecker & Niehrs 2001). In the forebrain, pallial and subpallial regions are specified by Shh secreted by the prechordal plate (Gunhaga et al. 2000). In the subpallial region, Shh from the neural plate induce the formation of the Anterior neural ridge which will become later on, the medial ganglionic eminence (Sousa & Fishell 2010).

Antero-posterior regionalization

Antero posterior (AP) regionalization generates distinct transverse domains at different axial positions which display distinct competence to respond to the same signal (Rubenstein 1998). Transverse domains of the nervous system are called prosomeres and appear in the prosencephalon (p1-6), rhombomeres in the rhombencephalon (r1-r7) and pseudorhombomeres (r8-r11), while the mesencephalon is considered as a single unit (Cambronero and Puelles, 2000). The first signal inducing AP patterning originates from the dorsal mesoderm ad specify the neuroectoderm of the forebrain and midbrain by the expression of Lim1 Otx2, Engrailed (En1) and Cerberus (Doniach, 1993). Then a other signals posteriorizes the neural plate, inducing

hindbrain and spinal cord via retinoic acid that (Durston et al., 1989) FGF2(Cox and Hemmati-Brivanlou, 1995;) and Hox genes signaling (Pearson et al.2005). Shh is expressed along the entire AP axis and triggers Shh, HNF3 β, Nkx2.2 expressions in all regions of the ventral neural tube, but specifically induces Nkx2.1 Nkx6.1 in posterior regions (Qiu et al., 1998). Similarly, Fgf8 applied to prosencephalon and mesencephalon induces distinct competence of receiving cells, inducing FoxG1 anteriorly and En2 posteriorly (Shimamura and Rubenstein, 1997).

Secondary organizers and brain patterning

Secondary patterning mechanisms arise during central nervous system development. The anterior neural ridge (ANR), defined by the early expression of Fgf8, drive the specification of the anterior areas of the forebrain. Fgf8 cooperate with Fgf15, Bmp4, Wnt and Shh to regulates prosencephalic regionalization through inhibition of Otx2 and Emx2 (Crossley et al., 2001; Storm et al., 2006) and activation of FoxG1 (Xuan et al., 1995; Shimamura and Rubenstein, 1997).

The zona limitans intrathalamica (ZLI) is the Shh expressing boundary region between prosomere 2 and prosomere 3. While prosomere 2 alar plate will develop into the thalamus, p3 alar plate will develop into the prethalamus (Martinez and Puelles, 2000). ZLI cells express the transcription factor Sim1, Nkx2.2, Wnt8b and Fgf15 (Fan et al., 1999 Price et al., 1992; Shimamura et al., 1995; Gimeno et al., 2002). Interstingly, Shh induction in the ZLI requires Wnt8b expression (A Martinez-Ferre 2014).

The Isthmic organizer (IsO) is localized at the midbrain-hindbrain boundary which controls the development of cerebellum, the isthmic and mesencephalic regions (for review see Martinez, 2001). The isthmic organizer develops exactly at the limit between Otx2 and Gbx2 expression domains. Mutant mice lacking Gbx2, Otx2, Wnt1, Pax2, En1, or Fgf8 do not develop isthmocerebellar structures (McMahon and Bradley, 1990).

Shh signaling pathway

Sonic Hedgehog is a cleaved protein that produce two secreted fragments: a 19 kDa N-terminal protein (N-Shh) that mediates signaling activities and a 25 kDa C-terminal protein (C-Shh) which possesses protease activity (Porter et al., 1995). N-Shh is modified by a cholesterol moiety to the C-terminus and a palmitoyl group to the N-terminus (Chamoun et al., 2001). Once secreted, Shh binds to patched (Ptc), a 12-transmembrane protein. That prevents the constitutive inhibition of smoothened (Smo), a 7transmembrane protein (Alcedo et al., 1996; Hynes et al., 2000). Hedgehog-interacting protein (Hip) is a transmembrane protein attenuating Shh signaling by binding N-Shh with high affinity (Chuang and McMahon, 1999), whereas vitronectin, an extracellular matrix glycoprotein, enhances Shh activity (Pons and Marti, 2000). Within the nucleus of Shh responding cells, zinc-finger transcription factors of the Gli family GL1/GL2/GLI3 are expressed (Hynes et al., 1997; Ruiz i Altaba, 1998; Cohen M2013). Combinatory effect of Gli1/Gli2 activation or Gli3 repression in different areas of the neural tube determines neural patterning, proliferation and cell survival (Blaess et al., 2006; Zervas et al. 2004). Later on, Shh signaling has to decrease because repressing activity of Gli3 is necessary for neuronal differentiation (Wang H, Ge 2011). Interestingly, decreasing Shh signaling mediates the switch from symmetric proliferative and asymmetric self-renewing divisions to symmetric neurogenic divisions through transcription of the transcription factor Hes1 (Saade M, 2013 ; Dave RK, 2011).

Shh mutant mice lack ventral structures in the CNS and die soon after birth (Machold R, Hayashi S 2003). However, Nestin-Cre transgenic mouse driving Shh or Smo conditional deletion in NSCs shows largely normal ganglionic eminences (Machold R, Hayashi S 2003), but disruption of postnatal neurogenic niches caused by proliferation decrease and increased apoptosis. (Balordi F, Fishell G. 2007). Interestingly, the function of Shh is dependent on the primary cilium. Ablation of the ciliary motor protein KIF3A block the formation of the primary cilia in NSC and results in decreased Shh signaling similar of Smo mutant mice animals (Han YG, Spassky 2008). Indeed,

smo is needs to be translocated to the primary cilia to siplay its proper function (Breunig JJ, 2008).

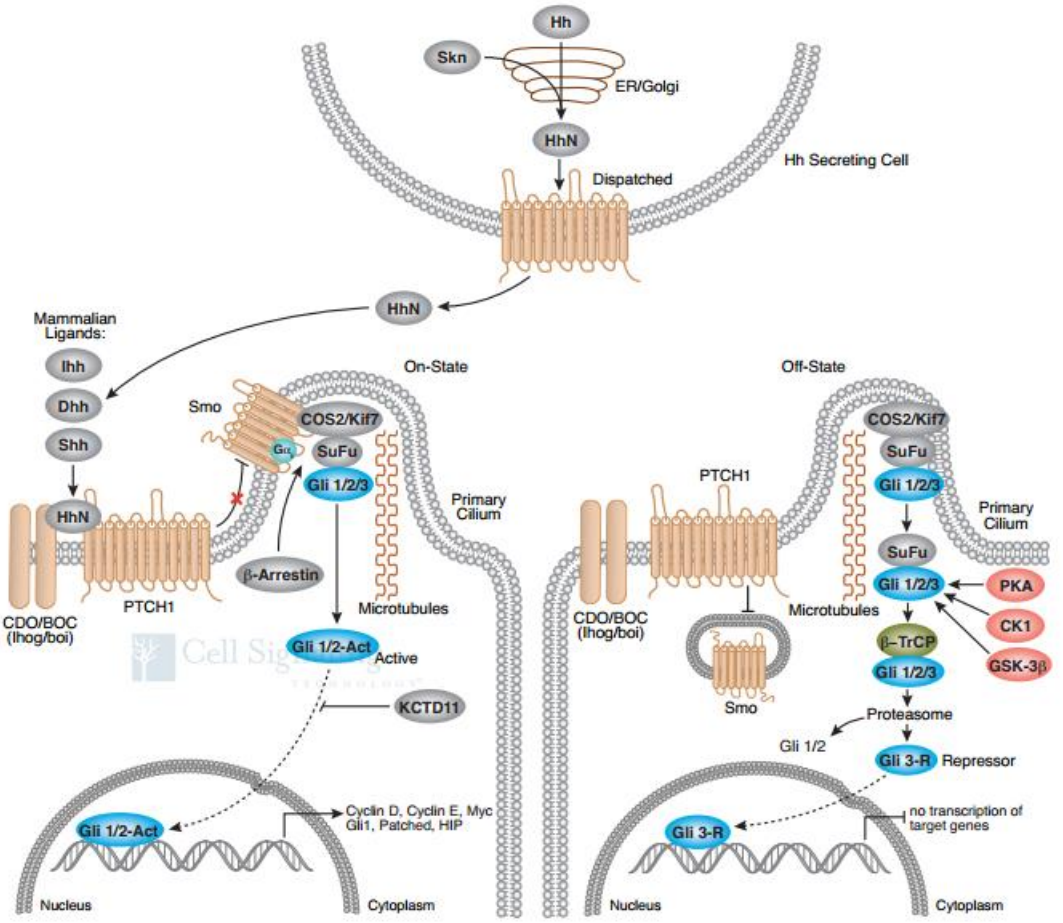

Figure 8. Sonic Hedgehog signaling pathway (adapted from Cell Signaling technology).

In the adult ventricular and subventricular zone and dentate gyrus, NSC are Shh-responsive expressing Ptc and Smo (Traiffort E, Charytoniuk D1999 1998). However in the adult, Shh expressing regions are rare and disparate with high Shh transcript found mainly in the basal forebrain and the brainstem (Traiffort 1999). However, Shh protein is also detected in neurogenic niches. In the adult SVZ, the Shh-is expressed in neurons and is detected in the cerebrospinal fluid (Ihrie RA, Shah JK,2011). In the dentate gyrus, Shh protein is also detected in the subgranular zone (Ihrie RA, Shah JK,2011). Interestingly, Shh can be anterogradely transported in neurons and tranfered

to neighboring cells, thus suggesting a transport mechanism to cells distant from the ventricule (Traiffort E, Moya KL, 2001). Finaly, a recent study in the limb bud showed that Shh can be transferred from one cell to another through a long extracellular filipodia, a mechanism that could also exist in the brain (Sanders TA 2013).

Shh is a well known morphogens that confer positional information to the NSC depending on the local concentration (Rogers and Schier, 2011). The classic ‗French flag model'' (Wolpert, 1969) was recently updated. Indeed, a recent study using time-lapse microscopy in developing zebrafish embryos tracked the relationships between Shh-GFP reporter activity and cell type patterning during the neural tube development (Xiong et al. 2013). Stricklingly, they found that specification of precursors does not occur in a highly ordered manner as expected. Instead, the progenitors of different lineages are mixed and specified in a salt-and-pepper pattern. Pattern precision is then recovered upon cell reorganization and migration along the dorsal-ventral axis. This reorganization is mediated by cadherin, suggesting that cellular adhesion is involved in cell sorting. In this revised ―French flag model", precise patterning arises from early heterogeneous specification that is corrected by subsequent positional sorting. (Xiong et al. 2013; Little SC.2013).

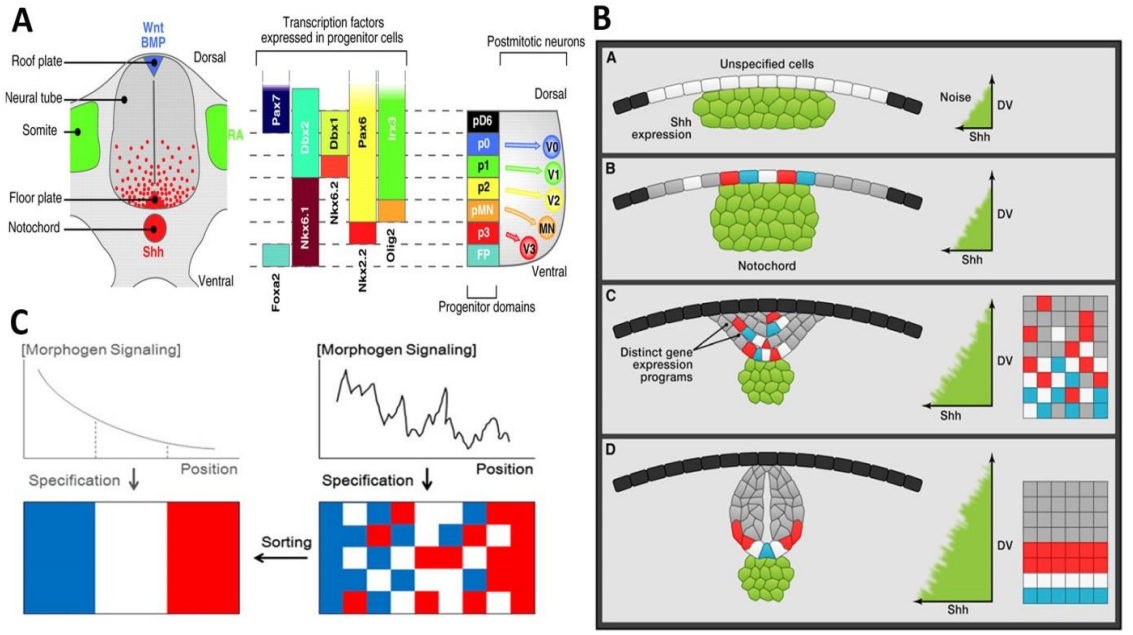

Figure 8. Cell sorting occurring after stochastic salt-and-pepper specification of neural progenitors. A. Patterning of the neural tube by signals (Shh, Wnt, BMP) triggers the expression of Olig2, Nkx2.2, Nkx6.1 and in restricted progenitor domains

(pMN, p0-p3, dP1-dP6) that each generate specific neuronal and glial subtypes. Embryonic OPCs arise from the pMN domain and is Shh dependent. A dorsal OPC-generating domain is active that is Shh- independent (Litlle SC 2013).

Notch signaling

Notch signaling pathway plays a central role in the regulation of embryonic and adult neurogenesis (Itaru Imayoshi 2008; Kageyama 2008). In the embryonic nervous system, NSC initially undergo proliferation only, then a subset of cells undergo neuronal differentiation, while others remain as progenitors for later neurogenic and gliogenic phases. During development, these processes proneural genes and Notch ligand genes are expressed at heterogenous levels in the ventricular zone also forming a _salt-and-pepper‘ gene expression pattern. This process, called lateral inhibition (Ishibashi et al. 1995). In this process, the membrane Notch ligands Delta and Jagged activate Notch receptors on adjacent cells. The Notch intracellular domain (NICD) is then cleaved from the membrane region of on cell and is transferred to the nucleus, where NICD forms a complex with RBPj and Maml (Jarriault et al. 1995; Honjo, 1996; Kopan and Ilagan, 2009). The NICD/RBPj/ Maml complex induces Hes1 and Hes5 genes. Hes genes are encode bHLH transcriptional repressors (Sasai et al., 1992; Kageyama et al., 2007). Through their bHLH domain, Hes factors form homodimers or heterodimers with Hes-related bHLH factors and bind to the DNA sequences called the N box (CACNAG) or the class C site (CACG(C/A)G) (Sasai et al. 1992; Iso et al., 2003; Kageyama et al., 2007). Hes1 and Hes5 directly repress proneural Ascl1 or Neurog2 expression, thereby inhibiting neural differentiation and leading to the maintenance of NSCs pool.

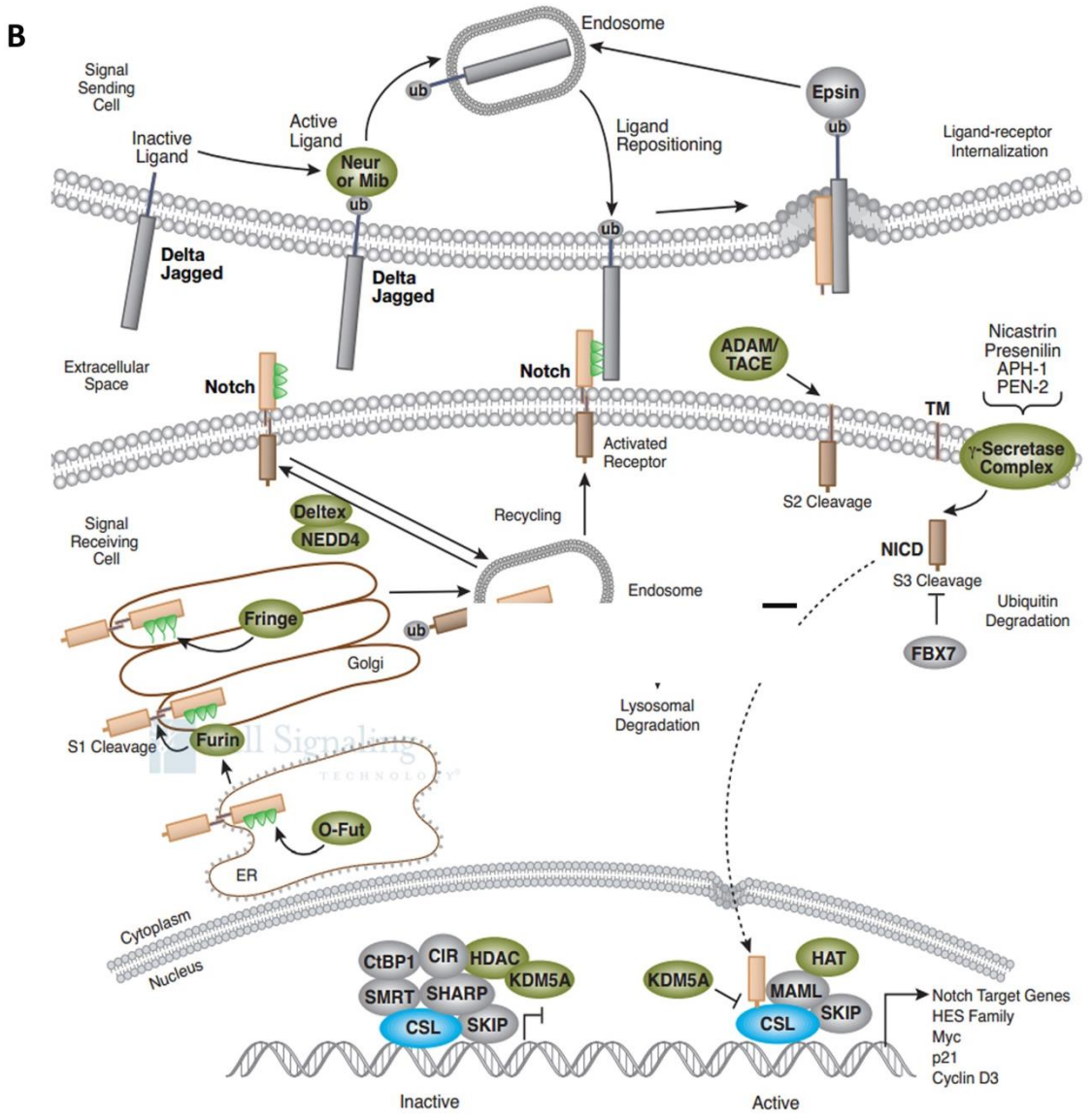

Figure 9. Notch signaling pathway. (adapted from Cell Signaling technology)

Wnt Wnt/ b -catenin signaling

Wnt ligands are a family of autocrine and paracrine secreted glycoproteins (L. Ciani, P.C. Salinas,2005; Faigle, Roland, 2013). In the absence of Wnt ligand, activated glycogen-synthetase-kinase-3 beta (GSK-3beta), forms a degradation complex, comprising axin, adenomatous polyposis coli (APC), and beta-transducing repeat-containing protein (beta-TrCP), which results in a phosphorylation and an ubiquitination of beta-catenin that lead to its degradation by the proteosome (R.H.

Chen, W.V. Ding, 2000). Continuous degradation of beta-catenin in the absence of Wnt maintains a low intracellular beta-catenin level (Faigle, Roland, 2013). However, in presence Wnt ligand, its receptor Frizzled and its co-receptor LRP5/6, activating phosphorylation of Dishevelled (Dvl) inactivates GSK-3beta by sequestering GSK-3beta from the degradation complex. (K. Tamai, M. Semenov, 2000). Beta-catenin is then stabilized and enters the nucleus to associates with TCF/LEF transcription factors which activate target genes (C.Y. Logan, R. Nusse, 2004).

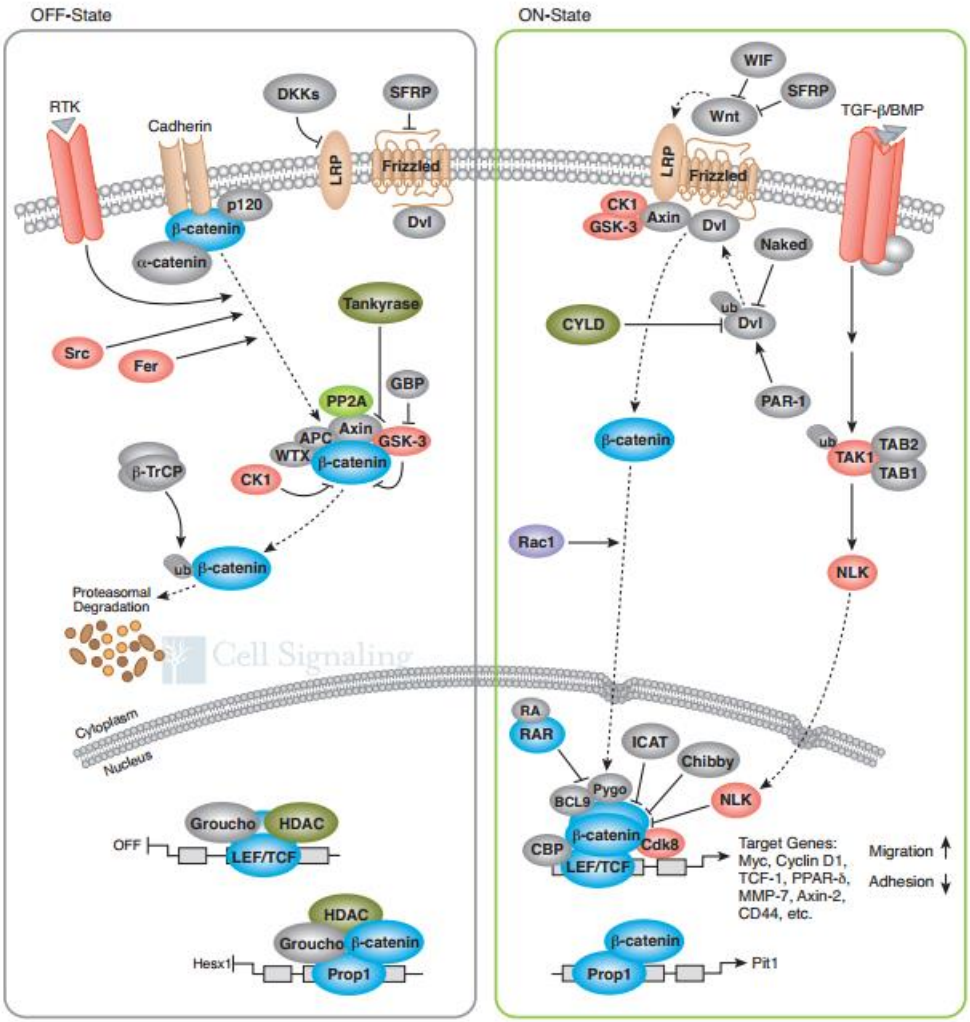

Figure 10. Wnt signaling pathway. (adapted from Cell Signaling technology)

Neural stem cell diversity and cell fate competency

Embryonic and early post-natal radial glial cells

Neural stem cells (NSC) generate all the neurons and glial cells that build the nervous system (McConnell, 1995; Breunig et al., 2011, Kriegstein and Alvarez-Buylla, 2009). After a first neurogenic phase, NSCs undergo gliogenesis producing oligodendrocytes progenitor cells (OPC) and astrocytes (Fujita 1986, 2003; Miller 1996; Temple 2001Noctor et al., 2004). The first NSCs to arise are the radial neuroepithelial cells that divide symmetrically to generate the neural plate and the neural tube. Neuroepithelial cells are oriented with a basal side attached to the pial surface and an apical side that contacts the lumen of the neural tube. After an early phase of neurogenesis, they transform into radial glial cells (RGC) increasing the size of their pial-contacting processes and through pseudostratification of the neuroepithelium by a switch from tight junctions to adherens junctions (Aaku-Saraste et al. 1997, Stoykova et al. 1997).

RGC express specific markers such as Nestin ,Glast,Tenascin C, vimentin , BLBP and glycogen granules (Morest and Silver, 2003, Gadisseux and Evrard, 1985, Hartfuss et al., 2001). First observed by Camillo Golgi in 1885, it is his student Ramon y Cajal who first suggested the glial identity for these cells based on the observation of morphological similarities with astrocytes. Later confirmed, RGC were shown to share with astrocytes GFAP expression, the main astrocyte marker (Choi, 1981; Levitt and Rakic, 1980) and the their ability to tightly contact endothelial cells (Taka1hashi et al. 1990, Misson et al. 1991). Many RGC subtypes have been identified, including tanycytes (hypothalamus), Müller glia (retina) and Bergmann glia (cerebellum) (Guo et al., 2013; Surzenko et al., 2013). Later on, Pasko Rakic demonstrated the multifunctionality of RGC showing that the pial surface-contacting processes was used as guidance cables for neuronal migration (Rakic, 1972 Xu et al., 2013). During development, RGC proliferate to form the ventricle zone (VZ) and subventricular zones (SVZ), a secondary germinal zone. RGC constitute the large majority of mitotic cells in ventricular zones (Lui et al., 2011; Malatesta and Gotz, 2013; Pilz et al., 2013). RGC undergo asymmetric division giving rise to one RGC and one differentiating cell

or an intermediate progenitor. Intermediate progenitors then migrate into the subventricular zone (SVZ), to further proliferate (Götz and Huttner, 2005; Miller and Gauthier, 2007). Recently, a new type of RGC, called outer SVZ progenitors (oSVZ), has been identified (Hansen et al., 2010; Fietz et al., 2010; Wang et al., 2011; Shitamukai et al., 2011). The expansion of the SVZ, and OSVZ progenitors, is the major cause of cortical expansion observed in mammals (Abdel-Mannan et al., 2008; Fish et al., 2008; Kriegstein et al., 2006).

Most of the RGC exhibit interkinetic nuclear migration (INM), a migration of their nucleus between the apical and the basal side in synchrony with their cell cycles. During cell division (M phase), the nuclei are located at the apical surface close to the ventricule. Then, they migrate basally during the G1 phase to remain in the basal region of the VZ during the S phase. In the G2 phase, the nuclei migrate back apically to undergo a second cell division when reaching the apical surface (LaMonica et al., 2013; Tsai et al., 2010, Taverna 2010). Observation of the INM directly by in-vivo time-lapse video imaging showed that INM has an intimate correlation with neurogenesis (Noctor SC, Flint AC 2001). However, some subtypes of neural progenitors do not exhibit INM (Kosodo et al. 2012). If INM is inhibited, cell cycle progression continues (Baye and Link, 2008; Murciano et al., 2002). However, RGC morphology seems to be involved in the long term maintenance of high proliferative capacity (Fietz SA, 2010). Notch signaling, which is known to prevent progenitor cells from differentiating, predominantly localizes to the apical side (Del Bene et al., 2008; Murciano et al., 2002). Interstingly, oSVZ SVZ cells undergo also some nuclear movements (Fietz et al., 2010; Hansen et al., 2010).

Much work has been done to understand why the nucleuses of neuroepithelial cells migrate toward the apical surface for mitosis. First postulated by Sauer in 1935: ~~–m~~itosis are confined to the region of the lumen not because only nuclei of that region divide, but because a nucleus that is about to divide moves to the region of the lumen to do so" (Sauer 1935). Indeed, in neuroepithelial cells and RGC, the apical plasma membrane is the location of the primary cilium, an organelle with a key role for setting up the mitotic spindle orientation (Chenn et al., 1998; Farkas and Huttner, 2008; Tamai et al., 2007; Dubreuil et al., 2007). The primary cilium persists until the onset of mitosis and provides, via its basal body, the necessary anchor for the centrosomes

which will drive mitotic spindle orientation (Dubreuil et al., 2007; Santos and Reiter, 2008, Chenn et al., 1998; Farkas and Huttner, 2008; Tamai et al., 2007). Despite its small size (1-5um), primary cilia are also important sensory organelle that detects signals in the ventricular cerebrospinal fluid such as IGF and Shh and PDGFA signalings (Lehtinen MK, Walsh CA, 2011; Willaredt MA, Tasouri E, Tucker KL 2013).Thus, the main function of INM is to drive pseudostratification of the V and maximize the apical progenitors mitosis by allowing the cell nucleus to reach the centrosome (Fish et al., 2008). The second main function is to control the extent to which RGC nuclei are exposed to different proliferative or differentiating signals (Taverna, Elena 2014). Interestingly, ventral RGC have a very different behavior. Basally dividing cells quickly outnumber the apical mitosis.These subapical progenitors (SAPs) increase from 7% (LGE) and 10% (MGE) at E14 to 20% at E16 to reach 60–70% of the total divinding cell in the LGE and MGE respectively. This particular mechanism contributes to SVZ enlargement of the ventral telencephalon and the generation of all the GABAergic interneurons as well as the early generation of oligodendrocytes progenitor cells (Pilz GA 2013).

Neural stem cells in the adult subventricular zone

In adult mammals, neurogenesis is maintained in the SVZ of the lateral ventricles (Altman, J. and Das, G.D. (1965) ; Kuhn, H.G. et al. (1996) Jessberger 2014). Indeed, neurogenic niches are conserved in the adulthood by maintenance of RGC-derived NSCs and ependymal cells (Spassky 2005). The adult SVZ contains slowly dividing NSCs (B cells), which give rise to actively proliferating cells (C cells) that function as the intermediate precursor cell (Doetsch et al. 1999). Type C cells give rise to immature neuroblasts (A cells) migrating in chains to the olfactory bulb in the rostral migrotary stream (RMS) where they differentiate into interneurons (Lois & AlvarezBuylla 1993, Alvarez-Buylla, A 2004). B cells display characteristics of astroglial cells, such as GFAP, GLAST, and other astroglial markers (Platel et al. 2008). B cells maintain some important properties of RGC such as long basal processes oriented tangentially which end feet contacting blood vessels, cell bodies located in the

ependymal cell layer with short apical processes extending on the ventricle or apical endings forming junctional complexes among themselves similarly to those of RGC (A Kriegstein; 2009). The ventricular surface observation reveals a striking ~~"p~~inwheel organization" containing the apical endings of B cells and in its periphery two types of ependymal cells: multiciliated (E1) whose beating cilia contribute to CSF flow and a type (E2) characterized by only two cilia that may work as sensors for CSF flow (Mirzadeh 2008). Interestingly, the adult SVZ neurogenic niche and the rostral migratory stream disappear quickly during human development (Sanai N 2011)

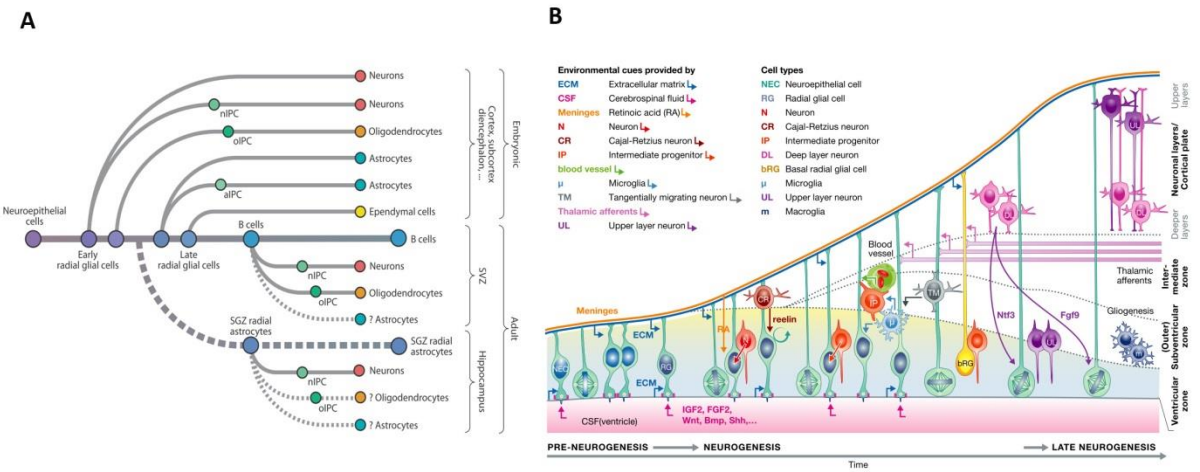

Figure 11. Overview of neurogenesis during development. The principal cell types of NPCs with the progeny they produce are indicated by different colors. Additional NPC types that are typically found in mammalian neocortex are indicated in the box..

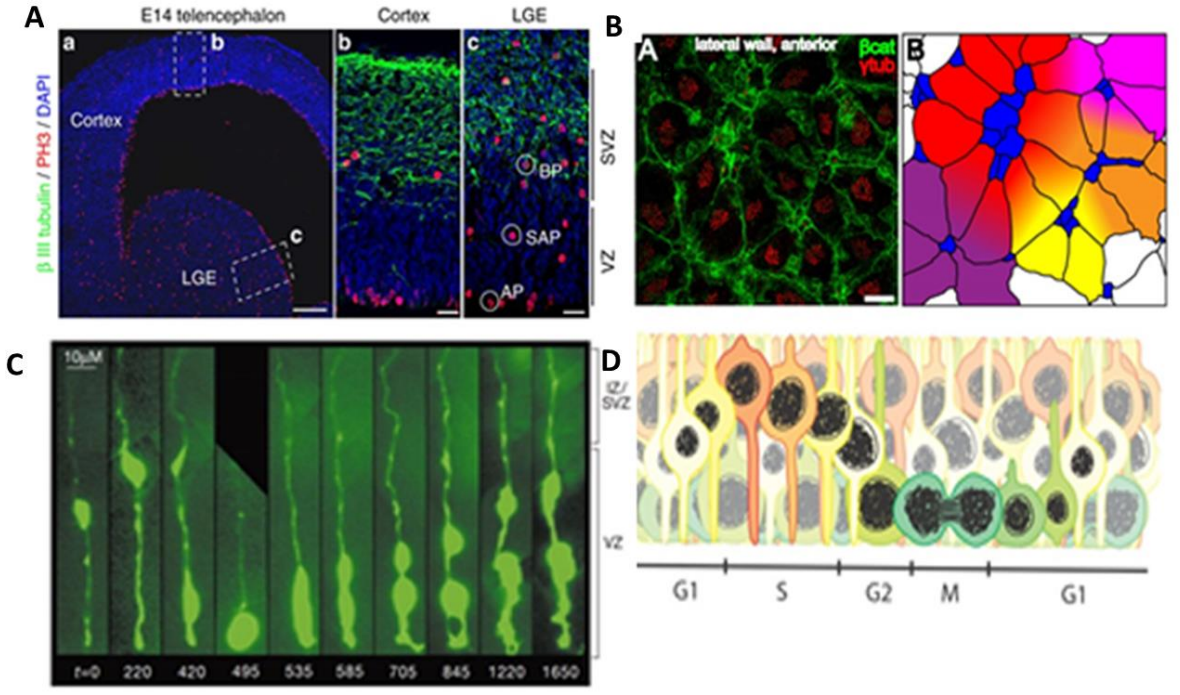

Figure 12. Ventricular zone organization. (**A**). Dividing NSCs are clustered in the cortical ventricular zone (VZ) but are scattered in the ganglionic eminence where subapical progenitors divide actively in the subventricular zone (SVZ). (**B**). Pinwheel architecture of the ventricular surface. Multiciliatted cells are the ependimal cells which circle proper NSCs which extend their primary cilia outside the ventricule. (**C**). Time laps imaging of interkinetic migration in mouse cortical slice. (**D**). Schematic of the nterkinetic migration. Nucleus move up and down depending on the cell cycle phase. Cells undergo mitosis at the ventricular surface where the primary cilia and the associated centromere was localized. Upon G1, they move toward the pial surface and receive less Shh and Notch signaling. This mechanism allow cells to differentiate and to migrate radialy toward the cortex thanks to the RGC processes (adapted from GA Pilz 2013; Mirzadeh J 2008; Paridaen JTML, 2014).

Neural stem cells in the adult hippocampus

Another major adult neurogenesis region in the adult mammalian brain is the dentate gyrus of the hippocampus (Altman & Das 1965, Kaplan & Hinds 1977, Gage 2000, Kempermann et al. 2004). Adult neurogenesis in the dentate gyrus has been involved in memory, mood disorder and epilepsy (Shors et al. 2002, Zhao et al. 2008, Dranovsky & Hen 2006, Parent et al. 2006). Adult neurogenesis takes place in the subgranular zone (SGZ). The SGZ contains two types of dividing cells: Radial astrocytes and darkly stained small cells (Altman & Das 1965, Kaplan & Hinds 1977, Cameron et al. 1993, Palmer et al. 2000). Radial astrocytes in the SGZ, also called type I progenitors (Filippov et al. 2003, Fukuda et al. 2003), have a long process crossing the granule cell layer as well as small horizontally oriented processes (Kosaka & Hama 1986, Seri et al. 2004). Nestin (Seri et al. 2004, Steiner et al. 2006). Similarly to the SV , the Radial astrocytes express NSC markers like Nestin….and contact the vascular system (Palmer et al. 2000). Radial astrocytes first generate intermediate progenitor cell, the small darkly stained cells called type II progenitors (Filippov et al. 2003, Fukuda et al. 2003) and differentiate into neurons characterized by the expression of doublecortin, PSA-NCAM, Tuc4, NeuroD, Prox1, and NeuN (Seki & Arai 1993, Fukuda et al. 2003, Seri et al. 2004) to progressively acquire electrophysiological characteristics of gabaergic neurons (Song et al. 2002, Filippov et

al. 2003). In addition to their role as neuronal precursors, radial astrocytes maintain their classical astrocytic functions of metabolic support Neurogenesis in the dentate gyrus is regulated by adrenal steroids (Gould et al. 1992, Cameron et al. 1998), glutamate signaling (Gould et al. 1994), seizures (Parent et al. 1997), enriched environment and exercise (Kempermann et al. 1997; 1998), inflammation (Monje et al. 2003), and antidepressants (Santarelli et al. 2003).

Oligodendrocytes progenitor cells are not adult neural stem cells

Besides self-renewal and multipotency capacities, other characteristics define stemness property. Indeed, stem cells need to have the capacity to clonally regenerate multiple different cell types in the tissue where they are, the ability to undergo asymmetric cell division and the potential to exist in as mitotically quiescent (Hall and Watt, 1989; Morrison et al., 1997; Potten and Loeffler, 1990). To determine if OPCs could fall into this definition, we have to look if they fit all the required criteria. At the time of their discovery by Raff et al in 1983, OPCs were already considered as bi-potential and able to generate both oligodendrocytes and type 2A astrocytes in vitro. Later on, OPCs were shown to produce free floating balls of cells in-vitro called neurospheres whose clonal cell analysis showed a tri-potent capacity able to generate oligodendrocytes, astrocytes and neurons (Kondo and Raff, 2000). However, we had to wait until recently to prove the OPCs asymmetric division capacity. A study using in vivo time lapse imaging showed that even if all OPCs visualised were generating oligodendrocytes, only 7 % differentiated directly after a cell division (Hughes et al., 2013). However, another study bring clear evidence that the proteoglycan NG2 segregates asymmetrically during OPCs cell division and generate two distinct daughter cells, one being OPC, the other differentiating OPC (Sugiarto et al., 2011). Thus, these studies validate the self-renewal and multipotency capacities of OPCs.

The rate of OPCs cell division is dependent on their location in the CNS and declines with age (Young et al., 20013). Moreover, in response to stress or injury OPCs become activated and undergo proliferation and differentiation (Zawadzka et al., 2010). Thus these studies demonstrate the quiescent capacity of OPCs as well as their tissue regenerating capacities. Finaly, Asymmetric cell division would imply an in-vivo differentiation into a different cell type i.e neuron, astrocytes or NSC. However, in-vivo evidence of physiological in-vivo asymmetric cell division is still lacking despite great effort to find such occurrence.Indeed, the only occurrence of asymmetric cell division was found on a verbB p53+/− mice where FACSorted NG2+ OPCs gave rise to a Nestin+/GFAP+ glioma precursor (Sugiarto 2011). In conclusion, even if many of stem cell properties are exhibited by OPCs, they cannot be defined as true neural stem cells.

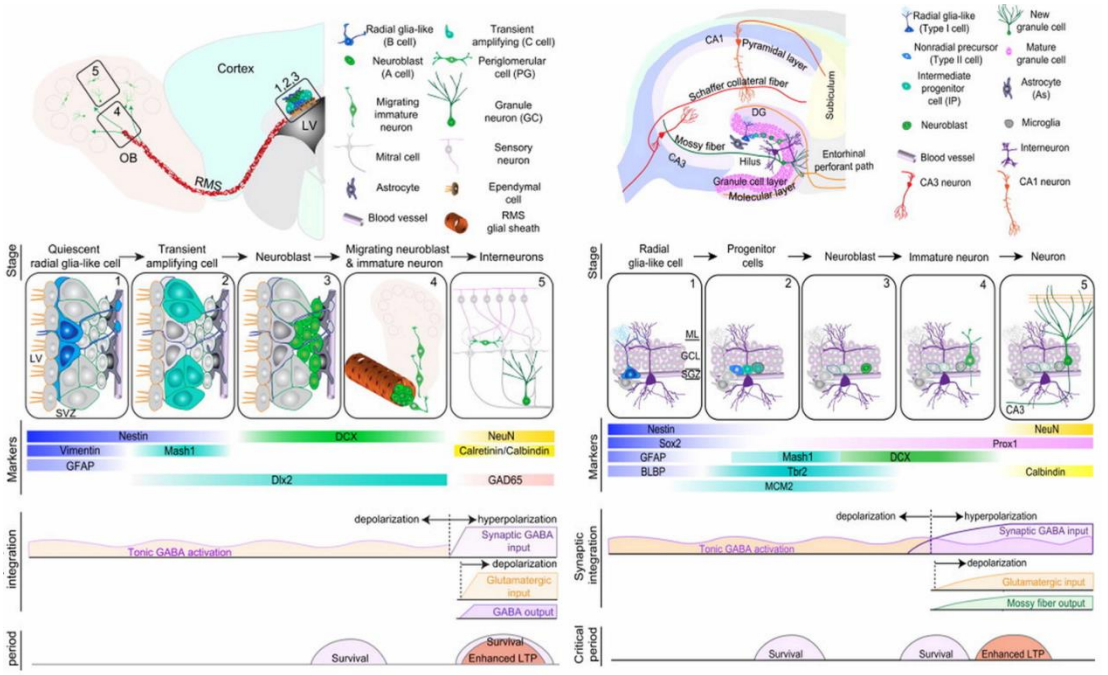

Figure 13. Comparison between SVZ and SGZ adult neurogenesis. None of the indicated NSCs marker is specific on its own. Combination of markers define the quiescent NSCs stage. (adapted from Ming Song 2011).

Mechanisms of Intrinsic and extrinsic regulations of neural stem cells

Stem cell niche, stemness maintance and growth factors

The NSC niche is composed of neural and vascular cells communicating by autocrine , paracrine or mechanical signallings.The embryonic NSCs niche is higly active during development but is maintained in a more quiescent stage in specif parts of the adult brain. Many factors regulate stemness maintenance and proliferation in NSCs niches (for review SJ Goldberg 2013). FGF and EGF are the main growth factors for the in vitro isolation of NSCs from the embryonic and adult brain. bFGF (FGF2) generate neurospheres in culture which differentiate into astrocytes, oligodendrocytes and neurons. Cell passaging generates secondary and tertiary neurospheres proving their self-renewal capacity. E8 to E10 NSCs are aleready responsive to bFGF rather than EGF. Similarly, EGF is a growth factor driving proliferation and NSCs survival. Cultures with bFGF alone divide slowly while those cultured with EGF alone divide at a faster rate. FGF-2 and EGF are mainly tranfered by endothelial cells contacting directly the NSCs. Other important factors regulate NSCs maintenance and survival such as VEGF, Wnt, Shh, Notch or CTNF (Fig. 15).

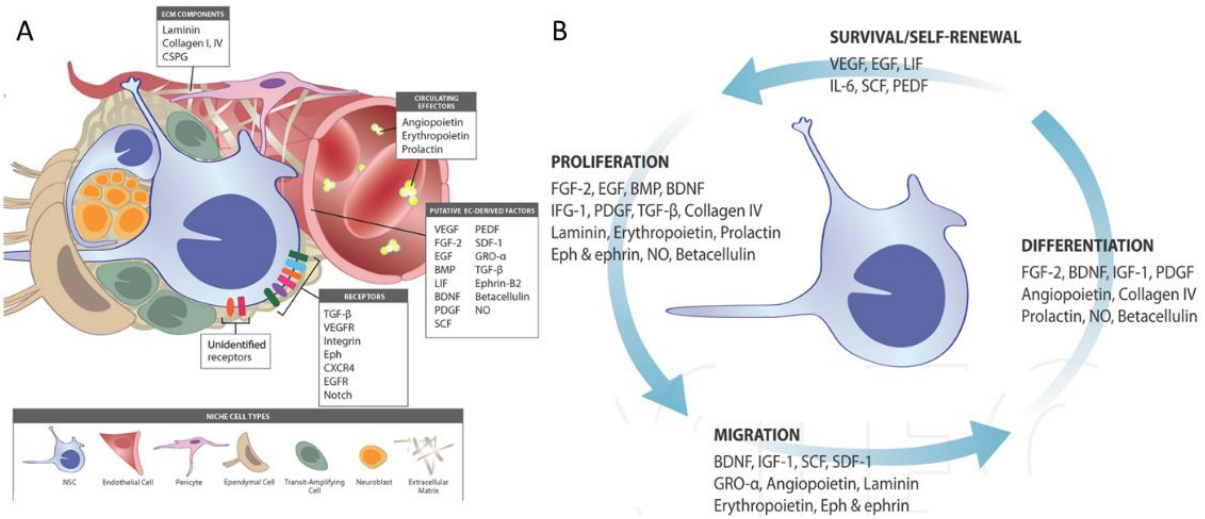

Figure 14. A. Sources of vascular – derived adult NSC niche effectors. Growth factors originate from the endothelial cell, blood circulation, extracellular matrix deposition, and perivascular cell types (adapted from SJ Goldberg 2013).

Table 1
NSC markers.

	Markers
(a) NSC *in vitro*	
NSCs	LeX (MMA^{LeX})[b]
	CD133 (human)/Prominin1 (mouse
	Notch1
	Syndecan-1
	Integrin-β1
	CD184^{+ve} CD271^{-ve} CD44^{-ve} CD24
	ABCG2
	CXCR4
	FGFR4
	Frizzled-9
	Glut1
	Notch2
	Exclusion of Hoechst 33342
	Cell size
	Granularity
(b) NSC *in vivo*	
	Nestin
	Sox2
	LeX
	CD15
	LeX (5750[L]
	GLAST
	Ephrin B1
	Prominin1
	CBF-1
	Pax6
	Vimentin
	BLBP
	RC2
	Nestin
	LeX
	GFAP

Survival factors for adult NSCs.

Class	Survival factors
A. Growth factors	bFGF and EGF
	HGF
	VEGF
	IGF-1
	PEDF
	MIF
B. Morphogens	Noggin
	Wnt (3 and 7b)
	Shh
	Notch
	Ephrins
C. Proteoglycans	CSPG
	Tenascin-C
D. Cytokines	LIF
	CNTF
	SDNSF
E. Hormones	Erythropoietin
	Insulin
	Adiponectin and leptin
F. Neurotransmitters	D-Serine
	Glutamate
	Dopamine
	Histamine
	NO
	GABA
	5HT
Other factors	Cystatin C

Survival factors for embryonic NSCs.

Class	Survival Factors
A. Growth factors	bFGF and EGF
	IGF-1
B. Morphogens	Wnt3a
	Shh
	Notch
C. Proteoglycans	HSPG
	CSPG
	Heparin
	DermatanPG/CSPG
D. Cytokines	Fractalkine
E. Hormones	Erythropoietin
F. Lipid transporter	ApoE

Figure 15. Table show in-vivo and in vitro –specific" markers together with survival factors involved in NSCs maintenance. Currently, a combination of marker is necessary to fully define the NSCs stage. (adapted from Ramasamy 2014).

Mitotic spindle orientation and asymmetric segregation of cellular components

During neurogenesis, NSCs can divide in one of three basic modes: symmetric proliferative (2NSCs) or differentiative (2 postmitotic cells) or asymmetric (1NSC and 1postmitotic cell). Recent studies have shown a link between cleavage orientation, centrosome asymmetries, ciliogenesis, asymmetric segregation of cellular components and cell fate (Paridaen J 2014). In the vertebrate developing brain, while early RGC symmetrical divisions feature cleavage planes perpendicular to the ventricular surface, later asymmetric divisions demonstrate oblique cleavage planes (Postiglione MP2011, LaMonica BE,2013). The spindle orientation of symmetric RGC divisions, regulated

by mechanisms involving centrosomes, microtubule positioning, and proteins of the internal plasma membrane, is essential to maintain symmetric RGC divisions (Konno D, 2008; Peyre E, Jaouen F,2011). For example, mutant mice for Lis1 severely disrupts the expansion of RGC pool by inducing random cleavage planes (Xie Y, Juschke C, 2013). Many proteins segregate differentialy during asymmetric cell division. For example, notch signaling proteins (Notch, Dll1/3, Mindbomb, Numb) are differentially segregated between daughter cells and lead to differential Notch signaling between daughter cells, thus driving different cell fate (Bultje RS, 2009 Kawaguchi D 2013)

In addition, the mouse Par3 protein segregates asymmetrically into the daughter cell that will remain RGC (Bultje RS 2009).

The centrosome inheritance is an other mechanism regulating asymmetric cell division. During interphase cells possess one mother and one daughter centriole constituting the centrosome. The mother centriole is the oldest centriole and mediates nucleation of the primary cilium while older centrioles are inherited by daughter. Interestingly, cells that inherit daughter centriole maintain their stem cell identity (Wang X, Tsai jw, 2009). A recent study shows the mother centriole is able to retain ciliary membrane and reforms a new cilium before its sister cell (Paridaen JT 2013). This earlier cilium reformation is thought to allow earlier ciliary signaling involved in RGC daughter cell fate such as IGF-1. Moreover, differentiating daughter cells form their primary cilia at their basolateral instead of their apical side, thus leading to asymmetrical daughter cell behavior (Wilsch-Brauninger M 2012).

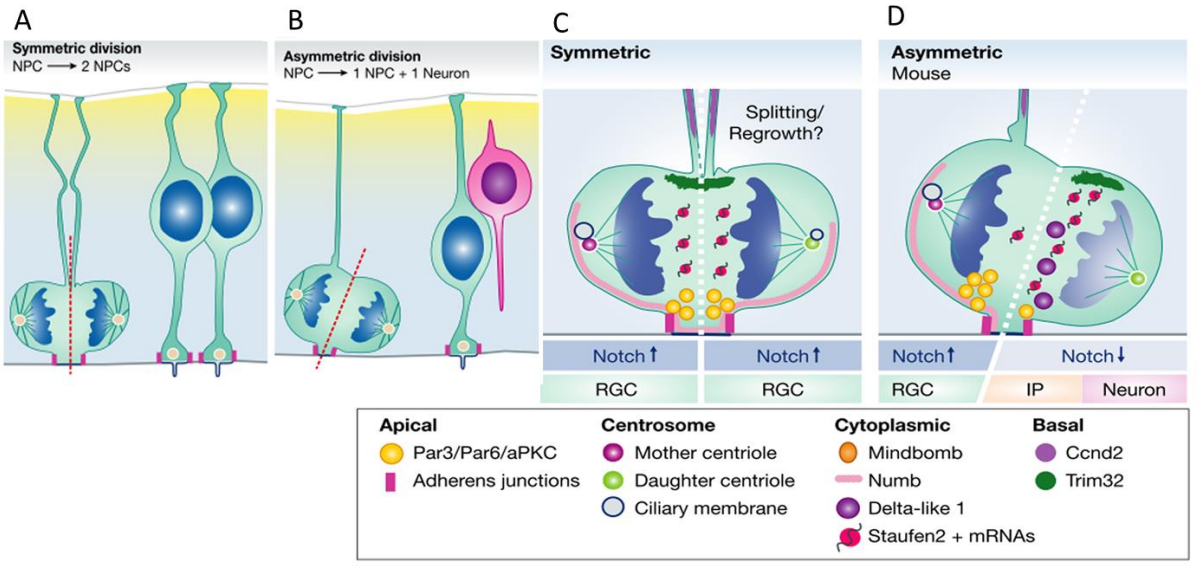

Figure 16. Asymetric segregation of cellular position and spindle orientation. Cell fate determinants may be equally (symmetric division, A) or unequally (Asymemetric B) distributed between daughter cells. (C, D) Examples of asymmetries between daughter cells that were introduced by asymmetric inheritance of differently aged centrioles, ciliary membrane, Par 3 and Notch signaling components (adapted from JTML Paridaen 2014).

Cell cycle length of neural precursors regulation of cell fate choice

Changes in cell cycle length have been implicated in cell fate decision (Dehay C,2007; Salomoni 2010). Cell cycle length in the mouse ventricular zone increases from 8 hours at the onset of neuron production at E11 to 18 hours at E16. This increase, due to a lengthening of G1 from 3 to 13 hours (Takahashi, T. et al 1995), is correlated with an increase in asymmetric division (Arai Y, Pulvers JN 2011; Lange C, Huttner WB,2009). To convert this correlation into causal explanation, a recent study, manipulation of overexpression cdk4/cyclinD1, two proteins thought have only a function in cell cycle control, lengthen the G1 phase, decreased neurogenesis at the expanse of RGCs. Conversely, their downregulation led to the opposite effects (Calegari, F. and Huttner, W.B. (2003), Lange, C. et al. (2009)).

Proneural basic helix-loop-helix factors (bHLHs) transcription factors in neural differentiation.

Basic helix-loop-helix transcription factors (bHLH) were found to play central roles in self-renewal of NSC and fate determination of neurons, oligodendrocytes, and astrocytes (Bertrand et al., 2002; Namihira and Nakashima, 2013). Indeed, early studies in Drosophila discovered „proneural" genes of the achaetescute complex (Garcia-Bellido, 1979). bHLH function through dimerization with ubiquitously expressed bHLH E-proteins such as E12, E47, HEB or TCF4 thanks to thei helix domain, and subsequent binding a to DNA sequence called the Ebox (CANNTG) thanks to their basic domain (Murre et al., 1989; Bertrand et al., 2002). The

mammalian homolog of drosophilia achaetescute complex genes (Ascl1), also called Ascl1 (Johnson et al., 1990), is now recognized as the master regulator of neurogenesis (Bertrand et al., 2002). Indeed, Ascl1 is required for specific subsets of neurons or oligodendrocytes in spinal cord, telencephalon, mesencephalon, hindbrain, olfactory sensory epithelium, as well as in the autonomic nervous system (Guillemot et al., 1993; Blaugrund et al., 1996; Cau et al., 1997; Hirsch et al., 1998; Casarosa et al., 1999; Akagi et al., 2004; Miyoshi et al., 2004; Pattyn et al., 2004; Helms et al., 2005; Parras et al., 2007; Sugimori et al., 2007; Sugimori et al., 2008). Other bHLH proneural genes such as Atoh1 (Math1), NeuroD, NeuroM, Neurog1/2, Ptf1a and Olig1/2 were discovered later on and shown to drive different cell type specifications or differentiations (Ma et al., 1996; Ben-Arie et al., 1997; Lu et al., 2000; Zhou et al., 2000; Glasgow et al., 2005; Ross et al., 2003).While Atoh1 is necessary for interneurons generation in the dorsal spinal cord, granule cells in the cerebellum and glutamatergic neurons in brain stem nuclei and inner ear epithelium (Ben-Arie et al., 1997; Gowan et al., 2001; Helms et al., 2001; Machold and Fishell, 2005), Neurog1/2 are necessary dorsal interneurons in the spinal cord, glutamatergic neurons in the cortex, and dopaminergic neurons in the midbrain (Ma et al., 1996; Sommer et al., 1996; Gowan et al., 2001; Parras et al., 2002; Kele et al., 2006), Ptf1a is essential for GABAergic neurons in the dorsal spinal cord, retina and cerebellum (Glasgow et al., 2005; Hoshino et al., 2005; Fujitani et al., 2006).

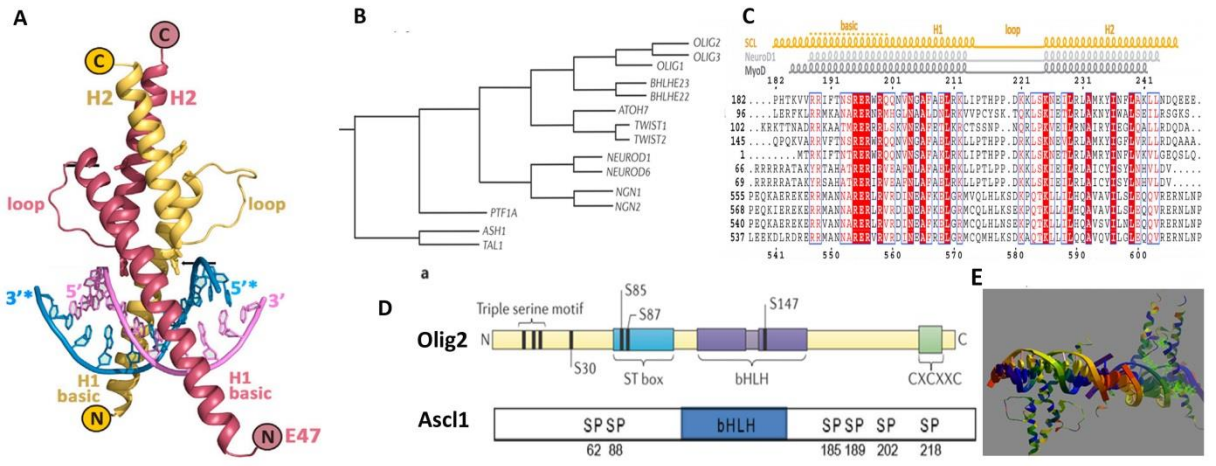

Figure 17. Ascl1 and Olig2 are Proneural bHLH transcription factors.
(A)Schematic of a DNA bound by a bHLH:E47 dimere (B) Phylogenetic tree of the proneural bHLH. Ash1 is the more ancient proneural HLH, gene evolved by

duplication and specialization. Olig2 /Olig1 evolved the most recently C. Sequence and structural alignment of bHLH domains od different bHLH proteins. Conserved amino acids are drawn in red boxes; similar amino acids are in red type. (D)Ascl1/Olig2 postranslational modification. Multiple phosphorylation sites a present on Ascl1 and Olig2 proteins. Regulatory function ae associated with the absence or presenc of phosphorymation (E) Structural representation conserved region in bHLH. Schematic of a DNA molecule bound by a bHLH. Green cross are amino acid conserved between different bHLH molecules. Basic domain is higly conserved and in close proximity to the DNA.

Neural bHLH factors promote neuronal differentiation through two main mechanisms. First, Ascl1 and Neurog1 drive differentiation through cell cycle exit thanks to the expression of p27 (Kip1), a cyclin-dependent kinase inhibitor (Farah et al., 2000). Second, Ascl1 and Neurog1 trigger neuronal differentiation through direct and indirect activation neural genes such as NeuroD or NeuroM (Fode et al., 1998; Cau et al., 2002). Ascl1 mutant mice display severe neuronal losses and proliferation defects (Casarosa et al., 1999; Horton et al., 1999; Wildner et al., 2006; Battiste et al., 2007). Conversely, overexpression of Ascl1 in neural cells drive cell cycle exit and early expression of neuronal specific markers such as Tuj1 or NeuN (Farah et al., 2000; Nakada et al., 2004; Helms et al., 2005; Kriks et al., 2005). Knock-in experiment where Neurog2 coding sequence was replaced by Ascl1 demonstrated distinct roles in the specification of glutamatergic and GABAergic neurons in dorsal and ventral telencephalon, respectively (Parras et al., 2002). A recent study demonstrated that Ascl1 is regulated by multisite phosphorylation on conserved serines-proline pairs by Cdk kinase activity during cell cycle and that dephosphorylation increase cell differentiation (Ali FR, Cheng K et al 2014).

Identifying transcriptional targets of bHLH factors is fundamental to provide mechanistic insights of bHLH functions in neurogenesis. However, it has been difficult to identify and validate Ascl1 direct in vivo downstream targets just based on the degenerate 6 base pair E-box DNA motif. With advanced technology using chromatin immuno-precipitation , microarray and bioinformatics, several in vivo transcriptional targets of bHLHs are beginning to be identified. Indeed, Notch ligands such as Dll1

and Dll3 were shown to be transcriptional targets of Ascl1 and Ascl1 interacts with Brn1/2 or Neurog2 on the promoter of Dll1 and Dll3 (Castro et al., 2006; Henke et al., 2009).

The Hes HLH family, the mammalian homologues of Drosophila hairy and Enhancer of split gene, and Ids, inhibitors of differentiation are transcriptional repressors. Hes1, Hes3, and Hes5 are expressed in undifferentiated neural stem cells of the VZ (Kageyama et al., 2008a). In mice mutant for Hes genes, Ascl1 and Neurog2 are upregulated and neuronal differentiation is promoted. The mechanism leads to a rapid depletion of the NSC pool (Ishibashi et al., 1995; Chen et al., 1997). Conversely, overexpression of Hes1 or Hes5 inhibits neurogenesis (Ohtsuka et al., 1999; Cau et al., 2000). Hes proteins were shown to bind Ascl1 enhancer regions and repress their transcription (Ishibashi et al., 1995; Chen et al., 1997). Interesingly, Hes proteins have oscillatory expression thanks to a cell autonomous negative auto-feedback loop (Kageyama et al., 2007). Ids proteins are HLH protein lacking the basic DNA binding domain. Ids proteins are able to inhibit neural differentiation working as a dominant negative heterodimere of bHLH proteins (Norton, 2000). Ids overexpression inhibits proneural genes and increase Hes1 expression. Interestingly, Ids interact with Hes1 and suppress Hes1 negative feedback loop (Bai et al., 2007).

The Notch signaling pathway and lateral inhibition

Notch signaling pathway is the main mechanism controlling cell cycle exit and differentiation in embryonic and adult neural development (Yoon and Gaiano, 2005; Louvi and Artavanis-Tsakonas, 2006). Notch signaling controls neural differentiation through lateral inhibition by controlling the balance between proneural and Hes transcription factors (Yoon and Gaiano, 2005; Louvi and Artavanis-Tsakonas, 2006).

At early stage, neural progenitors share similar levels of Notch receptor and ligand at their surface. Then, due to stochastic variation, a cell starts to express a higher level of Notch ligand Dll1. Upon activation of Notch receptor in a neighboring cell, the Notch intracellular domain (NICD) is translocated from the membrane to the nucleus. In the nucleus, NICD converts RBPj from a repressor to an activator and form an activating complex with Maml (mastermind-like) driving the expression of Hes1 or Hes5, thus

suppressing the transcription Ascl1 or Neurog1/2. As Dll1 is a direct target of Ascl1 and Neurog1/2, Notch ligand expression will follow the same down regulation. Consequently, a cell having higher levels of Dll1 and Ascl1 or Neurog1/2 expression will initiate differentiation whereas a cell having higher Notch activation and Hes gene expression will remain a progenitor. Recently, this classic view of lateral inhibition was improved by the discovery of the Hes/Ascl1 oscillation mechanism (Kageyama et al., 2008b). Indeed, Hes1 expression is periodically upregulated and downregulated with a 2-3 hour frequency (Shimojo et al., 2008). Dll1 and Neurog2 also oscillate but with an inverse periodicity (Shimojo et al., 2008).

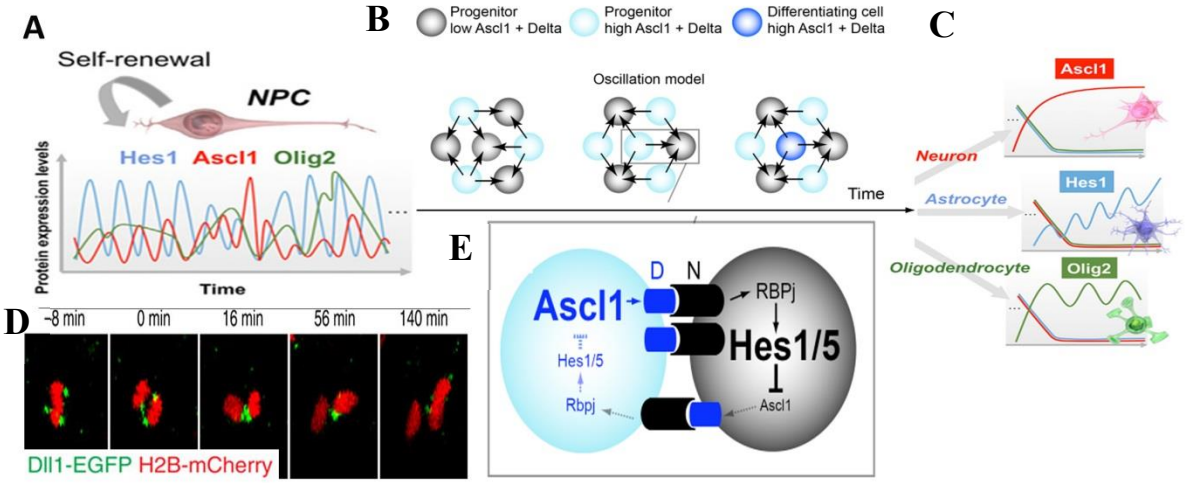

Figure 18 Dynamic Regulation of cell fate by Proneural bHLH Factors.
(A).Schematic representation of proneural gene oscillations NSCs. Time-lapse clearly showed that Hes1 and Ascl1 protein expression oscillate with a period of 2-3 hr, while Olig2 protein expression oscillates with a period of about 5 -8 hr in NSCs.**(B).Notch lateral inhibition.** Ascl1, Dll1 and Hes1 forming salt-and-pepper patterns. Substantial accumulation of Ascl1 and Delta or Hes1 is stabilized by their oscillatory dynamics. In the cell having higher level of Ascl1, Delta expression is increased and activates Notch signaling in the neighboring cell. In the cell having Notch signaling activation, RBPj upregulates Hes1 and Hes5. Then, the transcription Ascl1 is inhibited by Hes1 and Hes5 . (C) **Roles of bHLH Factors in NPC Self-Renewal and Cell Fate Determination.** Schematic representing Ascl1 up regulation upon neuron and oligodendrocyte differentiation, Hes1 cycling up-regulation upon Astrocyte differentiation and Olig2 up-regulation upon oligodendrocyte **(D) Dll1 asymmetric inheritance between sister cells.** Time-lapse of dividing NSCs. Cultured NSCs infected with retroviruses expressing Dll1-EGFP (green) and mCherry-Geminin

(red), which emits mCherry fluorescence in S/G2/M phases. Time is indicated relative to the timing of cytokinesis. Two cells are generated Dll1-inheriting and non-Dll1-inheriting sister cells, respectively differentiation (adapted from Imayoshi , 2014 Kawaguchi 2013 and EJ Kim 2009).

bHLH factors in oligodendrogenesis

During development, neurons and glia are produced from NSC in a sequential but overlapping manner. Olig1 and Olig2 bHLH transcription factors play a central role in oligodendrocyte specification and differentiation (Meijer et al., 2012).

In the developing spinal cord and hindbrain, motor neurons and oligodendrocytes are sequentially produced from the pMN domain (Goulding, 2009). In the VZ and SVZ of the ventral part of the telencephalon, the ganglionic eminences, Olig1 and Olig2 are expressed where GABAergic interneurons and oligodendrocyte precursors first emerge (Lu et al., 2002; Butt et al., 2005). Unlike Ascl1, the expression of Olig1 and Olig2 is maintained into mature oligodendrocytes. (Zhou et al., 2001; Lu et al., 2001).

In the absence of Olig2, the formation of the pMN domain is severely diminished, and both motoneurons and oligodendrocytes are missing, (Lu et al., 2000;Lu et al., 2002; Zhou and Anderson, 2002; Takebayashi et al., 2002). While Olig1 is requiered to Repress Dlx1/2 and inhibit GABAergic interneuron formation in the ventral telenephalon (Silbereis 2014), Olig1 knockout mice have broad defects in the maturation of oligodendrocytes (Lu et al., 2002; Xin et al., 2005) and a limited capacity to repair demyelinated lesions (Arnett et al., 2004). Conversely, overexpression of Olig1/2 in NPCs is sufficient to induce the specification of oligodendrocyte precursor cells (OPCs) (Zhou et al., 2001; Lu et al., 2001). Conditional deletions of Olig1 et Olig2 in NSC, OPCs and mature oligodendrocytes, revealed stage-specific regulatory roles. At early developmental stages, Olig2 promotes proliferation of self-renewing NPCs. Later on, Olig2 promotes motoneuron or oligodendrocytes specification (Yue et al., 2006; Cai et al., 2007; Zhu et al., 2012; Mei et al., 2013).

Interestingly, Olig2 functions mainly as a repressor (Novitch et al., 2001; Zhou et al., 2001) but also directly activates the expression of the oligodendrocyte-specific gene Sox10 (Küspert et al., 2011). Stage-specific functions of Olig2 are regulated by posttranscriptional modifications (Setoguchi and Kondo, 2004; Meijer et al., 2012).

Serine phosphorylation at the ST box of Olig2 by CK2 kinase activates OPCs generating function (Huillard et al., 2010). By contrast, while serine (S147) phosphorylation in its bHLH domain by PKA drives motor neuron formation, its dephosphorylation is involved in the transition from motor neuron to oligodendrocyte specification in the pMN domain (Li et al., 2011). This phosphorylation in the bHLH domain was shown to favor Olig2 homodimer formation, whereas dephosphorylation favor heterodimer formation with Neurog2. Olig2/ Neurog2heterodimer was shown to sequesters Neurog2 and thus prevents motoneuron formation (Li et al., 2011). In NPCs during the early stage of embryos, Olig2 is phosphorylated at 3 residues whereas in the postnatal white matter, the triple serine motif is nonphosphorylated (Sun et al., 2011).

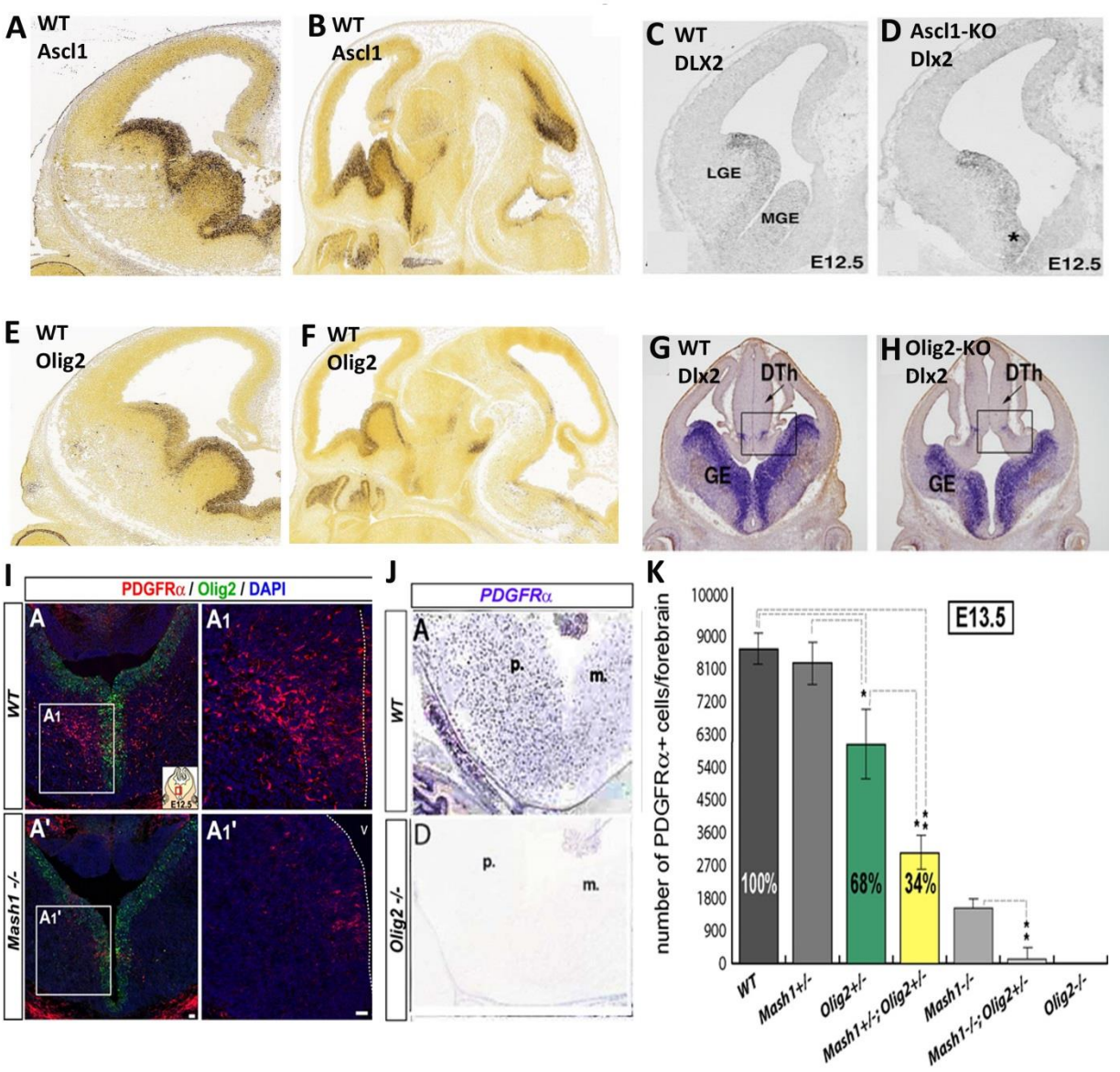

Fig 19. Ascl1 and Olig2 requirement for the generation of OPCs. (A-H) sections of E13.5 brain In-situ hybridization showing expression of *Ascl1* (**A,** coronal and **B,** sagittal) and *Olig2* (**E,F**). (**C,D**) *Ascl1* knock-out morphological changes observed in E13.5 sagital section of WT (G) and *Ascl1*-/- (H) mice. (**G,H**) *Olig2* knock-out morphological changes observed in E13.5 sagital section of WT (G) and *Olig2*-/- (H) mice. (**I**) Ascl1 requirement for OPCs specification in embryonic telencephalon: Telencephalic coronal sections of wild-type (A–A1) and *Ascl1*-/- (A'–A1') embryos at E14.5 (Parras et al 2007). (**J**) Olig2 requirement for OPCs specification in spinal cord coronal sections of wild-type (A) and *Olig2*-/- (D) embryos (Zhu et al 2001). (**K**) Genetic interaction between *Ascl1* and *Olig2*. Quantification of OPCS in the forebrain of E13.5embryos. Percentages represent the ratio of OPCs observed in embryos of indicated genotypes over wild-type embryos (Parras et al 2007).

bHLH factors in astrogenesis

With the exception of SCL (Stem cell leukemia), a bHLH transcription factor, necessary and sufficient to drive specificiation and differentiation of astrocytes in specific regions of the developing neural tube (M Nakanishi 2007), astrocyte fate seems to be the default differentiation path in absence of proneural or oligodendroneural genes (Ross et al., 2003; Namihira and Nakashima, 2013). Indeed, Many studies described the role of Notch/ Hes signaling and Id factors in astrocyte formation, but these factors are not sufficient (Cai et al., 2000; Ohtsuka et al., 2001; Tanigaki et al., 2001; Wu et al., 2003; Namihira et al., 2009). For example, overexpression of Hes or Id factors in early NSCs fail to prematurely induce astrocyte formation (Ohtsuka et al., 1999; Cai et al., 2000; Ohtsuka et al., 2001; Tanigaki et al., 2001; Wu et al., 2003; Namihira et al., 2009) and conversely, mutant mice for both Ascl1, Neurog2 or olig2 show precoce and increased astrogenesis development (Nieto et al., 2001, parras et al 2013). Rather, accumulating evidence indicate that astrocyte fate is driven by extrinsic cues such as leukemia inhibitory factor (LIF), cardiotrophin-1 (CT-1) and BMP signaling (Namihira and Nakashima, 2013).

Dynamic Regulation of Proneural bHLH Factors

Ascl1 is dynamically regulated at the mRNA and protein levels. Ascl1 protein is unstable in human NPCs with a half-life of only 14 min but is stabilized to a half-life of 50 min when NICD is mutated (Sriuranpong et al., 2002). Moreover, Ascl1 stability is post transcriptionally regulated. Indeed, nonphosphorylated Ascl1 is very unstable, whereas CK2-mediated phosphorylation of S152 stabilizes Ascl1 (Vin˜ als et al., 2004). In the cortex, Pax6 promotes RGC proliferation and spindle orientation (Asami M 2011), but also triggers neuronal differentiation through the induction of Neurog2 (Sansom 2009), Tbr1/2 (Götzand Huttner, 2005), Brn1/2, Sox4 and Sox11 (Martynoga B 2012).

However, even if Ascl1is predominantly expressed in the ventral telencephalon during embryonic development, dorsal Ascl1 positive cells also gives rise to cortical GABAergic interneurons and oligodendrocytes.

Ascl1 is expressed by NPCs in the ventral telencephalon, in the medial, lateral, and caudal ganglionic eminences. In Ascl1 knockout mice, the production of GABAergic neurons is largely abrogated, with a more profound phenotype in the medial ganglionic eminence (Casarosa et al., 1999; Horton et al., 1999). Conversely, overexpression of Ascl1 induces ectopic GABAergic neurons from dorsal cortical NPCs (Berninger et al., 2007; Poitras et al., 2007). Moreover, transient accumulation of Ascl1 in NPCs induces the expression of GABAergic differentiation associated with Dlx1/2/5/6 and Lhx6 expression (Yun et al., 2002; Petryniak et al., 2007; Miyoshi et al., 2010; Bartolini et al., 2013).

Expression dynamics of bHLH factors in multipotency and cell fate choice

Oscillating expression of bHLH factors, including Hes, Ascl1, Neurog2, and Olig2, in NPCs is important to maintain their proliferative and multipotent potentials (Imayoshi 2014). Single cell time-lapse imaging studies showed that in NPCs, Hes1 and Ascl1 protein expression oscillate with a period of 2-3 hr and that Olig2 protein expression oscillates with a 5-8 hr periodicity (Shimojo et al., 2008). While inactivation of Hes1 abolishes Ascl1 oscillation, it does not affect Olig2 oscillations (Imayoshi et al., 2013). An optogenetic approach has been employed to control the sustained Vs oscillatory Ascl1 and Olig2 mode of expressions (Wang, X., Chen, X., and Yang, Y. 2012). In this study, sustained Ascl1 expression enhances neuronal differentiation, whereas oscillatory Ascl1 expression with 3 hr periodicity activates proliferation of NPCs. These results indicate that sustained Ascl1 accumulation during 6-8h in G1 phase is necessary for neuronal fate determination. Thus, distinct expression dynamics of Ascl1 are important for the choice between proliferation and differentiation (Wang, X., Chen, X., and Yang, Y. 2012; Imayoshi et al., 2013). Interestingly, the 3 hr periodicity of Ascl1 oscillation is necessary for NPC proliferation as this effect was not observed with a 6 hr period (Imayoshi et al., 2013). Whether the period of oscillatory expression correlates with that of cell cycle remains

to be determined. During oligodendrocyte differentiation, oscillatory up-regulation of Olig2 occurs. When Olig2 becomes dominant the expression of Ascl1 and Hes1 is down-regulated (Imayoshi et al., 2013).

Before asymmetric cell division, where daughter cell remains NSC while the other differentiates, Ascl1, Hes1, and Olig2 are expressed together and oscillate. At the peak of Ascl1 or Olig2 oscillations, cells have a higher tendency to differentiate into neurons or oligodendrocytes respectively. However, this tendency is not decisive as posttranslational modifications are involved in fate choice process. Hes1 expression is first down regulated before cell division, and Ascl1 or Olig2 expression is up regulated in differentiating cells while the daughter NPC resumes Hes1 and Ascl1 oscillations. As oscillatory Ascl1 can promote cell cycle progression, such periodic production seems to be a driving force for cell-cycle progression, although the exact mechanism remains to be determined.

While sustained Hes1 expression is able to generate quiescent NPCs (Sang et al., 2008), Hes1 and Ascl1 oscillations may lead to accumulation of downstream factors in NPCs and serve as a molecular clock where the number of pulses may be used to drive differentiation at the right time. Such a molecular clock mechanism is supported by many studies. Indeed, interneurons born at different times would behave differently within the same environment (Pla et al., 2006; D.G. Southwell 2012) and the differentiation timing human IPScell converted into neurons takes several months and thus mimic the human neural development timing (C.R. Nicholas 2013). It has been proposed that the microRNA-9 (miR-9), regulating negatively Hes1 mRNA, accumulate progressively every round of division to a level sufficient to abrogate Hes1 oscillation (Bonev et al., 2012; Tan et al., 2012b). Moreover, new links between Hes genes and circadian control genes (Clock/Bmal1, Per1/2) were recently discovered outside the brain (Lee YJ1, Han DH, Pak YK, Cho SH.2012). Taken together, these results show that further analyses are required to determine whether Hes and proneural genes oscillations are involved in the cellular clock mechanism.

Epigenetic mechanism of neural stem cell regulation

NSCs multipotentiality is tightly regulated by DNA methylation. In early NSCs, astrocytic gene promoters are hypermethylated, thus blocking the access of the STAT3-p300／CBP-SMADs complex to its target sequence and thus prevent astrocytes differentiation (Takizawa et al. 2001). Later on, demethylation occurs and allows expression of astrocytic gene expression (Hatada et al. 2008). The most likely mechanism for DNA demethylation is the passive loss of CpG methylation due to successive rounds of DNA replication in the absence of DNMT1 methylase activity (Bestor 2000).Indeed, After conditional deletion of DNMT1 in NSCs lead a precoce astroglial differentiation (Fan et al. 2005).

The chromodomain protein family in neural stem cell

The Chromodomain Helicase DNA binding (CHD) gene family is a group of 9 chromatin reader proteins defined by the presence of two N-terminal chromodomains (chromatin modifier domain) and a sucrose non-fermenting (SNF2)-like helicase/ATPase associated with nucleosome remodeling (Feng, Weijun, 2013). Chromodomains mediate chromatin interactions through the direct binding of DNA and methylated histone H3 (Akhtar et al. 2000, Bouazoune et al. 2002, Fischle et al. 2003, Min et al. 2003, Brehm et al. 2004, Flanagan et al. 2005, Pray-Grant et al. 2005, Sims et al. 2005, Kim et al. 2006). The CHD family is further divided into 3 groups (Hall & Georgel 2007, Marfella & Imbalzano 2007). The group 1 is composed of CHD1/2 and which share 2 chromodomains, a SNF2-like helicase/ATPase domain and DNA-binding domains with a divergent N-terminus. The group 2 is composed of CHD3/4/5 and shares two N-terminal PHD zinc finger domains involved in chromatin remodeling (Eberharter et al. 2004, Ragvin et al. 2004, Pena et al. 2006, Shi et al. 2006, Sims & Wade 2011). The group 3 contains CHD6/7/8/9 and share two BRK domains (Brahma and Kismet domain) with unknown function and a SANT domain (Switching-

defective protein 3, Adaptor 2, Nuclear receptor corepressor, Transcription factor IIIB) which bind histone tails (Janssen et al. 2012; Boyer et al. 2004, Hall & Georgel 2007). CHD1 has been shown to assemble and slide nucleosomes (Lusser et al., 2005; Stockdale et al., 2006), and to associate with factors involved in transcription and centromeric maintenance (Simic et al., 2003; Walfridsson et al., 2007; Konev et al., 2007; Okada et al., 2009). Chd1 has a crucial role in regulating ESC pluripotency thanks to its ability to bind to H3K4me3 (Gaspar-Maia et al., 2009, Flanagan et al., 2005; Simic et al., 2003). CHD3 and CHD4 are members of the ~~"n~~ucleosome remodeling and deacetylase" (NuRD) complex (McDonel et al., 2009). The histone deacetylation activity of NuRD complexes was shown to facilitate the recruitment of PRC2 (polycomb repressor complex 2) mediating the deposition of inhibiting H3K27me3 marks (Reynolds et al., 2012). Chd4 is necessary for the localization of Ezh2, the enzymatic subunit of PRC2 and specifically inhibit astrocyte differentiation (Sparman et al 2013). However, recent studies also showed that CHD3/4 proteins were able to activate transcription (Reynolds et al., 2013, Hu and Wade, 2012). As CHD4, CHD5 has been shown to bind unmodified H3K4 (Musselman et al., 2009; Paul et al., 2013). CHD5 is predominantly expressed in the adult CNS in neurons of the neocortex, but is absent in astrocytes and oligodendrocytes (Garcia et al., 2010; Potts et al., 2011). CHD5 is a tumor-suppressor gene expressed in differentiating neurons (Brodeur, 2003; Okawa et al., 2008; Bagchi et al., 2007, Fujita et al., 2008, Garcia et al., 2010) and is able to bind to H3K27me3 to activate neuronal differentiation and the repress Polycomb target genes (egan et al 2013). Since the discovery that CHD7 mutations lead to CHARGE syndrome in human, numerous studies have investigated its function. Several animal models for CHARGE syndrome were created (Siebert et al. 1985, Bergman et al. 2005, Hurd et al. 2007, Bajpai et al. 2010, Schnetz el al. 2010, Zentner et al. 2010, Patten et al. 2012). CHARGE syndrome is an autosomal dominant disease caused by CHD7 mutations (Vissers et al. 2004). ~~"C~~HARGE" is an acronym for Coloboma, Heart malformation, Atresia of the choanae, Retardation of Growth and development and Genital anomalies which describe the main clinical symptoms (Pagon et al. 1981, Blake et al. 1998, Jongmans et al. 2006, Lalani et al. 2006, Bergman et al. 2011b). Anomalies of ear (90-100% of patients with CHD7 mutation), ocular coloboma and/or microphthalmia (80-90%), cranial nerve dysfunction, swallowing and

breathing difficulties (70-90%) are the major signs of CHARGE syndrome (Blake et al. 1998). Other symptoma could also reflect a CHARGE phenotype such as genital anomalies, growth retardation, congenital heart defects, and facial dysmorphism (Horsch & Scheele 2011). Later on, other criteria were included as hallmark for CHARGE syndrome (coloboma, choanal atresia, semicircular canals anomalies, rhombencephalic anomalies, hypothalamic-hypophyseal dysfunction, external/middle ear malformations, malformation of viscera, and mental retardation (Verloes 2005). Mutant mice for Chd7 develop many of the features observed in patients with CHARGE syndrome and mice that are homozygous for such mutations die at embryonic day 10.5 (Bosman et al. 2005; Hurd et al. 2007). CHD7 is composed of 38 exons spanning 188kb. CHD7 is highly conserved across evolution (Bosman et al. 2005, Aramaki et al. 2007, Shrinivasan et al. 2008, Bajpai et al. 2010). Mutations in the CHD7 gene lead to different form of the disease. Nonsense and frame shift mutations (75%), missense and splice site mutations (20 %) and more rarely, chromosomal rearrangements are found in CHARGE syndrome patients (Janssen et al. 2012). CHD7 mutations are detected in 60% of patients when using the criteria of Blake et al. (1998) and/or Verloes (2005) but mutation in other genes can trigger CHARGE syndrome (Jongmans et al. 2006, Lalani et al. 2006, Bergman et al. 2011a). Genetic heterogeneity in CHARGE syndrome could come from mutations in CHD7 interaction partners. The majority of CHARGE patients display mental retardation associated with olfaction deficit and anomalies of the olfactory bulb (Blustajn et al., 2008; Bergman et al., 2011). Moreover, CHARGE patients also develop autistic behavior (Hartshorne et al., 2005). Interestingly, mutation in CHD8, a protein which can physically interact with CHD7 (Batsukh et al., 2010) was identified as one of the major genetic causes of autism spectrum disorder (Neale et al., 2012; O'Roak et al., 2012; Talkowski et al., 2012). Functional studies showed that CHD7 binds predominantly to methylated histone H3K4 in a cell type and stage specific manner (Schnetz et al., 2009, 2010; Heintzman et al. 2009, Flanagan et al. 2005; Srinivasan et al. 2008). Moreover, it has been shown that CHD7 cooperates with PBAF (polybromo and BRG1-associated factor-containing complex) to regulate neural crest differentiation and migration through activation of Sox2, Slug, and Twist (Bajpai et al., 2010). Interestingly, Kismet, the drosophila ortholog of CHD7 regulates transcription by recruiting the TRX (Trithorax) histone

methyltransferases (Srinivasan et al. 2008). In the mouse brain, CHD7 and Sox2 are able to form a complex that cooperatively activates target genes that are essential for the development of neural stem cells (Engelen et al. 2011). A recent study showed that Chd7 is enriched in active NSCs and progenitors in the SVZ and SGZ of adult mice (Feng et al, 2013). This study showed that a NSCs specific conditional mutation of Chd7 leads triggers defects in adult neurogenesis. Indeed, loss of Chd7 in NSCs impedes the methylation of H3K4me1/3 in promoters of Sox4 and Sox11, two neuronal differentiation factors (Bergsland et al., 2006; Mu et al., 2012), thus inducing transcriptional repression by inhibitory chromatin remodeling of their promoters. In-situ hybridization and immunostaining data show that Chd7 is highly expressed in adult SVZ, RMS and SGZ regions of the mouse brain and in cells co-expressing GFAP, Mcm2, Nestin and Sox2, indicating that Chd7 is expressed in a subpopulation of dividing NSC. Moreover, most of Ascl1 and DCX positive cells express Chd7 thus showing Chd7 persistent expression in neural progenitors and neuroblasts. Using a Chd7 conditional knockout mouse line ($Chd7^{fl/fl}$) injected with BrdU and traced for 4 weeks showed a dramatic decrease of BrdU-positive cells and newborn DCX positive neurons in the olfactory bulb of Chd7 mutants. Interestingly, no changes were observed in Nestin and Sox2 positive cells in the SVZ of Chd7 knock-out mice, showing no direct effect on NSCs. Moreover, no significant difference of BrdU incorporation or Ki67 staining was observed in Chd7 mutants SVZ compared to control. Thus, loss of Chd7 impairs neurogenesis in the SVZ-OB without affecting the self-renewal of NSCs more likely indicating that Chd7 is required for the neuronal differentiation of NSCs (Feng, Weijun, 2013). Indeed, the number of transit amplifying cells marked by Ascl1 positive cells number was increased in Chd7 mutants suggesting an impairment of neuronal differentiation program. Indeed, Sox4 and Sox11, both necessary to the final differentiation of neurons were shown to be directly activated by Chd7 (Mu et al 2012). Finally, an increase of cell death of Chd7 mutant cells was observed thus suggesting that Chd7 mutant cells undergo apoptosis when unable to properly differentiate (Mu et al 2012). These important results bring to light the mechanism leading to the olfactory bulb and inner-ear defects and may explain some aspect of associated mental retardation and autistic behavior in CHARGE syndrome.

Direct reprogramming of fibroblasts to neurons and oligodendrocytes

Cellular reprogramming is a new emerging research field in which somatic cells can be turned into induced pluripotent stem cells (iPS cells) or other somatic cell types by the expression of specific combinations of genes (K Takahashi, 2006; Vierbuchen et al., 2010).

In this paradigm, Ascl1 was recently shown to be sufficient to directly convert mouse fibroblasts into induced neurons (iN) in-vitro and in-vivo (Vierbuchen et al., 2010; Torper et al., 2013). However, the addition of Brn2 and Myt1l (BAM factors) significantly improve the conversion efficacy and results in a full maturation of neuronal characteristics (Vierbuchen et al., 2010). Interestingly, the BAM factors are able to converts human fibroblasts into iN but need the addition of NeuroD1 or Zic1 to achieve similar efficacy. Moreover, dephosphorylated Ascl1 significantly promotes neuronal maturity in human fibroblast converted in neurons (Pang et al., 2011; Barker RA 2014). Stricklingly, most of the iN cells induced by the BAM factors are glutamatergic neurons and not GABAergic as expected based on physiological condition studies (Vierbuchen et al., 2010). While combinatorial use of Ascl1 and Neurog2 generate a mixtures of glutamatergic and GABAergic neurons (Ladewig et al., 2012), the combination of Ascl1 and Sox2 predominantly converts cells into GABAergic neurons (Karow et al., 2012). Other direct lineage reprogramming approaches have succefully generated dopaminergic neurons using Ascl, Nurr1 and Lmx1a (Caiazzo et al., 2011; Pfisterer et al., 2011), motoneuron using BAM, Lhx3, Hb9, Isl1, and Neurog2 (Son ey 2011) or oligodendrocyte precursor cells (OPCs) using Olig2, Sox10, Nkx6.2 or Zfp536 (Najm et al., 2013; Yang N, Zuchero JB2013). For NPCs, Direct conversion was shown using only one factor, Sox2 (Ring KL 2012), but improved yield was obtained using Sox2, Fo0xG1, Brn2/4, Klf4, E47 and c-Myc (E Lujan 2012, M Their 2012, DW Han 2012).

Interestingly, BAM factors are able to directly convert cells from different embryonic layer origin into iN (Marro S 2011). Indeed, recent genomic analysis of direct conversion by the BAM factors revealed the __pionеer factor‘‘ activity of Ascl1which is able to bind to its direct target and activate their expression irrespective of whether genomic sites are in nucleosome depleted region or nucleosome bound. In this study, a

specific histone marks (H3k4me1, H3k27ac and H3K9me3) was shown to favor Ascl1 access to its target sites (Wapinski et al., 2013).

Hoewever, protocols for direct cellular reprogramming based on overexpressing lentiviral vectors have really low efficiency (1-10%). As described above, the expression dynamic of those factors is critical for self-renewal, multipotency, and fate choice of NPCs (Imayoshi et al., 2013) and lentiviral vectors have only constitutively active promoters. Thus, new reprogramming protocols that control the range and mode of expression are now necessary to improve the low conversion efficacy of direct cellular reprogramming of neural cells. Moreover, the underlying mechanisms by which these reprogramming processes can be induced by just a small number of transcriptional factors remain largely unknown. To improve the efficacy and purity of direct reprogramming to neurons, it is essential to fully characterize the mechanisms by which reprogramming factors, including Ascl1 contribute to this process.

CHAPTER III: Oligodendrogenesis and myelination

Oligodendrocyte development comprises specification of oligodendrocyte precursor cells (OPCs) from NSCs and OPC differentiation into immature and mature myelinating oligodendrocytes (for review Rowitch D 2004, 2010 ; Gallo V 2014; Emery, 2010b; Liu and Casaccia, 2010; Meijer et al., 2012).

Myelination of the central nervous system

The term „myelin‘ (Greek word for „marrow‘, myelos), was first used by Rudolf Virchow in 1864 who was thinking that myelin was secreted by neurons. A century later, Pio del RioHortega revealed that myelin is actually formed as an extension of the plasma membrane of oligodendrocytes, a jawed-vertebrate specific cell type (Zalc et al 2008). Since, much progress has been achieved in the understanding of the myelination process (for review, see Mitew et al., 2013; Piaton et al., 2010; Taveggia et al., 2010; Simons and Lyons, 2013; Fancy et al., 2011; White and Kramer-Albers, 2014) . Indeed, myelin is now known to be a multi-layered lipid sheet periodically wrapped around neuronal axons and provide axonal insulation necessary for a rapid –saltatory

conduction" of the action potential (Lillie 1925; Tasaki 1939; Huxley and Stämpfli 1949), limit ephaptic conduction (Arvanitaki, 1942; Smith, K. J., and McDonald, W. I. 1999) and avoid the action potential conduction block observed in demyelinating disease (Davis FA. 1970; Rasminsky and Sears 1972). Moreover, myelin has been shown to sense axonal energy demands and provide an important trophic support to the neuron (Lee et al., 2012; Nave and Trapp, 2008, Nave 2010) for the high energy cost of fast electrical signaling (Attwell, D. & Laughlin, S.B 2001) and for axonal long term maintenance (Griffiths I, Klugmann M,1998). Axon myelination minimizes the membrane capacitance that has to be charged to trigger action potentials, thus reducing the metabolic cost of electrical signaling (Hartline , D. K. , and D. R. Colman . 2007). However, when taking into account the production of myelin and maintainance of the resting potential of oligodendrocytes, myelination has an overall positive energy cost (Harris JJ, Attwell D, 2012). Instead, myelin seems to be an evolutionary adaptation that allowed vertebrate to deal the need for a rapid information processing associated with large nervous systems and body (Zalc 2008). Indeed, myelination results in a 10 to 100-fold increase in nerve conduction velocity (Franz , D. N., A. Iggo . 1968, Waxman , S. G. 1980) reaching 100m/s.

Direct observation of myelination has been possible with the development of electron and light microscopy (Maturana, 1960; Peters, 1960a; Mobius et al., 2010). In mice, myelination starts postnatally and is almost completed at postnatal day 60 (P60) in most brain regions (Baumann and Pham-Dinh, 2001). We now know that myelin thickening is achieved with a single filipodia making axonal contact that spirally encircle the future internode and wrap the leading edge at the inner tongue around the axon forming microfilament-rich lamelipodia, underneath the previously deposited membrane, together with the lateral extension (Snaidero 2014). A growth zone at the inner tongue requires transport of newly synthesized membrane constituents from the soma through the oligodendroglial process. To this purpose, cytoplasmic channels transporting vesicules provides a connection from the outer and inner tongue of myelin. Present at the peak of myelination (postnatal day 10-15, P10-P15), cytoplasmic channels are almost absent at P60 when myelination is over (Snaidero 2014). The compaction of the myelin layers is achieved by myelin basic protein (MBP) and starts after only a few wraps (Readhead et al., 1987). Whereas membrane growth occurs

close to the axon at the innermost region of the myelin sheath, compaction starts in the outermost layers and progresses inward. MBP is the major cytoplasmic component, and its mRNA is transported in cytoplasmic granules to myelin (Colman et al., 1982) whose movements are oriented thanks to PI(3,4,5)P3 lipid signal activating the Rho GTPases at the leading edge of the innermost layer (Ridley, 2011). MBP protein is synthesised at the innermost layer close to the axon and is regulated by axonal signals such as electrical signal, neurotransmitters, ATP, ions, or growth factors (Colman et al., 1982; Barres and Raff, 1993; Demerens et al., 1996; Fields and Stevens-Graham, 2002; Wake et al., 2011; Laursen et al., 2011). Even if MBP is synthesized in innermost layers, compaction is not fast enough to keep up with the rapid extension of the myelin sheath (Snaidero 2014). Indeed, oligodendrocyte can make new myelin sheaths in only five hours (Czopka et al., 2013). Thus, MBP is synthesized close to the axon and diffuse backward to the outermost area at which compaction is initiated. MBP serves to bind two adjacent membranes by polymerizing into a fibrous network and establish an anchor point for myelin membrane zippering (Aggarwal et al., 2013). In the absence of CNP, myelin compaction occurs faster and extends to the inmost layers of the myelin sheath (Snaidero et al., 2014). Oligodendrocytes can myelinate up to 80 small-diameter axons or fewer long-calibre axons (Murray and Blakemore, 1980; Matthews and Duncan, 1971; Hildebrand et al., 1993). In-vitro, myelination occurs spontaneously when oligodendrocytes are cultured with axon-mimicking inert polystyrene tube with a diameter up to 4 mm (Lee S et al., 2012). In-vivo, oligodendrocytes are able to myelinate axons of a diameter from 0.2µm to ~1mm (Remahl and Hildebrand, 1982; Waxman and Bennett, 1972). The ratio of the inner axonal diameter to the total outer diameter (gratio) is used as an index of optimal axonal myelination. Theoretical considerations have shown that axons have an optimal g-ratio of 0.6. If myelin thickness deviates from this value, conduction velocity drops (Waxman and Bennett, 1972; Chomiak and Hu, 2009). Similar considerations apply for the internodal length. A linear relationship exists between the axon diameter, the number of myelin sheaths and the internodal length (Murray and Blakemore, 1980; Hildebrand and Hahn, 1978). For example, the increase in the diameter of the axon from 1 to 15 µm involves a lengthening of the internode from 100 to 1500 µm.

However, the maximum conduction velocity is reach at 600µm internodal distance (Waxman, 1997; Wu, L. M., Williams, A. et al., 2012).

Myelin is regulated by experience both during development and in adult life (Liu J Dietz et al., 2012; Mangin JM et al., 2012). Indeed, mice socially isolated between P21 and P35 show myelin defects driven by decreased neuregulin-1/ErbB3 signaling. Moreover, this time frame is important and constitutes a critical period, as mice isolated before or later does not develop such defects (Makinodan et al., 2012). Interestingly, neuronal overexpression of Nrg1 increases the thickness of myelin sheaths of myelinated axons and drive myelination of small calibre axons that would not be myelinated in wildtype (Brinkmann BG, 2008).

Functional organization of myelinated axons

To fulfill those functions, myelination structures the axons in different areas: i) The axon initial segment (AIS), an unmyelinated thin region where ion channels are clustered and action potentials are initiated; ii) the node of Ranvier, where sodium channels are clustered and action potentials are propagated (Kole MH, Stuart GJ 2012); iii) the paranode, where myelin tightly contact the axon; iv) the juxtaparanode, where potassium channels are clustered below the myelin sheath and v) the internode, the region between two node of Ranvier where the Na/K-ATPases are located (Young EA, Fowler CD 2008; Buttermore E 2013). The wrapping of oligodendrocyte stabilize the clustering of axonal Nav1.1 and Nav1.6 sodium channels at nodes of Ranvier and the Kv1, Kv3 and Kv 7 potassium channels at the paranode (Buttermore E 2013). Interestingly, clustering of Nav channels at the node of Ranvier occurs before myelination (feinberg et al. 2010)

Lipid composition of myelinating oligodendrocytes

Myelin is characterized by an unusual high lipid to protein ratio (Chrast R2011). Indeed, compared to other cells where around 30% of the dry weight consists

of lipids, myelin possesses more than 70% of lipids. Among the 700 lipid moieties identified by recent lipidomics studies (Gopalakrishnan G2013), three main classes are identified: phospholipids account for ~40%, glycosphingolipids for ~30%, and cholesterol for ~30%. (Gopalakrishnan G2013; Chrast R2011). More specifically, galactocerebrosides are the most abundant component of myelin, sulfatide (sGalCer) representing almost 20% alone. Phosphatidylethanolamine (plasmalogens) and Phosphatidylcholine (lecithin) are also major constituent, representing 16% and 12% respectively. Sphingomyelin, a minor component, associates with cholesterol in ~~–~~lipid rafts" and are involved in many processes, such as protein and lipid sorting or cell signaling (Dupree JL, 2010; K. Simons, D. Toomre 2001)

Interstingly, despite their abundance, glycosphingolipids are not essential for myelination. Indeed, mutant mice for CGT (UDP-galactose:ceramide galactosyltransferase) and CST (galactosylceramide 30 -sulfotransferase), two enzymes essential their synthesis, does not prevent formation of compact myelin sheaths despite paranodal and axonal defects (Coetzee T, Fujita 1996).

Paranodal disruption was shown to be partly due to the lack of SGalCer, since mice lacking galactosylceramide-3-Osulfotransferase (Gal3st1), the enzyme converting GalC into SGalC (Honke K, Hirahara Y, 2002– Hirahara Y, Bansal R2004), also showed nodes defects. Finaly, mice lacking Fa2h (fatty acid 2-hydroxylase), the enzyme hydroxylating GalC and SGalC showed important delay in myelination (Zoller I, Meixner M 2008). Together, these results highlight the importance of lipid synthesis and lipid signaling in oligodendrocytes metabolism and demyelinating diseases, a question that only begin to be tackled (Aggarwal 2011 ; Podbielska M 2011).

Structural and functional organization of myelin

Protein composition of myelin

Transcriptome microarray analysis of all the neural cell types in the brain released publicly data for the oligodendrocyte lineage in which purified PDGFRα+ (OPCs), GalC+ (pre-myelinating OLs) and MOG+ (myelinating OLs) are available. However, this study focused principally on astrocyte development and did not

exhaustively analysed the oligodendrocyte lineage (Cahoy JD et al 2008). Another study following the same cell purification protocol and allowed the identification of critical factors involved in myelination such as MRF (Emery B 2009). As those datasets are made available publicly on GEO database, they are now used by many others to analyse oligodendrocyte lineage and allow identification new critical factors (Monasterio-Schrader 2012). To date, mass-spectrometry is the most sensitive method to systematically identify the protein content of myelin. Up to now, eight proteomic studies of CNS myelin have been published, providing 11 datasets for myelin from mouse (Jahn O, Tenzer S 2009 Werner HB et al 2007; Vanrobaeys F et al 2005; Taylor CM et al 2004), Rat (Roth AD, Ivanova A, Colman DR 2006; Baer AS et al 2009), and human (Ishii A et al 2009; Dhaunchak AS et al 2010). The integration of all myelin proteomic datasets identified more than 1,280 proteins (Monasterio-Schrader 2012). Among them, the main myelin proteins identified are PLP/ DM20 (proteolipid protein) representing 17% of the protein content, MBP (myelin basic protein) representing 8% and CNP (2',3'-Cyclic-nucleotide 3'-phosphodiesterase) representing 4% (Monasterio-Schrader 2012). Other major compact myelin proteins are MOBP (myelinassociated oligodendrocytic basic protein), MAL (myelin and lymphocyte protein), MOG (myelin oligodendrocyte protein), MAG (myelin associated glycoprotein) representing each around 1% of the total protein content (Monasterio-Schrader 2012).

Plp1 (proteolipid protein) is the most expressed gene in myelinating oligodendrocyte (Eng et al. 1968; Norton and Poduslo 1973), but is also expressed in OPCs (Gudz et al., 2006), neurons (Bongarzone et al., 1999; Jacobs et al., 2003, 2004), neural precursors (Spassky et al., 1998; Delaunay et al., 2009) and non-neural cells (Campagnoni et al., 1992; Skoff et al., 2004a) suggesting other functions unrelated to myelination. PLP mutant mice triggers demyelination and premyelinating OL apoptosis (Knapp et al., 1986; Boison and Stoffel, Bongarzone et al., 2001). PLP has also been involved in the regulation of ion homeostasis Gudz et al., 2006), cell migration, proliferation, differentiation (Harburger and Calderwood, 2009) and OL apoptosis. Interestingly, PLP overexpression triggers acidification and mitochondrial dysfunction and reductions in ATP levels (Hüttemann et al., 2009). DM20, its isoform generated by alternative splicing lacks an internal 35 amino acid region and is expressed in neural tube OPCs but also in the heart or thymus (Macklin et al. 1987; Nave et al. 1987;

Simons et al. 1987; Campagnoni et al., 1992; Pribyl et al., 1996a,). PLP functions as an adhesive protein between two layers of the myelin sheath and it is involved in its compaction by conferring structural stability (Gow et al. 1997). PLP/DM20 is also involved in oligodendrocyte-neuron interactions (Yool et al. 2001), signaling (Gudz et al. 2003), and apoptosis regulation (Skoff et al. 2004; Heuttemann et al. 2009).

The MBP gene is very large (>100 kb) and generate mRNAs from different start site for classic oligodendrocyte-specific MBPs and peripheral golli MBPs (Campagnoni et al., 1993; Pribyl et al., 1993). The classic isoforms of MBP generate the 14 and 18.5-kDa isoforms which facilitate compaction of the myelin sheath, as well as the cytoplasmic and nuclear 17 and 21.5-kDa isoforms in pre-myelinating OLs (Allinquant et al., 1991; Hardy et al., 1996; Pedraza, 1997). MBP isoforms interact with Ca2+-CaM (calmodulin), actin, tubulin and SH3 domain (Src homology 3 domain)-containing proteins (Harauz and Libich, 2009). Morevover, Golli MBP isoforms are found in pre-myelinating OLs within cell processes surrounding axons (Pribyl et al., 1996). Overexpression of golli proteins can induce processes growth and OLs maturation (Reyes and Campagnoni, 2002) and OPC Ca2+ -mediated migration (Paez et al., 2009a). *MBP* mutant mice (*shiverer* mice) shows demyelination and myelin compaction defects (Privat and al. 1979). MBP binds to negatively charged lipids on the cytosolic surface of the OL membrane through electrostatic interactions (Boggs and Moscarello, 1982; Boggs et al., 1982) and are present in compact internodal myelin (Omlin et al., 1982; Kirschner and Blaurock, 1992). MBP is involved in microtubule stabilization (Dyer et al. 1994) and form a physical barrier, preventing the diffusion of proteins in large cytoplasmic domains (such as PLP, CNPase, MAG or Tspan2) to favor their integration in compact regions of the myelin (Fitzner et al., 2006. Aggarwal et al, 2011; Zuchero and Barres, 2011; Aggarwal and al., 2013) .

CNPase is a cytosolic membrane-anchored enzyme present in non-compact myelin (Drummond GI, I 1962 Trapp BD, Bernier L, 1988). Despite its ability to convert 2′,3′-cAMP into adenosine, the function of CNPase in myelin is still obscure. *CNPase* mutant mice display premature death through axonal swelling, while maintaining a normal myelin morphology. Conversely, CNPase overexpression results in oligodendrocyte process and myelin compaction defects and appear to be an auto-antigen in MS (Rösener M 1997 Lovato L, Cianti R, 2008). Thus, CNPase seems to

play a role in axonal maintenance after myelination, possibly through neuroprotection arising from a major contribution to the hydrolysis of 2′,3′-cAMP produced within myelinated axons (Verrier J, Jackson T 2012 Lappe-Siefke C2003)

Glial network in brain energy metabolism and axonal support

The brain is only 2% of the body‘s mass, but requires 20% of its energy consumption (Sokoloff, 1960). Based on the estimated energy consumption of each cell type, it is predicted that the majority ~70% should occur in neurons while the remaining ~30% should take place in glial cells (Attwell and Laughlin, 2001). In the cortical neurons, while housekeeping energy used on non-signaling tasks (macromolecules turnover, transport and mitochondria) accounts for 25% of the total enegy consumption, signaling energy account for 75%. Signaling energy could be divided as follow: while 50% of the energy is used for postsynaptic receptors, 21% is used for action potentials, 20% on resting potentials, 5% on presynaptic events, and 4% on neurotransmitter recycling (Attwell and Laughlin, 2012). Thus, action potentials account for a significant part of the consumed energy and thus need a corresponding supply. In optic nerve for example, action potentials consume ~6.10^{12} ATP/s on unmyelinated axons and ~$1.5.10^{11}$ ATP/s on myelinated axons (J Harris and D Attwell 2012) and most of the ATP is used for pumping of Na+ ions out of cells (Siesjo, 1978; Attwell and Laughlin, 2001). Indeed, in the neurons, action potentials cause a massive sodium entry at the nodes of Ranvier and a release of potassium below the oligodendrocyte membrane at the juxtaparanode (J.E. Rash 2010). Na+/K+-ATPases and mitochondria, located along the internodal region, are dedicated to the maintenance of membrane potential maintenance and to fit the high energetic demand of the axon, respectively (E.A. Young, C.D. Fowler,2008; N. Ohno, G.J. Kidd, D 2011). Thus, the highest energy requirements seems to occur along the internode and not at the node of Ranvier (Saab A 2013).

Astrocytes are the first metabolic support of neurons. Indeed, precise in-vitro and in-vivo metabolic analysis demonstrated that blood glucose is preferentially taken up by astrocytes which realease lactate to neurons by the ~~l~~actacte shuttle” mechanism

(Pellerin and Magistretti,1998, 2003) and that neurons preferentially use lactate as their main oxidative substrate (25% of glucose and 75% of lactate) (Bouzier-Sore et al., 2006). However, in myelinated fibers, axons are almost completely covered by myelin and evidence of axonal glucose transporters (GLT1/2) at the nodes of Ranvier or direct lactate transfert by perinodal astrocytes are lacking (K.A. Nave 2010). Interestingly, perinodal astrocytes can recycle neuronal mitochondria in a process called ―transmitophagy" (Davis CH, Kim KY 2014). Moreover, perinodal astrocytes and oligodendrocytes can form a glial (O/A) network through gap junctions in the cortex and optic nerve, (D.M. Menichella 2003). Gap junctions are channels formed of homo or heterotypic connexin hemichannels which are permeable to molecules smaller than 1.2 kDa, including ions, cyclic nucleotides, ATP, neurotransmitters and small metabolite such as glucose and lactate (Reyes EP 2014; L Hertz 2014). Oligodendrocytes express Cx47, Cx32, and Cx29 (Menichella et al., 2003, Dermietzel et al., 1989; Altevogt and Paul, 2004). Astrocytes express Cx43, Cx30 and Cx26 (Mercier and Hatton, 2001; Nagy et al., 2001). Oligodendrocytes are bidirectionaly coupled to astrocytes thanks to Cx47/Cx43 and Cx32/Cx30 heterotypic channels in the cortex (D.M. Menichella 2003, Wasseff 2011). However, in the corpus callosum, where only a few astrocytes reside, only oligodendrocyte to oligodendrocyte couplings occurs through Cx47/ Cx32 (Wasseff 2011, M. Maglione, 2011). Interestingly, Cx32/Cx47 mutant mice have no O/A or O/O coupling and exhibit a severe demyelination phenotype with myelin vacuolization phenotype, seizures, conduction block and increased oligodendrocytic input resistance typical of potassium homeostasis problems (D.M. Menichella 2003; M. Maglione, 2011). Similarly, in Cx43/Cx30 mutant mice, O/A coupling is disrupted and lead to vacuolization and myelination defect (S.E. Lutz, Y. Zhao 2009; A. Wallraff, R. Kohlin 2006). Those studies demonstrated that such O/A or O/O networks are involved in the buffering of the potassium generated at the periaxonal space (below the myelin membrane) through a mechanism called potassium syphonning (D.M. Menichella 2006).

An important question remaining to answer is how myelin may be directly beneficial for maintenance of the axon integrity. Many transgenic models allowed to tackled this question. *Shiverer* mice (*MBP* mutant mice) do not show axonopathy despite absence of compact myelin (Rosenbluth, 1980a,b; Griffiths et al., 1998). In the EAE

demyelinating model, early axonal defects occurs before myelin disruption (Nikic I, Merkler D, 2011). In contrary, *Plp1* null mutant mice develop progressive widespread axonal degeneration, with axonal transport defects, swellings (Klugmann M, Schwab MH, 1997). Similarly, *Cnp1* mutant mice develop progressive axonopathy and die prematurely despite normal myelination (Edgar JM, McLaughlin M, 2009). In another study, the specific ablation of oligodendrocytes by diphtheria toxin (DT) showed axon degeneration with axon damages occuring without complete demyelination and without involvement of inflammatory processes (Ghosh et al., 2011a; Pohl et al., 2011; Oluich et al., 2012). Thus, myelination and axonal support are not correlated but rather are two independent mechanisms, and oligodendrocytes play additional functions to just axonal myelination involved in axonal maintenance and energetic support.

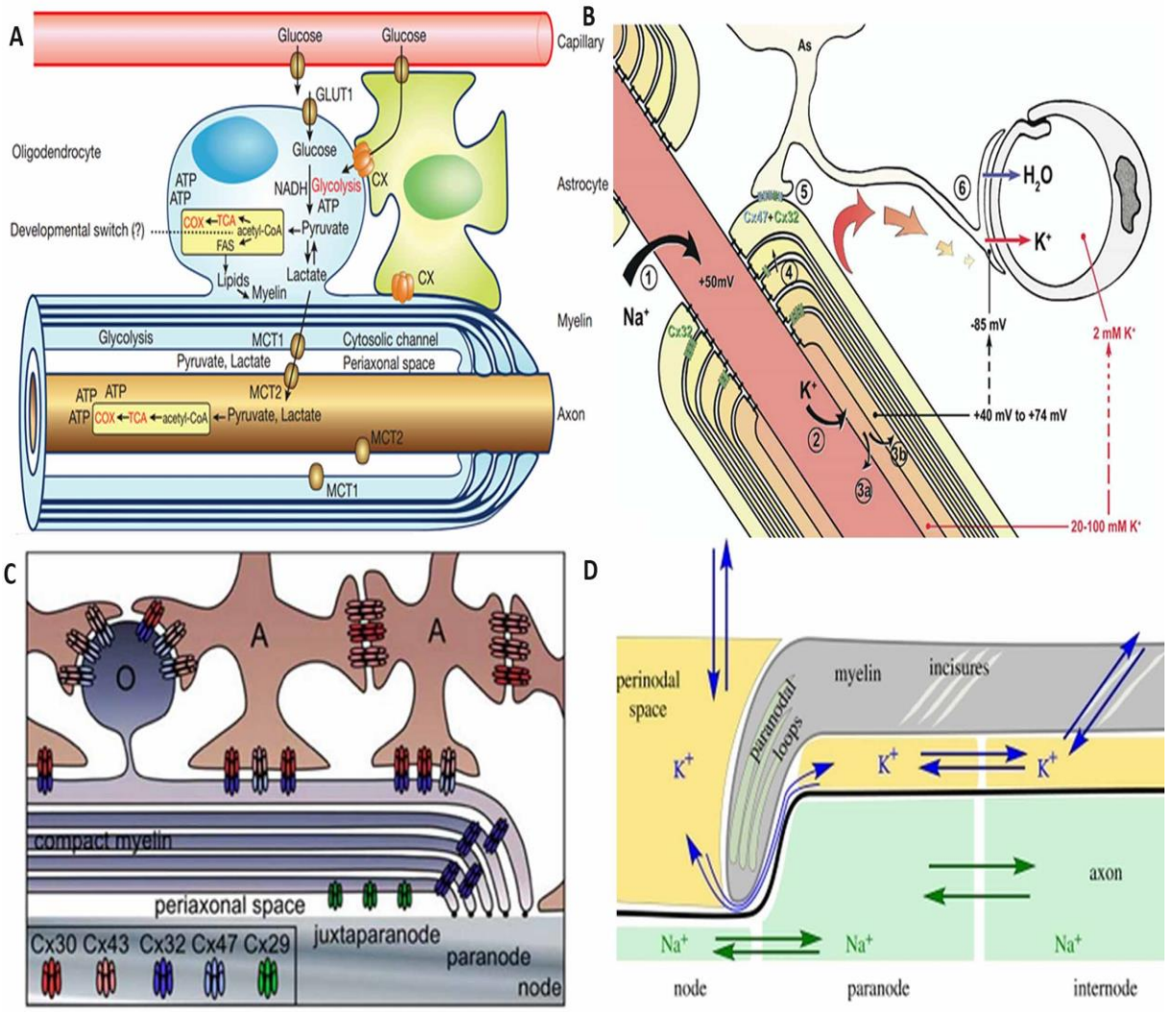

Figure 20. Glial metabolic network. A. This model of metabolic coupling between oligodendrocytes and axons shows oligodendrocytes glucose import through GLUT1, astrocytes and gap junctions. Pyruvate is metabolised in mitochondria for ATP generation. glucose serves the synthesis of fatty acid and support oligodendrocyte survival. Lactate and pyruvate can be directly transferred to axons via monocarboxylic acid transporters (MCT1, MCT2), which reside between the internodal myelin and the axonal compartment. B. Role of myelin in potassium clearance. Schematic representing myelinated axons isolated from the extracellular space by a thin periaxonal space from the oligodendroglial cytoplasm filling the inner loops of myelin (_cytosolic channel‘) and paranodal loops. Electrochemical gradient of K+ allow potassium to be released in the periaxonal space and to the oligodendrocyte via the gap junction network.C. Connexin nextwork. Schematic showing specific homo and heterometic connexin coupling. Oligodendrocyte is coupled to Astrocyte, oligodendrocyte and OPCs by gap junction.

Oligodendrogenesis throughout development

Transcriptional control of oligodendrocyte progenitor cells specification

Glial progenitor cells that give rise to oligodendrocytes were first identified in cultures of developing rat optic nerve cells as O-2A, a bi-potent progenitor able to generate oligodendrocyte and type-2A astrocyte (Raff et al., 1983). In the developing forebrain, generation of OPCs that will populate the entire brain and differentiate into myelinating oligodendrocytes occurs in ventro-dorsal and antero-posterior waves from separate domains (Kessaris et al., 2006). The anterior entopeduncular area (AEP) and the medial ganglionic eminences regions (Nkx2.1 positive) start to specify OPCs from E12.5 (Spassky et al., 2001; Tekki-Kessaris et al., 2001. Olivier, C. et al. 2001). As development progresses, the lateral and caudal ganglionic eminences (Gsh2 positive) generate OPCs from E15.5 and postnataly, the cortex (Emx1 positive precursors) start to produce OPCs (Tekki-Kessaris et al., 2006). All OPCs migrate from the VZ to populate the entire telencephalon. OPCs constitute the main proliferative population in the adult brain and around 5% of the total cell population of the brain (Levine et al., 2001; Dawson et al., 2003). Interestingly, Nkx2.1-derived OPCs are rapidly eliminated during postnatal life but if Nkx2.1, Gsh2 or Emx1 OPCs waves are ablated through

conditional deletion, the remaining OPCs quickly expand to regenerate a normal number of cells in the mature sebrain (Kessaris et al., 2006). A small proportion of OPCs generated during development are maintained throughout aldulthood as an immature slowly proliferative or quiescent state (Dawson et al., 2003). OPCs density is strickingly even in the adult brain even if a higher proliferation rate is observed in the white matter (Dimou et al., 2008). Indeed, while OPCs in the white matter are proliferative and differentiate into myelinating oligodendrocytes, gray matter OPCs are quiescent or slowly proliferative (Dimou et al., 2008). Despite regional expression marker differences, adult OPCs express the same markers as embryonic OPCs (Franklin and Ffrench-Constant, 2008). Known OPCs markers are proteoglycan NG2 (Nishiyama et al., 1999) and the platelet derived growth factor receptor α (PDGFRα), the O4 antigen and the transcription factors Olig2, Olig1, Nkx2.2 and Sox10 (Fancy et al., 2004). In the embryonic spinal cord, the ventral Olig2 pMN domain of the spinal cord generate sequentialy motoneuron and OPCs ((Pringle et al., 1996 and Lu et al., 2000). However, it is now recognized that spinal oligodendrocyte also have a dorsal origin from domains dP3-6 starting at E15.5. Indeed, Nkx6.1/Nkx6.2 double mutant mice, in which OPCs are lacking due to impaired Olig2 expression, are still producing OPCs in the dorsal spinal cord (Cai et al., 2005; Vallstedt et al., 2005). Embryonic dorsal OPCs arise from different domains and represent around 15% of dorsal OLs and are also generated later in development (Fogarty et al., 2005, Cai et al., 2005; Vallstedt et al., 2005). OPCs represent heterogeneous populations with distinct functions. Indeed, gray and white matter OPCs have different resting membrane potentials and ion channel expression profiles. Moreover, some OPCs generate action potentials and are able to sense neuronal activity by forming synapses with axons (Yuan et al., 2002; Karadottir et al., 2008). In support to this heterogeneity, dorsally or ventrally generated oligodendrocytes respectively myelinate specific axonal tracts (Tripathi et al., 2011) and have different proliferative potency depending on their origin (Vigano et al., 2013). While Shh gradient produced by the notochord and the floor plate triggers Olig2 expression in the pMN domain, Shh gradient produced by the AEP triggers Olig2 expression in the ventral telencephalon (Lu et al., 2002). While, dorsal BMPs and Wnts signal support generation of astrocytes and prevent OL generation at earlier embryonic stages (Mekki-Dauriac et al., 2002; Shimizu et al., 2005; Vallstedt et al., 2005), dorsal

FGF signaling was shown to overcome inhibiting signal and specify OPCs in the dorsal spinal cord (Vallstedt et al., 2005).

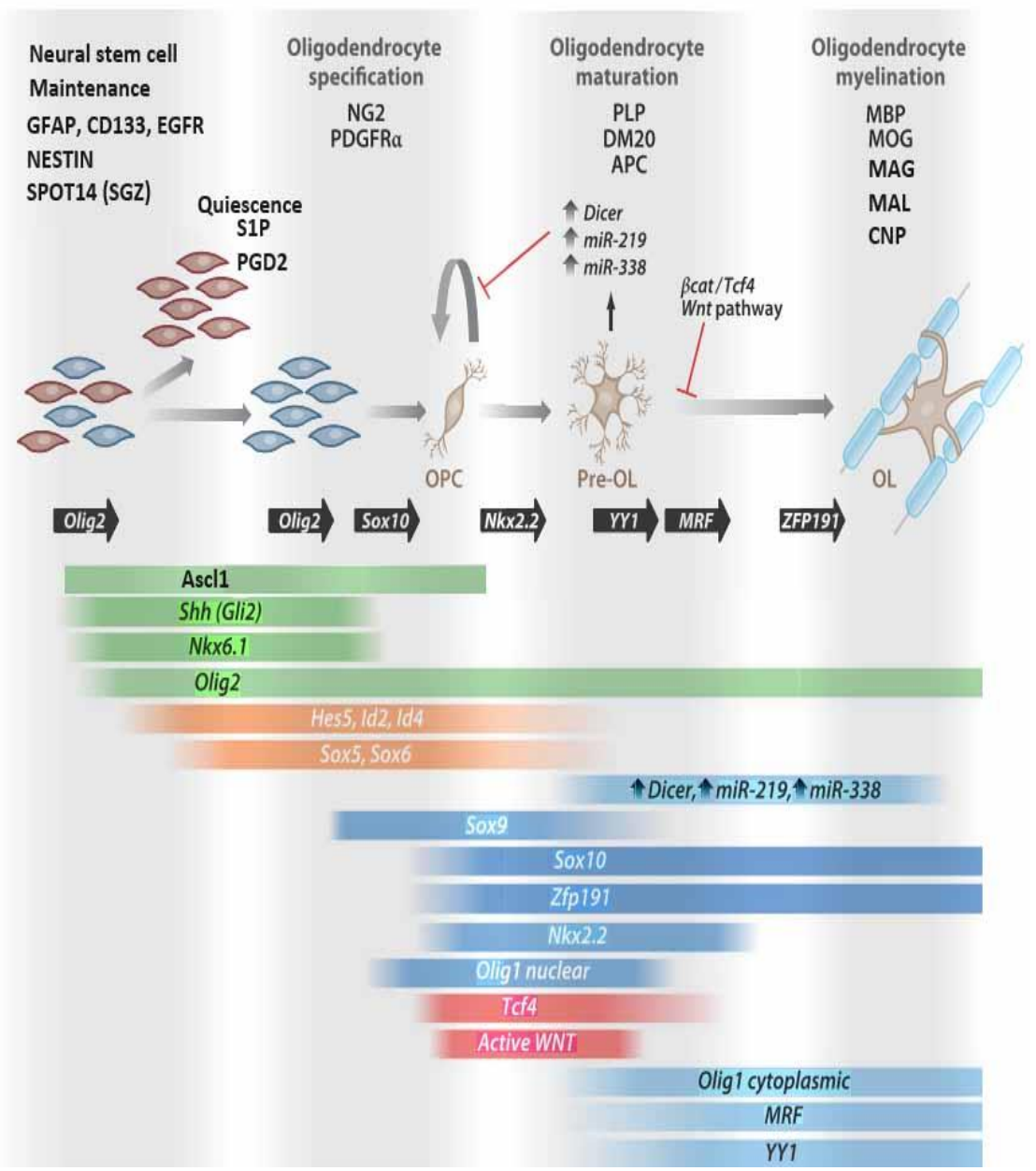

Figure 21. Schematic of the transcriptional control of oligodendrogensis. The diagram focuses on the NSCs to OPCs specification and maturation. Because of their undifferentiated state, stem cells defined by only few marker. Combination of marker is necessary to discriminate between active and quiescent NSCs.While the combination of GFAP, CD133 and EGFR define active NSCs, Spot14 or S1A and PGD were recently shown to define quiescent NSCs. OPCs are express only two specific markers, PDGFRα or NG2(CSPG4), whereas oligodendrocytes express APC (adenomatous polyposis coli) and proteolipid protein (PLP). Myelinating oligodendrocytes express

MBP, MOG and other myelin proteins. Transcription factors involved at each stage of maturation is indicated (adapted from S P J Fancy Chan).

Oligodendrogenesis during postnatal development and adulthood

In the mice postnatal and adult brain, transit amplifying precursors (also called C-type cells) are generate OPCs that migrate radially out of the SVZ into the overlying white matter and cortex where they stop dividing to differentiate into myelinating OLs (Aguirre et al., 2004; Aguirre et al., 2007; Menn et al., 2006; Nait Oumesmar et al., 1999). NSC in the SVZ generates OPCs or neuroblast but never both (Ortega et al., 2013). Interestingly, a ten fold higher number of OPCs are produced in the posterior part of the SVZ compared to rostral SVZ (Menn et al., 2006). Contrary to neuroblasts in the RMS, OPCs production from the adult SVZ is maintained with age (Capilla-Gonzalez et al., 2013). Another major source of OPCs comes from proliferation of OPCs present in the white matter and the brain parenchyma (Scafidi et al., 2014; Jablonska et al., 2012). OPCs are the major proliferative population of the adult brain and virtually all oligodendrocyte precursor cells continue to divide in adult mice with a cell-cycle time of 20 to 40 days (Young et al., 2013; Simon et al., 2011; Kang et al., 2010). Neonatal OPCs have been shown to divide either symmetrically, generating pairs of OPCs or mature oligodendrocytes, or asymmetrically to generate one OPC and one oligodendrocyte (Sugiarto et al., 2011; Zhu et al., 2011). In the adult brain, while half of the OPCs are dividing, the remaining OPCs are quiescent or divide even more slowly (Rivers et al., 2008). Different studies showed that adult OPCs have an increased cell cycle and migrate more slowly (Wolswijk and Noble, 1989; Simon et al., 2011; Clarke et al., 2012; Hughes et al., 2013; Young et al., 2013) but also differentiate more quickly than embryonic OPCs (Lin et al., 2009; Windrem et al., 2004). However, embryonic OPCs have better remyelinating capacity than adult OPCs thanks to their increased proliferative capacities (Ruckh et al., 2012; van Wijngaarden and Franklin, 2013).

Proliferation and survival of oligodendrocyte progenitor cells

While proliferation of OPCs depends in Cdk4 activation in the SVZ after demyelinating insult (Jablonska et al., 2012), OPC proliferation in WM depends on Cdk2/CyclinE activation in both developing and adult brains (Jablonska et al., 2012; Belachew et al., 2002).

PDGFRα is a specific marker of OPCs among neural cells (Heldin. C-H Westermark, B, 1981). PDGF-A, its ligand, is perhaps the most important mitogen for OPCs signaling (Noble et al., 1988; Richardson et al., 1988; Pringle et al., 1992). Indeed, OPC proliferation is tightly coupled to PDGF-A level (Calver et al., 1998; Fruttiger et al., 1999). Proliferative and pro-survival signaling through PDGFRα is linked to the α6β1 and αvβ3 integrin receptor interacting together in lipid rafts and driving phosphoinositide 3-kinase (PI3K)/PKC signaling (Baron et al., 2002, 2003; Decker and ffrench-Constant, 2004).

FGF-2 and FGF-18 act on FGFR1/2 or FGFR2/3, respectively, to stimulate OPC proliferation and inhibit differentiation (Chandran et al., 2003; Fortin et al., 2005). FGF-8 and FGF-17 primarily inhibit OPC differentiation through FGFR3 alone (Furusho et al., 2011). FGF-2 has also the capacity to promote PDGFRα expression and thus induces OPC proliferation and inhibits differentiation (McKinnon et al., 1990; Wolswijk and Noble, 1992; Baron et al., 2000).

IGF-1/ IGF-1R promote OPC proliferation and survival through the PI3K/Akt pathway phosphorylating GSK3β that prevent the phosphorylation and degradation of Cyclin-D1 (Pang et al., 2007; Zeger et al., 2007; Bibollet-Bahena and Almazan, 2009; Romanelli et al., 2009; Frederick et al., 2007). Moreover, FGF-2 and IGF-1 work synergistically to activate the ERK1/2 pathway that activate proliferating function of Cyclin-D1 in OPC (Frederick and Wood, 2004; Frederick et al., 2007).

Neuregulin-1 (NRG-1), an axonally-bound or secreted protein, has been shown to bind the OPC expressed ErbB tyrosine kinase receptors and promote OPC survival though the PI3K/ Akt pathway (Canoll et al., 1999; Fernandez et al., 2000; Flores et al., 2000).

Neurotransmitters released to OPCs by axonal synapses are involved in cell proliferation through IP3/Ca2+ signaling cascade (QK Yang Xiong 2013). Calcium enter in OPCs through GluR3/GluR4 receptors (P. P. Maldonado 2011; T. Itoh, J. Beesley, 2002, C. Y. Brazel, 2005), ATP /P2X and P2Y receptors (C. Agresti 2004–64), α-adrenergic receptors (R. Papay 2005), VDCC of the L-, N-, and R-type oligodendrocyte lineages in vivo (A. M. Butt, 2006).

During normal development, OPC proliferation and cell-cycle progression are positively regulated by two potent mitogenic factors—platelet-derived growth factor (PDGF) and fibroblast growth factor 2 (FGF2)—that act either individually or cooperatively through PDGFRα and FGFR1 to generate mature OLs (Calver et al., 1998; Fortin et al., 2005; McKinnon et al., 1990; Miller, 2002). Expression of the ligand PDGF-A is upregulated in reactive astrocytes of demyelinated lesions (Armstrong et al., 2002: Messersmith et al., 2000), and both FGF2 and FGFRs are upregulated in areas of acute or chronic cuprizone-induced demyelination (Messersmith et al., 2000). PDGF and FGF2 control differential responses in the OL lineage after demyelination (Murtie et al., 2005). Consistent with a role of PDGF in proliferation, OPC amplification and subsequent repopulation of demyelinated lesions are impaired in a heterozygote PDGFRα +/- or in a GFAP-driven PDGF-A null mouse (Murtie et al., 2005). Conversely, FGF2 acts to inhibit remyelination through FGFR1 (see below). Stimulation of epidermal growth factor (EGF) exerts multiple effects on the OL lineage, both OPCs and mature OLs (Aguirre et al., 2007; Scafidi et al., 2014). Selective EGFR overexpression in OL lineage cells promotes OPC proliferation and migration, enhancing the extent of functional remyelination of the corpus callosum after LPC-induced demyelination (Aguirre et al., 2007). Consistent with these findings, EGF infusion into the lateral ventricle (Gonzalez-Perez et al., 2009) or intranasal HB-EGF administration (Cantarella et al., 2008) promoted OPC recruitment from SVZ to demyelinated lesions. Furthermore, viral-mediated EGFR overexpression in WM OPCs increased proliferation and maintained an undifferentiated phenotype (Ivkovic et al., 2008).

brain-derived neurotrophic factor (BDNF) is required to regulate the number of OPCs during normal development and during remyelination (Vondran et al., 2010; VonDran et al., 2011).

Ciliary neurotrophic factor (CNTF) promote OL maturation during development and after demyelination (Stankoff et al., 2002; Albrecht et al., 2003).

The neurotrophin NT-3 promotes OPC proliferation and survival of mature OLs through TrkC receptors and MAPK phosphorylation (Cohen et al., 1996; Jean et al., 2003).

Insulin-like growth factor 1 (IGF-1) is a necessary factor for OL differentiation and myelination in vitro and in vivo (Mozell and McMorris, 1991; Werther et al., 1998; Beck et al., 1995; Ye et al., 2002). The IGF type 1 receptor (IGF-1R) is continuously expressed throughout the entire OL lineage, and IGF-1 appears to act at multiple developmental stages, promoting OPC proliferation, OL survival, and myelin synthesis (Barres et al., 1993; Ye and D'Ercole, 1999; e ger et al., 2007).

Hepatocyte growth factor (HGF) has been identified as a positive regulator of oligodendrocyte proliferation and migration and an inhibitor of differentiation (Yan and Rivkees, 2002: Ohya et al., 2007; Mela and Goldman, 2013).

MS occurs more frequently in females and undergoes remission during pregnancy (Confavreux et al., 1998), although the hormonal causes are poorly understood. Interestingly, pregnant mice demonstrate an increase in newly generated OLs and in the number of myelinated axons in corpus callosum (Gregg et al., 2007), prolactin has been identified as a major regulator of OL plasticity and WM repair during pregnancy, inducing OPC proliferation and enhancing OL regeneration in vivo (Gregg et al., 2007). Sexual dimorphism exists in rodent subcortical WM, where females display a higher proportion of unmyelinated axons (Kim and Juraska, 1997) and higher OL turnover (Cerghet et al., 2006).

Tumor necrosis factor α (TNFα) is an inflammatory cytokine which effects are mediated by the activation of TNFR1 (p55) and TNFR2 (p75) (Raine et al., 1998). In the brain, TNFα is synthesized and released by astrocytes and microglia (Liu et al., 1998). TNFα promote OPC proliferation (Arnett et al., 2001). More recent analysis demonstrated that TNFR2 also regulates expression of the chemokine CXCL12, which acts on the CXCR4 receptor to modulate remyelination. (Patel et al., 2012).

Cdk2 is necessary for OPC proliferation (Belachew et al., 2002) but after demyelination, loss of Cdk2 enhances OPCs differentiation (Caillava et al., 2011). The Cdk2 inhibitor p27 Kip1 inhibit recruitment of progenitors to demyelinated lesions (Crockett et al., 2005). The other Cdk inhibitor, p57 Kip2 prevents OL differentiation and remyelination (Kremer et al., 2009; Jadasz et al., 2012).

Migration of oligodendrocyte progenitor cells

OPCs achieve an homogenous distribution in the brain. it appears OPCs are a mediator of their own migration. Indeed, in vivo studies showed that contact between migrating OPCs is a powerful dispersal cue (Kirby et al., 2006; Hughes et al., 2013) and that this effect is mediated by the neurite outgrowth inhibitor, Nogo-A (Chong et al., 2012). SHH signaling acts as a chemoactrant through binding of the Patched-1 receptor (Mercha´n et al., 2007).Both PDGF-AA and FGF-2 act as potent chemoattractants to help direct OPCs (Noble et al., 1988; Zhang et al., 2004). While FGF-2/ FGFR1 has a pro-migratory role in a dose-dependent motogenic effect (Bansal et al., 1996; Osterhout et al., 1997;), PDGF acts through the Fyn/cdk5 pathway to promote WAVE2 phosphorylation which drive migration (Miyamoto et al., 2008). CXCL12/ CXCR4 acts as a chemoattractant and survival factor (Dziembowska et al., 2005). Extracellular matrix proteins have been implicated in OPC migration such as laminin, fibronectin, merosin, tenascin-C, and anosmin-1 (Frost et al., 1996; Garcion et al., 2001; Chun et al., 2003; , 2008; Hu et al., 2009; Relucio et al., 2009, 2012). Polysialylated neuronal cell adhesion molecule (PSANCAM) (Decker et al., 2000; Zhang et al., 2004), Eph/ ephrins (Prestoz et al., 2004), αvβ1integrins (Milner et al., 1996), claudin-11/OSP (oligodendrocyte-specific protein) (Tiwari-Woodruff et al., 2001, 2006), AN2/NG2 (neural/ glial antigen 2) (Stegmuller et al., 2002; Biname et al., 2013), and N-cadherin (Payne et al., 1996; Schnadelbach and Fawcett, 2001) have been linked to OPC motogenesis. Netrin-1/ DCC acts as a chemoattractant in the first wave of OPC migration in the optic nerve (Sugimoto et al., 2001; Spassky et al., 2002) NRG-1 has been shown to be chemoattractant during development but completely

dispensable for postnatal OPC migration (Ortega et al., 2012). Netrin-1/Unc5A receptor act as chemorepellent in the second wave of telencephalic and spinal OPCs Jarjour et al., 2003; Tsai et al., 2003, 2006). CXCL1/CXCR2 act as a stop signal and is central for proper OPC positioning (Tsai et al., 2002; Padovani-Claudio et al., 2006). Secreted Semaphorin-3A and membrane-bound Semaphorin-4D/ F (Spassky et al., 2002; Taniguchi et al., 2009).

Molecular mechanisms involved in myelination and remyelination

The mechanisms underlying the failure of remyelination in demyelinating diseases include depletion of the OPC pool, failure of correct migration of OPCs to the lesion, irreversible axonal loss, and presence of inhibitors of differentiation produced by reactive astrocytes, microglia or lymphocytes (Chong and Chan, 2010; Mason et al., 2004; Miron et al., 2013). In order to tackle each of those aspects, many studies tried to uncover the transcriptional network and the signaling pathways promoting or inhibiting myelination.

Transcriptional regulation of myelination

During development, Olig1, Olig2, and Nkx2.2 are central in OPCs specification and differentiation (Lu et al., 2002; Soula et al., 2001, Gallo, Vittorio 2014). Olig2 and Nkx2.2 are upregulated during acute phases of myelination and remyelination (Fancy et al., 2004). The role of Olig2 was recently extensively studied by Chip-seq and RNAseq analysis (Yu Chen Kim 2013). This groundbreaking study focuses on the collaborative role of Olig2 and Brg1 (Smarca4) in the transition between OPCs and myelinating oligodendrocyte. Olig2 was shown to activate different target genes depending on the differentiation stage and to recruit the chromatin-remodeling enzyme Brg1 (ATPase subunit of the SWI/SNF chromatin-remodeling complex) at the time of myelination (Yu Chen Kim 2013; Marathe HG 2013).This study made available important epigenetic data from H3K4me3, H3K27ac (active enhancers), RNA PolII, Olig2 and Brg1 Chip-seq in OPCs, pre-myelinating OLs and myelinating OLs (GSE42447). Olig2 was shown to be involved in almost all aspect of oligodendrocyte physiology such as specification, proliferation, survival, migration and

signalings of OPCs together with myelination, survival and signalings of mature oligodendrocyte. These processes are mainly controlled by the Olig2 phosphorylation status (Maire et al., 2010). While mutation of Olig2 in OPCs (CNPase-promoter) significantly inhibits differentiation, deletion in immature OLs (*Plp1* promoter) significantly enhances myelination. In contrast, ablation in the mature cells had no detrimental effect on myelination because of Olig1 compensatory role (Mei et al. 2013). As Olig2, Olig1 is expressed all along the oligodendrocyte lineage but is mainly involved in remyelination (Arnett et al., 2004). Indeed, while Olig1 function in OPCs is largely overlapping and compensated by Olig2, Olig1 mutant oligodendrocytes hardy differentiate into remyelinating oligodendrocytes (Arnett et al., 2004). Interestingly, Olig1 expression is nuclear in OPCs, immature oligodendrocytes and early remyelinating lesions, but become cytosolic in normal appearing white matter (Ligon et al., 2006). While the cytoplasmic function of Olig1 was recently shown to drive membrane extension and depend on the phosphorylation status of Olig1 (Niu et al., 2012), the nuclear function was shown to involve synergistic action with Olig2 and Sox10 on different promoters such as *Mbp* promoter (Xin et al., 2005; Li et al., 2007). This kind of localization switch is also observed for Myt1, a TFs involved in late maturation of oligodendrocytes (Nielsen et al., 2004; Vana et al., 2007).

Sox10 is also expressed all along the oligodendrocyte lineage. *Sox10* mutant mice have relatively normal numbers of OPCs thanks to transcriptional redundancy with *Sox9* and *Sox8* (Stolt C, 2002; Finzsch M 2008; Emery, B 2010). However, *Sox10* mutant mice display a complete loss of myelinating oligodendrocytes (Stolt et al., 2002; Finzsch M 2008; Takada et al., 2010; Hornig et al., 2013). *Sox10* mutant oligodendrocytes are able to ensheath axons but are unable to fully myelinate and finaly die by apoptosis (Takada N, 2010). Sox10 is necessary for *Mbp* promoter activation (Li et al., 2007) and it binds the mediator subunit 12 (Med12) and thus stabilize the general transcription machinery via the mediator complex (Vogl et al., 2013). Myrf and Sox10 share many common direct targets and work in a synergistic manner on many myelin specific genes (Bujalka et al., 2013; Hornig et al., 2013). Myrf is specifically induced by Sox10 during oligodendrocyte differentiation (Emery et al., 2009. Hornig et al., 2013). Conditional mutation of Myrf in oligodendrocytes results in a loss of myelin genes and progressive demyelination (Koenning et al., 2012). Sox17, which expression is maximal at the peak

of myelination (P15) is involved in cell-cycle exit and the initiation of differentiation (Sohn et al., 2006). Sox17 promotes myelination by inhibiting the Wnt/β-catenin pathway that maintain OPC proliferation (Chew et al., 2011; Ming et al., 2013). Interestingly, Sox17 is highly expressed in Multiple Sclerosis chronic active lesions (Moll et al., 2013).

Nkx2.2 mutant mice have a normal OPC numbers (Qi Y, Cai J, Wu Y 2001; Soula C, Danesin C2001) but display a severe defect in differentiation (Qi et al., 2001). Despite the fact that Nkx2.2 is required for myelination, it is transiently downregulated upon cytoplasmic translocation of Olig1, a process associated with Nkx6.2 upregulation (Cai et al., 2010). As Nkx2.2 inhibit *Mbp* (Wei et al., 2005) thus, its down-regulation may be necessary to initiate myelination. *Nkx6*.2 mutant mice display myelin defect and aberrant expression of the paranodal proteins stathmin1, neurofascin and contactin (Southwood et al., 2004). Nkx6.2 and Nkx2.2 may participate to paranodal region and axo-glial interactions (refXX).

Retinoid X receptor gamma (RXRγ) positively regulates OL differentiation during myelination and remyelination (Huang et al., 2011). RXRγ nuclear localization was demonstrated during OPC differentiation and OL regeneration in demyelinating lesions multiple sclerosis tissue. Moreover, treatment with 9-cis retinoic acid after demyelination promoted axonal remyelination (Huang et al., 2011).

Different other TFs were recently shown to be involved in myelination such as ZFP488 and ZFP191 which drive MBP or CNP expressions (Wang et al., 2006; Howng et al., 2010) but most of their genome-wide targets are yet to be discovered.

Specific role of Ascl1 in myelination

In addition to its function in OPCs generation in the neonatal olfactory bulb (Parras et al., 2004), Ascl1 is also involved in OLs specification in the embryonic wave of OPCs from the ventral telencephalon (Parras et al., 2007) and in the postnatal wave from the dorsal SVZ (Nakatani 2013). Indeed, *Ascl1* conditional knock-out mice in neonatal SVZ progenitors, show defects in the generation of OPC/oligodendrocytes at the profit of astrocyte generation (Nakatani et al., 2013). Moreover, conditional

deletion of *Ascl1* in OPCs results in an increase OPC proliferation at the expense of a reduce differentiation/maturation into myelinating oligodendrocytes. This could be explained by an increase of self-renewing symmetrical divisions of OPCs generating OPCs pairs at the expense of differentiating asymmetrical divisions generating OLs pairs (Nakatani et al., 2013). Interestingly, *Ascl1* knockout results in a decrease expression of Nkx2.2 in OLs (Sugimori et al., 2008) and could explain part of the myelination defects observed in the *Ascl1* knock-out (Sugimori M 2008, Nakatani et al 2013). In focal demyelination experiments, Ascl1 levels are upregulated both in the adult SVZ and OPCs close to the demyelinated region in cells co-expressing Olig2 and Nkx2.2 sugesting that this transcription factors could be part of a common transcriptional code promoting remyelination (Nakatani et al., 2013). Indeed, during OLs regeneration, Ascl1 function is also important for the normal differentiation of OPCs during the remyelination as shown by the conditional deletion of Ascl1 in adult OPCs before inducing a brain demyelinating lesion (Nakatani et al., 2013). Importantly, ASCL1 expression is also up-regulated around Multiple Sclerosis chronic active lesions suggesting that the function of Ascl1 in remyelination is conserved between rodents and humans (Nakatani et al., 2013). Thus these results show that Ascl1 is involved in a cell autonomous manner in the neural stem cell (NSC) cell-fate choice following cell division and regulate genes involved in the specification and differentiation of OPCs. However, most of the direct targets of Ascl1 are unknown. In this study, we aimed at uncovering the specific transcriptional role of Ascl1 in the process of OPCs to OLs differentiation.

Epigenetic Regulation of oligodendrogenesis

The oligodendrocyte epigenetics only begins to be unraveled compared to epigenetic in other lineages (Liu J, Casaccia P. 2010; JL Huynh, 2013, Yu Chen Kim 2013). Contrary to other neural lineages, OPC differentiation is initiated by histone deacetylation (Marin-Husstege et al., 2002). HDACs, which catalyses the removal of acetyl groups on histone lysine residues favoring transcription inhibition, repress

proliferative genes such as Sox2 or Sox9, whose downregulation is necessary for myelination (Lyssiotis et al., 2007; Shen and Casaccia-Bonnefil, 2008). HDAC inhibitors decrease the number of OPCs at the expanse of astrocytes and neurons (Siebzehnrubl et al., 2007). Oligodendrocyte differentiation is initiated by HDAC1/2 recruitement to the promoters of myelination inhibitors (Shen and Casaccia-Bonnefil, 2008) such as Hes5 (Kondo and Raff, 2000), Sox11 and Tcf4 (He al., 2007), Id2 and Id4 (Samanta and Kessler, 2004).

YY1, Yin Yang 1 facilitates the recruitment of HDAC1 to the promoters of some of these transcriptional inhibitors (He et al., 2007). SIRT2 another HDAC, is upregulated during differentiation. TCF7L2/TCF4 as described above mediates a cross talk between HDAC1/2 and Wnt signaling (Ye et al., 2009).

Histone methyltransferases catalyze the addition of methyl groups to histones. Methylation at H3K27 by Ezh2 plays a role in the selection of the oligodendrocyte lineage. Overexpression of Ezh2 in NSCs triggers oligodendrocyte fate choice, while Ezh2 silencing causes the opposite (Sher et al., 2008b). The dynamic changes in activation and repression of promoter and enhancers occurring during the process of OPCs differentiation and myelination was recently studied by Chip-seq analysis of H3K4me3 and H3K27ac marks at the stages of oligodendrogenesis: OPCs, premature OLs and myelinating OLs. (Yu Chen Kim 2013). This is nevertheless, just the begging of a deeper understanding of the logic undelaying the regulation of key regulatory genes promoting and inhibiting these stage transitions in the process of oligodendrogenesis.

Promoting signals of myelination

A multitude of growth and trophic factors regulate myelination (Casaccia-Bonnefil, 2000; Nave and Trapp, 2008 ; Mitew S 2014). The thyroid hormone signaling is maybe the most important pathway driving myelination. While, hypothyroidism is associated with myelin defects (Schoonover et al., 2004), hyperthyroidism results in early myelination (Pombo et al., 1998).

Triiodothyronine/thyroid hormone 3 (T3) triggers OPCs cell cycle exit and myelination through Thra and P53 mediated signalings (Barres et al., 1994; Tokumoto et al., 2001). IGF-1 signaling causes an increase in overall brain growth and an increased number of oligodendrocytes (Goddard et al., 1999). Fyn mutant mice display fewer myelinated axons with fewer mature oligodendrocytes and thinner myelin sheaths (Umemori et al., 1994; Osterhout et al., 1999; Goto et al., 2008). The fibronectin pathway blocks the myelin process outgrowth, while the laminin-2 and laminin-β1 integrin receptor pathway triggers process expansion (Chun et al., 2003; Relucio et al., 2009). Axons produce laminin-α2 before myelination (Colognato et al., 2002) which then binds to β1-integrin receptors on oligodendrocytes to promote the initial process extension through dephosphorylation of the tyrosine kinase Fyn (Hu et al., 2009; Liang et al., 2004; Bauer et al., 2009). Fyn induces actin and microtubule polymerization via FAK-mediated activation of the RhoGTPases Cdc42 and Rac1 (Chun et al., 2003; Bacon et al., 2007; Kim et al., 2008; O'Meara et al., 2013) .Brain-derived neurotrophic factor (BDNF) and FGF-2 activate the Raf-MEK-ERK pathway which favor myelination (Furusho et al., 2012; Xiao et al., 2012), and act through laminins, dystroglycan and integrin β1 receptors (Lee et al., 2006; Galvin et al., 2010).

The PI3K/Akt/mTOR (mammalian target of rapamycin) pathway is necessary to increase protein and lipid synthesis ability at the myelinating stage (Guardiola-Diaz et al., 2012). Interestingly, stimulation of this signaling triggers hypermyelination (Flores et al., 2008; Narayanan et al., 2009). Finally, LINGO-1, involved in cell-cell interactions, is specifically expressed in axons and OPCs being a key regulator of myelination timing because downregulation of LINGO-1 promotes OL differentiation and myelination during development (Mi et al., 2005).

Table 1. Secreted and contact-mediated extracellular factors that promote (green) or inhibit (red) specific stages of oligodendrocyte development

	OPC Specification	OPC Survival	OPC Migration	OPC Proliferation	Differentiation	Myelination
Secreted	SHH [1]	SHH	SHH / +	SHH	SHH	
	BMP				BMP	
					WNT	
	Autotaxin					Autotaxin
		PDGF-AA	PDGF-AA / +	PDGF-AA	PDGF-AA	
	FGF-2	FGF-2	FGF-2 / +	FGF-2	FGF-2	FGF-2 / §
		IGF-1		IGF-1	IGF-1	IGF-1 § / *
				BDNF	BDNF [2]	BDNF / §
				T3	TH3	
			HGF / + [3]			
			Netrin-1			Netrin-1
			Semaphorin 3A Semaphorin 3F			
			CXCL1	CXCL1	CXCL1 (?) [4]	
		CXCL12	CXCL12	CXCL12 [5]	CXCL12 [5,6]	
			Slit2 [7]			
Contact		NRG-1	NRG-1 +	NRG-1	NRG-1	NRG-1 * §
			PSA-NCAM			PSA-NCAM [8]
	Notch-1				Notch-1 / Notch-1 F3	Notch-1*
		Laminin α2			Laminin α2	Laminin α2 * §
		L1-Contactin				
		α6 Integrin				
		β1 Integrin				β1 Integrin *
					Lingo1	Lingo1*
					Gpr17	
		Fibronectin (via αvβ3)	Fibronectin (via αvβ1)	Fibronectin (via αvβ3)	Fibronectin (via αvβ5)	
			Dystroglycan		Dystroglycan [9]	Dystroglycan
		Semaphorin 4D [10]	Semaphorin 4F	Semaphorin 4D [10] Semaphorin 6A [11]	Semaphorin 6A [11]	
			Ephrins/Eph			
			OSP/Claudin-11	OSP/Claudin-11		OSP/Claudin-11
			N-cadherin [12]			N-cadherin [12]
			NG2 +			
			tenascin-C			
			Anosmin-1			

[+] Motogenic; [*]involved in size-sensing; [§]promotes myelin thickness.
[1]Orentas et al. (1999); [2]Vondran et al. (2010); [3]Yan and Rivkees (2002); [4]Kerstetter et al. (2009); [5]Patel et al. (2012); [6]Patel et al. (2010); [7]Liu et al. (2012); [8]Charles et al. (2000); [9]Galvin et al., 2010; [10]Yamaguchi et al. (2012); [11]Bernard et al. (2012); [12]Schnädelbach et al. (2000).

Figure 22. Table showing the main signaling controlling different aspect of the OPCs physiology (Adapted from S. Mitew et al.2013).

Inhibiting molecular mechanisms of myelination

BMP, FGF2, Notch, and Wnt signaling prevent oligodendrogenesis in favor of neurogenesis (Colak et al., 2008; Hsieh et al., 2004) and astrogliogenesis (Gomes et al., 2003; Samanta et al., 2007; See et al., 2007; Grinspan, 2009). These effects involve Id genes expression and inhibition of Olig2 (Samanta and Kessler, 2004; Chen and Panchision, 2007). The BMP antagonist Noggin increases the density of mature OLs during remyelination (Sabo et al., 2011) and the BMP antagonist chordin promotes oligodendrogenesis from GAD65 expressing neuroblasts of the adult SVZ (Jablonska et al., 2010). Blockade of Wnt/β-catenin signaling inhibit oligodendrogenesis

(Langseth et al., 2010), being the effects of Wnt mediated by BMPs (Feigenson et al., 2011).

Notch1 activation in OPCs inhibits myelination (Wang et al., 1998; Kondo and Raff, 2000; Genoud et al., 2002). Indeed Jag1 and Dll1 ligand are expressed on axons and binds to Notch1 in OPCs. Subsequent NICD nuclear transclocation increases the expression of the Hes1/5 that inhibit OPC differentiation (Wang et al., 1998; Kondo and Raff, 2000). In turn, Hes5 is inhibits Ascl1 and Sox10 (Liu et al., 2006; Wang et al., 1998). However, the presence of axonally expressed F3/contactin revert Notch1 signaling to a pro differentiation effect (Hu et al., 2003). Suppressors of Notch signaling enhance OPC maturation during normal development (Aguirre et al., 2010). Moreover, Notch signaling in adult brain is reactivated after demyelination (Hammond et al., 2014) and Jagged 1 is upregulated in MS chronic lesions (John et al., 2002). Eventually, a recent study showed that Endothelin-1 (ET-1) is a major regulator of Notch after demyelination (Hammond et al., 2014).

BMP and GPR17 signalings (Cheng et al., 2007, 2009) are inhibiting differentiation by inducing the bHLH molecules ID2/4, which directly inhibit Olig1 and Olig2 activity (Samanta and Kessler, 2004; Fumagalli et al., 2011). Wnt3A / Frizzled signaling, leads to the nuclear localization of β-catenin and strongly inhibits differentiation (Shimizu et al., 2005). β-catening recruits TCF7L2(TCF4) to *Id2* and *Id4* promoters but Tcf7l2 may act as a molecular switch between proliferation and differentiation depending on binding partners. (Fu et al., 2012; Memezawa et al., 2007). Finally, in *Sox5* and *Sox6* mutant mice present premature expression of PLP and MBP indicating that the also form part of an inhibitory mechanism of oligodendrocyte differentiation and myelination (Stolt 11C 2006)

Therapeutic Aspect of oligodendroglial pathologies

Multiple sclerosis is an inflammatory degenerative disease of the central nervous system, in which an autoimmune attack driven by infiltration of the brain by immune cells

causes a progressive or relapsing-remitting destruction of myelin sheaths together with the underlying axons and lead to action potential conduction block and associated

disabilities (Noseworthy et al., 2000; Compston and Coles, 2002). MS is a disease found in every region of the world, with increased prevalence in northern countries, affecting 2.3 million persons worldwide with a female to male sex ratio female/males has increased from 2:1 to 3:1 from data accumulated between 1941 to 1980. The development of therapies are mainly based on immunosuppressants, immuno-modulatory and anti-inflammatory drugs (Compston and Coles, 2002; Kieseier et al., 2007), but none is able to directly promote myelin repair and therefore, improve patients disabilities.

Demyelinated plaques can be normally repaired by endogenous OPCs proliferation and differentiation, especially in acute and early stages of the disease (Chang et al., 2002; Wolswijk, 2002). However, remyelination with time and desease progression becomes more and more ineffective, leading to chronically demyelinated lesions with substantial axonal loss (Trapp et al., 1998). Although endogenous myelin repair could be complete in some MS patients (Patrikios et al., 2006), this process is, in most cases, insufficient and abnormalities in myelin ultrastructure subsist even if the overall myelination appears normal (Jablonska et al., 2012)

As demonstrated in the experimental autoimmune-encephalomyelitis (EAE) and the cuprizone-induced demyelination models that are respectively used to tackle preferentialy the immune or the oligodendroglial aspect of the disease, axonal damage and neuronal loss play a central role in determining the extent of the disability of demyelinating diseases (Scafidi et al., 2014). Therefore, one of the major therapeutic challenges is to design new multi-steps treatments enhancing sequentially effective neuro-protection, OPCs proliferation, OL differentiation and axonal support.

Conclusions and Future Directions

Much progress have been made in the understanding of oligodendrocyte physiology since the discovery of Olig2 as the oligodendrocyte master gene (Zhou et al., 2001; Lu et al., 2001). However, really few therapeutic approaches have succeeded in driving potent remyelination. In order to find specific oligodendroglial therapeutic targets, it is now necessary to integrate the exhaustive genomic (Cahoy J 2008, Fu et al., 2009; Fancy et al., 2009) and epigenetic (Yu Chen Kim 2013) analysis of the oligodendroglial lineage together with the characterization of the intra and extra-cellular regulatory signaling pathways to bring a new understanding about the specificity of oligodendrocyte development and remyelination comparable to other cell types. Unravelling the particular transcriptional program of OPCs specification and differentiation will allow to progress in cell based therapies for example by increasing the yield of OPC production in direct lineage conversion experiments or to find new oligodendrocyte specific druggable molecules that avoid side effects.

PART II: EXPERIMENTAL WORK

Chapter I: Material and methods

Animals and genotyping

All animal procedures were performed according to the guidelines and regulations of the Inserm ethical committees (authorization #A75-13-19) and animal experimentation license A75-17-72 (C.P.). Both males and females were included in the study. Mice were maintained in standard conditions with food and water ad-libitum in the ICM animal facilities. Ascl1^{KO} and Olig2^{KO} mouse strains were used in this study. Because of the lethality in the first postnatal week in both knock-out mice, these strains were maintained by backcrossing to OF1 mice. For staging of embryos, midday of the vaginal plug was calculated as E0.5. Polymerase chain reaction was performed with wild type and knock-out primers to genotype the embryos. Wild-type,

heterozygous and homozygous mutant embryos were obtained from intercrosses of Ascl1 +/or Olig2+/mice. Genotyping of the different Ascl1 alleles was performed by PCR using the following primers and conditions: for the Ascl1 knock-out allele, forward primer 5‘-AGATGTAATTGTGGGCGAAG-3‘ and reverse primer 5‘-ACAGTTTGGCCCGGCATGGA-3‘ with 35 cycles of 95°C/1 min, 60°C/1 min, 72°C/1 min were used. For the wild type allele, forward primer 5‘-CTCCGGGAGCATGTCCCCAA-3‘ and reverse primer 5‘-CCAGGACTCAATACGCAGGG-3‘ with 35 cycles of 95°C/1 min, 58°C/1 min, 72°C/1 min were used. For the Olig2 wild type allele, forward primer 5‘-CTCGTAGCTCGGAGCTCAGCTCTGGCGGGC-3‘ and reverse primer 5‘-TAGAAGGCCAGACTGCCGCGGCGTAGATGC-3‘, and for the Olig2 knock-out allele forward primer 5‘-TGGCTACCCGTGATATTGCTGAAGAGCTTG-3‘ and reverse primer 5‘-GCATGCCGCCCCAGTGCTGGAAGCCACCGC-3‘, both with 35 cycles of 95°C/4 min, 62°C/1 min, 72°C/1 min were used. Because no differences in the phenotypes between Wild-type and heterozygous brains have been detected, they were both used as controls.

Immunofluorescence

Adult mice were perfused with freshly made chilled 2% paraformaldehyde (Sigma) with 25 ml, brain was dissected out, cryoprotected in PBS with 20% sucrose overnight, and included in OCT (BDH) before freezing and sectioning (14µ mthick) with a cryostated microtome (Leica). Sections were then either processed for immunohistochemistry or stored at -80°C. The following primary antibodies were used: mouse monoclonal antibodies to APC (Calbiochem, 1:200), Ascl1 (BD Biosciences, 1:200), Olig2 (Ligon et al., 2006), GFP (Invitrogen, 1:2000), Gpr17 (Cayman Chemical, 1:400), myelin basic protein (MBP, Millipore, 1:1000), Olig2 (Millipore, 1:1000), Ascl1 (gift from J. Johnson, 1:1000); PDGFRa (BD Biosciences, 1:800), and chicken polyclonal antibodies to GFP (Aves Laboratories, 1:2000) and MBP (Millipore, 1:50). Fluorescent secondary antibodies included the following: AlexaFluor-488, AlexaFluor-594, and AlexaFluor-647 Ig (1:1000, Invitrogen). Antigen retrieval for Ki67 antibody staining was performed using antigen retrieval solution

(Vector, H-330), heating sections in citrate-based solution up to boiling and then allowing cooling down at room temperature for 20 min. Immunofluorescence was visualized with Leica TC SP2 confocal or Zeiss AxioImagerApotome system microscopes. Pictures were taken as stacks of 5–10µm with 0.5µm between sections. Z-projections and orthogonal projections were done in ImageJ and processed with Adobe Photoshop. Figures were made using Adobe Illustrator. Human brain tissues were immunostained as previously described (Nait-Oumesmar et al., 2007) with mouse monoclonal antibodies for human Ascl1 (Cosmo Bio, 1:500), rabbit antibodies for Olig2 (Millipore, 1:100), Olig1 (R&D Systems, 1:50), and goat antibody for Sox10 (R&D Systems, 1:50).

Demyelinating lesions

Before surgery, adult (2-3months) WT mice were weighted and anesthetized by intraperitoneal injection of mixture of ketamine (0.1 mg/g) and xylacine (0.01 mg/g). An analgesic (buprenorphine, 30 mg/g) was administered intraperitoneally to prevent postsurgical pain. Focal demyelinating lesions were induced by stereotaxic injection of 1.5 llysolecithinsolution(LPC,Sigma, 1% in 0.9%NaCl) into the corpus callosum (CC; at coordinates: 1 mm lateral, 1.3 mm rostral to bregma, 1.7 mm deep to brain surface) using a glass-capillary connected to a 10µl Hamilton syringe. Animals were left to recover in a warm chamber before being returned into their housing cages.

Microarray experiments

Global gene expression analysis provides quantitative data about the population of RNA species in cells and tissues. Thus, microarray analysis is among the most commonly used methods in modern biology and there are more than a million expression datasets in the National Center for Biotechnology Information Gene Expression Omnibus (GEO) public database (Edgar et al., 2002). DNA microarrays are the most frequently used technique for RNA expression analysis. In this study, we performed microarray experiment using $Ascl1^{KO}$ (Guillemot et al., 1993) and $Olig2^{KO}$ (Lu et al., 2002) mice. Different genotypes ($Ascl1^{KO/KO}$, $Olig2^{KO/KO}$ and wild-type, i.e.

Ascl1$^{+/+}$, *Olig2*$^{+/+}$) were obtained from intercrosses of *Ascl1*$^{KO/+}$; *Olig2*$^{KO/+}$ doble heterozygous mice. RNA was purified from disected E13.5 ventral forebrain (Fig. 23B,C). RNA samples were prepared by pooling RNAs extracted from 3 brains to constitute one replicate and each sample type was prepared in five replicates. cRNA hybridization probes were hybridized to Affymetrix Mouse Whole Genome MOE430 2.0 arrays. The R-CRAN statistical language and Bioconductor software package (Gentleman et al., 2004) were used throughout the expression analyses. Raw image files were processed using Affymetrix GCOS. The probe signal levels were quantile-normalized, summarized and then transformed to the log 2 expression using GCRMA (gcrma R-package, Irizarry et al., 2003) and Frozen RMA (fRMA package; McCall and Irizarry., 2011). Gene filtering was performed using the Wilcoxon signed-rank test to select probe sets that were ~~–e~~onsistently expressed" ($p < 0.04$) in at least one group (mas5calls R-package; Bioconductor) (Fig. 24). All samples showed good quality control according to MAS5.0 guidelines and the AffyQC report (R-package; Bioconductor). Principle component analysis (PCA) was used to reduce the dimensionality of the whole dataset and measure the degree of similarity between samples (dudi.pca R-package; Thioulouse and Dray, 2007). We decided to withdraw two replicates from each sample type as they were outliers. The subsequent three-dimensional PCA plot confirmed a high degree of similarity among samples within the same genotype and much less similarity among samples of different genotypes. We used LIMMA statistical analysis (Smyt et al., 2004) to determine the differentially expressed genes. The resulting p-values were adjusted to FDR <5% with the Benjamini-Hochberg method to control the mean proportion of false positives (q-value R-package, Storey et al., 2003). Our microarray processing choices are explained below.

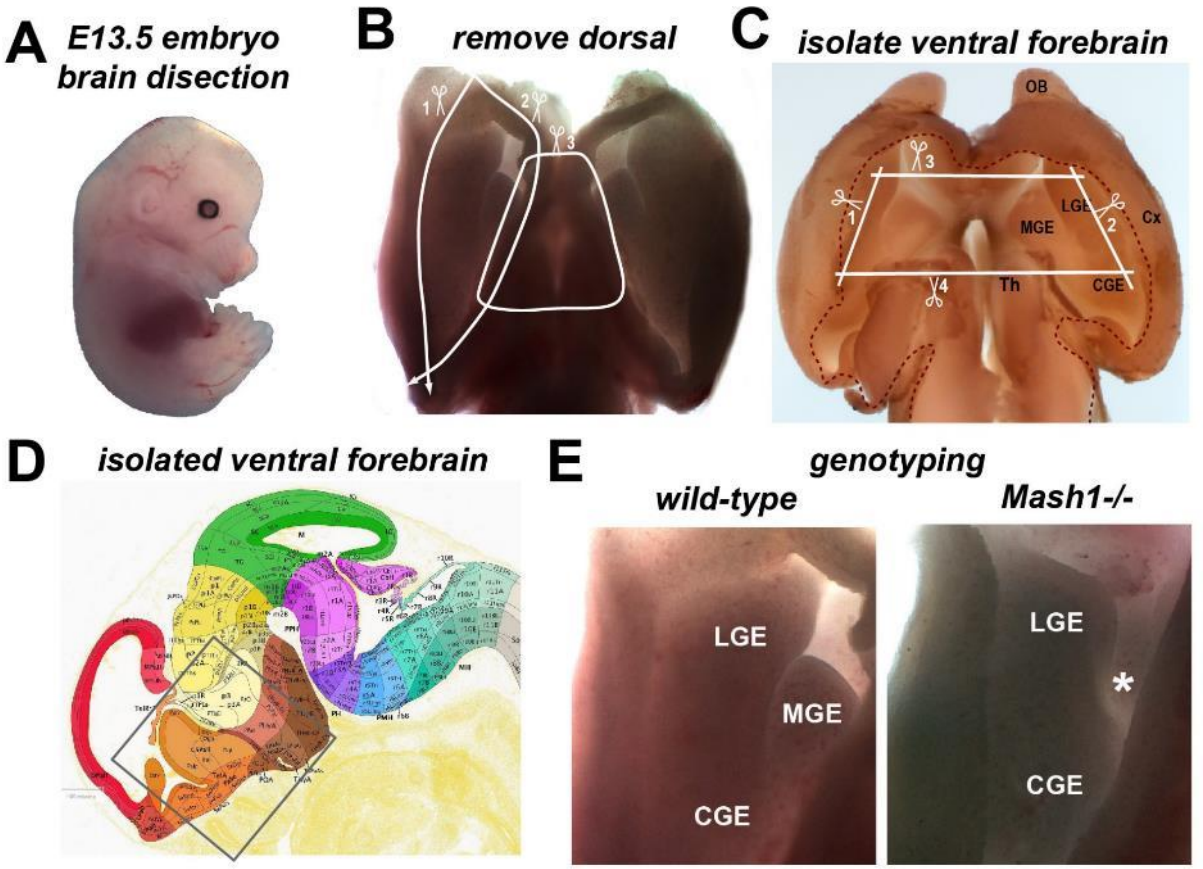

Figure 23. Isolation of the ventral forebrain region containing the ventral source of OPCs during development. (**A**) Picture of a mouse embryo at 13 days of gestation. (**B**) Dissected brain in a horizontal perspective with the dorsal telencephalon removed showing the dissection steps to follow to get remove the dorsal forebrain. (**C**) Steps to follow to dissect the ventral region containing the source of embryonic OPCs in the forebrain. Cutting steps, lines represent the cutting plane perpendicular to the plane of view, are represented by scissors and step numbers. (**D**) Brain sagittal section with the different regions represented schematically, according to the reference brain atlas of E13.5 embryo (Allen brain atlas: http://atlas.brain-map.org) that are contained in our dissected tissue (grey square). (**E**) Morphological difference between a wild-type and a Ascl1 mutant ventral telencephalon. Note that the MGE is absent in the mutant (asterisk). MGE, medial ganglionic eminence; LGE, lateral ganglionic eminence; CGE, caudal ganglionic eminence.

Technical aspects of microarray processing

A normalization step is necessary to remove non-biological variation among samples. Normalization comprises background correction, a within and between chip normalization and a probe summarization process to generate the final expression values for each probesets, a group of probes representing one particular mRNA. Several normalization protocols have been proposed based on different biological and statistical assumption. Thus, it is necessary to choose the method that most effectively normalizes the microarray data. In order to measure the background, Affymetrix microarrays includes for each gene 11 to 20 probesets that are composed by a perfect match (PM) and a mismatch (MM) probe. The PM is a 25-mer oligonucleotide designed to be complementary to its target cDNA and the MM probe contains a mutation at the 13th position of the probe. MAS 5.0 (Affymetrix algorithm) corrects for cross-hybridization by subtracting the MM signal from the PM to determine specific binding. A major problem of this approach is that the MM measures also cross-hybridization. Indeed, hybridization still occurs with the MM probe and leads to a MM intensity levels greater than expected. Thus, MAS5.0 normalization lead to false negatives and a great variability of the fold change estimate at low intensity (Irizarry et al., 2003). In our study, we preferred the GCRMA algorithm (GC-Robust Multichip Average) which uses the nearest-neighbor model (Santa Lucia, 1998) to estimate probe affinity to non specific binding. Taking into account the thermodynamics of binding (DNA duplex stability arises from hydrogen bonding between Crick‘s pairs and base stacking interactions between adjacent base pairs (Van der Waals interactions, electrostatic and hydrophobic interactions) as well as the biotin labeling interferences, GCRMA gives a more robust background correction and fold change estimate as well as less variability at low intensity (Mieczkowski et al., 2010). However, GCRMA is cannot normalize properly batch of experiments done in different condition or in different labs because variability in such case overcome the normalization capacity. In this study, we had to deal with dataset of multiple sources and had to find a proper normalization methods that allow good fold change estimate. We choose the frozen RMA (fRMA) method, which uses precomputed and ―frozen" information from the large publicly available microarray databases to estimates each probe-specific effects and variances (McCall and Irizarry, 2010). Even if GCRMA is best to compare a unique batch of experiment, fRMA greatly outperforms any other method to compare

different datasets and properly estimate fold changes and statistical significance when testing for differential expression. To assess statistical significance when comparing between different conditions, each gene could be tested independently from one another using a classical t-test or ANOVA. However, the incidence of false positives is proportional to the number of tests performed and the significance level (p-value cutoff). For example, a p-value of 0.05 signifies a 5% probability that a gene expression level is different between the two groups by chance. If 40,000 genes are tested, 2000 genes could be called significant by chance. Thus, it is important to correct the p-value to assess the false discovery rate of each gene when performing such statistical test. In this study, we used a recent approach to correct the p-value using LIMMA (Smyt, 2004). LIMMA is designed to easily analyze complex experiments involving comparisons between many arrays and correct for multiple testing using the bonferroni Hochberg FDR method thanks to a linear model of the whole dataset matrix that increase to normalization power of the pre-processing GCRMA or fRMA methods. In order to assess the quality of each microarray replicates, we used principal component analysis (PCA) and clustering methods (hierarchical clustering) to measure the degree of similarity between samples (Fig. 24C). These methods are used to determine the relationships among a group of variables when it is not appropriate to make a priori grouping decisions. They determine the effect of each variable on the total variance of the data set, and extract the maximum variance possible from the data to group similar replicates. All along our microarray analysis, we confirmed a high degree of similarity between samples within the same sample type and much less similarity between samples from different sample type and withdrowed of the analysis the necessary outlier replicates.

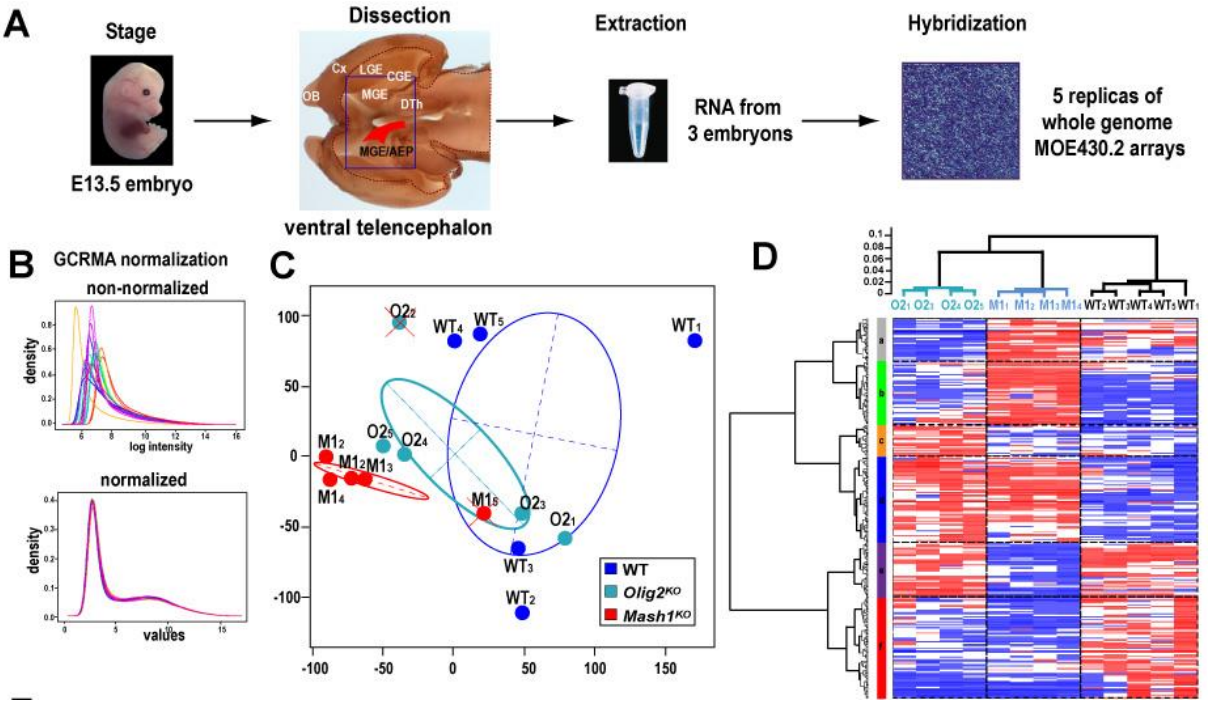

Figure 24. Generation, normalization and analysis of *Ascl1*^{KO} and *Olig2*^{KO} microarrays. (**A**) Scheme of arrays production. (**B**) Arrays samples before and after normalization by GCRMA showing a good normalization of all arrays after the treatment. (**C**) 2D projection of a 3D plot global representation of arrays showing the similarity of gene expression in each array, represented by the principal component analysis. One *Ascl1* and one *Olig2* arrays were not included in further analysis given their difference with respect of the others of the same genotype. Note the proximity of 4 *Ascl1*^{KO} arrays making the data of Ascl1 arrays very robust. (**D**) Clustering heat map of the 300 top genes more significantly regulated in the arrays, showing that selected arrays cluster together by genotype, presenting 6 different regulation pattern clusters. $M1_{1\text{-}5}$, *Ascl1KO* arrays; $O2_{1\text{-}5}$, *Olig2KO* arrays; $WT_{1\text{-}5}$, wild-type arrays. Dissection picture A in shows a forebrain where the dorsal region has been removed to show the ventral part; red are indicates the region generating OPC at embryonic stages (MGE/AEP). MGE, medial ganglionic eminence; AEP, anterior entopenduncular area; OB, olfactory bulb; LGE, lateral ganglionic eminence; Cx, cortex.

Cell culture

Neurospheres cultures

Neurospheres were isolated from CD1 mouse fetuses at embryonic day 13.5. Briefly, pregnant mice were euthanized by cervical dislocation and the fetuses were rapidly decapitated. After removal of meninges, the cortices were collected in Hanks' balanced salt solution without Ca2+ and Mg2+ (HBSS, Invitrogen, Carlsbad, USA) and dissociated in trypsin–EDTA (5 g/L trypsin–2 g/L EDTA, Sigma, St. Louis, USA) plus 1 U/mL DNAse I (Sigma) solution, for 30 min at 37 °C. Following trypsinization, cells were washed three times with HBSS, resuspended in a final volume of stem cell culture medium (xx) and mechanically dissociated using a pipette. Approximately 1×10^6 cells/mL were cultured in the presence of 10 ng/mL murine epidermal growth factor (EGF, PeproTech), 10 ng/mL murine basic fibroblast growth factor (bFGF, PeproTech) and 1% antibiotic peniciline /streptavidine (Sigma), and maintained at 37 °C in a humidified atmosphere of 5% CO2. Under these proliferating conditions, the cells grow as free-floating neurospheres. After mechanical dissociation of neurospheres, proliferating medium was changed after 2 DIV. For differentiation analysis, cells were plated on coated coverslips pre-coated with poly-d-lysine (PDL, Sigma) at 1×10^6 cells/mL. differentiate was induced by culturing dissociated neurospheres in differentiation medium (DMEM supplemented with 0.5 mM l-glutamine, 2% B-27 Supplement (Invitrogen), 30 mM glucose, 50 ng/mL bovine serum albumin, 1% fetal bovine serum and 1% AB/AM in tissue culture plates .Every 3 days, half of old medium was removed by aspiration and replaced by the same volume of fresh medium. cells were fixed with 4% paraformaldehyde (w/v) in PBS at 1, 3, 6, 9 and 15 DIV under differentiating conditions, and processed for characterization by immunocytochemistry

OPC purification protocol

OPCs were isolated from P2 Rat cortices using an immuno-panning method (Chen et al., 2007). Briefly, mixed cortices were cultured in 15% FBS medium for five days, then switched to B104 conditional medium for 2 days before isolation of OPCs

by mechanical shearing in an orbital shaker and then grown in the OPC Growth Medium (Sato medium supplemented mitogens 10 ng/ml PDGF-AA and 20 ng/ml bFGF). 20 million OPCs were fixed 10 min at room temperature with 1% formaldehyde-containing medium, then quenched by 125 mM glycine for 5 min at RT. Cells were washed in cell lysis buffer containing 50 mM HEPES (pH 7.6), 140 mM NaCl, 1 mM EDTA, 10% Glycerol, 0.25% Trit0on X-100 and 0.5% NP-40 and protease inhibitor cocktail (Roche) for 10 min at 4°C. Lysates were centrifuged and resuspended in nuclei washing buffer (200 mM NaCl, 1 mM EDTA, 1 mM EGTA, 10 mM Tris (pH 8.0), and protease inhibitor cocktail) and rocked for 10 min at 4°C. Nuclei were pelleted and resuspended in 300 µl sonication buffer (10 mM Tris-HCl (pH 8.0), 1 mM EDTA, 0.5 mM EGTA and protease inhibitor cocktail). The lysates were sonicated with a Bioruptor sonicator (Diagenode) for 30 minutes, with an interval cycle time of 30 seconds on, 30 seconds off into fragmented DNAs around 400 bp and precleared by adding 30 µl prerinsed protein A/G plus agarose beads for 1hr at 4°C. The concentration of the chromatin was checked by nanodrop and the integrity and size of fragments confirmed by running 1-3µg of sample in a 2% TAE gel. Sonicated chromatin (300 µg) was used for immuno-precipitation and incubated with appropriate antibodies (4 µg) overnight at 4°C. 10% of chromatin used for each ChIP reaction was kept as input DNA. Prerinsed protein A/G plus agarose beads (50 µl) was added to each ChIP reaction and incubated for 1 hr at 4°C. The beads were washed twice with low salt buffer (0.1% SDS, 1% Triton X-100, 2 mM EDTA, 20 mM Tris-HCl (pH 8.1), 150 mM NaCl), high salt buffer (0.1% SDS, 1% Triton X-100, 2 mM EDTA, 20 mM Tris-HCl (pH 8.1), 500 mM NaCl) and LiCl buffer (0.25 M LiCl, 1% IGEPAL CA630, 1% deoxycholic acid, 1 mM EDTA, 10 mM Tris (pH 8.1)), then rinsed with 1X TE. The beads were incubated in 200 µl elution buffer at 65°C for 20 min to elute immunoprecipitated materials. The eluted chromatin was subject to reversal of the crosslinking and DNA purification with phenol-chloroform. The ChIP-seq libraries were prepared using 5500 SOLiD Fragment Library Core Kit (PN 4464412) and run on the 5500xl SOLiD sequencer from Life Technologies. Antibodies for ChIP-seq are rabbit Ascl1 (gift from J. Johnson); Olig2 (Millipore, ab9610).

Cell transfection

Dissociated neurospheres were transfected with a NEON electroporation system (Invitrogen) using 100 µl cells at a concentration of 5×10^6 cells/ml in electroporation buffer and 400 nM *pCAG-Ascl1-ires-GFP* or *pCAG-Olig2-ires-GFP* plasmids. Electroporation was carried out using the following settings: 100 µl tip volume, 1300 V pulse voltage, 20 ms pulse width, one pulse. Electroporated cells were transferred to antibiotic-free EGF/FGF neurosphere medium, and experiments were carried out 24 h after transfection. Successful overexpression in 70% of living cells was confirmed by counting of the GFP positive cells 24h post-electroporation. Successful overexpression was then confirmed by real-time RT-PCR.

Drug screening

Drug repositioning is the process of finding new uses of existing drugs. The availability of several established clinical drug libraries and rapid advances in nextwork biology, genomics and bioinformatics has accelerated the development in silico drug screening. Here we used the Comparative Toxicogenomics Database (Davis AP, Murphy CG 2013) to searchevery drugs that were shown in a any system to modify the expression of one of the selected genes in enriched and specific gene lists generated for the oligodendrglial lineage cell types (OPCs, Premature OLs and myelinating OLs). Aiming at finding potential drug that could affect OPCs proliferation, survival or myelination. We selected drugs identified in at least two different studies with minimal toxic effect that were shown to significantly modify the expression of our gene of interest. We identified 184 drugs involved in OPC gene regulation and 519 drugs involved in myelin genes. As positive control, we identified many drugs already tested in the demyelinating/remyelinating context such as Cuprizone (demyelinating drug), Fingolimod, dimethyl fumarate (remyelinating drug in MS). Focusing on drugs that were untested in remyelinating studies, we selected

Creatine as genes involved in creatine metabolism Gatm and Gtam were found to be specific or enriched in myelinating oligodendrocytes.

Chapter II: Data analysis and interpretation

ChIP-Sequencing Peak-Calling and Data Analysis

All the Chip-sequencing analysis were done using Cisgenome2.0. Sequencing data were mapped to rat genome assembly (Baylor 3.4/rn4) using bowtie (version 0.12.7). Quality control and peak calling was performed using MACS (Model-based Analysis of ChIP-seq version 1.4.2) with default parameters. Filter was apply using a p value cutoff $< 10^{-9}$; an 5-fold enrichment compared to control; tag number > 20. The genome-wide distribution of protein binding regions was determined by genomatix in reference to Ensembl RGSC3.4.61 release and converted into mouse mm9 assembly for comparison with mouse data using the liftover tool of Cisgenome2.0. Phylogenetic conservation analysis was performed using Cisgenome2.0. Chip-sequencing peaks (BED file) were uploaded into genomtix to generate overview statistics of overlapping regions such as promoters, exons, introns, repeats, microRNAs etc. We then performed a next-neighbor analysis selecting all hit within a genes and genes associated with peaks in less than 5kb regions. We then associated integenic peaks with epigenetic and Hi-C data obtained from embryonic and adult brain tissue to detect long range promoter-enhancer interactions (Visel et al, 2010). Finally, we performed diverse gene set enrichment analysis with the identified direct targets either with pathway studio or genomatix and finally reconstructed the transcriptional network of Ascl1 and Olig2.

RT-PCR Analysis of ver-expression of Ascl1 and Olig2 in neurosphere

Total RNA was isolated from dissociated neurosphere cultures using the RNeasy Mini Lipid Kit (Qiagen) with DNase treatment. Tissues were homogenized in 1 mL QIAzol Lysis Reagent (Qiagen) using electric homogenizer. cDNA was generated from 500 ng of total RNA using SuperScript-III (Invitrogen). The integrity

of the RNA was assessed by nanodrop. 1/50 was amplified with Power SYBR Green (Applied Biosystems) and 100 nM of each primer in a Biorad iCycler real-time PCR machine: one cycle at 50 °C, 2 min;1 cycle 95° C, 10 min; 40 cycles 95° C, 15 sec, 60° C 1 min. Primers used :Ascl1r : —PCRfGCAACCGGGTCAAGTTGGT" ; Ascl1f : —PCRrGTCGTTGGAGTAGTTGGGGG» ; Olig2r : —TCCCCAGAACCCGATGATCTT Olig2f :—CGTGGACGAGGACACAGT";CHD7r:"TCTGGTTTTGTTCCCGAGTCL;CHD7f: "CCCTGAAGTAGAGGCGACAG";Scr_r:—GGATCAGCCTAACCGAATGA"scr_f:" CGGGATAGACTCCCATCTGA".

Transcription factor binding site enrichement analysis

Methods that detect occurrences of TFBSs and clusters of TFBSs from DNA sequence data are a usefull tool to understand the structure of cis-regulatory regions (Hardison and Taylor 2012). Methods used in this analysis detect clusters of motif matches appearing more frequently than expected given a promoter or whole-genome background model (Berman et al., 2002; Frith et al., 2002; Halfon et al., 2002; Markstein et al., 2002; Rebeiz et al., 2002). This Analysis searches transcription factor binding sites (TFBS) within the input sequences (BED files); and generates statistics on single TFBSs and TFBS pairs (modules) together with overrepresentation values and Z-scores. TFBS pairs are defined as two TFBS in a distance of 10-50 bp and allow to assess preferred distance ranges between TFBS. All occurrences of TFBS matches are calculated and the overrepresentation values are given based on the background of occurrences of the TFBS within the whole genomic sequence of the selected species or within all promoters as already annotated (500/100bp up/downstream of the TSS). Analysis output can be either to TFs family matrices or to individual TFs matrices. We also used de novo methods for the discovery of TFBS, such as MEME-CHIP (Timothy L. Bailey, 2009);

OBJECTIVES & HYPOTHESES

Our project aims to provide a new molecular understanding of the transcription program involved in neural stem cells differentiation into oligodendrocytes. The rational of this work relies on previous studies demonstrating that the bHLH transcription factors Olig2 and Ascl1 work in synergy to specify OPCs, the oligodendrocyte progenitor cells (Lu et al., 2002; Zhou and Anderson, 2002; Parras et al., 2004; Xin et al., 2005; Wang et al., 2006; Parras et al., 2007; Sugimori et al., 2007; Sugimori et al., 2008).

One central goal of this work was to understand at a genomic and transcriptomic level, how Ascl1 and Olig2 work together to specify OPCs. To do so, we followed a strategy using genome-wide transcriptome analysis and chromatin immuno-precipitation. We characterized Ascl1 and Olig2 regulated genes using genome-wide microarray analysis of embryonic ventral telencephalon from *Ascl1*^{KO}, *Olig2*^{KO} and wild-type (WT). Next, we identified functional high-confidence whole-genome transcription factor binding sites profiles for Ascl1 and Olig2 using chromatin-immuno-precipitation techniques in embryonic ventral telencephalon and purified OPCs. In order to perform an integrative analysis of the neural stem cell (NSCs) and oligodendroglial lineage differentiation processes, we coupled our Ascl1/Olig2 analysis with epigenetic information for active transcriptional enhancers in neural stem cells and OPCs that we combined with a cell-type specific transcriptomic analysis of the major cell types in the brain. We identified new specific markers of different neural lineages and new important genes driving OPCs differentiation. We focused on *Chd7* and *Tns3*, two genes whose expressions are driven by Ascl1 and Olig2 and enriched in the oligodendroglial lineage at two interesting stage, the early specification stage and the transition between migrating and differentiating oligodendrocytes, respectively.

Another major challenge of this work was to find therapeutical molecules promoting myelin repair. As currently, most of the available treatments for demyelinating diseases are based on immuno-modulatory and anti-inflammatory drugs and only a few are able to promote myelin repair, we used an approach of toxicogenomic and drug repositioning to identify new molecules known to modify OPCs and myelin genes but untested in the context of demyelinating diseases. We identified creatine as a potential metabolite important in the oligodendrocyte and axonal metabolism.

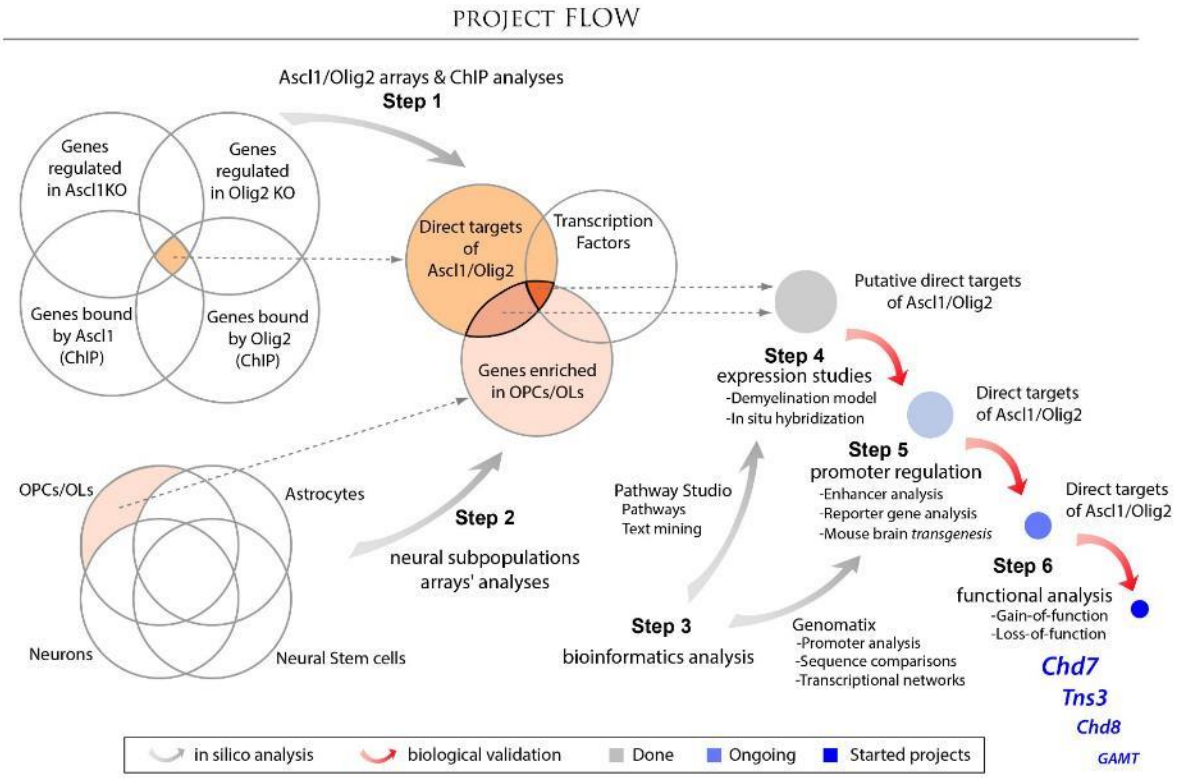

Figure 25. Project experimental design for identification of Ascl1/Olig2 common direct targets. Scheme representation of the different sets of data generated or processed to identify both the direct targets common to Aslc1 and Olig2, and those that are enriched in the oligodendroglial cells. Each Venn circle represents a gene dataset. Time flows from let to right. In silico studies are depictures with grey arrows and biological experiments with red arrows. Final focus in few selected genes is shown with relative size corresponding to the functional data cumulated for each selected gene (*Chd7, Tns3, Chd8, GAMT*).

RESULTS

Role of Ascl1 and Olig2 in neural stem cell and oligodendrocyte differentiation

Ascl1 and Olig2 regulated genes in embryonic ventral telencephalon identification by microarray analysis

In order to characterize the role of Ascl1 in NSCs and OPCs, we identified the Ascl1 regulated genes using genome-wide microarray analysis of E13.5 ventral telencephalon from *Ascl1*^{KO} and WT (Fig. 24A). The embryonic ventral telencephalon is formed by the ganglionic eminences and is mainly composed of NSCs and migrating neuroblasts but is also the first place of OPCs specification in the forebrain. We dissected part of ventral telencephalon containing the medial, lateral and caudal ganglionic eminences (Fig 24A-D), including also the following regions: subpallium (Spall), rostral secondary prosencephalon (RSP) and part of the prethalamus (PTh) according to Allen Brain E13.5 reference atlas (http://developingmouse.brain-map.org/static/atlas). We identified 2337 unique genes significantly regulated by Ascl1 (P-value < 0.05 and fold-change >1.2 fold) in this region. We subsequently analyzed the functional meaning of the genes identified using a "gene-set enrichment analysis" to detect statistically significant signalling pathways regulated by Ascl1 (Fig. 24). As expected, we found Notch/Hes pathway as significantly regulated. Interestingly, we found that Ascl1 regulates Notch signalling at different level: Ascl1 regulates Notch at the receptor level (*Notch1*), at the ligand level (*Jag1, Dll1, Dll3*), at the downstream target genes level (*Hes1, Hes5, Hes6, Hey1*) but also at the regulatory level (Mfng, Fbxw7, Itch). Similarly, Ascl1 regulates the Wnt pathway at different levels. Indeed, Ascl1 regulates the Wnt5a ligand gene, Fzd8 receptor gene, but also the *Gsk3b, Tcf7l2, Axin1 and Ctnnb1* effectors genes. We also found important regulators of the cell cycle and mitosis such as *Ccnd1, Ccnd2, Cdca8, Aurkb, Cdk7, Cdk6, Csnk2a1 Cdc25b,* as being significantly regulated, thus providing evidence of a functional control of Ascl1 in the G1-S and G2-M transitions. Moreover, Ascl1 is involved in other important signaling in NSCs such as, Integrin signaling (Itgb3bp, Itgb1, Itgb5), Semaphorin signaling (*Sema7a, Sema5a, Sema3a, Sema3e, Sema3c, Sema4c*) and Ephrin signaling (*Ephb2, Ephb3, Epha3, Epha4, Epha5*).

Then, we performed a genome-wide microarray analysis of E13.5 ventral telencephalon from *Olig2*^{KO} and WT and identified 1318 unique genes regulated by Olig2 (P-value < 0.05 and fold-change >1.2 fold, Fig. 26A). We identified 674 unique genes regulated by both Ascl1 and Olig2 and 644 unique genes regulated only by

Olig2. Interestingly, we found that a large proportion of genes regulated by both Ascl1 and Olig2 follow the same pattern of regulation (and really few having opposite regulation) thus demonstrating the synergistic action of Ascl1 and Olig2 in NSCs physiology. Moreover, the gene-set enrichment analysis of the shared and unique regulated genes showed that Olig2 and Ascl1 mostly regulate the same signalling pathways despite some specificity (Fig. 26B). Indeed, Olig2 also regulate genes involved in cell cycle (*Ccnl2, Cdc73, Mcm4, Ccnd2, Csnk2a2, Cenpl, Cdk5rap1, Atm, Ccnc, Ccnd1, Cdc27, Ccnt2*), Notch signalling (*Notch1, Notch2, Hes1, Itch, Jag1*), Wnt signalling (*Gsk3b, Tcf7l2, Fzd5 Fzd1, Dvl1, Axin1, Fbxw11*), Integrin signalling (*Itgb3bp, Itgav, Itgb1*), Semaphoring signalling (*Sema4b, Sema3e, Sema5a, Sema5b, Sema4b*) and Ephrin signalling (*Epha3, Epha5, Ephb1, Ephb2*). However, due to the non-conditional nature of the mutation in $Ascl1^{KO}$ and $Olig2^{KO}$, long term changes make impossible to discriminate between direct transcriptional targets and gene regulations occurring secondarily due to long term changes in cellular transcriptional state or changes in cell-type proportion in the ventral telencephalon. As such microarray analysis could not precisely identify direct targets, or discriminate in which cell type such regulations occurs, we used chromatin-immunoprecipitation experiments in ventral telencephalon or purified OPCs to further study the role of Ascl1 and Olig2 in OPCs.

A

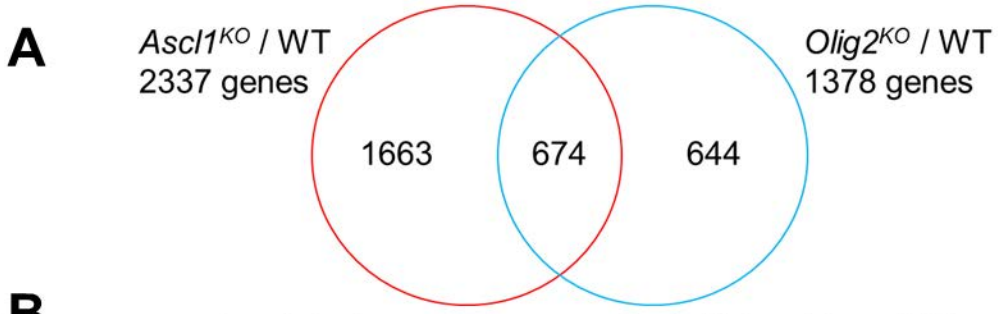

B

Canonical pathway	P-value	# Genes (observed)	# Genes (total)
Integrin Linked Kinase	2.10E-06	27	88
Akt Signaling	3.21E-06	66	317
Ribosomal Protein S6 Kinase	3.79E-06	35	133
Fbxw7 signaling	9.40E-06	15	37
Tcf/Lef Signaling	1.05E-05	30	191
Netrin Signaling Events	1.51E-05	14	31
Integrin-Linked Kinase Signaling	4.54E-05	17	46
Wnt-Beta Catenin Signaling	4.66E-05	25	83
Aurora Kinase Signaling	4.71E-05	31	125
Glycogen Synthase Kinase	1.10E-04	49	241
Telomerase Reverse Transcriptase	1.38E-04	19	65
G1-S And G2-M transition	1.85E-04	49	246
Nephrin/Neph1 Signaling	2.60E-04	11	26
Low Density Lipoprotein Receptor	3.51E-04	35	163
Notch Secretory Pathway	3.59E-04	15	44
Microtubule Regulating Kinase	3.63E-04	10	42
Mitogen-activated protein kinase (MAP Kinases)	3.70E-04	12	31
Cyclin E	4.41E-04	20	76
P21(Cdkn1a)	4.98E-04	27	117
Protein Degradation	6.07E-04	131	842
Glucocorticoid Regulated Kinase	6.74E-04	21	84
Semaphorin	7.06E-04	22	90
Estrogen Receptor	9.98E-04	23	170
Neurotrophic Tyrosine Kinase Receptor	1.00E-03	25	110
Focal Adhesion Kinase	1.08E-03	18	63
Ephb Signaling	1.13E-03	13	39
Notch	1.21E-03	21	79
Lim Domain Kinase	1.22E-03	15	54
Cdc42 Signaling Events	1.26E-03	20	74
Mixed Lineage Kinase	1.29E-03	40	207
Presenilin 1	1.31E-03	14	49
C-Myb Transcription Factor Network	1.76E-03	15	86
Cytokinesis	1.78E-03	10	30
Eph Receptor	2.21E-03	25	116
Cyclin A2	2.59E-03	14	90
Fyn Tyrosine Kinase	2.76E-03	33	169
Eukaryotic Protein Translation	2.78E-03	5	14
Tgf-Beta Signaling	2.83E-03	8	20
Cell Cycle	3.07E-03	51	514

Figure 26. Ascl1 and Olig2 commonly regulated genes. (**A**) Venn diagrams representing the gene subsets differently regaulated between *Ascl1* mutant versus wild-type and *Olig2* mutant versus wild-type. (**B**) Main pathways regulated in both *Ascl1* and *Olig2* mutant microarrays. Table showing significant signaling pathways regulated by Ascl1 (Yellow), Olig2 (Blue) or Ascl1 and Olig2 (Red). Most of the regulated pathways are regulted by both Ascl1 and Olig2. Important signaling, such as Notch,

Wnt, Sonic Hedgehog are regulated by Ascl1 and Olig2. The indicated number of gene (observed) correspond to the number of genes found to be regulated in E13.5 ventral telencephalon and belonging to a particular signaling pathway (gene total). Enrichment ratios are assessed statistically and p-value are indicated.

A

Gene Symbol	FC m1/wt	PValue	adjPVal	FcO2	PValue1	adjPVal1
Ascl1	0.030234	0.0000	0.0002	1.096	0.299	0.772
Dll3	0.136867	0.0000	0.0033	1.014	0.885	1
Srrm2	0.175114	0.0103	0.2469	0.377	0.087	0.748
Ddx6	0.199449	0.0453	0.4243	0.449	0.260	0.757
Brd4	0.211028	0.0018	0.1454	0.341	0.011	0.687
Gsk3b	0.212042	0.0231	0.3376	0.438	0.162	0.757
Gas2l3	0.216726	0.0089	0.2361	0.548	0.191	0.757
Bcan	0.217556	0.0000	0.1355	0.468	0.037	0.711
Eif2c2	0.227965	0.0140	0.2810	0.458	0.124	0.757
Xpr1	0.228525	0.0098	0.2418	0.515	0.151	0.757
Akap9	0.22877	0.0496	0.4335	0.434	0.217	0.757
Csnk2a1	0.229469	0.0219	0.3316	0.455	0.156	0.757
Rasal2	0.229857	0.0012	0.1252	0.504	0.039	0.711
Stk33	0.231351	0.0000	0.0326	1.034	0.829	1
A430081F14Rik	0.233254	0.0178	0.3078	0.572	0.266	0.757
Gas2l3	0.243505	0.0254	0.3486	0.573	0.293	0.767
Hes5	0.244936	0.0000	0.0094	0.896	0.292	0.767
Mll5	0.246158	0.0065	0.2135	0.428	0.051	0.711
Btg1	0.249387	0.0090	0.2361	0.439	0.068	0.727
Sgce	0.252843	0.0297	0.3700	0.464	0.167	0.757
Fancf	0.259928	0.0080	0.2266	0.477	0.080	0.737
Agap1	0.26341	0.0173	0.3048	0.469	0.117	0.757
Mll5	0.265957	0.0087	0.2335	0.370	0.029	0.711
Hmga2	2.472355	0.0091	0.2368	1.559	0.117	0.757
Tia1	2.483981	0.0401	0.4130	2.015	0.092	0.753
Lix1	2.492792	0.0101	0.2452	2.895	0.005	0.634
Kctd12b	2.509596	0.0020	0.1484	1.017	0.930	1
Lin7c	2.511138	0.0151	0.2906	2.198	0.029	0.711
Tmed2	2.521654	0.0066	0.2152	2.100	0.018	0.690
2810043O03Rik	2.555225	0.0152	0.2915	1.390	0.290	0.765
Asb4	2.580573	0.0000	0.0219	1.196	0.083	0.742
Tmed2	2.591533	0.0284	0.3630	2.323	0.044	0.711
Prkx	2.611488	0.0042	0.1859	1.424	0.158	0.757
Pax6	2.619862	0.0031	0.1707	1.344	0.204	0.757
Ctnnd1	2.653493	0.0025	0.1567	1.552	0.070	0.728
Pnoc	2.714899	0.0000	0.0085	1.181	0.042	0.711
Fscn1	2.862726	0.0042	0.1853	2.118	0.020	0.695
Eif4g3	2.902622	0.0026	0.1579	0.940	0.788	1
Gucy1a3	3.026879	0.0000	0.0054	1.127	0.111	0.757
Ascl1	3.067702	0.0000	0.0036	1.123	0.076	0.737
Armc9	3.268002	0.0367	0.3988	1.872	0.210	0.757
Thbs1	3.432003	0.0002	0.0604	1.247	0.203	0.757
Dyrk1a	3.589822	0.0043	0.1860	2.631	0.015	0.687
Grb10	3.689663	0.0264	0.3521	2.946	0.052	0.711
Cpa4	4.005338	0.0000	0.0005	1.708	0.000	0.182
Thbs1	4.023009	0.0008	0.1068	1.510	0.123	0.757
Dmrta1	4.158747	0.0001	0.0354	0.989	0.945	1
Npy	4.65679	0.0000	0.0100	1.027	0.822	1

B

Probe Set	Gene Symb	FcO2	PValue	adjPVal	FC m1/wt	PValue	adjPVal
1416149_	Olig1	3.4100	0.0100	0.6600	1.097246	0.7700	1.0000
1426438_	Ddx3y	3.2100	0.3400	0.8100	2.638428	0.4200	0.8600
1425457_	Grb10	2.9500	0.0500	0.7100	3.689663	0.0300	0.3500
1421180_	Lix1	2.8900	0.0000	0.6300	2.492792	0.0100	0.2500
1417210_	Eif2s3y	2.7500	0.3100	0.7800	1.98724	0.4800	0.9200
1454373_	Ubc	2.7400	0.0000	0.6200	2.034171	0.0200	0.3100
1423851_	Shisa2	2.0500	0.0000	0.3600	1.90497	0.0000	0.0900
1451314_	Vcam1	2.0100	0.0000	0.4800	0.85857	0.2500	0.6900
1426057_	Epha3	1.9500	0.0000	0.5000	2.152647	0.0000	0.0900
1427830_	Zfp260	1.7700	0.0000	0.4800	1.571678	0.0000	0.1800
1417187_	Ube2k	1.7600	0.0000	0.4800	1.863445	0.0000	0.0900
1416124_	Ccnd2	1.7200	0.0000	0.4600	2.17253	0.0000	0.0400
1453770_	Cpa4	1.7100	0.0000	0.1800	4.005338	0.0000	0.0000
1433891_	Lgr4	1.6600	0.0000	0.4600	0.932666	0.4300	0.8700
1455556_	Notch2	1.6200	0.0000	0.5000	1.133947	0.1900	0.6900
1453771_	Gulp1	1.6000	0.0000	0.4800	1.620033	0.0000	0.1100
1418246_	Rbm9	1.5200	0.0000	0.4600	1.53294	0.0000	0.0900
1418325_	Sephs2	1.5100	0.0000	0.2200	1.55992	0.0000	0.0300
1419484_	Gbas	1.5000	0.0000	0.3800	1.32692	0.0000	0.1500
1418286_	Efnb1	1.4600	0.0000	0.5000	1.41928	0.0000	0.1400
1427924_	Stx17	1.4200	0.0000	0.3100	1.371777	0.0000	0.0700
1460378_	Tes	1.4200	0.0000	0.4800	1.274947	0.0100	0.2100
1416711_	Tbr1	1.4000	0.0000	0.4600	2.098881	0.0000	0.0100
1452259_	Phf20	1.4000	0.0000	0.5100	1.302503	0.0000	0.1900
1418381_	Zfp148	1.3900	0.0000	0.3800	1.25297	0.0000	0.1500
1447513_	Kcnd3	1.3600	0.0000	0.4800	1.79824	0.0000	0.0200
1439163_	Zbtb16	0.6800	0.0000	0.4600	0.699845	0.0000	0.1200
1444778_	sept.-03	0.6700	0.0000	0.4200	0.854855	0.0400	0.4100
1459357_	Nfasc	0.6700	0.0000	0.4600	0.604063	0.0000	0.0500
1430290_	Gm10196	0.6600	0.0000	0.2200	0.700398	0.0000	0.0500
1439950_	Dync1h1	0.6400	0.0000	0.4600	0.595085	0.0000	0.0700
1417122_	Vav3	0.6300	0.0000	0.4800	0.975731	0.7700	1.0000
1440885_	Evl	0.6300	0.0000	0.4600	0.915897	0.2800	0.7000
1416232_	Olig2	0.6300	0.0000	0.2800	0.604686	0.0000	0.0300
1448147_	Tnfrsf19	0.6200	0.0000	0.3600	1.254691	0.0100	0.2600
1439578_	Lsm11	0.5400	0.0000	0.4600	0.690351	0.0100	0.2400
1429905_	Lhx9	0.5200	0.0000	0.4600	0.901211	0.3700	0.8000
1426936_	BC005512	0.4200	0.0000	0.4600	0.862563	0.3400	0.7600
1457268_	Dot1l	0.4200	0.0100	0.6900	0.410955	0.0100	0.2400
1420337_	Gbx2	0.4100	0.0000	0.6200	0.948732	0.8100	1.0000
1455165_	Rora	0.4100	0.0100	0.6900	0.744937	0.2700	0.6900
1460159_	Mysm1	0.3900	0.1100	0.7600	0.274112	0.0400	0.4200
1438688_	Srrm2	0.3800	0.0900	0.7500	0.175114	0.0100	0.2500
1419327_	Pdxdc1	0.3700	0.2000	0.7600	1.288309	0.7300	1.0000
1442222_	Ifnar1	0.3700	0.0200	0.6900	0.411992	0.0300	0.3600
1439107_	Mll5	0.3700	0.0300	0.7100	0.265957	0.0100	0.2300
1438042_	Shox2	0.3500	0.0100	0.6900	0.82073	0.5500	1.0000
1424922_	Brd4	0.3400	0.0100	0.6900	0.211028	0.0000	0.1500

Figure 27. Regulation of Ascl1 and Olig2 target genes in E13.5 vental telencephalon. (A-B) Table showing the most regulated and statistically significant genes (A) down and (B) up-regulated by Olig2 (maximal fold change and FDR 1%). A larger selection of Ascl1 regulated genes can be found in annex. Olig2 is not detected as significantly down regulated. However, Olig1 is higly up regulated and

oligodendrocyte expressed genes are down regulated such as brevican Smarca4 (Brg1). (**C**) Table showing the most down-regulated and statistically significant Ascl1 regulated genes (maximal fold change and FDR 1%). As expected, Ascl1 transcript is highly down-regulated, together with members of the Notch pathway such as Dll1, Dll3, Mnfg or Hes5. Interestingly, another Ascl1 probeset, measure an increase in gene expression in the knock-out. Partial transcription of the Ascl1 exon 1 region may be up-regulated larger selection of Ascl1 regulated genes can be found in annex.

Ascl1 direct target in embryonic ventral telencephalon identification by chromatin-immuno-precipitation

We used promoter-specific ChIP-on-chip and whole genome ChIP-sequencing techniques generated with Ascl1 antibody on whole E12.5 ventral telencephalon material to investigate which genes were regulated through direct binding of Ascl1 on gene promoter or associated cis-regulatory sequences (collaboration with D. Castro & F. Guillemot). First, we analyzed Ascl1 ChIP-on-chip experimental data (D. Castro 2011) and identified 1265 promoters significantly bound by Ascl1 (Fig. 28). Then, we analyzed Ascl1 in ChIP-sequencing experiment and identified 21902 regions significantly bound all along the genome by Ascl1 from which 8020 region were located inside a gene (promoter, intron, exon) and 13882 region were located in intergenic regions. We found a good overlap between the two experiments as 22013 unique regions bound by Ascl1 were found combining the two datasets. In order to infer regulatory capacities of those regions, we combined these datasets with NSCs H3K4me1, H3K4me3 and H3K27Ac epigenetic information to identify promoters and cis-regulatory regions that are actively regulated (GEO GSE12241). We then used a ~~"n~~ext neighbor's analysis" and we associated regions to the closest gene with a maximum distance of 5kb. Finally, we took advantage of recent Hi-C data obtained from embryonic and postnatal brain tissues to infer long range promoter-enhancer interactions from our ChIP-seq dataset (Y Shen 2012).

This integrative method (Fig. 28 and Fig. 29) allowed us to map the position of Ascl1 binding in the regulatory genetic landscape of NSCs and subsequent comparison with Ascl1/Olig2 knock-out microarray data allowed us to detect numerous high confidence functional Ascl1 binding sites.

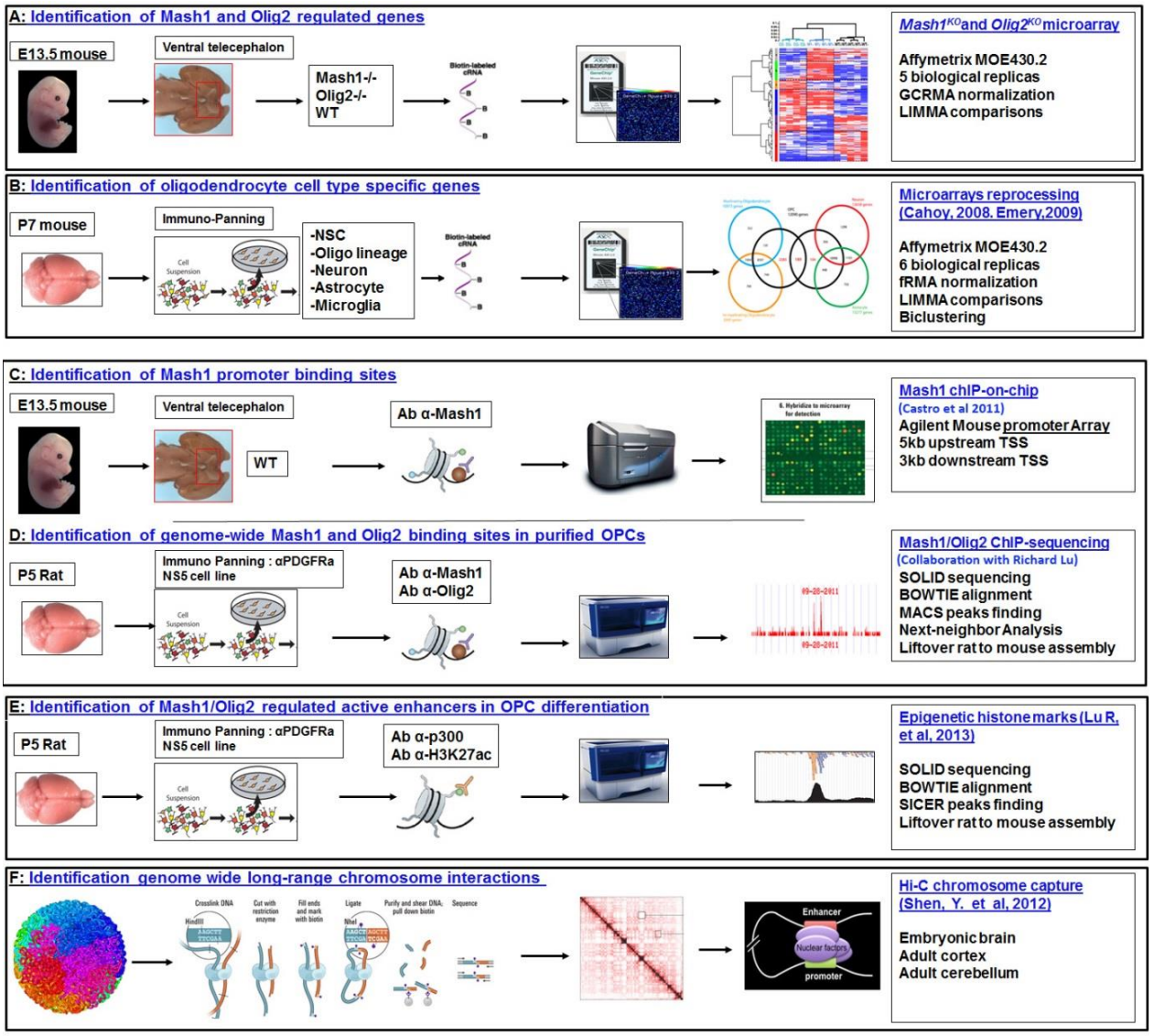

Figure 28. Analysis of Ascl1 and Olig2 function in oligodendrocyte differentiation. **(A)** Scheme of array production from *Ascl1*^{KO}, *Olig2*^{KO} and *WT*. Dissection picture shows the MGE/AEP region of mouse ventral forebrain (in red) where embryonic OPC are generated. MGE, medial ganglionic eminence; AEP, anterior entopenduncular area. (**B**) Identification of oligodendrocyte genes reprocessing published microarray data from all the main neural cell types. (**C,D**) Identification of Ascl1 and Olig2 binding sites using ChIP-Chip and Chip-seq analysis on mouse ventral forebrain (C), purified rat postnatal OPCs and NS5 cell line (D). **(E)** Identification of Ascl1/Olig2 regulated active enhancers using H3K27ac in the oligodendrocyte lineage. **(F)** Identification of genome-wide long range interactions in embryonic and adult mouse brain using Hi-C technics. Picture shows 3D organisation of chromosomes, each one occupying its own

territory.This technic mesure the interaction probability from two chromatin sites for the whole genome.

chr	start	end	length	summit	tags	_=-10*LOG10(pvalue)	fold_enrichment	FDR(%)	GeneIDs	Symbols
chr3	84741764	84742569	806	366	385	3100	235.88	0	50754	Fbxw7
chr3	126970642	126971796	1155	284	355	3100	200.88	0	109676	Ank2xA
chr16	35729081	35729820	740	370	203	3047.47	161.63	0	224132	Dirc2
chr6	96581372	96581954	583	334	191	3050.24	155.86	0	320265	Fam19a
chr5	116730210	116731154	945	392	416	3100	149.18	0	269693	Ccdc60
chr7	29086483	29087717	1235	874	447	3100	148.08	0	13389	Dll3
chr6	88931261	88932093	833	530	348	3100	134.48	0	232217	493342
chr11	80322042	80322908	867	445	308	3100	127.55	0	7	Myo1dx
chr7	119904052	119904759	708	395	225	3117.62	127.02	0	21676	Tead1
chr17	15508619	15509365	747	413	335	3100	124	0	13388	Dll1
chr12	100458536	100459083	548	229	216	3135.01	123.57	0	71375	Foxn3
chr3	7366318	7366959	642	335	154	2198.33	122.38	0	18767	Pkia
chr2	62645240	62646089	850	399	266	3100	118.01	0	170738	Kcnh7
chr6	52534162	52534883	722	359	267	3100	112.86	0	58875	Hibadh
chr4	5889606	5890170	565	267	140	1994.37	110.81	0	242297	Fam110
chr16	35564462	35565100	639	277	227	3094.19	110.29	0	20357	Sema5b
chr14	57506644	57507260	617	301	249	3100	105.18	0	76007	Zmym2
chr4	8726064	8727178	1115	760	266	3063.7	103.33	0	320790	Chd7
chr13	44847090	44847574	485	237	127	1871.58	102.75	0	16468	Jarid2
chr9	64957075	64957766	692	335	191	2515.72	101.13	0	56741	Igdcc4
chr11	80148973	80149679	707	392	215	2900.5	101	0	246104	Rhbdl3
chr1	140396592	140397227	636	295	133	1784.89	99.32	0	59125	Nek7
chr11	31900184	31900811	628	220	257	3100	98.57	0	18197	Nsg2
chr12	54354189	54354736	548	320	150	1998.51	94.55	0	27386	Npas3
chr4	131590149	131590714	566	221	102	1309.06	92.36	0	269587	Epb4.1
chr1	160196988	160197548	561	255	124	1614.56	91.26	0	240843	Brinp2
chr12	90039444	90040351	908	463	214	2831.24	90.29	0	18191	Nrxn3
chr7	17529549	17530357	809	360	276	3100	88.51	0	434128	Pnmal2
chr17	28173806	28174903	1098	374	412	3100	87.38	0	224650	Anks1
chr9	51957360	51958042	683	365	214	2695.78	87.38	0	244871	Zc3h12c
chr9	110108384	110108912	529	252	153	2051.86	86.57	0	20588	Smarcc1
chr5	123796093	123796933	841	462	273	3100	86.55	0	77045	Bcl7a
chr10	50630696	50631224	529	330	150	1915.76	85.84	0	20464	Sim1
chr9	112110108	112110905	798	448	371	3100	85.82	0	74100	Arpp21
chr2	78029670	78030274	605	267	164	2176.83	84.75	0	78158	493044
chr1	93310422	93311313	892	416	380	3100	84.6	0	55927	Hes6

Figure 29. Ascl1 direct targets in E12.5 ventral telencephalon. Table presenting a selection of Ascl1 direct tragets in E12.5 ventral telencephalon. Symbols of genes are indicated together with chromosomic position of the bindind peaks and associated Fold-change enrichement value compared to control and –log10(p-value). The list is sorted in decreasing order Fold-change enrichement. As expected, Notch genes are the main target of Ascl1 (Fbxw7, Dll3, Hes6. However, important epigenetic chromatin remodelers are aslo directly regulated by Ascl1 such as Chd7 or Smarcc1 (BRG1-Associated Factor 155). A list showing other directly regulated genes is available in the Annex 4.

Ascl1 and Olig2 direct target Identification in oligodendrocyte progenitor cells.

In order to find Ascl1 direct targets in OPCs, we generated Ascl1 ChIP-sequencing data from purified OPCs (see methods for details, in collaboration with Richard Q. Lu) and identified 3252 regions (Fig. 30A) significantly bound by Ascl1 from which 1507 region were located inside a gene and 1745 in intergenic regions. Following the same method previously mentioned, we inferred functional cis-regulatory regions from epigenetic information for H3K4me3 and H3K27Ac in OPCs (GSM1040159; GSM1040162), and from brain Hi-C data (Y Shen 2012). First, we compared the Ascl1 bound regions identified in OPCs with Ascl1 bound regions identified in ventral telencephalon. We found only 734 shared regions, while 2495/3252 regions were OPCs specific and 21213/22013 regions were ventral telencephalon specific. We show that the shared regions are involved in the same signalling pathways than in the ventral telencephalon but with some peculiarities. For example, genes involved in Notch signalling such as *Notch1, Notch2, Dll1, Fbxw7* are bound in OPCs; however, downstream targets like *Hes1, Hes5 or Hey1* are not bound anymore. Similarly some of the genes of the Wnt signalling are significantly bound by Ascl1 such as *Gsk3b, Fzd1, Dvl1, Axin1, Fbxw11, Tcf7l2* (for other signalling pathway, see Fig 31).

We then analysed Olig2 ChIP-sequencing data from purified OPCs (GSM1040156) and identified 21297 regions bound with high-confidence by Olig2. We compared the Ascl1 and Olig2 bound regions identified in OPCs and found 1514/3252 regions that are Ascl1 specific, 19588/21297 regions that are Olig2 specific and 1738 shared regions.

A

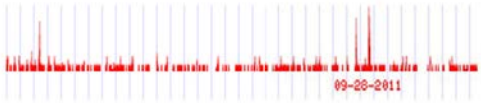

Mash1 chip chip/seq

14449 peaks on the genome in NSC and OPC (3252 in OPC)

Type of genomic element	Number of Regions	Percentage of Regions	Percentage in Genome	Enrichment compared to Genome
Exonic, complete	880	6.1%	5.5%	1.1
Exonic, partial	4671	32.3%	-	-
Intronic, complete	4334	30.0%	37.4%	0.8
Intergenic	4564	31.6%	57.1%	0.6
Sum of above	**14449**	**100.0%**	-	-
Promoter	5542	38.4%	2.6%	14.8

B

Olig2 chip seq

21297 peaks in OPC

Type of genomic element	Number of Regions	Percentage of Regions	Percentage in Genome	Enrichment compared to Genome
Exonic, complete	1342	6.7%	5.5%	1.2
Exonic, partial	2467	12.3%	-	-
Intronic, complete	9127	45.7%	37.4%	1.2
Intergenic	7044	35.3%	57.1%	0.6
Sum of above	**19980**	**100.0%**	-	-
Promoter	2954	14.8%	2.6%	5.7

Figure 30. Ascl1 and Olig2 ChIP binding sites analyses. (**A**) Table showing repartition of the Ascl1 peaks on the genome. Peaks originate from pooling datasets from the ventral telencephalon Chip-seq and Chip-on-chip and Chip-seq in OPCs. 38.4% of peaks are located in promoters. However, Chip-on-chip experiment are designed specifically for promoters, and thus bias proportions. (**B**) Table showing repartition of the OPCs Olig2 binding sites. Among the 21297 identified peaks in Olig2 Chip-seq in OPCs, 45% are intronic, 35% are intergenic and 14.8% of peaks are located in promoters. This reflects the enrichment of TFBS in promoters, enhancers and exon-intron junction where they play a role in the splicing regulation.

Interestingly, Ascl1 binding sites specific for OPCs are located in or near genes known to have key functions in the oligodendroglial lineage such as the early marker *Olig2, Pdgfra, Cspg4 (NG2)* or *Gpr17* but interestingly also in genes involved in later stages and myelination such as *Mbp, Qk, Plp1, Brg1, Myt1, Thra or Fa2h* (see Fig. 31).

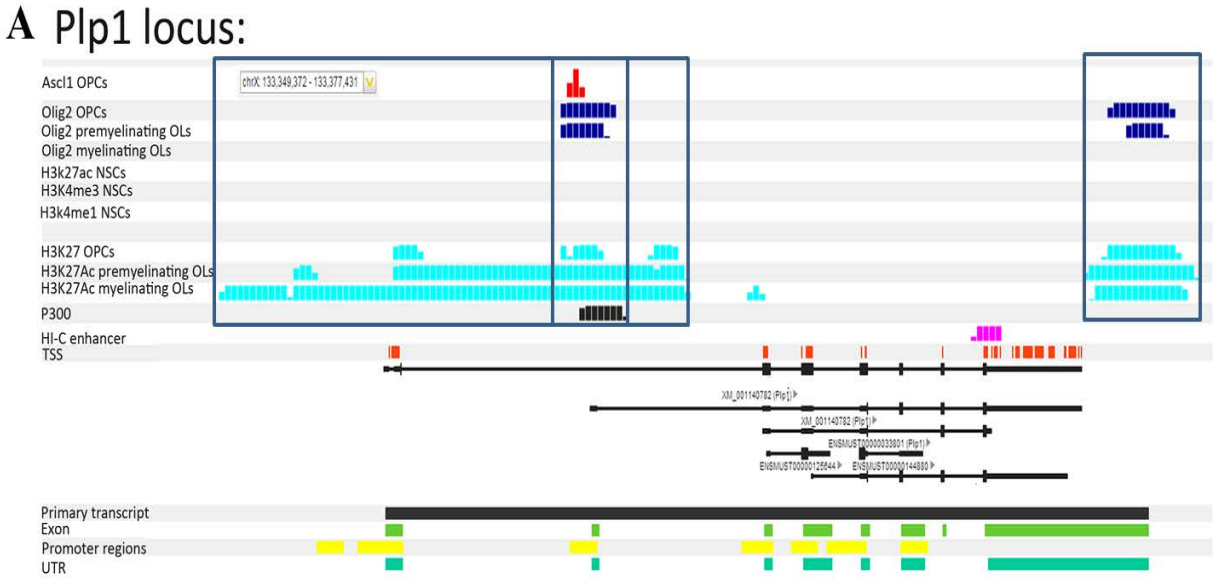

Figure 31. (A). Colaborative binding of Ascl1 and Olig2 on the Plp1 gene. Schematic representing the Plp1 locus. Plp1 gene is transcribed from left to right and indicated by different black horizontal lines representing different transcript existing for the Plp1 gene. Ascl1(red) and Olig2 (blue) binding region are indicated in parallel with H3K4me1/2 and HK27ac in neural stem cells (absent) as well as H3K27ac in the oligodendrogial lineage (light blue). This cobinding event of Ascl1 and Olig2 on active regulatory sites of genes involved in myelination demonstrate overlapping functions. Importantly, Chip-seq experiment are based on cell population pooling and thus reflect average chromatin state. Different mode of co-binding are possible and can occur at the same time. Ascl1 and Olig2 likely synergize via the mechanism of _assisted loading‘ or _hit and run model‘ where two TFs that compete for the same TFBS does not inhibit the activity of each other but rather increases the occupancy of each TFs via increased nucleosome depletion rate (Voss, T. C. 2011). Increased H3K27 acetylation of the chromatin promoter region is visible by the enlargement of the region between the OPC and the myelinating OLS stage. Ascl1 and Olig2 bind at secondary promoter site localized at the second exon of the gene and likely regulate the alternative promoter usage. Hi-C data (purple) indicate a long range interaction between the TSS of Plp1 and the region located at the last exon.

We then analysed Olig2 ChIP-sequencing data from purified OPCs (GSM1040156) and identified 21297 regions bound with high-confidence by Olig2. We compared the Ascl1 and Olig2 bound regions identified in OPCs and found 1514/3252 regions that are Ascl1 specific, 19588/21297 regions that are Olig2 specific and 1738 shared regions.

In order to construct a genomic profiles, we intrgrated our datasets to the Olig2 Chip-seq dataset from the whole oligodendrocyte lineage, (OPCs (21297regions), premyelinating OLs (25106regions),and myelinating OLs(2662 regions) , together with epigenetic marks from H3K27Ac, H3K4me1, and Brg1 (Yu et al 2013) as well as from Olig2-ChIPseq in SH-SY5Y (21523 regions) which is a neural proliferative cell line (Obtained from Ben Martinoga). This allowed us to map the genome with transcriptional and epigenetic information at different stages of the differentiation process and compare the overlapping and unique regions of botch Ascl1 and Olig2 in different contexts. This data integration is invaluable to generate hypothesis about transcriptional regulations, even in highly complex chromosomic regions such as the Olig2 locus or a simpler one such as THE Ascl1 locus (Fig32).

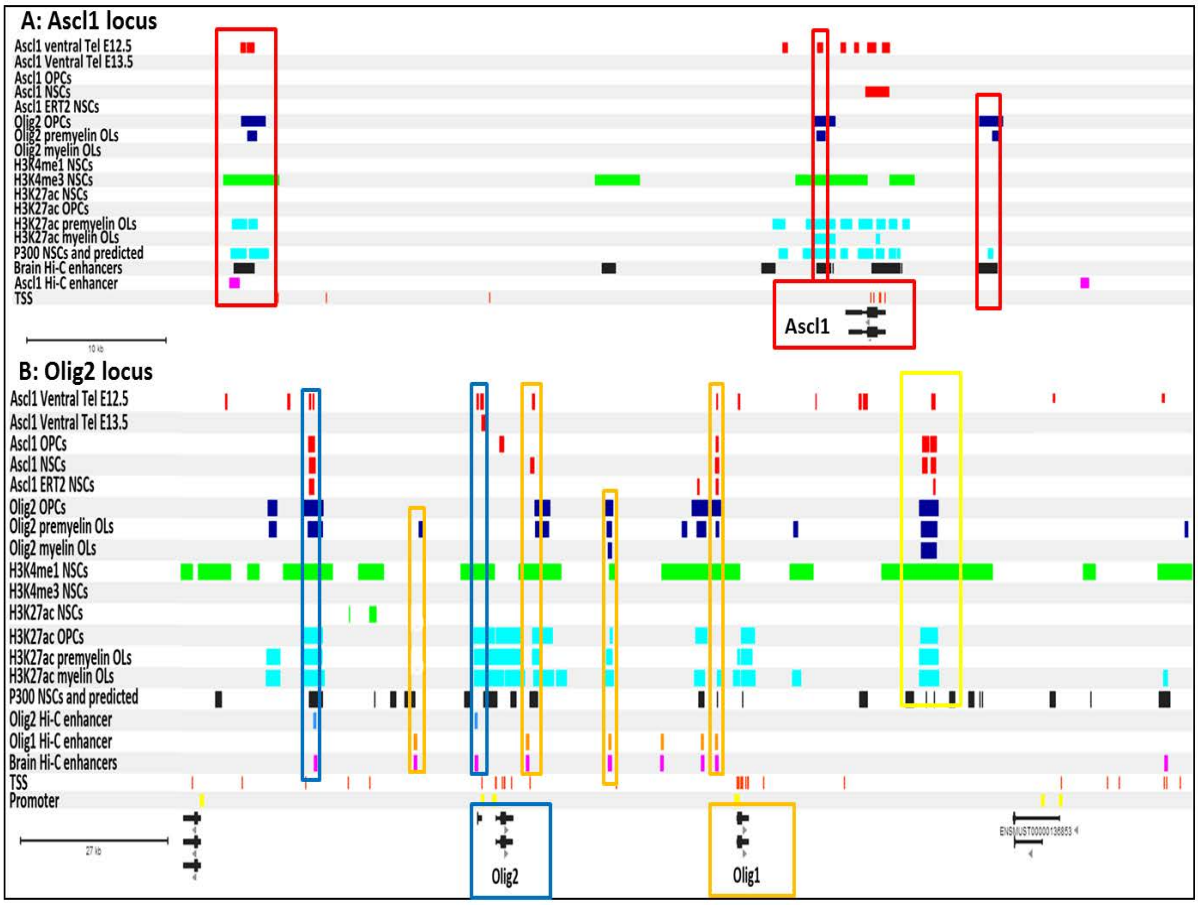

Figure 32. Integration of ChIP datasets in *Ascl1* and *Olig2* locus: Schematic representation of the Ascl1 (**A**) and Olig2 (**B**) loci integrating ChIP data depictured as vertical bars. Red rectangles indicate regulatory elements bound by Ascl1 and Olig2 in neural cells. Ascl1 binding are shown in red, Olig2 in blue, Epigenetic marks in NSCs in light green, Epigenetic marks in oligodendroglial lineage in light blue. In purple are indicated long range interacting enhancers identified by Hi-C analysis (data references in Fig. 31)

TF Matrices	Nr. of Matches in Input	Expected (genome)	Std.dev	Over representation (genome)	Z-Score (genome)	Expected (promoters)	Std.dev	Over representation (promoter)	Z-Score (promoters)
NRL	2	0.28	0.53	7.13	2.3	0.33	0.57	6.06	2.04
TTF1	2	0.33	0.57	6.07	2.04	0.34	0.58	5.93	2
ASCL2	12	1.53	1.24	7.86	8.07	2.71	1.65	4.43	5.34
SREBP	5	1.24	1.11	4.04	2.93	1.38	1.18	3.61	2.65
P53	9	2.32	1.52	3.88	4.06	2.68	1.64	3.36	3.55
PAX	7	2.06	1.44	3.4	3.09	2.09	1.45	3.34	3.05
AP4	9	1.62	1.27	5.56	5.41	2.75	1.66	3.27	3.47
RXR	7	1.42	1.19	4.92	4.26	2.19	1.48	3.2	2.91
TGFb	14	3.5	1.87	4	5.34	4.48	2.12	3.12	4.26
NF1	5	1.34	1.16	3.72	2.72	1.81	1.34	2.77	2
KKLF	32	6.17	2.48	5.19	10.2	11.96	3.46	2.68	5.66
GLI	14	3.01	1.73	4.65	6.05	5.23	2.29	2.67	3.61
ZNF219	31	5.98	2.44	5.18	10.03	11.66	3.41	2.66	5.52
INSM1	15	3.8	1.95	3.94	5.49	5.67	2.38	2.64	3.71
CARF	8	2.37	1.54	3.38	3.33	3.06	1.75	2.61	2.54
IRF4	8	3.16	1.78	2.54	2.45	3.21	1.79	2.49	2.4
WT1	23	4.93	2.22	4.67	7.92	9.43	3.07	2.44	4.26
SRF	11	4.77	2.18	2.31	2.63	4.54	2.13	2.42	2.79
ZBP89	25	5.88	2.43	4.25	7.68	10.55	3.25	2.37	4.3
PSE	8	3.31	1.82	2.42	2.31	3.39	1.84	2.36	2.23
GKLF	11	5.41	2.33	2.03	2.19	4.83	2.2	2.28	2.58
ZNF202	12	3.25	1.8	3.69	4.57	5.43	2.33	2.21	2.61
NGFIC	12	2.6	1.61	4.61	5.52	5.73	2.39	2.1	2.41
EGR2	11	3.72	1.93	2.96	3.52	5.58	2.36	1.97	2.09
MAZR	23	5.4	2.32	4.26	7.36	11.78	3.43	1.95	3.13
PLAG1	14	3.46	1.86	4.05	5.4	7.21	2.68	1.94	2.34

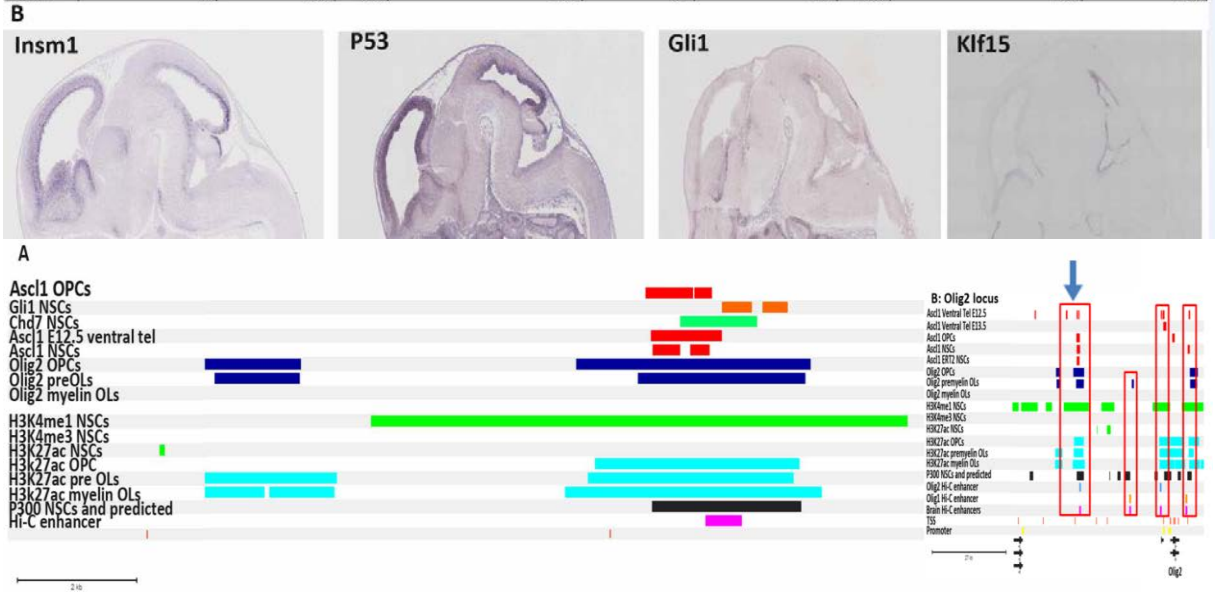

Figure 33. Ascl1/Olig2 enhancer TFBS clustering analysis. (A) Schematic representation of one enhancer of olig2 (magnification of top left enhancer in Olig2 loci Fig30B). Olig2 enhancer region (chr16: 91187670-91196090 (mm9)) is bound by Ascl1 (red), Olig2 (blue), Chd7(green), Gli1(orange) at region of active enhancer defined by the presence of H3K27Ac (light blue) and P300 binding site (Black). Dispite maintenance of the H3K27Ac marks all along the oligodendrocyte lineage, Olig2 binding disapear at the most mature stage. This regions is also identified as Olig2 enhancer in Hi-C and P300 binding site prediction. Table in A shows TFBS clustering in Olig2 enhancer. TFBS cluster for Ascl2 (12 TFBS), Gli (14 TFBS) or P53 (9 TFBS) are found in this regions. Other enriched TFBS are indicated. (**B** Sagital sections of E13.5 brain In-situ hybridization showing gene expression of the putative Olig2 co-factors on this Olig2 enhancer. The majority of the identified possible TFs co-factors share a similar expression pattern than Olig2 thus reinforcing the co-regulation inference probability.

Together, these results demonstrate the synergistic role played by Ascl and Olig2 in OPCs physiology in driving important signaling pathways such as Notch and Wnt but also their role in transcriptional activation of myelin genes whose protein expression will only be effective later on the development. Interestingly, the number of high confidence binding sites is much higher for Olig2. As similar binding site number differences were observed in different replicated Chip-seq experiment for Ascl1 and Olig2 in different contexts, this discrepancy is unlikely to be caused by technical or processing issues. In order to understand this difference, we identified all the binding site matrices of both Ascl1 and Olig2 searching for matrix specifity.

Ascl1 and Olig2 consensus DNA binding sequences analysis

bHLH proteins form heterodimers with E-proteins to bind DNA sequences called E- boxes (CANNTG). Thanks to ChIP sequencing data, it has been possible to define specificities in E-boxes for different bHLH proteins. In order to determine if Ascl1 and Olig2 have such binding preference for an E-box subtype, we searched in all the regions identified in Ascl1 and Olig2 ChIP-seq, all occurrences of E-boxes matches to perform a de-novo motif discovery and an E-box subtype overrepresentation analysis. We found that the E-boxes recognized in Ascl1 ChIP-seq correspond to degenerate TFBS matrices defined by binding frequency order as Ascl2, Ascl1, MyoD matrices (Fig. 35) and E-boxes recognized in Olig2 ChIP-seq correspond to Atoh1 (Fig. 35). As identified ChIP-seq regions can be bound by both Ascl1 and Olig2 and can display many E-boxes, we confirmed this sub-type specificity by selecting Ascl1 sepcific or Olig2 specific regions containing only one E-box. We obtained the same preferential binding order and confirmed the larger scale results (Fig. 35). Interestingly, Atoh1 and NeuroD1 matrices contain a CA/TC/TG E-box, while Ascl12 and Ascl1 contain a CA/CG/TG matrix. This difference could be in part explain the difference in binding frequence observed for each TFs in the Chip-seq datasets.

A

All site	Mash1 only	TF Matrices	Nr. Seq. with Match	Nr. of Matches	Expected (promoters)	Over representation (promoters)	Z-Score (promoter
	1	V$ASCL2.01	3736	4812	60.51	79.53	610.88
	2	V$MASH1.01	3642	3821	72.62	52.62	439.90
	3	V$ATOH1.01	3317	3646	82.86	44.00	391.47
	4	V$MYOGENIN.02	2371	2628	56.50	46.51	342.08
	5	V$AP4.02	2384	2741	60.92	45.00	343.38
	6	V$NEUROD1.01	3097	3205	91.73	34.94	325.08
	7	V$E47.01	1739	1760	50.38	34.94	240.83
	Olig2 only	TF Matrices	Nr. Seq. with Match	Nr. of Matches	Expected (promoters)	Over representation (promoters)	Z-Score (promoters
	1	V$ATOH1.01	4833	5361	88.23	60.76	561.42
	2	V$ASCL2.01	2674	3158	64.43	49.02	385.41
	3	V$NEUROD1.01	4313	4458	97.68	45.64	441.25
	4	V$NEUROG.01	4748	5114	108.33	47.21	481.02
	5	V$AP4.02	2532	3034	64.86	46.77	368.66
	6	V$MYOGENIN.02	2361	2688	60.17	44.68	338.77
	7	V$MASH1.01	2673	2828	77.32	36.57	312.82
	Mash1/Olig2	TF Matrices	Nr. Seq. with Match	Nr. of Matches	Expected (promoters)	Over representation (promoters)	Z-Score (promoters
	1	V$ASCL2.01	1423	2201	35.72	61.62	362.28
	2	V$MYOGENIN.02	1077	1442	33.36	43.23	243.85
	3	V$AP4.02	1089	1470	35.96	40.88	239.09
	4	V$ATOH1.01	1245	1767	48.91	36.13	245.64
	5	V$MASH1.01	1183	1494	42.87	34.85	221.61
	6	V$MYF5.01	741	1051	39.58	26.55	160.70
	7	V$NEUROD1.01	1007	1252	54.15	23.12	162.75

B

Unique site	Mash1Only	TF Matrices	Nr. Seq. with Match	Nr. of Matches	Expected (promoters)	Over representation (promoters)	Z-Score (promoters
	1	V$ASCL2.01	719	719	12.81	56.13	197.21
	2	V$MASH1.01	708	708	15.37	46.06	176.56
	3	V$MYOGENIN.02	465	500	11.96	41.80	140.99
	4	V$ATOH1.01	663	663	17.54	37.80	154.03
	5	V$AP4.02	452	498	12.90	38.62	134.97
	6	V$NEUROD1.01	622	622	19.42	32.03	136.66
	7	V$E47.01	374	374	10.66	35.07	111.12
	Olig2 only	TF Matrices	Nr. Seq. with Match	Nr. of Matches	Expected (promoters)	Over representation (promoters)	Z-Score (promoters
	1	V$ATOH1.01	3683	3689	64.89	56.85	449.95
	2	V$NEUROD1.01	3245	3245	71.83	45.17	374.43
	3	V$ASCL2.01	1991	1995	47.38	42.10	282.91
	4	V$NEUROG.01	3463	3465	79.67	43.49	379.32
	5	V$AP4.02	1812	2123	47.70	44.50	300.45
	6	V$MYOGENIN.02	1682	1876	44.25	42.40	275.34
	7	V$TCFE2A.02	2470	2470	59.17	41.74	313.40
	8	V$MASH1.01	2003	2003	56.87	35.22	258.06
	Mash1 Olig2	TF Matrices	Nr. Seq. with Match	Nr. of Matches	Expected (promoters)	Over representation (promoters)	Z-Score (promoters
	1	V$ASCL2.01	268	269	3.56	75.62	140.50
	2	V$MYOGENIN.02	196	216	3.32	65.03	116.44
	3	V$AP4.02	194	226	3.58	63.11	117.29
	4	V$ATOH1.01	238	241	4.87	49.48	106.79
	5	V$MASH1.01	201	201	4.27	47.08	94.99
	6	V$E47.01	123	123	2.96	41.53	69.47
	7	V$MYOD.01	123	124	3.68	33.68	62.45
	8	V$MYF5.01	120	133	3.94	33.74	64.76
	9	V$NEUROD1.01	167	169	5.39	31.34	70.26

C

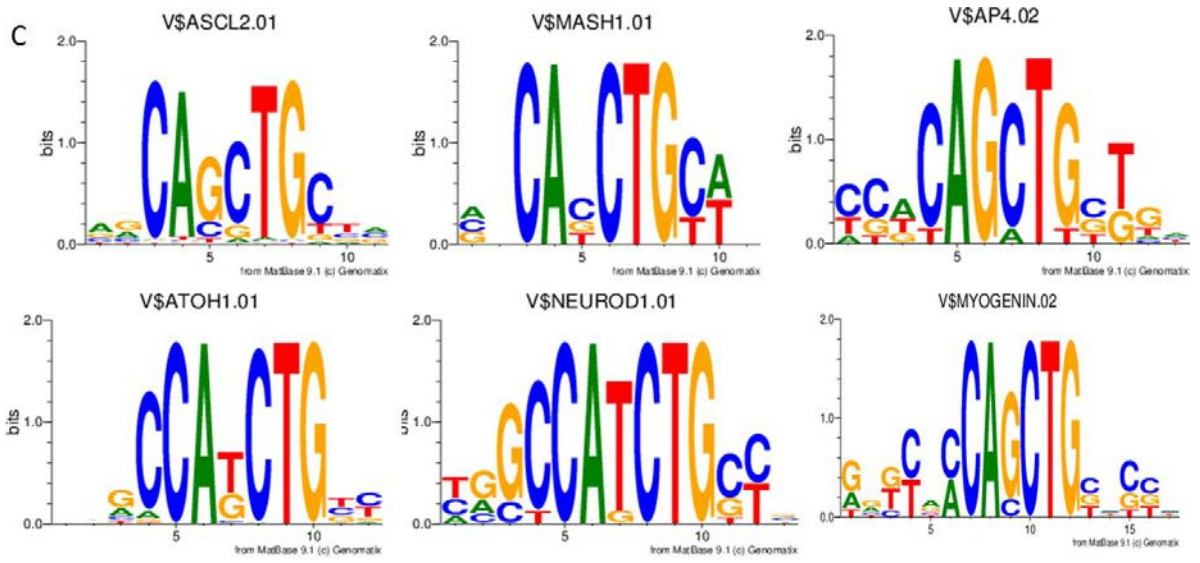

Figure 35: E-box subtype enrichment analysis in Ascl1 and Olig2 bound region (A) Table presenting E-box subtype analysis of all Ascl1 and Olig2 chip-seq peaks containing E-boxes (containing at least one E-box. peaks without E-boxes are withdrawn). Over representation of E-boxes subtypes is given for Ascl1 specific binding regions (Ascl1 only), Olig2 specific regions (olig2 only) and Ascl1/Olig2 shared regions. Enrichment is given compared to E-box average frequency in promoters. Associated statistical test is indicated (Z-score >2 are equivalent to a corrected p-value of 0.5). Ascl1 is more likely to bind Ascl2 or

Ascl1 matrices. Olig2 is more likely to bind Atoh1 or Ascl2. Ascl1/Olig2 shared regions contain more Ascl2 or Myogenin matrices **(B)**Table presenting E-box subtype analysis of unique E-box containing Ascl1 and Olig2 chip-seq peaks (containing only one E-box). Similar results and order are obtained when using regions containing only one E-box. (**C**) E-boxes subtype matrices.Each E-box subtype has defined nucleotide probability occurrence represented by the size of the letter. While Olig2 prefered binding is on (cCA/TC/TG) on Atoh1, NeuroD1 or NeuroG), Ascl1 prefered binding is on (CA/GC/TGc) on Ascl2, Ascl1, Myogenin or AP4.

Bioinformatic identification of Ascl1 and Olig2 cofactors

Models of combinatorial regulation by several TFs can be inferred from in-silico analysis of ChIP-seq binding regions (Hnisz D, Abraham BJ 2013). To identify potential transcription co-factors and identified the precise chromosomic position of all the E-boxes present in those regions. We extended those chromosomic positions of 50bp up and downstream to screen those regions in search of other known transcription factors TFBS matrices or transcription factor modules (one E-box flanking another TFBS matrix located a less than 50bp). This in-silico analysis showed that Ascl1 and Olig2 E-boxes are most frequently associated in pairs of E-boxes (tandem of TFBS) separated by a stable distance of 15bp (Fig. 37). We found that Ascl1 preferentially make TFBS clusters with E47, TCF15, MAZ, SP1, LHX8 (Fig 36), while Olig2 preferentially associate with Nf1, Evx1/2, Gsh2, Emx2, Zic1/2/3, Sox2/9, Gli2/3 (Fig. 40). Interestingly, the potential co-factors identified by this bioinformatics screen all share the same expression pattern than Ascl1 and Olig2 (as cross checked on Allen brain atlas), thus reinforcing the inference about their potential action as co-factors.

Ascl1 Top peaks (1000 peaks)						Olig2 Top peaks (1000peaks)					
Modules with ASCL2	Nr. of Input Seq. with Match	Nr. of Matches in Input	Expected in promoters	Over representation	Z-Score	Modules/with/ATOH1	Nr. of Input Seq. with Ma	Nr. of Matches in In	Expecte	Over representati	Z-Score
ASCL2/ASCL2	200	929	6.09	152.57	373.81	ATOH1/SOX9	260	320	110.79	2.89	19.83
ASCL2/ASCL1	240	1150	11.52	99.81	335.25	ATOH1/SOX2	289	353	128.74	2.74	19.72
ASCL2/E47	166	757	7.45	101.68	274.52	ATOH1/NF1	128	196	55.2	3.55	18.88
ASCL2/TCF15	101	294	8.02	36.65	100.8	ASCL2/ATOH1	186	284	100.56	2.82	18.24
ASCL2/MAZ	160	376	19.69	19.1	80.2	ATOH1/MYOGENIN	170	274	96.81	2.83	17.96
ASCL2/SP1	200	481	31.49	15.27	80.02	ATOH1/GAGA	115	337	137.88	2.44	16.92
ASCL2/LHX8	65	178	4.67	38.11	79.97	ATOH1/SOX11	203	247	92.91	2.66	15.93
ASCL2/KLF15	158	451	29.33	15.38	77.77	AP4/ATOH1	167	254	97.75	2.6	15.75
ASCL2/EMX2	74	218	7.56	28.83	76.35	ATOH1/LEF1	276	335	152.09	2.2	14.79
ASCL2/ARID1B	75	219	7.76	28.24	75.68	ATOH1/ISX	115	243	98.14	2.48	14.57
ASCL2/DLX5	87	216	7.68	28.11	74.97	ATOH1/SOX4	155	193	72.69	2.66	14.05
ASCL2/VAX1	86	208	7.15	29.08	74.91	ATOH1/HBP1	227	274	125.15	2.19	13.26
ASCL2/DLX1	99	207	7.09	29.19	74.89	ATOH1/GBX2	81	166	62.93	2.64	12.93
ASCL2/GSH2	106	205	7.25	28.28	73.26	ATOH1/NFAT5	239	274	130.07	2.11	12.58
ASCL2/PRRX2	64	177	5.48	32.31	73.07	ATOH1/HOX1-3	196	242	109.77	2.2	12.57
ASCL2/DLX2	84	204	7.31	27.9	72.55	ATOH1/HEN1	94	192	79.71	2.41	12.52
ASCL2/GBX1	55	160	4.56	35.05	72.52	ATOH1/LHX8	81	162	65.5	2.47	11.86
ASCL2/LHX6	81	213	8.99	23.7	67.89	ATOH1/OSNT	199	242	114.85	2.11	11.82
ASCL2/INSM1	139	280	15.39	18.2	67.33	ATOH1/MYOD	153	202	90.25	2.24	11.71
ASCL2/NRSF	56	185	7.42	24.94	65.02	ATOH1/TGIF2	196	236	112.35	2.1	11.62
ASCL2/ESX1	54	150	5.47	27.43	61.59	ATOH1/PKNOX2	178	209	95.33	2.19	11.59
ASCL2/BRN2	65	170	6.98	24.37	61.54	ATOH1/EVX1	120	227	106.88	2.12	11.57
ASCL2/LHX2	46	127	3.98	31.91	61.42	ATOH1/DBP	159	186	84.94	2.19	10.91
ASCL2/BSX	59	156	6.19	25.22	60.03	ATOH1/HMGA	156	193	89.47	2.16	10.89
ASCL2/CART1	64	172	7.52	22.88	59.82	ATOH1/MYF6	146	181	82.68	2.19	10.76
ASCL2/PKNOX2	92	171	7.51	22.78	59.49	ATOH1/ATOH1	116	150	64.57	2.32	10.57
ASCL2/ZIC2	120	220	12.57	17.5	58.37	ATOH1/HIC1	150	171	79.79	2.14	10.15
ASCL2/TCFE2A	106	166	7.8	21.28	56.47	ATOH1/YY2	143	173	81.12	2.13	10.15

Figure 36. Enrichment analysis of TFBS-module in Ascl1/H3K27Ac or Olig2/H3K27Ac bound regions. Table presenting most enriched Ascl1 (left) or Olig2 (right) associated modules of TFBS. Modules are defined as two TFBS located at less than 50bp to each other. As demonstrated by single TFBS analysis, Ascl2 matrix is more frequent than Ascl1 matrix. Interestingly, Ascl1 binds more frequently genomic region containing tandem repeat or clusters of E-boxes. Other binding sites enriched together with Ascl1/2 E-boxes binding site are indicated. Those TFs are likely to work in synergy or inhibit the action of Ascl1 on identified bound regions. We found Tcf15, Dlx1/2 or Gli to be significantly associated with Ascl1 TFBS. B. Table presenting most enriched Olig2 associated TFBS. Similarly, Olig2 binding region are screened for

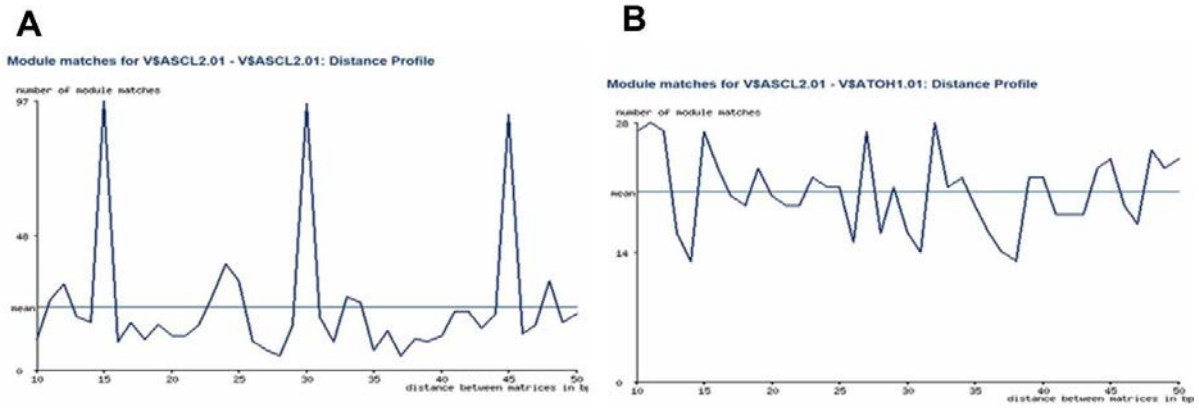

TFBS module enrichment. Atoh1 matrix is also found to frequently form tandem repeat of E-boxes. Other known or unknown TFBS matrices are identified such as Sox9, Sox2 or NF1

Figure 37 . Enrichment analysis of TFBS-module in Ascl1 or Olig2 bound regions. **(A)** Distance profile of Ascl1 tandem E-boxes. Schematic showing over representation of cluster of Ascl1/Ascl2 tandem E-boxes stably spaced by 15bp. (**B**) Distance profile of Olig2 tandem E-boxes. Schematic showing absence of regular spacing in Olig2/Atoh1 tandem E-boxes.

Gene expression cell-type specificity of the oligodendroglial lineage

In order to prioritize the genes regulated by Ascl1 and Olig2 in OPCs and the ventral telencephalon, we reprocessed microarray data obtained from purified OPCs, pre-myelinating and myelinating oligodendrocytes (GSE15303; GSE9566) that we compared using different clustering methods in order to identify the genes involved at each stage of the oligodendrocyte lineage (Emery et al., 2008, Cahoy et al., 2006). We identified the genes involved in the transition from NSCs to OPCs comparing microarray data obtained from purified OPCs with different microarray data obtained from embryonic and postanatal CD133/Prominin NSCs (GSE8034; GSE18326; GSE17760). We refined our screen using microarray data from all available brain cell-types such as different subtypes of postmitotic neurons (GABAergic, glutamatergic, dopaminergic, serotoninergic), astrocytes, microglia and endothelial cells to assess for strict cell-specificity (GSE29949; GSE9566; GSE11870). We validated our approach by the identification of known and unknown specific markers of each cell lineage, selected based on gene clustering analysis (see material and methods and annexes) and RNA expression pattern at E14.5 (*Eurexpress*) and P56 (*Allen brain atlas*). We selected different gene lists whose expressions are enriched in different stages of the oligodendrocyte lineage or from other cell types for subsequent analysis and paid particular attention to transcriptional factors (Fig. 38).

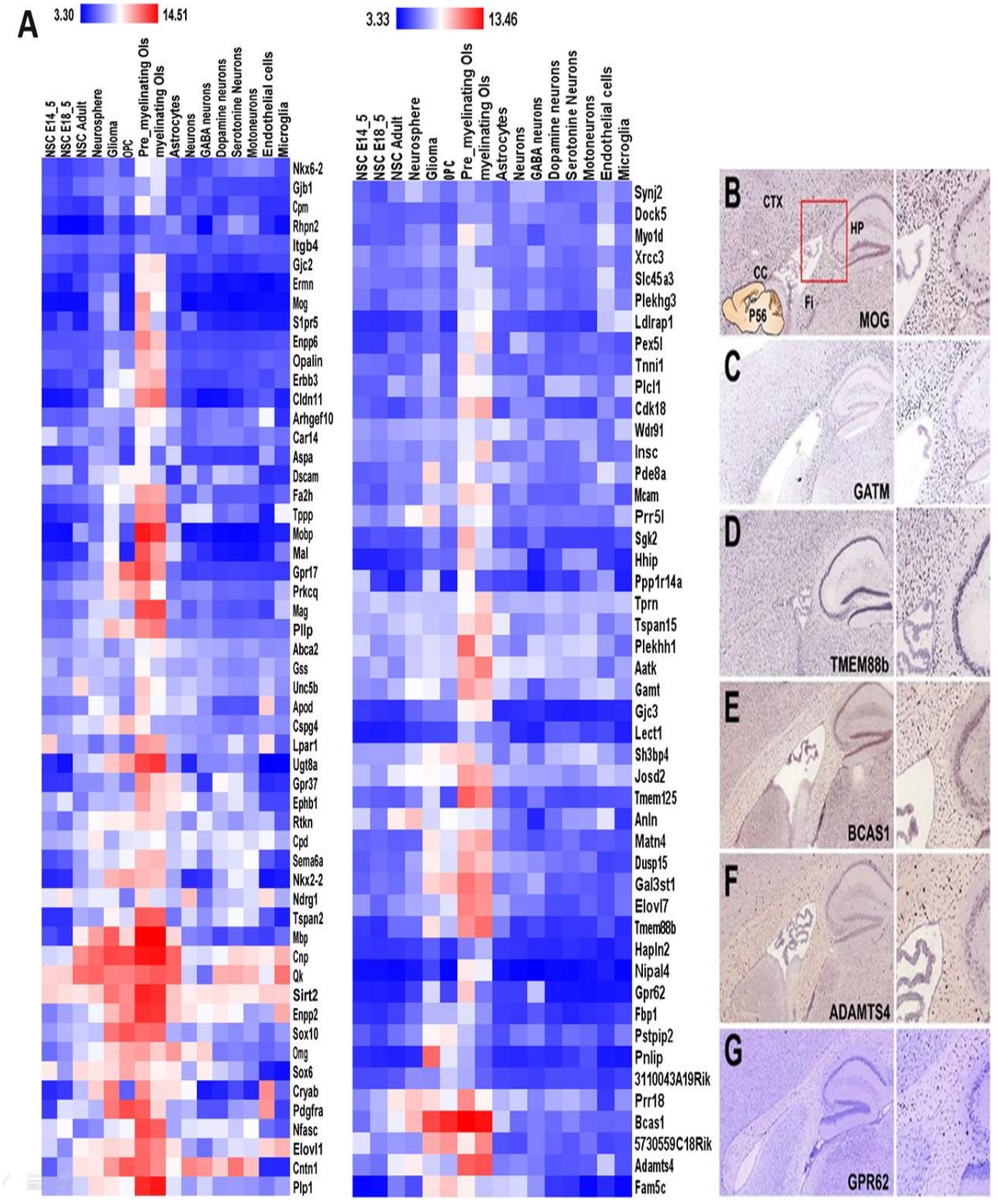

Figure 38. Identification of oligodendroglial enriched genes. (**A**) Clustering of expression data from different brain cell-type expression microarrays sorted for increasing expression in oligodendrocytes. Red indicates higher expression values and blue lower ones (data from (data from Cahoy et al 2009 and others cited in material and methods). (**B-G**) In situ hybridization of myelin oligodendrocyte glicoprotein (MOG) gene and selected candidates in sagittal sections of P56 mouse brains showing

specific expression in white matter regions (corpus callosum, CC and fimbria, Fi) and sparse expression in grey matter areas such as cortex (Ctx) and hippocampus (HP). Right side panels are higher magnifications of the region designated by the red inset in panel B.

A	OPC enriched genes								
Symbol	Name	NSCs	OPCs	preOLs	myOLs	Neurons	Astrocytes	Chr	Begin	End
Pdgfra	platelet derived growth factor receptor, alpha polypeptide	6.37	12.82	11.14	5.93	7.40	7.65	chr5	75578158	75580732
Serpine2	serine (or cysteine) peptidase inhibitor, clade E, member 2	8.77	12.77	12.35	9.92	11.59	13.01	chr1	79853926	79854994
Mbp	myelin basic protein	5.96	10.16	13.87	13.90	7.26	8.83	chr18	82704997	82707741
Arl4a	ADP-ribosylation factor-like 4A	5.64	9.72	8.72	7.65	8.95	6.61	chr12	40743385	40744181
Olig2	oligodendrocyte transcription factor 2	7.03	11.62	10.82	9.85	3.75	7.88	chr16	91227402	91230336
Eps8	epidermal growth factor receptor pathway substrate 8	5.86	9.61	9.32	7.34	8.78	10.11	chr6	137594972	137597373
Moxd1	monooxygenase, DBH-like 1	4.63	9.92	7.95	4.37	7.11	6.26	chr10	23947618	23948933
Ptpre	protein tyrosine phosphatase, receptor type, E	5.75	10.54	10.26	9.65	8.63	5.76	chr7	142770970	142771470
Dock10	dedicator of cytokinesis 10	5.49	9.94	10.55	12.13	7.20	6.40	chr1	80704838	80707407
Nkx2-2	NK2 transcription factor related, locus 2 (Drosophila)	5.19	10.86	10.34	8.23	4.20	6.31	chr2	147004761	147006597
Bcas1	breast carcinoma amplified sequence 1	7.06	12.63	13.28	13.14	5.58	6.91	chr2	170226519	170227691
Pcdh15	protocadherin 15	4.09	8.26	6.30	4.03	4.39	3.75	chr10	72847953	72848435
Enpp2	ectonucleotide pyrophosphatase/phosphodiesterase 2	7.13	11.46	13.39	13.83	10.41	9.50	chr15	54749717	54751708
Gsx1	GS homeobox 1	5.07	9.19	6.26	4.66	4.67	4.73	chr5	148000630	148001380
Gabrg1	gamma-aminobutyric acid (GABA) A receptor	5.20	9.13	7.37	4.15	7.46	9.02	chr5	71233192	71235050
Dbc1	deleted in bladder cancer 1 (human)	4.33	8.80	7.28	4.65	8.95	4.84	chr4	68613323	68615409
Cspg4	chondroitin sulfate proteoglycan 4	6.20	10.79	8.28	5.86	7.39	6.65	chr9	56723874	56724667
Cntn1	contactin 1	6.51	12.18	11.78	11.81	12.03	8.51	chr15	91951468	91952214
Sulf2	sulfatase 2	6.93	11.27	10.96	9.42	8.64	7.15	chr2	165967447	165970082
Fam5c	family with sequence similarity 5, member C	3.86	9.55	7.94	4.23	7.26	7.12	chr1	148341605	148342514
Spon1	spondin 1, (f-spondin) extracellular matrix protein	6.72	11.35	10.27	6.02	9.79	9.64	chr7	120910360	120914225
Sox10	SRY-box containing gene 10	7.08	12.58	12.12	11.99	6.61	7.04	chr15	78988874	78993911
B	Myelin enriched genes									
name	Name	NSCs	OPCs	preOLs	myOLs	Neurons	Astrocytes	Chr	Begin	End
Mobp	myelin-associated oligodendrocytic basic protein	4.24	5.03	13.59	14.04	4.55	6.36	chr9	120078671	120079177
Mog	myelin oligodendrocyte glycoprotein	4.32	3.86	9.90	12.77	3.47	4.52	chr17	37160231	37161061
Ugt8a	UDP galactosyltransferase 8A	5.14	10.89	13.13	13.31	4.03	5.84	chr3	125572698	125574764
Plp1	proteolipid protein (myelin) 1	6.14	8.72	13.12	13.44	5.07	7.87	chrX	133373090	133375164
Olig1	oligodendrocyte transcription factor 1	8.65	13.75	13.55	13.74	5.71	11.13	chr16	91270800	91272885
Cldn11	claudin 11	4.33	7.80	11.71	12.03	4.20	5.35	chr3	31050269	31051575
Mag	myelin-associated glycoprotein	6.15	7.16	12.87	13.18	5.38	6.46	chr7	31699224	31699815
Mbp	myelin basic protein	6.53	7.00	13.28	13.06	5.32	5.68	chr18	82704997	82707741
Tmem125	transmembrane protein 125	5.61	4.88	11.13	12.33	4.89	5.24	chr4	118210030	118214119
Cmtm5	CKLF-like MARVEL transmembrane domain containing 5	5.26	8.62	10.56	12.02	4.58	9.31	chr14	55553732	55557574
Tmem88B	transmembrane protein 88B	4.69	7.09	10.91	11.76	4.36	5.56	chr4	155158505	155159204
Aspa	aspartoacylase	5.31	4.65	7.41	12.24	4.86	7.33	chr11	73115552	73118107
Cnp	2',3'-cyclic nucleotide 3' phosphodiesterase	6.94	10.57	13.21	13.60	6.28	9.14	chr11	100445962	100446246
Opalin	oligodendrocytic myelin paranodal and inner loop protein	5.53	6.27	10.12	12.30	5.05	5.42	chr19	41147817	41149555
Fa2h	fatty acid 2-hydroxylase	5.79	8.39	10.93	12.18	5.26	6.13	chr8	113884946	113885762
Plxnb3	plexin B3	6.23	10.24	12.01	12.09	5.20	6.41	chrX	71005795	71006552
Erbb3	v-erb-b2 erythroblastic leukemia viral oncogene homolog	4.82	8.71	10.45	11.64	4.77	5.46	chr10	128023847	128025158
Gpr62	G protein-coupled receptor 62	4.15	4.69	7.59	11.56	4.85	4.35	chr9	106366731	106367126
Gsn	gelsolin	6.27	9.07	11.31	13.31	6.64	8.97	chr2	35126433	35128175
Efhd1	EF hand domain containing 1	5.12	4.65	7.64	11.34	4.69	8.53	chr1	89183997	89184599
Plekhb1	pleckstrin homology domain containing, family B (evectins	6.90	10.39	12.58	13.33	6.94	10.60	chr7	107800794	107803635
Anln	anillin, actin binding protein	7.43	8.44	7.97	11.56	5.21	6.77	chr9	22189782	22191346

Figure 38bis. Identification of cis-regulatory oligodendroglial specific genes. (**A**) Table presenting Olig2 regulated genes (microarray) and bound by Olig2 (Chip-seq) in H3k27ac region(Chip-seq) whose expression is enriched genes in OPCs compare to other cell types. Expression data for NSCs, OPCs, PremyelinatingOL, myelinating OLs, neurons and astrocytes. One regulatory chromosomic position is indicated for each gene. (**A**) Table presenting Olig2 bound by Olig2 (Chip-seq) in H3k27ac region(Chip-seq) whose expression is enriched genes in myelinating OLs compared to other cell types. Expression data for NSCs, OPCs, PremyelinatingOL, myelinating OLs, neurons and astrocytes. One regulatory chromosomic position is indicated for each gene. This kind of cis-regulatory sequence is higly enriched in TFBS cluster

specific to the defined cell-type and can be use in the context of genetic therapies to build synthetic promoters able to drive specific gene expression or repression.

Identification of Ascl1 and Olig2 regulated genes involved in oligodendrocyte lineage

Identification of Cdh7 as putative regulator of oligodendrogenesis and myelination.

As mentioned in the introduction, Chd7 is a member of the Chromodomain Helicase DNA binding domain (CHD) family that plays a role in controlling gene expression by ATP-dependent chromatin remodeling. Chd7 is known to interact with components of the BAF (Brahma associated factor complex) and PBAF complexes (Polybromo containing complex) and thus help recruiting transcriptional activators or repressors depending on the cellular context, such as embryonic stem cells (Schnetz et al., 2009) or neural crest cells where it interact with Brg1 (Li et al., 2013). We found that intronic regions of *Chd7* locus are bound by Ascl1 and Olig2 in OPCs, at regulatory elements presenting epigenetic marks associated with transcription activation such as H3K27Ac in OPCs, immature or myelinating oligodendrocytes (Fig. 39A, red rectangles). Moreover, Brg1 remodeling complex factor that interacts with Olig2 also binds in these elements in OPCs, suggesting that this gene is part of the regulatory mechanism of Olig2 function in oligodendrogenesis. Both *Chd7* expression pattern at embryonic (Fig. 39B) and postnatal/adult stages (Fig. 39C) indicate that *Chd7* is expressed like Ascl1 and Olig2 in VZ/SVZ progenitors and in oligodendroglial containing regions (such as the corpus callosum or the fimbria, arrowheads). Indeed, the transcriptome comparison of neural subpopulations clearly indicates that *Chd7* mRNA is expressed mainly in OPCs and immature oligodendrocytes (Fig. 39D). We investigated if *Chd7* was the only member of the chromodomain family expressed in OPCs and found that *Chd8*, the paralog of *Chd7* to the common Drosophila ortholog, Kismet, was also express in OPCs (Fig. 39E). We then searched for evidences that *Chd7* could be involved in de/remyelination and found that *CHD7* is significantly downregulated in human active MS plaque (Han et al., 2012; Fig. 39E) as well as in a FACSorted OPCs purified after a cuprizone induced demyelination (S. Moyon and C.

Lubetzki, unpublished; Fc=0.56 p-value=0.007; Fig. 39F). Transcriptional regulation of *Chd7* by Ascl1 and Olig2 was obtained not only by our microarrays analysis of $Ascl1^{KO}$ and $Olig2^{KO}$ (Fig. 39F) but also by overexpressing *Ascl1* or *Olig2* in neurosphere cultures, each of which was sufficient to upregulate *Cdh7* levels compared to controls (Fig. 39I,H). Finally, Chd7 has been shown to bind directly to different sequences located near the *Olig2* locus in the SH-SY5Y neural cell line known to express Olig2 (Schnetz et al., 2009). Base in data integration, we show here that those sites defined as active enhancers (H3k27ac, P300 marks) are able to interact with the *Olig2* transcription start site (Hi-C data) most likely due to the binding of Olig2, Ascl1, and Gli1 (Fig. 39K). Therefore, those sites may constitute important regulatory sequences for Olig2 expression in oligodendrogenesis suggesting that Chd7 together with Ascl1 and Olig2 play a role in this process. All these data strongly suggest that Chd7 is an important Ascl1/Olig2 target controlling oligodendrogenesis.

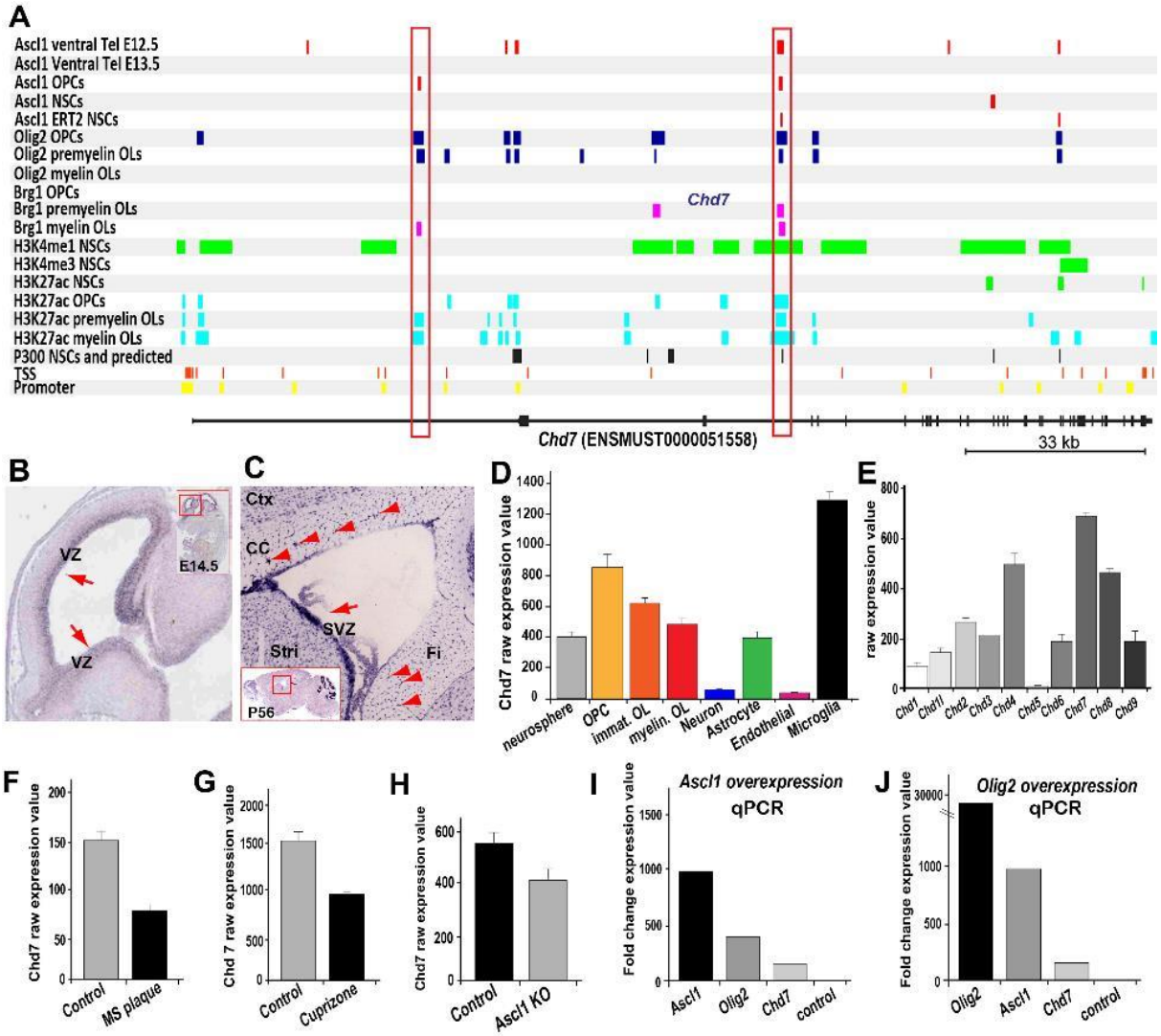
A
Ascl1 ventral Tel E12.5
Ascl1 Ventral Tel E13.5
Ascl1 OPCs
Ascl1 NSCs
Ascl1 ERT2 NSCs
Olig2 OPCs
Olig2 premyelin OLs
Olig2 myelin OLs
Brg1 OPCs
Brg1 premyelin OLs
Brg1 myelin OLs
H3K4me1 NSCs
H3K4me3 NSCs
H3K27ac NSCs
H3K27ac OPCs
H3K27ac premyelin OLs
H3K27ac myelin OLs
P300 NSCs and predicted
TSS
Promoter
Chd7
Chd7 (ENSMUST0000051558)
33 kb
B
VZ
E14.5
VZ
C
Ctx
CC
SVZ
Stri
Fi
P56
D
Chd7 raw expression value
neurosphere
OPC
immat. OL
myelin. OL
Neuron
Astrocyte
Endothelial
Microglia
E
raw expression value
Chd1
Chd1l
Chd2
Chd3
Chd4
Chd5
Chd6
Chd7
Chd8
Chd9
F
Chd7 raw expression value
Control
MS plaque
G
Chd 7 raw expression value
Control
Cuprizone
H
Chd7 raw expression value
Control
Ascl1 KO
I
Ascl1 overexpression
qPCR
Fold change expression value
Ascl1
Olig2
Chd7
control
J
Olig2 overexpression
qPCR
Fold change expression value
Olig2
Ascl1
Chd7
control

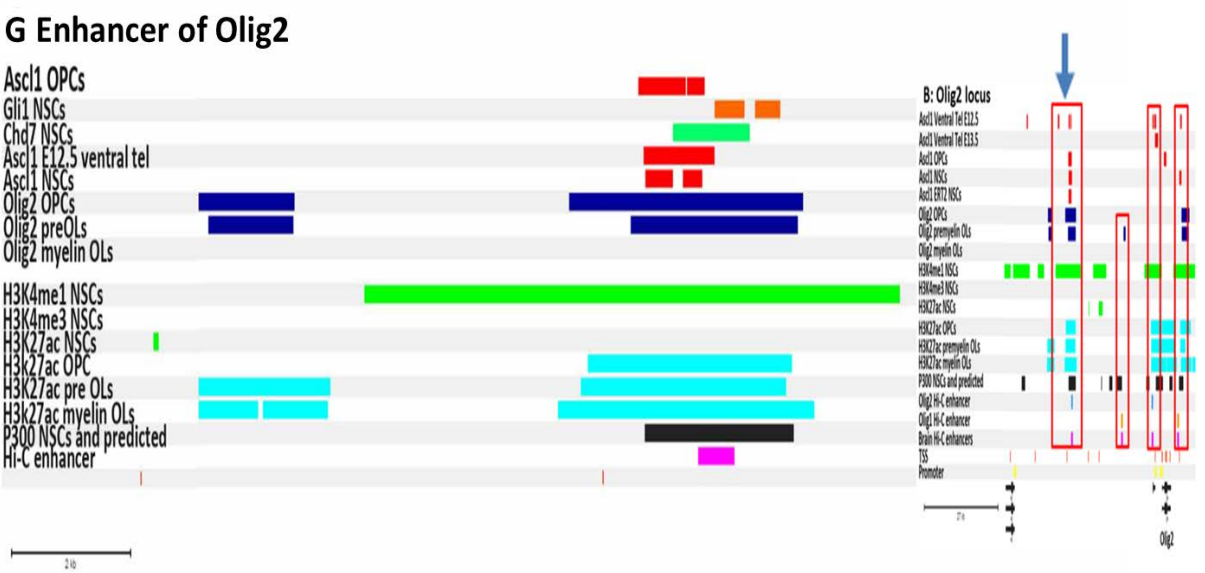

Figure 39. *Chd7* putative Ascl1-Olig2 target driving oligodendrogenesis. (**A**) Schematic representation from Genomatix genome browser of *Chd7* locus integrating ChIP data depictured as rectangles/bars in each line. Ascl1 and Olig2 ChIP binding peaks are shown in red and blue respectively, Brg1 ChIP sites in pink and epigenetic marks in cyan. Red vertical rectangles indicate regulatory elements bound by Ascl1 and Olig2 in OPCs and immature oligodendrocytes, presenting also Brg1 binding sites and active epigenetic marks in oligodendroglial cells. (**B**) Sagittal section of E14.5 embryo (www.euroexpress.org) showing *Chd7* expression pattern in the forebrain ventricular zone (VZ, arrows) by in situ hybridization; red square indicates the higher magnification area. (**C**) Brain sagittal section of P56 brain showing *Chd7* expression in telencephalic SVZ (arrow), and corpus callosum and fimbria (some cells highlighted by arrowheads); red square indicates the higher magnification area (**D**) Histograms representing raw expression levels of *Chd7* in different brain subtypes expression microarrays. Note the highest expression in OPCs, iOLs and microglia. (**E**) Histograms representing raw expression levels of different *Chd* genes in OPC expression microarrays. (**F**) Histograms representing raw expression levels of *Chd7* in human MS plaques compared to controls processed from GEO GSE38010 microarrays. (Fc=0.42, BH p-value=0.05). (**G**) Histograms representing raw expression levels of *Chd7* in FACSorted OPCs from corpus callosum tissue of cuprizone-treated demyelinated mice and controls (obtained from S. Moyon et al., C. Lubetzki J.Neurosci. in press. (**H**) Histograms representing raw expression levels of *Chd7* in ventral telencephalon expression microarrays of wild-type and Ascl1 mutant mice. (**I,J**) Histograms representing qPCR obtain fold change gene expression levels in neurosphere cells transfected with Ascl1 (I) or Olig2 (J) overexpressing vectors after 48 hours. (**K**) See figure Schematic representation of the Olig2 locus integrating ChIP data depictured as vertical bars. Red rectangles indicate regulatory elements bound by Ascl1 and Olig2 and Chd7 in neural cells. Chd7 Chip binding peaks are

shown in red, Ascl1 and Olig2 ChIP binding peaks are shown in blue, Brg1 ChIP sites in green and epigenetic marks in yellow. Epigenetic marks are shown in light blue.

Chd7 protein expression during myelination

Given the Chd7 mRNA expression in oligodendroglia and white matter regions, we characterized Chd7 protein expression by immunostaining at postnatal stages. Chd7 protein was coexpressed during neonatal stages (P3) with Ascl1 (but not Olig2) in the SVZ progenitors (expressing Mcm2 proliferation marker, Fig. 40C) and in all OPCs (Fig. 40B) as expected from our transcriptome analysis. During the peak of myelination, at 3 weeks postnatal (P24), we found Chd7 protein in all OPCs (PDGFRα^{+} cells, Fig. 40D-F) while its expression levels were highest in maturing oligodendrocytes (APC/CC1^{+} cells; Fig. 40E,F) and was reduced in mature oligodendrocytes (not shown). Therefore, Chd7 protein expression correlates with OPC differentiation suggesting a role in chromatin remodeling involved in this process

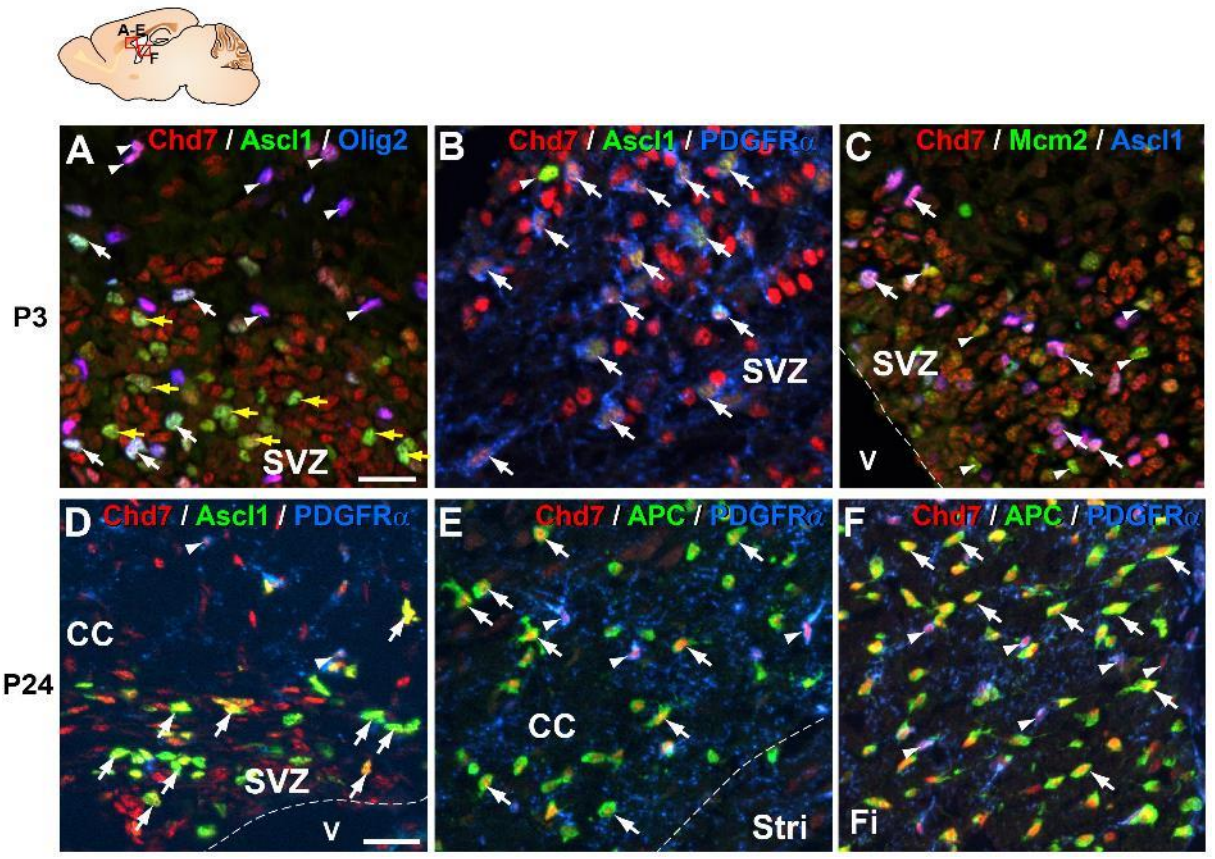

during myelination.

Figure 40. Chd7 protein expression during in postnatal brain. Sagittal sections of P3 (A-C) and P24 (D-F) brains immunostained for Chd7 antibody. Arrows and arrowheads indicate some examples of labelled cells. (**A**) Coexpression of Chd7 and Ascl1 in SVZ and CC cells either expressing Olig2 (arrowheads) or not (most likely transit amplifying precursors, arrows). (**B**) Chd7 and Ascl1 co-expression in PDGFRα+ (arrows), PDGFRα- (transit amplifying cells, arrowheads). Note that Chd7 is also expressed in Ascl1-negative cells in SVZ, most likely neuroblasts. (**C**) Chd7 and Aslc1 co-expression with Mcm2, proliferation marker in SVZ cells. (**D**) Chd7 and Ascl1 co-expression in SVZ cells (arrows) or PDGFRα+ OPCs in the CC (arrowheads). (**E, F**) Chd7-expressing cells in the CC (E) or in the fimbria (F) are either OPCs (PDGFRα$^+$ cells, arrowheads) or maturing oligodendrocytes (APC$^+$ cells, arrows). Note that the highest levels of Chd7 protein expression are found in APC$^+$ cells. V, ventricle; Fi, fimbria; CC, corpus callosum, Stri, striatum. Scale bar, 20 μm.

Given the expression pattern of Chd7, we investigated if its paralog gene, Chd8, was also expressed in oligodendrocyte lineage cells as expected from its expression in postnatal (P7) OPCs expression arrays (Fig. 39E). Indeed, Allen Brain Atlas in situ hybridization database (www.allen-brain-atlas) shows expression of Chd8 transcript in

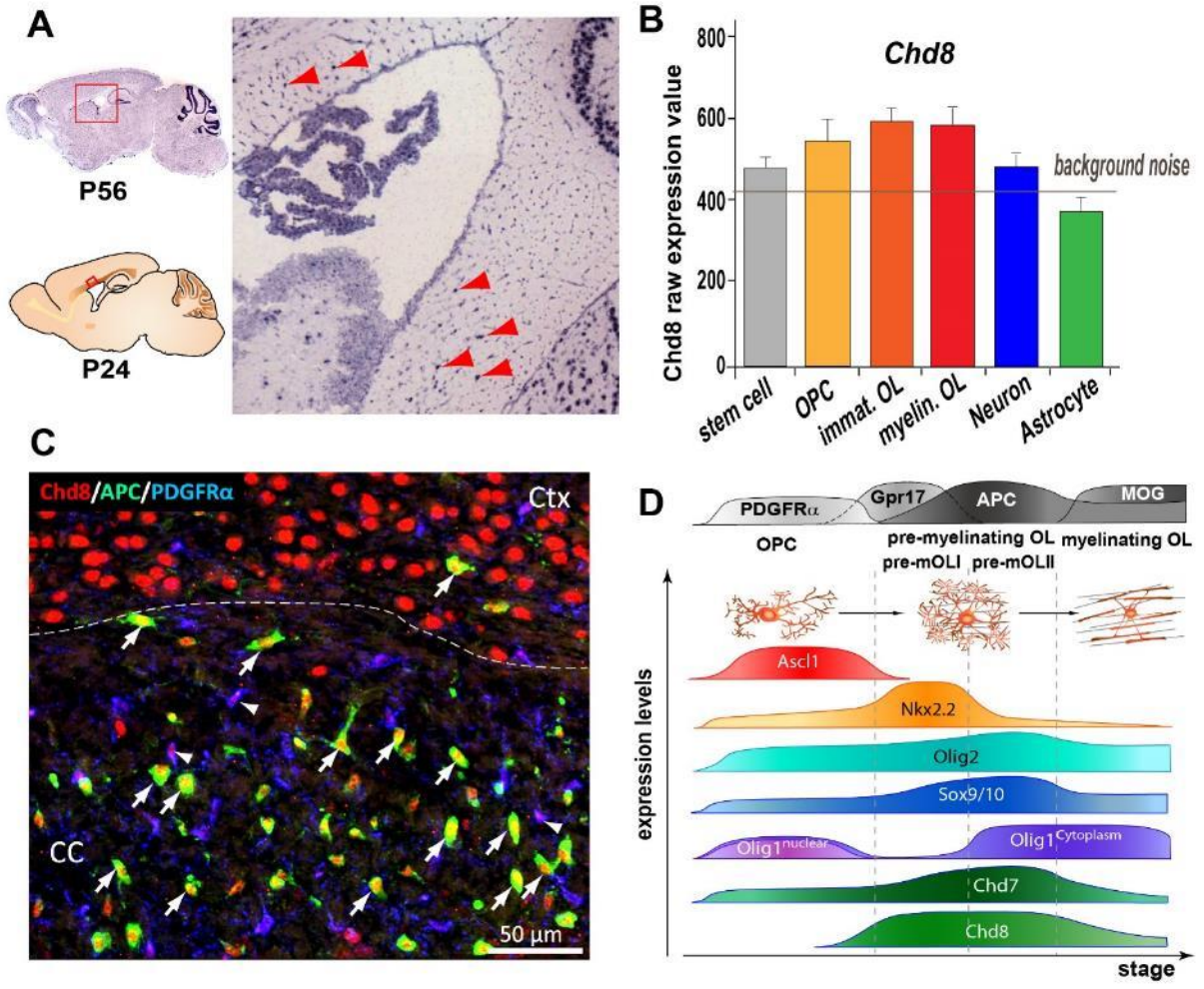

some myelinating cells in adult brain (P56, Fig. 41A) and microarray expression data from neonatal (P7) rat brain neural subtypes shows Chd8 expression in both OPCs and oligodendrocytes (Cajoy et al., 2007; Fig. 41B). We therefore investigated Chd8 protein expression in postnatal brain and found that it was strongly expressed in maturing oligodendrocytes (CC1/APC$^+$ cells, Fig. 41C,D), maintained at lower levels in mature oligodendrocytes (Fig. 41D) but differently to the mRNA, rarely detected in OPCs (PDGFRα+ cells, Fig. 41C,D). Therefore, during brain myelination while Chd7 is expressed both in OPCs and differentiating oligodendrocytes, Chd8 is only expressed in differentiating oligodendrocytes (Fig. 41D) suggesting a role in the process of differentiation and myelination.

Figure 41. Chd8 is expressed during myelination in differentiating OL. (A) Expression of *Chd8* mRNA in P56 brain showing expression in some cells of the white matter (arrows) and many neurons in the grey matter. (B) *Chd8* RNA expression levels in P7 rat brain neural subtypes showing enriched expression in immature and myelinating OL. (C) Chd8 immunoflurorescence in P24 brain sections showing expression with in all APC$^+$ cells but rarely in PDGFRα+ OPCs. (D) Summary schematic showing Chd7 and Chd8 expression at different stages of the oligodendroglial lineage together with transcription factors involved in oligodendrogenesis.

CHD7/8 protein expression during remyelination

We therefore, investigated if Chd7 and Chd8 could play a role during the process of remyelination. Using the LPC-induced focal demyelination model in the mouse corpus callosum, our preliminary analysis has found that soon after the demyelinating insult (2, 4 or 8 days post-injection, dpi), Chd7 (not shown) and Chd8 are highly expressed in and around the LPC demyelinating lesion (compare Fig. 42A and A‘) not only in the OLs close to the lesion region but also in the OPCs in/around the lesion (Fig. 42B,B_1). This upregulation in OPCs due to demyelination strongly suggests that Chd8 is mostlikely involved in promoting the remyelinating process.

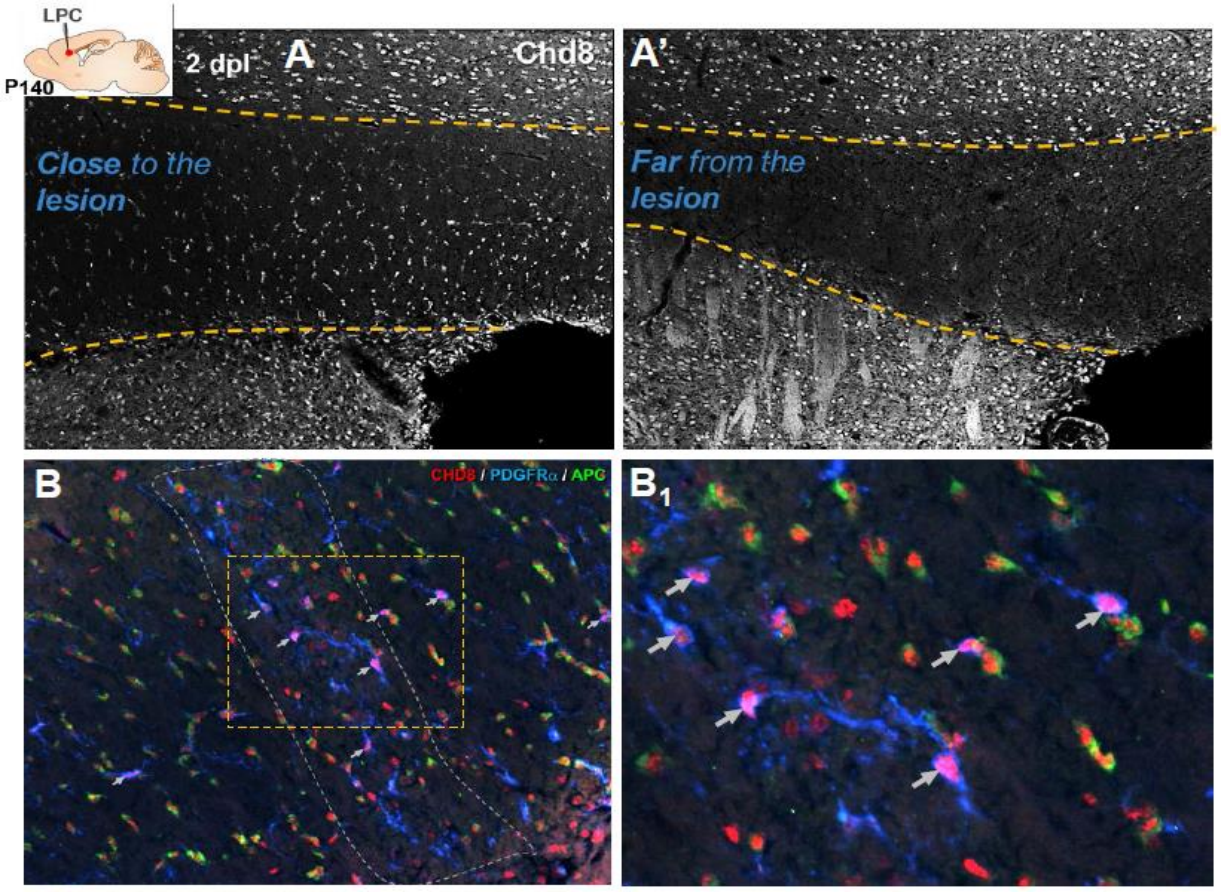

Figure 42. Figure. 5. Chd8 is upregulated in OPCs upon demyelination. (**A,A’**) Sagittal section of P140 brains at the level of the ventricle 2 days after LPC lesion (2dpi) showing increased levels of expression of Chd8 in the corpus calossum close to the lesion (A) compared to sections at a distance from the lesion (A‘). (**B,B**$_1$) The cells expressing high levels of Chd8 in the lesion territory are mostly PDGFRα$^+$ OPCs (arrows). (B_1) Higher magnification of the inset shown in B.

CHD8 protein expression in multiple sclerosis brain lesions

The data of Chd8 expression in demyelinating mouse models led us to investigate if CHD8 could also be expressed in oligodendroglia during remyelination in MS patients. We therefore have started to characterize CHD8 expression in different types of MS lesions, either chronic or actively remyelinating. Our preliminary data show that CHD8 can be found in oligodendroglial cells in the white matter close to demyelinated lesions (Fig. 43A,B) presenting typical alignments of white matter OLs (Fig. 43A). Moreover, we could find Chd8 co-expression with Sox10 oligodendroglial marker in cells at the border of the demyelinated lesion (Fig. 43C). We are currently characterizing CHD8 expression in different areas and lesions of MS patients to assess if CHD8 expression correlates with remyelination and it could be used as a hallmark of remyelination.

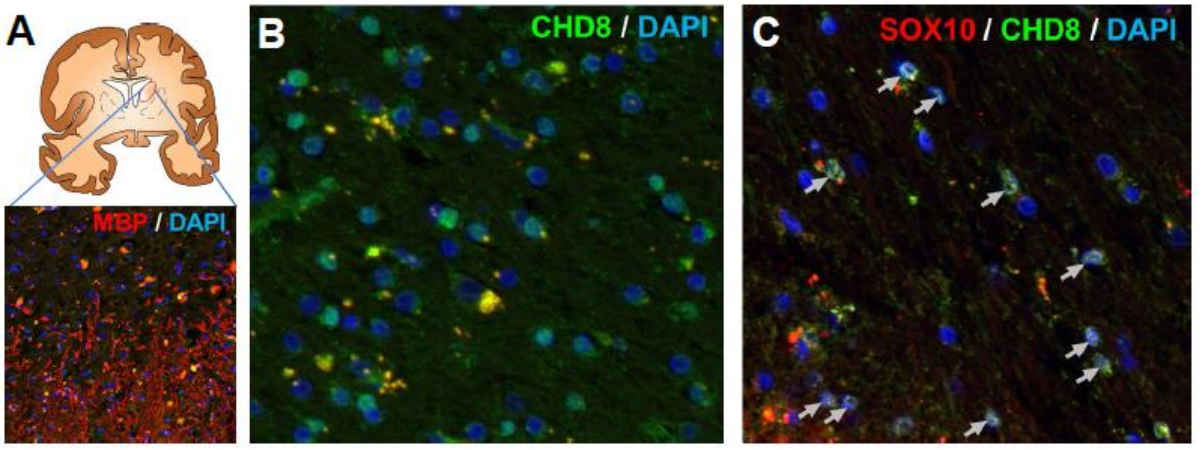

Figure 39. CHD8 is expressed oligodendroglial cells in MS brain. (A) Sagittal section of a periventricular brain tissue showing a demyelinated lesion by the absence of MBP expression. (B) CHD8 immunostaining in white matter region close to the demyelinating lesion showing $CHD8^{+}$ cells presenting typical alignments of OLs. (C) Coexpression of Sox10 and CHD8 in some cells close to lesion areas indicating that they are oligodendroglial cells.

Identification of TNS3 expression in premyelinating oligodendrocyte

Tensin 3 (*Tns3*) was one of the genes downregulated in *Ascl1*^{KO} (Fig. 44F) and *Olig2*^{KO} presenting binding by these two factor in an intragenic enhancer region showing active epigenetic marks in OPCs and differentiating oligodendrocytes (Fig. 44A). The expression pattern by in situ hybridization presented a strong specificity in white matter cells (such as the corpus callosum or the fimbria, Fig. 44B arrowheads) in the adult brain, and it was expressed like Ascl1 and Olig2 in the VZ zone of the embryonic (E14.5) ventral telencephalon (Fig. 44C). Moreover, the enrichment in the oligodendroglial cells was found also in the expression arrays of oligodendroglial cells in the postnatal brain (Fig. 44D), being Tns3 the only member of the family expressed

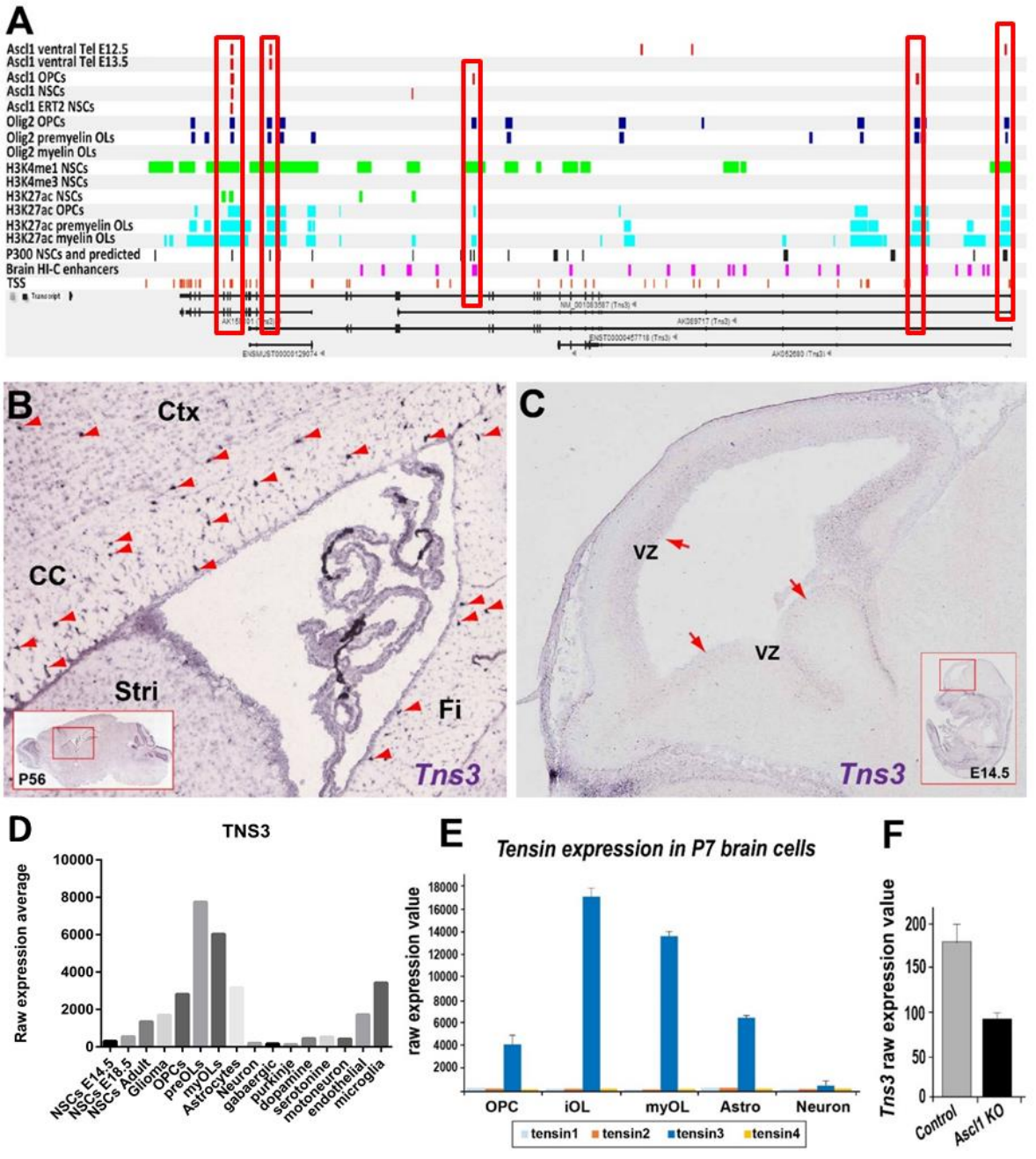

in the brain (Fig. 44E).

Figure 44. *Tns3* putative Ascl1-Olig2 target in oligodendrogenesis. (**A**) Schematic representation from Genomatix genome browser of *Tns3* locus integrating ChIP data depictured as rectangles/bars in each line. Ascl1 and Olig2 ChIP binding peaks are shown in red and blue respectively, Brg1 ChIP sites in pink and epigenetic marks in cyan. Red vertical rectangles indicate regulatory elements bound by Ascl1 and Olig2 in OPCs and immature oligodendrocytes, presenting also Brg1 binding sites and active epigenetic marks in oligodendroglial cells. (**B**) Sagittal section of E14.5 embryo showing *Tns3* expression pattern in the forebrain ventricular zone (VZ, arrows) by in situ hybridization; red square indicates the higher magnification area. (**C**) Brain sagittal section of P56 brain showing *Chd7* expression in corpus callosum (CC), cortex (Ctx) and fimbria (Fi) (some cells highlighted by arrowheads). (**D**) Histograms representing raw expression levels of *Tns3* in different brain subtypes expression microarrays. Note the higher expression in differentiating oligodendrocytes (OLs). (**E**) Histograms representing raw expression levels of different *Chd* genes in OPC expression microarrays. (**F**) Histograms representing raw expression levels of *Tns3* in ventral telencephalon expression microarrays of wild-type and Ascl1 mutant mice.

TNS3 EXPRESSION DURING MYELINATION

Tensin family is a group of focal adhesion proteins that interact with actin (by an actin binding motif), integrins and phosphotyrosine-containing proteins (through a SH-PBT motif). Tns3 has been found to be a negative regulator of cell migration and to be downregulated in human kidney cancer (Martuszewska et al., 2009). We therefore, investigated the expression of Tns3 in the postnatal brain. Indeed an anti-Tns3 polyclonal antibody showed specific expression in white matter regions correlating with the start of OPC differentiation in the brain (starting in the brainstem at P4 and appearing in the corpus callosum in the second postnatal week (Fig. 45A). Differently from the mRNA expression seen at P7 brain cell-types, we rarely detect Tns3 protein expression in PDGFRα^+ OPCs (Fig. 45A,B). As expected from the mRNA data mentioned before, its expression was strong in differentiating oligodendrocytes (strong APC-expressing cells). Surprisingly, Tns3 was localized mainly in the nucleus of the

differentiating oligodendrocytes and some neuronal population (Fig. 45A). The specificity of our anti-Tns3 antibody was confirm with a Tns3-LacZ gene-trap line,

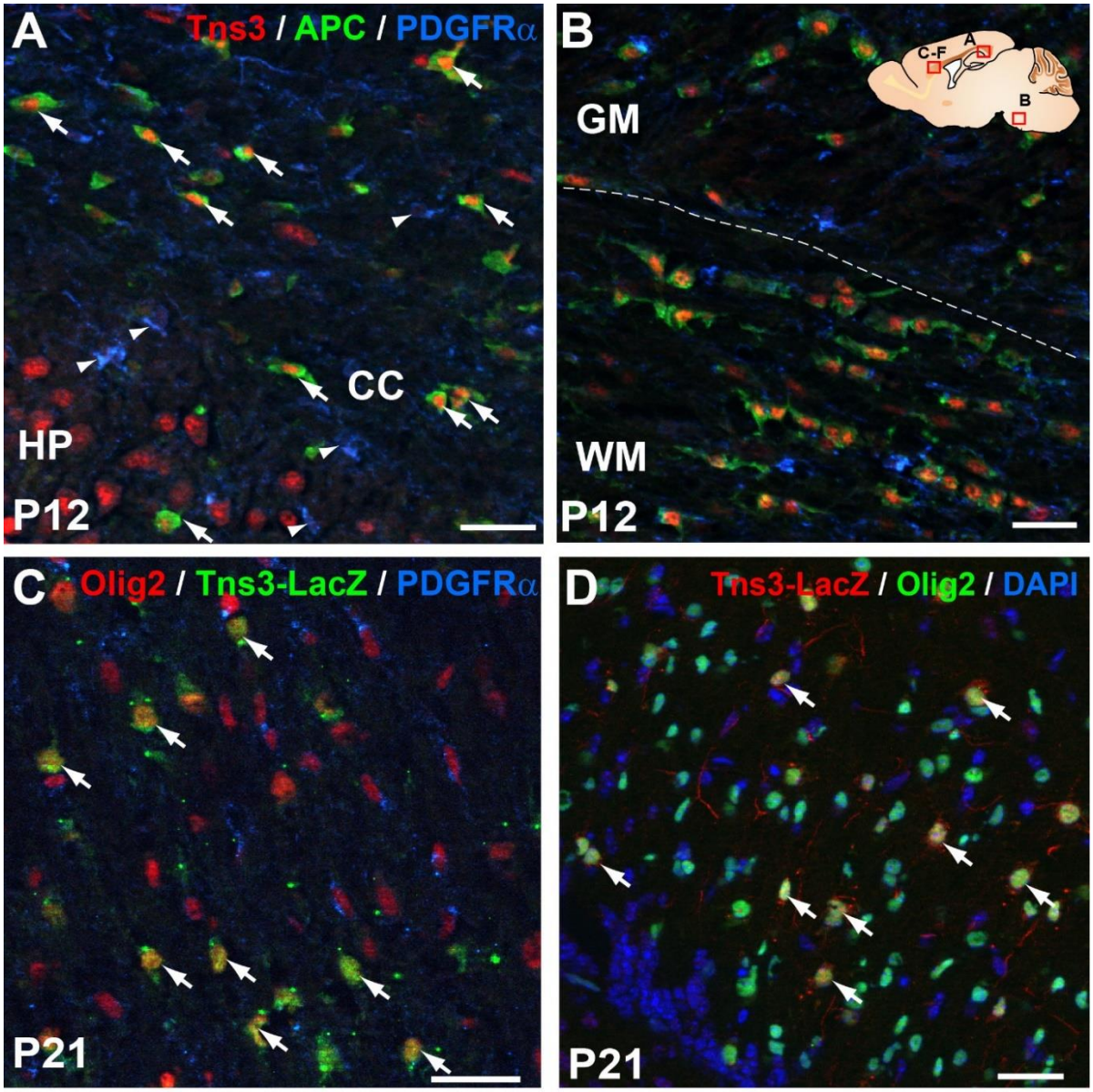

which show expression in Olig2^{+} / PDGFRα^{-} cells (oligodendrocytes) in the postnatal brain (Fig. 45C,D) and its by its cytoplasmic expression in the kidney and other regions outside the brain (data not shown). In line with the nuclear localization of Tns3, a role of nuclear actin in transcriptional regulation has been clearly demonstrated in the last decade (Miyamoto and Gurdon. Cell Mol Sci. 2013), suggesting that Tns3 nuclear expression in maturing oligodendrocytes could also be involved in the transcriptional regulation of myelination.

Figure 45: Tns3 protein expression during brain myelination. Sagittal sections of P12 (A,B), P21 (C,D) brains immunostained for Tns3 antibody. Arrows and arrowheads indicate some examples of labelled cells. (**A,B**) Expression of Tns3 in APC^+ oligodendrocytes but not in PDGFRα+ OPCs in the CC (A) or the brainstem (B) cells either expressing Olig2 (arrowheads) or not (most likely transit amplifying precursors, arrows). (**C,D**) βgal expression in the *Tns3-LacZ* mice showing expression with $Olig2^+$/$PDGFR\alpha^-$ cells (oligodendrocytes) but not in $Olig2^+$/$PDGFR\alpha^+$ cells (OPCs) and Ascl1 co-expression in PDGFRα+ (arrows), (transit amplifying cells, arrowheads). Note that Chd7 supporting specificity anti-Tns3 antibody. (**C**) Chd7 and Aslc1 co-expression with Mcm2, proliferation marker in SVZ cells. (**D**) Chd7 and Ascl1 co-expression in SVZ cells (arrows) or PDGFRα+ OPCs in the CC (arrowheads). HP, hippocampus; CC, corpus callosum, GM, grey matter, WM, white matter. Scale bar, 20 μm.

TNS3 EXPRESSION DURING REMYELINATION

Given the expression of Tns3 during myelination we investigated if it could also play a role during the process of remyelination. Using the LPC-induced focal demyelination model mentioned before, our preliminary studies has found that Tns3 is

strongly expressed soon after the demyelinating insult (2, 4 or 8 days post-injection, dpi), in and around the LPC demyelinating lesion (compare Fig. 46A-A_2) specifically

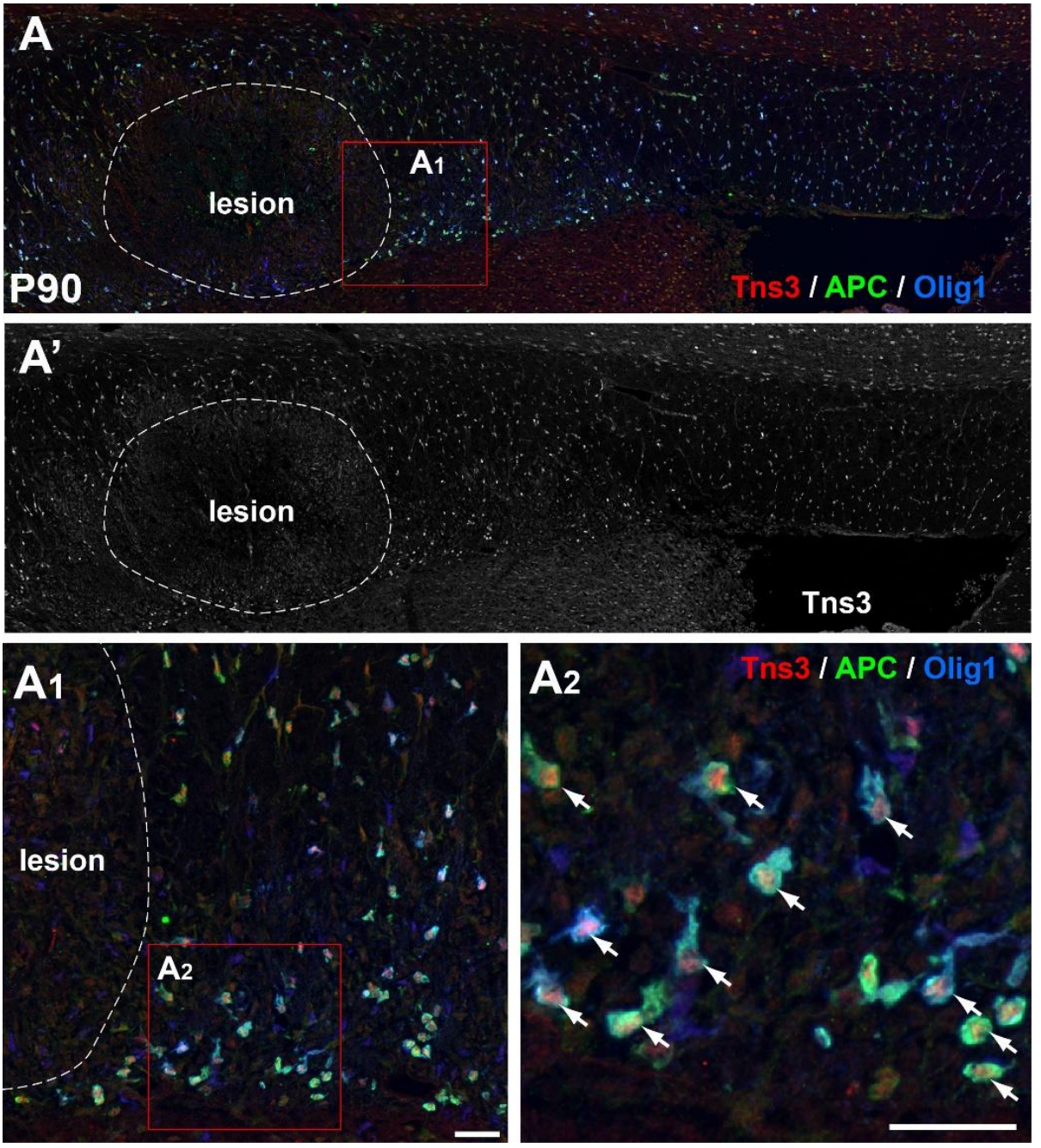

in maturing oligodendrocytes (cells expressing high levels of APC and Olig1 in the cytoplasm) suggesting that Tns3 could be involved in the mechanisms leading to remyelination.

Figure 46. Tns3 expression in newly generated remyelinating oligodendrocytes. (**A-A_2**) Tns3-expressing cells in the CC of adult (P90) mice, 4 days after demyelination

showing strong Tns3 expression in $APC^{+}/Olig1^{citoplasmic}$ cells (immature OLs) around the lesion. Note the absence of $APC^{+}/Olig1^{+}$ cells (oligodendrocytes) in the lesion. A_1 and A_2 are higher magnification of corresponding insets (red squares). Demyelinated lesion is shown by the dotted circle area. Note the absence of Tns3 expression and presence of $APC^{+}/Olig1^{+}$ oligodendrocytes in the lesion. Scale bar, 20 μm.

Together, all this data indicates that Tns3 expression clearly correlates with oligodendrocyte differentiation during myelination and remyelination and therefore it will be important to characterize its function in these processes and its possible implication in Multiple Sclerosis pathology.

Myelinating oligodendrocyte control the creatine metabolism in the brain

Creatine is a small metabolite that serves as an energy shuttle between the mitochondrial sites of production and the cytosol, the site of ATP utilization. As ATP diffusion is very limited, phosphocreatine and creatine, much smaller molecules, are able to diffuse very easily and they can accumulate to high concentrations without affecting metabolism (Wyss and Kaddurah- Daouk, 2000).

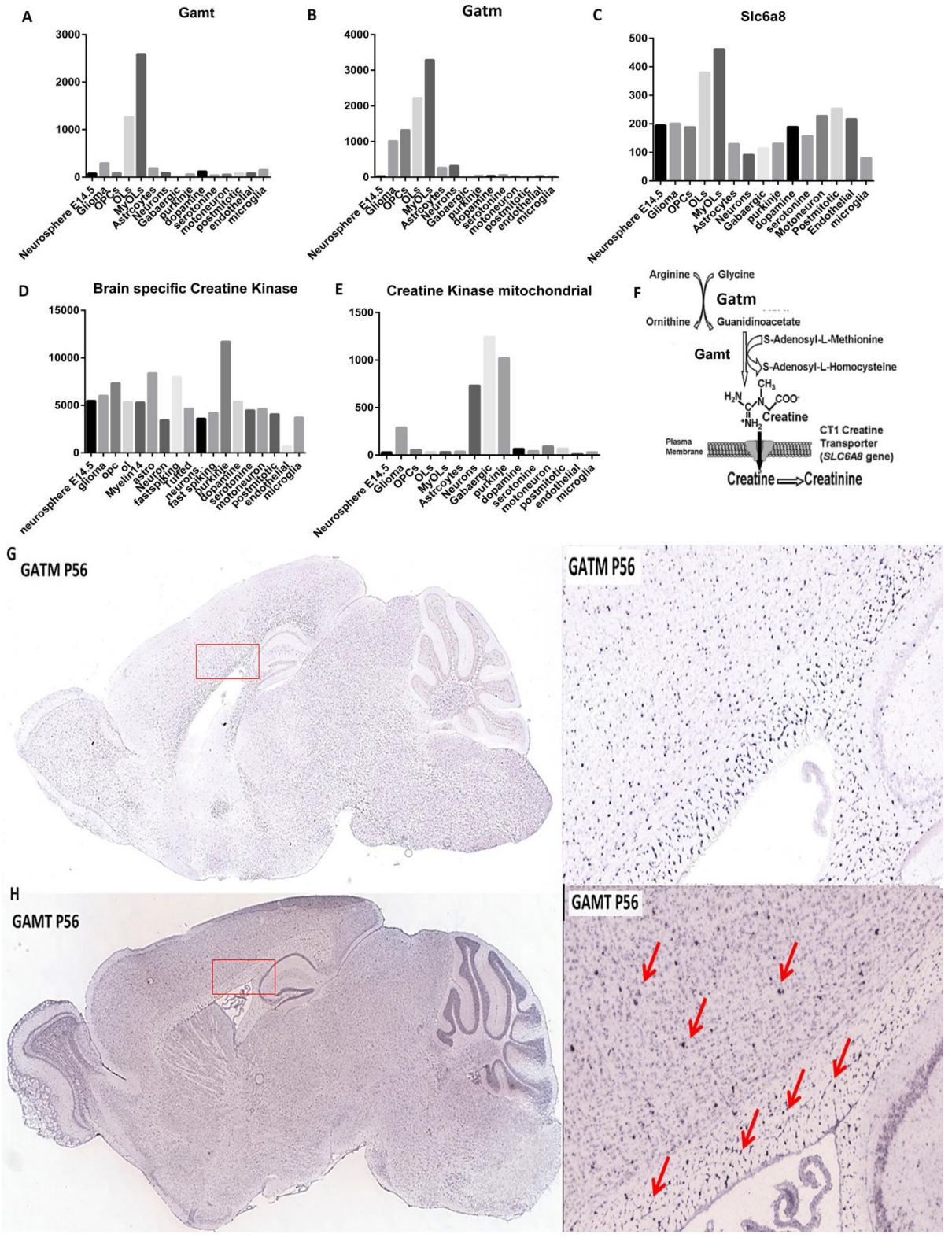

Figure 47. Creatine producing enzymes mRNA expression in the brain. (A-E). Cell-type specific microarray expression study of Gamt (**A**), Gatm (**B**), Slc68a (**C**),

Brain Creatine Kinase (**D**) and mitochondrial Creatine Kinase (**E**). Raw expression level for each gene is given for E14.5 neurosphere, glioma, OPCs, premyalinating oligodendrocyte, myelinating Oligodendrocytes, glutamatergic neurons, gabaergic neurons, purkinje cells, domapinergic, serotoninergic motoneuron, endothelial cell and microglia. Gamt et Gatm expressions show a clear specificity for myelinating oligodendocyte. Slc8a expression is highly enriched in oligodendrocyte dispite low expression in other cell types. While brain creatine kinase is expressed in all cell type (D), mitochondrial creatine kinase is neuron specific (E). (**F**) schematic representation of GATM et GAMT function in the creatine synthesis. One synthetized, creatine can be exported in the form of creatinine through the creatine transporter (CT1). (**G**) Sagittal section of P56 brain showing *Gatm* expression in the whole brain (left) or in corpus callosum (right). (**H**) Sagittal section of P56 brain showing *Gamt* expression in the whole brain (left) or in corpus callosum (right). Both gene are higly expressed in white matter region.

A

Chemical Name	Chemical ID	Disease Name	Inference Network	Inference Score
Chloroprene	D002737	Multiple Sclerosis	CD40|CIITA|CNR1|IL12A|IL1B|IL7R|IRF8|	9,97
Probucol	D011341	Multiple Sclerosis	APOE|SELE|VCAM1	9,93
Desoxycorticosterone	D003900	Multiple Sclerosis	IL1B|POMC|VCAM1	9,80
3'-O-(4-benzoyl)benzoyladenos	C033901	Multiple Sclerosis	IL1B|P2RX7	9,77
adenosine 5'-O-(3-thiotriphosp	C022571	Multiple Sclerosis	IL1B|P2RX7	9,77
N,N-diethyl-2-[(4-phenylmethy	C043062	Multiple Sclerosis	CD40|PTPRC	9,76
bicalutamide	C053541	Multiple Sclerosis	BCHE|CD40|ICAM1|VCAM1	9,70
Beryllium	D001608	Multiple Sclerosis	HLA-DPB1|IL1B	9,70
gadolinium chloride	C038958	Multiple Sclerosis	ICAM1|IL1B|TNFRSF1A	9,67
Pyrones	D011753	Multiple Sclerosis	IL1B|TNFAIP3	9,64
beta-hydroxy simvastatin acid	C483161	Multiple Sclerosis	HLA-DQB1|TNFSF14|VCAM1	9,60
Beclomethasone	D001507	Multiple Sclerosis	ICAM1|IL1B|IL2RA|PTPRC|SELE|VCAM1	9,56
GW 4064	C412815	Multiple Sclerosis	APOE|ICAM1|VCAM1	9,53
Dichlorvos	D004006	Multiple Sclerosis	BCHE|CNR1|IL1B|POMC	9,51
Naloxone	D009270	Multiple Sclerosis	ICAM1|IL1B|POMC|TNFRSF1A	9,50
hexadecafluoro-nonanoic acid	C018959	Multiple Sclerosis	IL1B|POMC	9,50
20-alpha-Dihydroprogesterone	D004092	Demyelinating Diseases	MBP|PMP22	9,47
capsiate	C470213	Multiple Sclerosis	ICAM1|IL2RA	9,45
CAP18 lipopolysaccharide-bind	C070646	Multiple Sclerosis	ICAM1|VCAM1	9,42
Carbon Tetrachloride	D002251	Multiple Sclerosis	APOE|ICAM1|IL1B|IL2RA|MCAM|P2RX7|F	9,39
iodopravadoline	C094023	Multiple Sclerosis	CNR1|ICAM1	9,39
diazoxon	C000912	Multiple Sclerosis	BCHE|CNR1	9,37
2-(2-cresyl)-4H-1-3-2-benzodio	C000516	Multiple Sclerosis	BCHE|IL1B	9,37
WR 1065	C020174	Multiple Sclerosis	IL2RA|TNFRSF1A	9,32

B

ChemicalName	ChemicalID	GeneSymbol	GeneID	InteractionActions	PubMedIDs
Bezafibrate	D001629	ACSL1	2180	increases expression	21640707
Dopamine	D004298	ADAMTS4	9507	increases expression	21983523
2-amino-3,8-dimethylimidazo(4,5-f)quinoxaline	C036990	ANLN	54443	increases expression	20816883
afimoxifene	C016601	APOD	347	increases expression	16514628
Polychlorinated Biphenyls	D011078	ARHGEF10	9639	affects expression	21334430
27-hydroxycholesterol	C076996	BACE1	23621	increases expression	19126211
Drugs, Chinese Herbal	D004365	CHN2	1124	increases expression	23811387
2,2,5,7,8-pentamethyl-1-hydroxychroman	C029141	CRYAB	1410	increases expression	21920950
2,2-bis(4-hydroxyphenyl)-1,1,1-trichloroethane	C404910	DHCR24	1718	increases expression	20826375
2,3-bis(3'-hydroxybenzyl)butyrolactone	C029497	EFHD1	80303	affects cotreatment|decreases expression	19167446
2,6-diisocyanatotoluene	C026942	ENPP2	5168	increases expression	22952646
Creatine	D003401	GAMT	1718	increases expression	18428409
beta-hexachlorocyclohexane	C023888	ERBB3	2065	affects binding|increases reaction	12439862
Amiodarone	D000638	ERMN	57471	increases expression	19774075
1-Methyl-4-phenyl-1,2,3,6-tetrahydropyridine	D015632	GAB1	2549	increases expression	20230807
3-dinitrobenzene	C017906	GALNT6	11226	increases expression	21983209
Ammonia	D000641	GAMT	2593	increases expression	20227315
halofuginone	C010176	GNG11	2791	increases expression	17180598
Leukotriene D4	D017998	GPR17	2840	increases activity	18974869
2-methoxy-5-(2',3',4'-trimethoxyphenyl)tropone	C030370	GPR37	2861	increases expression	20206263
2-tert-butylhydroquinone	C018855	GSS	2937	increases expression	19183254
4-hydroxy-2-nonenal	C027576	LPAR1	1902	increases expression	19191707
1,2-dithiol-3-thione	C049325	MAG	4099	increases expression	19162173
4,4'-diaminodiphenylmethane	C009505	MAL	4118	increases expression	18648102
2-(1'H-indolo-3'-carbonyl)thiazole-4-carboxylic acid methyl ester	C548651	MBP	4155	increases expression	19933214
Aspirin	D001241	MCAM	4162	increases expression	15456535
Capsaicin	D002211	MOBP	4336	increases expression	20349343
2,2',4,4'-tetrabromodiphenyl ether	C511295	NKX6-2	84504	increases expression	21394737
Flutamide	D005485	PADI2	11240	increases expression	21525395
gemcitabine	C056507	PAQR8	85315	increases expression	17039268
3,4,5,3',4'-pentachlorobiphenyl	C023035	PDLIM2	64236	increases expression	19692669
Pregnenolone Carbonitrile	D011285	PLEKHH1	57475	increases expression	22698814
Caffeine	D002110	PLP1	5354	increases expression	18444173
Diethylstilbestrol	D004054	PRR5L	79899	increases expression	19371625
Vinyl Chloride	D014752	RFTN1	23180	increases expression	18579281
Cephaloridine	D002509	RHPN2	85415	increases expression	18500788
methylformamide	C002950	SGK2	10110	increases expression	17040096
Bumetanide	D002034	SLC12A2	6558	increases response to substance	17259435
5-alpha-Dihydroprogesterone	D043582	SOX10	6663	increases expression	17478888
malaoxon	C100082	TJP2	9414	affects cotreatment|decreases expression	20970449
testosterone enanthate	C004648	TMBIM1	64114	affects expression	17440010
perfluoro-n-undecanoic acid	C101814	TPPP	11076	increases expression	23602845
Clofibric Acid	D002995	UNC5B	219699	affects expression	17602206

Figure 48. Toxicogenomic selection of drug affecting oligodendrocyte genes. A. Table showing the drug identified in this study as modifying oligodendrocyte gene expression and already testes in the context of demyelinating diseases. B. Table

showing drugs shown to affect oligodendrocyte genes and never tested in the context of demyelinating diseases. As creatine was among the identified molecules, we focused on its role in myelination and remyelination.

ARTICLE I: Ascl1/Mash1 Promotes Brain Oligodendrogenesis during Myelination and Remyelination

Development/Plasticity/Repair

Ascl1/Mash1 Promotes Brain Oligodendrogenesis during Myelination and Remyelination

Hiroko Nakatani,[1,2,3] Elodie Martin,[1,2,3]* Hessameh Hassani,[1,2,3]* Adrien Clavairoly,[1,2,3] Cécile L. Maire,[1,2,3] Arthur Viadieu,[1,2,3] Christophe Kerninon,[1,2,3] Aurélie Delmasure,[1,2,3] Magali Frah,[1,2,3] Melanie Weber,[4] Masato Nakafuku,[5] Bernard Zalc,[1,2,3,6] Jean-Léon Thomas,[1,2,3,6,7] François Guillemot,[4] Brahim Nait-Oumesmar,[1,2,3,6] and Carlos Parras[1,2,3]

[1]Université Pierre et Marie Curie-Paris 6, Centre de Recherche de l'Institut du Cerveau et de la Moelle épinière, 75013 Paris, France, [2]Inserm UMR_S 975, 75013 Paris, France, [3]Centre National de la Recherche Scientifique Unité Mixte de Recherche 7225, 75013 Paris, France, [4]Medical Research Council National Institute for Medical Research, Division of Molecular Neurobiology, London NW71 AA United Kingdom, [5]Division of Developmental Biology, Cincinnati Children's Hospital Research Foundation, Cincinnati, Ohio 45229, [6]Assistance Publique-Hôpitaux de Paris, GH Pitié-Salpêtrière, 75013 Paris, France, and [7]Department of Neurology, Yale School of Medicine, New Haven, Connecticut 06511

Oligodendrocytes are the myelin-forming cells of the CNS. They differentiate from oligodendrocyte precursor cells (OPCs) that are produced from progenitors throughout life but more actively during the neonatal period and in response to demyelinating insults. An accurate regulation of oligodendrogenesis is required to generate oligodendrocytes during these developmental or repair processes. We hypothesized that this regulation implicates transcription factors, which are expressed by OPCs and/or their progenitors. Ascl1/Mash1 is a proneural transcription factor previously implicated in embryonic oligodendrogenesis and operating in genetic interaction with Olig2, an essential transcriptional regulator in oligodendrocyte development. Herein, we have investigated the contribution of Ascl1 to oligodendrocyte development and remyelination in the postnatal cortex. During the neonatal period, Ascl1 expression was detected in progenitors of the cortical subventricular zone and in cortical OPCs. Different genetic approaches to delete *Ascl1* in cortical progenitors or OPCs reduced neonatal oligodendrogenesis, showing that Ascl1 positively regulated both OPC specification from subventricular zone progenitors as well as the balance between OPC differentiation and proliferation. Examination of remyelination processes, both in the mouse model for focal demyelination of the corpus callosum and in multiple sclerosis lesions in humans, indicated that *Ascl1* activity was upregulated along with increased oligodendro- genesis observed in remyelinating lesions. Additional genetic evidence indicated that remyelinating oligodendrocytes derived from Ascl1 progenitors/OPCs and that Ascl1 was required for proper remyelination. Together, our results show that Ascl1 function modulates multiple steps of OPC development in the postnatal brain and in response to demyelinating insults.

Introduction

During development, the basic-helix-loop-helix transcription factor (TF) Olig2 is both necessary and, in some contexts, sufficient for oligodendrocyte precursor cell (OPC) generation (Lu et al., 2001; Zhou et al., 2001; Zhou and Anderson, 2002; Yue et al., 2006; Zhu et al., 2012). Despite this key role, Olig2 is however not a master gene, and it acts in concert with additional cofactors to regulate oligodendrocyte specification. For example, Olig2 must interact with signaling pathways controlling its phosphorylation state to acquire an oligodendrogenic activity (Li et al., 2011). The multiple focal pattern of oligodendrogenesis in the embryonic brain also suggests that Olig2 interacts with multiple TFs providing positional cues and regulating locally its action in progenitor cells (Spassky et al., 1998; Tekki-Kessaris et al., 2001; Miguez et al., 2012).

Ascl1 is another basic-helix-loop-helix factor playing a major role at different stages of neurogenesis and having potent proneural and reprogramming activities (Bertrand et al., 2002; Vierbuchen et al., 2010; Vierbuchen and Wernig, 2012). *Ascl1* is also expressed by embryonic and neonatal OPCs (Kondo and Raff, 2000; Wang et al., 2001; Parras et al., 2004; Parras et al., 2007). *Ascl1* operates in genetic interaction with *Olig2* during OPC specification in the embryonic telencephalon, and the loss of *Ascl1* function reduces embryonic oligodendrogenesis (Parras et al., 2007; Sugimori et al., 2007). Therefore, beyond its role in neurogenesis, Ascl1 is involved in the regulation of oligodendrogenesis.

Received Feb. 21, 2013; revised April 4, 2013; accepted April 13, 2013.

Author contributions: B.N.-O. and C.P. designed research; H.N., E.M., H.H., A.C., C.L.M., A.V., C.K., A.D., M.F., M.W., and C.P. performed research; M.N. contributed unpublished reagents/analytic tools; H.N., E.M., H.H., A.C., M.N., B.Z., J.-L.T., F.G., B.N.-O., and C.P. analyzed data; B.Z., J.-L.T., F.G., B.N.-O., and C.P. wrote the paper.

This work was supported by Institut National de la Santé et de la Recherche Médicale Grant R05245DS to C.P. and H.N., National Multiple Sclerosis Society RG 4318A1/1 to H.N. and E.M., Fondation pour l'Aide à la Recherche sur la Sclerose En Plaques (H.N., H.H.), Neuropôle de Recherche Francilien/Région de l'Ile-de-France (H.H.), Fondation de France (C.P., H.N.), Université Pierre et Marie Curie-Paris 6 (A.C.), and "Investissements d'Avenir" ANR-10-IAIHU-06 at the Institut du Cerveau et de Moelle épinière (C.K., B.N.-O.). We thank Dr. W.D. Richardson for the *PDGFR ::CreER*^{T2} mice; A. Chedotal, J. Johnson, K. Campbell, G. Panganiban, M. Okabe, and M. Wegner for reagents; the UK Multiple Sclerosis Tissue Bank (Pr R. Reynolds, Imperial College, London), funded by the Multiple Sclerosis Society of Great Britain and Northern Ireland, registered charity 207495, for brain tissue samples; and A. Dauphin and D. Langui from the Plate-forme d'Imagerie Cellulaire de la Pitié-Salpêtrière for their advice, notably with EM analysis.

The authors declare no competing financial interests.

*E.M. and H.H. contributed equally to this work.

Correspondence should be addressed to Dr. Carlos Parras, Université Pierre et Marie Curie-Paris 6, Centre de Recherche de l'Institut du Cerveau et de la Moelle épinière, Hôpital de la Pitié-Salpêtrière 83, Boulevard de l'Hôpital ICM, 4ème étage (4.007), 75013 Paris, France. E-mail: carlos.parras@upmc.fr.

C.L. Maire's present address: Medical Oncology, Dana-Farber Cancer Institute, 44 Binney Street, Boston, MA 02115.

DOI:10.1523/JNEUROSCI.0805-13.2013

Copyright © 2013 the authors 0270-6474/13/339752-17$15.00/0

Table 1. Clinical and morphological characteristics of postmortem MS brain tissue

Case	Sex	Age (years)	PMD (hours)	Disease duration (years)	Cause of death	Course	Lesions analyzed			
							Active	Chronic active	Chronic silent	Shadow plaques
MS										
MS100	M	46	7	8	Pneumonia	SP	0	1	0	0
MS127	M	51	21	10	MS, bronchopneumonia	SP	1	1	0	0
MS136	M	50	10	9	Respiratory failure, sepsis, MS	SP	1	0	0	0
MS154	F	34	12	9	Pneumonia	SP	1	1	0	0
Control										
C20	F	84	24		Congestive cardiac failure		0	0	0	0
CO2	F	95	10		Bronchopneumonia		0	0	0	0

The importance of Ascl1 action in postnatal oligodendrogenesis and myelination as well as its requirement for proper myelin repair have however not yet been determined.

To ascertain its involvement in oligodendrogenesis during myelination and remyelination, we have examined *Ascl1* expression and function in oligodendroglial cells during the postnatal period of development and during myelin repair in the adult brain. At all ages examined, *Ascl1* expression was restricted to immature cell types (i.e., cortical subventricular zone [SVZ] progenitor cells and OPCs of gray matter and white matter). Using different genetic models to delete *Ascl1* in progenitor cells or OPCs, and to trace the *Ascl1*-cell lineage, we have characterized *Ascl1* requirement in oligodendrogenesis both under normal physiological conditions and after demyelinating lesions. We found that *Ascl1* was required in SVZ progenitors for oligodendroglial cell fate decision as well as in OPCs for their proper differentiation into oligodendrocytes. After demyelinating lesions, Ascl1 was expressed by intralesional SVZ progenitors and OPCs, which regenerated myelin-forming cells and thus participated in myelin repair of demyelinated lesions. Although *Ascl1* was dispensable for recruitment and maturation of intralesional progenitors and OPCs, we showed that it was required for a proper balance between the number of OPCs and oligodendrocytes. Finally, examination of human periventricular multiple sclerosis (MS) lesions confirmed that Ascl1 expression is a hallmark of OPCs involved in myelin repair, both in mice and humans. Together, our findings support a promoting role for Ascl1 during postnatal oligodendrogenesis and in the process of remyelination, both in progenitors for OPC specification as well as in OPCs for their differentiation.

Materials and Methods

Mouse breeding and genotyping. The following transgenic lines were used and genotyped using protocols previously described: *Ascl1* (Casarosa et al., 1999), $Ascl1^{fl}$ (Pacary et al., 2011), *Ascl1::Cre*, *Ascl1::GFP* (Parras et al., 2007), $Rosa26^{stop\text{-}YFP}$ (Srinivas et al., 2001), $Rosa26^{stop\text{-}LacZ}$ (Soriano, 1999), and *PDGFR ::CreER*^{T2} (Rivers et al., 2008). For simplicity, we renamed the different mice as follows: $Ascl1^{GFP}$ (for *Ascl1::GFP*), $Ascl1^{Cre/YFP}$ (for *Ascl1::Cre*; $Rosa26^{stop\text{-}YFP}$), $Ascl1^{Cre/LacZ}$ (for *Ascl1::Cre*; $Rosa26^{stop\text{-}LacZ}$), Cko^{OPC} (for conditional knock-out in OPCs: *PDGFR ::CreER*^{T2}; $Ascl1^{fl/}$; $Rosa26^{stop\text{-}YFP}$), Ctr^{OPC} (for control for Cko^{OPC}: *PDGFR ::CreER*^{T2}; $Ascl1^{fl/}$; $Rosa26^{stop\text{-}YFP}$), Cko^{dSVZ} (for dorsal Cre-electroporated $Ascl1^{fl/}$; $Rosa26^{stop\text{-}YFP}$), and Ctr^{dSVZ} (for dorsal Cre-electroporated $Ascl1^{fl/}$; $Rosa26^{stop\text{-}YFP}$). Both males and females were included in the study. All experiments were carried out in accordance to Inserm ethical committees (authorization #A75-13-19) and personal animal experimentation license A75-17-72 (C.P.).

Demyelinating mouse lesions. Before surgery, adult (4–6 months) $Ascl1^{GFP}$, $Ascl1^{Cre/YFP}$, amd $Ascl1^{Cre/LacZ}$ or Cko/Ctr^{OPC} mice were weighted and anesthetized by intraperitoneal injection of mixture of ketamine (0.1 mg/g) and xylacine (0.01 mg/g). An analgesic (buprenorphine, 30 mg/g) was administered intraperitoneally to prevent postsurgical pain. Focal demyelinating lesions were induced by stereotaxic injection of 1.5 l lysolecithin solution (LPC, Sigma, 1% in 0.9% NaCl) into the corpus callosum (CC; at coordinates: 1 mm lateral, 1.3 mm rostral to bregma, 1.7 mm deep to brain surface) using a glass-capillary connected to a 10 l Hamilton syringe. Animals were left to recover in a warm chamber before being returned into their housing cages.

Postnatal electroporation. Postnatal brain electroporation (Boutin et al., 2008) was adapted to target the dorsal SVZ. Briefly, postnatal day 2 (P2) pups were cryoanesthetized for 3 min on ice, and 2 l of plasmid solution (3 g *pCX-Cre*) was injected into the ventricle using a glass capillary. *pCX-Cre* plasmid drive *Cre* expression under the CMV-modified strong and ubiquitous promoter (kindly gift from Alain Chedotal, Institut de la Vision, Paris). Electrodes (Nepagene CUY650P10) were positioned in the dorsoventral axis with the positive pole dorsal. Five electric pulses of 100 V, 50 ms pulse ON, 850 ms pulse OFF were applied using a Nepagene CUY21-SC electroporator. Pups were immediately warmed up in a heating chamber and brought to their cages at the end of the experiment.

Tamoxifen administration. Tamoxifen (Sigma) was dissolved in corn oil (Sigma) at 20 mg/ml. Postnatal mice received one subcutaneous injection of 400 g (P5) or one intraperitoneal injection of 800 g (P8/P9). Adult animals received one intraperitoneal injection per day of 200 g for 5 consecutive days starting 7 d before LPC lesion.

MS and non-neurological control tissues. Autopsy brain tissue samples from 4 patients with confirmed secondary progressive MS and two patients without neurological diseases (Table 1) were obtained from the United Kingdom MS tissue bank (Richards Reynolds, Imperial College, London). MS and control brain samples were excised from matching periventricular regions or white matter. Four MS tissue blocks containing active (n 3) and chronic active lesions (n 3), periventricular lesions, and periplaque white matter were selected for further analysis. MS lesions were classified as previously reported (Lassmann, 1998).

Electron microscopy. $Ascl1^{Cre/LacZ}$ mice (P120) were perfused with 4% PFA and 0.5% glutaraldehyde in PBS buffer. Brains were sectioned (300 m) with a Tissue chopper (McIlwain) and subjected overnight to the X-gal reaction. Tissue was postfixed in 2.5% glutaraldehyde for 2 h. Regions containing the CC were dissected out under a binocular scope (MZ16, Leica). Tissue samples were osmicated, dehydrated in ethanol, and embedded in Epon. Ultrathin sections were made using a Leica electronic microscopy (EM) UC7 ultramicrotome, and micrographs were taken with a Philips CM120 electronic microscope.

Immunofluorescence. We optimized immunostaining for Ascl1, which is very sensitive to fixation conditions. Mice were perfused with freshly made chilled 2% paraformaldehyde (Sigma) with the following amounts (P0-P10, 15 ml; P10-P16, 20 ml; adult, 25 ml), brain was dissected out, cryoprotected in PBS with 20% sucrose overnight, and included in OCT (BDH) before freezing and sectioning (14 m thick) with a cryostated microtome (Leica). Sections were then either processed for immunohistochemistry or stored at 80°C. P0-P16 brain sections were postfixed with 4% PFA for 10 min. Sections were incubated in a blocking solution (PBS plus 10% normal goat serum, Vector Laboratories; and 0.1% Tween 20 or Triton X-100) and then with primary antibodies overnight at 4°C. The following primary antibodies were used: mouse monoclonal antibodies to APC (Calbiochem, 1:200), Ascl1 (BD Biosciences, 1:200), CNP (Millipore, 1:500), MOG (8-18C5, 1:5, Dr. C. Linington, Max-Planck

Institute, Tuebingen, Germany), Olig2 (Ligon et al., 2006), Nkx2.2 (clone 74.5A5, Developmental Studies Hybridoma Bank, 1:5); rabbit polyclonal antibodies to Caspase3 activated (R&D Systems, 1:200), pan-Dlx (gift from G. Panganiban, 1:100), GFP (Invitrogen, 1:2000), Gpr17 (Cayman Chemical, 1:400), Gsx2 (gift from K. Campbell, 1:1000), Ki67 (Novocastra, 1:1000), myelin basic protein (MBP, Millipore, 1:1000), NG2 (Millipore, 1:1000), Olig1 (Mizuguchi et al., 2001), Olig2 (Millipore, 1:1000), Sox9 (R&D Systems, 1:500); guinea pig antibodies to Sox10 (gift from M. Wegner, 1:1000), Ascl1 (gift from J. Johnson, 1:1000); rat monoclonal antibodies to Ki67 (Dako, 1:50), PDGFR (BD Biosciences, 1:800), and chicken polyclonal antibodies to GFP (Aves Laboratories, 1:2000) and MBP (Millipore, 1:50). Fluorescent secondary antibodies included the following: AlexaFluor-488, AlexaFluor-594, and AlexaFluor-647 Ig (1:1000, Invitrogen). Antigen retrieval for Ki67 antibody staining was performed using antigen retrieval solution (Vector, H-330), heating sections in citrate-based solution up to boiling and then allowing cooling down at room temperature for 20 min. Immunofluorescence was visualized with Leica TC SP2 confocal or Zeiss AxioImager-Apotome system microscopes. Pictures were taken as stacks of 5–10 m with 0.5 m between sections. Z-projections and orthogonal projections were done in ImageJ and processed with Adobe Photoshop. Figures were made using Adobe Illustrator.

Human brain tissues were immunostained as previously described (Nait-Oumesmar et al., 2007) with mouse monoclonal antibodies for human Ascl1 (Cosmo Bio, 1:500), CD68 (clone KP1, Dako, 1:100), rabbit antibodies for Olig2 (Millipore, 1:100), Olig1 (R&D Systems, 1:50), and goat antibody for Sox10 (R&D Systems, 1:50).

Quantification and statistical analysis. Confocal images were quantified for expression of TFs by manual or automated counting using ImageJ software. To quantify Ascl1 staining intensity at different stages studied (P2, P14, adult control, and adult 5 d after LPC lesion), confocal pictures of brain sections, immunolabeled for Ascl1 and PDGFR , were analyzed with ImageJ software to measure the mean nuclear Ascl1 intensity in CC OPCs (PDGFR cells) versus SVZ (PDGFR cells). Mean and SEM values obtained counting several sections (n 3–5) are shown as the ratio of Ascl1 intensity in CC OPCs versus SVZ cells. To estimate levels of TF expression at different stages of OPC differentiation, mean values of their relative intensity in cells at each stage were obtained using ImageJ from images (n 3), such as those shown in Figure 2. Data are presented as a line chart in Figure 2*J*. Values range from 0 to 255, with values 50 considered as background levels. All values are shown as mean SEM. Statistical analysis was performed using Student's t test in Prism 4, GraphPad Software. p values in graphic are represented as follows: *p 0.05, **p 0.01, ***p 0.001. Black bars in histograms correspond to SEM.

Results

Immature oligodendroglial cells of neonatal cortex express Ascl1

Although *Ascl1* is required for OPC generation in the embryonic forebrain and spinal cord (Parras et al., 2007; Sugimori et al., 2007), its roles during neonatal oligodendrogenesis and myelination are currently unknown. Postnatal OPCs derive from the cortical wall of lateral ventricles both in neonates (Gorski et al., 2002; Ivanova et al., 2003; Kessaris et al., 2006) and adults (Menn et al., 2006). To address Ascl1 function in postnatal oligodendrogenesis and myelination, we first examined its cortical expression in newborn mice (P2) by immunofluorescence. Ascl1 was detected in subsets of cells located in the cortical ventricle wall and in the CC (15% and 25% of total cells, respectively). The phenotype of Ascl1-expressing cells was characterized using antibodies against TFs expressed by oligodendroglial progenitors and precursors, including Olig1, Olig2, Sox9, Sox10, and Nkx2.2 (Qi et al., 2001; Sun et al., 2001; Zhou et al., 2001; Zhou and Anderson, 2002; Stolt et al., 2003, 2004; Arnett et al., 2004; Kitada and Rowitch, 2006; Liu et al., 2007; Cai et al., 2010). In the dorsal ventricle wall, Ascl1 cells expressed Olig2 (85%; Fig. 1*A*,*G*) and Sox9 (80%; Fig. 1*C*,*G*), two TFs expressed by immature neural progenitor/stem cells (Hack et al., 2004; Scott et al., 2010). The majority of Ascl1 /Olig2 /Sox9 cells expressed neither PDGFR , the most specific marker for OPCs (Hall et al., 1996; Kessaris et al., 2006), nor other OPC markers, such as NG2 (data not shown), or TFs expressed in OPCs, such as Olig1, Sox10, and Nkx2.2 TFs (Fig. 1*B*,*D*,*E*,*G*). In the CC, however, Ascl1 cells included equal populations (50%) of Olig2 /Sox9 / PDGFR progenitor cells (Fig. 1*A–E*,*G*) and PDGFR cells (Fig. 1*G*,*H*). It is noteworthy that all Ascl1 /PDGFR cells (10% of CC cells and 2% of SVZ cells) also expressed Olig2 (Fig. 1*A*, *G*,*H*) and both nuclear and cytoplasmic Olig1 (Fig. 1*B*,*G*,*H*), as well as Sox10 (Fig. 1*D*,*G*,*H*), Nkx2.2 (Fig. 1*E*,*G*,*H*), and Sox9 (Fig. 1*C*,*C*$_1$,*H*). This phenotype suggests that all Ascl1 /PDGFR cells are OPCs and a fraction of Ascl1 / PDGFR cells may correspond to immature neural progenitors in the process of generating OPCs (Fig. 1*G*,*H*). Supporting this possibility, we found that 48% of Ascl1 /PDGFR cells do not express either Dlx or Gsx2, two neurogenic cofactors (Petryniak et al., 2007; Waclaw et al., 2009) that are not expressed in OPCs (Fig. 1*F–H*). Therefore, Ascl1 /Olig2 /PDGFR / Dlx /Gsx2 cells (corresponding to 5–7% of SVZ or CC

Ascl1 in OPC is downregulated upon oligodendrocyte differentiation

We then investigated Ascl1 expression during OPC transition into myelinating oligodendrocytes. In the CC, when many OPCs start to differentiate during the second postnatal week, Ascl1 is still expressed in all PDGFR OPCs (Fig. 2*A*), but APC/CC1-expressing maturing oligodendrocytes (Bhat et al., 1996) were rarely Ascl1 (Fig. 2*B*,*B*$_1$) suggesting that maturing OPCs downregulate Ascl1 expression. Indeed, using the *Ascl1*^{GFP} transgenic line, in which GFP remains expressed longer than Ascl1, we found that most APC cells at this stage were GFP (Fig. 2*B*).

To assess Ascl1 coexpression with other TFs involved in OPC differentiation, we performed immunofluorescence for different TF combinations and for markers of different stages of oligodendroglial lineage, including Gpr17, which is expressed during OPC differentiation (Chen et al., 2009; Boda et al., 2011). At P14, when many oligodendroglial cells are at different stages of differentiation in the CC, Ascl1 is coexpressed with Sox9, Sox10, Olig2, Olig1, and Nkx2.2 in PDGFR cells (OPCs; labeled #1 in Fig. 2*C*,*D*,*J*,*K*). According to the expression levels of these TFs and oligodendroglial markers, we could divide premyelinating oligodendrocytes in two stages (Fig. 2*C–K*): (1) premyelinating oligodendrocyte stage I (mOLI) characterized by downregulation of Ascl1, Olig1, and PDGFR and upregulation of Nkx2.2/Gpr17/APC/Sox9/Sox10 (labeled #2 in Fig. 2*C–K*); and (2) premyelinating oligodendrocyte stage II (pre-mOLII), implicating the downregulation of Nkx2.2/Gpr17 and upregulation of Olig1-cytoplasmic expression while presenting the highest levels of Sox9/Sox10/Olig2 (labeled #3 in Fig. 2*C–K*). *Ascl1*^{GFP} transgene was still expressed at these premyelinating stages characterized by coexpression of high levels of Nkx2.2/Olig2 or Sox10/Olig2, indicating that Ascl1-expressing OPCs do differentiate into maturing oligodendrocytes (Fig. 2*I*,*K*). Eventually, APC cells starting to express myelin proteins, such as MOG, present a larger cytoplasm and intermediate levels of Olig2/Sox9/Sox10 expression with persistent Olig1 cytoplasmic expression (labeled #4 in Fig. 2*H*,*J*,*K*). Therefore, combinatorial expression of Ascl1 and other oligodendrogenic factors defines more precisely the successive stages of oligodendrogenesis. The initial stage of OPC differenti-

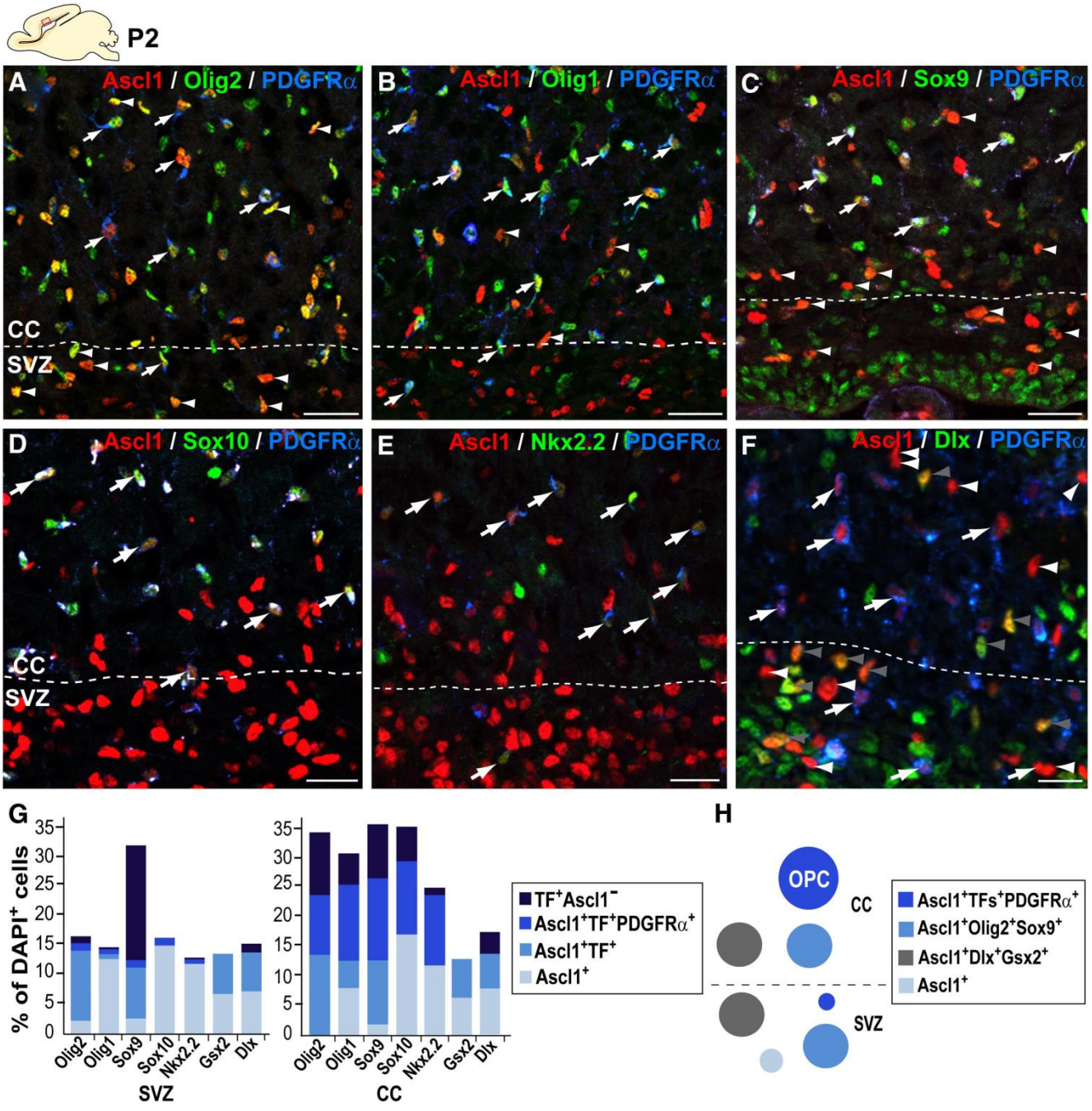

Figure 1. Neonatal subsets of Ascl1-expressing cells in SVZ and CC include neuronal or oligodendroglial progenitors and OPCs. ***A–E***, Sections through the dorsal SVZ and CC of P2 wild-type neonates showing by immunofluorescence the expression of Ascl1 protein together with Olig2, Sox9, Sox10, and Nkx2.2 in PDGFR cells (OPCs, arrows) or PDGFR cells (arrowheads). *A*, Ascl1 is coexpressed with Olig2 in immature progenitors (PDGFR cells) and OPCs both in SVZ and CC, whereas Ascl1 is coexpressed with Olig1 in PDGFR OPCs and few PDGFR cells of the CC (***B***). *C*, Ascl1 is coexpressed with Sox9 in all PDGFR OPCs and most Ascl1 /PDGFR cells, 30% of SVZ cells being Sox9 . Ascl1 is coexpressed with Sox10 (***D***) and Nkx2.2 (***E***) in all PDGFR OPCs but not in PDGFR cells. *F*, Pan-Dlx antibody (recognizing Dlx1/2/5/6 proteins) labels half of Ascl1 /PDGFR cells (gray arrowheads compared with white arrowheads) but not OPCs (arrows). *G*, Histograms representing the percentage of cells (DAPI) in the SVZ and CC that express Ascl1 together with other TFs, using PDGFR to label OPCs. Ascl1 represents Ascl1-only-expressing cells (light gray), Ascl1 TF are PDGFR /Ascl1 cells coexpressing the other TF (light blue), TF Ascl1 are TF-only-expressing cells (dark blue). *H*, Summary figure representing in circles the Ascl1 populations both in SVZ and CC. In the SVZ, 10% of Ascl1 ,PDGFR cells are Ascl1-only-expressing cells (light gray), whereas 90% are Olig2 /Sox9 , and these can be subdivided in two halves by their expression of Dlx/Gsx2 (gray) or not (light blue). These two last populations are also present in the forming CC, where half of Ascl1 cells are OPCs (expressing PDGFR , Olig2, Olig1, Sox9, Sox10, and Nkx2.2). Dlx and Gsx2 are not expressed in OPCs, and most likely Ascl1 /Olig2 /Sox9 /Gsx2 /Dlx cells are oligodendroglial progenitors. Dotted line represents the border between SVZ and CC. Scale bars, 20 m.

ation is marked by a transient upregulation of Nkx2.2/Gpr17 correlating with a downregulation of Ascl1/Olig1 (Fig. 2*J*,*K*), whereas further steps of transition toward a myelin-forming cell correlate with Nkx2.2/Gpr17 downregulation together with Olig1 cytoplasmic expression (Fig. 2*J*,*K*).

Ascl1 is required for OPC generation from SVZ progenitor cells

Given the expression of Ascl1 in SVZ-progenitors and in OPCs during the postnatal wave of oligodendrogenesis described above, we first investigated its role in cortical SVZ progenitors

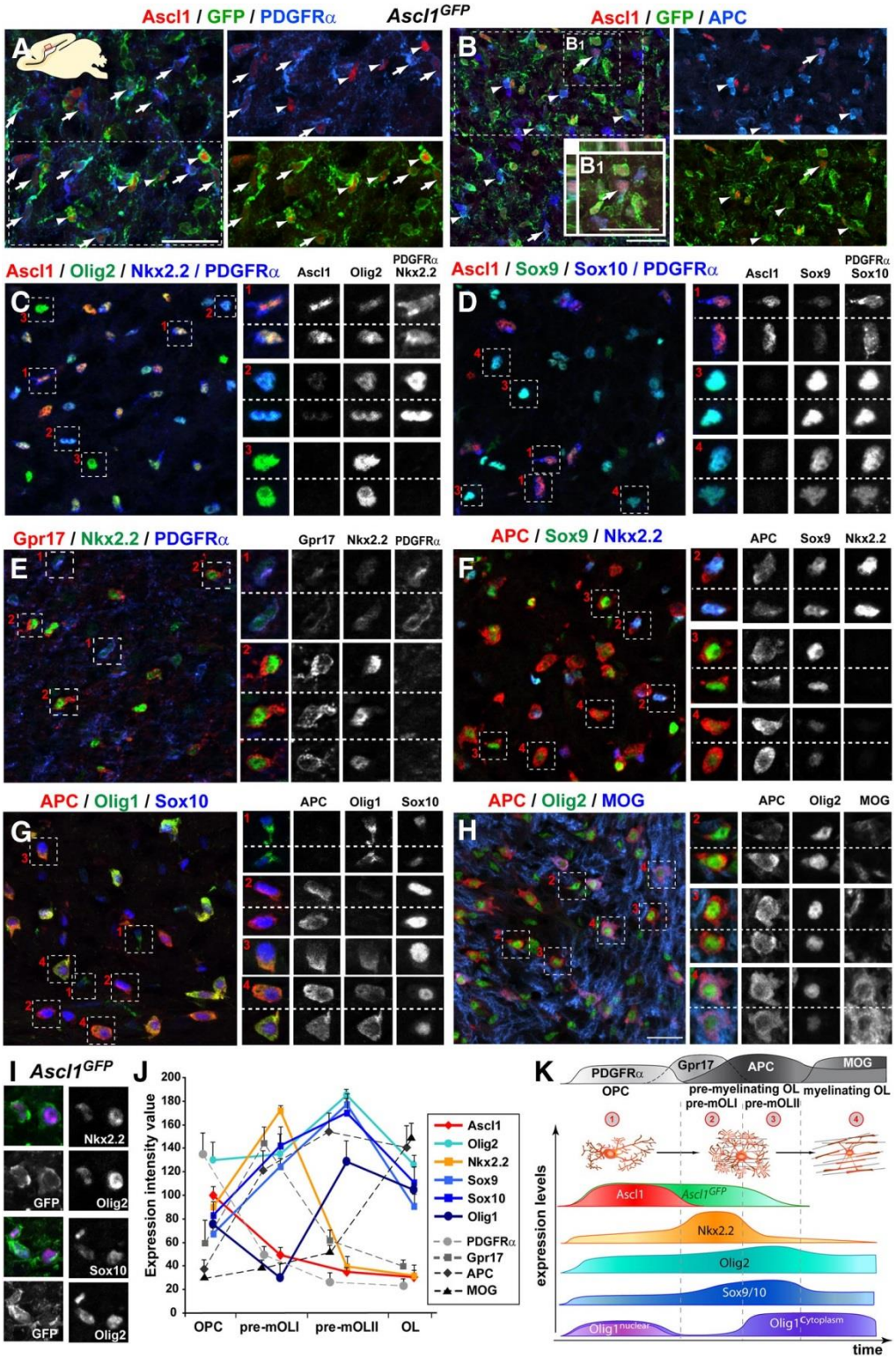

Figure 2. Expression pattern of Ascl1 and other TFs involved in oligodendrogenesis progression in the postnatal brain. *A–I*, Sections of P7 (*A*, *B*) or P14 (*C–I*) CC immunolabeled with antibodies against Ascl1, GFP, and main TFs involved in oligodendrogenesis. *A*, *B*, Sections of *Ascl1*^{GFP} P7 brain showing Ascl1 and GFP expression in all PDGFR OPCs (*A*, arrows) and some PDGFR cells (*A*, arrowheads), whereas APC oligodendrocytes express only GFP (*B*, arrowheads) and very rarely Ascl1 protein (*B* , arrow). *C–H*, Sections of P14 wild-type brains showing that: Ascl1 is coexpressed in PDGFR cells (OPCs, stage 1) together with Olig2 and Nkx2.2 (*C*) or Sox9 and Sox10 (*D*,*E*) but not in maturing oligodendrocytes that express high levels of Olig2, Nkx2.2, Sox9, and Sox10 (*C–E*). *E*, *F*, Nkx2.2 is expressed at high levels in cells being Gpr17 /PDGFR /APC and high levels of Olig2, Sox9 (*C*, *E*, *F*, named stage 2, pre-OLI). *G*, Olig1 is not expressed in some APC cells with high levels of Sox10 expression (stage 2, pre-OLI cells), but it is highly expressed in the cytoplasm of other APC cells with high or intermediate levels of Sox10/Sox9/Olig2 and low levels of Nkx2.2 (*C–F*; stage 3, pre-OLII). *H*, APC cells expressing high levels of Olig2 (stages 2 and 3) are MOG , corresponding to premyelinating oligodendrocytes, whereas APC cells expressing intermediate levels of Olig2 correspond to MOG myelinating oligodendrocytes (stage 4). *I*, *Ascl1*^{GFP} transgene is expressed in cells with high levels Nkx2.2, Olig2, and Sox10, suggesting that Ascl1-expressing cells give rise to maturing oligodendrocytes. *J*, Line chart representing the relative fluorescence intensity of each TF (color lines) and oligodendroglial markers (gray dotted lines) in stage of oligodendrogenesis. *K*, Summary scheme (based on values in *J*) for Ascl1 and other TFs expression profile during different stages of (*Figure legend continues.*)

and neonatal oligodendrogenesis. For this purpose, we deleted *Ascl1* in dorsal SVZ cells in a temporally controlled manner by targeting a Cre-expressing plasmid to the dorsal SVZ at P2 of *Ascl1*$^{fl/}$; *Rosa26*$^{stop\text{-}YFP}$ (mutant, *Cko*^{dSVZ}) or *Ascl1*$^{fl/}$; *Rosa26*$^{stop\text{-}YFP}$ (control, *Ctr*^{dSVZ}) mice, using a modified postnatal electroporation technique (Boutin et al., 2008). In control experiments using a GFP-expressing plasmid, many GFP SVZ cells showed radial glial-like processes, thus demonstrating that dorsal neural progenitor/stem cells were successfully targeted by our electroporation technique (Fig. 3*B*). In brains electroporated with Cre-expressing plasmids, Ascl1 protein was detected only in *Ctr*^{dSVZ} but not in *Cko*^{dSVZ} cells (Fig. 3*C*,*C*$_1$,*C* ,*C* $_1$), indicating that *Ascl1* could be efficiently deleted by Cre recombination. To assess the fate of electroporated cells, we analyzed the brains at 30 d postelectroporation (dpe). The majority of *Ctr*^{dSVZ}-YFP cells were oligodendrocytes (62.5 5.6%, *n* 5, APC^{high}), some were astrocytes (32.1 5.9%, *n* 5, GFAP /APC^{low}), and few were OPCs (9.3 0.8%, *n* 3, PDGFR) (Fig. 3*D*,*D* $_b$,*E*). In contrast, *Cko*^{dSVZ}-YFP cells were mostly astrocytes (82.9 4.1%, 2.7-fold), only 15.3 1.8% were oligodendrocytes (3.9-fold reduction), and 1.6 0.5% were OPCs (5.5-fold reduction) (Fig. 3*D* ,*D* $_1$,*E*), indicating that loss of *Ascl1* inhibits oligodendrogenesis for the benefit of astrogenesis. We did not observe a selective cell death of Ascl1-deficient cells at 3 dpe (as shown by the absence of activated caspase3 expression; data not shown). There was also a 1.7-fold increase in the number of *Ascl1*-deficient GFAP cells in the SVZ compared with controls (88.9 11.1% vs 48.3 4.7%; *p* 0.0082, *t* test, *n* 4; Fig. 3*D*,*D*$_1$). Ascl1 is therefore required for the proper generation of oligodendrocytes from the cortical SVZ; and, in the absence of Ascl1, the SVZ progenitor‘s fate is predominantly astroglial.

Ascl1 promotes the balance between OPC differentiation and proliferation

We next examined Ascl1 function specifically in neonatal OPCs by performing a temporal and conditional *Ascl1* deletion in OPCs of *Cko*^{OPC} and *Ctr*^{OPC} genotypes using *PDGFR ::CreER*^{T2} mice (Rivers et al., 2008; see Materials and Methods). We induced *Ascl1* deletion at early postnatal stages when OPC numbers peak in the brain (tamoxifen injection at P5 or P8-P9) and assessed their proliferative and differentiation capacity. Ki67 expression in OPCs was used as marker of proliferative OPCs. Seven days post-tamoxifen injection (dpi) *Cko*^{OPC} YFP OPCs showed a 1.7-fold increase in the proportion of Ki67 cells (36.4 5.2%, Fig. 4*A* ,*D*) compared with *Ctr*^{OPC} (21.3 0.7%, Fig. 4*A*,*D*), indicating an increase of OPC proliferation in the absence of Ascl1. Similar results were obtained when tamoxifen was injected at P5 or P8-P9 (Fig. 4*D*). Therefore, OPC proliferation increases in the absence of Ascl1.

Neonatal OPCs have been shown to divide either symmetrically, generating pairs of OPCs (OPC/OPC pairs) or mature oligodendrocytes (APC cells, named OL/OL pairs), or asymmetrically to generate one OPC and one oligodendrocyte (OPC/OL pairs) (Sugiarto et al., 2011; Zhu et al., 2011). To assess whether the difference in proliferation rate observed in the absence of Ascl1 could result from a change in OPC mode of division, we quantified the different types of YFP cell pairs in the CC at 7 dpi. *Ctr*^{OPC} (tamoxifen at P5) showed 23.1 4.0% of OPC/OPC pairs, 29.0 3.5% of OPC/OL pairs, and 47.8 3.7% of OL/OL pairs (Fig. 4*A*,*A*$_1$,*A*$_2$,*F*). In *Cko*^{OPC}, we observed a twofold increase in OPC/OPC pairs (48.4 2.7%; Fig. 4*A* ,*A* $_1$,*F*), a twofold decrease in OPC/OL pairs (14.6 3.1%), and no change in numbers of OL/OL pairs (37.0 5.9%; Fig. 4*A* ,*A* $_2$,*F*), suggesting that, in the absence of Ascl1, OPCs that would divide asymmetrically (OPC/OL pairs) divide instead symmetrically to generate two OPCs (Fig. 4*F*). Similar results were obtained when tamoxifen was injected at P5 or P8-P9 (Fig. 4*F*). Ascl1 thus regulates and promotes asymmetric divisions of OPCs. Consequently, the ratio of OPC/oligodendrocytes within the YFP population was increased in *Cko*^{OPC} cells (1.4-fold) compared with *Ctr*^{OPC} cells (*Cko*^{OPC}: 57.1 1.5% APC cells vs 42.8 1.5% PDGFR cells; *n* 5; *Ctr*^{OPC}: 47.6 1.8% APC cells vs 52.4 1.5% PDGFR cells; *n* 3, Fig. 4*E*), indicating that loss of Ascl1 in OPCs favors proliferation over differentiation. The differentiation defect of *Ascl1*-mutant cells appeared more pronounced regarding their expression of myelin proteins, such as CNP (Fig. 4*C–C* $_2$,*E*). To assess whether these differences were maintained at later stages, we studied the proportion of OPCs and oligodendrocytes present at 28 dpi. A similar ratio of 4:1 oligodendrocytes per OPC was found in *Cko*^{OPC} and *Ctr*^{OPC} cells (*Cko*^{OPC}: 79.6 0.9% APC cells vs 20.4 0.8% PDGFR cells, *n* 5; *Ctr*^{OPC}: 79.8 1.8% APC cells vs 20.1 1.8% PDGFR cells, *n* 4; Fig. 4*B*,*B* ,*G*), suggesting that other factors regulating OPC proliferation and differentiation compensate for the loss of *Ascl1* function over time.

Demyelination upregulates Ascl1 levels in adult OPCs

Because *Ascl1* expression is lost with oligodendrocyte differentiation, we then extended our study to adulthood to determine whether Ascl1 was still expressed in OPCs under normal and demyelinating conditions. Using an optimized protocol for Ascl1 immunofluorescence (see Materials and Methods), we detected intermediate to low levels of Ascl1 in young (P70) and aged (P200) brain, in virtually all OPCs (99%) in the CC, whereas high levels were observed in the neurogenic regions (i.e., SVZ/rostral migratory stream [RMS]; Fig. 5*A*,*B*,*G*). Ascl1 expression was also detected at low levels in a large majority of OPCs (90%) in other brain regions, including in the gray matter (in the hippocampus, thalamus, olfactory bulb; Fig. 5*C*; and data not shown) and the white matter (in the fimbria, striatum, cerebellum, brainstem; data not shown). In the cortex, Ascl1 expression was detectable in a large fraction (67%) of OPCs (Fig. 5*D*). These results are in accordance with the expression of the GFP reporter in *Ascl1*^{GFP} mice in the adult brain (Fig. 5*B*) (Parras et al., 2007).

In the adult CNS, demyelination results in the upregulation of several TF involved in oligodendrogenesis, including upregulation of *Olig2, Nkx2.2*, and *Sox10* transcripts (Fancy et al., 2004, 2009; Watanabe et al., 2004). To determine whether *Ascl1* expression is also altered in response to demyelination, we used adult *Ascl1*^{GFP} animals to perform LPC-induced focal demyelinating lesions in the CC, as previously reported (Nait-Oumesmar et al., 1999). At 5 d postlesion (dpl), cells expressing high to intermediate levels of Ascl1 and *Ascl1*^{GFP} (Ascl1^{high}/*Ascl1*^{GFP} cells) were detected both in the SVZ and within and around the lesion, which was characterized by a very dense cellularity (Fig. 5*E–E*$_2$). Ascl1^{high}/*Ascl1*^{GFP} cells were either OPCs (PDGFR) or more immature precursors (PDGFR cells), the latter having (as shown by GFP expression) characteristics of migrating cells (Fig.

4

(*Figure legend continued.*) oligodendrogenesis. Stage 1 OPCs are PDGFR cells. Premyelinating (APC cells) oligodendrocytes are divided in two stages: stage 2 (pre-OLI) are cells with high levels of Nkx2.2, Olig2, Sox9/10, and Gpr17 and negative for Olig1; stage 3 (pre-OLII) are cells with high levels of Olig2, Sox9/10, and cytoplasmic Olig1 and negative for Nkx2.2/Gpr17. Stage 4 (myelinating oligodendrocytes) are APC /MOG cells. OL, Oligodendrocyte. Dotted squares represent areas shown at higher magnification. Scale bars, 20 m.

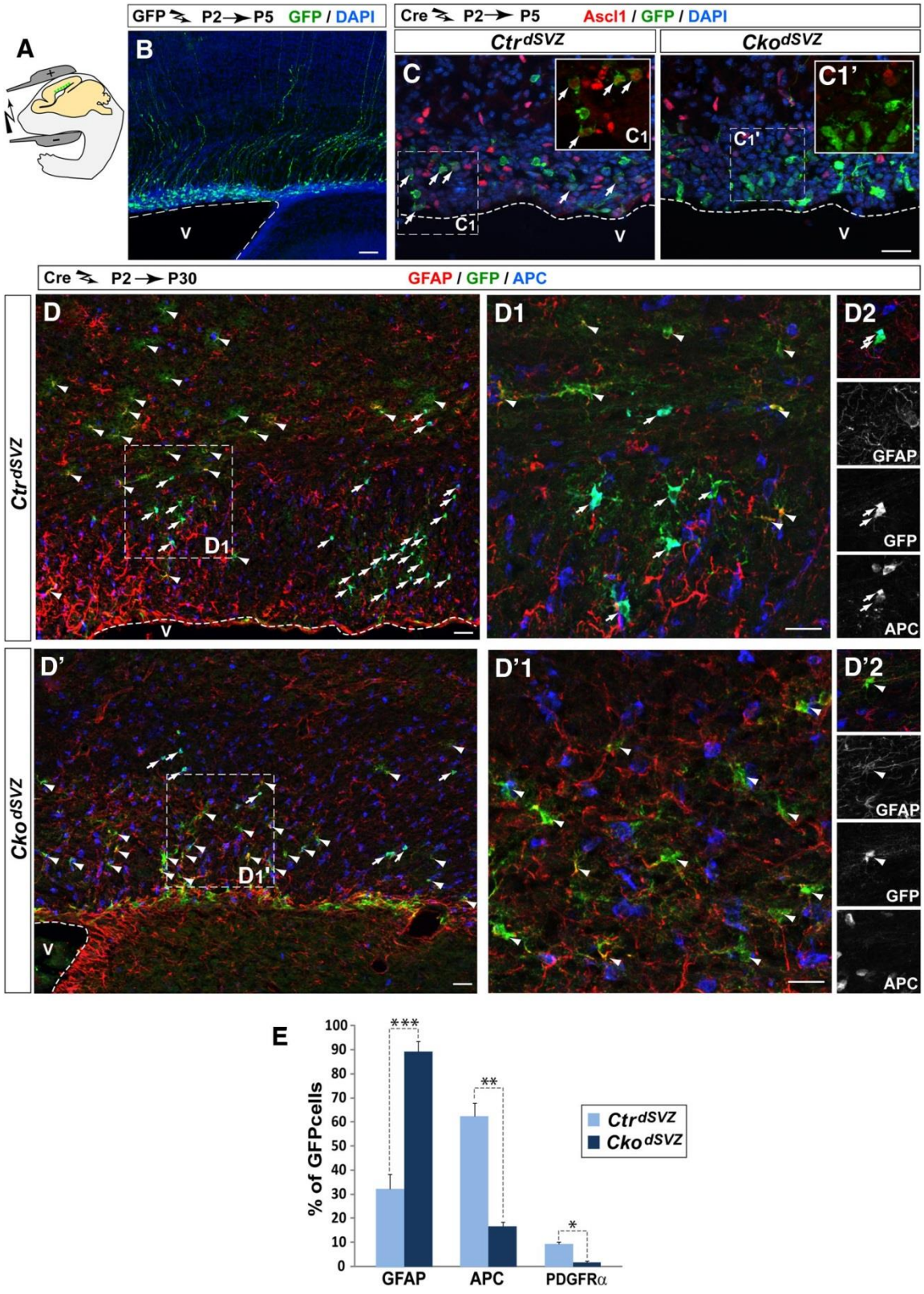

Figure 3. Ascl1 conditional ablation in dorsal SVZ cells reduces postnatal oligodendrogenesis. *A*, Schematic representation of the dorsal SVZ electroporation in P2 neonates. Green dots represent dorsal SVZ electroporated cells. ***B***, Sagittal section of GFP-electroporated wild-type brain at 3 dpl, showing GFP incorporation in dorsal precursors, including some containing radial glial processes. ***C–E***, Sagittal sections at the level ventricle of Cre-electroporated dorsal telencephalon from Ctr^{dSVZ} (control, ***C***, ***D***) and Cko^{dSVZ} (mutant, ***C*** , ***D***) genotypes. ***C–C*** $_1$, Brain sections at 3 dpl immunostained for Ascl1 and YFP showing that Ascl1 is present in some YFP -Ctr^{dSVZ} cells (arrows) but not in YFP -Cko^{dSVZ} cells; Ascl1 is still present in YFP -nonelectroporated cells. ***D***, ***D*** , Brain sections at 28 dpl immunostained for GFAP (red), YFP (green), and APC (blue). APC oligodendrocytes (arrows) are strongly reduced in YFP -Cko^{dSVZ} cells, most being GFAP cells (arrowheads). ***D*** $_1$, ***D*** $_1$, Higher magnifications of insets in ***D***, ***D*** . ***D*** $_2$, ***D*** $_2$, Examples of YFP cells coexpressing APC or GFAP cells in either genotype. ***E***, Histograms representing the percentage of YFP cells in the dorsal telencephalon coexpressing APC (oligodendrocytes), PDGFR (OPCs), or GFAP (astrocytes) at 28 dpl in Ctr^{dSVZ} and Cko^{dSVZ} genotypes. ***p 0.0001 (t test); n 5. **p 0.042 (t test); n 5. *p 0.035 (t test); n 3. Scale bars, 20 m.

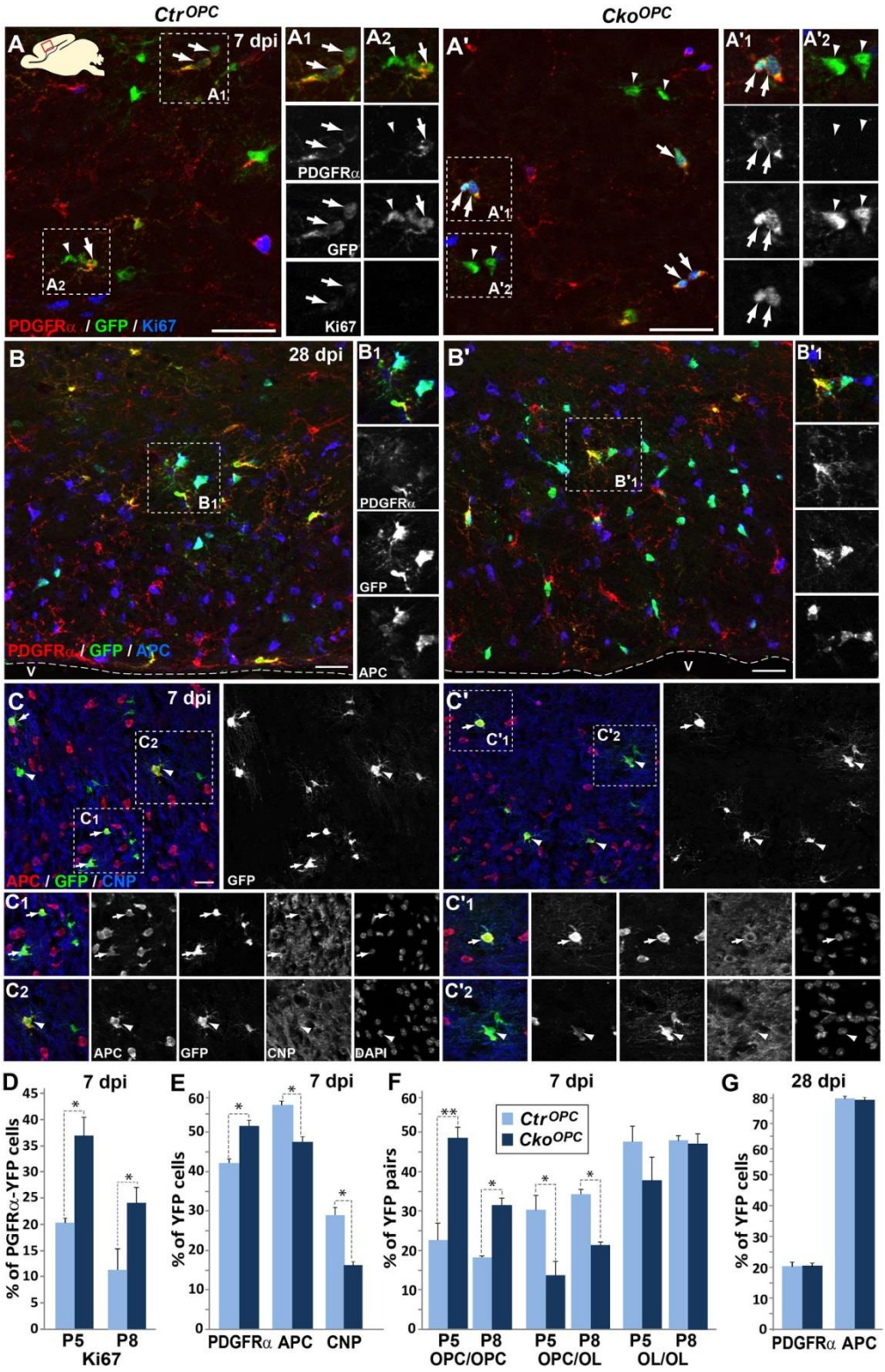

Figure 4. Ascl1 controls postnatal OPC division, proliferation, and differentiation. *A–C*, Sagittal sections through the CC of Ctr^{OPC} (control, *A–C*) or Cko^{OPC} (mutant, *A*, *B*, *C*) brains at P12 (*A*, *A*, *C*, *C*) or P33 (*B*, *B*) immunolabeled with antibodies against YFP and markers of oligodendroglial cells. *A*, *A*, Tamoxifen-injected brains analyzed at 7 dpi (P12) immunolabeled for cell cycle marker Ki67 illustrating the increase of proliferating YFP OPCs (Ki67 /YFP /PDGFR cells) in *Ascl1* mutant cells (*A*, *A*) compared with controls (*A*, *A*). YFP cells are often found as pairs of either two PDGFR cells (*A*, *A*), or either one (*A*) or two YFP /PDGFR cells (differentiating oligodendrocytes, *A*) and in Cko^{OPC} pairs of two PDGFR cells are increased and pairs with one PDGFR are decreased compared with Ctr^{OPC}. *B*, *B*, Tamoxifen-injected brains analyzed at 28 dpi (P33) illustrating that similar proportion YFP cells being either PDGFR or APC cells in Ctr^{OPC} (*B*) and Cko^{OPC} (*B*). *C*, *C*, Brain sections analyzed at 7 dpi immunolabeled for CNP myelin protein, APC, and YFP showing that less YFP -Cko^{OPC} cells (*C*) are APC /CNP (arrows) compared with Ctr^{OPC} cells (*C*) as illustrated at higher magnification in *C*–*C*. *D–G*, Histograms representing the quantification of the data illustrated in previous panels showing the following: (*D*) an increase in proliferation (Ki67) of mutant PDGFR OPCs at 7 pdi injected either at P5 (*p 0.016, *t* test, n 3) or P8 (*p 0.039, *t* test, n 3); (*E*) an increase in OPCs (0.038, *t* test, n 3) and a corresponding decrease of APC (*p 0.041, *t* test, n 3) or CNP /APC oligodendrocytes (*p 0.030, *t* test, n 3) in Cko^{OPC} cells compared with (*Figure legend continues.*)

5E_1). Ascl1 expression in OPCs (relative to its expression in SVZ cells) was upregulated to levels similar postnatal OPCs (Fig. 5*G*). Moreover, *Ascl1*^{GFP} cells in the lesion (Fig. 5*F*) and in the SVZ (data not shown) coexpressed high levels of Olig2 and Nkx2.2, suggesting that all three TFs are upregulated in progenitors and nearby OPCs involved in remyelination.

Ascl1 expression was not induced in oligodendrocytes upon/after demyelination given that Ascl1 protein was not detected in Olig2 /APC cells (Fig. 5*H*, arrowheads). However, the GFP transgene was expressed in maturing oligodendrocytes of *Ascl1*^{GFP} animals (cells expressing high levels of Olig2 and Sox10, Fig. 5*I*,I_1), as we previously observed at postnatal stages (Fig. 2). These data indicate that, in both the postnatal brain and in response to demyelination, a similar combination of TFs, including Ascl1 is induced in OPCs/progenitors and likely involved in (re)myelination.

Ascl1-expressing cells repopulate demyelinated lesions

Ascl1 progenitor/OPCs are localized in and around focal LPC lesions, suggesting that they may differentiate locally into myelinating oligodendrocytes and participate to myelin repair. In *Ascl1*^{GFP} mice, GFP expression persists long after that Ascl1 is downregulated, which allows cell fate mapping of Ascl1 progeny. We have examined the contribution of Ascl1-expressing cells to oligodendrocyte regeneration and lesion repair in *Ascl1*^{GFP} mice. The demyelinated lesion can be recognized by a dense cellularity, the absence of myelin proteins (such as MBP; Fig. 6*A*), and oligodendrocyte depletion (APC cells, Fig. 6*C*,*E*). At 2 dpl, there were many GFP cells in the lesion, most of them being OPCs (79%; PDGFR /Olig2 cells, Fig. 6*D*) and the remaining cells being immature progenitors. At 5 dpl, the number of GFP cells in the lesion was increased sevenfold, 60% being OPCs (Fig. 6*B*,*D*). At both time points, all OPCs were GFP , indicating that OPCs present within the lesion derive from Ascl1-expressing cells. In addition, at 5 dpl, 25% of GFP cells in the lesion were APC oligodendrocytes (Fig. 6*C*,*E*), suggesting that these cells had differentiated locally from Ascl1 OPCs/progenitors.

OPCs contributing to myelin lesion repair in the CC may derive from progenitors located in the SVZ (Nait-Oumesmar et al., 1999, 2008; Aguirre et al., 2007; Franklin and ffrench-Constant, 2008; Staugaitis and Trapp, 2009). LPC-induced *Ascl1*^{GFP} mice showed OPCs associated with GFP /PDGFR progenitors in the RMS, displaying a bipolar shape morphology and with the main cell body axis oriented toward the CC where the lesion is located (Fig. 6*F*,F_1). This observation suggests that Ascl1 progenitors and OPCs generated in the SVZ/RMS neurogenic zone can migrate away from the RMS toward CC lesions, likely recruited with signals delivered from the injured tissue.

Ascl1 progenitors differentiate into remyelinating oligodendrocytes

To assess the contribution of Ascl1 progenitors to the remyelination process, we used the Cre/loxP recombination system to trace the Ascl1-cell lineage in LPC-demyelinated mice. LPC-induced lesions were performed in the CC of adult *Ascl1*$^{Cre/YFP}$ mice, and the presence of intralesional APC /YFP oligodendrocytes was investigated at 5, 14, and 28 dpl. At all stages examined, the majority (67%) of intralesional PDGFR OPCs and APC oligodendrocytes expressed YFP and belong to the *Ascl1* cell lineage (Fig. 7*A*,*D*), with a similar proportion of YFP oli- godendrocytes present in nonlesion territories (Fig. 7*D*). At 14 dpl, intralesional APC /YFP cells expressed myelin proteins, such as MOG (Fig. 7*B*, *C*,C_1,C_2), suggesting that these cells were maturing into myelinating oligodendrocytes. We also used EM to identify intralesional -galactosidase /X-gal myelinating oli- godendrocytes using *Ascl1*$^{Cre/LacZ}$ mice. X-gal-reaction deposits were detected within the lesion area, in cells with ultrastructural characteristics of newly formed oligodendrocytes enwrapping multiple axons (Fig. 7*E*, E_1,E_2). These observations confirmed that Ascl1 progenitors/OPCs generate myelin-forming cells that participate in myelin repair.

Ascl1 is required for normal timing of OPC differentiation during remyelination

To determine Ascl1 requirement for proper remyelination, we deleted *Ascl1* expression specifically in OPCs before inducing CC myelin lesion. We assessed whether YFP -*Cko*^{OPC} cells were able to migrate into lesions, proliferate, and differentiate in the absence of Ascl1. At 8 and 15 dpl, remyelinating lesions in both *Cko*^{OPC} and *Ctr*^{OPC} displayed YFP cells being PDGFR OPCs and APC oligodendrocytes (Fig. 8*A*,*A* ,*B*,*B*). This result indicates that *Ascl1* is dispensable for OPC recruitment and subsequent oligodendrocyte maturation in demyelinated lesions. At 8 dpi, the proportion of YFP OPCs and YFP oligodendrocytes was similar in *Cko*^{OPC} and *Ctr*^{OPC}. Nevertheless, a relatively large number of YFP -*Cko*^{OPC} cells were negative for either oligodendroglial (PDGFR or APC) or astroglial (GFAP) markers at this stage (Fig. 8*B*,*B*). Some of them had typical oligodendrocyte morphology despite not expressing APC (Fig. 8*B*), most likely corresponding to cells with abnormal differentiation. In contrast at 15 dpl, YFP -*Cko*^{OPC} cells had a smaller ratio of oligodendrocyte to OPCs than *Ctr*^{OPC} cells (Fig. 8*C*,*C* ,*E*), whereas the glial marker-negative population was very much reduced (Fig. 8). Moreover, we found fewer YFP cells expressing CNP myelin protein in *Cko*^{OPC} than in *Ctr*^{OPC} (Fig. 8*D*,*D* ,*E*). Therefore, these data strongly suggest that Ascl1 is also required for normal OPC differentiation during remyelination and, as during myelination, other TFs most likely compensate its loss of function at later time points of the differentiation process.

Ascl1 is expressed in active MS lesions

In the mouse brain, Ascl1 expression is a hallmark of OPCs and precursor cells involved in remyelination. We hypothesized that, in humans, immature oligodendroglial cells in MS lesions may also express *Ascl1*. To test this hypothesis, we examined Ascl1 expression in four MS and two non-neurological control postmortem brain samples. Lesions were first characterized using Luxol fast blue/cresyl violet (Fig. 9*B*), MOG, and CD68 immunolabeling (Fig. 9*C*). The expression of Ascl1 and of oligodendroglial markers (Olig1 and Sox10) was examined in actively remyelinating borders (patchy MOG staining/CD68), in the chronic core of the lesions (MOG /CD68 ; Fig. 9*C*), and in normal-appearing white matter (Fig. 9*B*,*C*). Ascl1 cells were more numerous in active borders of MS lesions compared with chronic silent core or normal-appearing white matter. Moreover, the number of Ascl1 cells was reduced in the core of chronic lesions compared with the other regions studied. Interestingly, Ascl1 cells were more concentrated within the CD68

(*Figure legend continued.*) *Ctr*^{OPC} at 7 dpi; (*F*) an increase in PDGFR pairs (OPC/OPC) and a decrease of PDGFR -APC pairs (OPC/OL), with no change in APC pairs (OL/OL) in *Cko*^{OPC} cells at 7 dpi injected with tamoxifen at P5 (**p* 0.0073 and **p* 0.032, respectively, *t* test, *n* 3) or at P8 (**p* 0.041 and **p* 0.019, respectively, *t* test, *n* 3); and (*G*) no difference in the YFP cells being either PDGFR or APC cells between *Ctr*^{OPC} and *Cko*^{OPC} cells at later stages (28 dpi). OL, Oligodendrocyte; V, ventricle. Scale bars, 20 m.

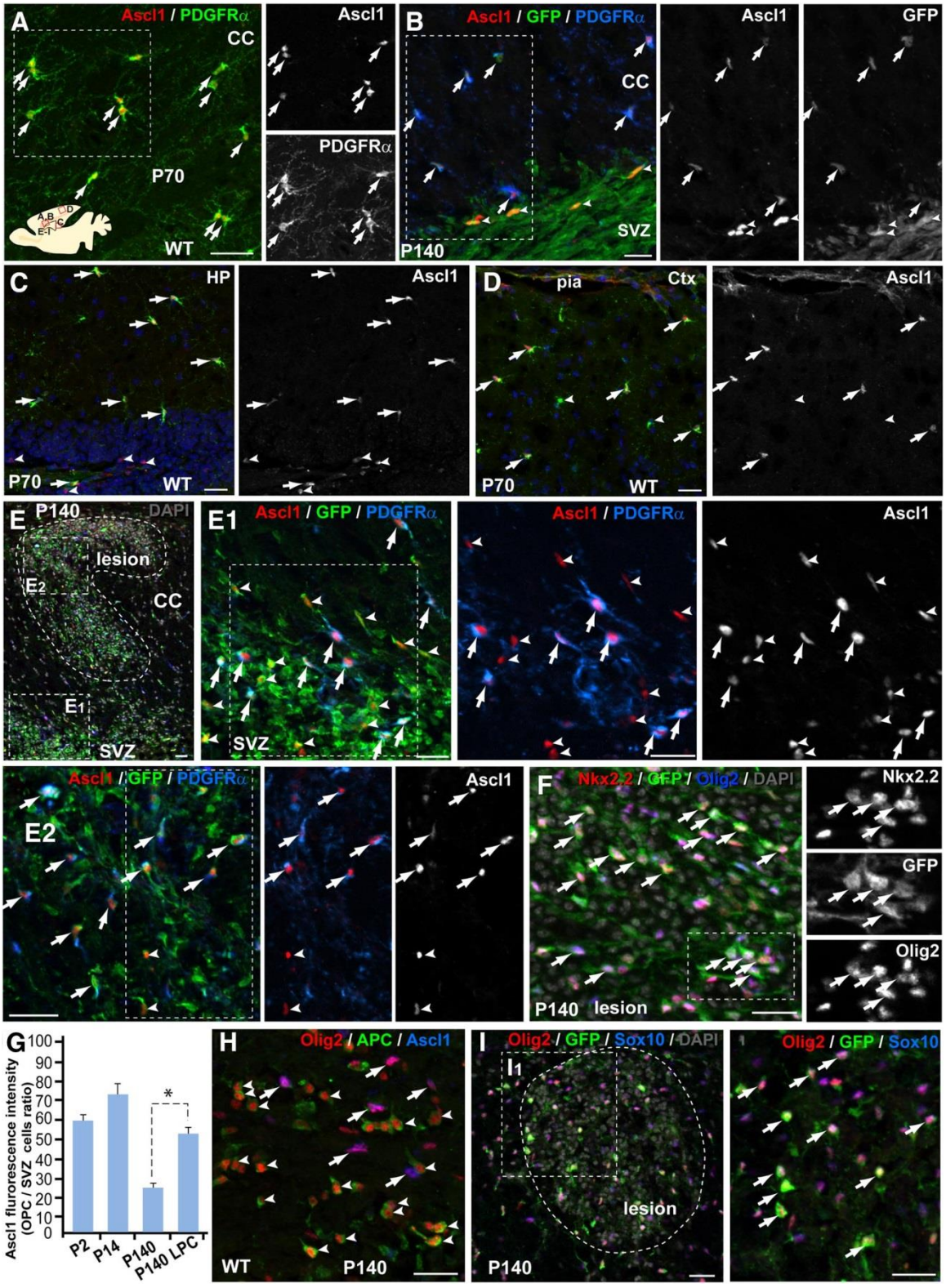

Figure 5. Ascl1-low expression in adult OPCs is upregulated upon demyelination. ***A–D***, Sections of adult wild-type (*A*, *C*, *D*, *H*) or *Ascl1*^{GFP} mice (*B*, *E*, *F*, *I*) in physiological conditions (***A–D***) or 5 d after focal demyelination of the CC (***E–I***). *A*, *C*, *D*, P70 brain showing Ascl1 expression in all OPCs (PDGFR cells, arrows) in CC (*A*), HP (*C*), and many OPCs in the Ctx (*D*, Ascl1-negative OPCs indicated by arrowheads). *B*, Ascl1 and *Ascl1*^{GFP} transgene expression in SVZ cells (arrowheads) and OPCs (arrows) in the CC. The low levels of Ascl1 in OPCs are compared with SVZ cells. *E*, LPC lesion in the CC showing high levels of Ascl1 expression in PDGFR OPCs (arrows) comparable with SVZ cells (arrowheads) both near the SVZ (*E* ,and the lesion (*E* ,high cellularity, DAPI). *F*, LPC lesion showing that cells coexpressing high levels of Olig2 and Nkx2.2 are *Ascl1*^{GFP} . *G*, Histograms representing the relative expression levels of Ascl1 immunofluorescence in OPCs compared with SVZ cells at P2, P14, P140, and LPC lesion P140. There is an increase after LPC at levels present in postnatal OPCs. *H*, *I*, After LPC demyelination, Ascl1 protein is still restricted to OPCs and never found in Olig2 /APC oligodendrocytes (arrowheads), whereas *Ascl1*^{GFP} transgene is expressed in cells with high levels of Olig2 and Sox10 (differentiation oligodendrocytes, *I*, *I*). Dotted squares represent areas shown at higher magnification. HP, Hippocampus; Ctx, cortex. **p* 0.025 (*t* test); *n* 3. Scale bars, 20 m.

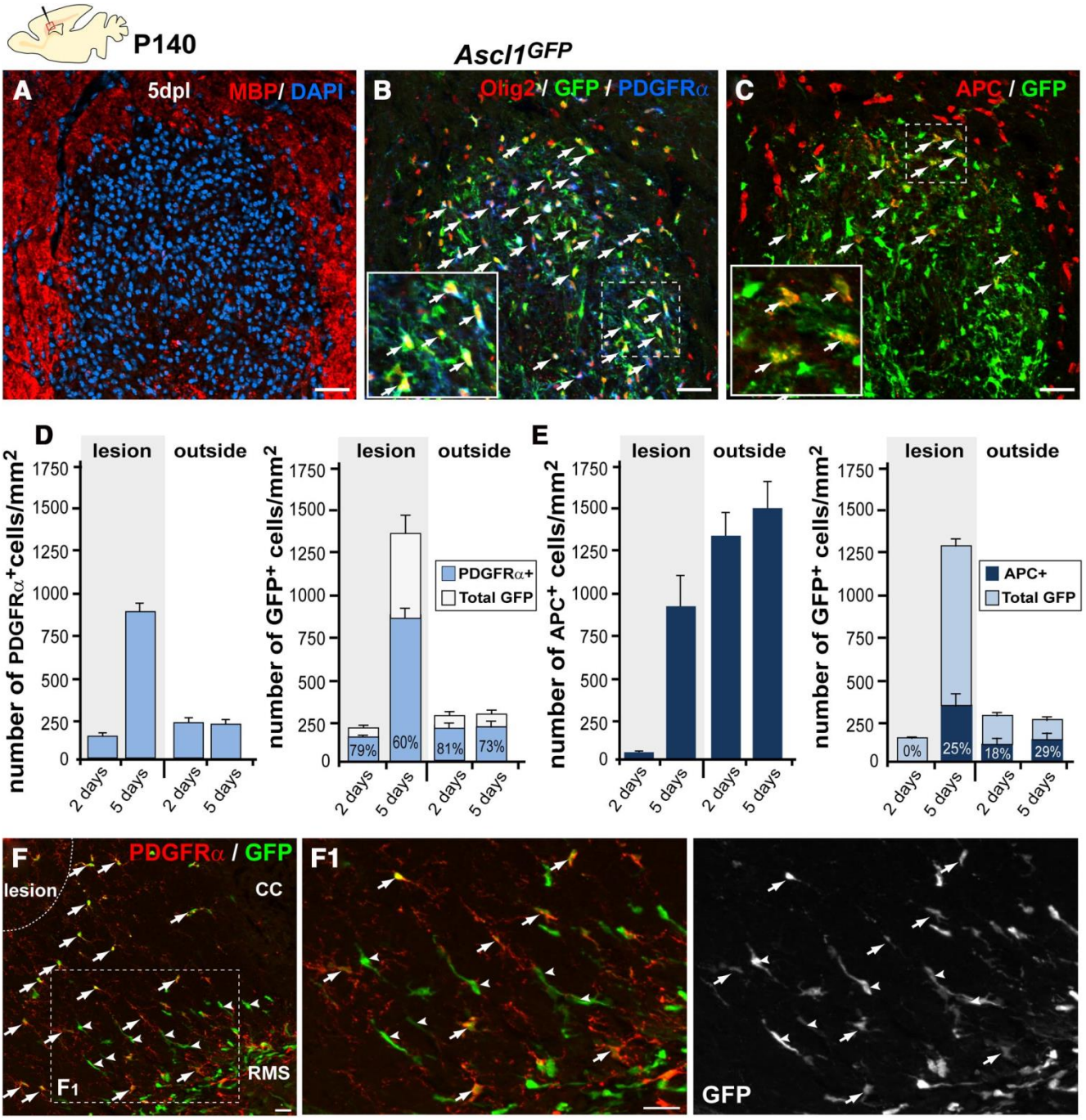

Figure 6. Ascl1-derived cells populated demyelinated lesions being mostly OPCs and maturing oligodendrocytes. Sections though the CC of adult (P140) *Ascl1*^{GFP} brain 5 d after LPC lesion labeled by immunofluorescence. ***A***, Demyelinated lesion shown by loss of MBP staining and dense cellularity (DAPI). ***B***, Many GFP cells are present in the lesion at 5 dpl coexpressing Olig2 and PDGFR . ***C***, Some GFP cells in the lesion express APCs, suggesting that they are differentiating oligodendrocytes. ***D***, ***E***, Histograms showing quantification of PDGFR (***D***) and APC cells (***E***) inside the lesion (lesion, gray background) and in regions of CC far from the lesion (outside) at 2 and 5 d after the LPC lesion. White bars represent the total GFP cells, a fraction of them expressing a given marker (blue). Almost all PDGFR cells in the lesion are GFP , and 60% of the GFP cells in the lesion are PDGFR and 25% express APCs. ***F***, *Ascl1*^{GFP} brain showing both OPCs (PDGFR / GFP cells, arrows) and GFP -only cells (arrowheads) with main axis perpendicularly oriented to the RMS, suggesting their migration toward the demyelinated lesion in the CC. Scale bars, 20 m.

borders of periventricular MS lesions (Fig. 9*D*) compared with other regions studied. Indeed, in other brain regions, including cortex and the normal-appearing white matter, Ascl1 expression level was very weak, most likely resulting from poor Ascl1 detection due to the fixation constraints of human brain samples. Nevertheless, the majority of Ascl1-expressing cells in active MS periventricular lesions were Olig1 and Sox10 (Fig. 9*E*,*F*), indicating that upregulation of Ascl1 in the endogenous OPCs may play a role in oligodendrocyte regeneration under pathological conditions. Overall, our findings on MS tissue are in agreement with our data on animal models of demyelination and demonstrate that Ascl1 is expressed at higher levels in oligodendroglial cells in MS plaques. Ascl1 may therefore be involved in oligodendrocyte differentiation and myelin repair in demyelinating pathology.

Discussion

In this paper, we show that Ascl1 is expressed during brain myelination and remyelination in SVZ progenitors and OPCs, play-

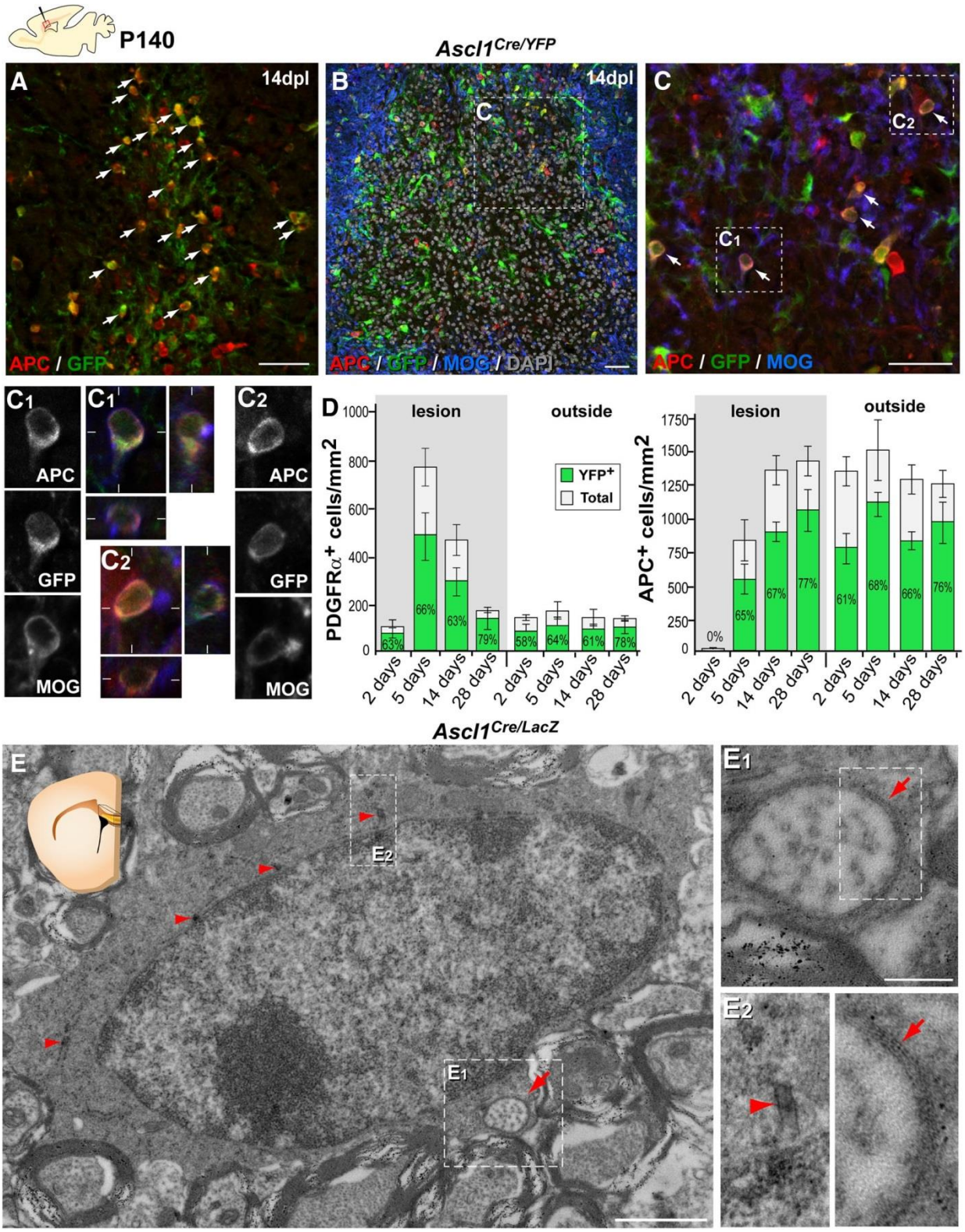

Figure 7. *Ascl1* progenitor-derived cells generate remyelinating oligodendrocytes. ***A–C***, Immunolabeling for YFP (green), APC (red), and MOG (blue) on coronal sections through the CC of an adult (P140) $Ascl1^{Cre/YFP}$ mouse at day 14 after LPC lesion. ***A***, There is a high number of APC /YFP cells (arrows) (i.e., *Ascl1* progenitor-derived cells) within the lesion. ***B***, Lower magnification of the demyelinated lesion characterized by the absence of MOG expression, high cellularity (DAPI, gray), and high number of YFP cells. ***C***, High magnification of inset in ***B*** showing APC and MOG coexpression in a few YFP cells (arrows). C_1, C_2, Individual channels and orthogonal projections of Z-stack pictures showing coexpression of MOG and APC in YFP cells. ***D***, Histograms representing the number of PDGFR or APC cells found in the lesion (lesion, gray background) or in regions of CC far from the lesion (outside) at different times after the lesion (2–28 d). Green bars represent the relative number of YFP cells among each of these populations. Oligodendrocytes (APC) mainly belong to the *Ascl1* cell lineage. ***E***, Electron micrograph images performed in a demyelinated zone of the CC, as shown in the schematic inset, from an $Ascl1^{Cre/LacZ}$ mouse, at day 60 after lesion. X-gal reaction deposits (arrowheads) in the cytoplasm of a young oligodendrocyte (big cytoplasm) assessing that this cell belongs to the *Ascl1* cell lineage (***E***, E_2). E_1, High magnification of the inset in ***E***, showing a thin myelinated axon (remyelinated, arrow). Scale bars: ***A–C***, 20 m; ***E***, 1 m; E_1, 200 nm.

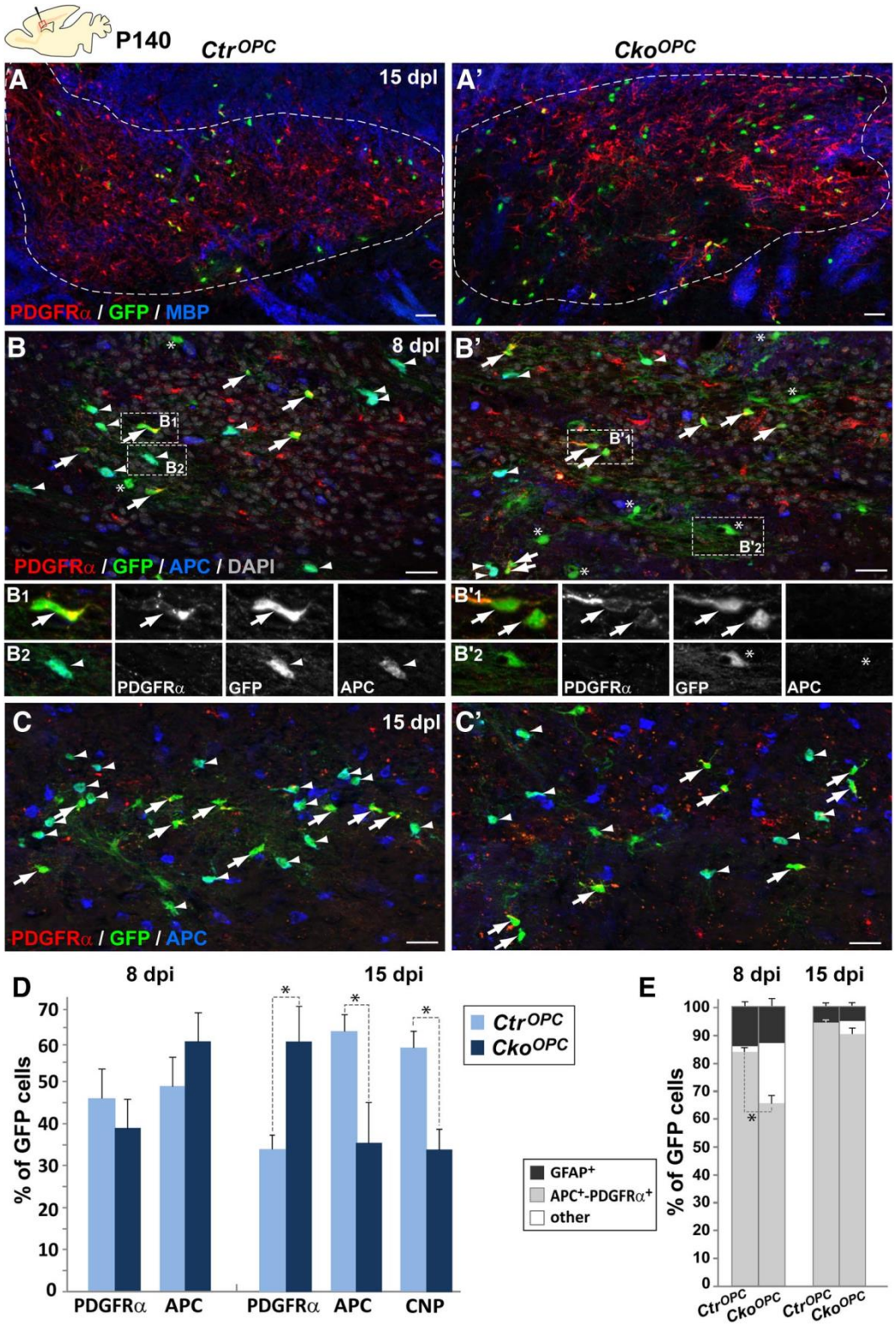

Figure 8. Ascl1 conditional deletion in adult OPCs reduces its differentiation during remyelination. ***A–D*** , Sagittal sections through the CC of adult (4 months), Ctr^{OPC} (control, ***A–D***) or Cko^{OPC} (mutant, ***A –D***) brains immunolabeled with antibodies against YFP and markers of oligodendroglial cells. ***A***, ***A*** , CC lesion (dotted area) shown by the absence of MBP and high density of PDGFR cells, illustrating the presence of YFP /PDGFR (arrows) and PDGFR (arrowheads) cells. ***B***, ***B*** , Lesion area illustrating that there is a similar proportion of YFP OPCs (arrows) that YFP oligodendrocytes (arrowheads) in Cko^{OPC} compared with Ctr^{OPC} at 8 dpl but more YFP-marker-negative cells (*) in Cko^{OPC}. ***B*** $_1$, ***B*** $_2$, Higher magnification of representative cells from each phenotype shown in separate color channels of the insets in ***B***, ***B*** . There are oligodendrocyte morphology and lack of APC staining in ***B*** $_2$. ***C***, ***C*** , Lesion area illustrating that there is a bigger proportion of YFP OPCs (arrows) that YFP oligodendrocytes (arrowheads) in Cko^{OPC} compared with Ctr^{OPC} at 15 dpl. ***D***, ***E***, Histograms representing the data shown above. ***D***, Cko^{OPC} present an increase PDGFR cells (*p 0.042, t test, n 4) and decrease in APC (*p 0.042, t test, n 4) and CNP cells (*p 0.038, t test, n 4) at 15 dpi. ***E***, Histograms representing the fate of YFP cells at 8 and 15 dpi by the expression of oligodendroglial markers (PDGFR or APC , gray bars), astroglial markers (GFAP , black), or negative for these markers (others, white bars). There are more Cko^{OPC} cells being neither oligodendroglial nor astroglial cells at 8 dpi (*p 0.021, t test, n 3), whereas this population is much smaller at 15 dpi. Scale bars, 20 m.

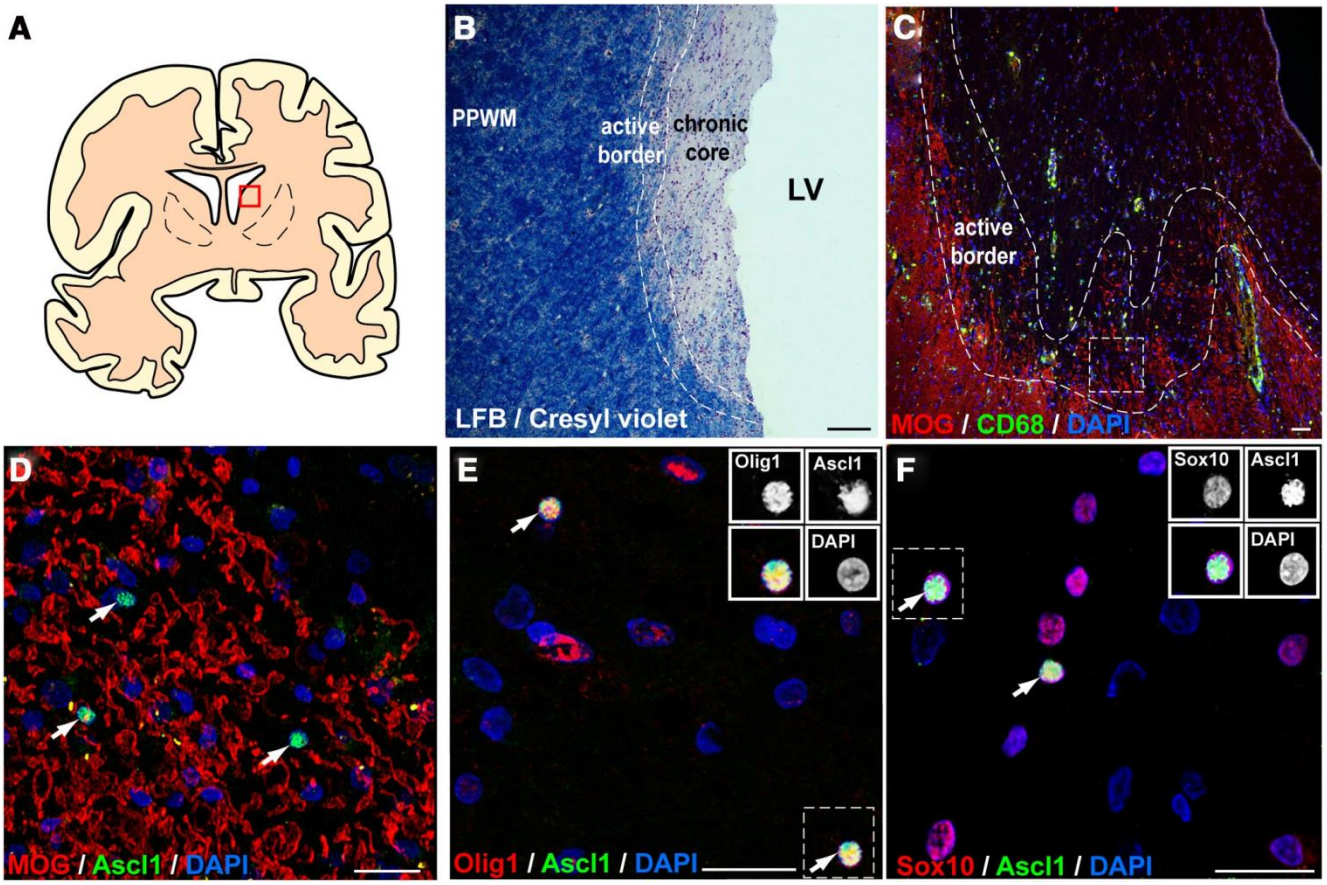

Figure 9. Ascl1 is expressed in oligodendroglial cells of active MS lesions. *A*, Schematic representation of a human brain coronal section at the level of the lateral ventricle illustrating the localization (boxed area) of a periventricular MS lesion shown in *B–F*. *B*, Luxol fast blue/cresyl violet staining reveals the typical feature of a chronic active periventricular lesion. *C*, Lesion activity was confirmed by immunolabeling for MOG and CD68, and subdivided into active borders (CD68 and MG myelin debris) and chronic inactive core lacking CD68 cells and MOG staining. *D*, Immunodetection of Ascl1 cells (arrows) in active regions. *E*, *F*, Double immunolabeling for Ascl1 and Olig1 (arrow, *E*) and Sox10 (arrow, *F*) confirmed the oligodendroglial expression of Ascl1 in active MS lesions. Scale bars, 20 m.

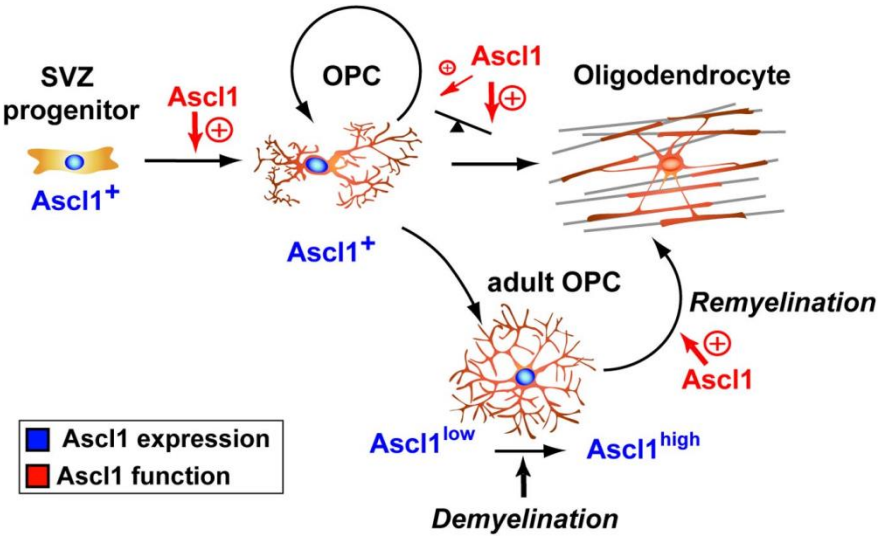

Figure 10. Working model for Ascl1 function in oligodendrogenesis. Ascl1 is expressed in cortical SVZ progenitors and the OPCs they generate, being downregulated upon oligodendrocyte differentiation. At postnatal stages, Ascl1 function is required in dorsal SVZ cells for normal OPC specification, and it is required in OPCs to balance OPC differentiation and proliferation. Ascl1 is maintained at low levels in adult OPCs, and its levels are upregulated upon demyelination being Ascl1 function required for normal OPC differentiation during remyelination. Arrow with plus symbol indicates functional requirement. Triangle with inclined line indicates Ascl1 function in the balance between OPC proliferation and differentiation, weighting more in the differentiation process.

ing a cell-autonomous role both in OPC specification and in fine-tuning of OPC proliferation versus differentiation (Fig. 10). First, we demonstrate that Ascl1 is expressed in neonatal cortical SVZ progenitors and that its conditional deletion strongly suppress OPC generation, thus demonstrating that Ascl1 is required for postnatal oligodendrocyte specification. Second, Ascl1 is expressed in all OPCs in most brain regions and its conditional ablation in OPCs favors proliferative over differentiative OPC divisions, leading to a reduced number of oligodendrocytes. Third, Ascl1 is not expressed in differentiating oligodendrocytes, but lineage-tracing studies show that Ascl1-expressing cells differentiate into myelinating and remyelinating oligodendrocytes. Fourth, Ascl1-expressing cells (OPCs and immature progenitors) are found in and around active lesions both in mouse and MS brain, Ascl1 being required for normal OPC differentiation during remyelination in mice and most likely implicated in human remyelination.

Ascl1 promotes OPC specification

Ascl1-conditional deletion in dorsal SVZ cells strongly reduces the generation of oligodendroglial cells in the dorsal telencephalon and the majority of *Ascl1*-deficient cells become instead astrocytes. This effect could be the result of the following: (1) selective cell death of *Ascl1*-deficient oligodendroglial cells; (2) reduced proliferation of oligodendroglial cells in the absence of *Ascl1*; (3) blocking of *Ascl1*-deficient SVZ cells at immature progenitor stage; or (4) specification switch from oligodendrocyte to astrocyte fate in the absence of *Ascl1*. We did not find preferential cell death of *Ascl1*-deficient SVZ cells or of their progeny. Also, *Ascl1*-deficient OPCs proliferate more than controls. In contrast, we found a 1.7-fold increase in the number of *Ascl1*-deficient GFAP cells in the SVZ compared with controls. Therefore, *Ascl1* is most likely required for OPC specification in the postnatal SVZ; and in the absence of *Ascl1,* the majority of SVZ cells be- come astrocytes or remain undifferentiated progenitors. *In vivo* clonal studies would be required to discriminate between these two possibilities. Indeed, a role in oligodendrocyte specification is supported by previous reports on *in vitro* experiments of *Ascl1* loss- and gain-of-function in progenitors. Clonal neurosphere cultures of *Ascl1*-deficient progenitors display a reduced capacity to generate oligodendrocytes (and neurons) and differentiate in- stead into astrocytes (Parras et al., 2004), whereas *Ascl1*- overexpressing progenitors favor oligodendrocyte differentiation at the expense

Cell-autonomous Ascl1 function in oligodendrogenesis

It has been suggested that Ascl1 plays an indirect role in oligodendrogenesis by Notch-mediated repression of the neurogenic determinants Dlx1/2 (Petryniak et al., 2007). However, in contrast with the embryonic expression of Ascl1 in a subset of OPCs (Parras et al., 2007; Sugimori et al., 2007), we demonstrate here that Ascl1 protein is present in the majority of postnatal brain OPCs, suggesting that Ascl1 plays a cell-autonomous function in oligodendrogenesis. Some immature progenitors coexpress Ascl1 and Dlx in oligodendrocyte-generating regions of embryonic (Petryniak et al., 2007) and postnatal telencephalon (current study), leaving space for Dlx inhibition of OPC specification. Nevertheless, Ascl1 conditional deletion in either SVZ cells or OPCs not only alters oligodendrocyte specification, but OPC proliferation versus differentiation balance, demonstrating a cell-autonomous role of Ascl1 at different stages of oligodendrogenesis. It is worth noting that Ascl1 and Olig2 are coexpressed in immature SVZ, suggesting that OPC specification likely requires the downregulation of Dlx1/2 in their progenitor cells.

Ascl1 function in OPC proliferation versus differentiation balance

Even though Ascl1 is expressed in proliferating cells, its conditional deletion in OPCs increased proliferation as measured by Ki67 expression. This could result from the fact that Ascl1 activates target genes involved either in proliferation or in cell cycle exit depending on the context, as recently reported for neurogenesis (Castro et al., 2011). In OPCs, the presence of inhibitors, such as Id2/4 (Wang et al., 2001; Yun et al., 2004) and other cofactors involved in proliferation and differentiation, could balance Ascl1 activation of proliferation versus cell cycle exit. Supporting this hypothesis, Ascl1 genome-wide chromatin immunoprecipitation data (ChIP-seq) in purified OPCs suggest that Ascl1 binds regulatory regions of both positive and negative factors controlling cell cycle (Clavairoly A, Parras C, unpublished observations). *Ascl1* deletion in OPCs also decreases differentiation during myelination (postnatal) or remyelination (adult). Indeed, one or 2 weeks after *Ascl1* deletion, more *Ascl1*-deficient cells are still OPCs and fewer have started differentiation. Our data suggest that Ascl1 cooperates with other factors to activate OPC differentiation and myelin protein expression. Nevertheless, Ascl1 requirement is compensated at later stages, and no myelination phenotype is found in *Ascl1*-mutant oligodendrocytes. Although Ascl1 is known to regulate *MBP* transcription *in vitro* (Gokhan et al., 2005), a genome-wide analysis of Ascl1 targets in oligodendrogenesis will be important to identify the Ascl1-target genes involved in the different stages of oligodendrocyte development (specification, proliferation, division mode, differentiation, and myelination).

Similar mechanisms of oligodendrogenesis during myelination and remyelination

Demyelination has been shown to upregulate *Olig2, Nkx2*.2, and *Sox10* transcript levels in and around lesion and also many other factors (Fancy et al., 2004, 2009), raising the question of the similarities and differences between oligodendrogenesis during myelination and remyelination. Our detailed characterization of the expression of Ascl1 and other TFs involved in oligodendrogenesis (Figs. 2 and 5) indicates that the same types of progenitors and OPCs, characterized by the same combined expression of markers, are involved in oligodendrogenesis during myelination and remyelination. After demyelination, we found that Ascl1 was upregulated in OPCs at levels found during myelination. Moreover, the levels of Ascl1, Olig2, Nkx2.2, and Sox9/10 expression at different stages of oligodendrogenesis were similar during remyelination and myelination (Fig. 5; and data not shown). Therefore, the upregulation of these factors during active remyelination likely results from the rejuvenation of a developmental genetic program enabling OPCs to actively proliferate, migrate, and differentiate into new remyelinating oligodendrocytes.

Demyelination induces axonal functional and structural loss, leading to major neurological and motor dysfunctions. In MS, despite the recent therapeutic advances aimed at reducing the inflammatory component and stopping demyelination, treatments to improve myelin repair are lacking because of the poor understanding of mechanisms leading to effective remyelination. In this context, our finding on the role of Ascl1 during myelin formation and in particular after demyelination, and future work characterizing its target genes, may pave the way toward a better understanding of the key players involved in oligodendrogenesis after demyelination and therefore help identifying new therapeutic targets aimed at favoring myelin repair.

References

Aguirre A, Dupree JL, Mangin JM, Gallo V (2007) A functional role for EGFR signaling in myelination and remyelination. Nat Neurosci 10:990–1002. CrossRef Medline

Arnett HA, Fancy SP, Alberta JA, Zhao C, Plant SR, Kaing S, Raine CS, Rowitch DH, Franklin RJ, Stiles CD (2004) bHLH transcription factor Olig1 is required to repair demyelinated lesions in the CNS. Science 306:2111–2115. CrossRef Medline

Bertrand N, Castro DS, Guillemot F (2002) Proneural genes and the specification of neural cell types. Nat Rev Neurosci 3:517–530. CrossRef Medline

Bhat RV, Axt KJ, Fosnaugh JS, Smith KJ, Johnson KA, Hill DE, Kinzler KW, Baraban JM (1996) Expression of the APC tumor suppressor protein in oligodendroglia. Glia 17:169–174. CrossRef Medline

Boda E, Viganò F, Rosa P, Fumagalli M, Labat-Gest V, Tempia F, Abbracchio MP, Dimou L, Buffo A (2011) The GPR17 receptor in NG2 expressing

cells: focus on in vivo cell maturation and participation in acute trauma and chronic damage. Glia 59:1958–1973. CrossRef Medline

Boutin C, Diestel S, Desoeuvre A, Tiveron MC, Cremer H (2008) Efficient in vivo electroporation of the postnatal rodent forebrain. PLoS One 3:e1883. CrossRef Medline

Cai J, Zhu Q, Zheng K, Li H, Qi Y, Cao Q, Qiu M (2010) Co-localization of Nkx6.2 and Nkx2.2 homeodomain proteins in differentiated myelinating oligodendrocytes. Glia 58:458–468. CrossRef Medline

Casarosa S, Fode C, Guillemot F (1999) Mash1 regulates neurogenesis in the ventral telencephalon. Development 126:525–534. Medline

Castro DS, Martynoga B, Parras C, Ramesh V, Pacary E, Johnston C, Drechsel D, Lebel-Potter M, Garcia LG, Hunt C, Dolle D, Bithell A, Ettwiller L, Buckley N, Guillemot F (2011) A novel function of the proneural factor Ascl1 in progenitor proliferation identified by genome-wide characterization of its targets. Genes Dev 25:930–945. CrossRef Medline

Chen Y, Wu H, Wang S, Koito H, Li J, Ye F, Hoang J, Escobar SS, Gow A, Arnett HA, Trapp BD, Karandikar NJ, Hsieh J, Lu QR (2009) The oligodendrocyte-specific G protein-coupled receptor GPR17 is a cell-intrinsic timer of myelination. Nat Neurosci 12:1398–1406. CrossRef Medline

Fancy SP, Zhao C, Franklin RJ (2004) Increased expression of Nkx2.2 and Olig2 identifies reactive oligodendrocyte progenitor cells responding to demyelination in the adult CNS. Mol Cell Neurosci 27:247–254. CrossRef Medline

Fancy SP, Baranzini SE, Zhao C, Yuk DI, Irvine KA, Kaing S, Sanai N, Franklin RJ, Rowitch DH (2009) Dysregulation of the Wnt pathway inhibits timely myelination and remyelination in the mammalian CNS. Genes Dev 23:1571–1585. CrossRef Medline

Franklin RJ, ffrench-Constant C (2008) Remyelination in the CNS: from biology to therapy. Nat Rev Neurosci 9:839–855. CrossRef Medline

Gokhan S, Marin-Husstege M, Yung SY, Fontanez D, Casaccia-Bonnefil P, Mehler MF (2005) Combinatorial profiles of oligodendrocyte-selective classes of transcriptional regulators differentially modulate myelin basic protein gene expression. J Neurosci 25:8311–8321. CrossRef Medline

Gorski JA, Talley T, Qiu M, Puelles L, Rubenstein JL, Jones KR (2002) Cortical excitatory neurons and glia, but not GABAergic neurons, are produced in the Emx1-expressing lineage. J Neurosci 22:6309–6314. Medline

Hack MA, Sugimori M, Lundberg C, Nakafuku M, Götz M (2004) Regionalization and fate specification in neurospheres: the role of Olig2 and Pax6. Mol Cell Neurosci 25:664–678. CrossRef Medline

Hall A, Giese NA, Richardson WD (1996) Spinal cord oligodendrocytes develop from ventrally derived progenitor cells that express PDGF alpha-receptors. Development 122:4085–4094. Medline

Ivanova A, Nakahira E, Kagawa T, Oba A, Wada T, Takebayashi H, Spassky N, Levine J, Zalc B, Ikenaka K (2003) Evidence for a second wave of oligodendrogenesis in the postnatal cerebral cortex of the mouse. J Neurosci Res 73:581–592. CrossRef Medline

Kessaris N, Fogarty M, Iannarelli P, Grist M, Wegner M, Richardson WD (2006) Competing waves of oligodendrocytes in the forebrain and postnatal elimination of an embryonic lineage. Nat Neurosci 9:173–179. CrossRef Medline

Kitada M, Rowitch DH (2006) Transcription factor co-expression patterns indicate heterogeneity of oligodendroglial subpopulations in adult spinal cord. Glia 54:35–46. CrossRef Medline

Kondo T, Raff M (2000) Basic helix-loop-helix proteins and the timing of oligodendrocyte differentiation. Development 127:2989–2998. Medline

Lassmann H (1998) Neuropathology in multiple sclerosis: new concepts. Mult Scler 4:93–98. CrossRef Medline

Li H, de Faria JP, Andrew P, Nitarska J, Richardson WD (2011) Phosphorylation regulates OLIG2 cofactor choice and the motor neuron-oligodendrocyte fate switch. Neuron 69:918–929. CrossRef Medline

Ligon KL, Fancy SP, Franklin RJ, Rowitch DH (2006) Olig gene function in CNS development and disease. Glia 54:1–10. CrossRef Medline

Liu Z, Hu X, Cai J, Liu B, Peng X, Wegner M, Qiu M (2007) Induction of oligodendrocyte differentiation by Olig2 and Sox10: evidence for reciprocal interactions and dosage-dependent mechanisms. Dev Biol 302:683–693. CrossRef Medline

Lu QR, Cai L, Rowitch D, Cepko CL, Stiles CD (2001) Ectopic expression of Olig1 promotes oligodendrocyte formation and reduces neuronal survival in developing mouse cortex. Nat Neurosci 4:973–974. CrossRef Medline

Menn B, Garcia-Verdugo JM, Yaschine C, Gonzalez-Perez O, Rowitch D, Alvarez-Buylla A (2006) Origin of oligodendrocytes in the subventricular zone of the adult brain. J Neurosci 26:7907–7918. CrossRef Medline

Miguez A, Ducret S, Di Meglio T, Parras C, Hmidan H, Haton C, Sekizar S, Mannioui A, Vidal M, Kerever A, Nyabi O, Haigh J, Zalc B, Rijli FM, Thomas JL (2012) Opposing roles for Hoxa2 and Hoxb2 in hindbrain oligodendrocyte patterning. J Neurosci 32:17172–17185. CrossRef Medline

Mizuguchi R, Sugimori M, Takebayashi H, Kosako H, Nagao M, Yoshida S, Nabeshima Y, Shimamura K, Nakafuku M (2001) Combinatorial roles of Olig2 and neurogenin2 in the coordinated induction of pan-neuronal and subtype-specific properties of motoneurons. Neuron 31:757–771. CrossRef Medline

Nait-Oumesmar B, Decker L, Lachapelle F, Avellana-Adalid V, Bachelin C, Baron-Van Evercooren A (1999) Progenitor cells of the adult mouse subventricular zone proliferate, migrate and differentiate into oligodendrocytes after demyelination. Eur J Neurosci 11:4357–4366. CrossRef Medline

Nait-Oumesmar B, Picard-Riera N, Kerninon C, Decker L, Seilhean D, Höglinger GU, Hirsch EC, Reynolds R, Baron-Van Evercooren A (2007) Activation of the subventricular zone in multiple sclerosis: evidence for early glial progenitors. Proc Natl Acad Sci U S A 104:4694–4699. CrossRef Medline

Nait-Oumesmar B, Picard-Riéra N, Kerninon C, Baron-Van Evercooren A (2008) The role of SVZ-derived neural precursors in demyelinating diseases: from animal models to multiple sclerosis. J Neurol Sci 265:26–31. CrossRef Medline

Pacary E, Heng J, Azzarelli R, Riou P, Castro D, Lebel-Potter M, Parras C, Bell DM, Ridley AJ, Parsons M, Guillemot F (2011) Proneural transcription factors regulate different steps of cortical neuron migration through Rnd-mediated inhibition of RhoA signaling. Neuron 69:1069–1084. CrossRef Medline

Parras CM, Galli R, Britz O, Soares S, Galichet C, Battiste J, Johnson JE, Nakafuku M, Vescovi A, Guillemot F (2004) Mash1 specifies neurons and oligodendrocytes in the postnatal brain. EMBO J 23:4495–4505. CrossRef Medline

Parras CM, Hunt C, Sugimori M, Nakafuku M, Rowitch D, Guillemot F (2007) The proneural gene Mash1 specifies an early population of telencephalic oligodendrocytes. J Neurosci 27:4233–4242. CrossRef Medline

Petryniak MA, Potter GB, Rowitch DH, Rubenstein JL (2007) Dlx1 and Dlx2 control neuronal versus oligodendroglial cell fate acquisition in the developing forebrain. Neuron 55:417–433. CrossRef Medline

Qi Y, Cai J, Wu Y, Wu R, Lee J, Fu H, Rao M, Sussel L, Rubenstein J, Qiu M (2001) Control of oligodendrocyte differentiation by the Nkx2.2 homeodomain transcription factor. Development 128:2723–2733. Medline

Rivers LE, Young KM, Rizzi M, Jamen F, Psachoulia K, Wade A, Kessaris N, Richardson WD (2008) PDGFRA/NG2 glia generate myelinating oligodendrocytes and piriform projection neurons in adult mice. Nat Neurosci 11:1392–1401. CrossRef Medline

Scott CE, Wynn SL, Sesay A, Cruz C, Cheung M, Gomez Gaviro MV, Booth S, Gao B, Cheah KS, Lovell-Badge R, Briscoe J (2010) SOX9 induces and maintains neural stem cells. Nat Neurosci 13:1181–1189. CrossRef Medline

Soriano P (1999) Generalized lacZ expression with the ROSA26 Cre reporter strain. Nat Genet 21:70–71. CrossRef Medline

Spassky N, Goujet-Zalc C, Parmantier E, Olivier C, Martinez S, Ivanova A, Ikenaka K, Macklin W, Cerruti I, Zalc B, Thomas JL (1998) Multiple restricted origin of oligodendrocytes. J Neurosci 18:8331–8343. Medline

Srinivas S, Watanabe T, Lin CS, William CM, Tanabe Y, Jessell TM, Costantini F (2001) Cre reporter strains produced by targeted insertion of EYFP and ECFP into the ROSA26 locus. BMC Dev Biol 1:4. CrossRef Medline

Staugaitis SM, Trapp BD (2009) NG2-positive glia in the human central nervous system. Neuron Glia Biol 5:35–44. CrossRef Medline

Stolt CC, Lommes P, Sock E, Chaboissier MC, Schedl A, Wegner M (2003) The Sox9 transcription factor determines glial fate choice in the developing spinal cord. Genes Dev 17:1677–1689. CrossRef Medline

Stolt CC, Lommes P, Friedrich RP, Wegner M (2004) Transcription factors Sox8 and Sox10 perform non-equivalent roles during oligodendrocyte development despite functional redundancy. Development 131:2349–2358. CrossRef Medline

Sugiarto S, Persson AI, Munoz EG, Waldhuber M, Lamagna C, Andor N,

Hanecker P, Ayers-Ringler J, Phillips J, Siu J, Lim DA, Vandenberg S, Stallcup W, Berger MS, Bergers G, Weiss WA, Petritsch C (2011) Asymmetry-defective oligodendrocyte progenitors are glioma precursors. Cancer Cell 20:328–340. CrossRef Medline

Sugimori M, Nagao M, Bertrand N, Parras CM, Guillemot F, Nakafuku M (2007) Combinatorial actions of patterning and HLH transcription factors in the spatiotemporal control of neurogenesis and gliogenesis in the developing spinal cord. Development 134:1617–1629. CrossRef Medline

Sun T, Echelard Y, Lu R, Yuk DI, Kaing S, Stiles CD, Rowitch DH (2001) Olig bHLH proteins interact with homeodomain proteins to regulate cell fate acquisition in progenitors of the ventral neural tube. Curr Biol 11:1413–1420. CrossRef Medline

Tekki-Kessaris N, Woodruff R, Hall AC, Gaffield W, Kimura S, Stiles CD, Rowitch DH, Richardson WD (2001) Hedgehog-dependent oligodendrocyte lineage specification in the telencephalon. Development 128:2545–2554. Medline

Vierbuchen T, Wernig M (2012) Molecular roadblocks for cellular reprogramming. Mol Cell 47:827–838. CrossRef Medline

Vierbuchen T, Ostermeier A, Pang ZP, Kokubu Y, Südhof TC, Wernig M (2010) Direct conversion of fibroblasts to functional neurons by defined factors. Nature 463:1035–1041. CrossRef Medline

Waclaw RR, Wang B, Pei Z, Ehrman LA, Campbell K (2009) Distinct temporal requirements for the homeobox gene Gsx2 in specifying striatal and olfactory bulb neuronal fates. Neuron 63:451–465. CrossRef Medline

Wang S, Sdrulla A, Johnson JE, Yokota Y, Barres BA (2001) A role for the helix-loop-helix protein Id2 in the control of oligodendrocyte development. Neuron 29:603–614. CrossRef Medline

Watanabe M, Hadzic T, Nishiyama A (2004) Transient upregulation of Nkx2.2 expression in oligodendrocyte lineage cells during remyelination. Glia 46:311–322. CrossRef Medline

Yue T, Xian K, Hurlock E, Xin M, Kernie SG, Parada LF, Lu QR (2006) A critical role for dorsal progenitors in cortical myelination. J Neurosci 26:1275–1280. CrossRef Medline

Yun K, Mantani A, Garel S, Rubenstein J, Israel MA (2004) Id4 regulates neural progenitor proliferation and differentiation in vivo. Development 131:5441–5448. CrossRef Medline

Zhou Q, Anderson DJ (2002) The bHLH transcription factors OLIG2 and OLIG1 couple neuronal and glial subtype specification. Cell 109:61–73. CrossRef Medline

Zhou Q, Choi G, Anderson DJ (2001) The bHLH transcription factor Olig2 promotes oligodendrocyte differentiation in collaboration with Nkx2.2. Neuron 31:791–807. CrossRef Medline

Zhu X, Hill RA, Dietrich D, Komitova M, Suzuki R, Nishiyama A (2011) Age-dependent fate and lineage restriction of single NG2 cells. Development 138:745–753. CrossRef Medline

Zhu X, Zuo H, Maher BJ, Serwanski DR, LoTurco JJ, Lu QR, Nishiyama A (2012) Olig2-dependent developmental fate switch of NG2 cells. Development 139:2299–2307. CrossRef Medline

ARTICLE II: Development of the prethalamus is crucial for thalamocortical projection formation and is regulated by Olig2

© 2014. Published by The Company of Biologists Ltd | Development (2014) 141, 2075-2084 doi:10.1242/dev.097790

RESEARCH ARTICLE

Development of the prethalamus is crucial for thalamocortical projection formation and is regulated by Olig2

Katsuhiko Ono[1,*,‡], Adrien Clavairoly[2,*], Tadashi Nomura[1,3], Hitoshi Gotoh[1], Aoi Uno[1], Olivier Armant[4], Hirohide Takebayashi[3,5], Qi Zhang[6], Kenji Shimamura[7], Shigeyoshi Itohara[6], Carlos M. Parras[2] and Kazuhiro Ikenaka[8]

ABSTRACT

Thalamocortical axons (TCAs) pass through the prethalamus in the first step of their neural circuit formation. Although it has been supposed that the prethalamus is an intermediate target for thalamocortical projection formation, much less is known about the molecular mechanisms of this targeting. Here, we demonstrated the functional implications of the prethalamus in the formation of this neural circuit. We show that Olig2 transcription factor, which is expressed in the ventricular zone (VZ) of prosomere 3, regulates prethalamus formation, and loss of Olig2 results in reduced prethalamus size in early development, which is accompanied by expansion of the thalamic eminence (TE). Extension of TCAs is disorganized in the Olig2-KO dorsal thalamus, and initial elongation of TCAs is retarded in the Olig2-KO forebrain. Microarray analysis demonstrated upregulation of several axon guidance molecules, including Epha3 and Epha5, in the Olig2-KO basal forebrain. In situ hybridization showed that the prethalamus in the wild type excluded the expression of Epha3 and Epha5, whereas loss of Olig2 resulted in reduction of this Ephas-negative area and the corresponding expansion of the Ephas-positive TE. Dissociated cultures of thalamic progenitor cells demonstrated that substrate-bound EphA3 suppresses neurite extension from dorsal thalamic neurons. These results indicate that Olig2 is involved in correct formation of the prethalamus, which leads to exclusion of the EphA3-expressing region and is crucial for proper TCA formation. Our observation is the first report showing the molecular mechanisms underlying how the prethalamus acts on initial thalamocortical projection formation.

KEY WORDS: Dorsal thalamus, Thalamic eminence, EphA3, Microarray, In situ hybridization, Mouse

INTRODUCTION

The cerebral cortex and dorsal thalamus have reciprocal connections, which are essential morphological bases for cortical functions. Thalamocortical axons (TCAs) send sensory information and feedback of motor programming from the caudal brain areas, and these connections are organized in a topographical manner (Vanderhaeghen and Polleux, 2004). Formation of the topographic connections is regulated by several axon guidance molecules (Braisted et al., 2000, 2009; Dufour et al., 2003; Vanderhaeghen and Polleux, 2004; Torii and Levitt, 2005; Uemura et al., 2007). Developing thalamic neurons send axons towards the ventral telencephalon through the prethalamus (or ventral thalamus). Special guidance cells named corridor cells in the ventral telencephalon guide TCAs to the pallium (López-Bendito et al., 2006). Thus, the ventral telencephalon is regarded as an important intermediate target for the formation of reciprocal connections.

TCAs need to pass through the prethalamus on exiting from the dorsal thalamus to the ventral telencephalon as the prethalamus occupies exiting points of TCAs. The prethalamus has been supposed to be an intermediate target of TCAs (Deng and Elberger, 2003; Molnár et al., 2012); however, evidence is scarce that identifies the molecular mechanisms underlying the axon guidance role of the prethalamus, and functions of the prethalamus in thalamocortical projection are not fully understood (Leyva-Diaz and Lopez-Bendito, 2013). Mouse lines showing defects in prethalamus formation would be a useful model for analyzing the functional role of the prethalamus in thalamocortical projection formation.

Olig2 is a bHLH transcription factor that is essential for oligodendrocyte and somatic motoneuron development (Lu et al., 2002; Takebayashi et al., 2002b; Zhou and Anderson, 2002), and is also involved in dorsoventral patterning of the spinal cord, which is required for pMN domain specification. In the diencephalon, Olig2 is expressed in the VZ of the prethalamus at early fetal stages, such as E9.5 in mice (Ono et al., 2008). These Olig2+ cells differentiate into GABAergic neurons in the thalamic reticular nucleus (TRN) as well as into macroglial cells in the diencephalon, whereas loss of Olig2 does not affect GABAergic neuron differentiation (Takebayashi et al., 2008). The function of Olig2 in this area has not been elucidated. Here, we report that loss of Olig2 results in hypoplasia of the prethalamus, which leads to defects of TCA extension. The prethalamus is devoid of Epha3 and Epha5 expression whereas ventrally adjacent thalamic eminence (TE) expresses Epha3 and Epha5 (referred to here as Ephas positive) and, in the E13.5 Olig2-KO diencephalon, Ephas-positive TE expanded dorsally. Furthermore, the substrate-bound Epha3 suppresses neurite extension in cultured thalamic neurons. These results together indicate that Olig2 regulates proper formation of the prethalamus, which leads to exclusion of the EphA3-expressing non-permissive region for TCA and is crucial for proper TCA formation.

RESULTS

Reduced size of the prethalamus in Olig2-KO mice

We first explored early development of the prethalamus in the Olig2-KO mouse to examine whether Olig2-KO mice can be used to

[1]Department of Biology, Kyoto Prefectural University of Medicine, Kyoto 603-8334, Japan. [2]Sorbonne Universites, UPMC Univ Paris 06 UMR S 1127, and Inserm U 1127, and CNRS UMR 7225, and ICM, 75013, Paris, France. [3]PRESTO, JST, Kawaguchi 332-0012, Japan. [4]Institute of Toxicology and Genetics, KIT Campus Nord, Eggenstein-Leopoldshafen D-76344, Germany. [5]Division of Neurobiology and Anatomy, Graduate School of Medical and Dental Sciences, Niigata University, Niigata 951-8510, Japan. [6]Laboratory for Behavioral Genetics, RIKEN BSI, Wako 351-0198, Japan. [7]Department of Brain Morphogenesis, Institutes for Molecular and Embryological Genetics, Kumamoto University, Kumamoto 860-8556, Japan. [8]Division of Neurobiology and Bioinformatics, National Institute for Physiological Sciences, Okazaki 444-8787, Japan.
*These authors contributed equally to this work

‡Author for correspondence (katsono@koto.kpu-m.ac.jp)

Received 19 April 2013; Accepted 11 March 2014

Development (2014) 141, 2075-2084 doi:10.1242/dev.097790

analyze functions in the prethalamus for thalamocortical projection formation. The prethalamus is demarcated by Dlx2, as well as by Islet1/2, expression (Bulfone et al., 1993).

As Olig2 expression in the diencephalon is observed as early as E9.5 (Ono et al., 2008; supplementary material Fig. S1), whole-mount Dlx2 in situ hybridization was performed in the E10.5 forebrain. Dlx2+ prethalamus was much smaller in Olig2-KO mice (n=3) than in wild-type animals (n=4) (Fig. 1A,B, arrows). To observe prethalamus formation more precisely, coronal sections of the E11.5 forebrain were double-stained with Dlx2 in situ hybridization and Islet1/2 immunohistochemistry. In wild-type or heterozygous mice, Dlx2+ cells were observed in the middle part of the diencephalon (Fig. 1C,E,G,I). Islet1/2+ cells were located laterally to Dlx2+ cells (Fig. 1I). Because no significant difference was observed between wild-type and Olig2 heterozygous animals, they are both referred to as normal control animals. Dlx2+ cells in the Olig2-KO diencephalon were also observed at a similar level; however, as shown in the whole-mount in situ hybridization, the Dlx2+ area was much smaller than that in normal control animals (Fig. 1D,F,H,J). The mean area of the Dlx2+ region in each section of Olig2-KO was ~60% smaller than that of the wild type (Fig. 1K). In addition, the Islet1/2+ region was also greatly decreased in the Olig2-KO prethalamus (Fig. 1I,J). The prethalamus in E13.5 Olig2-KO mice was also smaller (not shown); thus, loss of Olig2 results in hypoplasia of the prethalamus in early development, as early as E10.5.

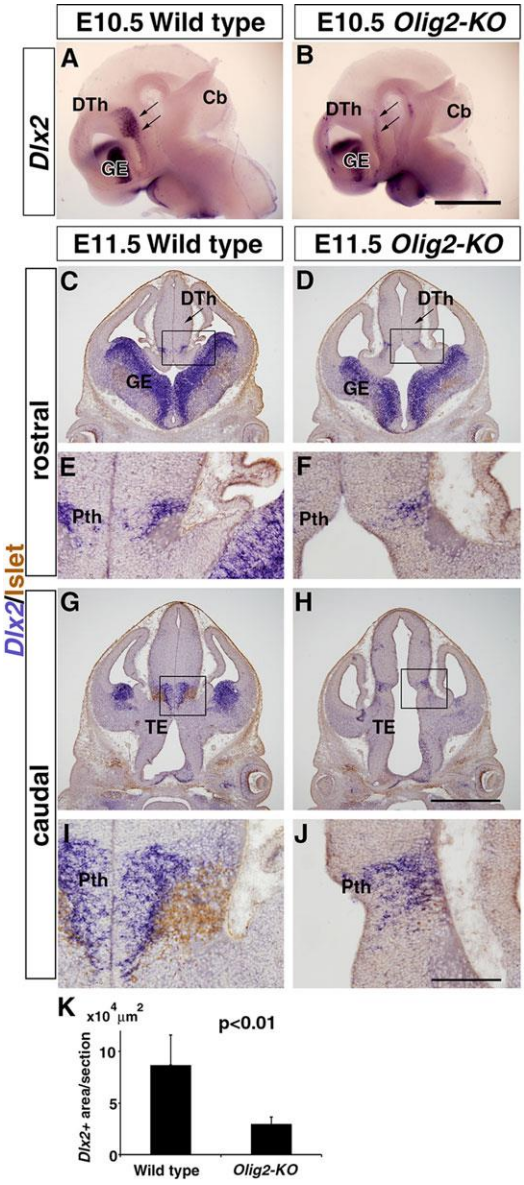

Fig. 1. Defective prethalamus development in the Olig2-KO mouse. (A,B) Whole-mount in situ hybridization of E10.5 forebrain with Dlx2. Arrows indicate prethalamus. The prethalamus of the Olig2-KO mouse shows hypoplasia. (C-J) Double staining with Dlx2 in situ hybridization (purple) and Islet1/2 immunohistochemistry (brown). (C,E,G,I) E11.5 wild-type mouse. (D,F,H,J) E11.5 Olig2-KO mouse. The Dlx2+ and Islet1/2+ area is much smaller in Olig2-KO mouse than in normal control animals. Cb, cerebellum; DTh, dorsal thalamus; GE, ganglionic eminence; Pth, prethalamus; TE, thalamic eminence. (K) Quantitative analysis of E11.5 Dlx2+ prethalamus region, showing 60% reduction of the area in the Olig2-KO mouse. Data are mean±s.e.m. (wild type, n=3; Olig2-KO, n=3; Student's t-test). Scale bars: 1 mm in B; 500 µm in H; 100 µm in J.

We then examined whether reduced proliferation or elevated apoptosis contributes to the hypoplasia of the Olig2-KO prethalamus. Sections of control and Olig2-KO mice at E10.5 and E11.5 were double labeled with Dlx2 in situ hybridization and cleaved caspase 3 immunohistochemistry (a marker of apoptotic cells) or pH3 immunohistochemistry (a marker of mitotic cells). At E10.5, cleaved caspase 3+ spots were more abundantly observed in the prethalamus of Olig2-KO than in control mice (supplementary material Fig. S2A-E), whereas pH3+ cell density was similar between the control and Olig2-KO (supplementary material Fig. S2G). At E11.5, the density of cleaved caspase 3+ cells was similar between the control and Olig2-KO prethalamus, whereas that of pH3+ cells was slightly higher in the Olig2-KO prethalamus than in the normal control (supplementary material Fig. S2F,H). These results indicate that transiently elevated apoptosis at E10.5 may be, at least in part, involved in reduction of the size of the prethalamus in Olig2-KO mice.

Dorsal shift of the border between the prethalamus and thalamic eminence in the Olig2-KO diencephalon

To better understand the defects of prethalamus formation in Olig2-KO mice, areas adjacent to the prethalamus were examined by the expression of region marker molecules. The thalamic eminence (TE) is a dorsal part of prosomere 3, although, in coronal sections of the fetal diencephalon, TE is observed ventral to the prethalamus (Fig. 2; López-Bendito and Molnár, 2003; Puelles, 2001). The TE is demarcated by the expression of calretinin (Abbott and Jacobowitz, 1999), Tbr1 and Tbr2 (Eomes – Mouse Genome Informatics) (Bulfone et al., 1995; Puelles, 2001). Tbr2 is expressed in basal progenitors of the TE, and calretinin and Tbr1 are expressed in the mantle layer. In normal control animals, Tbr2 expression was observed ventrally to the Olig2+ domain (Fig. 2A). In the Olig2-KO diencephalon, Tbr2 was also expressed ventral to the CreER expression that recapitulates intrinsic Olig2 expression (Fig. 2B), and the Tbr2+ area was much wider than that in normal control animals (Fig. 2A,B, flanked by arrows), whereas the CreER+ prethalamus was narrower (Fig. 2B, flanked by arrowheads). Although Lhx5 expression was reported to demarcate the prethalamus, in our observation, Lhx5 was expressed in the dorsal border of the prethalamus and the main body of the TE whereas the main part of the prethalamus was devoid of Lhx5 expression (supplementary material Fig. S3A,F). In the E12.5 Olig2-KO diencephalon, the Lhx5-negative area was much reduced in size and was compatible with the reduction of the Dlx2+ area (supplementary material Fig. S3B,G). We then measured the relative positions of Tbr2- and Olig2- or Cre-expressing domains within the dorsoventral axis of the E13.5

Development (2014) 141, 2075-2084 doi:10.1242/dev.097790

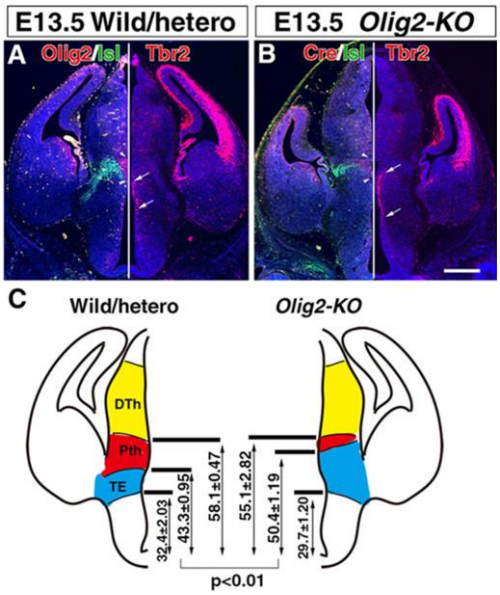

Fig. 2. Altered formation of the prethalamus and TE in Olig2-KO mice. (A,B) Comparison of formation of the prethalamus and thalamic eminence in normal control and Olig2-KO mouse at E13.5. Both are composite pictures, in which left and right halves are adjacent sections immunostained with Islet1/2 (green in left half), Olig2 or Cre (red in left half), and Tbr2 (red in right half). The prethalamus is shown by Islet1/2 and the TE by Tbr2. The VZ of the prethalamus is indicated by arrowheads and that of the TE by arrows. The mutant embryo brain was taken at a slightly caudal level compared with the wild-type embryo brain. Scale bar: 500 μm in B. (C) Relative position of borders of the dorsal thalamus (yellow), prethalamus (red) and TE (blue) in coronal sections of the diencephalon. Total height of the diencephalon in the coronal section is regarded as 100% height, and relative position is expressed as percentage from the bottom (mean±s.d.; wild type, n=3; Olig2-KO, n=3; Student's t-test).

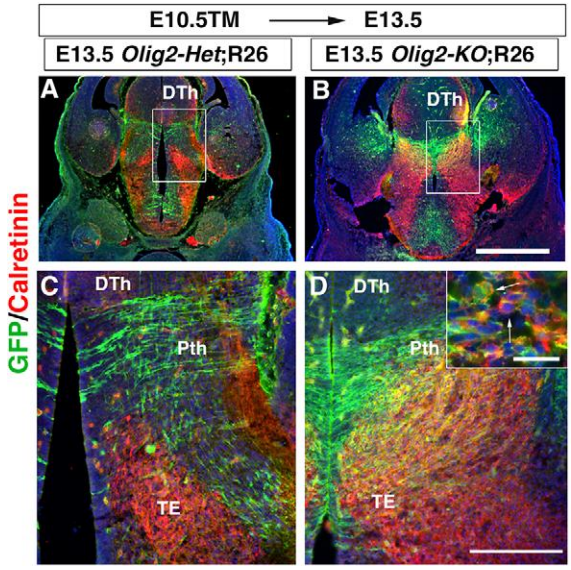

Fig. 3. Fate change of Olig2 lineage cells in the absence of Olig2. (A,B) E13.5 Olig2-hetero;Rosa26^{GFP} and Olig2-KO;Rosa26^{GFP} mouse diencephalon, stained with calretinin (red) and GFP (green). Boxed areas in A and B are magnified in C and D, respectively. (C,D) Higher magnification pictures. In the heterozygous mouse, GFP+ and calretinin+ cells are mutually exclusive (C), whereas overlapping distribution is apparent in Olig2-KO mouse (D). Inset shows representative double-labeled cells (arrows). Scale bars: 500 μm in B; 200 μm in D; 20 μm in inset.

diencephalon (Fig. 2C). Total height of the diencephalon in a coronal section was regarded as 100% height. As shown in Fig. 2C, the dorsal border of the prethalamus and the ventral border of the TE were unchanged in the Olig2-KO diencephalon. However, the border between the prethalamus and TE was significantly shifted dorsally in knockout mice. In addition, the Tbr2-expressing thalamic eminence occupied 10±1.44% width within the total height of the diencephalon in control animals, whereas that in Olig2-KO mice was 20.7±2.38%, which was also statistically significant (P<0.01). These observations clearly demonstrate hypoplasia of the prethalamus accompanied by expansion of the TE in Olig2-KO mice.

To examine whether the reduction of the prethalamus with dorsal expansion of the TE involves a fate change of Olig2 lineage cells, we performed genetic fate mapping. We generated Olig2$^{KICreER/+}$; Rosa26-GAP-EGFP and Olig2$^{KICreER/KICreER}$;Rosa26-GAP-EGFP (hereafter named Olig2-hetero;Rosa26^{GFP} and Olig2-KO;Rosa26^{GFP}, respectively) mice, and tamoxifen was administered to dams at E10.5 to induce GFP expression in Olig2+ cells. Animals were analyzed at E13.5, and sections were double-stained with calretinin, Tbr1 or Islet1/2 and with GFP immunohistochemistry. In the Olig2-hetero;Rosa26^{GFP} diencephalon, GFP+ cells and calretinin+ cells were mostly mutually exclusive and thus only a few cells were double immunoreactive (Fig. 3A,C). By contrast, calretinin+ cells, as well as Tbr1+ cells, expanded dorsally and showed overlapping distribution with GFP+ cells in the Olig2-KO;Rosa26^{GFP} diencephalon (Fig. 3B,D; supplementary material Fig. S4A,B), and many calretinin+ cells were also GFP+, indicating a fate change of Olig2 lineage cells (Fig. 3D, inset). Islet1/2+ cells in the Olig2-KO prethalamus were also GFP+ (supplementary material Fig. S4C,D) and therefore Olig2 lineage cells in the Olig2-KO diencephalon showed dual phenotypes, both prethalamus and TE.

Although the border between the prethalamus and the TE was dorsally shifted in Olig2-KO mice, other areas of the forebrain seemed to be properly formed. For example, the Olig3+ dorsal thalamus was positioned dorsal to the prethalamus (Vue et al., 2009; supplementary material Fig. S3C,H). Whereas the ventral and dorsal borders of the Olig3+ area were unchanged in the Olig2-KO mouse (supplementary material Fig. S3C,H), the relative width of the Olig3 domain within the dorsoventral axis was slightly reduced in the Olig2-KO diencephalon (supplementary material Fig. S3K). Shh and Fgf8 expression in ZLI was unchanged in the absence of Olig2 (supplementary material Fig. S3D,E,I,J). In addition, Islet1/2+ cells, including corridor cells (López-Bendito et al., 2006), were positioned normally in the ventral telencephalon at E13.5 in both the normal control and Olig2-KO mice (supplementary material Fig. S5). Overall, the prethalamus and TE are specifically malformed in the early forebrain development of the Olig2-KO mouse, although a slight defect was noticed in the dorsal thalamus.

Defect of TCA extension in the Olig2-KO diencephalon

We next examined whether the prethalamus has an impact on the formation of the thalamocortical projection. Axons in the fetal forebrain were stained with anti-neurofilament M (NF-M) antibody. At E13.5, when TCAs start to extend into the prethalamus and the ventral telencephalon (López-Bendito et al., 2006), NF-M+ axons extended dorsoventrally and in parallel in the mantle layer, and they gradually converged in the ventral part (Fig. 4A,B, arrowheads). In age-matched Olig2-KO mice, NF-M+ axons were disorganized and followed a tortuous course in the dorsal thalamus; they sometimes formed small aggregates (Fig. 4C,D, arrowheads). To elucidate whether these NF-M+ axons are TCAs, they were co-immunostained with anti-netrin G1 antibody (Niimi et al., 2007) because netrin G1 is

Development (2014) 141, 2075-2084 doi:10.1242/dev.097790

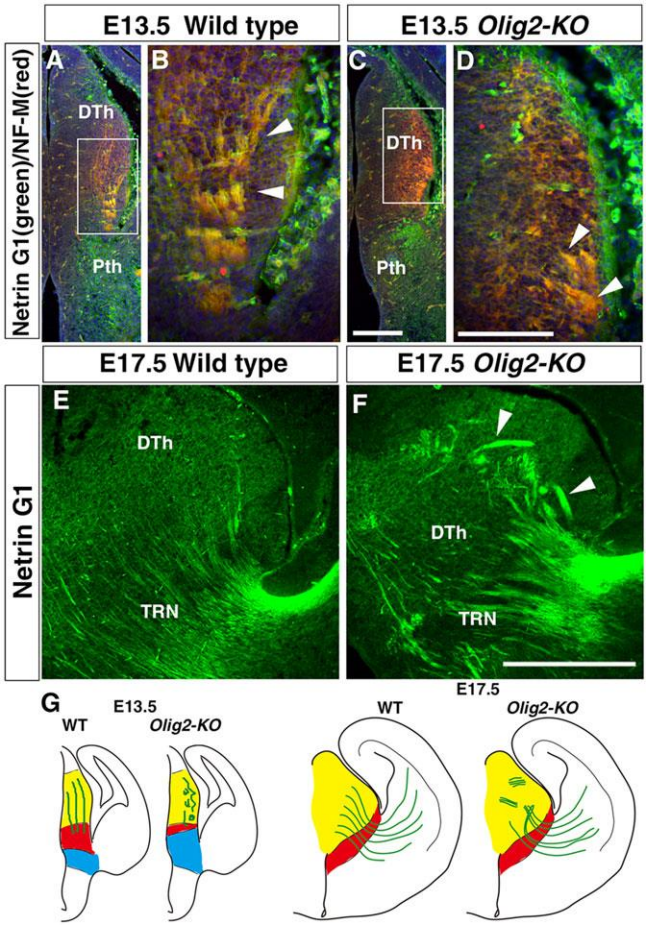

Fig. 4. Disorganization of TCAs in the Olig2-KO dorsal thalamus. (A-D) E13.5 diencephalon immunostained with anti-NF-M (red) and anti-netrin G1 (green) antibodies. NF-M+ axons in the dorsal thalamus (DTh) are also netrin-G1+, indicating that they are TCAs. Wild-type TCAs extend in parallel and converge ventrally in the prethalamus (A,B; arrowheads in B). TCAs in the Olig2-KO mouse show disorganized extension and sometimes form axon aggregates (C,D; arrowheads in D). (E,F) Netrin G1+ TCAs in the E17.5 DTh and prethalamus (thalamic reticular nucleus, TRN). In the wild type, netrin G1+ axons are extended in parallel in the DTh and TRN (E), whereas those in the Olig2-KO mouse form abnormal thick axon bundles orienting randomly (arrowheads in F). (G) Summary of the observed defects in Olig2-KO diencephalon. Scale bars: 200 μm in C; 100 μm in D; 500 μm in F.

expressed by developing dorsal thalamic neurons (Nakashiba et al., 2002). Indeed, NF-M+ axons co-expressed netrin G1 in both the wild-type and Olig2-KO dorsal thalamus (Fig. 4B,D, arrowheads), indicating that the disorganized axons in Olig2-KO mice were TCAs (Fig. 4D). By E17.5, wild-type TCAs had formed a thin fasciculus in the dorsal thalamus and prethalamus including TRN, which extended in parallel, orienting ventrolaterally (Fig. 4E). By contrast, Olig2-KO netrin G1+ fibers formed an abnormally thick fasciculus and extended randomly in the dorsal thalamus (Fig. 4F, arrowheads). These observations indicate that, in the Olig2-KO diencephalon, the initial changes in prethalamus/TE regionalization are followed by later disorganized axonal fasciculation and extension (Fig. 4G).

Retarded and disorganized thalamocortical projection in the Olig2-KO forebrain

The Olig2-KO mouse prethalamus shows defects as early as E10.5, before the onset of TCA formation, suggesting that the initial stage of projection formation would be disorganized in Olig2-KO mice. We thus examined TCA at E13.5 using DiI axonal tracing. DiI-labeled TCAs were observed, orienting dorsolaterally in the ventral telencephalon of wild-type animals (Fig. 5A). By contrast, in Olig2-KO mice, DiI-labeled TCAs had just crossed the telencephalon-diencephalon boundary (TDB), and had not yet reached the lateral ganglionic eminence (Fig. 5B). Measuring the length of the TCAs in the ventral telencephalon between the growing tip and the TDB, Olig2-KO TCAs were much shorter (around 60% reduction) than those of wild-type animals (Fig. 5C). The result clearly shows a reduction of TCA extension at early stages in the absence of Olig2 (Fig. 5A,B, insets).

We further examined whether TCAs reach the cerebral cortex and whether topographic thalamocortical projection is formed in the Olig2-KO mouse. DiI was injected into the middle part of the E18.5 cortex, and DiA was injected into the frontal and occipital poles of the same brain (Fig. 6A,B, insets). The frontal cortex had a connection with the medial part of the thalamus, the middle part with the central part, and occipital cortex with the lateral part in both normal control and Olig2-KO mice (Fig. 6C,D). Therefore, the topography of the reciprocal projection was roughly preserved in the absence of Olig2. However, axon arrangement was markedly disorganized in the Olig2-KO thalamus: whereas axons were arranged in parallel in the wild-type thalamus, those in Olig2-KO formed a thick fasciculus and crossed each other with abnormal overlapping course of axons (Fig. 6C-F). On closer examination, retrogradely labeled cell bodies were observed in the Olig2-KO dorsal thalamus (Fig. 6F, arrows), indicating that TCAs in Olig2-KO reached the cerebral cortex in spite of the initial delay of their extension.

Disorganized TCAs extend from non-Olig2 lineage cells

Olig2 is strongly expressed in the VZ of the prethalamus and weakly in the caudoventral part of the dorsal thalamus, whereas TCAs have defects of axon extension; therefore, we examined whether the axonal extension defect in the Olig2-KO dorsal thalamus is induced in a cell-autonomous or a non-cell-autonomous manner. If TCA defects in Olig2-KO mice are induced in a cell-autonomous manner, they should be shown by Olig2 lineage neurons. To analyze this, we again used Olig2-KO;Rosa26^{GFP} mice, and tamoxifen was administered to pregnant mice at E11.5 and/or E12.5 to label Olig2+ cells. At E13.5, when NF-M+ axons were disorganized in the lateral part of the dorsal thalamus of Olig2-KO;Rosa26^{GFP} mouse, axon aggregates were found in the nucleus-free zones (supplementary material Fig. S6A,B, arrows). Nevertheless, processes of GFP+ Olig2-lineage cells were present in the prethalamus showing radial extension, but were not present in cell-free zones (supplementary material Fig. S6C,D, asterisks). At E17.5, GFP+ axons of Olig2-KO;Rosa26^{GFP} mice were observed in the TRN, whereas no GFP+ axons were present in the dorsal thalamus (supplementary material Fig. S6E). Abnormally oriented axons extending randomly were GFP negative (supplementary material Fig. S6F, arrowheads). These results indicated that axons showing disorganized elongation do not belong to Olig2 lineage neurons, suggesting non-cell autonomous defect of axonal extension in the Olig2-KO dorsal thalamus.

Altered expression of axon guidance molecules in the Olig2-KO prethalamus

As axon arrangement was impaired in the Olig2-KO mouse dorsal thalamus, and axonal disorganization occurred in a non-cell-autonomous manner, it is highly probable that the expressions of axon guidance molecules are altered in the terrain through which

Development (2014) 141, 2075-2084 doi:10.1242/dev.097790

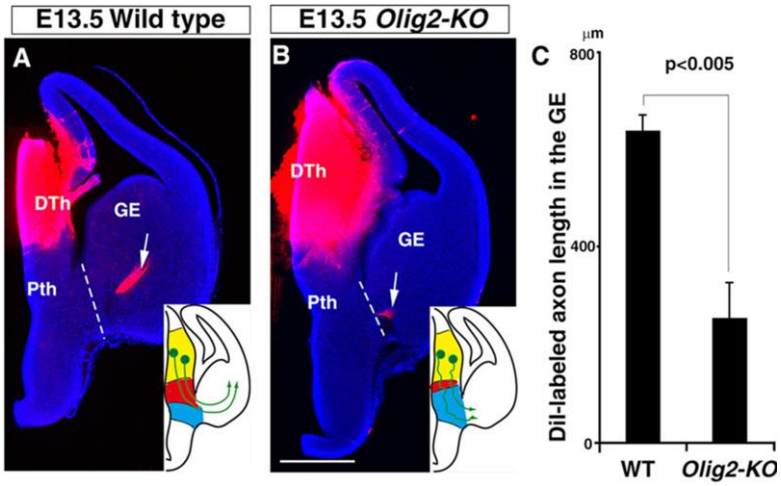

Fig. 5. Arrest of TCA extension at the initial stage of projection formation. (A,B) E13.5 forebrain with DiI crystal injection into the dorsal thalamus. Broken lines indicate the telencephalon-diencephalon boundary (TDB). Labeled TCAs had reached the lateral ganglionic eminence of the ventral telencephalon in the wild-type animal (arrow in A) whereas those in the Olig2-KO mouse had just crossed the TDB in the ventral telencephalon (arrow in B). DTh, dorsal thalamus; GE, ganglionic eminence; Pth, prethalamu. Insets show schematics of diencephalon regionalization and TCA extension. Scale bar: 500 μm. (C) Mean distance between the distal tip of DiI-labeled fibers and the TDB. Data are mean±s.e.m. (wild type, n=3; Olig2-KO, n=3; Student's t-test)

TCAs pass, including the prethalamus and the TE. We therefore conducted a microarray analysis for changes in the gene expression of axon guidance molecules in the diencephalon or basal forebrain comparing the transcriptomes of wild-type and Olig2-KO mice at E13.5 (Table 1). Efna, Epha and Sema genes, and Unc5c were shown to change their expression in the absence of Olig2. Using Allen Institute for Brain Science Web in situ hybridization data (http://developingmouse.brain-map.org/), we confirmed that Epha3 and Epha5 were expressed in the E13.5 diencephalon. We then examined the expression pattern of these molecules in the Olig2-KO diencephalon by in situ hybridization. In the E13.5 wild-type forebrain, the prethalamus is devoid of mRNA for Epha3 and Epha5, and the Ephas-negative region continues to the TDB (Fig. 7A,C, asterisks), and both Epha3 and Epha5 are expressed in the TE (Fig. 7A,C; supplementary material Fig. S7A,C,E,G,I,K,M,O; Kudo et al., 2005). In the age-matched Olig2-KO forebrain, the Epha3- and Epha5-expressing TE was dorsally expanded and, conversely, the Ephas-negative prethalamus were reduced in size (Fig. 7B,D; supplementary material Fig. S7B,D,F,H,J,L,N,P). Thus, malformed formation of the prethalamus and TE was accompanied with the altered expression of axon guidance molecules, likely leading to the altered extension of TCAs. EphrinA5 (Efna5), which encodes one of the ligands for EphA3, was expressed in the dorsal thalamus, which seemed to be unchanged in the absence of Olig2 (Fig. 7E,F).

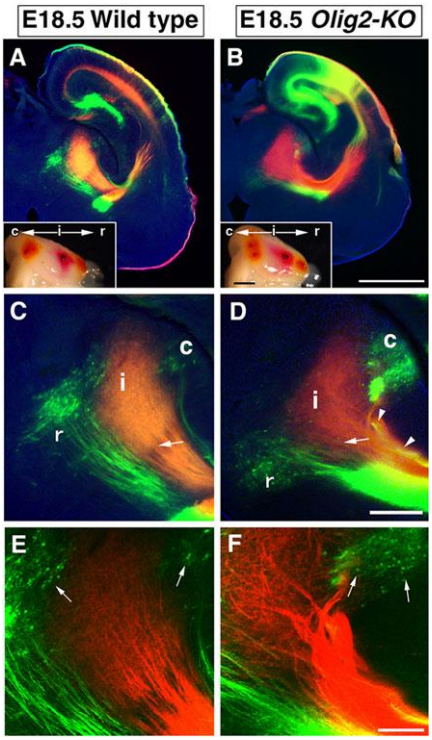

Fig. 6. Axonal tracing of reciprocal connection between the thalamus and cortex at E18.5. (A,B) Low-magnification pictures. Insets show injection sites of DiI (i, intermediate) and DiA (r, rostral; c, caudal). (C,D) Higher magnification pictures of the dorsal thalamus. c, i, r of the thalamus represent connections from c, i, r, respectively, of the cortical injection site. Arrows in C and D indicate positions of the external medullary laminae. Arrowheads in D indicate abnormal overlapping course of axons showing yellow color. (E,F) Laser scanning confocal micrographs. Arrows indicate retrogradely labeled cell bodies. Axons in the wild type are arranged in parallel (E), whereas those in Olig2-KO cross each other (F). Scale bars: 1 mm in B and inset; 200 μm in D; 100 μm in F.

Sema5a and Unc5c also showed changed expression in microarray analysis (Table 1); however, in situ hybridization analysis demonstrated that the expression patterns of Sema5a and Unc5c were not altered in the E13.5 diencephalon of Olig2-KO mice (not shown).

EphA3 suppresses axonal extension from cultured thalamic neurons

The above results strongly suggest that EphA3 and EphA5 are candidate molecules affecting the initial extension of TCAs. We next examined the roles of EphA3 in the neurite extension of dorsal thalamic neurons in vitro. Dissociated dorsal thalamic progenitor cells were cultured on the substrate double coated with PLL and either EphA3-Fc chimeric protein or human Fc for 40 h. Neurons were identified with class-III β tubulin immunohistochemistry (Fig. 8A,B). Neurite length on Fc-coated substrate was slightly but definitely different from that on EphA3 (33.3±2.38 μm and 24.4±2.90 μm, respectively, mean±s.e.m.) (Fig. 8C); thus, substrate-bound EphA3 apparently inhibited neurite extension from dorsal thalamic neurons.

Ectopic Olig2 does not affect EphA3 expression

We then examined whether Olig2 affects or suppresses EphA3 expression. In this experiment, we used a chick embryo neural tube, because gene expression hierarchy is well known in this region of the chick embryo (Liu et al., 2007; Mizuguchi et al., 2001) when compared with the fetal mouse diencephalon. Epha3 expression in the

Development (2014) 141, 2075-2084 doi:10.1242/dev.097790

Table 1. Microarray expression analysis of control versus Olig2-KO brains at E13.5

Gene name	Gene symbol	RefSeq transcript ID	Probe set ID	FcOlig2/wild type	P value
Ephrin A1	Efna1	NM_001162425 /NM_010107	1416895_at	1.37	0.01
Ephrin B1	Efnb1	NM_010110	1418286_a_at	1.46	0.00
Ephrin B2	Efnb2	NM_010111	1449549_at	1.75	0.02
Ephrin B2	Efnb2		1419639_at	1.40	0.03
Eph receptor A3	Epha3	NM_010140	1426057_a_at	1.95	0.00
Eph receptor A3	Epha3		1425574_at	1.59	0.00
Eph receptor A3	Epha3		1455426_at	1.35	0.00
Eph receptor A3	Epha3		1425575_at	1.29	0.01
Eph receptor A5	Epha5	NM_007937	1420557_at	1.67	0.01
Eph receptor A5	Epha5		1435286_at	1.12	0.04
Semaphorin 3E	Sema3e	NM_011348	1442226_at	1.56	0.00
Semaphorin 4B	Sema4b	NM_013659	1455678_at	1.41	0.03
Semaphorin 5A	Sema5a	NM_009154	1437422_at	0.61	0.01
UNC-5 homolog C	Unc5c	NM_009472	1449522_at	0.79	0.01

Significant changes were observed in genes encoding these axon guidance molecules.

normal E6 chick spinal cord was observed in the ventral VZ and ventral horn (VH). In the VZ, Epha3 expression was partially overlapped with Olig2, whereas motoneurons in the ventral horn, which are of Olig2 lineage, do not express Olig2. Olig2 was transfected to the E3 chick neural tube and E6 spinal cord was examined with GFP, Olig2, Islet1/2 and HB9 immunohistochemistry, and Epha3 in situ hybridization. Olig2 was overexpressed on the electroporated side (supplementary material Fig. S8A,B), which induced ectopic Islet1/2 but did not induce HB9 (not shown). Signal intensity of Epha3 expressed in the VZ and VH was measured with ImageJ software, and the ratio of electroporated side/non-electroporated side was calculated and compared between Olig2-transfected and GFP-transfected samples. Signal intensity was not changed after Olig2 or EGFP transfection in both VZ and the ventral horn (supplementary material Fig. S8F). The ratio was 0.94-1.01 and was not statistically significant. The results indicate that ectopic overexpression of Olig2 does not affect Epha3 expression.

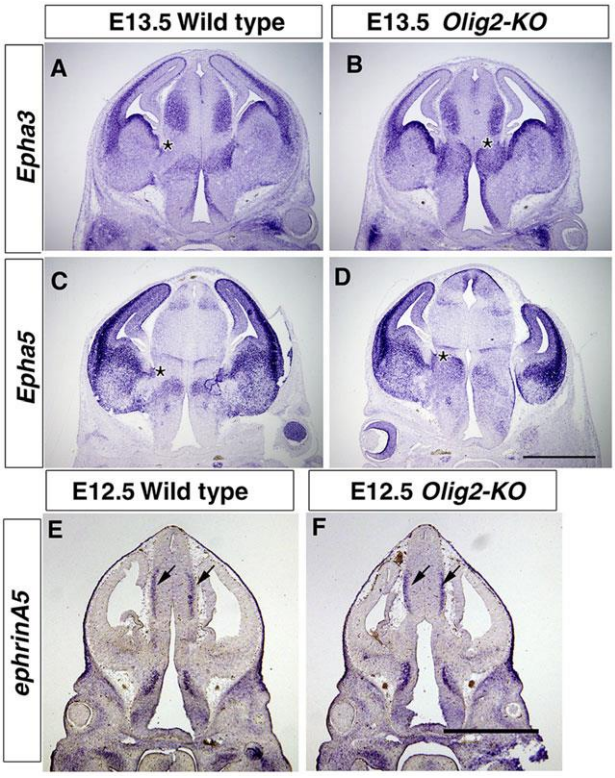

Fig. 7. Altered expression of Epha3 and Epha5 in the E13.5 Olig2-KO mouse diencephalon. (A,B) Epha3 in situ hybridization. (C,D) Epha5 in situ hybridization. Note that an Ephas-negative area is observed in the control prethalamus, being intercalated between the dorsal thalamus and the ventral telencephalon (asterisks in A and C). By contrast, the Ephas-negative area is very narrow in the Olig2-KO diencephalon (asterisks in B and D). (E,F) EphrinA5 (Efna5) in situ hybridization. EphrinA5 is expressed in both the wild-type and Olig2-KO dorsal thalamus (arrows). Scale bars: 1 mm.

DISCUSSION

In the present study, the Olig2-KO mouse diencephalon was examined morphologically, and we found malformation of the prethalamus and TE, followed by disorganized extension of TCAs. These results indicate that Olig2 controls proper formation of the prethalamus and also that proper formation of the prethalamus controls the initial extension of TCAs. Together, our results provide possible molecular mechanisms underlying initial TCA extension in the prethalamus.

Olig2 regulates proper formation of the prethalamus

Olig2 is expressed in VZ cells of the prethalamus, which develops into TRN and the zona incerta (Inamura et al., 2011), which are mostly composed of GABAergic neurons (Ottersen and Storm-Mathisen, 1984). We previously demonstrated that distribution of GABAergic neurons is nearly normal in the Olig2-KO forebrain compared with normal control animals (Ono et al., 2008), and a fate-mapping study demonstrated that Olig2 lineage cells differentiate into GABAergic neurons in the absence of Olig2 (Takebayashi et al., 2008). In the present study, we examined the formation of the prethalamus at much younger stages: E10.5-E13.5. The Dlx2-positive, as well as Lhx5-negative, prethalamus in Olig2-KO mice was markedly reduced in size (Figs 1, 2). Accompanying the size reduction of the prethalamus, the TE expanded dorsally. The reduced size of the prethalamus is probably caused both by elevated apoptosis at E10.5 (supplementary material Fig. S2) and by the fate change of Olig2 lineage cells from prethalamus cells to TE cells (Fig. 3; supplementary material Fig. S4). It is noteworthy that this is the first demonstration of Olig2 function in early forebrain patterning beyond its known role in glial development (Cai et al., 2007; Lu et al., 2002; Ono et al., 2008, 2009). We previously

Development (2014) 141, 2075-2084 doi:10.1242/dev.097790

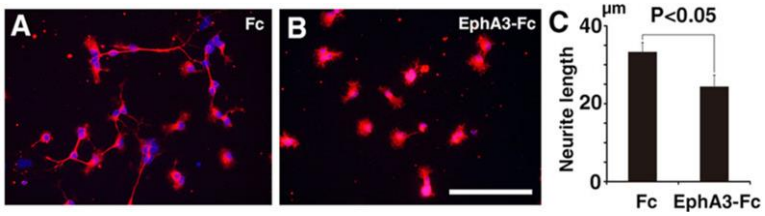

Fig. 8. Suppression of neurite extension from cultured thalamic neurons by EphA3. (A,B) Dissociated thalamus progenitor cells were cultured on substrate double-coated with poly-L-lysine and with human Fc (A) or mouse EphA3-human Fc (B) chimeric protein. Cultured cells were stained with class-III β tubulin immunohistochemistry (red). (C) Neurite extension was apparently impaired on substrate coated with EphA3. n=3 independent cultures. Scale bar: 100 μm in B.

reported that loss of Olig2 does not affect apoptosis in the pMN domain (Takebayashi et al., 2008). Other parts of the E10.5 forebrain regions, such as the Dlx2-positive ganglionic eminence or (Dlx2-negative) cerebral cortex, revealed a similar level of apoptosis (not shown). Therefore, involvement of Olig2 in the apoptotic pathway might be dependent on the stage or region of the central nervous system. In addition, it is probable that Olig2 interacts with other transcription factors, such as Tbr2, for proper boundary formation in the TE, as has been reported in the developing neural tube (Helms and Johnson, 2003). Further studies are necessary to clarify the mechanisms of Olig2 function in forebrain patterning.

Proper formation of the prethalamus and TE is required for early thalamocortical projection

Another important new finding is that loss of Olig2 results in retardation of initial TCA extension, which leads to abnormal fasciculation and random orientation of TCA at the late fetal stage (Figs 4-6). It is highly probable that the delay of TCA extension is caused by reduction of prethalamus formation and expansion of the TE, both of which are induced by loss of Olig2: (1) the prethalamus occupies an exit region for TCAs; (2) a defect in the thalamocortical projection was probably induced in a non-cell-autonomous manner (see supplementary material Fig. S6); (3) EphA3 and EphA5 expression is observed in the TE but not in the prethalamus; (4) EphA3 and EphA5 expression occupies the route of TCA extension in the Olig2-KO diencephalon (Fig. 7; supplementary material Fig. S7); (5) ephrinA5, a possible counterpart molecule of EphA3, is expressed in the dorsal thalamus; (6) substrate-bound EphA3 suppresses neurite extension from thalamic neurons in vitro (Fig. 8). Eph receptors and ephrin ligands act as a repellant molecule system in neural circuit formation. In addition, ephrin A proteins also recognize and transduce the reverse signaling of EphA proteins, which also includes axon repulsion (Rashid et al., 2005; Xu and Henkemeyer, 2012). Together, these observations suggest that the Epha3- and Epha5-negative prethalamus may provide a permissive or less inhibitory substrate for TCAs, and that occupation of Epha3 and Epha5 in the exit route impairs initial extension of TCAs in the Olig2-KO diencephalon. It is probable that EphA3 negatively regulates TCA elongation, and, therefore, expansion of Ephas-positive TE may impair initial TCA extension in the Olig2-KO forebrain (Figs 4, 5).

Another possible functional role of the prethalamus in TCA extension is contact guidance of prethalamic axons to TCAs. Mitrofanis and Baker (Mitrofanis and Baker, 1993) proposed that pioneer fibers from the prethalamus extending into the thalamus guide TCAs to the prethalamus. Our observation might support the possible association of thalamic and prethalamic axons as these axons do not express a combination of repellant molecules; while thalamic axons may express ephrinA5, its counterpart molecules EphA3 and EphA5 are not expressed in prethalamic axons (Fig. 7). It remains unknown whether these axons express molecules that mediate contact attraction.

The Olig2-KO forebrain includes other minor defects. For example, the prethalamus region at E11.5 and E12.5 was constricted in Olig2-KO mice (Fig. 1, Fig. 7E,F). This constriction was, however, partially recovered by E13.5 (Figs 2, 3, Fig. 7A-D) [probably owing to elevated proliferation in the Olig2-KO prethalamus (supplementary material Fig. S2H)], and cytoarchitecture, such as radial arrangement of the prethalamic cells and radial fiber extension, was preserved normally in the absence of Olig2 (Fig. 3D; supplementary material Fig. S6). Therefore, the constriction of the prethalamus at early stages may not be the cause of the retardation of TCAs in the Olig2-KO forebrain, although this possibility cannot be ruled out completely. In addition, the dorsal thalamus of the Olig2-KO mouse shows slight hypoplasia (supplementary material Fig. S3K), and the EphA3-positive region is also slightly reduced in the Olig2-KO thalamus (Fig. 7). We could not clarify whether the slight reduction of EphA3 expression in the dorsal thalamus affects the initial delay of TCA extension. However, as EphA3 negatively regulates TCA extension, reduction of EphA3 expression might not have a strong effect on the initial delay of axon elongation. As hypoplasia of the prethalamus is the severest defect within the Olig2-KO diencephalon, it is the most likely cause of the initial retardation and impairment of TCA guidance.

The prethalamus and TE have been supposed to be intermediate targets for formation of the thalamocortical projection, as loss of transcription factors expressed in these regions induces defects of thalamocortical projection, which includes Pax6, Mash1 (Ascl1 – Mouse Genome Informatics), Tbr1 (López-Bendito and Molnár, 2003), Dlx1/2 and Ebf1 (Garel et al., 2002) and Olig2 (present study). Transcription factors regulate region identity in the rostral-caudal axis (Kiecker and Lumsden, 2004; Puelles and Rubenstein, 2003; Rubenstein et al., 1998) and cell-fate determination in the dorsoventral axis (Helms and Johnson, 2003; Tanabe and Jessell, 1996). Recently, evidence has supported that transcription factors regulating cell-type specification also regulate cell migration and neural circuit formation (Chédotal and Rijli, 2009; Shirasaki et al., 2006). Cell-fate determination may include the cell-type-specific behavior of committed cells through regulation of the expression of cytoskeletal molecules and receptors for axon guidance molecules.

In our observations, prethalamus formation is controlled by Olig2, which leads to EphA3- and EphA5-negative terrain for the initial extension of TCAs; therefore, transcription factors also control the milieu or environment for axon elongation, regulating neural circuit formation indirectly. As Olig2 may not suppress or regulate EphA3 expression directly (supplementary material Fig. S8) and as the expression of morphogen molecules that may affect EphA3 expression was not altered in the Olig2-KO diencephalon (supplementary material Fig. S3D,E,I,J), it is probable that putative programs for TE formation regulate EphA3 expression. Olig2 is involved in multistep processes of diencephalon formation and may indirectly repress EphA3 expression through interacting with transcription factors involved in TE development.

In conclusion, the present study elucidates that Olig2 is crucial for proper formation of the prethalamus, especially the boundary between the prethalamus and TE, and that proper formation of the prethalamus is crucial for correct extension of TCAs. Therefore,

Development (2014) 141, 2075-2084 doi:10.1242/dev.097790

appropriate regionalization of the prethalamus and TE provides a pathway from the dorsal thalamus to the ventral telencephalon.

MATERIALS AND METHODS

Animals and tissue preparation

The animals used in this study were Olig2^{KICreER} (Takebayashi et al., 2002b), Olig2$^{-/-}$ (Lu et al., 2002), ROSA26-GAP43-EGFP (Nakahira et al., 2006) and wild-type ICR mice (Slc, Shizuoka, Japan). Genotyping was performed as described previously (Takebayashi et al., 2002b; Tatsumi et al., 2008). Fertilized chick eggs were purchased from Yamagishi Corporation (Mie, Japan) and were incubated at 37°C. Embryonic stages of chicks were determined according to Hamburger and Hamilton (Hamburger and Hamilton, 1951). At least three independent experiments were carried out in all histological and culture analyses, including DiI tracing. All animal procedures were approved by the Animal Research Committee of Kyoto Prefectural University of Medicine and of the National Institute for Physiological Sciences.

To obtain Olig2-KO mice, Olig2^{KICreER} heterozygous mice were mated and the day when the vaginal plug was found was regarded as embryonic day 0.5 (E0.5). To label Olig2 lineage cells, Olig2^{KICreER};ROSA26-GAP43-EGFP double heterozygous mice were mated, and tamoxifen (TM; 3 mg/animal) was injected intraperitoneally into pregnant mothers with fetuses at E10.5, E11.5 or E11.5 and E12.5, as described previously (Masahira et al., 2006). Pregnant mice were deeply anesthetized with pentobarbital (100 mg/kg body weight), and fetal mice were removed from the uterus. Fetal mouse brains were fixed with 4% paraformaldehyde (PFA) in PBS overnight, and subsequently with 20% sucrose in PBS. Fixed brains were cut coronally with a cryostat at 20 µm, and sections were thaw-mounted onto MAS-coated glass slides (Matsunami Glass, Tokyo, Japan).

In situ hybridization

In situ hybridization was performed using digoxygenin-labeled antisense riboprobes, as described previously (Ding et al., 2005; Wilkinson, 1998). cDNAs used in this study were as follows: mDlx2 (NM_010054, nt_746-1355), mephrinA5 (NM_207654, nt204-831), mUuc5c (Watanabe et al., 2006), mEpha3 (NM_010140, nt_2760-3340), mEpha5 (NM_007937, nt_1135-2100), mFgf8 (Ohuchi et al., 1994), mOlig3 (Takebayashi et al., 2002a), mLhx5 (Hirata et al., 2006), mShh (Iseki et al., 1996), mSema5a (NM_009154, nt_634-1162) and chick EphA3 (Iwamasa et al., 1999). Sense probes were used as a negative control, which did not show specific signals.

Immunohistochemistry

Immunohistochemistry was carried out as previously described (Ono et al., 2004, 2008). The GFP signal in the Rosa26-GAP43-EGFP reporter mouse brain was enhanced by incubation with fluorescein-conjugated tyramide (Tyramide Signal Amplification-Fluorescein Systems; PerkinElmer Life Science, Boston, MA, USA). Primary antibodies used were: rabbit anti-Olig2 (1:1000, AB9610; Millipore, Temecula, CA, USA; 1:500, 0B-905; IBL, Takasaki, Japan), rabbit anti-GFP (1:1000, AB3080; Millipore), rat anti-GFP (1:1000, 04404-84; Nacalai Tesque, Kyoto, Japan), rabbit anti-calretinin (1:1000, 7697; Swant, Marly, Switzerland), rabbit anti-Tbr1 (1:500, ab31940; Abcam, Cambridge, UK), rabbit anti-Tbr2 (1:500, ab23345; Abcam), mouse anti-Islet1/2 (4D5, 1:50; DSHB), mouse anti-neurofilament M (Watanabe et al., 2006), mouse anti-netrin G1 (1:500; Niimi et al., 2007), rabbit anti-netrin G1 (1:10; Niimi et al., 2007), mouse anti-HB9 (1:50, 5C10; DSHB), rabbit anti-cleaved caspase 3 (1:500, 9661; Cell Signaling, Danvers, MA), rabbit anti-Cre (1:1000, 69050-3; Novagen, San Diego, CA) and rabbit anti-phospho-histone H3 (pH3; 1:500, 06-570; Millipore). Stained sections were observed under a bright field and epifluorescent microscope (BX-51; Olympus, Tokyo, Japan), and images were captured via a CCD camera (DP-71; Olympus).

Axonal tracing with lipophilic carbocyanine dye

In order to label early TCAs in the E13.5 brain, crystals of lipophilic dye DiI (1,1^{0}-dioctadecyl-3,3,3^{0},3^{0}-tetramethylindocarbocyanine perchlorate; Invitrogen, Eugene, OR, USA) were applied to the dorsal thalamus of wild-type and Olig2-KO animals after fixation. Tissues were kept in 4% PFA at 37°C for 4 days. To label reciprocal connections between the dorsal thalamus and cortex in the E17.5 and E18.5 cortex, 2% solutions of DiI and DiA [4-(4-(dihexadecylamino)styryl)-N-methylpyridinium iodide; Invitrogen] were used as tracers. DiA was injected into the frontal and occipital poles, and DiI was injected into the middle part of the cortex (Fig. 6A,B, insets). They were kept at 37°C in the fixative for 2 weeks and then cut coronally with a vibratome at 100 µm. Sections were stained with Hoechst33342, and observed under an epifluorescent microscope and a confocal laser scanning microscope (FV-1000; Olympus).

Microarray preparation, processing and statistical analysis

The samples were grouped into two sample types: Olig2-KO (Lu et al., 2002) and the wild type. RNA was purified from the E13.5 ventral forebrain from Olig2-KO (Olig2$^{-/-}$) and the wild type (Olig2$^{+/+}$). RNA samples were prepared by pooling RNAs extracted from three brains to constitute one replicate and each sample type was prepared in five replicates. cRNA hybridization probes were hybridized to Affymetrix Mouse Whole Genome MOE430 2.0 arrays. The R-CRAN statistical language and Bioconductor software package (Gentleman et al., 2004) were used throughout the expression analyses. Raw image files were processed using Affymetrix GCOS and the Microarray Suite (MAS) 5.0 algorithm. The probe signal levels were quantile normalized, summarized and then transformed to the log 2 expression using GCRMA (gcrma R-package; Irizarry et al., 2003) and Frozen RMA (fRMA package; McCall and Irizarry, 2011). Gene filtering was performed using the Wilcoxon signed-rank test to select probe sets that were ‗consistently expressed' ($P<0.04$) in at least one group (mas5calls R-package; Bioconductor). All samples showed good quality control according to MAS5.0 guidelines and the AffyQC report (R-package; Bioconductor). Principal component analysis (PCA) was used to reduce the dimensionality of the whole dataset and measure the degree of similarity between samples (dudi.pca R-package; Thioulouse and Dray, 2007). We had to withdraw two replicates from each sample type as they were aberrant. The subsequent three-dimensional PCA plot confirmed a high degree of similarity among samples of the same sample type and much less similarity among samples of different sample types. We used LIMMA statistical analysis (Smyt, 2004) to determine the differentially expressed genes in Olig2-KO. The resulting P-values were adjusted to FDR <5% with the Benjamini-Hochberg method to control the mean proportion of false positives (q-value R-package; Storey and Tibshirani, 2003) and a kernel-based FDR method to assess the probability of being false positive for a specific gene (kerfdr R-package; Guedj et al., 2009). Microarray data have been deposited in Gene Expression Omnibus with accession number GSE56389.

Dissociation culture of dorsal thalamus neurons

The dorsal thalamus at E12.5 was dissected free from the fetal brain, minced into small pieces, treated with 0.1% trypsin for 15 min at 37°C, and then triturated with a fire-polished pasture pipette. Dissociated cell suspension (1×10^{5} cells/ml) was prepared in culture medium (MEM containing 5% fetal bovine serum and 5% horse serum). For analyses of the substrate-bound form of EphA3, plastic dishes (35 mm in diameter) were sequentially coated with poly-L lysine (PLL, 80 µg/ml; Sigma, St Louis, MO, USA) overnight at 4°C and then with mouse EphA3-human Fc or human Fc (100 nM; R&D Systems, Minneapolis, MN, USA) for 5 h at 37°C. After rinsing the culture substrates with PBS, 2 ml thalamic cell suspension was plated onto the culture dishes. Cultures were maintained for 40 h. They were fixed with 4% PFA and stained with anti-class III β tubulin antibody (1:1000, G7121; Promega) to examine neurite extension. Three independent culture experiments were performed. In each experiment, epifluorescent photomicrographs were taken of 9-15 randomly chosen fields and the length of neurites with more than 50 labeled cells was measured with ImageJ software (NIH).

Electroporation

In ovo electroporation was performed as previously described (Ono et al., 2004). E3 chick embryos (HH stage 17-20; Hamburger and Hamilton, 1951) were used. DNA of pCAGGS-EGFP (Gotoh et al., 2011) solution with or

without pCAGGS-mOlig2 (Mizuguchi et al., 2001) was injected into the central canal, and square pulses (30 V, 50 ms, twice; Nihon Koden, SEN-3401) were delivered to the embryos. The embryos were fixed at E6 (HH stage 27-29) and analyzed histologically. Gene expression was analyzed as the ratio of signal intensity between the electroporated side and non-electroporated side, and the ratio of Olig2-transfected samples was compared with that of EGFP-transfected samples.

Image analysis

The area of the Dlx2+ region and neurite length both in vivo and in vitro was measured with ImageJ software after images were captured with a CCD camera as above. In all cases, quantitative analysis was carried out using at least three Olig2-KO or wild-type/heterozygous mice.

Acknowledgements

Some monoclonal antibodies were obtained from DSHB. We thank Dr Martyn Goulding (The Salk Institute) for providing the reporter mouse, and Drs Hideaki Tanaka (Kumamoto University), Hideyo Ohuchi (Okayama University), Masahiko Hibi (Nagoya University), Jun-ichi Miyazaki (Osaka University) and Kazunori Nakajima (Keio University) for cDNAs and helpful comments.

Competing interests

The authors declare no competing financial interests.

Author contributions

The project was designed by K.O., H.T., K.S. and K.I. Histological and culture experiments were performed by K.O., A.C., T.N., H.G., A.U., O.A., Q.Z. and S.I., and microarray analysis was carried out by A.C., C.M.P. and O.A. The manuscript was written by K.O. and H.T. with the remaining authors commenting on the manuscript.

Funding

This work was supported by Grants-in-Aid for Scientific Research (C) and an Innovated Area (Neural Diversity and Neocortical Organization) provided by JSPS and MEXT, Japan (to K.O.); by the Cooperative Study Program of NIPS (to K.O., H.T., H.G. and K.I.); by Kumamoto University (K.O., H.T., H.G. and K.S.); by FIRST program (to S.I.); by ARSEP scholarships (A.C.); and by Institut National de la Sante et de la Recherche Medicale and the program ‗Investissements d'Avenir' [ANR-1-IAIHU-06] (C.M.P).

Supplementary material

Supplementary material available online at
http://dev.biologists.org/lookup/suppl/doi:10.1242/dev.097790/-/DC1

References

Abbott, L. C. and Jacobowitz, D. M. (1999). Developmental expression of calretinin-immunoreactivity in the thalamic eminence of the fetal mouse. Int. J. Dev. Neurosci. 17, 331-345.

Braisted, J. E., Catalano, S. M., Stimac, R., Kennedy, T. E., Tessier-Lavigne, M., Shatz, C. J. and O'Leary, D. M. (2000). Netrin-1 promotes thalamic axon growth and is required for proper development of the thalamocortical projection. J. Neurosci. 20, 5792-5801.

Braisted, J. E., Ringstedt, T. and O'Leary, D. D. M. (2009). Slits are chemorepellents endogenous to hypothalamus and steer thalamocortical axons into ventral telencephalon. Cereb. Cortex 19 Suppl. 1, i144-i151.

Bulfone, A., Puelles, L., Porteus, M. H., Frohman, M. A., Martin, G. R. and Rubenstein, J. L. (1993). Spatially restricted expression of Dlx-1, Dlx-2 (Tes-1), Gbx-2, and Wnt-3 in the embryonic day 12.5 mouse forebrain defines potential transverse and longitudinal segmental boundaries. J. Neurosci. 13, 3155-3172.

Bulfone, A., Smiga, S. M., Shimamura, K., Peterson, A., Puelles, L. and Rubenstein, J. L. R. (1995). T-Brain-1: a homolog of Brachyury whose expression defines molecularly distinct domains within the cerebral cortex. Neuron 15, 63-78.

Cai, J., Chen, Y., Cai, W.-H., Hurlock, E. C., Wu, H., Kernie, S. G., Parada, L. F. and Lu, Q. R. (2007). A crucial role for Olig2 in white matter astrocyte development. Development 134, 1887-1899.

Chedotal, A. and Rijli, F. M. (2009). Transcriptional regulation of tangential neuronal migration in the developing forebrain. Curr. Opin. Neurobiol. 19, 139-145.

Deng, J. and Elberger, A. J. (2003). Corticothalamic and thalamocortical pathfinding in the mouse: dependence on intermediate targets and guidance axis. Anat. Embryol. 207, 177-192.

Ding, L., Takebayashi, H., Watanabe, K., Ohtsuki, T., Tanaka, K. F., Nabeshima, Y.-i., Chisaka, O., Ikenaka, K. and Ono, K. (2005). Short-term lineage analysis of dorsally derived Olig3 cells in the developing spinal cord. Dev. Dyn. 234, 622-632.

Dufour, A., Seibt, J., Passante, L., Depaepe, V., Ciossek, T., Frisen, J., Kullander, K., Flanagan, J. G., Polleux, F. and Vanderhaeghen, P. (2003). Area specificity and topography of thalamocortical projections are controlled by ephrin/Eph genes. Neuron 39, 453-465.

Garel, S., Yun, K., Grosschedl, R. and Rubenstein, J. L. R. (2002). The early topography of thalamocortical projections is shifted in Ebf1 and Dlx1/2 mutant mice. Development 129, 5621-5634.

Gentleman, R. C., Carey, V. J., Bates, D. M., Bolstad, B., Dettling, M., Dudoit, S., Ellis, B., Gautier, L., Ge, Y. C., Gentry, J. et al. (2004). Bioconductor: open software development for computational biology and bioinformatics. Genome Biol. 5, R80.

Gotoh, H., Ono, K., Takebayashi, H., Harada, H., Nakamura, H. and Ikenaka, K. (2011). Genetically-defined lineage tracing of Nkx2.2-expressing cells in chick spinal cord. Dev. Biol. 349, 504-511.

Guedj, M., Robin, S., Celisse, A. and Nuel, G. (2009). Kerfdr: a semi-parametric kernel-based approach to local false discovery rate estimation. BMC Bioinformatics 10, 84.

Hamburger, V. and Hamilton, H. L. (1951). A series of normal stages in the development of the chick embryo. J. Morphol. 88, 49-92.

Helms, A. W. and Johnson, J. E. (2003). Specification of dorsal spinal cord interneurons. Curr. Opin. Neurobiol. 13, 42-49.

Hirata, T., Nakazawa, M., Muraoka, O., Nakayama, R., Suda, Y. and Hibi, M. (2006). Zinc-finger genes Fez and Fez-like function in the establishment of diencephalon subdivisions. Development 133, 3993-4004.

Inamura, N., Ono, K., Takebayashi, H., Zalc, B. and Ikenaka, K. (2011). Olig2 lineage cells generate GABAergic neurons in the prethalamic nuclei, including the zona incerta, ventral lateral geniculate nucleus and reticular thalamic nucleus. Dev. Neurosci. 33, 118-129.

Irizarry, R. A., Ooi, S. L., Wu, Z. and Boeke, J. D. (2003). Use of mixture models in a microarray-based screening procedure for detecting differentially represented yeast mutants. Stat. Appl. Genet. Mol. Biol. 2, Article1.

Iseki, S., Araga, A., Ohuchi, H., Nohno, T., Yoshioka, H., Hayashi, F. and Noji, S. (1996). Sonic hedgehog is expressed in epithelial cells during development of whisker, hair, and tooth. Biochem. Biophys. Res. Commun. 218, 688-693.

Iwamasa, H., Ohta, K., Yamada, T., Ushijima, K., Terasaki, H. and Tanaka, H. (1999). Expression of Eph receptor tyrosine kinases and their ligands in chick embryonic motor neurons and hindlimb muscles. Dev. Growth Differ. 41, 685-698.

Kiecker, C. and Lumsden, A. (2004). Hedgehog signaling from the ZLI regulates diencephalic regional identity. Nat. Neuroci. 7, 1242-1249.

Kudo, C., Ajioka, I., Hirata, Y. and Nakajima, K. (2005). Expression profiles of EphA3 at both the RNA and protein level in the developing mammalian forebrain. J. Comp. Neurol. 487, 255-269.

Leyva-Diaz, E. and Lopez-Bendito, G. (2013). In and out from the cortex: development of major forebrain connections. Neuroscience 254, 26-44.

Liu, Z., Hu, X., Cai, J., Liu, B., Peng, X., Wegner, M. and Qiu, M. (2007). Induction of oligodendrocyte differentiation by Olig2 and Sox10: evidence for reciprocal interactions and dosage-dependent mechanisms. Dev. Biol. 302, 683-693.

Lopez-Bendito, G. and Molnar, Z. (2003). Thalamocortical development: how are we going to get there? Nat. Rev. Neurosci. 4, 276-289.

Lopez-Bendito, G., Cautinat, A., Sanchez, J. A., Bielle, F., Flames, N., Garratt, A. N., Talmage, D. A., Role, L. W., Charnay, P., Marın, O. and Garel, S. (2006). Tangential neuronal migration controls axon guidance: a role for neuregulin-1 in thalamocortical axon navigation. Cell 125, 127-142.

Lu, Q. R., Sun, T., Zhu, Z., Ma, N., Garcia, M., Stiles, C. D. and Rowitch, D. H. (2002). Common developmental requirement for Olig function indicates a motor neuron/oligodendrocyte connection. Cell 109, 75-86.

Masahira, N., Takebayashi, H., Ono, K., Watanabe, K., Ding, L., Furusho, M., Ogawa, Y., Nabeshima, Y.-i., Alvarez-Buylla, A., Shimizu, K. et al. (2006). Olig2-positive progenitors in the embryonic spinal cord give rise not only to motoneurons and oligodendrocytes, but also to a subset of astrocytes and ependymal cells. Dev. Biol. 293, 358-369.

McCall, M. N. and Irizarry, R. A. (2011). Thawing frozen robust multi-array analysis (fRMA). BMC Bioinformatics 12, 369.

Mitrofanis, J. and Baker, G. E. (1993). Development of the thalamic reticular and perireticular nuclei in rats and their relationship to the course of growing corticofugal and corticopetal axons. J. Comp. Neurol. 338, 575-587.

Mizuguchi, R., Sugimori, M., Takebayashi, H., Kosako, H., Nagao, M., Yoshida, S., Nabeshima, Y.-i., Shimamura, K. and Nakafuku, M. (2001). Combinatorial roles of olig2 and neurogenin2 in the coordinated induction of pan-neuronal and subtype-specific properties of motoneurons. Neuron 31, 757-771.

Molnar, Z., Garel, S., Lopez-Bendito, G., Maness, P. and Price, D. J. (2012). Mechanisms controlling the guidance of thalamocortical axons through the embryonic forebrain. Eur. J. Neurosci. 35, 1573-1585.

Nakahira, E., Kagawa, T., Shimizu, T., Goulding, M. D. and Ikenaka, K. (2006). Direct evidence that ventral forebrain cells migrate to the cortex and contribute to the generation of cortical myelinating oligodendrocytes. Dev. Biol. 291, 123-131.

Nakashiba, T., Nishimura, S., Ikeda, T. and Itohara, S. (2002). Complementary expression and neurite outgrowth activity of netrin-G subfamily members. Mech. Dev. 111, 47-60.
Niimi, K., Nishimura-Akiyoshi, S., Nakashiba, T. and Itohara, S. (2007). Monoclonal antibodies discriminating netrin-G1 and netrin-G2 neuronal pathways. J. Neuroimmunol. 192, 99-104.
Ohuchi, H., Yoshioka, H., Tanaka, A., Kawakami, Y., Nohno, T. and Noji, S. (1994). Involvement of androgen-induced growth factor (FGF-8) gene in mouse embryogenesis and morphogenesis. Biochem. Biophys. Res. Commun. 204, 882-888.
Ono, K., Yasui, Y. and Ikenaka, K. (2004). Lower rhombic lip-derived cells undergo transmedian tangential migration followed by radial migration in the chick embryo brainstem. Eur. J. Neurosci. 20, 914-922.
Ono, K., Takebayashi, H., Ikeda, K., Furusho, M., Nishizawa, T., Watanabe, K. and Ikenaka, K. (2008). Regional- and Temporal-dependent changes in the differentiation of Olig2 progenitors in the forebrain, and the impact on astrocyte development in the dorsal pallium. Dev. Biol. 320, 456-468.
Ono, K., Takebayashi, H. and Ikenaka, K. (2009). Olig2 transcription factor in the developing and injured forebrain; Cell lineage and glial development. Mol. Cells 27, 397-401.
Ottersen, O. P. and Storm-Mathisen, J. (1984). GABA-containing neurons in the thalamus and pretectum of the rodent. An immunohistochemical study. Anat. Embryol. 170, 197-207.
Puelles, L. (2001). Brain segmentation and forebrain development in amniotes. Brain Res. Bull. 55, 695-710.
Puelles, L. and Rubenstein, J. L. R. (2003). Forebrain gene expression domains and the evolving prosomeric model. Trends Neurosci. 26, 469-476.
Rashid, T., Upton, A. L., Blentic, A., Ciossek, T., Knoll, B., Thompson, I. D. and Drescher, U. (2005). Opposing gradients of ephrin-As and EphA7 in the superior colliculus are essential for topographic mapping in the mammalian visual system. Neuron 47, 57-69.
Rubenstein, J. L. R., Shimamura, K., Martinez, S. and Puelles, L. (1998). Regionalization of the prosencephalic neural plate. Annu. Rev. Neurosci. 21, 445-477.
Shirasaki, R., Lewcock, J. W., Littieri, K. and Pfaff, S. L. (2006). FGF as a target-derived chemoattractant for developing motor axons genetically programmed by the LIM code. Neuron 50, 841-853.
Smyth, G. K. (2004). Linear models and empirical bayes methods for assessing differential expression in microarray experiments. Stat. Appl. Genet. Mol. Biol. 3, Article3.
Storey, J. D. and Tibshirani, R. (2003). Statistical significance for genomewide studies. Proc. Natl. Acad. Sci. U.S.A. 100, 9440-9445.
Takebayashi, H., Ohtsuki, T., Uchida, T., Kawamoto, S., Okubo, K., Ikenaka, K., Takeichi, M., Chisaka, O. and Nabeshima, Y.-i. (2002a). Non-overlapping expression of Olig3 and Olig2 in the embryonic neural tube. Mech. Dev. 113, 169-174.
Takebayashi, H., Nabeshima, Y., Yoshida, S., Chisaka, O., Ikenaka, K. and Nabeshima, Y.-i. (2002b). The basic helix-loop-helix factor olig2 is essential for the development of motoneuron and oligodendrocyte lineages. Curr. Biol. 12, 1157-1163.
Takebayashi, H., Usui, N., Ono, K. and Ikenaka, K. (2008). Tamoxifen modulates apoptosis in multiple modes of action in CreER mice. Genesis 46, 775-781.
Tanabe, Y. and Jessell, T. M. (1996). Diversity and pattern in the developing spinal cord. Science 274, 1115-1123.
Tatsumi, K., Takebayashi, H., Manabe, T., Tanaka, K. F., Makinodan, M., Yamauchi, T., Makinodan, E., Matsuyoshi, H., Okuda, H., Ikenaka, K. et al. (2008). Genetic fate mapping of Olig2 progenitors in the injured adult cerebral cortex reveals preferential differentiation into astrocytes. J. Neurosci. Res. 86, 3494-3502.
Thioulouse, J. and Dray, S. (2007). Interactive multivariate data analysis in R with the ade4 and ade4TkGUI packages. J. Stat. Soft. 22, 1-14.
Torii, M. and Levitt, P. (2005). Dissociation of corticothalamic and thalamocortical axon targeting by an EphA7-mediated mechanism. Neuron 48, 563-575.
Uemura, M., Nakao, S., Suzuki, S. T., Takeichi, M. and Hirano, S. (2007). OL-protocadherin is essential for growth of striatal axons and thalamocortical projections. Nat. Neurosci. 10, 1151-1159.
Vanderhaeghen, P. and Polleux, F. (2004). Developmental mechanisms patterning thalamocortical projections: intrinsic, extrinsic and in between. Trends Neurosci. 27, 384-391.
Vue, T. Y., Aaker, J., Taniguchi, A., Kazemzadeh, C., Skidmore, J. M., Martin, D. M., Martin, J. F., Treier, M. and Nakagawa, Y. (2009). Sonic hedgehog signaling controls thalamic progenitor identity and nuclei specification in mice. J. Neurosci. 29, 4484-4497.
Watanabe, K., Tamamaki, N., Furuta, T., Ackerman, S. L., Ikenaka, K. and Ono, K. (2006). Dorsally derived netrin 1 provides an inhibitory cue and elaborates the ‚waiting period' for primary sensory axons in the developing spinal cord. Development 133, 1379-1387.
Wilkinson, D. G. (1998). In situ Hybridization, A Practical Approach. Oxford, UK: Oxford University Press.
Xu, N.-J. and Henkemeyer, M. (2012). Ephrin reverse signaling in axon guidance and synapstogenesis. Semin. Cell Dev. Biol. 23, 58-64.
Zhou, Q. and Anderson, D. J. (2002). The bHLH transcription factors OLIG2 and OLIG1 couple neuronal and glial subtype specification. Cell 109, 61-73.

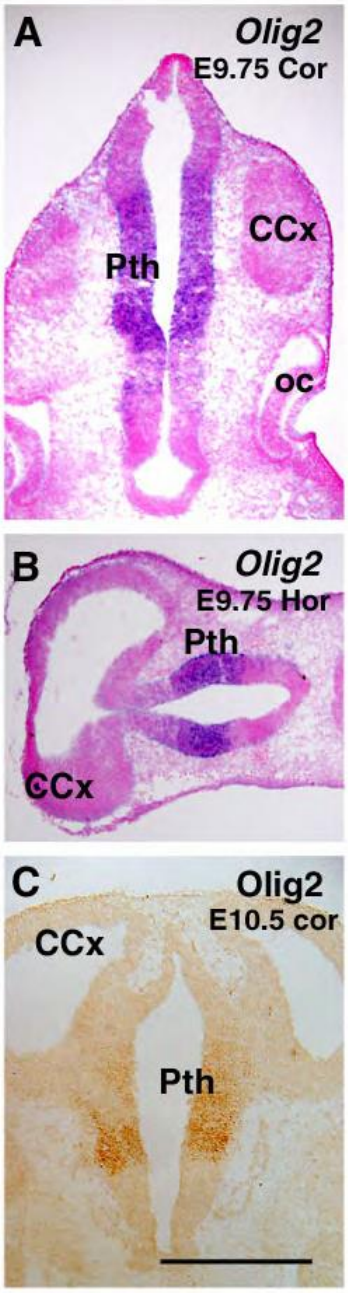

Supplementary Fig. 1 Expression of Olig2 in early diencephalon development
Expression of Olig2 was examined in the E9.75 (A,B) and E10.5 (C) diencephalon with *Olig2* ISH (dark blue) and Olig2 IHC (brown), respectively. A and C are coronal sections and B is a horizontal section. Note that Olig2 mRNA or protein is expressed in the diencephalon of these stages. Red in A and B is nuclear fast red for counter-staining. CCx, cerebral cortex. oc, optic cup. Pth, prethalamus. Bar in C = 500μm.

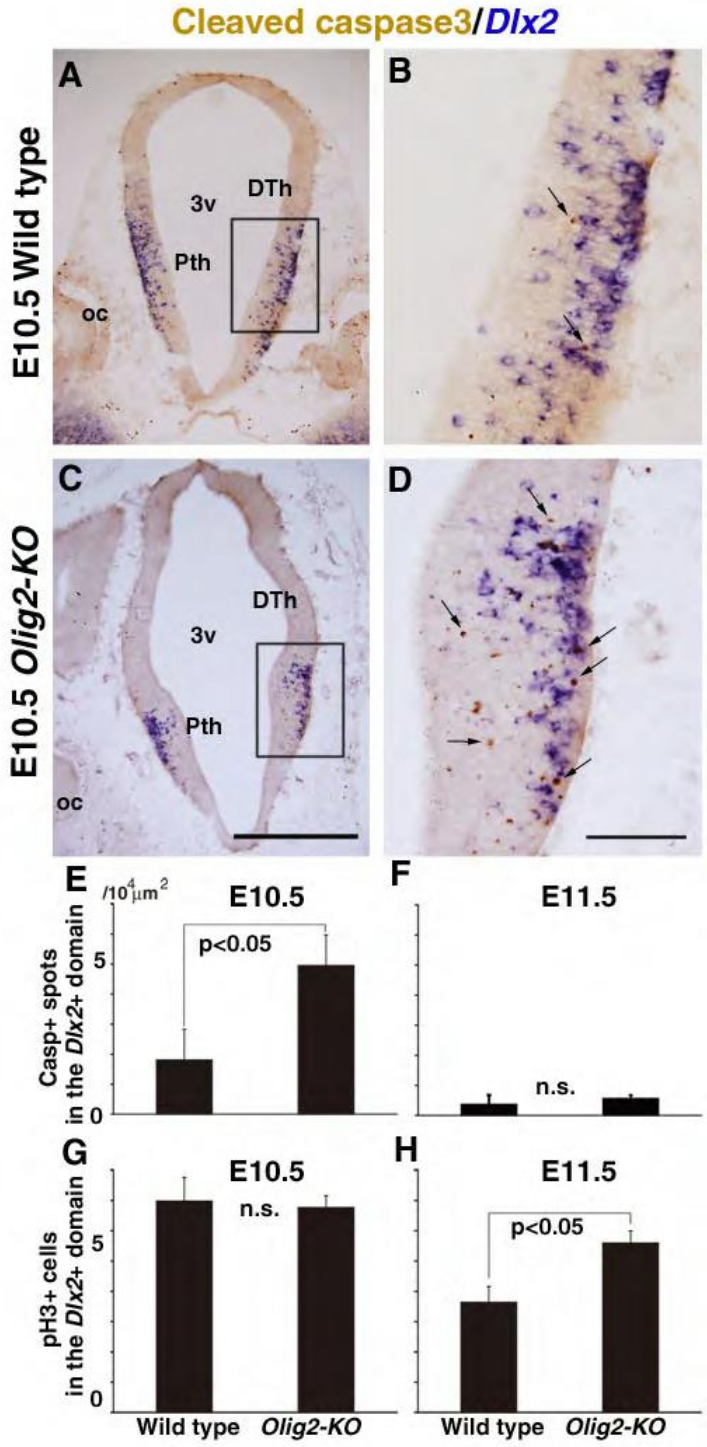

Supplementary Fig. 2 Apoptosis and proliferation in the prethalamus of *Olig2-KO* mice
A-D: E10.5 diencephalon of normal control (A,B) and *Olig2-KO* (C,D) was double-stained with *Dlx2* ISH and cleaved (activated) caspase-3 IHC. Caspase-3+ spots (arrows) were observed in the diencephalon, including the Dlx2+ prethalamus, and were more abundant in the *Olig2-KO* than in the control prethalamus. 3v, third ventricle. oc, optic cup. Bar in B = 200μm; in D = 100μm. E, F: Density of cleaved caspase-3+ spots in the E10.5 and E11.5 prethalamus. G,H: Density of pH3+ mitotic cells in the E10.5 and E11.5 prethalamus.

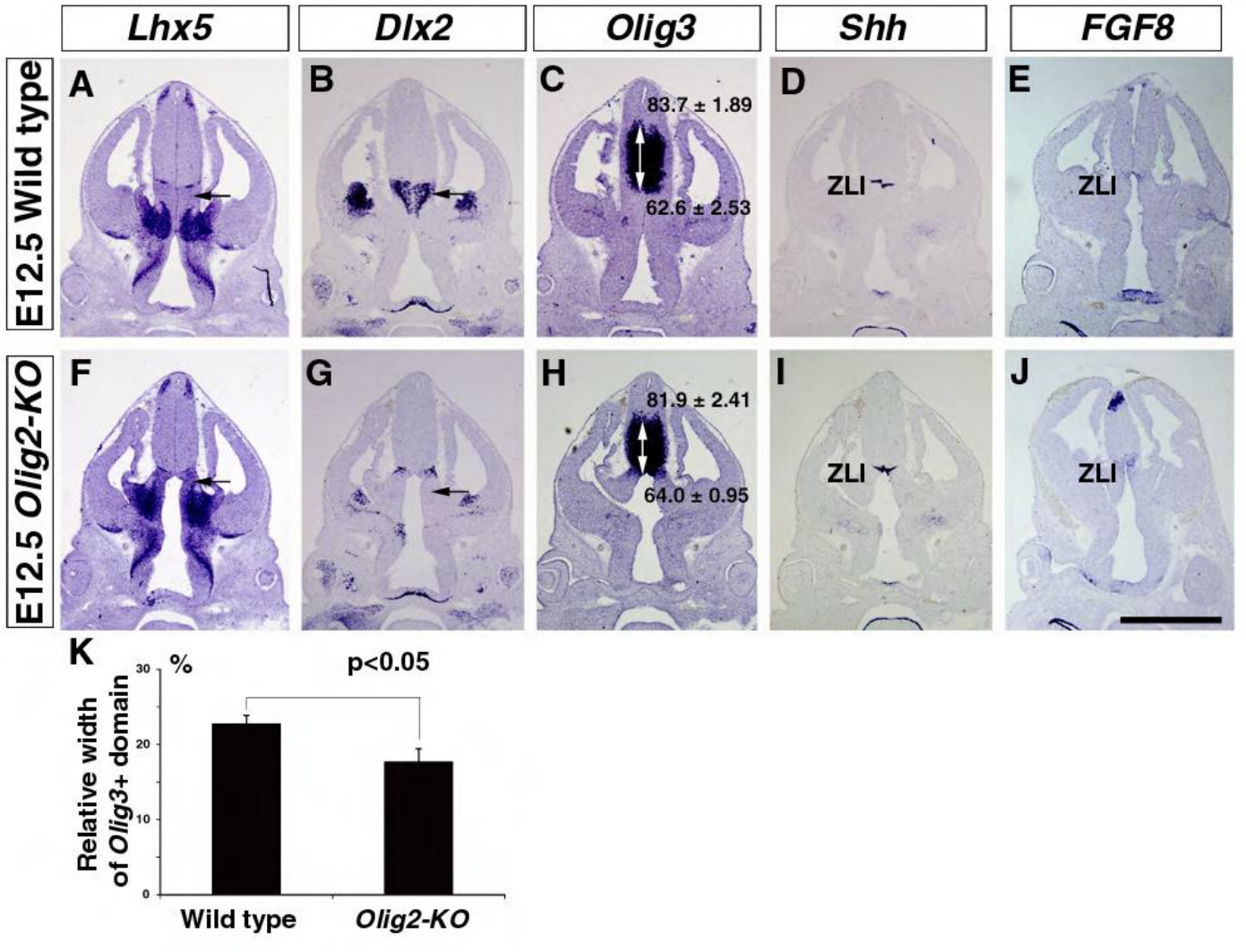

Supplementary Fig. 3 Expression of transcription factors and morphogen molecules in the E12.5 diencephalon
A-E: E12.5 wild-type. F-J: E12.5 *Olig2-KO*. Arrows in A, B, F, G indicate the prethalamus which shows hypoplasia. A, F: *Lhx5* is expressed in the dorsal border of the prethalamus and thalamic eminence while the main part of the prethalamus is devoid of *Lhx5* expression. In the *Olig2-KO* diencephalon, *Lhx5*-negative region is much smaller (F) than the control (A). B, G: *Dlx2* expression in the prethalamus. C, H: *Olig3* is mainly expressed in the dorsal thalamus. Double-direction arrows in images indicate an extend of Olig3+ domain, and numbers indicate the relative position of the dorsal and ventral borders, which are unchanged in *Olig2-KO* mouse (see text), while the relative width of the *Olig3*-expressing domain is slightly reduced in the *Olig2-KO* mouse (K). D, I: *Shh* expression is observed in the zona limitans intrathalamica (ZLI) in both wild-type and *Olig2-KO* mice. E, J: *FGF8* expression is mostly restricted to the rostralmost part of the diencephalon and ZLI shows very weak expression of *FGF8*, which is similar between wild-type and *Olig2-KO*. Bar = 1mm.

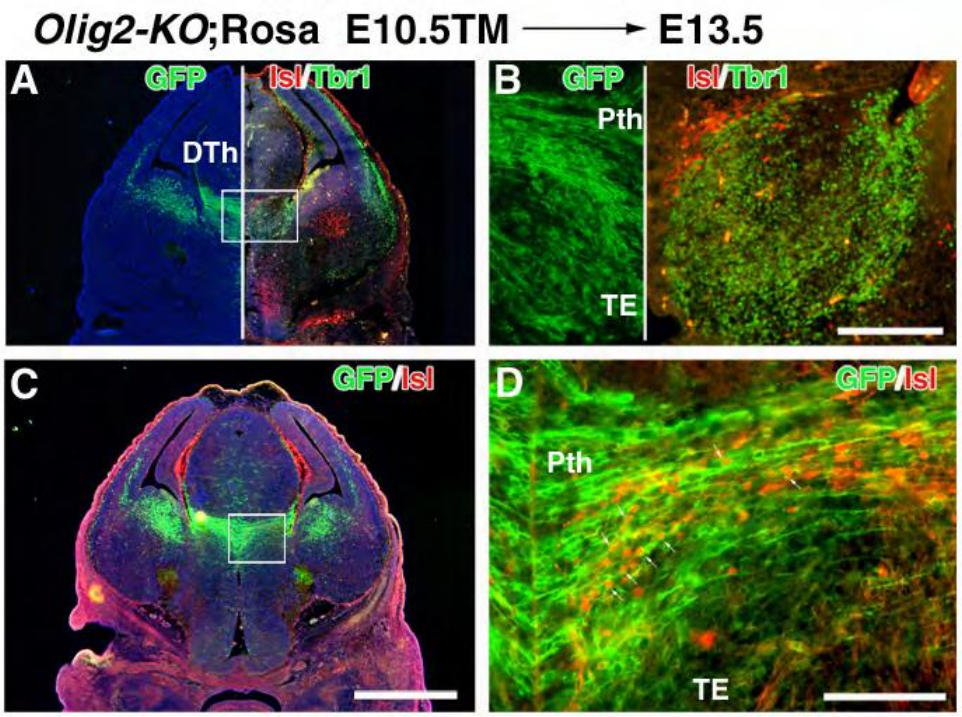

Supplementary Fig. 4 Dual phenotype of Olig2 lineage cells in the Olig2-KO diencephalon
E13.5 *Olig2-KO*;Rosa26^{GFP} mouse diencephalon with tamoxifen treatment at E10.5. Boxed areas in A and C are magnified in B and D, respectively. A, B: Composite pictures in which left and right halves are adjacent sections immunostained with GFP (green in left half), Islet1/2 (red in right half), and Tbr1 (green in right half) IHC. Note that GFP+ area shows Tbr1 and Islet1/2 expression. C, D: A section double-stained with anti-GFP and anti-Islet1/2 antibodies. Arrows in D indicate double-labeled cells. The results, together with those in Fig. 3, elucidate that Olig2 lineage cells in the *Olig2-KO* diencephalon are dual phenotypes, both prethalamus and thalamic eminence. Bars in C = 1mm; in D = 200μm.

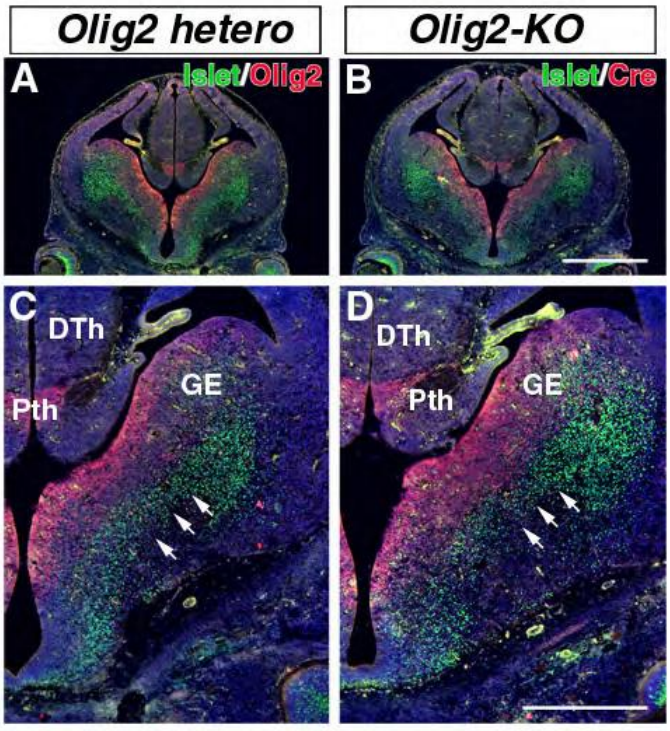

Supplementary Fig. 5 Normal arrangement of Islet1/2+ cells including corridor cells in the *Olig2-KO* ventral telencephalon
E13.5 forebrain is double-stained with Islet1/2 (green) and Olig2 (red in A and C) or CreER (red in B and D). Islet1/2+ cells are aligned dorsolaterally (arrows in C and D) in the ventral telencephalon, which contains corridor cells, in both Olig2 heterozygous and KO mice. Bars in B = 1 mm; in D =500μm.

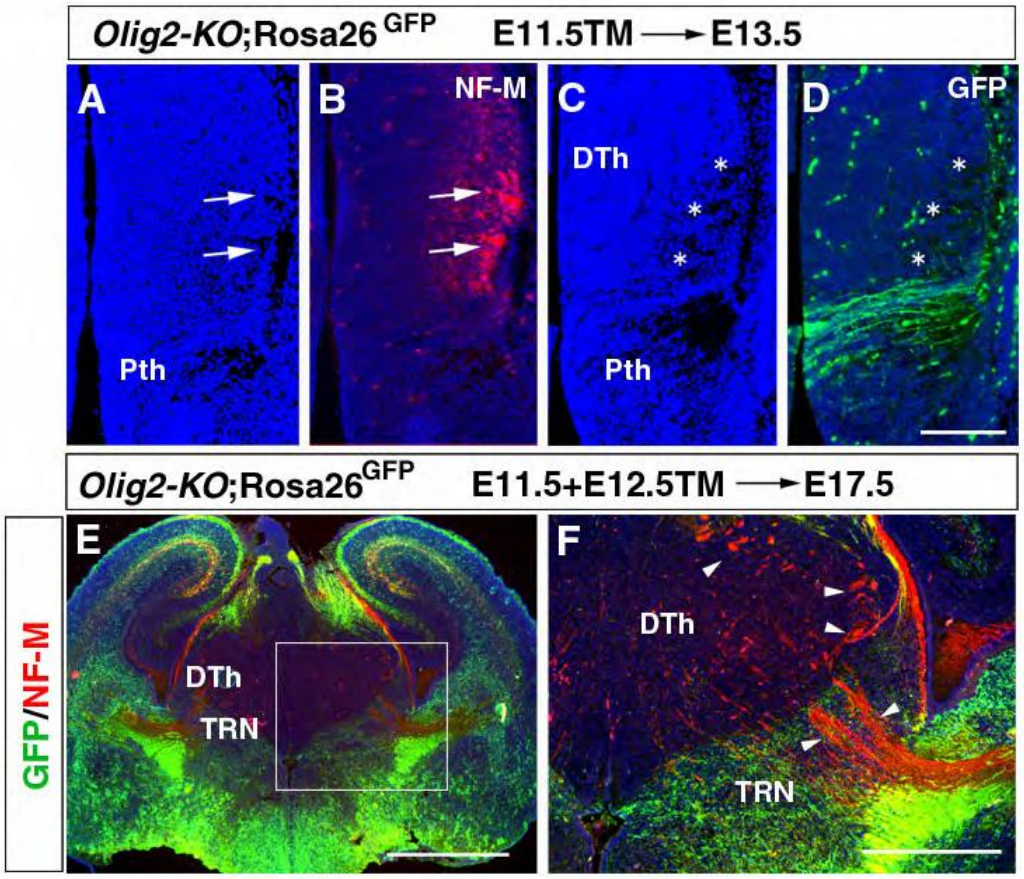

Supplementary Fig. 6 Distribution of Olig2 lineage cells and axons in the prethalamus
A-D: E13.5 dorsal thalamus of the *Olig2-KO*;Rosa26^{GFP} mouse with E11.5 TM treatment is stained by NF-M (B) or GFP (D) immunohistochemistry. Nuclear staining with Hoechst reveals small cell-free zones (arrows in A) that are filled with NF-M+ axons (B). However, when the adjacent sections are stained with anti-GFP antibody, which labels Olig2 lineage cells and processes, GFP+ processes are observed in the prethalamus (Pth) and the marginal zone of the dorsal thalamus (DTh in C), but not in cell-free zones in the dorsal thalamus. E, F: E17.5 diencephalon of the *Olig2-KO*;Rosa26^{GFP} with tamoxifen treatment at E11.5 and E12.5. Most of the NF+ axons (red) in the dorsal thalamus are not labeled with GFP, so that disorganized axons are not extended from Olig2 lineage neurons. Bar in D = 200μm; in E = 1mm; in F = 500μm.

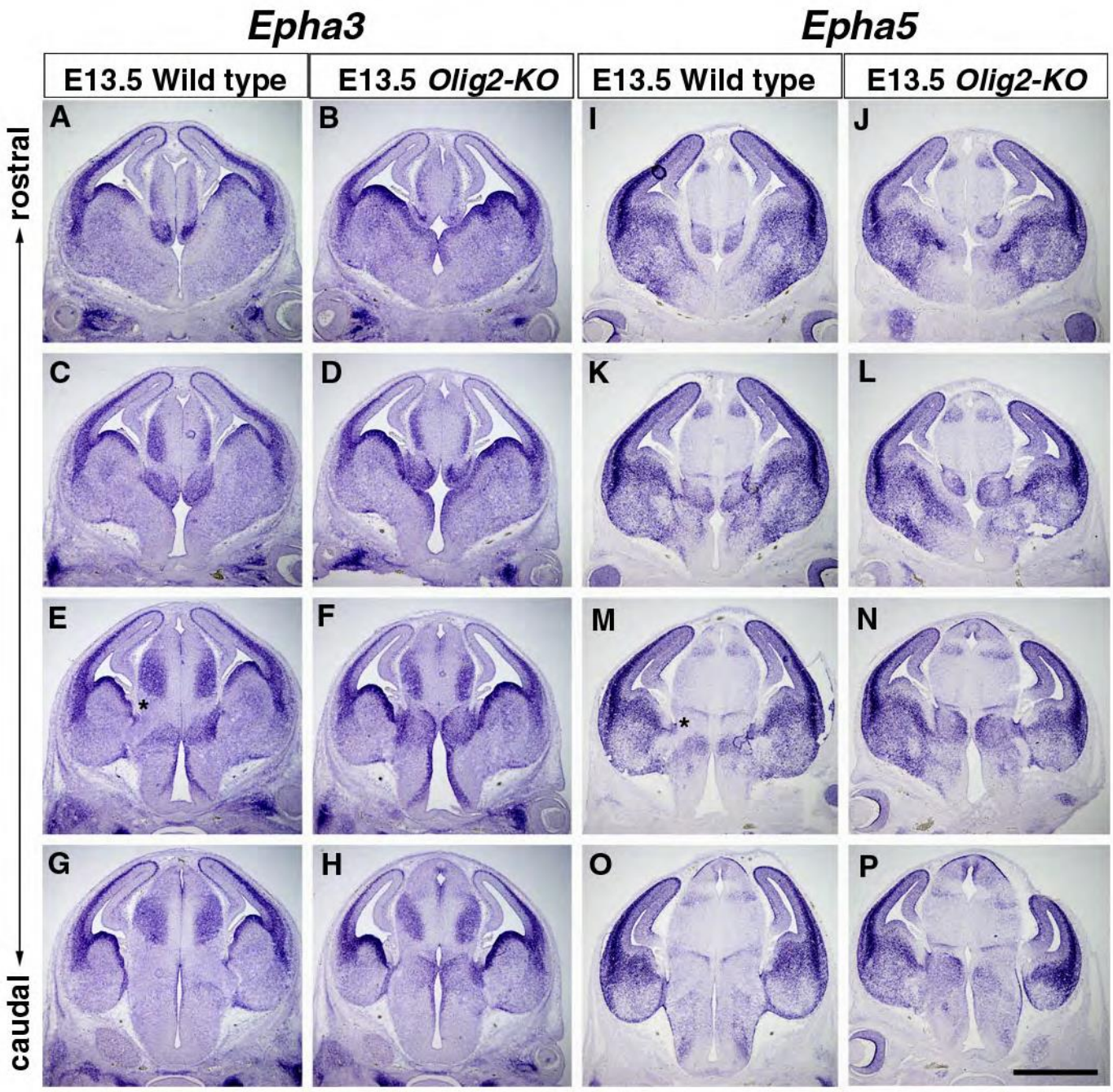

Supplementary Fig. 7 Details of *Epha3* and *Epha5* expression in the E13.5 diencephalon
Rostral to caudal arrangement of E13.5 forebrain stained with *Epha3* ISH (A-H) or with *Epha5* ISH (I-P) in the wild-type and *Olig2-KO* mice. Note that prethalamus in the wild-type is devoid of *Epha3* and *Epha5* expression that continues to the ventral telencephalon (asterisks in E and M). Such a *Epha*-negative region is missing in the *Olig2-KO* mouse. E, F, M and N are the same picture to Fig. 7A-D. Bar = 1mm.

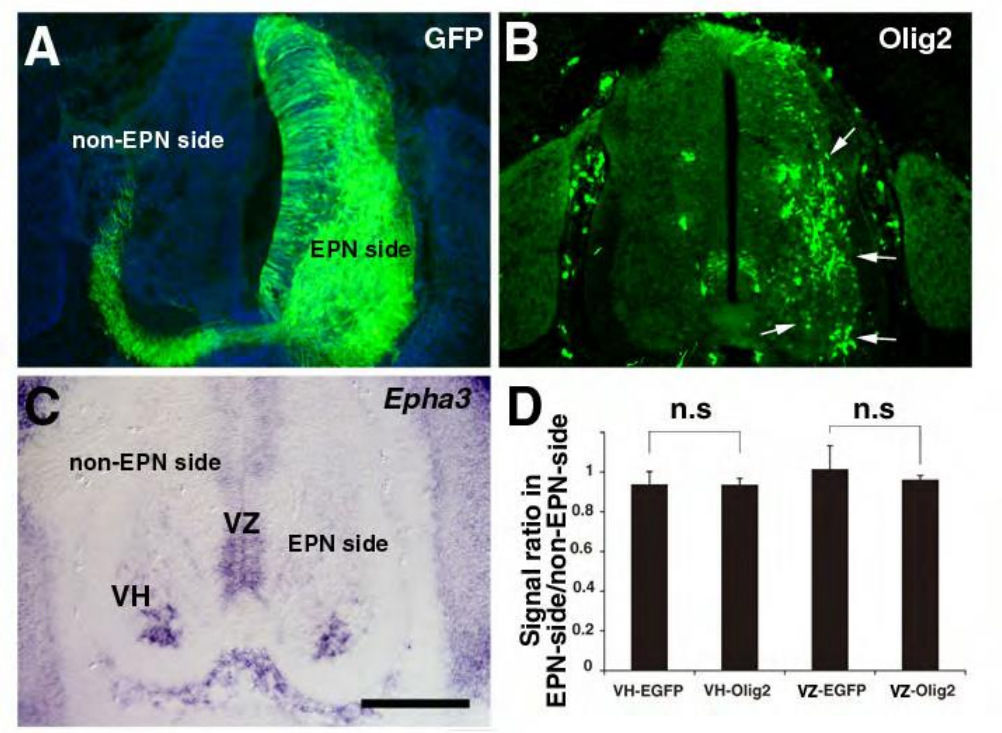

Supplementary Fig. 8 No effect of ectopic Olig2 on *Epha3* expression
Olig2 expression vector was electroporated to the E3 chick neural tube together with EGFP expression vector, and the spinal cord was analyzed at E6 to identify whether *Epha3* expression was affected by ectopic overexpression of Olig2. A, B: Serial sections of the E6 spinal cord with co-electroporation of GFP and Olig2. Ectopic Olig2 was indicated by arrows, which includes ventral horn (VH). C: *EphA3* expression was observed in the ventral VZ and VH. D: Ratio of signal intensity between electroporated (EPN) side (Olig2 and GFP or GFP alone) and non-electroporated (non-EPN) side was nearly 1, which means that *Epha3* expression was unaffected by ecto- pic Olig2. Bar in C = 200µm.

PART III: DISCUSSION

Since 2010, the year of publication of the groundbreaking discovery of the direct conversion mechanism of fibroblast into neuron by the BAM factors, Brn2, Ascll1 and Myt1l (Vierbuchen et al., 2010), more than 500 article about Ascl1 were published. Most of them followed the same approach of viral transduction of combination of TFs. Starting from a constructs combining more than 20 different TFs, Verbruchen et al, identified the core BAM factors sufficient to induce neurogenesis. Similar experiments were done to generate OPCs and oligodendrocytes through direct conversion (Najm et al., 2013; Yang N, Zuchero JB 2013). Despite successful, this approach display really low yield and do not explain the chromosomic remodeling mechanisms which triggers direct cell lineage conversion. Recent

studies tackled this question for Ascl1 (D. Castro 2011; Wapinski et al., 2013. MD Borromeo, 2014) and for Olig2 (Yu et al 2013) and unraveled some of the mechanisms of action of Ascl1 and Olig2 at a genome-wide level. While Castro et al, focused on the role of Ascl1 in the ventral telencephalon using promoter-specific Chip-on-chip, Borromero et al, focused on the role of Ascl1 in the spinal cord using genome-wide Chip-sequencing analysis. Wapinsky et al demonstrated the preferential binding of Ascl1 on H3k27Ac/H3K4me1 active enhancers and characterized its role of pioneer TFs. Yu et al characterized the whole oligodendrocyte lineage and provide a great insight in the epigenetic of differentiating oligodendrocytes. Another great progress was made by the characterization of oscillatory expression of Ascl1 and Olig2 in proliferating neural stem cells (Imayoshi , 2014). This study shed a light on a regulatory process involving an oscillatory or stable mode of expression to regulate cell proliferation or cell fate choice respectively. This kind of regulation involving the mode of expression rather than specific expression of a new TFs opens the way for wider comprehension of the genetic regulatory logic.

One particular goal of this study was to untangle the specific and shared role of Ascl1 and Olig2 in the specification of oligodendrocyte progenitors. We demonstrated that Ascl1 directly binds and regulates key genes involved in the specification, proliferation and differentiation of OPCs. Using comparison of transcriptomic and binding profile of Ascl1 and Olig2, we showed that the downstream direct targets of both TFs were highly overlapping despite clear specificities in regulated genes, in binding sequence preferences and on average coverage of the genome. Four time more peaks were identified in OPCs in Olig2 Chip-seq compared to Ascl1 Chip-seq.

Our work confronted us with the multiple testing problem. In microarray and chip-seq experiments, several thousand events are simultaneously measured across different conditions. When testing for differential expression, each gene is tested independently from one another using a t-test or ANOVA. The incidence of false positives is proportional to the number of tests performed and the significance level (p-value cut-off). A p-value of 0.05 signifies a 5% probability that a gene expression level is different between the two groups by chance. If 40,000 genes are tested, 2,000 genes could be called significant by chance. Thus, it is important to correct the p-value to assess the false discovery rate (FDR) for each gene when performing such large statistical test. In this study, we used a combination of algorithm (GCRMA, fRMA, LIMMA) to normalize perform the multiple comparisons and estimate the best FDR cut-off. A FDR of 5% signifies a 5% probability that a particular test result is a false positive. Using this strategy is really of helped when we compared multiple conditions.

Stringent FDR coupled to clustering allowed us to identify previously unknown genes that are both co-regulated and specific of the process we studied during this work, the differentiation of oligodendrocytes. In our Ascl1/Olig2 microarray experiment, the different replicates displayed rather high variability (see PCA in material and methods Fig. 24C). Dissection variability is the most likely explanation; however, this could also be caused by biological or other technical variability. Mice of the same genetic background and the same parents were used to generate the samples. Despite this variability, comparison with $Ascl1^{KO}$ yield robust results. Control genes such as *Ascl1 Dll1*, *Hes5* (*Dlx* genes being stable) were highly regulated and statistically significant and were used to define the appropriate FDR cut-off. *Ascl1* had two different probe-sets which undergo differential up and down regulation. The detection of an up-regulated transcript in the $Ascl1^{-/-}$ mice is in accordance with the up-regulation of the in-situ-hybridization signal observed with RNA probe targeting the most 5‘ region of the gene (Cau et al., 1997). To avoid to miss information, being too stringent, FDR of 20% and Fold-change >1.2 were used to compare microarray and ChIP-seq experiments further down the workflow. $Olig2^{KO}$ results were more puzzling because of the detection of only a small down-regulation for Olig2 (Fc 0.63 FDR 3%; Fig 24B) while a complete absence was expected. However, Olig2 targets were identified as control, such as Olig1 or Brevican. Corrected p-value were set also at 20% (p-value <0.01) for subsequent analysis. Both datasets behave similarly, with only few genes strongly regulated and many genes regulated (2300 by Ascl1 and 1200 by Olig2) with low amplitude. This result could be attributed to technical biases described above, however, it also fit with the ~~–e~~ontinuous model” described in the introduction and perhaps reflect some biological causality (Biggin 2011). The small number of replicates used was initially 5 per condition but only 3 were available for subsequent analysis, as 2/5 replicates were discarded for each condition after being identified by principal component analysis as outliers (see material and methods and annex for R-script). As demonstrated by the reprocessing of published data, increasing the replicate number rapidly overcome the biological and technical variability (see annex 12). In humans, hundreds of microarrays are necessary. Using statistical tests as a proxy to prioritize the genes identified, we always used internal controls as well as external control (*Allen brain atlas*, *Eurexpress* In situ hybridization databases) to define the necessary stringency. Inspired by the work of Cahoy et al 2009 and Emery et al 2009, we took advantage of their published microarrays done in the whole oligodendrocyte lineage as well as post-mitotic neurons and astrocytes. Combined with other cell type specific microarrays such as different neural stem cells, microglia, endothelial cells and neural subtypes (see material and methods for complete

references), the global cell type comparison presented in this work allowed us to identify for each cell type, genes involved in the shaping of the epigenetic landscape such as transcription factor network and epigenetic regulators. The information contained in those gene lists was used to generate functional hypothesis about the oligodendrocyte physiology. For example, the gene up/down-regulated between the NSCs to OPC are involved in OPCs activation or inhibition. The gene highly expressed in NSCs and OPCs but not in post-mitotic cells must be involved in cell cycle control and mitosis. However, differential expression is not sufficient to detect important functions. Olig2 being stable but highly expressed from the NSCs to the myelinating stage, would not have been detected only based on fold-change consideration. As mentioned above, the mode of regulation is a key determinant of the gene signaling. Gene regulation involves that both the expression level and the mode of expression are important to keep in mind to understand the complete regulatory logic. In this regards, assessing the oscillatory expression of Ascl1 and Hes genes in OPCs will bring a new understanding of OPCs specificity. Indeed, stable expression of Ascl1 and down regulation of Hes1 is necessary for the NSCs to become post-mitotic and start to differentiate. However, OPCs maintain their Ascl1 expression and continue to divide after the embryonic and postnatal gliogenic phase, constituting the main proliferative population of the brain. Thus, an interesting question is to know is if Ascl1 maintain its oscillatory activity in order to maintain its proliferative state. This parameter may explain why conversion yield are so low in OPCs generation experiment. Generation of new kind of synthetic promoters able to drive different mode of gene activation will be of great help in controlling cell reprogramming more precisely. On other central question is the possible link between Ascl1 / Hes1 / Hes5 and the circadian gene such as clock or Bma1 which are also bHLH proteins. A recent study showed an intrinsic timing of differentiation for the gabaergic neuroblast migrating tangentially from the ganglionc eminence to the cortex. When grafting cell from the MGE, directly in the cortex, cells took the same time to differentiate or undergo apoptosis than the one that were travelling in-vivo *DG* (DG *Southwell 2012*).

Recent technological progresses in biology, such as high throughput sequencing favored the emergence of high dimensional data. Our ability to benefit from this large knowledge was only made possible since the organization of a publicly accessible data repository (GEO) and the emergence of the computational tool necessary to process the high-throughput sequencing data. The emergence of internet profoundly changed the scientific potentialities. Having access to raw data of studies performed by other laboratory is particularly important to assess their validity and compare with ours. Indeed, we realized during this work how most of the

experiments were done when dealing with sequencing and microarray analysis. Most of the time, the minimal amount (3) of replicates is used, while many studies (even on human) does not reach this requirement. In this line, only a few microarray analysis of demyelinated and remyelinating lesions in mice were performed. Having robust data about the process of remyelination is indeed necessary to tackle the complexity of the phenomenon at work in Human diseases. The most careful experimental approach of demyelination and remyelination to date was performed in rat where demyelination was induced by *0.1 % ethidium bromide* injection and lesions where micro-dissected at 5, 14 and 28 days post lesion and analysed by microarray experiment (*Huang JK, Jarjour* A et al ., *2010*). Microdissected lesions are enriched in inflammatory, and cell death associated genes, comparing day 14 with d5 captured genes regulated upon remyelination. Interrogating this dataset with our oligodendrocyte screen discriminated the inflammatory part from the oligodendroglial part. However, this brilliant study suffered from the lack of statistical robustness with only 3 replicates. A far more exhaustive view of the remyelination process would have been gained with only few more replicates.

In contrast, w*e have been fortunate to* benefit from replicated Chip-seq experiments analysis done in different cellular contexts for Ascl1, Chip-seq from purified OPCs, whole ventral telencephalon, SH-SY5Y neuronal cultures (B martynoga) cell line and in different species (rat OPCs, mouse ventral telencephalon, mouse cell line). Established algorithm pipeline to process chip-seq data from sequencing to peak calling (BOWTIE for reads alignement, MACS for peak calling) are now available online and make the procedure rather standard (see material and methods).

The recent discovery allowing to question the role of the genome structure in gene regulation (Dekker 2013) made us reconsidering carefully the classical next neighbor analysis method to infer regulatory region to the closest gene. Indeed, only 7% of the cis-regulatory regions interact with their closest gene. We used epigenetic information about active enhancers and active promoters to assess the functionality of the Ascl1 and Olig2 binding event and infer long-distance regulation from available Hi-C data capturing interaction profile from embryonic and postnatal brain. Chip-seq peak detection and comparisons of the Chip-seq experiments were done using cistrome genome and Genomatix. Those powerful bioinformatics tools allowed us to convert Ascl1 bound chromosomic position in rat into mouse chromosomic position (*liftover tool*) and update from previous genome assembly (mm9 to mm10). Mouse genome is much better annotated than the rat genome. Results were loaded on a genome browser for subsequent analysis and observation of ChIP-seq binding

profile (Genomatix, UCSC). This general overview of the chromatin state associated to particular genomic loci is a powerful tool. We identification high confidence Ascl1 and Olig2 binding site as well as the enriched regulated signaling pathway they compose. Ascl1 and Olig2 regulate overlapping function by clusters of modules of TFBS. We generated new hypotheses about gene regulatory networks and validate them by different approaches paying particular attention to the chromatin remodelers. A precise analysis of promoter-enhancer interactions involved in the oligodendrocyte lineage allowed the construction of a catalogue of regulatory sequence greatly enriched in oligodendrocyte specific regulatory sequence(Annex). This information was used to define short synthetic promoter for viral construction that could efficiently drive gene expression to the oligodendrocytes. We also analyzed OPCs specific cis-regulatory element such as the Pdgfrα or Cspg4. Transfection analysis of miniTOL2-Tomato integrative plasmids containing 6 putative enhancers of *Pdgfra* or *MOG* were done in differentiating neurospheres (data not shown). We obtained preliminary successful expression in *Pdgfra* positive OPCs for the *Pdgfra* construct. However, NSCs were also expressing the construct, likely because of one of the enhancer being involved in another process. The *MOG* miniTOL2-Tomato construct was expressed in myelinating oligodendrocyte but replication of the experiment has to be performed.

Creatine

The creatine metabolism seems to be a function of the oligodendrocytes. Creatine was thought to come principally from periphery through the blood brain barrier (Wyss and Kaddurah-Daouk, 2000) In situ hybridization shows stronger GATM expression in white matter region compared to grey matter (Fig. 47G). It will be of great interest to explore further the metabolic coupling between myelin, axons and astrocytes. As phosphocreatine acts as a metabolic intermediate transported from mitochondria to areas with high energy demands. This gradient of GATM expression could indeed be correlated to the specific metabolic needs of the axonal fibers passing by the white matter structures such as the corpus callosum or the fimbria. If so, specific transporter such as CT1 or specific channels such as gap junction could be involved. The role of creatine in myelination has already been explored and shown to be beneficial in different neurological diseases. A clinical trial is currently in phase III in the context of Huntington‘s disease (M. Flint Beal 2011). Moreover, increased creatine is found in MS lesion (M Inglese 2003; M. V. Davydovskaya 2013). These results suggest that the increased creatine content in MS lesion is due to the release of its content by the dying

oligodendrocyte and associated metabolic changes. A recent study demonstrated the expression of CT1, the creatin transporter in neurons and oligodendrocytes. This finding is in accordance with the microarray data. Moreover, *Gamt* and *Gatm* are clearly expressed in young adult white matter. *Gatm* knock-out mice was recently generated and they provide a good model to test the role of creatine in myelin formation (Choe et al. 2012; C. I. Nabuurs 2013). *Gatm* mutant mice are viable, despite growth retardation and weight loss. Overall size is reduced despite normal gross morphology appearance. However, precise characterization of its role in oligodendrogenesis and myelin methabolism has not yet been assessed. We are currently exploring this function in the lab using 2 and 3 weeks old brains from *Gatm* mutant mice.

Chd7

Chd7 was our first selected candidate, Bcas being already understudy in another lab. Indeed, all the criteria made from it an interesting factor to study in the role of oligodendrocyte differentiation and myelination: i) it was downregulated in both Ascl1and Olig2 mutant arrays; ii) it presented binding of Ascl1 and Olig2 in intragenic regions by ChIP-seq made in purified OPCs; iii) it was expressed in the ventricular zone of the ventral telencephalon like Ascl1 and Olig2; iv) its expression was enriched in oligodendroglia in expression microarrays; v) its expression in white matter was confirmed by in situ hybridization datasets; vi) it was downrelated both in demyelinating mouse models (cuprizone and lysolecytine) and in MS microarrays; vii) tools for its expression and functional characterization were available (antibody working in immunofluorescence) and both regular and conditional mutant mice (*Chd7*^{Gt} and *Chd7*^{Flox} mice); viii) Chd7

We therefore, started a detailed characterization of Chd7 protein expression demonstrating that like the *Chd7* mRNA, Chd7 protein is found both in OPCs and in immature OLs being downregulated to very low levels in mature OLs (Fig. 40). We also demonstrated that Chd7 was co-expressed with Ascl1 in SVZ progenitors (confirming the data that was published at that time by the lab of HK Liu (Feng et al., 2013) suggesting that both factors likely regulate each other and/or function in the same transcriptional complex. Our recent data also indicates that Chd7 is strongly upregulated in maturing oligodendrocytes in and around remyelinating lesions in mice (not shown), suggesting an important role in both myelination and remyelination. We obtained *Chd7*^{Gt} and *Chd7*^{Flox} mice from Dr. Donna Martin (Michigan, USA) but due to health status of the mice and cold weather during last winter, plus the 6 months needed to combine the three alleles to trace mutant cells (*Cre*, *Chd7*^{fl}, *tracer*), all our functional studies have been delayed until now. We are nevertheless, starting the first experiments using two *Chd7* conditional mutations in oligodendroglia. One using *Olig1*^{Cre} mice, that will remove *Chd7* in around 50% of oligodendroglia from embryonic stages (experience from RQ. Lu‘s lab). Another, *PDGFR□::CreER*^{T}, that will permit us to specifically delete *Chd7* in some OPCs the postnatal brain during myelination (Tamoxifen injection in the first week postnatal) or after a focal demyelinating lesion (lysolecytin, LPC) in the adult brain (Tamoxifen injection before demyelination). In both cases, we are going to trace the Chd7 mutant cells using a Cre-induceable reporter background (*Rosa26*$^{stop\text{-}Tomato}$). We hope from this studies to demonstrate the function/requirement of Chd7 in oligodendrocyte differentiation and myelination.

Moreover, in collaboration with RQ Lu‘s lab we have started to improve ChIP protocols to make Chd7 ChIP-seq in purified OPCs and immature oligodendrocytes. From this data we expect to characterize the Chd7 transcriptional regulation mechanisms in oligodendrogenesis during (re)myelination.

Chd8

The choice of Chd7 as a important candidate to regulate OPC/OL differentiation pushed us to investigate the role of its paralog gene, *Chd8,* given its expression in oligodendroglia from microarray neural subtypes. Indeed, this data was confirmed by in situ hybridization expression data from postnatal and adult stages showing enrichment in white matter cells. Our immunofluorescence characterization of Chd8 protein expression in the postnatal brain has confirmed that Chd8 is present during the phase of OL differentiation and being downregulated to very low levels in mature/myelinating OL. Moreover, Chd8 is induced in OPCs close to demyelinating lesions and its expression timing correlates with factors inducing remyelination such as Olig2, Ascl1 or Nkx2.2. This function in remyelination could be conserved up to humans given that our preliminary data shows that Chd8 is expressed in active remyelinating MS lesions. Given that *Chd7* conditional mutations (Olig1-Cre, on-going work in collaboration with Richard Q. Lu‘s lab) shows strong impairment in oligodendrocyte differentiation, we could assume and the upregulation of Chd8 in OPCs during remyelination we could expect that Chd7 and Chd8 regulate different steps/genes in OL differentiation and myelination. Therefore, the characterization of Chd8 function in (re)myelination and its target genes in chromatin remodeling could constitute an important step forward in our understanding of the (re)myelination process, and future therapeutic strategies could be derived from this knowledge.

Tns3

From our microarray and ChIP integrative strategy we found that Tns3 was an interesting common target of Ascl1 and Olig2 given the expression pattern similar to these TFs in the ventral thelencephalon and from the expression in oligodendroglial cell-types in the postnatal brain. These data was confirmed by the expression found in *Allen brain* and *Euroexpress* In situ hybridization databases, which shown an enriched expression in white matter regions at postnatal and adult stages, in sparse cells that could constitute a precise stage of oligendroglial lineage different to OPCs given the it was less dense than *Pdgfra* in situ expression pattern. We could confirm the oligodendroglial expression using an antibody for Tns3, and moreover, characterize that its expression perfectly match the start of OPC/OL differentiation, being downregulation to very low levels in the mature OL. This specific expression of Tns3 to the moment of OL differentiation and myelination suggests that it plays a relevant role in these processes and that is therefore the kind of genes that we set off to find in our analysis.

Another criteria for which Tns3 was selected was its implication human tumors. Contrary to the expression data in tumors and mouse kidney, Tns3 antibody signal was localized to the nucleus. Given that Tns3 has been shown to mediate integrin signaling from the cell surface to the actin skeleton, we were surprise to find Tns3 nuclear localization. Nevertheless, search for actin functions led us to discover more than ten years of documenting the nuclear function of actin in transcriptional regulation, that place Tns3 in the center of the research focus of the lab. We have started to analyze brains of Tns3 mutant mice (from a gene-trap line) but our preliminary data (from two and three postnatal mice) have not yet unravel a phenotype in the process of oligodendrogenesis or myelination. This contrary to our expectation rises the

problem of gene functional redundancy and reliability of expression databases. We have explored all the data published for other *Tensin* family members without finding a clear signal in oligodendroglial cells. *Tns2* is expressed in vessels of the brain and maybe there is a weak signal in the white matter that needs to be confirm. We recently got an antibody working in immunofluorescence showing weak signal of Tns2 in white matter regions and we are testing the possibility of an upregulation of Tns2 levels in *Tns3* mutant white matter and therefore a possible functional compensation of Tns3 function by Tns2.

CONCLUSION AND PERSPECTIVES

In the present work we used integrated analyses of expression microarrays and chromatin immuno-precipitation analysis to characterize the genes that are regulated by Ascl1 and Olig2 in NSCs and the oligodendroglial lineage. We identified Ascl1 and Olig2 target genes in Notch, Wnt and Sonic Hedgehog signaling pathways. We identified Chd7 and Tns3 as new important players regulated by both Ascl1 and Olig2 during the oligodendrocyte differentiation and compared the transcriptome of OPC and differentiating oligodendrocytes with other neural cell types to identify genes with specific function at different stages of the oligodendroglial lineage. We also brought attention to the creatine metabolism function in oligodendrocyte. We found a highly enriched expression of Gatm, Gamt and Slc68a, two genes that code for the enzymes necessary for creatine synthesis. Finally, we generated a list of potential beneficial drugs able to change myelin gene expression and which were never tested in the context of remyelination. we hope that these identified genes and regulatory sequence involved in oligodendrogenesis and whose expression are regulated in demyelinated lesions will allow the development of new therapeutic strategies promoting an efficient remyelination in demyelinating diseases such as Multiple sclerosis or leukodystrophies.

ANNEX

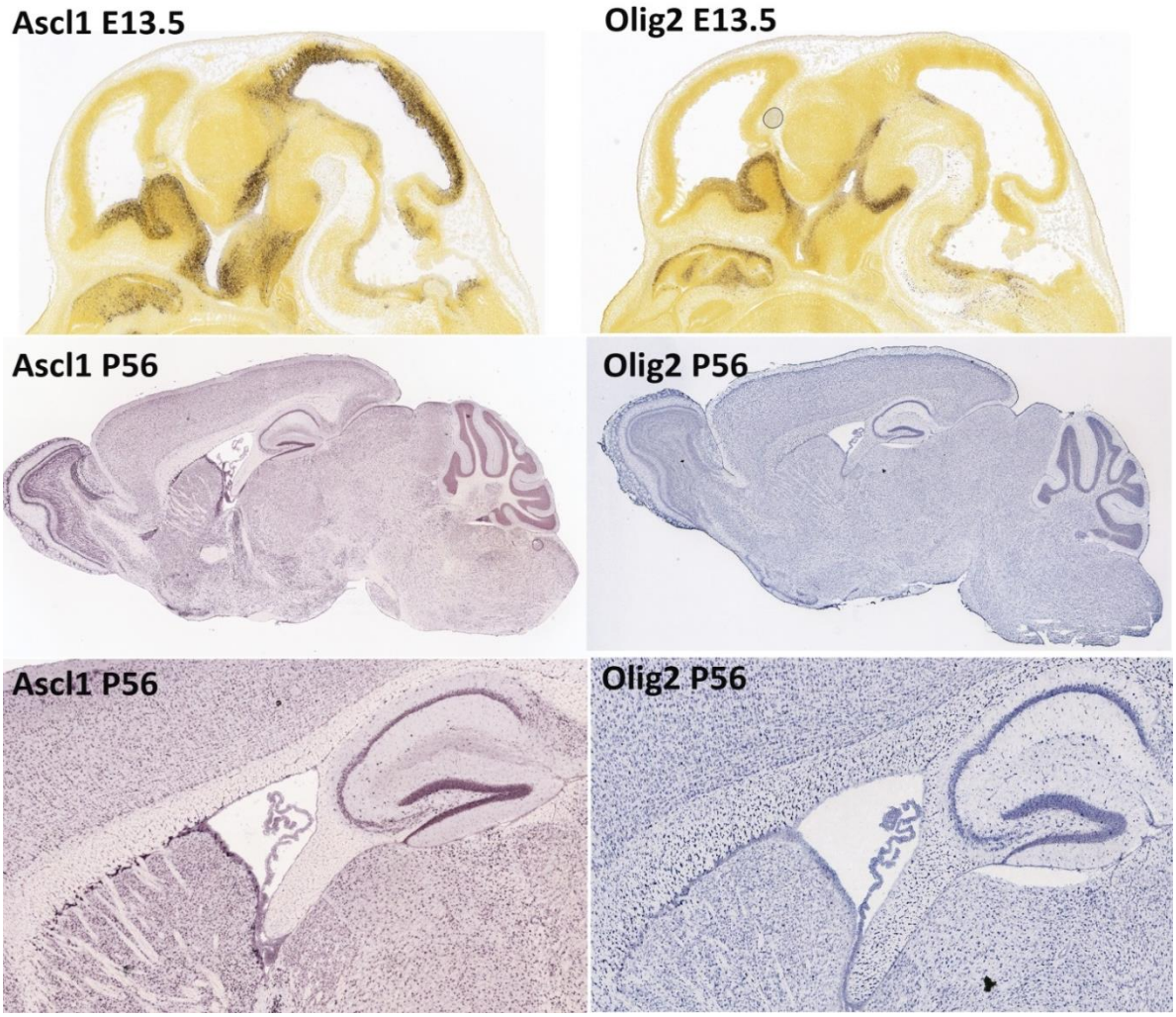

Annex1 Sagittal section of Ascl1 and Olig2 in-situ hybridization of E13.5 and P56 mouse brain .Similar expression pattern in the major part of the ventricular zone at E13.5. At P56, Ascl1 expression is scatterd in the brain and highly enriched in the neurogenic zone in the adult SVZ and SGZ in the hippocampus. Olig2 expression is strong all over the brain and more visible in white matter regions such as the corpus callosum and the fimbria.

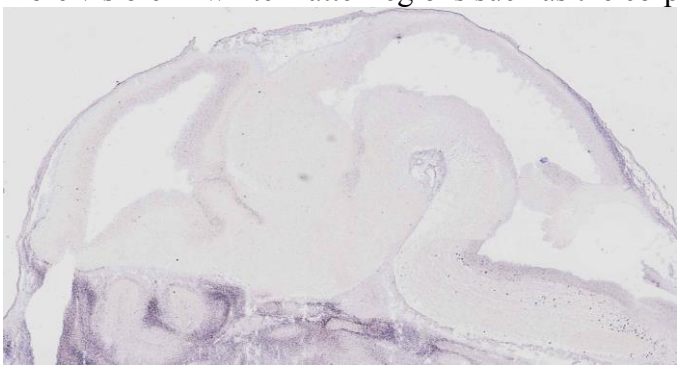

Annex 2: Sagital view of in-situ hybridization of Chd7 in E14.5 mice (eurexpress). early appearance of OPCs is visible in the rhombencephalon. Expression of Chd7 is mainly in the SVZ and VZ.

Gene Symbol	Gene Title	Fc O2-KO/WT	PValue
Prkci	protein kinase C, iota	1.84	3.34E-02
Apbb2	amyloid beta (A4) precursor protein-binding, family B, member 2	1.85	8.12E-03
Eif2s3x	eukaryotic translation initiation factor 2, subunit 3, structural gene X-linked	1.85	2.72E-02
Hnrnpl	heterogeneous nuclear ribonucleoprotein L	1.85	3.40E-02
Ywhag	tyrosine 3-monooxygenase/tryptophan 5-monooxygenase activation protein	1.85	3.39E-02
Dcun1d1	DCN1, defective in cullin neddylation 1, domain containing 1 (S. cerevisiae)	1.86	1.77E-02
Clasp2	CLIP associating protein 2	1.88	9.35E-03
Tmx4	thioredoxin-related transmembrane protein 4	1.88	9.90E-03
Srpk2	serine/arginine-rich protein specific kinase 2	1.90	3.94E-02
Tgoln1	trans-golgi network protein	1.90	2.67E-02
Plxnc1	similar to plexin C1 /// plexin C1	1.91	6.63E-03
Sepw1	selenoprotein W, muscle 1	1.92	3.41E-02
Dclk1	doublecortin-like kinase 1	1.93	2.68E-02
Epha3	Eph receptor A3	1.95	1.07E-03
Sp3	trans-acting transcription factor 3	1.98	3.86E-02
Plekhj1	pleckstrin homology domain containing, family J member 1	1.98	1.43E-02
Soat1	sterol O-acyltransferase 1	1.98	8.50E-03
Mapk6	mitogen-activated protein kinase 6	1.99	1.52E-02
Usp22	ubiquitin specific peptidase 22	1.99	3.04E-02
Prpf39	PRP39 pre-mRNA processing factor 39 homolog (yeast)	2.00	4.34E-02
Tspyl1	testis-specific protein, Y-encoded-like 1	2.00	2.43E-02
Vcam1	vascular cell adhesion molecule 1	2.01	9.24E-04
Ppp1r12a	protein phosphatase 1, regulatory (inhibitor) subunit 12A	2.04	2.62E-02
Pitpnc1	phosphatidylinositol transfer protein, cytoplasmic 1	2.04	1.45E-02
Arl8b	ADP-ribosylation factor-like 8B	2.04	2.58E-02
Tfrc	transferrin receptor	2.05	4.05E-02
Zfa /// Zfx	zinc finger protein, autosomal /// zinc finger protein X-linked	2.05	2.33E-02
Adam10	a disintegrin and metallopeptidase domain 10	2.05	3.50E-02
Rab2a	RAB2A, member RAS oncogene family	2.05	1.06E-02
Shisa2	shisa homolog 2 (Xenopus laevis)	2.05	2.45E-04
Taf7	TAF7 RNA polymerase II, TATA box binding protein (TBP)-associated factor	2.08	2.56E-02
Rcan2	regulator of calcineurin 2	2.09	2.87E-02
Fscn1	fascin homolog 1, actin bundling protein (Strongylocentrotus purpuratus)	2.12	1.96E-02
Bpnt1	bisphosphate 3'-nucleotidase 1	2.14	1.42E-02
Zfx	zinc finger protein X-linked	2.15	1.25E-02
Lin7c	lin-7 homolog C (C. elegans)	2.20	2.85E-02
Canx	calnexin	2.20	2.00E-02
Nucks1	nuclear casein kinase and cyclin-dependent kinase substrate 1	2.21	1.10E-02
Sfpq	splicing factor proline/glutamine rich (polypyrimidine tract binding protein a	2.22	1.98E-02
4932431P20Rik	RIKEN cDNA 4932431P20 gene	2.31	6.03E-03
Tmed2	transmembrane emp24 domain trafficking protein 2	2.32	4.44E-02
Mier1	mesoderm induction early response 1 homolog (Xenopus laevis	2.36	2.16E-02
Gm7536	Predicted gene 7536	2.43	1.19E-02
Xiap	X-linked inhibitor of apoptosis	2.44	7.69E-03
Pnpt1	polyribonucleotide nucleotidyltransferase 1	2.45	3.37E-02
Actb	actin, beta	2.51	2.86E-03
Dyrk1a	dual-specificity tyrosine-(Y)-phosphorylation regulated kinase 1a	2.63	1.54E-02
Ubc	ubiquitin C	2.74	3.50E-03
Lix1	limb expression 1 homolog (chicken)	2.89	4.95E-03
Olig1	oligodendrocyte transcription factor 1	3.41	6.03E-03

Annex

Annex 3 : Table showing the gene the most significantly upregulated in Olig2 knock-out compared to wild type. Fold change are indicated Fc and associated p-value.

Gene Symbol	Gene Title	Fc O2-KO/WT	PValue
Zkscan1	zinc finger with KRAB and SCAN domains 1	0.30	5.89E-03
Brd4	bromodomain containing 4	0.34	1.12E-02
Shox2	short stature homeobox 2	0.35	1.46E-02
Ifnar1	interferon (alpha and beta) receptor 1	0.37	1.63E-02
Mll5	myeloid/lymphoid or mixed-lineage leukemia 5	0.37	2.89E-02
F630007L15Rik	RIKEN cDNA F630007L15 gene	0.38	1.91E-04
Gbx2	gastrulation brain homeobox 2	0.41	4.23E-03
Rora	RAR-related orphan receptor alpha	0.41	9.47E-03
4933407C03Rik	RIKEN cDNA 4933407C03 gene	0.42	1.42E-02
Eif4ebp2	eukaryotic translation initiation factor 4E binding protein 2	0.42	1.32E-02
Dot1l	DOT1-like, histone H3 methyltransferase (S. cerevisiae)	0.42	1.07E-02
D10Ertd638e	DNA segment, Chr 10, ERATO Doi 638, expressed	0.43	3.95E-02
Bptf	bromodomain PHD finger transcription factor	0.43	3.77E-02
Pde4b	phosphodiesterase 4B, cAMP specific	0.44	3.16E-02
Hipk2	homeodomain interacting protein kinase 2	0.45	1.19E-02
Nav3	neuron navigator 3	0.46	1.11E-02
Samd5	sterile alpha motif domain containing 5	0.46	2.05E-02
Pak7	p21 protein (Cdc42/Rac)-activated kinase 7	0.46	6.72E-03
D630030B22Rik	RIKEN cDNA D630030B22 gene	0.46	1.24E-02
E130308A19Rik	RIKEN cDNA E130308A19 gene	0.47	4.61E-03
Bcan	brevican	0.47	3.67E-02
C78516	expressed sequence C78516	0.48	1.54E-03
Smarca4	SWI/SNF related, matrix associated, actin dependent regulator	0.49	1.46E-02
Kdm2a	lysine (K)-specific demethylase 2A	0.49	1.26E-02
Asxl3	additional sex combs like 3 (Drosophila)	0.49	3.80E-02
Brd3	bromodomain containing 3	0.49	8.37E-03
Auts2	autism susceptibility candidate 2	0.50	2.46E-02
Trio	Triple functional domain (PTPRF interacting)	0.50	4.17E-02
Spnb2	spectrin beta 2	0.50	2.73E-02
5830407P18Rik	RIKEN cDNA 5830407P18 gene	0.50	3.79E-02
Rasal2	RAS protein activator like 2	0.50	3.93E-02
2410137F16Rik	RIKEN cDNA 2410137F16 gene	0.50	7.25E-03
Atxn2	Ataxin 2	0.51	1.40E-02
Pdzrn3	PDZ domain containing RING finger 3	0.51	3.21E-03
Ssbp3	Single-stranded DNA binding protein 3	0.51	1.39E-03
Lhx9	LIM homeobox protein 9	0.52	7.25E-04
Ccdc97	coiled-coil domain containing 97	0.52	3.50E-02
Myo16	myosin XVI	0.52	6.78E-03
Oaz2	Ornithine decarboxylase antizyme 2	0.52	6.73E-03
Tmem57	transmembrane protein 57	0.52	5.35E-03
Tcf7l2	transcription factor 7-like 2, T-cell specific, HMG-box	0.53	7.00E-03
Rab14	RAB14, member RAS oncogene family	0.53	3.88E-02
D15Wsu126e	DNA segment, Chr 15, Wayne State University 126, expressed	0.53	9.74E-03
Kdm6a	4lysine (K)-specific demethylase 6A	0.54	1.36E-02
Tmem109	transmembrane protein 109	0.54	2.72E-02
Rnmt	RNA (guanine-7-) methyltransferase	0.54	1.01E-02
Usp7	ubiquitin specific peptidase 7	0.54	3.56E-02
Dtl	denticleless homolog (Drosophila)	0.54	3.52E-02
Lsm11	U7 snRNP-specific Sm-like protein LSM11	0.54	7.26E-04
Prokr2	prokineticin receptor 2	0.55	3.77E-03

Annex 4: Table showing the gene the most significantly downregulated in Olig2 knock-out compared to wild type. Fold change are indicated Fc and associated p-value.

Gene Symbol	Gene Title	Ascl1KO/WT	PValue	adjPVal	Olig2KO/WT	PValue	adjPVal
Ascl1	achaete-scute complex homolog 1 (Drosophila)	0.03	0.000	0.000	1.10	0.299	0.772
6330415B21Rik	RIKEN cDNA 6330415B21 gene	0.12	0.145	0.655	0.21	0.273	0.757
Dll3	delta-like 3 (Drosophila)	0.14	0.000	0.003	1.01	0.885	1
Srrm2	serine/arginine repetitive matrix 2	0.18	0.010	0.247	0.38	0.087	0.748
C430003N24Rik	RIKEN cDNA C430003N24 gene	0.21	0.010	0.247	0.50	0.161	0.757
Gsk3b	glycogen synthase kinase 3 beta	0.21	0.023	0.338	0.44	0.162	0.757
Bcan	brevican	0.22	0.002	0.136	0.47	0.037	0.711
Eif2c2	eukaryotic translation initiation factor 2C, 2	0.23	0.014	0.281	0.46	0.124	0.757
Xpr1	xenotropic and polytropic retrovirus receptor 1	0.23	0.010	0.242	0.52	0.151	0.757
Csnk2a1	casein kinase 2, alpha 1 polypeptide /	0.23	0.022	0.332	0.46	0.156	0.757
Rasal2	RAS protein activator like 2	0.23	0.001	0.125	0.50	0.039	0.711
Stk33	serine/threonine kinase 33	0.23	0.000	0.033	1.03	0.829	1
Gas2l3	growth arrest-specific 2 like 3	0.24	0.025	0.349	0.57	0.293	0.767
Hes5	hairy and enhancer of split 5 (Drosophila)	0.24	0.000	0.009	0.90	0.292	0.767
Btg1	B-cell translocation gene 1, anti-proliferative	0.25	0.009	0.236	0.44	0.068	0.727
Sgce	sarcoglycan, epsilon	0.25	0.030	0.370	0.46	0.167	0.757
Fancf	Fanconi anemia, complementation group F	0.26	0.008	0.227	0.48	0.080	0.737
Agap1	ArfGAP with GTPase domain, ankyrin repeat and PH domai	0.26	0.017	0.305	0.47	0.117	0.757
Krit1	KRIT1, ankyrin repeat containing	0.26	0.060	0.462	0.52	0.303	0.776
Slc8a1	solute carrier family 8 (sodium/calcium exchanger), memb	0.26	0.070	0.487	0.49	0.287	0.763
Mll5	myeloid/lymphoid or mixed-lineage leukemia 5	0.27	0.009	0.233	0.37	0.029	0.711
Crim1	cysteine rich transmembrane BMP regulator 1 (chordin like	0.27	0.034	0.391	0.45	0.149	0.757
Gdap10	ganglioside-induced differentiation-associated-protein 10	0.27	0.008	0.224	0.51	0.091	0.752
Slc10a4	solute carrier family 10	0.27	0.000	0.009	1.02	0.864	1
Mysm1	myb-like, SWIRM and MPN domains 1	0.27	0.042	0.419	0.39	0.109	0.757
Crebbp	CREB binding protein	0.28	0.052	0.441	0.47	0.203	0.757
D10Ertd638e	DNA segment, Chr 10, ERATO Doi 638, expressed	0.28	0.007	0.222	0.43	0.039	0.711
Ttr	transthyretin	0.28	0.468	0.910	0.77	0.879	1
Zfp280d	zinc finger protein 280D	0.29	0.061	0.466	0.70	0.537	1
9130404D08Rik	RIKEN cDNA 9130404D08 gene	0.29	0.044	0.423	0.40	0.109	0.757
Saps3	SAPS domain family, member 3	0.29	0.025	0.345	0.59	0.253	0.757
Ttc3	tetratricopeptide repeat domain 3	0.29	0.122	0.611	0.90	0.880	1
Nisch	nischarin	0.29	0.071	0.491	0.55	0.328	0.797
Cacng4	calcium channel, voltage-dependent, gamma subunit 4	0.30	0.001	0.131	0.56	0.038	0.711
Eif4ebp2	eukaryotic translation initiation factor 4E binding protein 2	0.30	0.003	0.160	0.42	0.013	0.687
Mast4	microtubule associated serine/threonine kinase family mer	0.30	0.006	0.205	0.48	0.046	0.711
Id2	inhibitor of DNA binding 2	2.05	0.000	0.082	1.72	0.002	0.541
Npy2r	neuropeptide Y receptor Y2	2.06	0.000	0.003	1.01	0.662	1.000
Ube3a	Ubiquitin protein ligase E3A	2.07	0.005	0.196	1.80	0.013	0.687
Igfbp5	insulin-like growth factor binding protein 5	2.08	0.000	0.034	1.00	0.995	1
Peg3	paternally expressed 3	2.09	0.000	0.041	1.25	0.035	0.711
Jhdm1d	jumonji C domain-containing histone demethylase 1 homc	2.09	0.001	0.114	1.55	0.012	0.687
Tbr1	T-box brain gene 1	2.10	0.000	0.011	1.40	0.001	0.463
C630043F03Rik	RIKEN cDNA C630043F03 gene	2.14	0.000	0.070	1.46	0.009	0.687
Pik3ip1	phosphoinositide-3-kinase interacting protein 1	2.14	0.003	0.169	1.23	0.259	0.757
Epha3	Eph receptor A3	2.15	0.000	0.094	1.95	0.001	0.500
Prss23	protease, serine, 23	2.17	0.000	0.017	1.23	0.016	0.687
Ccnd2	cyclin D2	2.17	0.000	0.041	1.72	0.001	0.456
E030016H06Rik	RIKEN cDNA E030016H06 gene	2.19	0.003	0.168	1.42	0.081	0.739
Kcnmb2	potassium large conductance calcium-activated channel, s	2.19	0.000	0.005	0.94	0.192	0.757
4632427E13Rik	RIKEN cDNA 4632427E13 gene	2.20	0.002	0.157	1.73	0.014	0.687
Fam181b	family with sequence similarity 181, member B	2.20	0.000	0.011	1.12	0.109	0.757
Apbb2	amyloid beta (A4) precursor protein-binding, family B, mer	2.22	0.002	0.152	1.85	0.008	0.670
Mab21l1	mab-21-like 1 (C. elegans)	2.25	0.001	0.112	1.61	0.012	0.687
Txnrd1	thioredoxin reductase 1	2.26	0.004	0.184	1.56	0.051	0.711
Prr15	proline rich 15	2.30	0.001	0.125	0.88	0.422	0.898
Cck	cholecystokinin	2.36	0.002	0.152	1.14	0.489	0.972
Pcdh18	protocadherin 18	2.36	0.004	0.183	1.49	0.085	0.743
Tcfap2c	transcription factor AP-2, gamma	2.44	0.002	0.150	1.26	0.235	0.757
Kctd12b	potassium channel tetramerisation domain containing 12b	2.51	0.002	0.148	1.02	0.930	1.000
Asb4	ankyrin repeat and SOCS box-containing 4	2.58	0.000	0.022	1.20	0.083	0.742
Prkx	protein kinase, X-linked	2.61	0.004	0.186	1.42	0.158	0.757
Pax6	paired box gene 6	2.62	0.003	0.171	1.34	0.204	0.757
Ctnnd1	catenin (cadherin associated protein), delta 1	2.65	0.002	0.157	1.55	0.070	0.728
Pnoc	prepronociceptin	2.71	0.000	0.008	1.18	0.042	0.711
Fscn1	fascin homolog 1, actin bundling protein (Strongylocentrot	2.86	0.004	0.185	2.12	0.020	0.695
Eif4g3	Eukaryotic translation initiation factor 4 gamma, 3	2.90	0.003	0.158	0.94	0.788	1.000
Gucy1a3	guanylate cyclase 1, soluble, alpha 3	3.03	0.000	0.005	1.13	0.111	0.757
Ascl1	achaete-scute complex homolog 1 (Drosophila)	3.07	0.000	0.004	1.12	0.076	0.737
Thbs1	similar to thrombospondin 1 /// thrombospondin 1	3.43	0.000	0.060	1.25	0.203	0.757
Dyrk1a	dual-specificity tyrosine-(Y)-phosphorylation regulated kin	3.59	0.004	0.186	2.63	0.015	0.687
Cpa4	carboxypeptidase A4	4.01	0.000	0.001	1.71	0.000	0.182
Thbs1	thrombospondin 1	4.02	0.001	0.107	1.51	0.123	0.757
Dmrta1	doublesex and mab-3 related transcription factor like famil	4.16	0.000	0.035	0.99	0.945	1.000
Npy	neuropeptide Y	4.66	0.000	0.010	1.03	0.822	1.000

Annex 5: Table showing the gene the most significantly downregulated in Ascl1 knock-out compared to wild type. Fold change are indicated Fc and associated p-value.

Gene Symbol	Gene Title	FC Ascl1-KO/WT	PValue	Fc Olig2-KO/WT	PValue
Brd4	bromodomain containing 4	0.21	1.85E-03	0.34	1.12E-02
Bcan	brevican	0.22	1.52E-03	0.47	3.67E-02
Rasal2	RAS protein activator like 2	0.23	1.19E-03	0.50	3.93E-02
Mll5	myeloid/lymphoid or mixed-lineage leukemia 5	0.27	8.67E-03	0.37	2.89E-02
D10Ertd638e	DNA segment, Chr 10, ERATO Doi 638, expressed	0.28	7.36E-03	0.43	3.95E-02
Cacng4	calcium channel, voltage-dependent, gamma subunit 4	0.30	1.34E-03	0.56	3.81E-02
Eif4ebp2	eukaryotic translation initiation factor 4E binding protein 2	0.30	2.69E-03	0.42	1.32E-02
5730478J17Rik	RIKEN cDNA 5730478J17 gene	0.31	1.42E-03	0.57	4.22E-02
Bptf	bromodomain PHD finger transcription factor	0.33	1.28E-02	0.43	3.77E-02
Cdca7	Cell division cycle associated 7	0.34	1.13E-03	0.56	2.29E-02
Zkscan1	zinc finger with KRAB and SCAN domains 1	0.35	1.14E-02	0.30	5.89E-03
Cacna1b	calcium channel, voltage-dependent, N type, alpha 1B subunit	0.35	2.53E-03	0.56	3.63E-02
5830407P18Rik	RIKEN cDNA 5830407P18 gene	0.36	7.36E-03	0.50	3.79E-02
Brd3	bromodomain containing 3	0.36	1.32E-03	0.49	8.37E-03
Samd5	sterile alpha motif domain containing 5	0.36	6.66E-03	0.46	2.05E-02
E130308A19Rik	RIKEN cDNA E130308A19 gene	0.37	1.08E-03	0.47	4.61E-03
Asxl3	additional sex combs like 3 (Drosophila)	0.37	9.26E-03	0.49	3.80E-02
4933407C03Rik	RIKEN cDNA 4933407C03 gene	0.37	7.78E-03	0.42	1.42E-02
Nav3	neuron navigator 3	0.38	4.44E-03	0.46	1.11E-02
Dtl	denticleless homolog (Drosophila)	0.39	5.48E-03	0.54	3.52E-02
Rgs17	regulator of G-protein signaling 17	0.40	1.63E-03	0.64	4.23E-02
Atxn2	Ataxin 2	0.40	3.42E-03	0.51	1.40E-02
D630030B22Rik	RIKEN cDNA D630030B22 gene	0.41	6.27E-03	0.46	1.24E-02
Dot1l	DOT1-like, histone H3 methyltransferase (S. cerevisiae)	0.41	9.03E-03	0.42	1.07E-02
Rab14	RAB14, member RAS oncogene family	0.41	9.81E-03	0.53	3.88E-02
Ifnar1	interferon (alpha and beta) receptor 1	0.41	2.73E-02	0.37	1.63E-02
Usp7	ubiquitin specific peptidase 7	0.42	8.91E-03	0.54	3.56E-02
Strbp	spermatid perinuclear RNA binding protein	0.42	2.89E-03	0.56	1.75E-02
D15Wsu126e	DNA segment, Chr 15, Wayne State University 126, expressed	0.43	2.36E-03	0.53	9.74E-03
Anks1	ankyrin repeat and SAM domain containing 1	0.44	6.38E-04	0.67	2.03E-02
Gsk3b	glycogen synthase kinase 3 beta	0.44	9.59E-03	0.55	3.64E-02
Pak7	p21 protein (Cdc42/Rac)-activated kinase 7	0.46	6.54E-03	0.46	6.72E-03
Cuedc1	CUE domain containing 1	0.46	4.35E-04	0.57	2.82E-03
Vps29	vacuolar protein sorting 29 (S. pombe)	0.47	8.53E-04	0.57	4.02E-03
Smarca4	SWI/SNF related, matrix associated, actin dependent regulator of chromatin, subfamily a, member 4	0.47	1.13E-02	0.49	1.46E-02
Rcor2	REST corepressor 2	0.48	2.19E-03	0.63	1.93E-02
Zfp644	zinc finger protein 644	0.48	1.26E-02	0.55	3.00E-02
Dis3l2	DIS3 mitotic control homolog (S. cerevisiae)-like 2	0.48	2.04E-03	0.61	1.35E-02
Fam40a	family with sequence similarity 40, member A	0.48	8.08E-03	0.59	3.39E-02
2410137F16Rik	RIKEN cDNA 2410137F16 gene	0.49	5.57E-03	0.50	7.25E-03
Trio	Triple functional domain (PTPRF interacting)	0.49	3.66E-02	0.50	4.17E-02
Tmem57	transmembrane protein 57	0.49	3.46E-03	0.52	5.35E-03
C78516	expressed sequence C78516	0.49	1.98E-03	0.48	1.54E-03
Nav1	neuron navigator 1	0.49	1.47E-03	0.57	4.84E-03
Fbxo32	F-box protein 32	0.50	4.87E-03	0.61	2.23E-02
Kalrn	kalirin, RhoGEF kinase	0.50	9.11E-03	0.62	4.09E-02
6430501K19Rik	RIKEN cDNA 6430501K19 gene	0.50	5.98E-06	0.70	3.29E-04
Bat2l2	HLA-B associated transcript 2-like 2	0.50	7.93E-03	0.60	2.92E-02
Klf13	Kruppel-like factor 13	0.50	5.49E-03	0.61	2.45E-02
Prox1	prospero-related homeobox 1	0.50	8.09E-03	0.62	3.84E-02

Annex : Table of Ascl1/Olig2 down regulated genes in ventral telencephalon

Pitpnc1	phosphatidylinositol transfer protein, cytoplasmic 1	1.97	1.78E-02	2.04	1.45E-02
Prkci	protein kinase C, iota	1.98	2.16E-02	1.84	3.34E-02
Hnrnpl	heterogeneous nuclear ribonucleoprotein L	1.99	2.20E-02	1.85	3.40E-02
Clasp2	CLIP associating protein 2	2.00	6.06E-03	1.88	9.35E-03
Sp3	trans-acting transcription factor 3	2.00	3.66E-02	1.98	3.86E-02
Tmtc3	transmembrane and tetratricopeptide repeat containing 3	2.00	5.07E-04	1.78	1.43E-03
Tfrc	transferrin receptor	2.02	4.32E-02	2.05	4.05E-02
Zfx	zinc finger protein X-linked	2.02	1.76E-02	2.15	1.25E-02
Ubc	ubiquitin C	2.03	1.76E-02	2.74	3.50E-03
G2e3	G2/M-phase specific E3 ubiquitin ligase	2.04	1.03E-02	1.82	2.10E-02
Rabgap1	RAB GTPase activating protein 1	2.04	1.80E-02	1.79	3.94E-02
Neurod1	neurogenic differentiation 1	2.04	5.78E-03	1.56	4.19E-02
Id2	inhibitor of DNA binding 2	2.05	3.31E-04	1.72	1.51E-03
Klf6	Kruppel-like factor 6	2.06	7.73E-03	1.73	2.58E-02
Ttc3	tetratricopeptide repeat domain 3	2.07	3.53E-04	1.40	1.68E-02
Arl8b	ADP-ribosylation factor-like 8B	2.07	2.38E-02	2.04	2.58E-02
Ube3a	Ubiquitin protein ligase E3A	2.07	5.07E-03	1.80	1.33E-02
Ywhaz	tyrosine 3-monooxygenase/tryptophan 5-monooxygenase activation protein, zeta polypeptide	2.08	6.57E-03	1.75	2.17E-02
Armc9	armadillo repeat containing 9	2.09	9.75E-03	1.71	3.60E-02
Peg3	paternally expressed 3	2.09	7.81E-05	1.25	3.53E-02
Jhdm1d	jumonji C domain-containing histone demethylase 1 homolog D (S. cerevisiae)	2.09	8.96E-04	1.55	1.20E-02
Tmx4	thioredoxin-related transmembrane protein 4	2.09	4.78E-03	1.88	9.90E-03
Tbr1	T-box brain gene 1	2.10	6.65E-06	1.40	7.49E-04
Soat1	sterol O-acyltransferase 1	2.12	5.45E-03	1.98	8.50E-03
Prpf39	PRP39 pre-mRNA processing factor 39 homolog (yeast)	2.13	3.18E-02	2.00	4.34E-02
Rp2h	retinitis pigmentosa 2 homolog (human)	2.13	3.56E-03	1.65	2.30E-02
C630043F03Rik	RIKEN cDNA C630043F03 gene	2.14	2.27E-04	1.46	9.20E-03
Epha3	Eph receptor A3	2.15	4.95E-04	1.95	1.07E-03
Zfa/Zfx	zinc finger protein, autosomal /// zinc finger protein X-linked	2.16	1.74E-02	2.05	2.33E-02
Prss23	protease, serine, 23	2.17	1.40E-05	1.23	1.63E-02
Ccnd2	cyclin D2	2.17	7.54E-05	1.72	5.98E-04
Adam10	a disintegrin and metallopeptidase domain 10	2.18	2.54E-02	2.05	3.50E-02
Sfpq	splicing factor proline/glutamine rich (polypyrimidine tract binding protein associated)	2.19	2.10E-02	2.22	1.98E-02
Usp22	ubiquitin specific peptidase 22	2.19	1.80E-02	1.99	3.04E-02
4632427E13Rik	RIKEN cDNA 4632427E13 gene	2.20	2.47E-03	1.73	1.36E-02
Apbb2	amyloid beta (A4) precursor protein-binding, family B, member 2	2.22	2.27E-03	1.85	8.12E-03
Eif2s3x	eukaryotic translation initiation factor 2, subunit 3, structural gene X-linked	2.23	8.93E-03	1.85	2.72E-02
Ppp1r12a	protein phosphatase 1, regulatory (inhibitor) subunit 12A	2.24	1.57E-02	2.04	2.62E-02
Mab21l1	mab-21-like 1 (C. elegans)	2.25	8.69E-04	1.61	1.25E-02
Nucks1	nuclear casein kinase and cyclin-dependent kinase substrate 1	2.28	9.14E-03	2.21	1.10E-02
Sfrp1	secreted frizzled-related protein 1	2.38	9.04E-03	1.89	3.22E-02
Tcfap2c	transcription factor AP-2, gamma	2.38	5.65E-06	1.24	1.25E-02
Tgoln1	trans-golgi network protein	2.40	6.96E-03	1.90	2.67E-02
Xiap	X-linked inhibitor of apoptosis	2.41	8.28E-03	2.44	7.69E-03
Lix1	limb expression 1 homolog (chicken)	2.49	1.01E-02	2.89	4.95E-03
Lin7c	lin-7 homolog C (C. elegans)	2.51	1.51E-02	2.20	2.85E-02
Tmed2	transmembrane emp24 domain trafficking protein 2	2.59	2.84E-02	2.32	4.44E-02
Fscn1	fascin homolog 1, actin bundling protein (Strongylocentrotus purpuratus)	2.86	4.22E-03	2.12	1.96E-02
Dyrk1a	dual-specificity tyrosine-(Y)-phosphorylation regulated kinase 1a	3.59	4.25E-03	2.63	1.54E-02
Cpa4	carboxypeptidase A4	4.01	2.29E-08	1.71	8.97E-06

Annex3: Table of Ascl1/Olig2 up regulated genes in ventral telencephalon

Annex 5: Scripts for R.-CRAN:

R-CRAN scripts and Packages used for microarray analysis

```
#################################################################
###########
```

Bioconductor Packages to install from www.bioconductor.org or R-cran repository:

```
Affy; gcrma; oligo; frma; rgl ; mass; Ade4;limma;kerfdr

#################################################################
###########
```

Load packages:

```
library(affy)
library(gcrma)
library(oligo)
library(frma)
library(ade4)
library(rgl)
library(MASS)
library(limma)
library(kerfdr)

#################################################################
###########
```

Fonctions to source in R-CRAN:

```
pxt.h1Proportion = function(pv, method = "storey", lambda =
0.5){
   method = match.arg(method)
  pi1 = 1 - mean(pv > lambda, na.rm = TRUE)/(1 - lambda)
  if (pi1 < 0) {
        warning(paste("estimated pi1 =", round(pi1, digit =
4),
            "set to 0.0"))
        pi1 = 0
    }
    if (pi1 > 1) {
        warning(paste("estimated pi1 =", round(pi1, digit =
4),
            "set to 1.0"))
        pi1 = 1
    }

  return(pi1)
```

```
}

pxt.rainbow = function(n, default2Col =
c("darkgrey","orange"), default6Col = c("red", "green",
"blue", "orange", "purple", "pink" ), mode = c("rainbow",
"gray", "grey")){
  mode = match.arg(mode)
  if (mode == "grey")
    mode = "gray"
  if (n == 1)
    return(default2Col[1])
  if (n == 2)
    return(default2Col )
  if (n > 6 & mode == "rainbow")
    return(rainbow(n))
  if (n < 7 & n > 2 & mode == "rainbow")
    return (default6Col[1:n])
  if (n > 2 & mode == "gray")
    return(gray (seq (0.8, 0.2, length = n)))
}


pxt.plotGroup3d = function(xyz, group = NULL, group.display =
TRUE, group.font = 4, group.family = c("serif", "sans",
"mono", "symbol"), group.cex = 1.5, group.xyz = NULL, labels =
NULL, type = c("s", "p", "l", "h"), alpha = 0.6, box = FALSE,
size = 0.4, col = NULL, fcol = pxt.rainbow, star = FALSE,
ellipse = TRUE, ellipse.alpha = 0.1,ellipse.back = c("fill",
"line"), labels.col = "black", labels.cex = 0.6, labels.adj =
c(0,-1), labels.family = c("serif", "sans", "mono",
"symbol"),labels.font = 2, ...) {

  require(rgl)
  require(MASS)

  ellipse.back = match.arg(ellipse.back)
  type = match.arg(type)
  labels.family = match.arg(labels.family)
  group.family = match.arg(group.family)


  if (is.null(group)){
    group.display = FALSE
    star = FALSE
    ellipse = FALSE
  # color definition
  col3d = col
    if (is.null(col))
      col3d = "darkgrey"
  }
  else{
```

```
  if (!is.factor(group))
    group = factor(as.character(group), exclude = "NA")

  if (is.null(col))
    col = fcol(nlevels(as.factor(group)))
  col3d = col[match(group, levels(group))]
  col3d[which(is.na(col3d))] = "white"
  }

  # main plot
  open3d()
  plot3d(x = xyz, type = type, size = size, box = box, col =
col3d, alpha = alpha, ...)
  MU = NULL
  if (!is.null(group)){
    # barycenter computation & plot
    for (iii in 1:length(levels(group))){
      aa = which(group == levels(group)[iii])
      mu = c(mean(xyz[aa, 1]),mean(xyz[aa, 2]), mean(xyz[aa,
3]))
      MU = rbind(MU, mu)
      if (length(aa) > 1){
        sigma = cov.trob(xyz[aa, ])$cov
        if (star)
          for (jjj in aa)
            rgl.lines(rbind(mu, as.numeric(xyz[jjj, ])), color
= col[iii])
        if (ellipse)
          plot3d(ellipse3d(sigma, centre = mu), col=col[iii],
alpha=ellipse.alpha, add = TRUE, back = ellipse.back)
      }
    }

    # groups
    if (group.display){
      if (is.null(group.xyz))
        group.xyz = MU
        text3d(group.xyz, text=levels(group), color = col,
font = group.font, family = group.family, cex = group.cex)
      }
  }

  # labels
  if (!is.null(labels))
    text3d(xyz, text=labels,adj = labels.adj, color =
labels.col, family = labels.family, cex = labels.cex, font =
labels.font)

}
```

```
pxt.plotGroup2d = function(xy, group = NULL, group.display =
FALSE, group.font = 4, group.family = c("serif", "sans",
"mono", "symbol"), group.cex = 1.5, group.xy = NULL, pch = 16,
labels = NULL, col = NULL, fcol = pxt.rainbow, star = FALSE,
star.lty = "dotted", ellipse = TRUE, ellipse.axes = TRUE,
labels.cex = 0.8, labels.adj = c(0,-1), labels.family =
c("serif", "sans", "mono", "symbol"),labels.font = 2, legend =
TRUE, legend.location = "bottomright", legend.title = NULL,
legend.cex = 1, ...) {

  require(ade4)

  labels.family = match.arg(labels.family)
  group.family = match.arg(group.family)


  if (is.null(group)){
    group.display = FALSE
    star = FALSE
    ellipse = FALSE
  # color definition
  col2d = col
    if (is.null(col))
      col2d = "darkgrey"
  }
  else{
    if (!is.factor(group))
      group = factor(as.character(group), exclude = NA)

    if (is.null(col))
      col = fcol(nlevels(group))
    col2d = rep(NA, length(group))
    col2d = col[match(group, levels(group))]
    col2d[which(is.na(col2d))] = "lightgrey"
  }

  # main plot

  plot(x = xy, col = col2d, pch = pch, asp = 1,...)
  MU = NULL
  if (!is.null(group)){
    # barycenter computation & plot
    for (iii in 1:length(levels(group))){
      aa = which(group == levels(group)[iii])
      mu = c(mean(xy[aa, 1]),mean(xy[aa, 2]))
      MU = rbind(MU, mu)
      if (length(aa) > 1){
        if (star)
          for (jjj in aa)
            lines(rbind(mu, as.numeric(xy[jjj, ])), col =
col[iii], lty = star.lty)
```

```
        if (ellipse)
          scatterutil.ellipse(xy[aa, 1], xy[aa, 2], rep(1,
length(aa)), coul=col[iii], ax = ellipse.axes, cell = 1)
      }
    }

    # groups
    if (group.display){
      if (is.null(group.xy))
        group.xy = MU
        text(group.xy, labels=levels(group), col = col, font =
group.font, family = group.family, cex = group.cex)
      }
    if (legend){
      legend(legend.location, legend = levels(group), fill =
col, bty = "n", title = legend.title, cex = legend.cex)
    }
  }

  # labels
  if (!is.null(labels))
    text(xy, labels=labels,adj = labels.adj, col = col2d,
family = labels.family, cex = labels.cex, font = labels.font)

 return(list(xy = xy, labels = labels, group = group))
}

pxt.cv = function(x, robust = TRUE){
  if (robust)
    cv = mad(x, na.rm = TRUE)/mean(x, na.rm = TRUE)
  else cv = sd(x, na.rm = TRUE)/mean(x, na.rm = TRUE)
  return(cv)
}



##############################################################
###########

Define working directory:

setwd("C:/Users/Desktop")

##############################################################
###########

Read and load Affymetrix MOE430 2.0 arrays CEL files:

Mydata<-ReadAffy()
```

```
##########################################################################
###########
```

Normalize affymetrix MOE430 2.0 arrays data:

```
eset <- gcrma(Mydata)
(choose rma, gcrma or frma)

##########################################################################
###########
```

Export résults:

```
write.exprs(eset, file="file_name.txt", sep=",")

##########################################################################
###########
```

Load data for statistical analysis:

```
exp.norm = read.table("name_file.txt", sep = "\t", h = TRUE,
stringsAsFactors = FALSE)
rownames(exp.norm) = exp.norm[, 1]
exp.norm = exp.norm[, 2:ncol(exp.norm)]

##########################################################################
###########
```

Expression data distribution :

```
pdf("distributionExpression.pdf")
hist(as.numeric(as.matrix(exp.norm)), main  = "distribution
expression")
dev.off()

##########################################################################
###########
```

Probeset selection for Principal component analysis:

```
d90 <- apply(exp.norm,1,function(x)quantile(x,probs=.9))
cv = apply(exp.norm, MARGIN = 1, FUN = pxt.cv)
pbsok = rownames(exp.norm)[which(d90>log(10,2) & cv > 0.0005)]

##########################################################################
###########
```

Principle component analysis:

```
grp = rep(c("KO", "WT"), each = 5)
```

```
pca = dudi.pca(t(exp.norm[pbsok, ]), nf = 3, scannf = FALSE)

pxt.plotGroup3d(pca$li, group = grp)
pdf("pca.pdf")
pxt.plotGroup2d(pca$li[, 1:2], , group = grp, labels =
names(exp.norm))
dev.off()

##############################################################
###########
```

ANOVA analysis:

```
pv = NULL
for (iii in 1:nrow(exp.norm[pbsok, ] )){print(iii)
  model = aov(as.numeric(exp.norm[pbsok[iii],
])~as.factor(grp))
  pv[iii] = summary(model)[[1]][1, 5]
}
names(pv) = pbsok

##############################################################
###########
```

P-values Distribution :

```
pxt.h1Proportion(pv)
pdf("distributionPv.pdf")
hist(pv, main = "percent of differentialy expressed genes")
dev.off()

##############################################################
###########
```

Multiple testing correction:

Bonferonni method:

```
bonf = pv*length(pv)
bonf[which(bonf > 1)] = 1
names(bonf) = pbsok
```

Bonferoni-Hochberg method:

```
FDR_bh = pv*length(pv)/rank(pv)
FDR_bh[which(FDR_bh > 1)] = 1
names(FDR_bh) = pbsok
```

Kernel based methods:

```
kerfdr = kerfdr(pv)$localfdr
```

```
names(kerfdr)

results = data.frame(pbsok, pv, bonf, FDR_bh, kerfdr)
write.table(resultats, file = "resultats_pvalues.txt", sep =
"\t", quote = FALSE, row.names = FALSE)

############################################################
###########
```

Limma Analysis:

```
library(limma)
exp.norm = read.table("name_file.txt", sep = "\t", h = TRUE,
stringsAsFactors = FALSE)
rownames(exp.norm) = exp.norm[, 1]
exp.norm = exp.norm[, 2:ncol(exp.norm)]
design <- model.matrix(~ -1+factor(c(1,1,1,2,2,2,3,3,3)))
colnames(design) <- c("group1", "group2", "group3")
fit <- lmFit(exp.norm, design)
contrast.matrix <- makeContrasts(group2-group1, group3-group2,
group3-group1, levels=design)
fit2 <- contrasts.fit(fit, contrast.matrix)
fit2 <- eBayes(fit2)
write.table(topTable(fit2, coef=1, adjust="fdr", sort.by="B",
number=50000), file="name_comparison1.xls", row.names=F,
sep="\t")
write.table(topTable(fit2, coef=2, adjust="fdr", sort.by="B",
number=50000), file=" name_comparison2.xls", row.names=F,
sep="\t")
Increase coefficient for more comparisons:
write.table(topTable(fit2, coef=3…, adjust="fdr", sort.by="B",
number=50000), file=" name_comparison3….xls", row.names=F,
sep="\t")

############################################################
###########
```

Affymetrix mogene 1 0 st v1 analysis:

```
library(oligo)
geneCELs <- list.celfiles("C:/Users/Desktop/geneExperiment",
full.names = TRUE)
affyGeneFS <- read.celfiles(geneCELs)
genePS <- rma(affyGeneFS, target = "probeset")
theIDs  <-  getBM(attributes  =  "affy_mogene_1_0_st_v1",
filters  =  "entrezgene",  mart  =  ensembl)
geneCore <- rma(affyGeneFS, target = "core")
featureData(genePS) <- getNetAffx(genePS, "probeset")
featureData(geneCore) <- getNetAffx(geneCore, "transcript")
featureData(exonCore)
varLabels(featureData(geneCore))
```

```
write.exprs(genePS, file="Myproject_oligo_rma.xls", sep=",")
```

REFERENCES

1. E. Aaku-Saraste, B. Oback, A. Hellwig, W. B. Huttner, Neuroepithelial cells downregulate their plasma membrane polarity prior to neural tube closure and neurogenesis. Mechanisms of Development 69, 71-81 (1997).
2. O. Abdel-Mannan, A. F. P. Cheung, Z. Molnár, Evolution of cortical neurogenesis. Brain Research Bulletin 75, 398-404 (2008).
3. K. Adelman et al., Immediate mediators of the inflammatory response are poised for gene activation through RNA polymerase II stalling. Proceedings of the National Academy of Sciences of the United States of America 106, 18207-18212 (2009).
4. S. Aggarwal et al., Myelin membrane assembly is driven by a phase transition of myelin basic proteins into a cohesive protein meshwork. PLoS biology 11, (2013).
5. M. Aida et al., Transcriptional pausing caused by NELF plays a dual role in regulating immediate-early expression of the junB gene. Molecular and Cellular Biology 26, 6094-6104 (2006).
6. T. Akagi et al., Requirement of multiple basic helix-loop-helix genes for retinal neuronal subtype specification. The Journal of Biological Chemistry 279, 28492-28498 (2004).
7. A. Akhtar, D. Zink, P. B. Becker, Chromodomains are protein-RNA interaction modules. Nature 407, 405-409 (2000).
8. J. Alcedo, M. Ayzenzon, T. Von Ohlen, M. Noll, J. E. Hooper, The Drosophila smoothened gene encodes a seven-pass membrane protein, a putative receptor for the hedgehog signal. Cell 86, 221-232 (1996).
9. F. R. Ali et al., The phosphorylation status of Ascl1 is a key determinant of neuronal differentiation and maturation in vivo and in vitro. Development (Cambridge, England) 141, 2216-2224 (2014).
10. M. Altaf et al., NuA4-dependent acetylation of nucleosomal histones H4 and H2A directly stimulates incorporation of H2A.Z by the SWR1 complex. The Journal of Biological Chemistry 285, 15966-15977 (2010).
11. M. Altaf-Ul-Amin, F. M. Afendi, S. K. Kiboi, S. Kanaya, Systems biology in the context of big data and networks. BioMed Research International 2014, (2014).
12. J. Altman, G. D. Das, Autoradiographic and histological evidence of postnatal hippocampal neurogenesis in rats. The Journal of Comparative Neurology 124, 319-335 (1965).
13. A. Alvarez-Buylla, D. A. Lim, For the long run: maintaining germinal niches in the adult brain. Neuron 41, 683-686 (2004).
14. Y. Arai et al., Neural stem and progenitor cells shorten S-phase on commitment to neuron production. Nature Communications 2, (2011).
15. M. Aramaki et al., Embryonic expression profile of chicken CHD7, the ortholog of the causative gene for CHARGE syndrome. Birth Defects Research. Part A, Clinical and Molecular Teratology 79, 50-57 (2007).
16. M. B. Ardehali et al., Drosophila Set1 is the major histone H3 lysine 4 trimethyltransferase with role in transcription. The EMBO journal 30, 2817-2828 (2011).
17. H. A. Arnett et al., bHLH transcription factor Olig1 is required to repair demyelinated lesions in the CNS. Science (New York, N.Y.) 306, 2111-2115 (2004).
18. C. D. Arnold et al., Quantitative genome-wide enhancer activity maps for five Drosophila species show functional enhancer conservation and turnover during cis-regulatory evolution. Nature Genetics 46, 685-692 (2014).
19. P. Aroca, L. Puelles, Postulated boundaries and differential fate in the developing rostral hindbrain. Brain Research. Brain Research Reviews 49, 179-190 (2005).
20. A. Arvanitaki, Effects Evoked in an Axon by the Activity of a Contiguous One. Journal of Neurophysiology 5, 89-108 (1942).
21. M. Asami et al., The role of Pax6 in regulating the orientation and mode of cell division of progenitors in the mouse cerebral cortex. Development (Cambridge, England) 138, 5067-5078 (2011).
22. M. Ashburner, Drosophila. A laboratory handbook. Cold Spring Harbor Laboratory Press, Cold Spring Harbor, NY, xliii-+ 1331pp. (1989).

23. D. Attwell, S. B. Laughlin, An energy budget for signaling in the grey matter of the brain. Journal of Cerebral Blood Flow and Metabolism: Official Journal of the International Society of Cerebral Blood Flow and Metabolism 21, 1133-1145 (2001).
24. G. Badis et al., Diversity and complexity in DNA recognition by transcription factors. Science (New York, N.Y.) 324, 1720-1723 (2009).
25. J. Baedke, The epigenetic landscape in the course of time: Conrad Hal Waddington's methodological impact on the life sciences. Studies in History and Philosophy of Biological and Biomedical Sciences 44, 756-773 (2013).
26. A. Bagchi et al., CHD5 is a tumor suppressor at human 1p36. Cell 128, 459-475 (2007).
27. S. Bai et al., NOTCH1 regulates osteoclastogenesis directly in osteoclast precursors and indirectly via osteoblast lineage cells. The Journal of Biological Chemistry 283, 6509-6518 (2008).
28. R. Bajpai et al., CHD7 cooperates with PBAF to control multipotent neural crest formation. Nature 463, 958-962 (2010).
29. F. Balordi, G. Fishell, Hedgehog signaling in the subventricular zone is required for both the maintenance of stem cells and the migration of newborn neurons. The Journal of Neuroscience: The Official Journal of the Society for Neuroscience 27, 5936-5947 (2007).
30. F. Balordi, G. Fishell, Mosaic removal of hedgehog signaling in the adult SVZ reveals that the residual wild-type stem cells have a limited capacity for self-renewal. The Journal of Neuroscience: The Official Journal of the Society for Neuroscience 27, 14248-14259 (2007).
31. C. R. S. Banerji et al., Cellular network entropy as the energy potential in Waddington's differentiation landscape. Scientific Reports 3, (2013).
32. J. Banerji, S. Rusconi, W. Schaffner, Expression of a beta-globin gene is enhanced by remote SV40 DNA sequences. Cell 27, 299-308 (1981).
33. R. A. Barker, F. Cicchetti, Neurodegenerative disorders: the Glia way forward. Frontiers in Pharmacology 5, (2014).
34. B. A. Barres, M. C. Raff, Proliferation of oligodendrocyte precursor cells depends on electrical activity in axons. Nature 361, 258-260 (1993).
35. G. Bartolini, G. Ciceri, O. Marín, Integration of GABAergic interneurons into cortical cell assemblies: lessons from embryos and adults. Neuron 79, 849-864 (2013).
36. T. Batsukh et al., CHD8 interacts with CHD7, a protein which is mutated in CHARGE syndrome. Human Molecular Genetics 19, 2858-2866 (2010).
37. J. Battiste et al., Ascl1 defines sequentially generated lineage-restricted neuronal and oligodendrocyte precursor cells in the spinal cord. Development (Cambridge, England) 134, 285-293 (2007).
38. P. Batut, A. Dobin, C. Plessy, P. Carninci, T. R. Gingeras, High-fidelity promoter profiling reveals widespread alternative promoter usage and transposon-driven developmental gene expression. Genome Research 23, 169-180 (2013).
39. N. Baumann, D. Pham-Dinh, Biology of oligodendrocyte and myelin in the mammalian central nervous system. Physiological Reviews 81, 871-927 (2001).
40. L. M. Baye, B. A. Link, Nuclear migration during retinal development. Brain Research 1192, 29-36 (2008).
41. P. B. Becker, W. Hörz, ATP-dependent nucleosome remodeling. Annual Review of Biochemistry 71, 247-273 (2002).
42. R. Belotserkovskaya et al., FACT facilitates transcription-dependent nucleosome alteration. Science (New York, N.Y.) 301, 1090-1093 (2003).
43. N. Ben-Arie et al., Math1 is essential for genesis of cerebellar granule neurons. Nature 390, 169-172 (1997).
44. J. E. H. Bergman et al., CHD7 mutations and CHARGE syndrome: the clinical implications of an expanding phenotype. Journal of Medical Genetics 48, 334-342 (2011).
45. M. Bergsland, M. Werme, M. Malewicz, T. Perlmann, J. Muhr, The establishment of neuronal properties is controlled by Sox4 and Sox11. Genes & Development 20, 3475-3486 (2006).
46. B. Berninger, F. Guillemot, M. Götz, Directing neurotransmitter identity of neurones derived from expanded adult neural stem cells. The European Journal of Neuroscience 25, 2581-2590 (2007).
47. B. E. Bernstein et al., A bivalent chromatin structure marks key developmental genes in embryonic stem cells. Cell 125, 315-326 (2006).
48. N. Bertrand, D. S. Castro, F. Guillemot, Proneural genes and the specification of neural cell types. Nature Reviews. Neuroscience 3, 517-530 (2002).

49. T. H. Bestor, The DNA methyltransferases of mammals. Human Molecular Genetics 9, 2395-2402 (2000).
50. W. A. Bickmore, B. van Steensel, Genome architecture: domain organization of interphase chromosomes. Cell 152, 1270-1284 (2013).
51. M. Bieda, X. Xu, M. A. Singer, R. Green, P. J. Farnham, Unbiased location analysis of E2F1-binding sites suggests a widespread role for E2F1 in the human genome. Genome Research 16, 595-605 (2006).
52. Mark D. Biggin, Animal Transcription Networks as Highly Connected, Quantitative Continua. Developmental Cell 21, 611-626 (2011).
53. S. Blaess, J. D. Corrales, A. L. Joyner, Sonic hedgehog regulates Gli activator and repressor functions with spatial and temporal precision in the mid/hindbrain region. Development (Cambridge, England) 133, 1799-1809 (2006).
54. K. D. Blake et al., CHARGE association: an update and review for the primary pediatrician. Clinical Pediatrics 37, 159-173 (1998).
55. E. Blaugrund et al., Distinct subpopulations of enteric neuronal progenitors defined by time of development, sympathoadrenal lineage markers and Mash-1-dependence. Development (Cambridge, England) 122, 309-320 (1996).
56. J. Blustajn, C. F. E. Kirsch, A. Panigrahy, I. Netchine, Olfactory anomalies in CHARGE syndrome: imaging findings of a potential major diagnostic criterion. AJNR. American journal of neuroradiology 29, 1266-1269 (2008).
57. O. Bogdanovic et al., Dynamics of enhancer chromatin signatures mark the transition from pluripotency to cell specification during embryogenesis. Genome Research 22, 2043-2053 (2012).
58. S. F. Boj et al., Functional targets of the monogenic diabetes transcription factors HNF-1alpha and HNF-4alpha are highly conserved between mice and humans. Diabetes 58, 1245-1253 (2009).
59. H. Bolouri, E. H. Davidson, Transcriptional regulatory cascades in development: initial rates, not steady state, determine network kinetics. Proceedings of the National Academy of Sciences of the United States of America 100, 9371-9376 (2003).
60. L. Boltzmann, in Sitzungsber. Kais. Akad. Wiss. Wien Math. Naturwiss. Class e 76. (1877), chap. 373-435.
61. B. Bonev, P. Stanley, N. Papalopulu, MicroRNA-9 Modulates Hes1 ultradian oscillations by forming a double-negative feedback loop. Cell Reports 2, 10-18 (2012).
62. S. Bonn et al., Tissue-specific analysis of chromatin state identifies temporal signatures of enhancer activity during embryonic development. Nature Genetics 44, 148-156 (2012).
63. T. Borggrefe, X. Yue, Interactions between subunits of the Mediator complex with gene-specific transcription factors. Seminars in Cell & Developmental Biology 22, 759-768 (2011).
64. E. A. Bosman et al., Multiple mutations in mouse Chd7 provide models for CHARGE syndrome. Human Molecular Genetics 14, 3463-3476 (2005).
65. K. Bouazoune et al., The dMi-2 chromodomains are DNA binding modules important for ATP-dependent nucleosome mobilization. The EMBO journal 21, 2430-2440 (2002).
66. L. A. Boyer, R. R. Latek, C. L. Peterson, The SANT domain: a unique histone-tail-binding module? Nature Reviews. Molecular Cell Biology 5, 158-163 (2004).
67. M. R. Branco, A. Pombo, Intermingling of chromosome territories in interphase suggests role in translocations and transcription-dependent associations. PLoS biology 4, (2006).
68. A. Brehm, K. R. Tufteland, R. Aasland, P. B. Becker, The many colours of chromodomains. BioEssays: News and Reviews in Molecular, Cellular and Developmental Biology 26, 133-140 (2004).
69. J. J. Breunig, T. F. Haydar, P. Rakic, Neural stem cells: historical perspective and future prospects. Neuron 70, 614-625 (2011).
70. J. J. Breunig et al., Primary cilia regulate hippocampal neurogenesis by mediating sonic hedgehog signaling. Proceedings of the National Academy of Sciences of the United States of America 105, 13127-13132 (2008).
71. B. G. Brinkmann et al., Neuregulin-1/ErbB signaling serves distinct functions in myelination of the peripheral and central nervous system. Neuron 59, 581-595 (2008).
72. J. Briscoe, A. Pierani, T. M. Jessell, J. Ericson, A homeodomain protein code specifies progenitor cell identity and neuronal fate in the ventral neural tube. Cell 101, 435-445 (2000).
73. G. M. Brodeur, Neuroblastoma: biological insights into a clinical enigma. Nature Reviews. Cancer 3, 203-216 (2003).

74. C. E. Brown, T. Lechner, L. Howe, J. L. Workman, The many HATs of transcription coactivators. Trends in Biochemical Sciences 25, 15-19 (2000).
75. C. Buecker, J. Wysocka, Enhancers as information integration hubs in development: lessons from genomics. Trends in Genetics 28, 276-284 (2012).
76. M. Bulger, M. Groudine, Functional and mechanistic diversity of distal transcription enhancers. Cell 144, 327-339 (2011).
77. R. S. Bultje et al., Mammalian Par3 regulates progenitor cell asymmetric division via notch signaling in the developing neocortex. Neuron 63, 189-202 (2009).
78. J. Cai et al., A crucial role for Olig2 in white matter astrocyte. Development 134, 1887-1899 (2007).
79. L. Cai, E. M. Morrow, C. L. Cepko, Misexpression of basic helix-loop-helix genes in the murine cerebral cortex affects cell fate choices and neuronal survival. Development (Cambridge, England) 127, 3021-3030 (2000).
80. M. Caiazzo et al., Direct generation of functional dopaminergic neurons from mouse and human fibroblasts. Nature 476, 224-227 (2011).
81. F. Calegari, W. B. Huttner, An inhibition of cyclin-dependent kinases that lengthens, but does not arrest, neuroepithelial cell cycle induces premature neurogenesis. Journal of Cell Science 116, 4947-4955 (2003).
82. E. Calo, J. Wysocka, Modification of enhancer chromatin: what, how and why? Molecular cell 49, (2013).
83. F. Cambronero, L. Puelles, Rostrocaudal nuclear relationships in the avian medulla oblongata: a fate map with quail chick chimeras. The Journal of Comparative Neurology 427, 522-545 (2000).
84. H. A. Cameron, P. Tanapat, E. Gould, Adrenal steroids and N-methyl-D-aspartate receptor activation regulate neurogenesis in the dentate gyrus of adult rats through a common pathway. Neuroscience 82, 349-354 (1998).
85. H. A. Cameron, C. S. Woolley, B. S. McEwen, E. Gould, Differentiation of newly born neurons and glia in the dentate gyrus of the adult rat. Neuroscience 56, 337-344 (1993).
86. E. I. Campos, D. Reinberg, Histones: annotating chromatin. Annual Review of Genetics 43, 559-599 (2009).
87. Y. Cao et al., Genome-wide MyoD binding in skeletal muscle cells: a potential for broad cellular reprogramming. Developmental Cell 18, 662-674 (2010).
88. A. Carr, M. D. Biggin, A comparison of in vivo and in vitro DNA-binding specificities suggests a new model for homeoprotein DNA binding in Drosophila embryos. The EMBO journal 18, 1598-1608 (1999).
89. K. Cartharius et al., MatInspector and beyond: promoter analysis based on transcription factor binding sites. Bioinformatics (Oxford, England) 21, 2933-2942 (2005).
90. S. Casarosa, C. Fode, F. Guillemot, Mash1 regulates neurogenesis in the ventral telencephalon. Development (Cambridge, England) 126, 525-534 (1999).
91. D. S. Castro et al., Proneural bHLH and Brn proteins coregulate a neurogenic program through cooperative binding to a conserved DNA motif. Developmental Cell 11, 831-844 (2006).
92. E. Cau, G. Gradwohl, S. Casarosa, R. Kageyama, F. Guillemot, Hes genes regulate sequential stages of neurogenesis in the olfactory epithelium. Development (Cambridge, England) 127, 2323-2332 (2000).
93. E. Cau, G. Gradwohl, C. Fode, F. Guillemot, Mash1 activates a cascade of bHLH regulators in olfactory neuron progenitors. Development (Cambridge, England) 124, 1611-1621 (1997).
94. E. Cau, S. Casarosa, F. Guillemot, Mash1 and Ngn1 control distinct steps of determination and differentiation in the olfactory sensory neuron lineage. Development (Cambridge, England) 129, 1871-1880 (2002).
95. M. Center for History and New, Guide rapide pour débuter.
96. C. E. Chamberlain, J. Jeong, C. Guo, B. L. Allen, A. P. McMahon, Notochord-derived Shh concentrates in close association with the apically positioned basal body in neural target cells and forms a dynamic gradient during neural patterning. Development (Cambridge, England) 135, 1097-1106 (2008).
97. Z. Chamoun et al., Skinny hedgehog, an acyltransferase required for palmitoylation and activity of the hedgehog signal. Science (New York, N.Y.) 293, 2080-2084 (2001).
98. H. Chen et al., Conservation of the Drosophila lateral inhibition pathway in human lung cancer: a hairy-related protein (HES-1) directly represses achaete-scute homolog-1 expression. Proceedings of the National Academy of Sciences of the United States of America 94, 5355-5360 (1997).

99. L. Chen, S. J. Bush, J. M. Tovar-Corona, A. Castillo-Morales, A. O. Urrutia, Correcting for differential transcript coverage reveals a strong relationship between alternative splicing and organism complexity. Molecular Biology and Evolution 31, 1402-1413 (2014).
100. R. H. Chen, W. V. Ding, F. McCormick, Wnt signaling to beta-catenin involves two interactive components. Glycogen synthase kinase-3beta inhibition and activation of protein kinase C. The Journal of Biological Chemistry 275, 17894-17899 (2000).
101. X. Chen, X. Wang, Z. Du, Z. Ma, Y. Yang, Spatiotemporal control of gene expression in mammalian cells and in mice using the LightOn system. Current Protocols in Chemical Biology 5, 111-129 (2013).
102. X. Chen et al., Integration of external signaling pathways with the core transcriptional network in embryonic stem cells. Cell 133, 1106-1117 (2008).
103. B. Cheng et al., Functional Association of Gdown1 with RNA Polymerase II Poised on Human Genes. Molecular Cell 45, 38-50 (2012).
104. J. Cheng et al., Transcriptional Maps of 10 Human Chromosomes at 5-Nucleotide Resolution. Science 308, 1149-1154 (2005).
105. A. Chenn, Y. A. Zhang, B. T. Chang, S. K. McConnell, Intrinsic polarity of mammalian neuroepithelial cells. Molecular and Cellular Neurosciences 11, 183-193 (1998).
106. C. Chiang et al., Cyclopia and defective axial patterning in mice lacking Sonic hedgehog gene function. Nature 383, 407-413 (1996).
107. A. Chlebowski, M. Lubas, T. H. Jensen, A. Dziembowski, RNA decay machines: the exosome. Biochimica Et Biophysica Acta 1829, 552-560 (2013).
108. B. H. Choi, Radial glia of developing human fetal spinal cord: Golgi, immunohistochemical and electron microscopic study. Brain Research 227, 249-267 (1981).
109. T. Chomiak, B. Hu, What is the optimal value of the g-ratio for myelinated fibers in the rat CNS? A theoretical approach. PloS One 4, (2009).
110. P. T. Chuang, A. P. McMahon, Vertebrate Hedgehog signalling modulated by induction of a Hedgehog-binding protein. Nature 397, 617-621 (1999).
111. L. Ciani, P. C. Salinas, WNTs in the vertebrate nervous system: from patterning to neuronal connectivity. Nature Reviews. Neuroscience 6, 351-362 (2005).
112. C. R. Clapier, B. R. Cairns, The biology of chromatin remodeling complexes. Annual Review of Biochemistry 78, 273-304 (2009).
113. M. B. Clark et al., The Reality of Pervasive Transcription. PLoS Biol 9, (2011).
114. S. L. Clarke et al., Human developmental enhancers conserved between deuterostomes and protostomes. PLoS genetics 8, (2012).
115. I. Cobos, L. Puelles, S. Martínez, The avian telencephalic subpallium originates inhibitory neurons that invade tangentially the pallium (dorsal ventricular ridge and cortical areas). Developmental Biology 239, 30-45 (2001).
116. I. Cobos, K. Shimamura, J. L. Rubenstein, S. Martínez, L. Puelles, Fate map of the avian anterior forebrain at the four-somite stage, based on the analysis of quail-chick chimeras. Developmental Biology 239, 46-67 (2001).
117. M. Cohen, J. Briscoe, R. Blassberg, Morphogen interpretation: the transcriptional logic of neural tube patterning. Current Opinion in Genetics & Development 23, 423-428 (2013).
118. J. F. Colas, G. C. Schoenwolf, Towards a cellular and molecular understanding of neurulation. Developmental Dynamics: An Official Publication of the American Association of Anatomists 221, 117-145 (2001).
119. D. R. Colman, G. Kreibich, A. B. Frey, D. D. Sabatini, Synthesis and incorporation of myelin polypeptides into CNS myelin. The Journal of Cell Biology 95, 598-608 (1982).
120. B. Corominas-Murtra, J. Goñi, R. V. Solé, C. Rodríguez-Caso, On the origins of hierarchy in complex networks. Proceedings of the National Academy of Sciences of the United States of America 110, 13316-13321 (2013).
121. J. Cotney et al., The Evolution of Lineage-Specific Regulatory Activities in the Human Embryonic Limb. Cell 154, 185-196 (2013).
122. W. G. Cox, A. Hemmati-Brivanlou, Caudalization of neural fate by tissue recombination and bFGF. Development (Cambridge, England) 121, 4349-4358 (1995).
123. M. P. Creyghton et al., Histone H3K27ac separates active from poised enhancers and predicts developmental state. Proceedings of the National Academy of Sciences of the United States of America 107, 21931-21936 (2010).

124. P. H. Crossley, S. Martinez, Y. Ohkubo, J. L. Rubenstein, Coordinate expression of Fgf8, Otx2, Bmp4, and Shh in the rostral prosencephalon during development of the telencephalic and optic vesicles. Neuroscience 108, 183-206 (2001).
125. T. Czopka, C. Ffrench-Constant, D. A. Lyons, Individual oligodendrocytes have only a few hours in which to generate new myelin sheaths in vivo. Developmental Cell 25, 599-609 (2013).
126. J. K. Dale et al., Cooperation of BMP7 and SHH in the induction of forebrain ventral midline cells by prechordal mesoderm. Cell 90, 257-269 (1997).
127. S. Darras, J. Gerhart, M. Terasaki, M. Kirschner, C. J. Lowe, β-catenin specifies the endomesoderm and defines the posterior organizer of the hemichordate Saccoglossus kowalevskii. Development (Cambridge, England) 138, 959-970 (2011).
128. C. Darwin, On the Origin of Species by Means of Natural Selection, or the Preservation of Favoured Races in the Struggle for Life. (ed. London: John Murray, 1859).
129. C. Das, J. K. Tyler, Histone exchange and histone modifications during transcription and aging. Biochimica Et Biophysica Acta 1819, 332-342 (2013).
130. R. K. Dave et al., Sonic hedgehog and notch signaling can cooperate to regulate neurogenic divisions of neocortical progenitors. PloS One 6, (2011).
131. E. H. Davidson, Emerging properties of animal gene regulatory networks. Nature 468, 911-920 (2010).
132. F. A. Davis, Axonal conduction studies based on some considerations of temperature effects in multiple sclerosis. Electroencephalography and Clinical Neurophysiology 28, 281-286 (1970).
133. R. L. Davis, H. Weintraub, A. B. Lassar, Expression of a single transfected cDNA converts fibroblasts to myoblasts. Cell 51, 987-1000 (1987).
134. R. Dawkins, The Selfish Gene: 30th Anniversary Edition. (Oxford University Press, 2006), pp. 386.
135. B. A. de Boer et al., OccuPeak: ChIP-Seq peak calling based on internal background modelling. PloS One 9, (2014).
136. H. de Jong, M. Page, Search for steady states of piecewise-linear differential equation models of genetic regulatory networks. IEEE/ACM transactions on computational biology and bioinformatics / IEEE, ACM 5, 208-222 (2008).
137. P. de Lanerolle, L. Serebryannyy, Nuclear actin and myosins: life without filaments. Nature Cell Biology 13, 1282-1288 (2011).
138. E. M. De Robertis, H. Kuroda, Dorsal-ventral patterning and neural induction in Xenopus embryos. Annual Review of Cell and Developmental Biology 20, 285-308 (2004).
139. E. de Wit, W. de Laat, A decade of 3C technologies: insights into nuclear organization. Genes & Development 26, 11-24 (2012).
140. B. M. Degnan, M. Vervoort, C. Larroux, G. S. Richards, Early evolution of metazoan transcription factors. Current Opinion in Genetics & Development 19, 591-599 (2009).
141. C. Dehay, H. Kennedy, Cell-cycle control and cortical development. Nature Reviews. Neuroscience 8, 438-450 (2007).
142. J. Dekker, L. Mirny, Biological techniques: Chromosomes captured one by one. Nature 502, 45-46 (2013).
143. J. Dekker, K. Rippe, M. Dekker, N. Kleckner, Capturing chromosome conformation. Science (New York, N.Y.) 295, 1306-1311 (2002).
144. F. Del Bene, A. M. Wehman, B. A. Link, H. Baier, Regulation of neurogenesis by interkinetic nuclear migration through an apical-basal notch gradient. Cell 134, 1055-1065 (2008).
145. C. Demerens et al., Induction of myelination in the central nervous system by electrical activity. Proceedings of the National Academy of Sciences of the United States of America 93, 9887-9892 (1996).
146. E. Dessaud, A. P. McMahon, J. Briscoe, Pattern formation in the vertebrate neural tube: a sonic hedgehog morphogen-regulated transcriptional network. Development (Cambridge, England) 135, 2489-2503 (2008).
147. E. Dessaud et al., Interpretation of the sonic hedgehog morphogen gradient by a temporal adaptation mechanism. Nature 450, 717-720 (2007).
148. D. E. Dickel, A. Visel, L. A. Pennacchio, Functional anatomy of distant-acting mammalian enhancers. Philosophical Transactions of the Royal Society of London. Series B, Biological Sciences 368, (2013).
149. J. R. Dixon et al., Topological domains in mammalian genomes identified by analysis of chromatin interactions. Nature 485, 376-380 (2012).

150. S. Djebali et al., Landscape of transcription in human cells. Nature 489, 101-108 (2012).
151. F. Doetsch, I. Caillé, D. A. Lim, J. M. García-Verdugo, A. Alvarez-Buylla, Subventricular zone astrocytes are neural stem cells in the adult mammalian brain. Cell 97, 703-716 (1999).
152. A. Dranovsky, R. Hen, Hippocampal neurogenesis: regulation by stress and antidepressants. Biological Psychiatry 59, 1136-1143 (2006).
153. Dubreuil.
154. V. Dubreuil, A.-M. Marzesco, D. Corbeil, W. B. Huttner, M. Wilsch-Bräuninger, Midbody and primary cilium of neural progenitors release extracellular membrane particles enriched in the stem cell marker prominin-1. The Journal of Cell Biology 176, 483-495 (2007).
155. I. Dunham, ENCODE-ing the Future. Genetic Engineering & Biotechnology News 33, 38-39 (2013).
156. A. J. Durston et al., Retinoic acid causes an anteroposterior transformation in the developing central nervous system. Nature 340, 140-144 (1989).
157. A. Eberharter, I. Vetter, R. Ferreira, P. B. Becker, ACF1 improves the effectiveness of nucleosome mobilization by ISWI through PHD-histone contacts. The EMBO journal 23, 4029-4039 (2004).
158. Y. Echelard et al., Sonic hedgehog, a member of a family of putative signaling molecules, is implicated in the regulation of CNS polarity. Cell 75, 1417-1430 (1993).
159. D. Echevarría, C. Vieira, L. Gimeno, S. Martínez, Neuroepithelial secondary organizers and cell fate specification in the developing brain. Brain Research. Brain Research Reviews 43, 179-191 (2003).
160. L. B. Edelman, P. Fraser, Transcription factories: genetic programming in three dimensions. Current Opinion in Genetics & Development 22, 110-114 (2012).
161. R. Edgar, M. Domrachev, A. E. Lash, Gene Expression Omnibus: NCBI gene expression and hybridization array data repository. Nucleic Acids Research 30, 207-210 (2002).
162. S. Efroni et al., Global transcription in pluripotent embryonic stem cells. Cell Stem Cell 2, 437-447 (2008).
163. C. M. Egan et al., CHD5 is required for neurogenesis and has a dual role in facilitating gene expression and polycomb gene repression. Developmental Cell 26, 223-236 (2013).
164. C. F. Ehret, G. De Haller, Origin, development, and maturation of organelles and organelle systems of the cell surface in Paramecium. Journal of Ultrastructure Research 9, Supplement 1, 1-42 (1963).
165. J. Elf, G.-W. Li, X. S. Xie, Probing transcription factor dynamics at the single-molecule level in a living cell. Science (New York, N.Y.) 316, 1191-1194 (2007).
166. B. Emery, Regulation of oligodendrocyte differentiation and myelination. Science (New York, N.Y.) 330, 779-782 (2010).
167. E. P. Consortium, An integrated encyclopedia of DNA elements in the human genome. Nature 489, 57-74 (2012).
168. E. P. Consortium et al., Identification and analysis of functional elements in 1% of the human genome by the ENCODE pilot project. Nature 447, 799-816 (2007).
169. E. Engelen et al., Sox2 cooperates with Chd7 to regulate genes that are mutated in human syndromes. Nature Genetics 43, 607-611 (2011).
170. A. V. Ereskovsky, E. Renard, C. Borchiellini, Cellular and molecular processes leading to embryo formation in sponges: evidences for high conservation of processes throughout animal evolution. Development Genes and Evolution 223, 5-22 (2013).
171. J. T. Erler, R. Linding, Network medicine strikes a blow against breast cancer. Cell 149, 731-733 (2012).
172. J. Ernst, M. Kellis, Discovery and characterization of chromatin states for systematic annotation of the human genome. Nature Biotechnology 28, 817-825 (2010).
173. J. Ernst et al., Mapping and analysis of chromatin state dynamics in nine human cell types. Nature 473, 43-49 (2011).
174. M. Esteller, Non-coding RNAs in human disease. Nature Reviews Genetics 12, 861-874 (2011).
175. R. Faigle, H. Song, Signaling mechanisms regulating adult neural stem cells and neurogenesis. Biochimica Et Biophysica Acta 1830, 2435-2448 (2013).
176. J. V. Falvo, D. Thanos, T. Maniatis, Reversal of intrinsic DNA bends in the IFN beta gene enhancer by transcription factors and the architectural protein HMG I(Y). Cell 83, 1101-1111 (1995).
177. C. M. Fan et al., "Expression patterns of two murine homologs of Drosophila single-minded suggest possible roles in embryonic patterning and in the pathogenesis of Down syndrome.". Molecular and Cellular Neurosciences 7, (1996).

178. G. Fan et al., DNA methylation controls the timing of astrogliogenesis through regulation of JAK-STAT signaling. Development (Cambridge, England) 132, 3345-3356 (2005).
179. S. P. J. Fancy, J. R. Chan, S. E. Baranzini, R. J. M. Franklin, D. H. Rowitch, Myelin regeneration: a recapitulation of development? Annual Review of Neuroscience 34, 21-43 (2011).
180. M. H. Farah et al., Generation of neurons by transient expression of neural bHLH proteins in mammalian cells. Development (Cambridge, England) 127, 693-702 (2000).
181. L. M. Farkas, W. B. Huttner, The cell biology of neural stem and progenitor cells and its significance for their proliferation versus differentiation during mammalian brain development. Current Opinion in Cell Biology 20, 707-715 (2008).
182. J. Feng, T. Liu, B. Qin, Y. Zhang, X. S. Liu, Identifying ChIP-seq enrichment using MACS. Nature Protocols 7, 1728-1740 (2012).
183. W. Feng, H.-K. Liu, Epigenetic regulation of neuronal fate determination: the role of CHD7. Cell Cycle (Georgetown, Tex.) 12, 3707-3708 (2013).
184. J. E. Ferrell, Bistability, bifurcations, and Waddington's epigenetic landscape. Current biology: CB 22, R458-466 (2012).
185. R. D. Fields, B. Stevens-Graham, New insights into neuron-glia communication. Science (New York, N.Y.) 298, 556-562 (2002).
186. S. A. Fietz et al., OSVZ progenitors of human and ferret neocortex are epithelial-like and expand by integrin signaling. Nature Neuroscience 13, 690-699 (2010).
187. G. J. Filion et al., Systematic protein location mapping reveals five principal chromatin types in Drosophila cells. Cell 143, 212-224 (2010).
188. P. Filippakopoulos, S. Knapp, The bromodomain interaction module. FEBS letters 586, 2692-2704 (2012).
189. V. Filippov et al., Subpopulation of nestin-expressing progenitor cells in the adult murine hippocampus shows electrophysiological and morphological characteristics of astrocytes. Molecular and Cellular Neurosciences 23, 373-382 (2003).
190. W. Fischle et al., Molecular basis for the discrimination of repressive methyl-lysine marks in histone H3 by Polycomb and HP1 chromodomains. Genes & Development 17, 1870-1881 (2003).
191. J. L. Fish, C. Dehay, H. Kennedy, W. B. Huttner, Making bigger brains–the evolution of neural-progenitor-cell division. Journal of Cell Science 121, 2783-2793 (2008).
192. J. F. Flanagan et al., Double chromodomains cooperate to recognize the methylated histone H3 tail. Nature 438, 1181-1185 (2005).
193. C. Fode et al., The bHLH protein NEUROGENIN 2 is a determination factor for epibranchial placode-derived sensory neurons. Neuron 20, 483-494 (1998).
194. N. J. Francis, R. E. Kingston, C. L. Woodcock, Chromatin compaction by a polycomb group protein complex. Science (New York, N.Y.) 306, 1574-1577 (2004).
195. D. N. Franz, A. Iggo, Conduction failure in myelinated and non-myelinated axons at low temperatures. The Journal of Physiology 199, 319-345 (1968).
196. M. Fuccillo, A. L. Joyner, G. Fishell, Morphogen to mitogen: the multiple roles of hedgehog signalling in vertebrate neural development. Nature Reviews. Neuroscience 7, 772-783 (2006).
197. K. Fujita et al., Abnormal basiocciput development in CHARGE syndrome. AJNR. American journal of neuroradiology 30, 629-634 (2009).
198. S. Fujita, Transitory differentiation of matrix cells and its functional role in the morphogenesis of the developing vertebrate CNS. Current Topics in Developmental Biology 20, 223-242 (1986).
199. S. Fujita, The discovery of the matrix cell, the identification of the multipotent neural stem cell and the development of the central nervous system. Cell Structure and Function 28, 205-228 (2003).
200. T. Fujita et al., CHD5, a tumor suppressor gene deleted from 1p36.31 in neuroblastomas. Journal of the National Cancer Institute 100, 940-949 (2008).
201. Y. Fujitani et al., Ptf1a determines horizontal and amacrine cell fates during mouse retinal development. Development (Cambridge, England) 133, 4439-4450 (2006).
202. S. Fukuda et al., Two distinct subpopulations of nestin-positive cells in adult mouse dentate gyrus. The Journal of Neuroscience: The Official Journal of the Society for Neuroscience 23, 9357-9366 (2003).
203. M. J. Fullwood et al., An oestrogen-receptor-alpha-bound human chromatin interactome. Nature 462, 58-64 (2009).
204. E. Fussner, R. W. Ching, D. P. Bazett-Jones, Living without 30 nm chromatin fibers. Trends in Biochemical Sciences 36, 1-6 (2011).

205. D. V. Fyodorov, J. T. Kadonaga, Dynamics of ATP-dependent chromatin assembly by ACF. Nature 418, 897-900 (2002).
206. J. F. Gadisseux, P. Evrard, Glial-neuronal relationship in the developing central nervous system. A histochemical-electron microscope study of radial glial cell particulate glycogen in normal and reeler mice and the human fetus. Developmental Neuroscience 7, 12-32 (1985).
207. F. H. Gage, Mammalian neural stem cells. Science (New York, N.Y.) 287, 1433-1438 (2000).
208. F. Gao, B. C. Foat, H. J. Bussemaker, Defining transcriptional networks through integrative modeling of mRNA expression and transcription factor binding data. BMC bioinformatics 5, (2004).
209. I. Garcia et al., Expression of the neuron-specific protein CHD5 is an independent marker of outcome in neuroblastoma. Molecular Cancer 9, (2010).
210. A. Garcia-Bellido, J. Moscoso del Pradio, Genetic analysis of maternal information in Drosophila. Nature 278, 346-348 (1979).
211. A. Gaspar-Maia et al., Chd1 regulates open chromatin and pluripotency of embryonic stem cells. Nature 460, 863-868 (2009).
212. M. Geertz, S. J. Maerkl, Experimental strategies for studying transcription factor-DNA binding specificities. Briefings in Functional Genomics 9, 362-373 (2010).
213. M. B. Gerstein et al., Integrative analysis of the Caenorhabditis elegans genome by the modENCODE project. Science (New York, N.Y.) 330, 1775-1787 (2010).
214. Y. Ghavi-Helm, E. E. M. Furlong, Analyzing transcription factor occupancy during embryo development using ChIP-seq. Methods in Molecular Biology (Clifton, N.J.) 786, 229-245 (2012).
215. A. Ghazalpour et al., Comparative analysis of proteome and transcriptome variation in mouse. PLoS genetics 7, (2011).
216. S. Ghisletti et al., Identification and characterization of enhancers controlling the inflammatory gene expression program in macrophages. Immunity 32, 317-328 (2010).
217. J. H. Gibcus, J. Dekker, The hierarchy of the 3D genome. Molecular Cell 49, 773-782 (2013).
218. D. G. Gibson, J. C. Venter, Synthetic biology: Construction of a yeast chromosome. Nature 509, 168-169 (2014).
219. D. A. Gilchrist et al., Regulating the regulators: the pervasive effects of Pol II pausing on stimulus-responsive gene networks. Genes & Development 26, 933-944 (2012).
220. L. Gimeno, R. Hashemi, P. Brûlet, S. Martínez, Analysis of Fgf15 expression pattern in the mouse neural tube. Brain Research Bulletin 57, 297-299 (2002).
221. L. Giorgetti et al., Noncooperative interactions between transcription factors and clustered DNA binding sites enable graded transcriptional responses to environmental inputs. Molecular Cell 37, 418-428 (2010).
222. S. M. Glasgow, R. M. Henke, R. J. Macdonald, C. V. E. Wright, J. E. Johnson, Ptf1a determines GABAergic over glutamatergic neuronal cell fate in the spinal cord dorsal horn. Development (Cambridge, England) 132, 5461-5469 (2005).
223. A. D. Goldberg et al., Distinct factors control histone variant H3.3 localization at specific genomic regions. Cell 140, 678-691 (2010).
224. R. H. Goodman, S. Smolik, CBP/p300 in cell growth, transformation, and development. Genes & Development 14, 1553-1577 (2000).
225. S. M. Görisch, P. Lichter, K. Rippe, Mobility of multi-subunit complexes in the nucleus: accessibility and dynamics of chromatin subcompartments. Histochemistry and Cell Biology 123, 217-228 (2005).
226. M. Götz, W. B. Huttner, The cell biology of neurogenesis. Nature Reviews. Molecular Cell Biology 6, 777-788 (2005).
227. E. Gould, H. A. Cameron, D. C. Daniels, C. S. Woolley, B. S. McEwen, Adrenal hormones suppress cell division in the adult rat dentate gyrus. The Journal of Neuroscience: The Official Journal of the Society for Neuroscience 12, 3642-3650 (1992).
228. E. Gould, H. A. Cameron, B. S. McEwen, Blockade of NMDA receptors increases cell death and birth in the developing rat dentate gyrus. The Journal of Comparative Neurology 340, 551-565 (1994).
229. S. J. Gould, The Structure of Evolutionary Theory. (Harvard University Press, 2002), pp. 1460.
230. M. Goulding, Circuits controlling vertebrate locomotion: moving in a new direction. Nature Reviews. Neuroscience 10, 507-518 (2009).
231. K. Gowan et al., Crossinhibitory activities of Ngn1 and Math1 allow specification of distinct dorsal interneurons. Neuron 31, 219-232 (2001).

232. D. Graur et al., On the Immortality of Television Sets: "Function" in the Human Genome According to the Evolution-Free Gospel of ENCODE. Genome Biology and Evolution 5, 578-590 (2013).
233. I. Griffiths et al., Axonal swellings and degeneration in mice lacking the major proteolipid of myelin. Science (New York, N.Y.) 280, 1610-1613 (1998).
234. A. I. Grosberg, S. K. Nechaev, E. I. Shakhnovich, [The role of topological limitations in the kinetics of homopolymer collapse and self-assembly of biopolymers]. Biofizika 33, 247-253 (1988).
235. A. Y. Grosberg, A. R. Khokhlov, in American Insitute of Physics, NY. (1994).
236. D. S. Gross, W. T. Garrard, Nuclease hypersensitive sites in chromatin. Annual Review of Biochemistry 57, 159-197 (1988).
237. L. Guelen et al., Domain organization of human chromosomes revealed by mapping of nuclear lamina interactions. Nature 453, 948-951 (2008).
238. F. Guillemot et al., Mammalian achaete-scute homolog 1 is required for the early development of olfactory and autonomic neurons. Cell 75, 463-476 (1993).
239. L. Gunhaga, T. M. Jessell, T. Edlund, Sonic hedgehog signaling at gastrula stages specifies ventral telencephalic cells in the chick embryo. Development (Cambridge, England) 127, 3283-3293 (2000).
240. Z. Guo et al., Early postnatal GFAP-expressing cells produce multilineage progeny in cerebrum and astrocytes in cerebellum of adult mice. Brain Research 1532, 14-20 (2013).
241. J. B. Gurdon, On the origin and persistence of a cytoplasmic state inducing nuclear DNA synthesis in frogs' eggs. Proceedings of the National Academy of Sciences of the United States of America 58, 545-552 (1967).
242. J. B. Gurdon, From nuclear transfer to nuclear reprogramming: the reversal of cell differentiation. Annual Review of Cell and Developmental Biology 22, 1-22 (2006).
243. J. A. Hall, P. T. Georgel, CHD proteins: a diverse family with strong ties. Biochemistry and Cell Biology = Biochimie Et Biologie Cellulaire 85, 463-476 (2007).
244. P. A. Hall, F. M. Watt, Stem cells: the generation and maintenance of cellular diversity. Development (Cambridge, England) 106, 619-633 (1989).
245. G. Hallson et al., dSet1 is the main H3K4 di- and tri-methyltransferase throughout Drosophila development. Genetics 190, 91-100 (2012).
246. Dong W. Han et al., Direct Reprogramming of Fibroblasts into Neural Stem Cells by Defined Factors. Cell Stem Cell 10, 465-472 (2012).
247. Y.-G. Han et al., Hedgehog signaling and primary cilia are required for the formation of adult neural stem cells. Nature Neuroscience 11, 277-284 (2008).
248. D. V. Hansen, J. H. Lui, P. R. L. Parker, A. R. Kriegstein, Neurogenic radial glia in the outer subventricular zone of human neocortex. Nature 464, 554-561 (2010).
249. J. J. Harris, D. Attwell, The energetics of CNS white matter. The Journal of Neuroscience: The Official Journal of the Society for Neuroscience 32, 356-371 (2012).
250. Y. Hart, Y. E. Antebi, A. E. Mayo, N. Friedman, U. Alon, Design principles of cell circuits with paradoxical components. Proceedings of the National Academy of Sciences of the United States of America 109, 8346-8351 (2012).
251. Y. Hart et al., Robust control of nitrogen assimilation by a bifunctional enzyme in E. coli. Molecular Cell 41, 117-127 (2011).
252. E. Hartfuss, R. Galli, N. Heins, M. Götz, Characterization of CNS precursor subtypes and radial glia. Developmental Biology 229, 15-30 (2001).
253. D. K. Hartline, D. R. Colman, Rapid conduction and the evolution of giant axons and myelinated fibers. Current biology: CB 17, R29-35 (2007).
254. T. S. Hartshorne, T. L. Grialou, K. R. Parker, Autistic-like behavior in CHARGE syndrome. American Journal of Medical Genetics. Part A 133A, 257-261 (2005).
255. I. Hatada et al., Astrocyte-specific genes are generally demethylated in neural precursor cells prior to astrocytic differentiation. PloS One 3, (2008).
256. Q. He et al., High conservation of transcription factor binding and evidence for combinatorial regulation across six Drosophila species. Nature Genetics 43, 414-420 (2011).
257. M. Hecker, S. Lambeck, S. Toepfer, E. van Someren, R. Guthke, Gene regulatory network inference: data integration in dynamic models-a review. Bio Systems 96, 86-103 (2009).
258. N. D. Heintzman et al., Histone modifications at human enhancers reflect global cell-type-specific gene expression. Nature 459, 108-112 (2009).
259. N. D. Heintzman et al., Distinct and predictive chromatin signatures of transcriptional promoters and enhancers in the human genome. Nature Genetics 39, 311-318 (2007).

260. A. W. Helms, K. Gowan, A. Abney, T. Savage, J. E. Johnson, Overexpression of MATH1 disrupts the coordination of neural differentiation in cerebellum development. Molecular and Cellular Neurosciences 17, 671-682 (2001).
261. A. W. Helms et al., Sequential roles for Mash1 and Ngn2 in the generation of dorsal spinal cord interneurons. Development (Cambridge, England) 132, 2709-2719 (2005).
262. R. M. Henke et al., Neurog2 is a direct downstream target of the Ptf1a-Rbpj transcription complex in dorsal spinal cord. Development (Cambridge, England) 136, 2945-2954 (2009).
263. D. Hernandez-Verdun, P. Roussel, M. Thiry, V. Sirri, D. L. J. Lafontaine, The nucleolus: structure/function relationship in RNA metabolism. Wiley interdisciplinary reviews. RNA 1, 415-431 (2010).
264. C. Hildebrand, R. Hahn, Relation between myelin sheath thickness and axon size in spinal cord white matter of some vertebrate species. Journal of the Neurological Sciences 38, 421-434 (1978).
265. C. Hildebrand, S. Remahl, H. Persson, C. Bjartmar, Myelinated nerve fibres in the CNS. Progress in Neurobiology 40, 319-384 (1993).
266. M. R. Hirsch, M. C. Tiveron, F. Guillemot, J. F. Brunet, C. Goridis, Control of noradrenergic differentiation and Phox2a expression by MASH1 in the central and peripheral nervous system. Development (Cambridge, England) 125, 599-608 (1998).
267. K. Hizume, S. H. Yoshimura, K. Takeyasu, Linker histone H1 per se can induce three-dimensional folding of chromatin fiber. Biochemistry 44, 12978-12989 (2005).
268. D. Hnisz et al., Super-enhancers in the control of cell identity and disease. Cell 155, 934-947 (2013).
269. B. G. Hoffman et al., Locus co-occupancy, nucleosome positioning, and H3K4me1 regulate the functionality of FOXA2-, HNF4A-, and PDX1-bound loci in islets and liver. Genome Research 20, 1037-1051 (2010).
270. P. Hogeweg, Toward a theory of multilevel evolution: long-term information integration shapes the mutational landscape and enhances evolvability. Advances in Experimental Medicine and Biology 751, 195-224 (2012).
271. T. Honjo, The shortest path from the surface to the nucleus: RBP-J kappa/Su(H) transcription factor. Genes to Cells: Devoted to Molecular & Cellular Mechanisms 1, 1-9 (1996).
272. R. A. Horowitz, D. A. Agard, J. W. Sedat, C. L. Woodcock, The three-dimensional architecture of chromatin in situ: electron tomography reveals fibers composed of a continuously variable zig-zag nucleosomal ribbon. The Journal of Cell Biology 125, 1-10 (1994).
273. U. Horsch, A. Scheele, Compendium on CHARGE syndrome multi-disciplinary and international perspectives. (Median-Verl. von Killisch-Horn, Heidelberg, 2011).
274. S. Horton, A. Meredith, J. A. Richardson, J. E. Johnson, Correct coordination of neuronal differentiation events in ventral forebrain requires the bHLH factor MASH1. Molecular and Cellular Neurosciences 14, 355-369 (1999).
275. M. Hoshino et al., Ptf1a, a bHLH transcriptional gene, defines GABAergic neuronal fates in cerebellum. Neuron 47, 201-213 (2005).
276. G. Hu, P. A. Wade, NuRD and pluripotency: a complex balancing act. Cell Stem Cell 10, 497-503 (2012).
277. Z. Hu, P. J. Killion, V. R. Iyer, Genetic reconstruction of a functional transcriptional regulatory network. Nature Genetics 39, 683-687 (2007).
278. E. G. Hughes, S. H. Kang, M. Fukaya, D. E. Bergles, Oligodendrocyte progenitors balance growth with self-repulsion to achieve homeostasis in the adult brain. Nature Neuroscience 16, 668-676 (2013).
279. E. Huillard et al., Disruption of CK2beta in embryonic neural stem cells compromises proliferation and oligodendrogenesis in the mouse telencephalon. Molecular and Cellular Biology 30, 2737-2749 (2010).
280. E. A. Hurd et al., Loss of Chd7 function in gene-trapped reporter mice is embryonic lethal and associated with severe defects in multiple developing tissues. Mammalian Genome: Official Journal of the International Mammalian Genome Society 18, 94-104 (2007).
281. A. F. Huxley, R. Stämpfli, Evidence for saltatory conduction in peripheral myelinated nerve fibres. The Journal of Physiology 108, 315-339 (1949).
282. J. Huxley, Evolution: The Modern Synthesis. (ed. London: George Allen and Unwin Ltd, 1942).
283. M. Hynes et al., Control of cell pattern in the neural tube by the zinc finger transcription factor and oncogene Gli-1. Neuron 19, 15-26 (1997).
284. M. Hynes et al., The seven-transmembrane receptor smoothened cell-autonomously induces multiple ventral cell types. Nature Neuroscience 3, 41-46 (2000).

285. R. A. Ihrie et al., Persistent sonic hedgehog signaling in adult brain determines neural stem cell positional identity. Neuron 71, 250-262 (2011).
286. I. Imayoshi et al., Oscillatory control of factors determining multipotency and fate in mouse neural progenitors. Science (New York, N.Y.) 342, 1203-1208 (2013).
287. I. Imayoshi, R. Kageyama, Oscillatory control of bHLH factors in neural progenitors. Trends in Neurosciences, (2014).
288. I. Imayoshi, T. Shimogori, T. Ohtsuka, R. Kageyama, Hes genes and neurogenin regulate non-neural versus neural fate specification in the dorsal telencephalic midline. Development (Cambridge, England) 135, 2531-2541 (2008).
289. M. Ishibashi et al., Targeted disruption of mammalian hairy and Enhancer of split homolog-1 (HES-1) leads to up-regulation of neural helix-loop-helix factors, premature neurogenesis, and severe neural tube defects. Genes & Development 9, 3136-3148 (1995).
290. T. Iso, L. Kedes, Y. Hamamori, HES and HERP families: multiple effectors of the Notch signaling pathway. Journal of Cellular Physiology 194, 237-255 (2003).
291. D. A. Jackson, A. B. Hassan, R. J. Errington, P. R. Cook, Visualization of focal sites of transcription within human nuclei. The EMBO journal 12, 1059-1065 (1993).
292. A. Jacquier, The complex eukaryotic transcriptome: unexpected pervasive transcription and novel small RNAs. Nature Reviews. Genetics 10, 833-844 (2009).
293. R. Jansen, D. Greenbaum, M. Gerstein, Relating whole-genome expression data with protein-protein interactions. Genome Research 12, 37-46 (2002).
294. N. Janssen et al., Mutation update on the CHD7 gene involved in CHARGE syndrome. Human Mutation 33, 1149-1160 (2012).
295. S. Jarriault et al., Signalling downstream of activated mammalian Notch. Nature 377, 355-358 (1995).
296. R. G. Jenner et al., The transcription factors T-bet and GATA-3 control alternative pathways of T-cell differentiation through a shared set of target genes. Proceedings of the National Academy of Sciences of the United States of America 106, 17876-17881 (2009).
297. K. W. Jeong et al., Recognition of enhancer element-specific histone methylation by TIP60 in transcriptional activation. Nature Structural & Molecular Biology 18, 1358-1365 (2011).
298. S. Jessberger, F. H. Gage, Adult neurogenesis: bridging the gap between mice and humans. Trends in Cell Biology, (2014).
299. C. Jin et al., H3.3/H2A.Z double variant-containing nucleosomes mark 'nucleosome-free regions' of active promoters and other regulatory regions. Nature Genetics 41, 941-945 (2009).
300. F. Jin et al., A high-resolution map of the three-dimensional chromatin interactome in human cells. Nature 503, 290-294 (2013).
301. Q. Jin et al., Distinct roles of GCN5/PCAF-mediated H3K9ac and CBP/p300-mediated H3K18/27ac in nuclear receptor transactivation. The EMBO journal 30, 249-262 (2011).
302. S. John et al., Chromatin accessibility pre-determines glucocorticoid receptor binding patterns. Nature Genetics 43, 264-268 (2011).
303. J. E. Johnson, S. J. Birren, D. J. Anderson, Two rat homologues of Drosophila achaete-scute specifically expressed in neuronal precursors. Nature 346, 858-861 (1990).
304. F. C. Jones et al., The genomic basis of adaptive evolution in threespine sticklebacks. Nature 484, 55-61 (2012).
305. M. C. J. Jongmans et al., CHARGE syndrome: the phenotypic spectrum of mutations in the CHD7 gene. Journal of Medical Genetics 43, 306-314 (2006).
306. R. Kageyama, T. Ohtsuka, T. Kobayashi, The Hes gene family: repressors and oscillators that orchestrate embryogenesis. Development (Cambridge, England) 134, 1243-1251 (2007).
307. R. Kageyama, T. Ohtsuka, H. Shimojo, I. Imayoshi, Dynamic Notch signaling in neural progenitor cells and a revised view of lateral inhibition. Nature Neuroscience 11, 1247-1251 (2008).
308. R. Kalhor, H. Tjong, N. Jayathilaka, F. Alber, L. Chen, Genome architectures revealed by tethered chromosome conformation capture and population-based modeling. Nature Biotechnology 30, 90-98 (2012).
309. Y. Kao-Huang et al., Nonspecific DNA binding of genome-regulating proteins as a biological control mechanism: measurement of DNA-bound Escherichia coli lac repressor in vivo. Proceedings of the National Academy of Sciences of the United States of America 74, 4228-4232 (1977).
310. M. S. Kaplan, J. W. Hinds, Neurogenesis in the adult rat: electron microscopic analysis of light radioautographs. Science (New York, N.Y.) 197, 1092-1094 (1977).

311. P. Kapranov et al., RNA maps reveal new RNA classes and a possible function for pervasive transcription. Science (New York, N.Y.) 316, 1484-1488 (2007).
312. M. Karow et al., Reprogramming of pericyte-derived cells of the adult human brain into induced neuronal cells. Cell Stem Cell 11, 471-476 (2012).
313. D. Kawaguchi, S. Furutachi, H. Kawai, K. Hozumi, Y. Gotoh, Dll1 maintains quiescence of adult neural stem cells and segregates asymmetrically during mitosis. Nature Communications 4, (2013).
314. J. Kele et al., Neurogenin 2 is required for the development of ventral midbrain dopaminergic neurons. Development (Cambridge, England) 133, 495-505 (2006).
315. G. Kempermann, H. G. Kuhn, F. H. Gage, More hippocampal neurons in adult mice living in an enriched environment. Nature 386, 493-495 (1997).
316. G. Kempermann, H. G. Kuhn, F. H. Gage, Experience-induced neurogenesis in the senescent dentate gyrus. The Journal of Neuroscience: The Official Journal of the Society for Neuroscience 18, 3206-3212 (1998).
317. G. Kempermann, S. Jessberger, B. Steiner, G. Kronenberg, Milestones of neuronal development in the adult hippocampus. Trends in Neurosciences 27, 447-452 (2004).
318. B. N. Kholodenko et al., Untangling the wires: a strategy to trace functional interactions in signaling and gene networks. Proceedings of the National Academy of Sciences of the United States of America 99, 12841-12846 (2002).
319. S. Khorasanizadeh, The nucleosome: from genomic organization to genomic regulation. Cell 116, 259-272 (2004).
320. C. Kiecker, C. Niehrs, A morphogen gradient of Wnt/beta-catenin signalling regulates anteroposterior neural patterning in Xenopus. Development (Cambridge, England) 128, 4189-4201 (2001).
321. C. Kiecker, A. Lumsden, The role of organizers in patterning the nervous system. Annual Review of Neuroscience 35, 347-367 (2012).
322. M.-S. Kim, X. Merlo, C. Wilson, J. Lough, Co-activation of atrial natriuretic factor promoter by Tip60 and serum response factor. The Journal of Biological Chemistry 281, 15082-15089 (2006).
323. T.-K. Kim et al., Widespread transcription at neuronal activity-regulated enhancers. Nature 465, 182-187 (2010).
324. A. H. Knoll, The Multiple Origins of Complex Multicellularity. Annual Review of Earth and Planetary Sciences 39, 217-239 (2011).
325. F. Koch, J.-C. Andrau, Initiating RNA polymerase II and TIPs as hallmarks of enhancer activity and tissue-specificity. Transcription 2, 263-268 (2011).
326. N. L. Komarova, X. Zou, Q. Nie, L. Bardwell, A theoretical framework for specificity in cell signaling. Molecular Systems Biology 1, n/a-n/a (2005).
327. T. Kondo, M. Raff, Oligodendrocyte precursor cells reprogrammed to become multipotential CNS stem cells. Science (New York, N.Y.) 289, 1754-1757 (2000).
328. A. Y. Konev et al., CHD1 motor protein is required for deposition of histone variant H3.3 into chromatin in vivo. Science (New York, N.Y.) 317, 1087-1090 (2007).
329. D. Konno et al., Neuroepithelial progenitors undergo LGN-dependent planar divisions to maintain self-renewability during mammalian neurogenesis. Nature Cell Biology 10, 93-101 (2008).
330. I. E. Konstantinov, In search of Alexander A. Maximow: the man behind the unitarian theory of hematopoiesis. Perspectives in Biology and Medicine 43, 269-276 (2000).
331. R. Kopan, M. X. G. Ilagan, The canonical Notch signaling pathway: unfolding the activation mechanism. Cell 137, 216-233 (2009).
332. R. D. Kornberg, Mediator and the mechanism of transcriptional activation. Trends in Biochemical Sciences 30, 235-239 (2005).
333. T. Kosaka, K. Hama, Three-dimensional structure of astrocytes in the rat dentate gyrus. The Journal of Comparative Neurology 249, 242-260 (1986).
334. Y. Kosodo, Interkinetic nuclear migration: beyond a hallmark of neurogenesis. Cellular and molecular life sciences: CMLS 69, 2727-2738 (2012).
335. T. Kouzarides, SnapShot: Histone-modifying enzymes. Cell 131, (2007).
336. S. Krauss, J. P. Concordet, P. W. Ingham, A functionally conserved homolog of the Drosophila segment polarity gene hh is expressed in tissues with polarizing activity in zebrafish embryos. Cell 75, 1431-1444 (1993).
337. A. Kriegstein, A. Alvarez-Buylla, The glial nature of embryonic and adult neural stem cells. Annual Review of Neuroscience 32, 149-184 (2009).

338. A. Kriegstein, S. Noctor, V. Martínez-Cerdeño, Patterns of neural stem and progenitor cell division may underlie evolutionary cortical expansion. Nature Reviews. Neuroscience 7, 883-890 (2006).
339. S. Kriks, G. M. Lanuza, R. Mizuguchi, M. Nakafuku, M. Goulding, Gsh2 is required for the repression of Ngn1 and specification of dorsal interneuron fate in the spinal cord. Development (Cambridge, England) 132, 2991-3002 (2005).
340. J. N. Kuehner, E. L. Pearson, C. Moore, Unravelling the means to an end: RNA polymerase II transcription termination. Nature Reviews. Molecular Cell Biology 12, 283-294 (2011).
341. H. G. Kuhn, H. Dickinson-Anson, F. H. Gage, Neurogenesis in the dentate gyrus of the adult rat: age-related decrease of neuronal progenitor proliferation. The Journal of Neuroscience: The Official Journal of the Society for Neuroscience 16, 2027-2033 (1996).
342. M. Küspert, A. Hammer, M. R. Bösl, M. Wegner, Olig2 regulates Sox10 expression in oligodendrocyte precursors through an evolutionary conserved distal enhancer. Nucleic Acids Research 39, 1280-1293 (2011).
343. J. Ladewig et al., Small molecules enable highly efficient neuronal conversion of human fibroblasts. Nature Methods 9, 575-578 (2012).
344. S. R. Lalani et al., Spectrum of CHD7 mutations in 110 individuals with CHARGE syndrome and genotype-phenotype correlation. American Journal of Human Genetics 78, 303-314 (2006).
345. B. E. LaMonica, J. H. Lui, D. V. Hansen, A. R. Kriegstein, Mitotic spindle orientation predicts outer radial glial cell generation in human neocortex. Nature Communications 4, (2013).
346. F. Lan et al., Recognition of unmethylated histone H3 lysine 4 links BHC80 to LSD1-mediated gene repression. Nature 448, 718-722 (2007).
347. E. S. Lander et al., Initial sequencing and analysis of the human genome. Nature 409, 860-921 (2001).
348. S. G. Landt et al., ChIP-seq guidelines and practices of the ENCODE and modENCODE consortia. Genome Research 22, 1813-1831 (2012).
349. C. Lange, W. B. Huttner, F. Calegari, Cdk4/cyclinD1 overexpression in neural stem cells shortens G1, delays neurogenesis, and promotes the generation and expansion of basal progenitors. Cell Stem Cell 5, 320-331 (2009).
350. B. Langmead, C. Trapnell, M. Pop, S. L. Salzberg, Ultrafast and memory-efficient alignment of short DNA sequences to the human genome. Genome Biology 10, (2009).
351. C. Larroux et al., Genesis and expansion of metazoan transcription factor gene classes. Molecular Biology and Evolution 25, 980-996 (2008).
352. L. S. Laursen, C. W. Chan, C. Ffrench-Constant, Translation of myelin basic protein mRNA in oligodendrocytes is regulated by integrin activation and hnRNP-K. The Journal of Cell Biology 192, 797-811 (2011).
353. P. J. Laybourn, J. T. Kadonaga, Role of nucleosomal cores and histone H1 in regulation of transcription by RNA polymerase II. Science (New York, N.Y.) 254, 238-245 (1991).
354. J.-H. Lee, D. G. Skalnik, Wdr82 is a C-terminal domain-binding protein that recruits the Setd1A Histone H3-Lys4 methyltransferase complex to transcription start sites of transcribed human genes. Molecular and Cellular Biology 28, 609-618 (2008).
355. K. K. Lee, J. L. Workman, Histone acetyltransferase complexes: one size doesn't fit all. Nature Reviews. Molecular Cell Biology 8, 284-295 (2007).
356. M. J. Lee et al., Sequential application of anticancer drugs enhances cell death by rewiring apoptotic signaling networks. Cell 149, 780-794 (2012).
357. S. Lee et al., A culture system to study oligodendrocyte myelination processes using engineered nanofibers. Nature Methods 9, 917-922 (2012).
358. T. I. Lee et al., Control of Developmental Regulators by Polycomb in Human Embryonic Stem Cells. Cell 125, 301-313 (2006).
359. Y. J. Lee, D. H. Han, Y. K. Pak, S. H. Cho, Circadian regulation of low density lipoprotein receptor promoter activity by CLOCK/BMAL1, Hes1 and Hes6. Experimental & Molecular Medicine 44, 642-652 (2012).
360. Y. Lee et al., Oligodendroglia metabolically support axons and contribute to neurodegeneration. Nature 487, 443-448 (2012).
361. M. K. Lehtinen, C. A. Walsh, Neurogenesis at the brain-cerebrospinal fluid interface. Annual Review of Cell and Developmental Biology 27, 653-679 (2011).

362. Q. Lei, A. K. Zelman, E. Kuang, S. Li, M. P. Matise, Transduction of graded Hedgehog signaling by a combination of Gli2 and Gli3 activator functions in the developing spinal cord. Development 131, 3593-3604 (2004).
363. B. Lenhard, A. Sandelin, P. Carninci, Metazoan promoters: emerging characteristics and insights into transcriptional regulation. Nature Reviews. Genetics 13, 233-245 (2012).
364. M. Levine, R. Tjian, Transcription regulation and animal diversity. Nature 424, 147-151 (2003).
365. M. Levine, Transcriptional enhancers in animal development and evolution. Current biology: CB 20, R754-763 (2010).
366. P. Levitt, P. Rakic, Immunoperoxidase localization of glial fibrillary acidic protein in radial glial cells and astrocytes of the developing rhesus monkey brain. The Journal of Comparative Neurology 193, 815-840 (1980).
367. H. Li, J. P. de Faria, P. Andrew, J. Nitarska, W. D. Richardson, Phosphorylation regulates OLIG2 cofactor choice and the motor neuron-oligodendrocyte fate switch. Neuron 69, 918-929 (2011).
368. E. Lieberman-Aiden et al., Comprehensive mapping of long-range interactions reveals folding principles of the human genome. Science (New York, N.Y.) 326, 289-293 (2009).
369. R. S. Lillie, FACTORS AFFECTING TRANSMISSION AND RECOVERY IN THE PASSIVE IRON NERVE MODEL. The Journal of General Physiology 7, 473-507 (1925).
370. S. Lin, A. D. Riggs, The general affinity of lac repressor for E. coli DNA: implications for gene regulation in procaryotes and eucaryotes. Cell 4, 107-111 (1975).
371. C. Linker et al., Cell communication with the neural plate is required for induction of neural markers by BMP inhibition: evidence for homeogenetic induction and implications for Xenopus animal cap and chick explant assays. Developmental Biology 327, 478-486 (2009).
372. S. C. Little, M. Tikhonov, T. Gregor, Precise developmental gene expression arises from globally stochastic transcriptional activity. Cell 154, 789-800 (2013).
373. J. Liu, P. Casaccia, Epigenetic regulation of oligodendrocyte identity. Trends in Neurosciences 33, 193-201 (2010).
374. J. Liu et al., Impaired adult myelination in the prefrontal cortex of socially isolated mice. Nature Neuroscience 15, 1621-1623 (2012).
375. C. Y. Logan, R. Nusse, The Wnt signaling pathway in development and disease. Annual Review of Cell and Developmental Biology 20, 781-810 (2004).
376. C. Lois, A. Alvarez-Buylla, Proliferating subventricular zone cells in the adult mammalian forebrain can differentiate into neurons and glia. Proceedings of the National Academy of Sciences of the United States of America 90, 2074-2077 (1993).
377. G. Longo, P. A. Miquel, C. Sonnenschein, A. M. Soto, Is information a proper observable for biological organization? Progress in Biophysics and Molecular Biology 109, 108-114 (2012).
378. A. Louvi, S. Artavanis-Tsakonas, Notch signalling in vertebrate neural development. Nature Reviews. Neuroscience 7, 93-102 (2006).
379. Q. R. Lu et al., Oligodendrocyte lineage genes (OLIG) as molecular markers for human glial brain tumors. Proceedings of the National Academy of Sciences of the United States of America 98, 10851-10856 (2001).
380. Q. R. Lu et al., Sonic hedgehog--regulated oligodendrocyte lineage genes encoding bHLH proteins in the mammalian central nervous system. Neuron 25, 317-329 (2000).
381. Q. R. Lu et al., Common developmental requirement for Olig function indicates a motor neuron/oligodendrocyte connection. Cell 109, 75-86 (2002).
382. K. Luger, A. W. Mäder, R. K. Richmond, D. F. Sargent, T. J. Richmond, Crystal structure of the nucleosome core particle at 2.8 A resolution. Nature 389, 251-260 (1997).
383. J. H. Lui, D. V. Hansen, A. R. Kriegstein, Development and evolution of the human neocortex. Cell 146, 18-36 (2011).
384. E. Lujan, S. Chanda, H. Ahlenius, T. C. Südhof, M. Wernig, Direct conversion of mouse fibroblasts to self-renewing, tripotent neural precursor cells. Proceedings of the National Academy of Sciences of the United States of America 109, 2527-2532 (2012).
385. G. Lupo, W. A. Harris, K. E. Lewis, Mechanisms of ventral patterning in the vertebrate nervous system. Nature Reviews. Neuroscience 7, 103-114 (2006).
386. A. Lusser, D. L. Urwin, J. T. Kadonaga, Distinct activities of CHD1 and ACF in ATP-dependent chromatin assembly. Nature Structural & Molecular Biology 12, 160-166 (2005).
387. Q. Ma, C. Kintner, D. J. Anderson, Identification of neurogenin, a vertebrate neuronal determination gene. Cell 87, 43-52 (1996).

388. S. MacArthur et al., Developmental roles of 21 Drosophila transcription factors are determined by quantitative differences in binding to an overlapping set of thousands of genomic regions. Genome Biology 10, (2009).
389. R. Machold et al., Sonic hedgehog is required for progenitor cell maintenance in telencephalic stem cell niches. Neuron 39, 937-950 (2003).
390. R. Machold, G. Fishell, Math1 is expressed in temporally discrete pools of cerebellar rhombic-lip neural progenitors. Neuron 48, 17-24 (2005).
391. K. Maeshima, S. Hihara, M. Eltsov, Chromatin structure: does the 30-nm fibre exist in vivo? Current Opinion in Cell Biology 22, 291-297 (2010).
392. P. K. Maini, T. E. Woolley, R. E. Baker, E. A. Gaffney, S. S. Lee, Turing's model for biological pattern formation and the robustness problem. Interface Focus 2, 487-496 (2012).
393. M. Makinodan, K. M. Rosen, S. Ito, G. Corfas, A critical period for social experience-dependent oligodendrocyte maturation and myelination. Science (New York, N.Y.) 337, 1357-1360 (2012).
394. A. Maksimov, in Folia Haematologica 8. (1909), pp. 125-134.
395. P. Malatesta, M. Götz, Radial glia - from boring cables to stem cell stars. Development (Cambridge, England) 140, 483-486 (2013).
396. S. Malik, R. G. Roeder, The metazoan Mediator co-activator complex as an integrative hub for transcriptional regulation. Nature Reviews. Genetics 11, 761-772 (2010).
397. J. R. Manak et al., Biological function of unannotated transcription during the early development of Drosophila melanogaster. Nature Genetics 38, 1151-1158 (2006).
398. P. K. Mandal, H. H. Kazazian, SnapShot: Vertebrate transposons. Cell 135, 192-192.e191 (2008).
399. S. Mangan, U. Alon, Structure and function of the feed-forward loop network motif. Proceedings of the National Academy of Sciences of the United States of America 100, 11980-11985 (2003).
400. J.-M. Mangin, P. Li, J. Scafidi, V. Gallo, Experience-dependent regulation of NG2 progenitors in the developing barrel cortex. Nature Neuroscience 15, 1192-1194 (2012).
401. Y. S. Mao, B. Zhang, D. L. Spector, Biogenesis and function of nuclear bodies. Trends in genetics: TIG 27, 295-306 (2011).
402. L. Marcon, J. Sharpe, Turing patterns in development: what about the horse part? Current Opinion in Genetics & Development 22, 578-584 (2012).
403. C. G. A. Marfella, A. N. Imbalzano, The Chd family of chromatin remodelers. Mutation Research 618, 30-40 (2007).
404. R. Margueron, D. Reinberg, Chromatin structure and the inheritance of epigenetic information. Nature Reviews. Genetics 11, 285-296 (2010).
405. S. Marro et al., Direct lineage conversion of terminally differentiated hepatocytes to functional neurons. Cell Stem Cell 9, 374-382 (2011).
406. G. R. Martin, Isolation of a pluripotent cell line from early mouse embryos cultured in medium conditioned by teratocarcinoma stem cells. Proceedings of the National Academy of Sciences of the United States of America 78, 7634-7638 (1981).
407. S. Martínez, The isthmic organizer and brain regionalization. The International Journal of Developmental Biology 45, 367-371 (2001).
408. S. Martínez, L. Puelles, Neurogenetic compartments of the mouse diencephalon and some characteristic gene expression patterns. Results and Problems in Cell Differentiation 30, 91-106 (2000).
409. A. Martinez-Ferre, M. Navarro-Garberi, C. Bueno, S. Martinez, Wnt signal specifies the intrathalamic limit and its organizer properties by regulating Shh induction in the alar plate. The Journal of Neuroscience: The Official Journal of the Society for Neuroscience 33, 3967-3980 (2013).
410. B. Martynoga, D. Drechsel, F. Guillemot, Molecular control of neurogenesis: a view from the mammalian cerebral cortex. Cold Spring Harbor Perspectives in Biology 4, (2012).
411. G. A. Maston, S. G. Landt, M. Snyder, M. R. Green, Characterization of enhancer function from genome-wide analyses. Annual Review of Genomics and Human Genetics 13, 29-57 (2012).
412. A. Mathelier et al., JASPAR 2014: an extensively expanded and updated open-access database of transcription factor binding profiles. Nucleic Acids Research 42, D142-147 (2014).
413. M. A. Matthews, D. Duncan, A quantitative study of morphological changes accompanying the initiation and progress of myelin production in the dorsal funiculus of the rat spinal cord. The Journal of Comparative Neurology 142, 1-22 (1971).
414. H. R. Maturana, The fine anatomy of the optic nerve of anurans--an electron microscope study. The Journal of Biophysical and Biochemical Cytology 7, 107-120 (1960).

415. H. R. Maturana, F. J. Varela, Autopoiesis and Cognition: The Realization of the Living. (ed. Boston Studies in the Philosophy of Science, Vol. 42, 1973), pp. 184.
416. H. Maturana, F. Varena, De Maquinas y Seres Vivos. On Machines and Living Beings. (Santiago de Chile, ed. 1 edition, 1972), pp. 140.
417. V. Matys et al., TRANSFAC and its module TRANSCompel: transcriptional gene regulation in eukaryotes. Nucleic Acids Research 34, D108-110 (2006).
418. S. K. McConnell, Strategies for the generation of neuronal diversity in the developing central nervous system. The Journal of Neuroscience: The Official Journal of the Society for Neuroscience 15, 6987-6998 (1995).
419. P. McDonel, I. Costello, B. Hendrich, Keeping things quiet: roles of NuRD and Sin3 co-repressor complexes during mammalian development. The International Journal of Biochemistry & Cell Biology 41, 108-116 (2009).
420. J. D. McGhee, J. M. Nickol, G. Felsenfeld, D. C. Rau, Higher order structure of chromatin: orientation of nucleosomes within the 30 nm chromatin solenoid is independent of species and spacer length. Cell 33, 831-841 (1983).
421. A. P. McMahon, A. Bradley, The Wnt-1 (int-1) proto-oncogene is required for development of a large region of the mouse brain. Cell 62, 1073-1085 (1990).
422. F. Mei et al., Stage-specific deletion of Olig2 conveys opposing functions on differentiation and maturation of oligodendrocytes. The Journal of Neuroscience: The Official Journal of the Society for Neuroscience 33, 8454-8462 (2013).
423. D. H. Meijer et al., Separated at birth? The functional and molecular divergence of OLIG1 and OLIG2. Nature Reviews. Neuroscience 13, 819-831 (2012).
424. H. Meinhardt, Primary body axes of vertebrates: Generation of a near-cartesian coordinate system and the role of Spemann-type organizer. Developmental Dynamics 235, 2907-2919 (2006).
425. S. Melnik et al., The proteomes of transcription factories containing RNA polymerases I, II or III. Nature Methods 8, 963-968 (2011).
426. E. M. Mercer et al., Multilineage priming of enhancer repertoires precedes commitment to the B and myeloid cell lineages in hematopoietic progenitors. Immunity 35, 413-425 (2011).
427. F. D. Miller, A. S. Gauthier, Timing is everything: making neurons versus glia in the developing cortex. Neuron 54, 357-369 (2007).
428. R. H. Miller, Oligodendrocyte origins. Trends in Neurosciences 19, 92-96 (1996).
429. S. L. Miller, A production of amino acids under possible primitive earth conditions. Science (New York, N.Y.) 117, 528-529 (1953).
430. J. Min, Y. Zhang, R.-M. Xu, Structural basis for specific binding of Polycomb chromodomain to histone H3 methylated at Lys 27. Genes & Development 17, 1823-1828 (2003).
431. Z. Mirzadeh, F. T. Merkle, M. Soriano-Navarro, J. M. Garcia-Verdugo, A. Alvarez-Buylla, Neural stem cells confer unique pinwheel architecture to the ventricular surface in neurogenic regions of the adult brain. Cell Stem Cell 3, 265-278 (2008).
432. J. P. Misson, C. P. Austin, T. Takahashi, C. L. Cepko, V. S. Caviness, The alignment of migrating neural cells in relation to the murine neopallial radial glial fiber system. Cerebral Cortex (New York, N.Y.: 1991) 1, 221-229 (1991).
433. S. Mitew et al., Mechanisms regulating the development of oligodendrocytes and central nervous system myelin. Neuroscience 276C, 29-47 (2014).
434. G. Miyoshi, Y. Bessho, S. Yamada, R. Kageyama, Identification of a novel basic helix-loop-helix gene, Heslike, and its role in GABAergic neurogenesis. The Journal of Neuroscience: The Official Journal of the Society for Neuroscience 24, 3672-3682 (2004).
435. G. Miyoshi, G. Fishell, GABAergic interneuron lineages selectively sort into specific cortical layers during early postnatal development. Cerebral Cortex (New York, N.Y.: 1991) 21, 845-852 (2011).
436. G. Miyoshi et al., Genetic fate mapping reveals that the caudal ganglionic eminence produces a large and diverse population of superficial cortical interneurons. The Journal of Neuroscience: The Official Journal of the Society for Neuroscience 30, 1582-1594 (2010).
437. W. Möbius et al., in Methods in Cell Biology, M.-R. Thomas, Ed. (Academic Press, 2010), vol. Volume 96, pp. 475-512.
438. E. C. mod et al., Identification of functional elements and regulatory circuits by Drosophila modENCODE. Science (New York, N.Y.) 330, 1787-1797 (2010).
439. M. L. Monje, H. Toda, T. D. Palmer, Inflammatory blockade restores adult hippocampal neurogenesis. Science (New York, N.Y.) 302, 1760-1765 (2003).

440. D. K. Morest, J. Silver, Precursors of neurons, neuroglia, and ependymal cells in the CNS: what are they? Where are they from? How do they get where they are going? Glia 43, 6-18 (2003).
441. S. J. Morrison, N. M. Shah, D. J. Anderson, Regulatory mechanisms in stem cell biology. Cell 88, 287-298 (1997).
442. L. Mu et al., SoxC transcription factors are required for neuronal differentiation in adult hippocampal neurogenesis. The Journal of Neuroscience: The Official Journal of the Society for Neuroscience 32, 3067-3080 (2012).
443. A. Y. Mulkidjanian, M. Y. Galperin, E. V. Koonin, Co-evolution of primordial membranes and membrane proteins. Trends in Biochemical Sciences 34, 206-215 (2009).
444. F. Müller, L. Tora, Chromatin and DNA sequences in defining promoters for transcription initiation. Biochimica Et Biophysica Acta 1839, 118-128 (2014).
445. I. Muñoz-Sanjuán, A. H. Brivanlou, Neural induction, the default model and embryonic stem cells. Nature Reviews. Neuroscience 3, 271-280 (2002).
446. A. Murciano, J. Zamora, J. López-Sánchez, J. M. Frade, Interkinetic nuclear movement may provide spatial clues to the regulation of neurogenesis. Molecular and Cellular Neurosciences 21, 285-300 (2002).
447. J. A. Murray, W. F. Blakemore, The relationship between internodal length and fibre diameter in the spinal cord of the cat. Journal of the Neurological Sciences 45, 29-41 (1980).
448. C. Murre et al., Interactions between heterologous helix-loop-helix proteins generate complexes that bind specifically to a common DNA sequence. Cell 58, 537-544 (1989).
449. C. A. Musselman, M.-E. Lalonde, J. Côté, T. G. Kutateladze, Perceiving the epigenetic landscape through histone readers. Nature Structural & Molecular Biology 19, 1218-1227 (2012).
450. C. A. Musselman et al., Binding of the CHD4 PHD2 finger to histone H3 is modulated by covalent modifications. The Biochemical Journal 423, 179-187 (2009).
451. N. Nady et al., Recognition of multivalent histone states associated with heterochromatin by UHRF1 protein. The Journal of Biological Chemistry 286, 24300-24311 (2011).
452. F. J. Najm et al., Transcription factor-mediated reprogramming of fibroblasts to expandable, myelinogenic oligodendrocyte progenitor cells. Nature Biotechnology 31, 426-433 (2013).
453. Y. Nakada, T. L. Hunsaker, R. M. Henke, J. E. Johnson, Distinct domains within Mash1 and Math1 are required for function in neuronal differentiation versus neuronal cell-type specification. Development (Cambridge, England) 131, 1319-1330 (2004).
454. A. Nakamoto, L. M. Nagy, T. Shimizu, Secondary embryonic axis formation by transplantation of D quadrant micromeres in an oligochaete annelid. Development 138, 283-290 (2011).
455. M. Nakanishi et al., Microglia-derived interleukin-6 and leukaemia inhibitory factor promote astrocytic differentiation of neural stem/progenitor cells. The European Journal of Neuroscience 25, 649-658 (2007).
456. H. Nakatani et al., Ascl1/Mash1 promotes brain oligodendrogenesis during myelination and remyelination. The Journal of Neuroscience: The Official Journal of the Society for Neuroscience 33, 9752-9768 (2013).
457. H. Nam et al., Network context and selection in the evolution to enzyme specificity. Science (New York, N.Y.) 337, 1101-1104 (2012).
458. M. Namihira et al., Committed neuronal precursors confer astrocytic potential on residual neural precursor cells. Developmental Cell 16, 245-255 (2009).
459. M. Namihira, K. Nakashima, Mechanisms of astrocytogenesis in the mammalian brain. Current Opinion in Neurobiology 23, 921-927 (2013).
460. G. J. Narlikar, R. Sundaramoorthy, T. Owen-Hughes, Mechanisms and functions of ATP-dependent chromatin-remodeling enzymes. Cell 154, 490-503 (2013).
461. K. Nasmyth, C. H. Haering, Cohesin: its roles and mechanisms. Annual Review of Genetics 43, 525-558 (2009).
462. G. Natoli, J.-C. Andrau, Noncoding transcription at enhancers: general principles and functional models. Annual Review of Genetics 46, 1-19 (2012).
463. K.-A. Nave, Myelination and the trophic support of long axons. Nature Reviews. Neuroscience 11, 275-283 (2010).
464. K.-A. Nave, B. D. Trapp, Axon-glial signaling and the glial support of axon function. Annual Review of Neuroscience 31, 535-561 (2008).
465. B. M. Neale et al., Patterns and rates of exonic de novo mutations in autism spectrum disorders. Nature 485, 242-245 (2012).

466. A. Németh, G. Längst, Genome organization in and around the nucleolus. Trends in genetics: TIG 27, 149-156 (2011).
467. C. R. Nicholas et al., Functional maturation of hPSC-derived forebrain interneurons requires an extended timeline and mimics human neural development. Cell Stem Cell 12, 573-586 (2013).
468. C. Niehrs, On growth and form: a Cartesian coordinate system of Wnt and BMP signaling specifies bilaterian body axes. Development (Cambridge, England) 137, 845-857 (2010).
469. M. Nieto, C. Schuurmans, O. Britz, F. Guillemot, Neural bHLH genes control the neuronal versus glial fate decision in cortical progenitors. Neuron 29, 401-413 (2001).
470. S. C. Noctor, A. C. Flint, T. A. Weissman, R. S. Dammerman, A. R. Kriegstein, Neurons derived from radial glial cells establish radial units in neocortex. Nature 409, 714-720 (2001).
471. S. C. Noctor, V. Martínez-Cerdeño, L. Ivic, A. R. Kriegstein, Cortical neurons arise in symmetric and asymmetric division zones and migrate through specific phases. Nature Neuroscience 7, 136-144 (2004).
472. Alex S. Nord et al., Rapid and Pervasive Changes in Genome-wide Enhancer Usage during Mammalian Development. Cell 155, 1521-1531 (2013).
473. J. D. Norton, ID helix-loop-helix proteins in cell growth, differentiation and tumorigenesis. Journal of Cell Science 113 (Pt 22), 3897-3905 (2000).
474. B. G. Novitch, A. I. Chen, T. M. Jessell, Coordinate regulation of motor neuron subtype identity and pan-neuronal properties by the bHLH repressor Olig2. Neuron 31, 773-789 (2001).
475. B. J. O'Roak et al., Sporadic autism exomes reveal a highly interconnected protein network of de novo mutations. Nature 485, 246-250 (2012).
476. U. Ohler, D. A. Wassarman, Promoting developmental transcription. Development 137, 15-26 (2010).
477. S. Ohno, So much "junk" DNA in our genome. Brookhaven Symposia in Biology 23, 366-370 (1972).
478. T. Ohtsuka et al., Hes1 and Hes5 as notch effectors in mammalian neuronal differentiation. The EMBO journal 18, 2196-2207 (1999).
479. T. Ohtsuka, M. Sakamoto, F. Guillemot, R. Kageyama, Roles of the basic helix-loop-helix genes Hes1 and Hes5 in expansion of neural stem cells of the developing brain. The Journal of Biological Chemistry 276, 30467-30474 (2001).
480. M. Okada, K. Okawa, T. Isobe, T. Fukagawa, CENP-H-containing complex facilitates centromere deposition of CENP-A in cooperation with FACT and CHD1. Molecular Biology of the Cell 20, 3986-3995 (2009).
481. E. R. Okawa et al., Expression and sequence analysis of candidates for the 1p36.31 tumor suppressor gene deleted in neuroblastomas. Oncogene 27, 803-810 (2008).
482. C.-T. Ong, V. G. Corces, Enhancer function: new insights into the regulation of tissue-specific gene expression. Nature Reviews. Genetics 12, 283-293 (2011).
483. C.-T. Ong, V. G. Corces, Enhancers: emerging roles in cell fate specification. EMBO reports 13, 423-430 (2012).
484. S. K. T. Ooi et al., DNMT3L connects unmethylated lysine 4 of histone H3 to de novo methylation of DNA. Nature 448, 714-717 (2007).
485. C. Pack, K. Saito, M. Tamura, M. Kinjo, Microenvironment and effect of energy depletion in the nucleus analyzed by mobility of multiple oligomeric EGFPs. Biophysical Journal 91, 3921-3936 (2006).
486. R. A. Pagon, J. M. Graham, J. Zonana, S. L. Yong, Coloboma, congenital heart disease, and choanal atresia with multiple anomalies: CHARGE association. The Journal of Pediatrics 99, 223-227 (1981).
487. T. D. Palmer, A. R. Willhoite, F. H. Gage, Vascular niche for adult hippocampal neurogenesis. The Journal of Comparative Neurology 425, 479-494 (2000).
488. Q. Pan, O. Shai, L. J. Lee, B. J. Frey, B. J. Blencowe, Deep surveying of alternative splicing complexity in the human transcriptome by high-throughput sequencing. Nature Genetics 40, 1413-1415 (2008).
489. C. H. Pander, Wurzburg., (1817).
490. Z. P. Pang et al., Induction of human neuronal cells by defined transcription factors. Nature 476, 220-223 (2011).
491. J. M. Parent et al., Dentate granule cell neurogenesis is increased by seizures and contributes to aberrant network reorganization in the adult rat hippocampus. The Journal of Neuroscience: The Official Journal of the Society for Neuroscience 17, 3727-3738 (1997).

492. J. M. Parent, R. C. Elliott, S. J. Pleasure, N. M. Barbaro, D. H. Lowenstein, Aberrant seizure-induced neurogenesis in experimental temporal lobe epilepsy. Annals of Neurology 59, 81-91 (2006).
493. J. T. M. L. Paridaen, W. B. Huttner, Neurogenesis during development of the vertebrate central nervous system. EMBO reports 15, 351-364 (2014).
494. J. T. M. L. Paridaen, M. Wilsch-Bräuninger, W. B. Huttner, Asymmetric inheritance of centrosome-associated primary cilium membrane directs ciliogenesis after cell division. Cell 155, 333-344 (2013).
495. C. M. Parras et al., The proneural gene Mash1 specifies an early population of telencephalic oligodendrocytes. The Journal of Neuroscience: The Official Journal of the Society for Neuroscience 27, 4233-4242 (2007).
496. C. M. Parras et al., Divergent functions of the proneural genes Mash1 and Ngn2 in the specification of neuronal subtype identity. Genes & Development 16, 324-338 (2002).
497. D. Pasini et al., Characterization of an antagonistic switch between histone H3 lysine 27 methylation and acetylation in the transcriptional regulation of Polycomb group target genes. Nucleic Acids Research 38, 4958-4969 (2010).
498. S. A. Patten et al., Role of Chd7 in zebrafish: a model for CHARGE syndrome. PloS One 7, (2012).
499. A. Pattyn et al., Ascl1/Mash1 is required for the development of central serotonergic neurons. Nature Neuroscience 7, 589-595 (2004).
500. A. Pattyn et al., Coordinated temporal and spatial control of motor neuron and serotonergic neuron generation from a common pool of CNS progenitors. Genes & Development 17, 729-737 (2003).
501. S. Paul et al., Chd5 requires PHD-mediated histone 3 binding for tumor suppression. Cell Reports 3, 92-102 (2013).
502. A. Pavlopoulos, M. Akam, Hox gene Ultrabithorax regulates distinct sets of target genes at successive stages of Drosophila haltere morphogenesis. Proceedings of the National Academy of Sciences of the United States of America 108, 2855-2860 (2011).
503. J. C. Pearson, D. Lemons, W. McGinnis, Modulating Hox gene functions during animal body patterning. Nature Reviews. Genetics 6, 893-904 (2005).
504. A. Pekowska et al., H3K4 tri-methylation provides an epigenetic signature of active enhancers. The EMBO journal 30, 4198-4210 (2011).
505. P. V. Peña et al., Molecular mechanism of histone H3K4me3 recognition by plant homeodomain of ING2. Nature 442, 100-103 (2006).
506. L. A. Pennacchio, E. M. Rubin, Genomic strategies to identify mammalian regulatory sequences. Nature Reviews Genetics 2, 100-109 (2001).
507. E. M. Pera, M. Kessel, Patterning of the chick forebrain anlage by the prechordal plate. Development (Cambridge, England) 124, 4153-4162 (1997).
508. A. Peters, The formation and structure of myelin sheaths in the central nervous system. The Journal of Biophysical and Biochemical Cytology 8, 431-446 (1960).
509. A. Peters, The structure of the peripheral nerves of the lamprey (Lampetra fluviatilis). Journal of Ultrastructure Research 4, 349-359 (1960).
510. M. A. Petryniak, G. B. Potter, D. H. Rowitch, J. L. R. Rubenstein, Dlx1 and Dlx2 control neuronal versus oligodendroglial cell fate acquisition in the developing forebrain. Neuron 55, 417-433 (2007).
511. E. Peyre et al., A lateral belt of cortical LGN and NuMA guides mitotic spindle movements and planar division in neuroepithelial cells. The Journal of Cell Biology 193, 141-154 (2011).
512. U. Pfisterer et al., Direct conversion of human fibroblasts to dopaminergic neurons. Proceedings of the National Academy of Sciences of the United States of America 108, 10343-10348 (2011).
513. R. D. Phair et al., Global nature of dynamic protein-chromatin interactions in vivo: three-dimensional genome scanning and dynamic interaction networks of chromatin proteins. Molecular and Cellular Biology 24, 6393-6402 (2004).
514. J. E. Phillips, V. G. Corces, CTCF: master weaver of the genome. Cell 137, 1194-1211 (2009).
515. G. Piaton, R. M. Gould, C. Lubetzki, Axon-oligodendrocyte interactions during developmental myelination, demyelination and repair. Journal of Neurochemistry 114, 1243-1260 (2010).
516. H. Pickersgill et al., Characterization of the Drosophila melanogaster genome at the nuclear lamina. Nature Genetics 38, 1005-1014 (2006).
517. G.-A. Pilz et al., Amplification of progenitors in the mammalian telencephalon includes a new radial glial cell type. Nature Communications 4, (2013).

518. R. Pla, V. Borrell, N. Flames, O. Marín, Layer acquisition by cortical GABAergic interneurons is independent of Reelin signaling. The Journal of Neuroscience: The Official Journal of the Society for Neuroscience 26, 6924-6934 (2006).
519. M. Placzek, M. Tessier-Lavigne, T. Yamada, T. Jessell, J. Dodd, Mesodermal control of neural cell identity: floor plate induction by the notochord. Science (New York, N.Y.) 250, 985-988 (1990).
520. M. Placzek, J. Briscoe, The floor plate: multiple cells, multiple signals. Nature Reviews. Neuroscience 6, 230-240 (2005).
521. J.-C. Platel, K. A. Dave, A. Bordey, Control of neuroblast production and migration by converging GABA and glutamate signals in the postnatal forebrain. The Journal of Physiology 586, 3739-3743 (2008).
522. L. Poitras, N. Ghanem, G. Hatch, M. Ekker, The proneural determinant MASH1 regulates forebrain Dlx1/2 expression through the I12b intergenic enhancer. Development (Cambridge, England) 134, 1755-1765 (2007).
523. A. Pombero, S. Martinez, Telencephalic morphogenesis during the process of neurulation: an experimental study using quail-chick chimeras. The Journal of Comparative Neurology 512, 784-797 (2009).
524. S. Pons, E. Martí, Sonic hedgehog synergizes with the extracellular matrix protein vitronectin to induce spinal motor neuron differentiation. Development (Cambridge, England) 127, 333-342 (2000).
525. J. A. Porter et al., The product of hedgehog autoproteolytic cleavage active in local and long-range signalling. Nature 374, 363-366 (1995).
526. Z. C. Poss, C. C. Ebmeier, D. J. Taatjes, The Mediator complex and transcription regulation. Critical Reviews in Biochemistry and Molecular Biology 48, 575-608 (2013).
527. M. P. Postiglione et al., Mouse inscuteable induces apical-basal spindle orientation to facilitate intermediate progenitor generation in the developing neocortex. Neuron 72, 269-284 (2011).
528. C. S. Potten, M. Loeffler, Stem cells: attributes, cycles, spirals, pitfalls and uncertainties. Lessons for and from the crypt. Development (Cambridge, England) 110, 1001-1020 (1990).
529. R. C. Potts et al., CHD5, a brain-specific paralog of Mi2 chromatin remodeling enzymes, regulates expression of neuronal genes. PloS One 6, (2011).
530. M. G. Pray-Grant, J. A. Daniel, D. Schieltz, J. R. Yates, P. A. Grant, Chd1 chromodomain links histone H3 methylation with SAGA- and SLIK-dependent acetylation. Nature 433, 434-438 (2005).
531. M. Price et al., Regional expression of the homeobox gene Nkx-2.2 in the developing mammalian forebrain. Neuron 8, 241-255 (1992).
532. I. Prigogine, Self-Organization in Nonequilibrium Systems: From Dissipative Structures to Order through Fluctuations. (Wiley, New York, ed. 1 edition, 1977), pp. 512.
533. I. Prigogine, I. Stengers, Order Out of Chaos: Man's New Dialogue with Nature. (Bantam Books, 1984), pp. 390.
534. A. V. Probst, E. Dunleavy, G. Almouzni, Epigenetic inheritance during the cell cycle. Nature Reviews. Molecular Cell Biology 10, 192-206 (2009).
535. L. Puelles, G. Domenech-Ratto, M. Martinez-de-la-Torre, Location of the rostral end of the longitudinal brain axis: review of an old topic in the light of marking experiments on the closing rostral neuropore. Journal of Morphology 194, 163-171 (1987).
536. M. Qiu, K. Shimamura, L. Sussel, S. Chen, J. L. Rubenstein, Control of anteroposterior and dorsoventral domains of Nkx-6.1 gene expression relative to other Nkx genes during vertebrate CNS development. Mechanisms of Development 72, 77-88 (1998).
537. A. Rada-Iglesias et al., Epigenomic annotation of enhancers predicts transcriptional regulators of human neural crest. Cell Stem Cell 11, 633-648 (2012).
538. A. Rada-Iglesias et al., A unique chromatin signature uncovers early developmental enhancers in humans. Nature 470, 279-283 (2011).
539. M. C. Raff, R. H. Miller, M. Noble, A glial progenitor cell that develops in vitro into an astrocyte or an oligodendrocyte depending on culture medium. Nature 303, 390-396 (1983).
540. A. Ragvin et al., Nucleosome binding by the bromodomain and PHD finger of the transcriptional cofactor p300. Journal of Molecular Biology 337, 773-788 (2004).
541. A. Raj, A. van Oudenaarden, Nature, nurture, or chance: stochastic gene expression and its consequences. Cell 135, 216-226 (2008).
542. P. Rakic, Mode of cell migration to the superficial layers of fetal monkey neocortex. The Journal of Comparative Neurology 145, 61-83 (1972).
543. O. Ram et al., Combinatorial patterning of chromatin regulators uncovered by genome-wide location analysis in human cells. Cell 147, 1628-1639 (2011).

544. C. M. Rands, S. Meader, C. P. Ponting, G. Lunter, 8.2% of the Human Genome Is Constrained: Variation in Rates of Turnover across Functional Element Classes in the Human Lineage. PLoS Genet 10, (2014).
545. J. M. Raser, E. K. O'Shea, Noise in gene expression: origins, consequences, and control. Science (New York, N.Y.) 309, 2010-2013 (2005).
546. M. Rasminsky, T. A. Sears, Internodal conduction in undissected demyelinated nerve fibres. The Journal of Physiology 227, 323-350 (1972).
547. C. Readhead et al., Expression of a myelin basic protein gene in transgenic shiverer mice: correction of the dysmyelinating phenotype. Cell 48, 703-712 (1987).
548. S. Remahl, C. Hildebrand, Changing relation between onset of myelination and axon diameter range in developing feline white matter. Journal of the Neurological Sciences 54, 33-45 (1982).
549. G. Rey et al., Genome-wide and phase-specific DNA-binding rhythms of BMAL1 control circadian output functions in mouse liver. PLoS biology 9, (2011).
550. N. Reynolds, A. O'Shaughnessy, B. Hendrich, Transcriptional repressors: multifaceted regulators of gene expression. Development (Cambridge, England) 140, 505-512 (2013).
551. N. Reynolds et al., NuRD-mediated deacetylation of H3K27 facilitates recruitment of Polycomb Repressive Complex 2 to direct gene repression. The EMBO journal 31, 593-605 (2012).
552. H. S. Rhee, B. F. Pugh, Genome-wide structure and organization of eukaryotic pre-initiation complexes. Nature 483, 295-301 (2012).
553. A. J. Ridley, Life at the leading edge. Cell 145, 1012-1022 (2011).
554. K. L. Ring et al., Direct reprogramming of mouse and human fibroblasts into multipotent neural stem cells with a single factor. Cell Stem Cell 11, 100-109 (2012).
555. T. O. Ririe, J. S. Fernandes, P. W. Sternberg, The Caenorhabditis elegans vulva: a post-embryonic gene regulatory network controlling organogenesis. Proceedings of the National Academy of Sciences of the United States of America 105, 20095-20099 (2008).
556. H. Roelink et al., Floor plate and motor neuron induction by vhh-1, a vertebrate homolog of hedgehog expressed by the notochord. Cell 76, 761-775 (1994).
557. H. Roelink et al., Floor plate and motor neuron induction by different concentrations of the amino-terminal cleavage product of sonic hedgehog autoproteolysis. Cell 81, 445-455 (1995).
558. K. W. Rogers, A. F. Schier, Morphogen gradients: from generation to interpretation. Annual Review of Cell and Developmental Biology 27, 377-407 (2011).
559. S. E. Ross, M. E. Greenberg, C. D. Stiles, Basic helix-loop-helix factors in cortical development. Neuron 39, 13-25 (2003).
560. S. B. Rothbart, B. D. Strahl, Interpreting the language of histone and DNA modifications. Biochimica Et Biophysica Acta 1839, 627-643 (2014).
561. A. Routh, S. Sandin, D. Rhodes, Nucleosome repeat length and linker histone stoichiometry determine chromatin fiber structure. Proceedings of the National Academy of Sciences of the United States of America 105, 8872-8877 (2008).
562. D. H. Rowitch, Glial specification in the vertebrate neural tube. Nature Reviews. Neuroscience 5, 409-419 (2004).
563. D. H. Rowitch, A. R. Kriegstein, Developmental genetics of vertebrate glial-cell specification. Nature 468, 214-222 (2010).
564. J. L. Rubenstein, K. Shimamura, S. Martinez, L. Puelles, Regionalization of the prosencephalic neural plate. Annual Review of Neuroscience 21, 445-477 (1998).
565. A. Ruiz i Altaba, Combinatorial Gli gene function in floor plate and neuronal inductions by Sonic hedgehog. Development (Cambridge, England) 125, 2203-2212 (1998).
566. A. J. Ruthenburg, H. Li, D. J. Patel, C. D. Allis, Multivalent engagement of chromatin modifications by linked binding modules. Nature Reviews. Molecular Cell Biology 8, 983-994 (2007).
567. M. Saade et al., Sonic hedgehog signaling switches the mode of division in the developing nervous system. Cell Reports 4, 492-503 (2013).
568. A. Saha, J. Wittmeyer, B. R. Cairns, Mechanisms for nucleosome movement by ATP-dependent chromatin remodeling complexes. Results and Problems in Cell Differentiation 41, 127-148 (2006).
569. P. Salomoni, F. Calegari, Cell cycle control of mammalian neural stem cells: putting a speed limit on G1. Trends in Cell Biology 20, 233-243 (2010).
570. N. Sanai et al., Corridors of migrating neurons in the human brain and their decline during infancy. Nature 478, 382-386 (2011).

571. A. Sandelin et al., Mammalian RNA polymerase II core promoters: insights from genome-wide studies. Nature Reviews. Genetics 8, 424-436 (2007).
572. T. A. Sanders, E. Llagostera, M. Barna, Specialized filopodia direct long-range transport of SHH during vertebrate tissue patterning. Nature 497, 628-632 (2013).
573. L. Sang, H. A. Coller, J. M. Roberts, Control of the reversibility of cellular quiescence by the transcriptional repressor HES1. Science (New York, N.Y.) 321, 1095-1100 (2008).
574. S. N. Sansom et al., The level of the transcription factor Pax6 is essential for controlling the balance between neural stem cell self-renewal and neurogenesis. PLoS genetics 5, (2009).
575. L. Santarelli et al., Requirement of hippocampal neurogenesis for the behavioral effects of antidepressants. Science (New York, N.Y.) 301, 805-809 (2003).
576. N. Santos, J. F. Reiter, Building it up and taking it down: the regulation of vertebrate ciliogenesis. Developmental Dynamics: An Official Publication of the American Association of Anatomists 237, 1972-1981 (2008).
577. A. Sanyal, B. R. Lajoie, G. Jain, J. Dekker, The long-range interaction landscape of gene promoters. Nature 489, 109-113 (2012).
578. Y. Sasai, R. Kageyama, Y. Tagawa, R. Shigemoto, S. Nakanishi, Two mammalian helix-loop-helix factors structurally related to Drosophila hairy and Enhancer of split. Genes & Development 6, 2620-2634 (1992).
579. F. C. Sauer, Mitosis in the neural tube. The Journal of Comparative Neurology 62, 377-405 (1935).
580. D. Schmidt et al., Five-Vertebrate ChIP-seq Reveals the Evolutionary Dynamics of Transcription Factor Binding. Science 328, 1036-1040 (2010).
581. M. P. Schnetz et al., Genomic distribution of CHD7 on chromatin tracks H3K4 methylation patterns. Genome Research 19, 590-601 (2009).
582. M. P. Schnetz et al., CHD7 targets active gene enhancer elements to modulate ES cell-specific gene expression. PLoS genetics 6, (2010).
583. B. Schwanhäusser et al., Global quantification of mammalian gene expression control. Nature 473, 337-342 (2011).
584. M. A. Schwartz, H. D. Madhani, Principles of MAP kinase signaling specificity in Saccharomyces cerevisiae. Annual Review of Genetics 38, 725-748 (2004).
585. A. Scott, J. Song, R. Ewing, Z. Wang, Regulation of protein stability of DNA methyltransferase 1 by post-translational modifications. Acta Biochimica Et Biophysica Sinica 46, 199-203 (2014).
586. A. Sebé-Pedrós, A. de Mendoza, B. F. Lang, B. M. Degnan, I. Ruiz-Trillo, Unexpected repertoire of metazoan transcription factors in the unicellular holozoan Capsaspora owczarzaki. Molecular Biology and Evolution 28, 1241-1254 (2011).
587. T. Seki, Y. Arai, Highly polysialylated neural cell adhesion molecule (NCAM-H) is expressed by newly generated granule cells in the dentate gyrus of the adult rat. The Journal of Neuroscience: The Official Journal of the Society for Neuroscience 13, 2351-2358 (1993).
588. A. A. Sérandour et al., Epigenetic switch involved in activation of pioneer factor FOXA1-dependent enhancers. Genome Research 21, 555-565 (2011).
589. B. Seri, J. M. García-Verdugo, L. Collado-Morente, B. S. McEwen, A. Alvarez-Buylla, Cell types, lineage, and architecture of the germinal zone in the adult dentate gyrus. The Journal of Comparative Neurology 478, 359-378 (2004).
590. T. Setoguchi, T. Kondo, Nuclear export of OLIG2 in neural stem cells is essential for ciliary neurotrophic factor-induced astrocyte differentiation. The Journal of Cell Biology 166, 963-968 (2004).
591. K. Sha et al., Distributed probing of chromatin structure in vivo reveals pervasive chromatin accessibility for expressed and non-expressed genes during tissue differentiation in C. elegans. BMC genomics 11, (2010).
592. J. Shandilya, S. G. E. Roberts, The transcription cycle in eukaryotes: From productive initiation to RNA polymerase II recycling. Biochimica et Biophysica Acta (BBA) - Gene Regulatory Mechanisms 1819, 391-400 (2012).
593. Y. Shen et al., A map of the cis-regulatory sequences in the mouse genome. Nature 488, 116-120 (2012).
594. X. Shi et al., ING2 PHD domain links histone H3 lysine 4 methylation to active gene repression. Nature 442, 96-99 (2006).
595. K. Shimamura, D. J. Hartigan, S. Martinez, L. Puelles, J. L. Rubenstein, Longitudinal organization of the anterior neural plate and neural tube. Development (Cambridge, England) 121, 3923-3933 (1995).

596. K. Shimamura, J. L. Rubenstein, Inductive interactions direct early regionalization of the mouse forebrain. Development (Cambridge, England) 124, 2709-2718 (1997).
597. H. Shimojo, T. Ohtsuka, R. Kageyama, Oscillations in notch signaling regulate maintenance of neural progenitors. Neuron 58, 52-64 (2008).
598. A. Shitamukai, D. Konno, F. Matsuzaki, Oblique radial glial divisions in the developing mouse neocortex induce self-renewing progenitors outside the germinal zone that resemble primate outer subventricular zone progenitors. The Journal of Neuroscience: The Official Journal of the Society for Neuroscience 31, 3683-3695 (2011).
599. T. J. Shors, D. A. Townsend, M. Zhao, Y. Kozorovitskiy, E. Gould, Neurogenesis may relate to some but not all types of hippocampal-dependent learning. Hippocampus 12, 578-584 (2002).
600. O. Shoval, U. Alon, SnapShot: network motifs. Cell 143, 326-e321 (2010).
601. J. R. Siebert, J. M. Graham, C. MacDonald, Pathologic features of the CHARGE association: support for involvement of the neural crest. Teratology 31, 331-336 (1985).
602. T. Siggers, M. H. Duyzend, J. Reddy, S. Khan, M. L. Bulyk, Non-DNA-binding cofactors enhance DNA-binding specificity of a transcriptional regulatory complex. Molecular Systems Biology 7, (2011).
603. J. C. Silbereis et al., Olig1 function is required to repress dlx1/2 and interneuron production in Mammalian brain. Neuron 81, 574-587 (2014).
604. R. Simic et al., Chromatin remodeling protein Chd1 interacts with transcription elongation factors and localizes to transcribed genes. The EMBO journal 22, 1846-1856 (2003).
605. D. N. Simon, K. L. Wilson, The nucleoskeleton as a genome-associated dynamic 'network of networks'. Nature Reviews. Molecular Cell Biology 12, 695-708 (2011).
606. M. A. Simon, D. D. Bowtell, G. S. Dodson, T. R. Laverty, G. M. Rubin, Ras1 and a putative guanine nucleotide exchange factor perform crucial steps in signaling by the sevenless protein tyrosine kinase. Cell 67, 701-716 (1991).
607. M. Simonis et al., Nuclear organization of active and inactive chromatin domains uncovered by chromosome conformation capture-on-chip (4C). Nature Genetics 38, 1348-1354 (2006).
608. M. Simons, D. A. Lyons, Axonal selection and myelin sheath generation in the central nervous system. Current Opinion in Cell Biology 25, 512-519 (2013).
609. J. K. Sims, P. A. Wade, SnapShot: Chromatin remodeling: CHD. Cell 144, 626-626.e621 (2011).
610. R. J. Sims et al., Human but not yeast CHD1 binds directly and selectively to histone H3 methylated at lysine 4 via its tandem chromodomains. The Journal of Biological Chemistry 280, 41789-41792 (2005).
611. M. R. Singleton, M. S. Dillingham, D. B. Wigley, Structure and mechanism of helicases and nucleic acid translocases. Annual Review of Biochemistry 76, 23-50 (2007).
612. G. Sirinakis et al., The RSC chromatin remodelling ATPase translocates DNA with high force and small step size. The EMBO journal 30, 2364-2372 (2011).
613. J. M. Slack, Inducing factors in Xenopus early embryos. Current biology: CB 4, 116-126 (1994).
614. S. T. Smale, Transcription initiation from TATA-less promoters within eukaryotic protein-coding genes. Biochimica Et Biophysica Acta 1351, 73-88 (1997).
615. J. M. Smith. (2000), pp. 177-194.
616. K. J. Smith, W. I. McDonald, The pathophysiology of multiple sclerosis: the mechanisms underlying the production of symptoms and the natural history of the disease. Philosophical Transactions of the Royal Society of London. Series B, Biological Sciences 354, 1649-1673 (1999).
617. N. Snaidero et al., Myelin membrane wrapping of CNS axons by PI(3,4,5)P3-dependent polarized growth at the inner tongue. Cell 156, 277-290 (2014).
618. E. H. Snoussi, Necessary Conditions for Multistationarity and Stable Periodicity. Journal of Biological Systems 06, 3-9 (1998).
619. L. Sommer, Q. Ma, D. J. Anderson, neurogenins, a novel family of atonal-related bHLH transcription factors, are putative mammalian neuronal determination genes that reveal progenitor cell heterogeneity in the developing CNS and PNS. Molecular and Cellular Neurosciences 8, 221-241 (1996).
620. E. Y. Son et al., Conversion of mouse and human fibroblasts into functional spinal motor neurons. Cell Stem Cell 9, 205-218 (2011).
621. D. Song, Z. Wang, T. W. Berger, Contribution of T-type VDCC to TEA-induced long-term synaptic modification in hippocampal CA1 and dentate gyrus. Hippocampus 12, 689-697 (2002).
622. V. H. Sousa, G. Fishell, Sonic hedgehog functions through dynamic changes in temporal competence in the developing forebrain. Current Opinion in Genetics & Development 20, 391-399 (2010).

623. D. G. Southwell et al., Intrinsically determined cell death of developing cortical interneurons. Nature 491, 109-113 (2012).
624. A. Sparmann et al., The chromodomain helicase Chd4 is required for Polycomb-mediated inhibition of astroglial differentiation. The EMBO journal 32, 1598-1612 (2013).
625. N. Spassky et al., Adult ependymal cells are postmitotic and are derived from radial glial cells during embryogenesis. The Journal of Neuroscience: The Official Journal of the Society for Neuroscience 25, 10-18 (2005).
626. H. Spemann, H. Mangold, Induction of embryonic primordia by implantation of organizers from a different species. Roux's Arch. Entw. Mech., 599-638 (1924).
627. A. V. Spirov, D. M. Holloway, Modeling the evolution of gene regulatory networks for spatial patterning in embryo development. Procedia Computer Science 18, (2013).
628. F. Spitz, E. E. M. Furlong, Transcription factors: from enhancer binding to developmental control. Nature Reviews. Genetics 13, 613-626 (2012).
629. S. Srinivasan, K. M. Dorighi, J. W. Tamkun, Drosophila Kismet regulates histone H3 lysine 27 methylation and early elongation by RNA polymerase II. PLoS genetics 4, (2008).
630. V. Sriuranpong et al., Notch signaling induces rapid degradation of achaete-scute homolog 1. Molecular and Cellular Biology 22, 3129-3139 (2002).
631. D. Stamataki, F. Ulloa, S. V. Tsoni, A. Mynett, J. Briscoe, A gradient of Gli activity mediates graded Sonic Hedgehog signaling in the neural tube. Genes & Development 19, 626-641 (2005).
632. B. Steiner et al., Type-2 cells as link between glial and neuronal lineage in adult hippocampal neurogenesis. Glia 54, 805-814 (2006).
633. C. D. Stern, Neural induction: old problem, new findings, yet more questions. Development (Cambridge, England) 132, 2007-2021 (2005).
634. C. D. Stern, Evolution of the mechanisms that establish the embryonic axes. Current Opinion in Genetics & Development 16, 413-418 (2006).
635. C. Stockdale, A. Flaus, H. Ferreira, T. Owen-Hughes, Analysis of nucleosome repositioning by yeast ISWI and Chd1 chromatin remodeling complexes. The Journal of Biological Chemistry 281, 16279-16288 (2006).
636. E. E. Storm et al., Dose-dependent functions of Fgf8 in regulating telencephalic patterning centers. Development (Cambridge, England) 133, 1831-1844 (2006).
637. A. Stoykova, M. Götz, P. Gruss, J. Price, Pax6-dependent regulation of adhesive patterning, R-cadherin expression and boundary formation in developing forebrain. Development (Cambridge, England) 124, 3765-3777 (1997).
638. B. D. Strahl, C. D. Allis, The language of covalent histone modifications. Nature 403, 41-45 (2000).
639. S. Sugiarto et al., Asymmetry-defective oligodendrocyte progenitors are glioma precursors. Cancer Cell 20, 328-340 (2011).
640. M. Sugimori et al., Combinatorial actions of patterning and HLH transcription factors in the spatiotemporal control of neurogenesis and gliogenesis in the developing spinal cord. Development (Cambridge, England) 134, 1617-1629 (2007).
641. M. Sugimori et al., Ascl1 is required for oligodendrocyte development in the spinal cord. Development (Cambridge, England) 135, 1271-1281 (2008).
642. Y. Sun et al., Phosphorylation state of Olig2 regulates proliferation of neural progenitors. Neuron 69, 906-917 (2011).
643. N. Surzenko, T. Crowl, A. Bachleda, L. Langer, L. Pevny, SOX2 maintains the quiescent progenitor cell state of postnatal retinal Muller glia. Development (Cambridge, England) 140, 1445-1456 (2013).
644. Y. Takagi, R. D. Kornberg, Mediator as a general transcription factor. The Journal of Biological Chemistry 281, 80-89 (2006).
645. K. Takahashi, S. Yamanaka, Induction of pluripotent stem cells from mouse embryonic and adult fibroblast cultures by defined factors. Cell 126, 663-676 (2006).
646. T. Takahashi, J. P. Misson, V. S. Caviness, Glial process elongation and branching in the developing murine neocortex: a qualitative and quantitative immunohistochemical analysis. The Journal of Comparative Neurology 302, 15-28 (1990).
647. T. Takahashi, R. S. Nowakowski, V. S. Caviness, The cell cycle of the pseudostratified ventricular epithelium of the embryonic murine cerebral wall. The Journal of Neuroscience: The Official Journal of the Society for Neuroscience 15, 6046-6057 (1995).

648. H. Takebayashi et al., Non-overlapping expression of Olig3 and Olig2 in the embryonic neural tube. Mechanisms of Development 113, 169-174 (2002).
649. T. Takizawa et al., DNA methylation is a critical cell-intrinsic determinant of astrocyte differentiation in the fetal brain. Developmental Cell 1, 749-758 (2001).
650. M. E. Talkowski et al., Sequencing chromosomal abnormalities reveals neurodevelopmental loci that confer risk across diagnostic boundaries. Cell 149, 525-537 (2012).
651. H. Tamai et al., Pax6 transcription factor is required for the interkinetic nuclear movement of neuroepithelial cells. Genes to Cells 12, 983-996 (2007).
652. K. Tamai et al., LDL-receptor-related proteins in Wnt signal transduction. Nature 407, 530-535 (2000).
653. M. Tan et al., Identification of 67 histone marks and histone lysine crotonylation as a new type of histone modification. Cell 146, 1016-1028 (2011).
654. S.-L. Tan, T. Ohtsuka, A. González, R. Kageyama, MicroRNA9 regulates neural stem cell differentiation by controlling Hes1 expression dynamics in the developing brain. Genes to Cells: Devoted to Molecular & Cellular Mechanisms 17, 952-961 (2012).
655. K. Tanigaki et al., Notch1 and Notch3 instructively restrict bFGF-responsive multipotent neural progenitor cells to an astroglial fate. Neuron 29, 45-55 (2001).
656. I. Tasaki, The Electro-Saltatory Transmission of the Nerve Impulse and the Effect of Narcosis Upon the Nerve Fiber. American Journal of Physiology -- Legacy Content 127, 211-227 (1939).
657. C. Taveggia, M. L. Feltri, L. Wrabetz, Signals to promote myelin formation and repair. Nature Reviews. Neurology 6, 276-287 (2010).
658. E. Taverna, M. Götz, W. B. Huttner, The Cell Biology of Neurogenesis: Toward an Understanding of the Development and Evolution of the Neocortex. Annual Review of Cell and Developmental Biology, (2014).
659. E. Taverna, W. B. Huttner, Neural progenitor nuclei IN motion. Neuron 67, 906-914 (2010).
660. S. D. Taverna, H. Li, A. J. Ruthenburg, C. D. Allis, D. J. Patel, How chromatin-binding modules interpret histone modifications: lessons from professional pocket pickers. Nature Structural & Molecular Biology 14, 1025-1040 (2007).
661. S. Temple, The development of neural stem cells. Nature 414, 112-117 (2001).
662. E. P. C. The, A User's Guide to the Encyclopedia of DNA Elements (ENCODE). PLoS Biol 9, (2011).
663. M. Thier et al., Direct conversion of fibroblasts into stably expandable neural stem cells. Cell Stem Cell 10, 473-479 (2012).
664. F. Tie et al., CBP-mediated acetylation of histone H3 lysine 27 antagonizes Drosophila Polycomb silencing. Development (Cambridge, England) 136, 3131-3141 (2009).
665. O. Torper et al., Generation of induced neurons via direct conversion in vivo. Proceedings of the National Academy of Sciences of the United States of America 110, 7038-7043 (2013).
666. B. D. Towbin, P. Meister, S. M. Gasser, The nuclear envelope--a scaffold for silencing? Current Opinion in Genetics & Development 19, 180-186 (2009).
667. E. Traiffort et al., Discrete localizations of hedgehog signalling components in the developing and adult rat nervous system. The European Journal of Neuroscience 11, 3199-3214 (1999).
668. E. Traiffort, K. L. Moya, H. Faure, R. Hässig, M. Ruat, High expression and anterograde axonal transport of aminoterminal sonic hedgehog in the adult hamster brain. The European Journal of Neuroscience 14, 839-850 (2001).
669. J.-W. Tsai, K. H. Bremner, R. B. Vallee, Dual subcellular roles for LIS1 and dynein in radial neuronal migration in live brain tissue. Nature Neuroscience 10, 970-979 (2007).
670. A. M. Turing, in Philosophical Transactions of the Royal Society of London. (1952), pp. 37-72.
671. J. G. van Bemmel et al., A network model of the molecular organization of chromatin in Drosophila. Molecular Cell 49, 759-771 (2013).
672. B. van Steensel, Chromatin: constructing the big picture. The EMBO Journal 30, 1885-1895 (2011).
673. H. W. van Straaten, J. W. Hekking, F. Thors, E. L. Wiertz-Hoessels, J. Drukker, Induction of an additional floor plate in the neural tube. Acta Morphologica Neerlando-Scandinavica 23, 91-97 (1985).
674. H. W. van Straaten, F. Thors, L. Wiertz-Hoessels, J. Hekking, J. Drukker, Effect of a notochordal implant on the early morphogenesis of the neural tube and neuroblasts: histometrical and histological results. Developmental Biology 110, 247-254 (1985).

675. A. Vaquero, A. Loyola, D. Reinberg, The constantly changing face of chromatin. Science of aging knowledge environment: SAGE KE 2003, (2003).
676. J. C. Venter et al., The Sequence of the Human Genome. Science 291, 1304-1351 (2001).
677. A. Verloes, Updated diagnostic criteria for CHARGE syndrome: a proposal. American Journal of Medical Genetics. Part A 133A, 306-308 (2005).
678. P. J. Verschure et al., Condensed chromatin domains in the mammalian nucleus are accessible to large macromolecules. EMBO reports 4, 861-866 (2003).
679. C. Vieira, R. Garcia-Lopez, S. Martínez, Positional regulation of Pax2 expression pattern in mesencephalic and diencephalic alar plate. Neuroscience 137, 7-11 (2006).
680. T. Vierbuchen et al., Direct conversion of fibroblasts to functional neurons by defined factors. Nature 463, 1035-1041 (2010).
681. D. Villar, P. Flicek, D. T. Odom, Evolution of transcription factor binding in metazoans — mechanisms and functional implications. Nature Reviews Genetics 15, 221-233 (2014).
682. F. Viñals et al., BMP-2 decreases Mash1 stability by increasing Id1 expression. The EMBO journal 23, 3527-3537 (2004).
683. A. Visel et al., ChIP-seq accurately predicts tissue-specific activity of enhancers. Nature 457, 854-858 (2009).
684. A. Visel et al., A high-resolution enhancer atlas of the developing telencephalon. Cell 152, 895-908 (2013).
685. L. E. L. M. Vissers et al., Mutations in a new member of the chromodomain gene family cause CHARGE syndrome. Nature Genetics 36, 955-957 (2004).
686. P. Voigt, D. Reinberg, Histone tails: ideal motifs for probing epigenetics through chemical biology approaches. Chembiochem: A European Journal of Chemical Biology 12, 236-252 (2011).
687. P. Voigt, D. Reinberg, Putting a halt on PRC2 in pediatric glioblastoma. Nature Genetics 45, 587-589 (2013).
688. P. Voigt, W.-W. Tee, D. Reinberg, A double take on bivalent promoters. Genes & Development 27, 1318-1338 (2013).
689. T. C. Voss et al., Dynamic exchange at regulatory elements during chromatin remodeling underlies assisted loading mechanism. Cell 146, 544-554 (2011).
690. T. Wada et al., DSIF, a novel transcription elongation factor that regulates RNA polymerase II processivity, is composed of human Spt4 and Spt5 homologs. Genes & Development 12, 343-356 (1998).
691. C. H. Waddington, The epigenotype. Endeavour 1, 18-20 (1942).
692. C. H. Waddington, The strategy of the genes; a discussion of some aspects of theoretical biology. (Allen & Unwin, London, 1957).
693. C. H. Waddington, The nature of life. (Atheneum, New York, 1962).
694. C. H. Waddington, Experiments on embryonic induction. I. The competence of the extra-embryonic ectoderm in the chick. II. Experiments on coagulated organisers in the chick. III. A note on induction by chick primitive streak transplanted to the rabbit embryo. J. exp. Biol. 11, (1934).
695. C. H. Waddington, D. M. Needham, Studies on the nature of the amphibian organization centre II. Induction by synthetic polycyclic hydrocarbons. Proc. Roy. Soc. (Lond.), 310-317 (1935).
696. H. Wake, P. R. Lee, R. D. Fields, Control of local protein synthesis and initial events in myelination by action potentials. Science (New York, N.Y.) 333, 1647-1651 (2011).
697. J. Walfridsson, O. Khorosjutina, P. Matikainen, C. M. Gustafsson, K. Ekwall, A genome-wide role for CHD remodelling factors and Nap1 in nucleosome disassembly. The EMBO journal 26, 2868-2879 (2007).
698. J. A. Wamstad et al., Dynamic and Coordinated Epigenetic Regulation of Developmental Transitions in the Cardiac Lineage. Cell 151, 206-220 (2012).
699. E. T. Wang et al., Alternative isoform regulation in human tissue transcriptomes. Nature 456, 470-476 (2008).
700. H. Wang, G. Ge, Y. Uchida, B. Luu, S. Ahn, Gli3 is required for maintenance and fate specification of cortical progenitors. The Journal of Neuroscience: The Official Journal of the Society for Neuroscience 31, 6440-6448 (2011).
701. X. Wang et al., Asymmetric centrosome inheritance maintains neural progenitors in the neocortex. Nature 461, 947-955 (2009).
702. X. Wang, J.-W. Tsai, B. LaMonica, A. R. Kriegstein, A new subtype of progenitor cell in the mouse embryonic neocortex. Nature Neuroscience 14, 555-561 (2011).

703. O. L. Wapinski et al., Hierarchical mechanisms for direct reprogramming of fibroblasts to neurons. Cell 155, 621-635 (2013).
704. S. G. Waxman, Determinants of conduction velocity in myelinated nerve fibers. Muscle & Nerve 3, 141-150 (1980).
705. S. G. Waxman, Axon-glia interactions: building a smart nerve fiber. Current biology: CB 7, R406-410 (1997).
706. S. G. Waxman, M. V. Bennett, Relative conduction velocities of small myelinated and non-myelinated fibres in the central nervous system. Nature: New Biology 238, 217-219 (1972).
707. V. M. Weake, J. L. Workman, Inducible gene expression: diverse regulatory mechanisms. Nature Reviews. Genetics 11, 426-437 (2010).
708. H. Weintraub, M. Groudine, Chromosomal subunits in active genes have an altered conformation. Science (New York, N.Y.) 193, 848-856 (1976).
709. R. White, E.-M. Krämer-Albers, Axon-glia interaction and membrane traffic in myelin formation. Frontiers in Cellular Neuroscience 7, (2014).
710. W. A. Whyte et al., Enhancer decommissioning by LSD1 during embryonic stem cell differentiation. Nature 482, 221-225 (2012).
711. W. A. Whyte et al., Master transcription factors and mediator establish super-enhancers at key cell identity genes. Cell 153, 307-319 (2013).
712. H. Wildner et al., dILA neurons in the dorsal spinal cord are the product of terminal and non-terminal asymmetric progenitor cell divisions, and require Mash1 for their development. Development (Cambridge, England) 133, 2105-2113 (2006).
713. M. A. Willaredt, E. Tasouri, K. L. Tucker, Primary cilia and forebrain development. Mechanisms of Development 130, 373-380 (2013).
714. M. Wilsch-Bräuninger, J. Peters, J. T. M. L. Paridaen, W. B. Huttner, Basolateral rather than apical primary cilia on neuroepithelial cells committed to delamination. Development (Cambridge, England) 139, 95-105 (2012).
715. D. Wilson, V. Charoensawan, S. K. Kummerfeld, S. A. Teichmann, DBD--taxonomically broad transcription factor predictions: new content and functionality. Nucleic Acids Research 36, D88-92 (2008).
716. E. Wingender, T. Schoeps, J. Dönitz, TFClass: an expandable hierarchical classification of human transcription factors. Nucleic Acids Research 41, D165-170 (2013).
717. L. Wittler, M. Kessel, The acquisition of neural fate in the chick. Mechanisms of Development 121, 1031-1042 (2004).
718. L. Wolpert, Positional information and the spatial pattern of cellular differentiation. Journal of Theoretical Biology 25, 1-47 (1969).
719. L. Wolpert, I. Macpherson, I. Todd, Cell spreading and cell movement: an active or a passive process? Nature 223, 512-513 (1969).
720. C. L. Woodcock, A. I. Skoultchi, Y. Fan, Role of linker histone in chromatin structure and function: H1 stoichiometry and nucleosome repeat length. Chromosome Research: An International Journal on the Molecular, Supramolecular and Evolutionary Aspects of Chromosome Biology 14, 17-25 (2006).
721. n. Wu Ct, J. R. Morris, Genes, genetics, and epigenetics: a correspondence. Science (New York, N.Y.) 293, 1103-1105 (2001).
722. L. M. N. Wu, A. Williams, A. Delaney, D. L. Sherman, P. J. Brophy, Increasing internodal distance in myelinated nerves accelerates nerve conduction to a flat maximum. Current biology: CB 22, 1957-1961 (2012).
723. M. Wu et al., Molecular regulation of H3K4 trimethylation by Wdr82, a component of human Set1/COMPASS. Molecular and Cellular Biology 28, 7337-7344 (2008).
724. Y. Wu, Y. Liu, E. M. Levine, M. S. Rao, Hes1 but not Hes5 regulates an astrocyte versus oligodendrocyte fate choice in glial restricted precursors. Developmental Dynamics: An Official Publication of the American Association of Anatomists 226, 675-689 (2003).
725. Y. Xie, C. Jüschke, C. Esk, S. Hirotsune, J. A. Knoblich, The phosphatase PP4c controls spindle orientation to maintain proliferative symmetric divisions in the developing neocortex. Neuron 79, 254-265 (2013).
726. M. Xin et al., Myelinogenesis and axonal recognition by oligodendrocytes in brain are uncoupled in Olig1-null mice. The Journal of Neuroscience: The Official Journal of the Society for Neuroscience 25, 1354-1365 (2005).
727. F. Xiong et al., Specified neural progenitors sort to form sharp domains after noisy Shh signaling. Cell 153, 550-561 (2013).

728. H. Xu et al., Bergmann glia function in granule cell migration during cerebellum development. Molecular Neurobiology 47, 833-844 (2013).
729. J. Xu et al., Pioneer factor interactions and unmethylated CpG dinucleotides mark silent tissue-specific enhancers in embryonic stem cells. Proceedings of the National Academy of Sciences of the United States of America 104, 12377-12382 (2007).
730. S. Xuan et al., Winged helix transcription factor BF-1 is essential for the development of the cerebral hemispheres. Neuron 14, 1141-1152 (1995).
731. Y. Yamaguchi et al., NELF, a multisubunit complex containing RD, cooperates with DSIF to repress RNA polymerase II elongation. Cell 97, 41-51 (1999).
732. N. Yang et al., Generation of oligodendroglial cells by direct lineage conversion. Nature Biotechnology 31, 434-439 (2013).
733. S. W. Yang, H. A. Nash, Comparison of protein binding to DNA in vivo and in vitro: defining an effective intracellular target. The EMBO journal 14, 6292-6300 (1995).
734. K. Yoon, N. Gaiano, Notch signaling in the mammalian central nervous system: insights from mouse mutants. Nature Neuroscience 8, 709-715 (2005).
735. N. Yosef, A. Regev, Impulse control: temporal dynamics in gene transcription. Cell 144, 886-896 (2011).
736. K. M. Young et al., Oligodendrocyte dynamics in the healthy adult CNS: evidence for myelin remodeling. Neuron 77, 873-885 (2013).
737. R. A. Young, Control of the embryonic stem cell state. Cell 144, 940-954 (2011).
738. N. Yudkovsky, J. A. Ranish, S. Hahn, A transcription reinitiation intermediate that is stabilized by activator. Nature 408, 225-229 (2000).
739. T. Yue et al., A critical role for dorsal progenitors in cortical myelination. The Journal of Neuroscience: The Official Journal of the Society for Neuroscience 26, 1275-1280 (2006).
740. K. Yun et al., Modulation of the notch signaling by Mash1 and Dlx1/2 regulates sequential specification and differentiation of progenitor cell types in the subcortical telencephalon. Development (Cambridge, England) 129, 5029-5040 (2002).
741. B. Zalc, D. Goujet, D. Colman, The origin of the myelination program in vertebrates. Current biology: CB 18, R511-512 (2008).
742. K. S. Zaret, J. S. Carroll, Pioneer transcription factors: establishing competence for gene expression. Genes & Development 25, 2227-2241 (2011).
743. M. Zawadzka et al., CNS-resident glial progenitor/stem cells produce Schwann cells as well as oligodendrocytes during repair of CNS demyelination. Cell Stem Cell 6, 578-590 (2010).
744. G. E. Zentner et al., CHD7 functions in the nucleolus as a positive regulator of ribosomal RNA biogenesis. Human Molecular Genetics 19, 3491-3501 (2010).
745. G. E. Zentner, P. J. Tesar, P. C. Scacheri, Epigenetic signatures distinguish multiple classes of enhancers with distinct cellular functions. Genome Research 21, 1273-1283 (2011).
746. M. Zervas, S. Millet, S. Ahn, A. L. Joyner, Cell behaviors and genetic lineages of the mesencephalon and rhombomere 1. Neuron 43, 345-357 (2004).
747. J. Zhang et al., ChIA-PET analysis of transcriptional chromatin interactions. Methods (San Diego, Calif.) 58, 289-299 (2012).
748. Y. Zhang et al., Spatial organization of the mouse genome and its role in recurrent chromosomal translocations. Cell 148, 908-921 (2012).
749. C. Zhao, W. Deng, F. H. Gage, Mechanisms and functional implications of adult neurogenesis. Cell 132, 645-660 (2008).
750. S. Zhao, W.-P. Fung-Leung, A. Bittner, K. Ngo, X. Liu, Comparison of RNA-Seq and Microarray in Transcriptome Profiling of Activated T Cells. PLoS ONE 9, (2014).
751. Q. Zhou, G. Choi, D. J. Anderson, The bHLH transcription factor Olig2 promotes oligodendrocyte differentiation in collaboration with Nkx2.2. Neuron 31, 791-807 (2001).
752. Q. Zhou, T. Li, D. H. Price, RNA Polymerase II Elongation Control. Annual Review of Biochemistry 81, 119-143 (2012).
753. Q. Zhou, D. J. Anderson, The bHLH transcription factors OLIG2 and OLIG1 couple neuronal and glial subtype specification. Cell 109, 61-73 (2002).
754. X. Zhu et al., Olig2-dependent developmental fate switch of NG2 cells. Development (Cambridge, England) 139, 2299-2307 (2012).

ABSTRACT

Our project aims to provide a new molecular understanding of the transcription program involved in neural stem cells differentiation into oligodendrocytes. The rational of this work relies on previous studies demonstrating that the bHLH transcription factors Olig2 and Ascl1 work in synergy to specify OPCs, the oligodendrocyte progenitor cells. One central goal of this work was to understand at a genomic and transcriptomic level, how Ascl1 and Olig2 work together to specify OPCs. We followed a strategy using genome-wide transcriptome analysis and chromatin immuno-precipitation to characterize Ascl1 and Olig2 directly regulated genes in OPCs and during oligodendrocyte differentiation. We identified new specific markers of different stage of the neural lineages and new important genes correlated to OPCs differentiation. We focused on *Chd7* and *Tns3*, two genes which expressions are driven by Ascl1 and Olig2 and enriched in the oligodendroglial lineage at two interesting stage, the early specification stage and the transition between migrating and differentiating oligodendrocytes, respectively. Moreover, we identified the myelinating oligodendrocyte as the cell in charge of the creatine synthesis in the brain and potentially driving axonal metabolic support. We also used an approach a toxicogenomic and drug repositioning approach to identify new molecules known to modify OPCs and myelin genes but untested in the context of demyelinating diseases. As currently, most of the available treatments for demyelinating diseases are based on immuno-modulatory and anti-inflammatory drugs but none are able to directly promote myelin repair, we expect that these identified genes involved in oligodendrogenesis and whose expression are regulated in demyelinated lesions will allow the development of new therapeutic strategies promoting an efficient remyelination in demyelinating diseases such as Multiple sclerosis or leukodystrophies.

RESUME EN FRANÇAIS

Ce projet vise à fournir une nouvelle compréhension moléculaire du programme de transcription impliqué dans la différenciation des cellules souches neurales en oligodendrocytes myélinisant. La logique de ce travail repose sur des études antérieures ayant montré le rôle des facteurs de transcription bHLH Olig2 et Ascl1, opérant en synergie dans la spécification des OPCs, les cellules progénitrices d'oligodendrocytes . L'objectif central de ce travail était de comprendre au niveau génomique et transcriptomique les mécanismes par lesquels Ascl1 et Olig2 agissent pour spécifier les OPCs. Nous avons suivi une stratégie utilisant l'analyse du transcriptome et des profils de fixation des facteurs de transcription par immuno- précipitation de la chromatine . Nous avons pu identifier les cibles directes de Ascl1 et Olig2 dans les OPC et lors de la différenciation des oligodendrocytes. Nous avons également identifié de nouveaux marqueurs spécifiques des différents stades des lignées oligodendrocyte et nous sommes concentrés sur *Chd7* et *Tns3*, deux gènes régulé par Ascl1 et Olig2 et enrichis dans la lignée oligodendrogliale à deux stades intéressants, la phase de spécification précoce et la transition entre la migration et la différenciation des oligodendrocytes, respectivement. De plus, nous avons porté notre attention sur le rôle spécifique des oligodendrocyte dans la synthèse de la créatine et son rôle possible de support métabolique dans la synthèse de myéline et de support axonal. Nous avons également initié une approche de repositionnement toxicogénomique pour identifier de nouvelles molécules à tester dans le cadre de maladie demyélinisantesLa plupart des traitements disponibles pour traiter les maladies démyélinisantes sont basées sur une approche immune modulatrice et anti-inflammatoire. A ce jour, aucun n'est en mesure de promouvoir directement la réparation de la myéline de manière efficace. Nous espérons que les gènes dont l'expression est régulée dans les lésions de démyélinisation identifiés lors de cette étude permettront de mieux comprendre le mécanisme de remyelinisation et le développement de nouvelles stratégies dans les maladies démyélinisantes telles que la sclérose en plaques ou dans les leucodystrophies.